R-08-46

# Hydrochemistry of surface water and shallow groundwater

## Site descriptive modelling SDM-Site Laxemar

Mats Tröjbom, Mopelikan

Björn Söderbäck, Birgitta Kalinowski,
Svensk Kärnbränslehantering AB

October 2008

**Svensk Kärnbränslehantering AB**
Swedish Nuclear Fuel
and Waste Management Co

Box 250, SE-101 24 Stockholm
Phone +46 8 459 84 00

ISSN 1402-3091
SKB Rapport R-08-46

# Hydrochemistry of surface water and shallow groundwater

## Site descriptive modelling SDM-Site Laxemar

Mats Tröjbom, Mopelikan

Björn Söderbäck, Birgitta Kalinowski,
Svensk Kärnbränslehantering AB

October 2008

*Keywords:* Surface water, Shallow groundwater, Groundwater, Precipitation, Hydrochemistry, Hydrogeochemistry, Chemical composition, Environmental isotopes, Regolith, Major constituents, Minor constituents, Dissolved ions, Trace elements, Nutrient salts, Nutrients, Mass balance, Integrated evaluation, Laxemar, Simpevarp, Oskarshamn.

# Preface

This investigation was conducted for SKB within the framework of SurfaceNet, the group working with site description and modelling of surface systems, for the purpose of evaluating hydrochemical issues with a specific bearing on the surface system. Most of the work was done by Mats Tröjbom (Mopelikan) and Björn Söderbäck (Svensk Kärnbränslehantering AB), with assistance from Birgitta Kalinowski (Svensk Kärnbränslehantering AB). The following persons contributed many relevant comments during the internal review of the report (listed in alphabetical order): Eva Andersson (Sweco Environment AB), Sten Berglund (Svensk Kärnbränslehantering AB), Gustav Sohlenius (SGU), Bill Wallin (Geokema AB) and Kent Werner (EmpTec AB). Russel Alexander (Bedrock Geosciences) added a large number of valuable comments during the external review.

# Abstract

Based on a mathematical/statistical approach, a large number of visualisations and models reflect the hydrochemistry of the Laxemar-Simpevarp area, with the intention of providing an understanding of important processes and factors that affect the hydrochemistry of the surface systems. In order to widen the perspective, all data from Laxemar stage 2.3, including observations from different levels of the bedrock, as well as hydrological measurements and characterisations of the Quaternary deposits, have been included in the analyses. The purpose of this report is to provide a general understanding of the site and to explain observed overall patterns and anomalies, and ultimately to present a conceptual model that explains the present hydrochemistry of the surface system in the light of the past. The report may also serve as a basis for further evaluation and testing of scenarios, and may be regarded as an intermediate step between raw data compilations from the vast Sicada database and specialised expert models.

The topography in the Laxemar-Simpevarp area is characterised by elevated areas covered by thin or no Quaternary deposits, intersected by deep fissure valleys filled with thick sediments. This topography, in combination with the withdrawal of the Baltic Sea due to isostatic land uplift, are two important factors determining the hydrochemistry of the Laxemar-Simpevarp area. Furthermore, marine remnants in the Quaternary deposits influence the hydrochemistry in areas at low elevation close to the coast, whereas higher-lying areas are mostly influenced by atmospheric deposition and weathering processes. The vegetation cover has also great impact on the hydrochemistry of the surface system. Degradation of biogenic carbon generates large numbers of $H^+$ ions, which drive weathering processes in the Quaternary deposits as well as in the upper parts of the bedrock.

The present situation in the surface system is a consequence of the palaeohydrological past. In higher elevated areas, meteoric recharge has a great influence on the observed hydrochemistry, which is usually characterised by dilute fresh waters of low ionic strength. In lower areas close to the coast, there are indications of ongoing flushing of marine relicts since the area was covered by sea water. At most locations in the Laxemar-Simpevarp area, this flushing is more or less completed and concentrations of marine ions may be explained by deposition and anthropogenic sources. As much as 2/3 of the Cl input to the surface system has been estimated to originate from anthropogenic sources as road salt.

One important question in the hydrochemical evaluation is whether there are any indications of deep groundwater discharge in the surface system. It can be concluded from observations in shallow groundwater that deep groundwater signatures are present in the Quaternary deposits in potential deep discharge areas beneath lakes and brackish bays. On land, no deep signatures have been detected neither in surface water nor in groundwater, which indicates that shallow meteoric recharge/discharge patterns dominate and that potential regional deep discharge is too dilute to be detected in surface water.

# Sammanfattning

Med en matematisk/statistisk utgångspunkt beskrivs i den här rapporten hydrokemin i Laxemar-Simpevarpsområdet med ett stort antal visualiseringar och modeller av olika komplexitet, med avsikten att spegla de viktigaste faktorerna som styr hydrokemin i ytsystemet. För att bredda perspektivet har också samtliga data från olika nivåer i berget inkluderats i analysen, liksom hydrologiska mätdata och karaktäriseringar av de kvartära avlagringarna. Syftet med denna rapport är dels att ge en generell förståelse för platsen och att förklara storskaliga mönster och anomalier, dels att presentera en konceptuell modell som beskriver dagens hydrokemi i ytsystemet med utgångspunkt från den paleohydrologiska utvecklingen. Rapporten, som kan betraktas som ett mellansteg mellan sammanställningar av rådata från databasen Sicada och specialiserade expertmodeller, kan också utgöra en bas för fortsatta utvärderingar av scenarion och alternativa hypoteser.

Topografin i Laxemar-Simpevarp området kännetecknas av att högre liggande områden täckta av tunna avlagringar eller hällar, genomkorsas av djupa sprickdalar fyllda med tjocka sediment. Den lokala topografin har tillsammans med den pågående landhöjningen haft stor betydelse för bildningen av den hydrokemi som observeras i ytsystemet idag. I de kvartära avlagringarna i de lägre liggande områdena nära kusten finns relikt marina lämningar som fortfarande påverkar hydrokemin, medan kemin i högre liggande områden främst påverkas av atmosfärisk deposition och vittringsprocesser. Vegetationsskiktet har också haft en mycket viktig inverkan på hydrokemin i ytsystemet. Nedbrytning av organiskt material genererar vätejoner, $H^+$, vilka i sin tur driver vittringsprocesser i de kvartära avlagringarna och de övre delarna av berget.

Den nuvarande hydrokemiska situationen har också formats av den paleohydrologiska historiken. I högre liggande områden påverkas hydrokemin i hög grad av nederbörd och inströmmande grundvatten, vilket leder till utspädda yt- och grundvatten med lågt innehåll av joner. I lägre liggande områden nära kusten finns det indikationer på en pågående urspolning av relikt marina lämningar som härrör från tiden då området täcktes av havsvatten. På de flesta ställena i Laxemar-Simpevarpsområdet är denna urspolning mer eller mindre fullbordad och förekomsten av marina joner kan främst förklaras av deposition och antropogena källor. Så mycket som 2/3 av den totala tillförseln av klorid till ytsystemet har uppskattats ha sitt ursprung i antropogena källor såsom vägsalt.

En viktig frågeställning vid den hydrokemiska utvärderingen har varit om det finns några indikationer på utströmning av djupt grundvatten i ytsystemet. Det finns indikationer på att det förekommer djupsalina signaturer i de kvartära avlagringarna i potentiella utströmningsområden under sjöar och havsvikar. På land har dock inga djupsalina signaturer påvisats, varken i ytvatten eller ytligt grundvatten. Detta tyder på att lokala ytliga strömningsmönster dominerar i dessa områden och att en potentiell regional utströmning sannolikt är alltför utspädd för att den skall vara möjlig att upptäcka.

# Extended summary

Based on a mathematical/statistical approach, a large number of visualisations and models reflecting the hydrochemistry of the Laxemar-Simpevarp area have been produced, with the intention of providing an understanding of important processes and factors that affect the hydrochemistry of the surface systems. In order to widen the perspective, all data from Laxemar stage 2.3, including observations from different depths in the bedrock, as well as hydrological measurements and characterisation of the Quaternary deposits (QD), have been included in the analyses. The purpose of this report is to provide a detailed understanding of the hydrochemistry of the site and to explain observed overall patterns and anomalies, and ultimately to present a conceptual model that explains the present hydrochemistry of the surface system in the light of the past. One major concern in the report is whether there are any indications of deep groundwater discharge in the surface system.

### *Important factors influencing the hydrochemistry of the surface systems*

The topography in the Laxemar-Simpevarp area is characterised by elevated areas covered by thin or no Quaternary deposits, intersected by deep fissure valleys filled with thick sediments. This topography, in combination with the withdrawal of the Baltic Sea due to isostatic land uplift, are two important factors determining the hydrochemistry of the Laxemar-Simpevarp area. Furthermore, marine remnants in the Quaternary deposits influence the hydrochemistry in areas at low elevation close to the coast, whereas higher-lying areas are mostly influenced by atmospheric deposition and weathering processes.

Glacial residues in the form of till were deposited during the Weichselian glaciation and deglaciation. When the ice cover retreated about 12000 BC, the whole area was covered by water and the deposits were exposed on the sea floor. The deep fissure valleys which overlay the major deformation zones in the bedrock are now filled with thick sediment layers of glacial and post-glacial origin. The gradual isolation of these former brackish bays has resulted in sucession from brackish water to freshwater followed by formation of wetlands (in the Laxemar-Simpevarp area there was usually no lake stage). In modern times, fertile soils such as wetlands have often been converted into agricultural land by ditching and drainage, further altering the hydrochemical parameters in the area.

The formation of vegetation and a soil layer on the emerging land had a profound impact on the hydrochemistry of the surface system, for example due to the input of $H^+$ of biogenic origin. The distribution and fate of elements utilised by the biosphere, e.g. nutrients and essential trace elements, are significantly affected by biochemical cycles and retention processes.

Road salt has a significant impact on the concentrations of major ions measured in the surface waters in the area. In the catchment of the Laxemarån River, winter road salt spread on the E22 motorway constitutes about 50% of the total Cl flux in this catchment. Summer road salt spread on gravel roads for dust control is also a potential source of Cl which has been shown to have significant influence in some areas. As much of 2/3 of the total Cl input into surface waters in the Laxemar-Simpevarp area may be of anthropogenic origin according to estimations.

### *The palaeohydrological perspective*

Over the geological eras, the parameters influencing the hydrology and hydrochemistry of the Laxemar-Simpevarp area have undergone dramatic changes. Recurring glaciations covering the area with several kilometres of ice have alternated with interglacials when the area was covered by sea water or, as at present, by thin soils. Since the latest deglaciation around 12000 BC, land uplift in combination with changes in water level have resulted in a gradual withdrawal of the sea and establishment of the present coastline.

During the last glaciation, the Quaternary deposits and the bedrock were infiltrated by glacial meltwater to a depth of at least 500 metres. Nowadays, this glacial water has to a varying extent been replaced by sea water due to density intrusion during the Littorina stage, and later due to meteoric recharge in areas above sea level. During the most saline part of the Littorina Sea period, 4000–3000 BC, sea water with salinity almost twice that of the present Baltic Sea covered large parts of the Laxemar sub-area and the entire Simpevarp sub-area. There are indications that this marine water percolated into the upper 500 metres of the bedrock in at least the low altitude, near-coastal areas, driven by the density gradient. Carbon isotope measurements may be interpreted as indicating that the inorganic carbon that predominates at these depths originates from organic carbon. According to the estimates this carbon may have an average age of between 6,000 and 14,000 years, which suggests that the carbon input from the surface system must have occurred since the latest glaciation. The presence of carbon with biogenic isotope signatures also implies that meteoric recharge probably has an impact even at depths of several hundred metres in the bedrock.

### *Conceptual model for the hydrochemistry of the surface system*

The present situation in the surface system is a consequence of the palaeohydrological past. In higher elevated areas, meteoric recharge has a great influence on the observed hydrochemistry, which is usually characterised by dilute fresh waters of low ionic strength. In lower areas close to the coast, there are indications of ongoing flushing of marine relicts since the area was covered by sea water. At most locations in the Laxemar-Simpevarp area, this flushing is more or less completed and observed concentrations of marine ions may be explained by deposition and anthropogenic sources as road salt.

The formation of a vegetation cover has also had a great impact on the hydrochemistry of the surface system. Degradation of biogenic carbon generates large numbers of $H^+$ ions, which drive weathering processes in the Quaternary deposits as well as in the bedrock. According to isotope measurements, also a significant fraction of the carbon in the upper 400 metres of the bedrock seems to originate from a biogenic source, probably supplied through meteoric recharge. The distribution of other elements associated with organic matter, such as N, P, K and Si, is also affected by uptake and cycling in the biosphere.

On a regional scale, meteoric recharge and subsequent flushing of ions results in the large scale hydrochemistry according to the conceptual model described in Figure E-1. Marine relicts in combination with regional groundwater flow patterns may explain the anomalous composition in shallow groundwater sampling points in till below lake and sea sediments. These sites are predominantly located close to major facture zones, which are potential deep groundwater discharge points. When all the pieces are put together, the following conceptual model may explain the hydrochemistry of the area on a regional scale:

- In the lower-lying areas close to the coast, relict marine water prevails in the deeper parts of the deposits and in the upper parts of the bedrock. The high salinity, compared with present Baltic Sea water, in combination with negative values of deuterium excess indicates that this sea water is probably a remnant of the Littorina stage when sea water with a Cl concentration of approximately 6,500 $mg \cdot L^{-1}$ infiltrated the deposits and the bedrock.
- In the deposits closer to the surface, intermediate Cl concentrations in combination with meteoric isotope signatures indicates ongoing flushing of relict marine remnants of Littorina or younger age.
- In slightly higher-lying areas, which should also have been covered by sea water after the latest glaciation, meteoric isotope signatures and low Cl concentrations indicate that marine influences have been washed out due to the meteoric recharge. This process has also affected the groundwater in the upper parts of the bedrock, resulting in signatures similar to the shallow groundwater at a few hundred metres depth.
- In areas located above the highest coastline of the Littorina Sea, relict marine remnants are probably almost absent. Cl concentrations in these areas can be fully explained by deposition and point sources such as road salt.

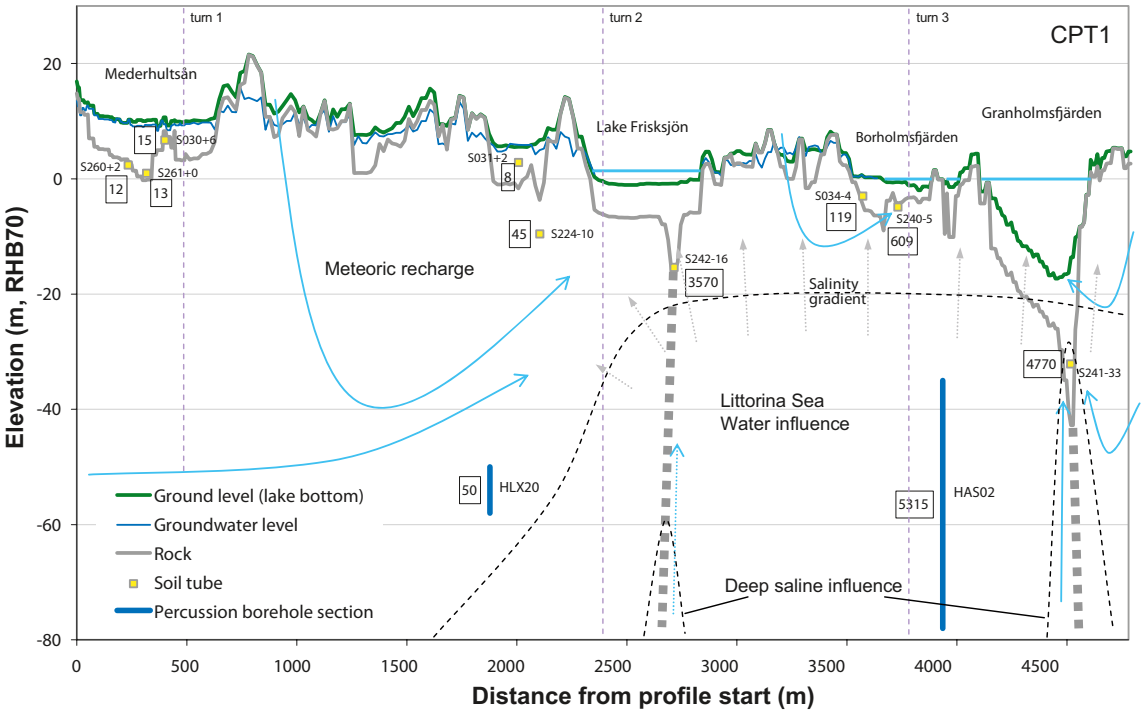


***Figure E-1.*** *This profile summarises the regional conceptual model, which attempts to explain the large-scale hydrochemical patterns of the Laxemar-Simpevarp area (cf Section 8.3). Blue arrows represent hypothetical groundwater flow lines and dashed grey lines the approximate location of fracture zones in the bedrock.*

- Deep saline signatures present in two soil tubes located in till below thick lake and sea sediments may be explained by the influence of deep groundwater discharge. Both these sites are located in the vicinity of major fracture zones in the area, which have been proposed as potential areas for deep groundwater discharge. The differing water isotope signatures between these both sites indicates, however, that SSM000241 is attributable to regional or local meteoric discharge originating from the higher elevated area in the north, whereas SSM000242 may reflect a more stagnant relict marine groundwater less influenced by ongoing meteoric recharge.

### *Indications of deep groundwater discharge in the surface system*

One important question in this evaluation is whether there are any indications of deep groundwater discharge in the surface system. The Ion Source Model (cf Section 3.2.5) is a powerful tool for detecting deviations in relative composition among elements in the surface system that may be attributed to discharging groundwater. The following conclusions are primarily based on the patterns identified in the Ion Source Model, with support from other models and bivariate visualisations:

- The most pronounced deep signature in the surface system is found in SSM000241, located in till below thick sea sediments in the Granholmsfjärden Basin. This soil tube is located close to a major deformation zone, which has been identified as a candidate area for deep groundwater discharge. The groundwater chemistry in this object is influenced by degradation of organic matter. However, the composition between marine and deep saline sources, with a substantial deviation towards the deep saline composition as indicated in the Ion Source Model, is probably attributable to the influence of deep saline groundwater. This conclusion is also supported by other visualisations including Li and Cl. In addition, the Water Origin Model indicates that this shallow groundwater sampling site located below sea level probably contains meteoric discharge from the surrounding higher elevated areas.

- SSM000242, located in till below sediments in Lake Frisksjön, shows in many respects similar chemical characteristics to SSM000241 with regard to deep saline signatures. There is however one important difference: SSM000242 displays a stronger marine signature, with regard to both the ion composition and the isotope signature of the water. This may be interpreted as indicating more stagnant conditions, which also is indicated by the hydrological pump test conducted.
- SSM000022, located on the island of Ävrö, has previously been identified as a candidate for deep discharge. According to findings in this report, deep groundwater discharge is less probable, although there are some contradictory indications. There are also no indications of any significant presence of a deep saline component in the surface water discharge from this area.

It can be concluded from observations of major elements, trace elements and environmental isotopes in shallow groundwater that potential deep groundwater signatures are present in the Quaternary deposits in potential deep discharge areas. On land, no deep signatures have been detected neither in surface water nor in groundwater, which indicates that shallow meteoric recharge/discharge patterns dominate and that potential regional deep discharge is too dilute to be detected in surface water.

# Contents


**1 Introduction** 15
1.1.1 This report 16
1.1.2 Objectives 16
1.1.3 Definitions of water types 17

**2 Background and methods** 19
2.1 The Laxemar-Simpevarp area 19
2.2 Data used in this report 22
2.2.1 Compilation of hydrochemical parameters 22
2.2.2 Hydrological parameters 22
2.2.3 Overview of sampling sites and sampled objects 23
2.2.4 Hydrochemical data from surface systems 24
2.2.5 Hydrochemical reference data from the bedrock 25
2.2.6 Influence of flushing water content on data from cored boreholes 32
2.2.7 Chemical composition of the regolith 33
2.3 Statistical methods and visualisation techniques 33
2.3.1 Statistical processing of data 33
2.3.2 Handling of values below reporting limits 34
2.3.3 Representation of isotope measurements 34
2.3.4 Cross plots (scatter plots) 35
2.3.5 Piper plot 35
2.3.6 Projection plots 35
2.3.7 Cross sections and profiles 35
2.3.8 Multivariate analysis and visualisation 36
2.3.9 Principal component analysis (PCA) 36
2.3.10 Partial least squares modelling (PLS) 36
2.3.11 Coding and labelling in figures 36
2.3.12 Marking of trendlines and scenarios in figures 37

**3 Hydrochemical overview of the Laxemar-Simpevarp area** 39
3.1 Traditional water type classifications 39
3.1.1 Ludwig-Langelier plot 39
3.1.2 Piper plot 40
3.2 Exploring sources of dissolved ions 41
3.2.1 Summary of methodology 42
3.2.2 Calibration of the Ion Source Model 42
3.2.3 Spatial visualisation of the Ion Source Model 43
3.2.4 Comparisons with results of the M3-model 45
3.2.5 Projections onto the Ion Source Model 47
3.2.6 Interpretation of sources and water types in the Ion Source Model 48
3.2.7 Interpretation of chemical reactions in the Ion Source Model 50
3.3 Exploring the origin of water – the solvent 51
3.3.1 Global and local meteoric water lines 51
3.3.2 The Water Origin Model 54
3.3.3 Detailed evaluation of two lakes in the Laxemar area 56
3.4 Exploring concentration trends and mixtures 58
3.4.1 Calibration of the the Mixing Model 58
3.4.2 Comparisons between the the Mixing Model and the M3-model 59
3.4.3 Projections onto the Mixing Model 60
3.4.4 Interpretation of the Mixing Model 61

3.5 Age dating and residence time 63
3.5.1 Age estimations by $^{3}H$ activity 65
3.5.2 Age estimations by $^{14}C$ activity 66
3.6 Summary of the four models 69

**4 Detailed chemical evaluations** 71
4.1 Origin and fate of selected elements 71
4.1.1 Marine influences (Na, Cl, Br) 71
4.1.2 Deep saline influences (Ca, Cl, $^{37}Cl$, Li) 76
4.1.3 On the origin of sulphur 82
4.1.4 On the origin of calcium, strontium and magnesium (Ca, Sr, Mg) 86
4.1.5 On the origin of carbon, nitrogen and phosphorus (C, N, P) 91
4.2 Chemical reactions and processes 98
4.2.1 Weathering of minerals 98
4.2.2 Cation exchange in the Quaternary deposits 100
4.2.3 Redox processes 102
4.2.4 Microbially mediated processes 104
4.3 Deep signatures in the shallow system 105
4.3.1 Reporting limits and dilution constraints 106
4.3.2 Summary of possible deep signatures in shallow objects 106

**5 Integrated evaluation of hydrochemical and hydrological data in the surface system** 109
5.1 Evaluation of observed hydrochemistry in relation to hydrological recharge/discharge characteristics 109
5.1.1 Hydrological classification compared to traditional hydrochemical classification 109
5.1.2 Exploration by Principal Component Analysis 110
5.1.3 Conclusions – recharge/discharge characteristics 111
5.2 Evaluation of concentrations and water flow 113
5.2.1 Conclusions – concentrations and water flow 120
5.3 Estimation of mass transport in streams in the Laxemar-Simpevarp area 120
5.3.1 Water discharge measurements used for transport estimates 120
5.3.2 Hydrochemical data used for transport estimates 125
5.3.3 Compilation of transport, area-specific transport and flow-weighted concentrations 126
5.3.4 Estimated transport of trace elements 132

**6 Evaluation of hydrochemistry on catchment scale** 137
6.1 Catchment model VBX-VII. 137
6.1.1 Hydrological network and water balance 137
6.1.2 Mathematical description of the VBX-VI model 139
6.1.3 Distributed land characteristics and prerequisites for retention 141
6.1.4 Model setup, calibration and verification 141
6.2 Mass balance scenarios 142
6.2.1 Mass balance for chloride (Cl) 142
6.2.2 Mass balance for sodium (Na) 146
6.2.3 Mass balance for potassium (K) 149
6.2.4 Mass balance for calcium (Ca) 153
6.2.5 Mass balance for strontium (Sr) 156
6.2.6 Mass balance for magnesium (Mg) 158
6.2.7 Mass balance for sulphate ($SO_4^{2-}$) 161
6.2.8 Mass balance for bicarbonate ($HCO_3^-$) 164
6.2.9 Mass balance for total organic carbon (TOC) 168
6.2.10 Mass balance for total nitrogen (Tot-N) 171
6.2.11 Mass balance for total phosphorus (Tot-P) 174
6.2.12 Mass balance for total silicon (Si) 177
6.3 Summary and conclusions of catchment modelling 179

**7 Integrated hydrochemical evaluation of selected objects and sub-areas** 185
7.1 Identification of objects and sub-areas of special interest 185
7.2 Shallow groundwater beneath lakes and the Baltic Sea 186
7.2.1 Major elements and environmental isotopes ($^{2}H$ and $^{18}O$) 188
7.2.2 Comparisons among trace elements and isotopes 189
7.2.3 The highly deviant hydrochemistry in SSM000241 and SSM000242 190
7.2.4 Conclusions 191
7.3 The soil tube SSM000022 located on Ävrö 192
7.4 Elevated concentrations of Ca and $HCO_3^-$ in Ekerumsån 193
7.5 Anthropogenic sources of salts (Cl) 194
7.5.1 Winter road salt 194
7.5.2 Summer road salt 195
7.5.3 Salt emissions from SKB drilling of cored boreholes. 197
7.5.4 Anthropogenic influence on shallow groundwater 198

**8 A conceptual model for the hydrochemistry in surface systems in the Laxemar-Simpevarp area** 199
8.1 Important factors for the hydrochemistry of the surface systems 199
8.2 Evolution of the groundwater in the bedrock 199
8.3 Conceptual model for the hydrochemistry of the surface system 203
8.3.1 Regional model 203

**9 Evaluation of uncertainities** 207
9.1 Selection and representativity of data 207
9.2 Statistical testing and significance 207
9.3 Uncertainties associated with specific chapters 209
9.3.1 Uncertainties in Chapter 3 209
9.3.2 Uncertainties in Chapter 4 210
9.3.3 Uncertainties in Chapter 5 210
9.3.4 Uncertainties in Chapter 6 211
9.3.5 Uncertainties in Chapter 7 212

**10 References** 213

**Appendix A** Hydrochemical data and hydrological characteristics of oil tubes 217

**Appendix B** Data used for catchment model VBXVII 221

**Appendix C** Detailed model results from the catchment model VBXII 227

**Appendix D** Number of observations of data selection C. Surface water, shallow groundwater and groundwater from the bedrock 241

**Appendix E** Mean values of data selection C. Surface water, shallow groundwater and groundwater from the bedrock 245

# 1 Introduction

The Swedish Nuclear Fuel and Waste Management Co (SKB) has been conducting site investigations at two sites, the Laxemar-Simpevarp area and Forsmark, with the objective of siting a geological repository for spent nuclear fuel. The site investigations were initiated in 2002 and completed in 2007. The results of the investigations provide basic input to the site descriptive modelling. A Site Descriptive Model (SDM) is an integrated description of the site and its regional setting, including the current state of the geosphere and the biosphere, as well as ongoing natural processes of importance for long-term safety. The SDM should summarise the current state of knowledge concerning the site and provide parameters and models to be used in further analyses within Safety Assessment, Repository Design and Environmental Impact Assessment.

The site investigation programme involves extensive studies of the surface ecosystem as well as of the bedrock in order to provide a detailed characterisation of the site (see /SKB 2001/ for a description of the general execution programme). The strategy adopted by SKB for developing a descriptive ecosystem model based on site data is described in /Löfgren and Lindborg 2003/. The site investigation in the Laxemar-Simpevarp area involves many disciplines, as outlined in Figure 1-1, which describes the current preliminary hierarchical report structure behind the SDM-Site main report. The present report is a level-III reference report which focuses on the chemistry of the surface system, but also includes data and conclusions from the disciplines of geology, hydrogeology and hydrogeochemistry.

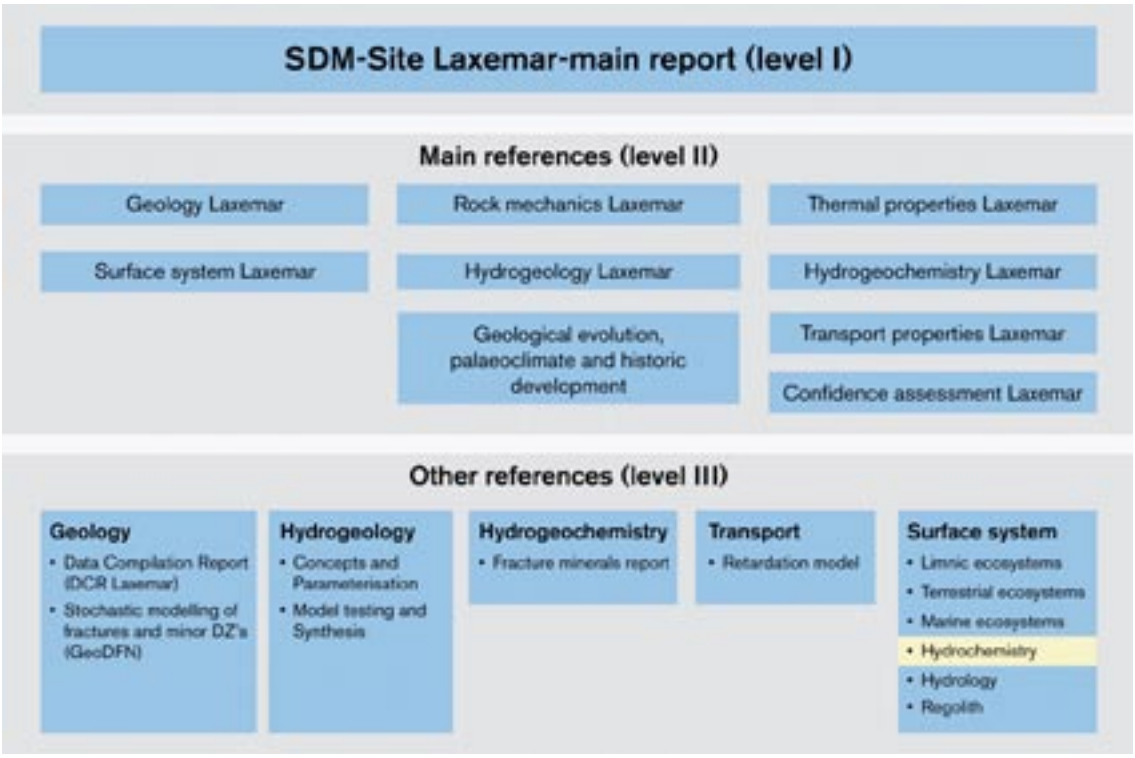


***Figure 1-1.*** *The hierarchical report structure (preliminary) of references behind the SDM-Site main report.*

### 1.1.1 This report

This report focuses on the surface system and evaluates hydrochemical data from surface water and shallow groundwater in relation to observations from deep groundwater, based on data from the Laxemar 2.3 'data freeze' (data available in the SKB Sicada database in August 2007). It also attempts to couple hydrochemical data with observations from other disciplines, e.g. hydrological measurements and land use and regolith characteristics.

According to Figure 1-2, most shallow groundwater observations reflect the first 10 metres from the ground surface to the upper fractured parts of the bedrock. Deep bedrock hydrochemistry, with the main purpose of describing the conditions at the planned repository depth, primarily focuses on depths below c 150 metres, leaving an intermediate zone of approximately 150 metres where the areas of interest overlap. Some objects attributed to the surface system, such as private wells, reach this intermediate zone as well.

In order to understand the characteristics of the objects that reach the intermediate zone, deeper observations from the bedrock are included in all models as a reference. No attempt is made in this report to add interpretations of the deep hydrochemistry to the interpretations made by the ChemNet hydrochemistry group (see /SKB 2004, SKB 2006a and Laaksoharju (ed) 2008/ for evaluations of deep groundwater hydrochemistry). Comments on patterns regarding these deep levels are mainly added as a service to the reader in order to provide a wider picture.

The focus in this report is on answering fundamental questions regarding the origin and fate of elements and identifying important processes within the surface system of the Laxemar-Simpevarp area, rather than giving an overall description of the hydrochemical sampling programme. A complete, element-by-element statistical compilation of all hydrochemical data from surface systems in the Laxemar-Simpevarp area was conducted in /Tröjbom and Söderbäck 2006/.

The report contains a large number of visualisations and models. However, due to the enormous amount of possible element combinations, and to the multitude of chemical processes that may influence the hydrochemistry of the site, all possible combinations could not be evaluated. Accordingly, the report focus on a limited number of questions that may be regarded as important for an overall understanding of the hydrochemistry of the site, but there are undoubtedly potentially important patterns and questions that remain unexplored. The report may therefore serve as a basis for further evaluation and testing of scenarios, and may be regarded as an intermediate step between raw data compilations from the vast Sicada database and specialised expert models.

### 1.1.2 Objectives

The overall objective of this report is to contribute to a better understanding of the surface system in the Laxemar-Simpevarp area by adding a wider perspective, including deeper hydrochemical observations from the bedrock and data from other disciplines, e.g. regolith data and hydrological measurements, as well as multi-element analyses considering combinations of elements and isotopes. In the last chapter of the report, important conclusions from the many visualisations and models are used to develop a conceptual model for the purpose of explaining the present hydrochemistry of the surface systems in the light of the past.

Some more specific objectives, each relating to one or several chapters in the report, are:

- To use mathematical/statistical methods as the baseline for modelling (Chapter 3 and 6).
- To explain the overall hydrochemical patterns in the Laxemar-Simpevarp area in terms of water origin (Chapter 3), sources and sinks for different elements (Chapters 4 and 6), and chemical reactions and processes (Chapter 4).
- To explain the hydrochemistry of anomalous objects in the Laxemar-Simpevarp area (Chapter 7).
- To identify potential areas for surface discharge of deep groundwater from the bedrock (Chapter 3, 4 and 7).
- To quantify mass flows in the surface system (Chapter 5 and 6).

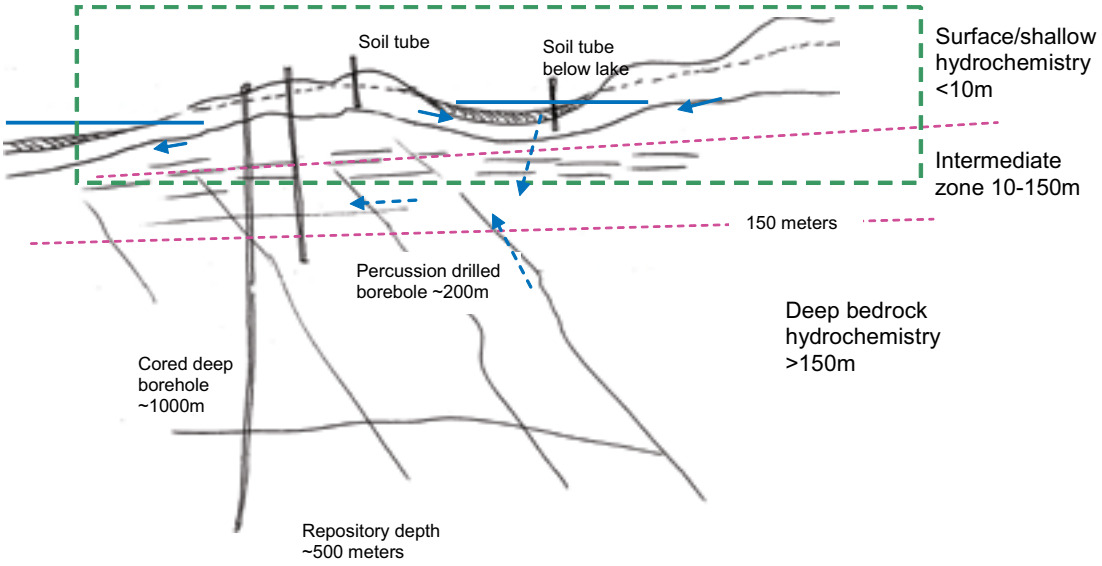


***Figure 1-2.*** *Schematic profile of the Laxemar-Simpevarp area identifying the area of interest focused on in this report, surface and shallow hydrochemistry, and approximate boundaries with other disciplines and fields of responsibility.*

### 1.1.3 Definitions of water types

In this section a few important terms regarding water types used in the report are defined. Three main water types representing different depth levels are defined below (cf Table 1-1):

- **Meteoric water** denotes input to the surface system from precipitation. A significant proportion of the precipitation reenters the atmosphere through evapotranspiration.
- **Surface water** denotes fresh or brackish water sampled in lakes, streams and the Baltic Sea.
- **Shallow groundwater** denotes groundwater in the overburden sampled in soil tubes (in other SKB reports these are sometimes called soil pipes or wells or groundwater monitoring wells in Quaternary deposits), or private wells.
- **Groundwater** denotes all waters contained in water-conducting fractures sampled in the bedrock, e.g. in percussion or cored boreholes, and in drilled private wells.
- **Deep (saline) groundwater** refers to groundwater originating from greater depths in the bedrock and is a subset of the "groundwater" type above. This water type also includes brine (alternatively shield brine), which is a designation of the highly saline groundwater present at great depths in the granitic Fennoscandian shield.

Within the ChemNet reporting (e.g. /SKB2005b/), the use of 'end-members' is an important concept describing the composition of a number of ideal water types. The observed water composition of samples from the site is interpreted as mixtures of the different end-members. An end-member is defined by the absolute concentrations of the constituents and consequently reflects a very specific water type, e.g. the Baltic Sea, at a specific point and time. The end-members used in Laxemar stage 2.3 are listed in Table 1-1 /Laaksoharju (ed) 2008/.

**Table 1-1. End-members used in the Laxemar 2.3 modelling stage.**

| End-member | *Comment* | Na mg/L | K mg/L | Ca mg/L | Mg mg/L | $HCO_3$ mg/L | Cl mg/L | $SO_4$ mg/L | $\delta^2H$ ‰SMOW | $\delta^{18}O$ ‰SMOW |
|---|---|---|---|---|---|---|---|---|---|---|
| Deep saline | *KLX02* | 8,200 | 45.5 | 19,300 | 2.12 | 14.1 | 47,200 | 10 | –44.9 | –8.9 |
| Littorina Sea | | 3,674 | 134 | 151 | 448 | 92.5 | 6,500 | 890 | –37.8 | –4.7 |
| Altered meteoric groundwater | *HLX28* | 110 | 2.97 | 11.2 | 3.60 | 265 | 23 | 35.8 | –76.5 | –10.9 |
| Glacial | | 0.17 | 0.4 | 0.18 | 0.1 | 0.12 | 0.5 | 0.5 | –158 | –21 |
| Old meteoric – glacial | | 0.17 | 0.4 | 0.18 | 0.1 | 0.12 | 0.5 | 0.5 | –118 | –16 |

### 1.1.4 Chemical abbreviations used in the text

In order to achieve a compact presentation, elements, compounds and isotopes are usually referred to in text and figures by their chemical notation. Abbreviations used in the report are listed and explained in Table 1-2 below.

**Table 1-2. Compilation of chemical abbreviations used in the report.**

| Abbreviation | Description | Abbreviation | Description |
|---|---|---|---|
| Ba | Barium | Mg | Magnesium |
| Br | Bromine | N | Nitrogen |
| $^{12}C$ | Stable carbon isotope | Na | Sodium |
| $^{13}C$ | Stable carbon isotope | $N_{tot}$ | Total nitrogen |
| $^{14}C$ | Radioactive carbon isotope | $NH_4$-N | Ammonium nitrogen |
| Ca | Calcium | $NO_3$-N | Nitrate nitrogen |
| Cl | Chlorine | $^{18}O$ | Stable oxygen isotope |
| $^{37}Cl$ | Stable chlorine isotope | P | Phosphorus |
| $CO_2$ | Carbon dioxide | pH | Hydrogen ion activity |
| DIC | Dissolved inorganic carbon | $PO_4^{3-}$-P | Phosphate phosphorus |
| DOC | Dissolved organic carbon | $P_{tot}$ | Total phosphorus |
| Eu | Europium (rare earth element) | REE | Rare earth elements |
| F | Fluorine | $^{222}Rn$ | Radon isotope (radioactive) |
| Fe | Iron | S | Sulphur |
| $^{2}H$ | Deuterium (stable hydrogen isotope) | $^{34}S$ | Stable sulphur isotope |
| $^{3}H$ | Tritium (radioactive hydrogen isotope) | $S^{2-}$ | Sulphide ion |
| $HCO_3^-$ | Bicarbonate ion | Si | Silicon |
| I | Iodine | $SO_4^{2-}$ | Sulphate ion |
| K | Potassium | Sr | Strontium |
| La | Lanthanum (rare earth element) | $^{86}Sr$ | Radioactive strontium isotope |
| Li | Lithium | $^{87}Sr$ | Radioactive strontium isotope |
| Mn | Manganese | TOC | Total organic carbon |

# 2 Background and methods

The two candidate sites for siting of the repository for spent nuclear fuel are referred to as the Forsmark area and the Laxemar-Simpevarp area. The hydrochemistry of the surface system in the latter area is evaluated in the present report, whereas the Forsmark area is evaluated in a parallel report /Tröjbom et al. 2007/.

At the start of the site investigations in 2002, regional model areas with clearly defined boundaries were defined for each site for the purpose of regional scale modelling. These areas were denominated the Forsmark regional model area and the Simpevarp regional model area, respectively. Furthermore, two smaller areas within the Simpevarp regional model area, the Simpevarp subarea and the Laxemar subarea, were defined, and preliminary site descriptions were produced for both subareas. Since the two subareas are included in the same regional model area, the former Simpevarp regional area is in a SDM-Site context denoted the Laxemar-Simpevarp regional model area, for clarity and to avoid confusion.

## 2.1 The Laxemar-Simpevarp area

The Laxemar-Simpevarp area is located in the County of Kalmar within the municipality of Oskarshamn, about 350 km south of Stockholm. In Figure 2-1, an aerial photograph gives a picture of topography, land use and vegetation in the Laxemar-Simpevarp area. In Figure 2-2, the boundaries of the Laxemar and Simpevarp sub-areas are shown within the Simpevarp regional model area (the outer box).

Different aspects of the Laxemar-Simpevarp area have been described in many reports from different disciplines, and it is beyond the scope of this report to provide a résumé of all these models. Instead, a selection of important background reports is compiled in Table 2-1, together with references to site descriptions from other disciplines. This report is based on data from the Laxemar 2.3 ‘data freeze’.

***Figure 2-1.*** *Aerial photo showing the central parts of the Laxemar-Simpevarp area.*

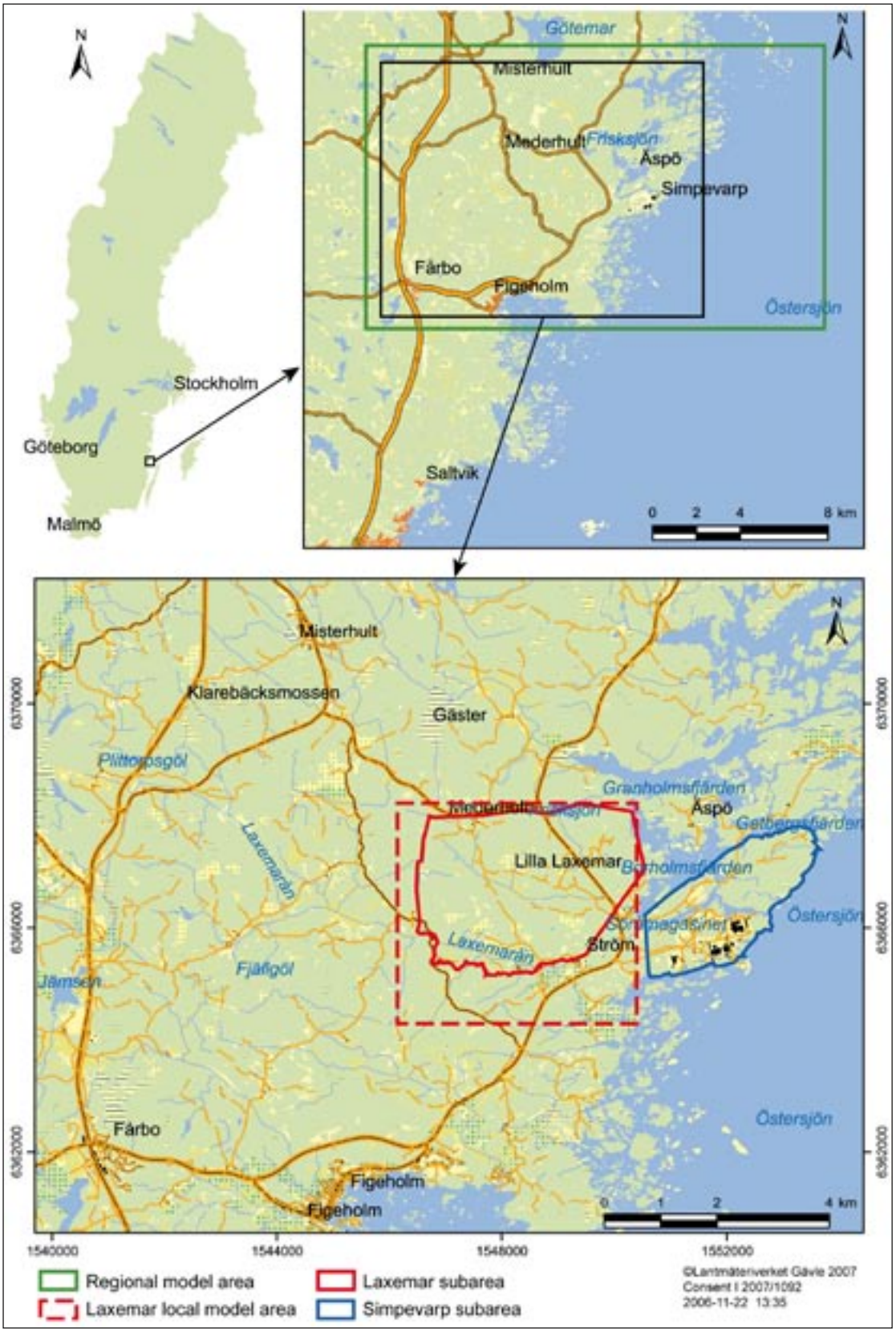


***Figure 2-2.*** *The location of the Laxemar-Simpevarp area. The black rectangles show the spatial extension of the enlarged map.*

**Table 2-1. Compilation of previous reports on surface hydrochemistry in the Laxemar-Simpevarp area, and a selection of reports from other disciplines that contain descriptions of the Laxemar-Simpevarp area.**

| Report title | SKB Report number | Reference |
|---|---|---|
| **Reports on hydrochemistry in surface water and shallow groundwater** | | |
| Evaluating hydrochemical data from shallow groundwater in Laxemar from a microbiological perspective. | R-09-02 | /Hallbeck 2009/ |
| Chemical characteristics of surface systems in the Simpevarp area. | R-06-18 | /Tröjbom and Söderbäck 2006/ |
| Surface water sampling at Simpevarp 2005. | P-06-155 | /Ericsson and Engdahl 2007a/ |
| Sampling of precipitation at Simpevarp, 2004. | P-05-175 | /Ericsson 2005/ |
| Sampling and analysis of precipitation at Simpevarp 2005. | P-06-324 | /Ericsson and Engdahl 2007b/ |
| Sampling and analysis of shallow groundwater at Simpevarp 2005. | P-06-325 | /Ericsson and Engdahl 2007c/ |
| Surface water sampling at Simpevarp 2004. | P-05-118 | /Ericsson and Engdahl 2005/ |
| Surface water sampling at Simpevarp 2002–2003. | P-04-13 | /Ericsson and Engdahl 2004a/ |
| Sampling of precipitation at Äspö, 2003. | P-04-14 | /Ericsson 2004/ |
| Surface water sampling in Oskarshamn October 2003 to February 2004. | P-04-75 | /Ericsson and Engdahl 2004b/ |
| **Preliminary site descriptions** | | |
| Geological evolution, palaeoclimate and historical development of the Forsmark and Laxemar-Simpevarp areas. | R-08-19 | /Söderbäck (ed) 2008/ |
| Preliminary site description Laxemar subarea – version 1.2. | R-06-10 | /SKB 2006b/ |
| Description of surface systems. Preliminary site description Laxemar subarea – version 1.2. | R-06-11 | /Lindborg (ed) 2006/ |
| Preliminary site description Laxemar stage 2.1. | R-06-110 | /SKB 2006c/ |
| Description of surface systems. Preliminary site description Simpevarp subarea – version 1.2. | R-05-01 | /Lindborg (ed) 2005/ |
| Preliminary site description Simpevarp subarea – version 1.2. | R-05-08 | /SKB 2005/ |
| **Hydrogeochemical evaluations** | | |
| Bedrock hydrogeochemistry Laxemar, Site descriptive modelling, SDM-Site Laxemar. | R-08-93 | /Laaksoharju (ed) 2008/ |
| Explorative analyses of microbes, colloids and gases together with microbial modelling. Site descriptive model, SDM-Site Laxemar. | R-08-109 | /Hallbeck 2008/ |
| Hydrogeochemical evaluation. Preliminary site description Laxemar subarea – version 1.2. | R-06-12 | /SKB 2006a/ |
| Hydrogeochemical evaluation. Preliminary site description Simpevarp subarea – version 1.2. | R-04-74 | /SKB 2004/ |
| **Hydrology and hydrogeology** | | |
| Near-surface hydrogeological model of Laxemar. Open repository – Laxemar 1.2. | R-06-66 | /Bosson 2006/ |
| Description of climate, surface hydrology, and near-surface hydrogeology. Simpevarp 1.2. | R-05-04 | /Werner et al. 2005a/ |
| Description of climate, surface hydrology, and near-surface hydrogeology. Preliminary site description Laxemar subarea – version 1.2. | R-05-61 | /Werner et al. 2005b/ |
| **Geology** | | |
| Description of the regolith at Laxemar. | R-08-05 | /Sohlenius and Hedenström 2008/ |
| Depth and stratigraphy of regolith at Laxemar. | R-08-06 | /Nyman et al. 2008/ |
| Geology Laxemar. Site descriptive modelling, SDM-Site Laxemar. | R-08-54 | /Wahlgren et al. 2008/ |

## 2.2 Data used in this report

This report is based on hydrochemical data from the Laxemar 'data freeze 2.3', which cover observations from March 2002 to August 2007. The dataset is presented briefly in this section. More detailed descriptions of data from surface water and shallow groundwater are found in /Tröjbom and Söderbäck 2006/. Information about deeper boreholes is compiled in ChemNet hydrogeochemical evaluations /Laaksoharju (ed) 2008/. See Table 2-1 for further references.

### 2.2.1 Compilation of hydrochemical parameters

A large number of hydrochemical parameters have been measured within the different sampling campaigns in the Laxemar-Simpevarp area. The parameters can be grouped into a number of categories, based on the sampling interval of each parameter. Parameter categories used in evaluations in this report are listed in Table 2-2, along with a representative element for each group. The total number of observations of these representative elements in different objects is listed in Appendix D.

In Section 5.1.2 a number of aggregated parameters, derived from e.g. chemical and hydrological site data from soil tubes, are correlated with a field-estimated recharge-discharge characteristic for each soil tube. These parameters, which are listed in Table 2-3, either represent mean values or the variability around the mean value, expressed as the coefficient of variation or the standard deviation. The variability of concentration parameters that can take a value of zero, but not negative values, is expressed as the coefficient of variation, CV, which reflects the relative dispersion from the mean, whereas the standard deviation is used for most other parameters. Soil tubes with less than three observations were excluded in the analysis in Section 5.1.2 as no measure of variability could be estimated for these objects.

### 2.2.2 Hydrological parameters

The semi-quantitative recharge-discharge parameter denoted "RD", is based on a hydrological field classification according to Table 2-4. Five discrete classes ranging from recharge to discharge are coded to form the semi-quantitative parameter ranging from 1 to 5. This parameter is further evaluated in /Werner et al. 2008/. A compilation of data is found in Appendix A.

**Table 2-2. Different parameter categories and representative parameters in the Sicada database. The grouping is based on the sampling interval of each parameter.**

| Representative parameter | Other parameters in category |
|---|---|
| pH | Conductivity |
| Cl | Na, K, Ca, Mg, $HCO_3$ $SO_4$ |
| Sr | Li, I, F, Br |
| Si | $SiO_2$ |
| Fe | Mn |
| $S^2$ | $O_2$ |
| Tot-N | $NH_4$-N, $NO_{23}$-N, tot-P, $PO_4$-P, TOC, DIC |
| DOC | |
| $^{2}H$ | $^{3}H$, $^{18}O$ |
| $^{13}C$ | |
| $^{14}C$ | |
| $^{34}S$ | |
| $^{87}Sr$ | $^{10}B$, $^{37}Cl$ |
| Cu | Zn, Pb, Cd, Cr, Al, Ni, Hg, Co, V |
| La | Sc, Rb, Y, Zr, Mo, In, Sb, Cs, Ba, Hf, Tl, Ce, Pr, Nd, Sm, Eu, Gd, Tb, Dy, Ho, Er, Tm, Yb, Lu |
| U | Th |
| $^{222}Rn$ | $^{226}Ra$, $^{238}U$, $^{235}U$, $^{234}U$, $^{232}Th$, $^{230}Th$ |

**Table 2-3. A selection of hydrochemical parameters measured in soil tubes, which in Section 5.1.2 are correlated with a field-estimated hydrological parameter that describes a recharge-discharge characteristic in each soil tube. The suffix "cv" denotes the coefficient of variation and "ss" the standard deviation.**

| | Abbreviation of aggregated parameter | |
|---|---|---|
| **Original parameter** | **Variability** | **Mean value** |
| Bicarbonate | HCO3_cv | - |
| Chloride | Cl_cv | Cl |
| Conductivity (field) | Cond_cv | - |
| Deuterium ($^{2}H$) | D_ss | - |
| DOC | DOC_cv | DOC |
| Groundwater level | GWL_ss | GWL |
| ORP (field) | ORP_ss | ORP |
| Oxygen | Ox_ss | Ox |
| Oxygen-18 ($^{18}O$) | O18_ss | O18 |
| pH (field) | pH_ss | - |
| Radon-222 ($^{222}Rn$) | - | Rn222 |
| Sulphate | SO4_cv | SO4 |
| Temperature | Temp_ss | Temp |
| Tritium ($^{3}H$) | Tr_ss | Tr |

**Table 2-4. Explanation of the hydrological classification parameter RD. Most soil tubes in the Laxemar-Simpevarp area are classified as class 1 or 5 (cf Appendix A).**

| Field classification (categorical variable) | RD (semi-quantitative variable) |
|---|---|
| Recharge | 1 |
| Probable recharge | 2 |
| Varying | 3 |
| Probable discharge | 4 |
| Discharge | 5 |

### 2.2.3 Overview of sampling sites and sampled objects

Hydrochemical sampling is conducted in a number of different object types represented by a unique id code in the SKB Sicada database. A three letter prefix and a serial number identify each object shown in Figure 2-3 below, e.g. SSM000001 is the soil tube with serial number 1. There are water samples from five different object types:

- Surface water samples (PSM) – precipitation, lake, stream and sea water.
- Private wells and springs (PSM) – drilled or dug wells and natural springs either representing shallow groundwater in the overburden or groundwater in the bedrock.
- Soil tubes (SSM) – groundwater monitoring wells drilled in the overburden, usually not extending more than 10 metres deep. The representative sampling depth corresponds to the location of the intake screen, usually the last meter of the soil tube.
- Percussion boreholes are drilled in the bedrock, usually extending to a depth of approximately 200 metres, sometimes sectioned by packers. Different three letter prefixes starting with "H" denote the geographical area of the percussion borehole: HLX – Laxemar, HSH – Simpevarp, HAV – Ävrö, HBH – Bockholmen, HAS – Äspö.
- Cored boreholes, usually extending towards a depth of 1,000 metres and sectioned at several levels with packers. Different three letter prefixes starting with "K" denote the geographical area of the cored borehole: KLX – Laxemar, KSH – Simpevarp, KAV – Ävrö, KBH – Bockholmen, KAS – Äspö.

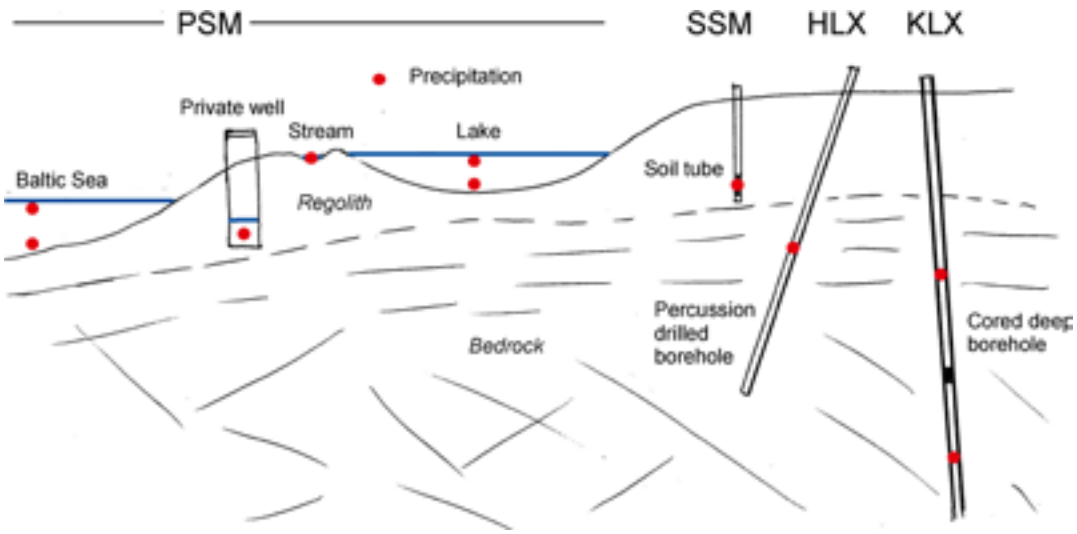


***Figure 2-3.*** *Schematic picture showing the different object types which are sampled for hydrochemistry of the Laxemar-Simpevarp area. The red dots denote the representative sampling level.*

Surface water sampling is conducted in the few lakes within the Laxemar-Simpevarp area, in the major streams and at five locations in the Baltic Sea, according to Figure 2-4 to Figure 2-6. Sampling of shallow groundwater is conducted in soil tubes and private wells according to Figure 2-7. Surface water divides that form the sub-catchments of the Laxemar-Simpevarp area are also marked in these maps. A comprehensive summary of the hydrochemistry of the surface system is given in /Tröjbom and Söderbäck 2006/.

Groundwater sampling in the bedrock is conducted in cored boreholes and percussion boreholes according to Figure 2-8. Deep boreholes are clustered at 'drill sites', surrounded by percussion boreholes used for flushing water supply (cf Table 2-5) and monitoring purposes. Soil tubes are also located around the drill sites for environmental monitoring purposes. There are also a relatively large number of soil tubes and percussion boreholes located outside drill sites for monitoring and characterisation purposes. Many soil tubes and percussion drilled wells are mainly used for hydrological monitoring of groundwater levels and hydrological characterisations e.g. by pumping and so called 'slug tests', and hydrochemical sampling has been carried out in only about half of the soil tubes.

Physical and hydrological information on soil tubes is compiled in Appendix A, whereas information on private wells is found in /Morosini and Hultgren 2003/. Cored boreholes are described and evaluated in detail in /Laaksoharju (ed) 2008/, and some depth and hydrochemical data from percussion boreholes are compiled in Appendix E.

### 2.2.4 Hydrochemical data from surface systems

Hydrochemical data from surface systems (precipitation, stream water, lake water, sea water, shallow groundwater in soil tubes and private wells) are based on the Laxemar 2.3 'data freeze', covering the 5-year period from July 2002 to August 2007. Due to revisions of the monitoring programme and different extensions of sampling campaigns, there is a large variation in representativity and available number of samples from different objects. A charge balance error of ±15% had to be accepted for samples from the surface system in order to achieve acceptable geographical coverage. The large charge balance errors are attributed to the selected analytical methods, which in combination with the dilute waters present in this area give analytical errors greater influence (cf Section 9.1). Two different selections of hydrochemical data from the surface system are used in combination with three different sets of reference data from the bedrock described in Section 2.2.5. Three major datasets named A, B and C are formed:

A. All available data from the surface system. This set of data, which represents individual samples, is used to give an idea of the total variation in the material.

B. All samples from selection A with a charge balance error within ±15%. This set of data contains mean values per object and depth level.

C. Same as selection B for the surface system but with a different selection of reference data from the bedrock compared to selection B (cf Section 2.2.5).

An overview of all available samples from the surface system is compiled in Appendix D. A statistical compilation of mean values is found in Appendix E. The geographical locations are shown in Figure 2-4 and Figure 2-7.

### 2.2.5 Hydrochemical reference data from the bedrock

Hydrochemical reference data for groundwater sampled from different types of boreholes in the bedrock are based on the Laxemar 2.3 'data freeze' covering the period to November 2007 (the extended 2.3 'data freeze'). Groundwater samples with large charge balance errors have been omitted in accordance with the ChemNet 2.3 data categorisation /Laaksoharju (ed) 2008/. Groundwater data from the bedrock are mainly included in the visualisations and analyses in this report as a reference for shallow observations. The following groundwater reference data from the bedrock are added to the three data selections A, B, and C for surface water data described above (cf Section 2.2.4):

A. All available groundwater data with an acceptable charge balance (±5%) and measurements, for the KFM samples, of flushing water content. So called 'drilling samples' and 'experiment water samples' were excluded. This set of data, which represents individual samples, is used to give an idea of the total variation in the material.

B. All samples from selection A, but with samples exhibiting unreliable depth information deselected, e.g. 'tube samples' and 'drilling samples'. This set of data contains mean values per object and depth level.

C. Expert selection of single samples representing the groundwater hydrochemistry in the bedrock with satisfactory depth accuracy, stable redox conditions, acceptable charge balance and probable isotope values, according to the ChemNet 2.3 data categorisation in January 2008 (cf /Laaksoharju (ed) 2008/ for a description of this work). Data from ChemNet categories 1 to 3 are included in selection C.

Data selection C is used in most visualisations and models throughout this report in order to harmonise with the hydrogeochemical reporting of deeper groundwater data. In some visualisations, dataset B is used to reflect the greater variability of a larger number of samples, at the expense of slightly more unreliable depth information. To give an idea of the total variability of the dataset, selection A is sometimes included in the background as grey marks, or specially labelled for individual objects.

A compilation of all available groundwater samples from the bedrock is provided in Appendix D. This compilation is based on data selection C (see bullet list above). A statistical compilation of mean values are found in Appendix E. The geographical locations of the objects are shown in Figure 2-8.


***Figure 2-4.*** *Surface water sampling points and private wells in the Laxemar-Simpevarp area.*

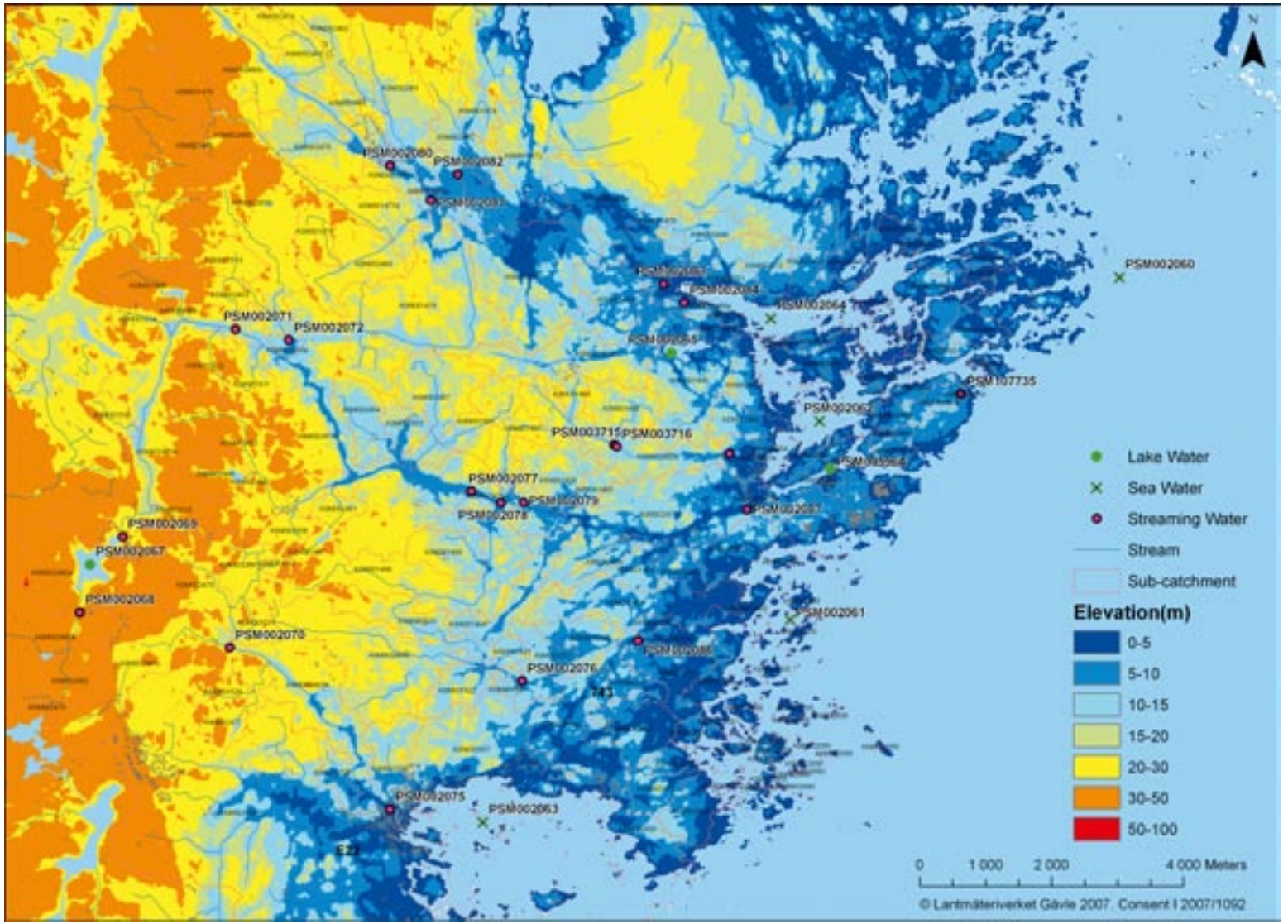


***Figure 2-5.*** *The location of the surface water sampling points in relation to the digital elevation model in the Laxemar-Simpevarp area.*

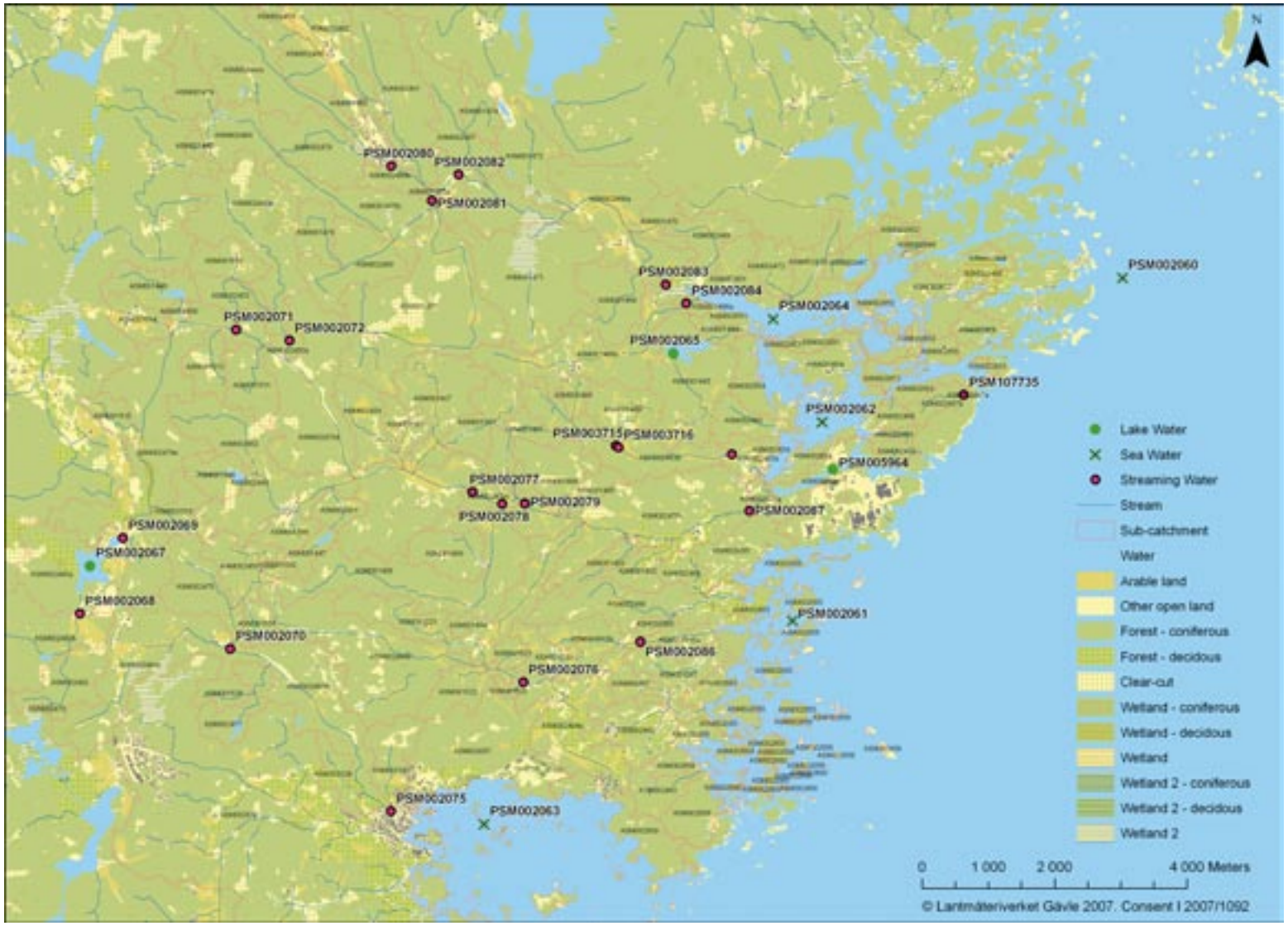


***Figure 2-6.*** *The location of the surface water sampling points in relation to the land use map in the Laxemar-Simpevarp area.*


***Figure 2-7.*** *Shallow groundwater sampling points in the Laxemar-Simpevarp area (soil tubes and private wells).*


***Figure 2-8.*** *Groundwater sampling points in the bedrock in the Laxemar-Simpevarp area (cored- and percussion drilled boreholes).*

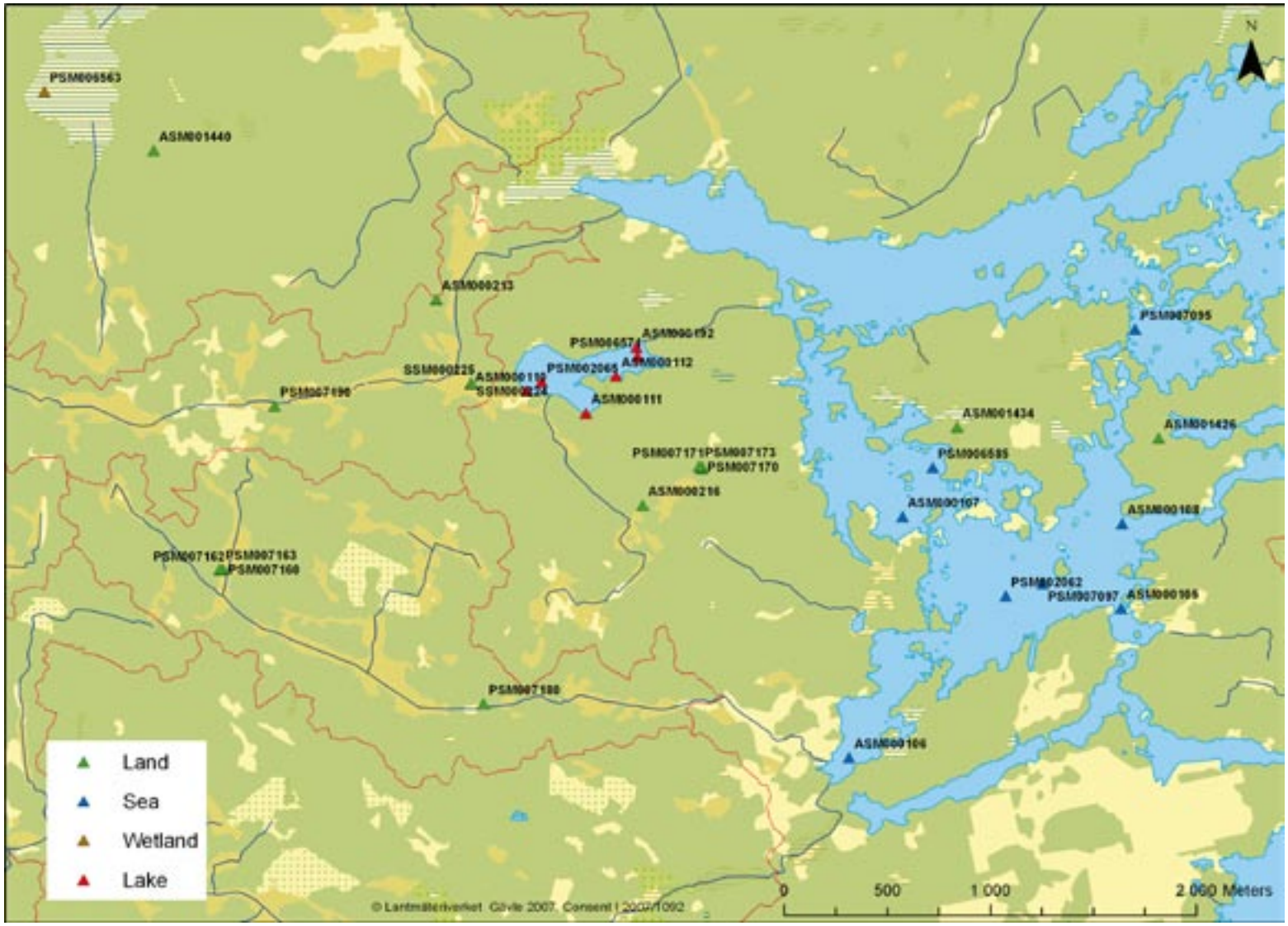


***Figure 2-9.*** *Regolith sampling sites in the Laxemar-Simpevarp area.*

### 2.2.6 Influence of flushing water content on data from cored boreholes

Flushing water used during drilling of the cored boreholes is labelled with uranine. If the composition of the flushing water source is known, it is theoretically possible to correct the measurements and recalculate the original composition. Percussion boreholes are used as flushing water wells, and the approximate chemical composition of this water is documented by the hydrochemical sampling. A detailed investigation of the impact during drilling and the possibilities to use uranine to label drilling water is found in /Laaksoharju (ed) 2008/. The correction is complicated by the following factors:

- Element concentrations in percussion boreholes are not constant.
- Non-uranine-labelled surface water may cause contamination during drilling and pumping.
- The altered chemical environment due to the flushing water may cause reactions that affect the chemical composition measured in the groundwater in the bedrock.

A rough recalculation based on a simple linear binary mixing model was performed per element to correct for the influence of flushing water contamination in the cored boreholes. The correction was based on the average composition of the flushing water wells used, according to Table 2-5.

The results of the flushing water correction can be seen in Figure 2-10, where original and corrected values for Cl and $HCO_3^-$ are shown. The correction has little effect on most Cl measurements, whereas $HCO_3^-$ generally decreases and the resulting negative concentrations make the non-conservative behaviour of this ion evident (no negative values occur after correction for any other ions).

Due to its small impact on the concentrations of samples from the bedrock, the flushing water correction was discarded in all models and visualisations throughout this report. As most visualisations are based on data selection C, where groundwater samples were specially selected for low flushing water contents, flushing water contamination has little influence on the conclusions in this report.

**Table 2-5. Flushing water wells (percussion boreholes) used in drilling of cored boreholes.**

| Cored borehole | Flushing water well | Cored borehole | Flushing water well |
|---|---|---|---|
| KSH01A | HSH03 | KLX11B | HLX28 |
| KSH01B | HSH03 | KLX11C | HLX28 |
| KSH02 | HLX10 | KLX11D | HLX28 |
| KSH03A | HSH03 | KLX11E | HLX28 |
| KSH03B | HSH03 | KLX11F | HLX28 |
| KAV04A | HLX10 / HSH03 | KLX12A | HLX10 |
| KAV04B | HSH03 | KLX13A | HLX14 |
| KLX03 | HLX14 | KLX14A | HLX28 |
| KLX04 | HLX10 | KLX15A | HLX14 |
| KLX05 | HLX10 | KLX16A | HLX10 |
| KLX06 | HLX20 | KLX17A | HLX14 |
| KLX07A | HLX10 | KLX18A | HLX14 |
| KLX07B | HLX10 | KLX19A | HLX28 |
| KLX08 | HLX10 | KLX20A | HLX28 |
| KLX09 | HLX20 | KLX21B | HLX10 |
| KLX09B | HLX20 | KLX22A | HLX28 |
| KLX09C | HLX20 | KLX22B | HLX28 |
| KLX09D | HLX20 | KLX23A | HLX28 |
| KLX09E | HLX20 | KLX23B | HLX28 |
| KLX09F | HLX20 | KLX24A | HLX28 |
| KLX09G | HLX20 | KLX25A | HLX28 |
| KLX10 | HLX27 / HLX10 | KLX26A | HLX14 |
| KLX10B | HLX20 | KLX26B | HLX14 |
| KLX10C | HLX20 | KLX28A | HLX14 |
| KLX11A | HLX28 | KLX29A | HLX14 |

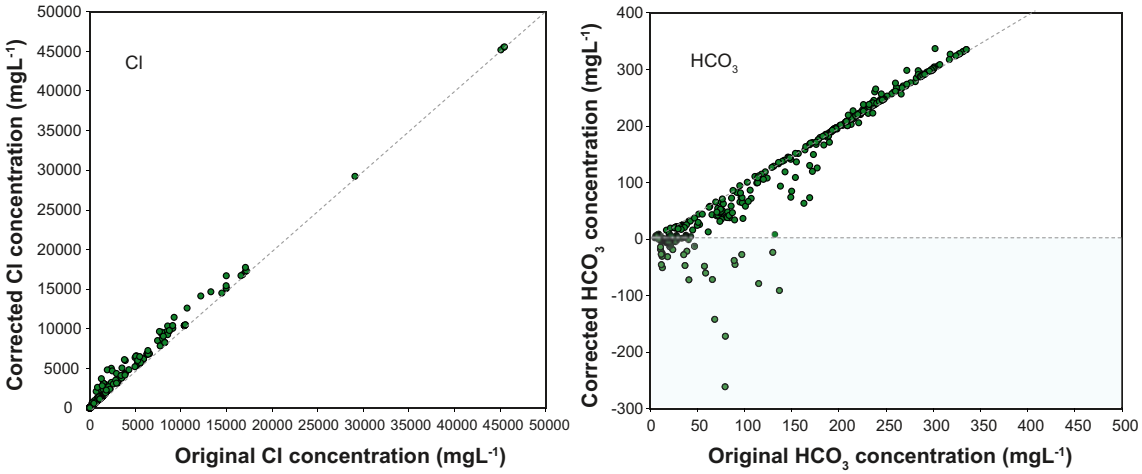


***Figure 2-10.*** *The result of the flushing water correction of measurements from cored boreholes. Original (horizontal axis) and corrected (vertical axis) Cl concentrations to the left and corresponding measurements for $HCO_3^-$ to the right. All available data corresponding to selection A from cored boreholes in the Laxemar-Simpevarp area are included in these plots (cf Section 2.2.5).*

### 2.2.7 Chemical composition of the regolith

The chemical composition of the regolith has been analysed for both major constituents and a large number of trace elements. These samples are taken from a broad range of environments including till, glacial clay, marine and lacustrine sediments and sediments below wetlands according to Figure 2-9. See /Sohlenius and Hedenström 2008/ for further evaluations of regolith data.

## 2.3 Statistical methods and visualisation techniques

Statistical methods and visualisation techniques used in this report are described in this section. Symbols and labels included in the figures to facilitate interpretations are also explained.

### 2.3.1 Statistical processing of data

The extensive data sets described in Section 2.2 are processed by statistical methods in order to simplify visualisations. In most figures the arithmetic mean is used to get a single value representing all samples from a specific object or depth level, and individual samples are included in only a few plots to reflect the dispersion of the whole dataset (cf Section 9.1 for further discussions on this topic). According to the compilations in Sections 2.2.4 and 2.2.5, these mean values are based on a varying number of samples depending on object type and sampling campaign.

A set of aggregated parameters is used in Section 5.1.2 to explore correlations with hydrological parameters (cf Section 2.2.1). These parameters either represent arithmetic mean values or measures of dispersion such as standard deviation or coefficient of variation. Standard deviation, which is expressed in the same unit as the measurements, is used for parameters such as temperature and isotope deviations, whereas coefficient of variation is used for concentration data that may take on values of zero (the coefficient of variation is unitless and describes the relative dispersion around the mean value).

### 2.3.2 Handling of values below reporting limits

Measurements of all elements have reporting limits that reflect the accuracy of the analytical method used. There may also be a variation in the reporting limit for a specific element depending on differences between analytical methods or laboratories. Environmental factors such as salinity may also influence the reporting limits. In all statistical calculations, values below reporting limits were set to a value equivalent to half of the reporting limit. When different reporting limits occur for a single object, the highest limit is shown in statistics and figures. See appendix 8 in /Laaksoharju (ed) 2008/ for an evaluation of analytical uncertainties.

### 2.3.3 Representation of isotope measurements

Isotope measurements are usually expressed as relative deviations from an international standard according to the oxygen isotope example in Equation 2-1. International standards from /Clark and Fritz 1997/ are shown in Table 2-6.

*Equation 2-1. Example showing the calculation of the oxygen isotopic deviation from the international reference. The usually very small deviation is multiplied by 1,000 and is therefore expressed in per mille (‰).*

$$\delta^{18}O_{sample} = \left( \frac{(^{18}O/^{16}O)_{sample} - (^{18}O/^{16}O)_{reference}}{(^{18}O/^{16}O)_{reference}} \right) \cdot 1000 \ \text{(‰ SMOW)}$$

Isotope measurements of $^{2}H$ and $^{18}O$ in precipitation from a wide range of climatic regions follow a general relationship called the Global Meteoric Water Line (GMWL – see Equation 2-2). Local precipitation measurements form Local Meteoric Water Lines (LMWL), which diverge slightly from GMWL due to of factors varying from place to place. Isotope measurements of groundwater or surface water may be related to GMWL or LMWL, and significant deviations from these lines may reflect processes influencing the water cycle, such as evaporation.

*Equation 2-2. The Global Meteoric Water Line /Clark and Fritz 1997/, originally derived from /Rozaniski et al. 1993/.*

$$\delta^{2}H = 8.17(\pm 0.07)\,\delta^{18}O + 11.27(\pm 0.65) \text{ ‰ VSMOW}$$

Radiogenic isotopes of hydrogen ($^{3}H$) and carbon ($^{14}C$) are measured as the activity of the radioactive decay. In the case of $^{14}C$, this activity is expressed as the proportion of modern carbon that corresponds to the measured activity (abbreviated pmC).

**Table 2-6. International isotope standards for isotopes used in this report. From /Clark and Fritz 1997/.**

| Isotope ratio | Abbreviation in this report | International reference | Reference ratio |
|---|---|---|---|
| $^{2}H/^{1}H$ | $^{2}H$ | VSMOW | $1.5575 \cdot 10^{-4}$ |
| $^{11}B/^{10}B$ | Not included | NBS 951 | 4.404362 |
| $^{13}C/^{12}C$ | $^{13}C$ | VPDB | $1.1237 \cdot 10^{-2}$ |
| $^{18}O/^{16}O$ | $^{18}O$ | VSMOW | $2.0052 \cdot 10^{-3}$ |
| $^{34}S/^{32}S$ | $^{34}S$ | CDT | $4.5005 \cdot 10^{-2}$ |
| $^{37}Cl/^{35}Cl$ | $^{37}Cl$ | SMOC | 0.324 |
| $^{87}Sr/^{86}Sr$ | $^{87}Sr$ | Absolute ratio measured | - |

### 2.3.4 Cross plots (scatter plots)

Combinations of variables are visualised in standard cross plots with two axes. To facilitate interpretations with regard to specific issues, the original variables are sometimes transformed in order to focus on the range of interest. Logarithmic scales on one or two axes are used for the same purpose (cf Section 2.3.11 and 2.3.12 for descriptions of labels and trendlines).

Time series consisting of discrete measurements are shown as points connected by lines to facilitate interpretation, although these lines may not represent the actual trajectories between these points.

### 2.3.5 Piper plot

The Piper plot is a specialised plot for water classification. Compositional data (the relative molar amounts) of cations and anions are plotted into the ternary (triangular) coordinate systems, which as a second step are projected onto the central prism. This methodology may be seen as a dimension-reducing technique that reduces the original concentrations of seven major constituents (7 dimensions) into a two dimensional visualisation (the central prism), where dominating ions may be distinguished (Figure 2-11).

### 2.3.6 Projection plots

Many figures in this report are used to visualise how a third parameter relates to two parameters in a two-dimensional scatter-plot. The magnitude of the third parameter is shown by a colour code representing a varying number of discrete classes. This type of plot, here called ‘projection plot’, visualises 3 parameters at the same time, corresponding to 3 dimensions.

### 2.3.7 Cross sections and profiles

In Section 7, cross sections of the 3-dimensional regolith layer model /Nyman et al. 2008/ are used to visualise how hydrochemical sampling points relate to various spatial information. Profiles in these cross sections were created in ArcGis 9.1 by the plug-in /ESRI 2007/.

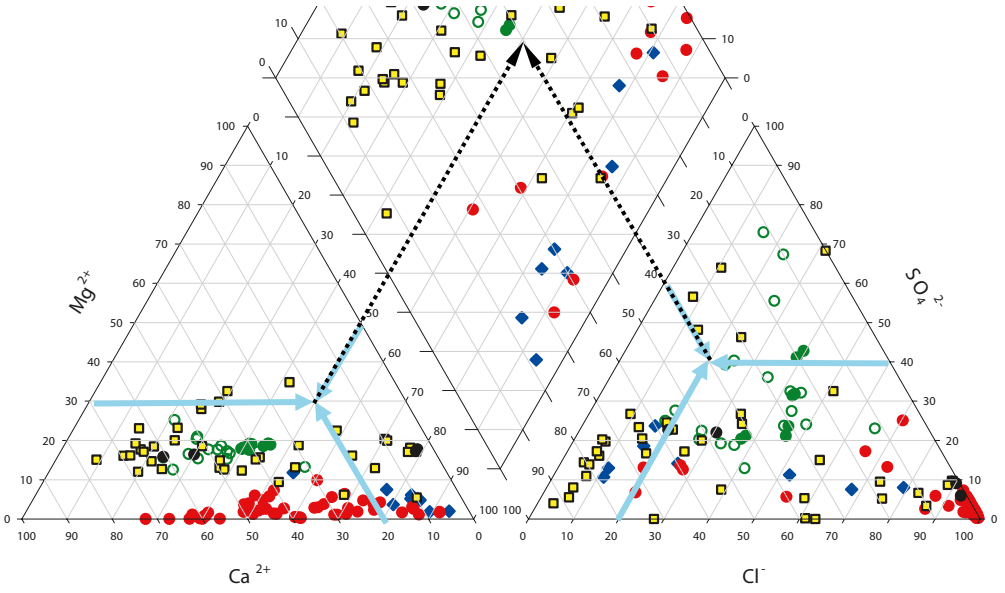


***Figure 2-11.*** *The principle of a Piper classification plot. The blue-green arrows show how the relative composition of Ca:Mg:Na+K (20%:30%:50%) and Cl:$SO_4$:$HCO_3$ (20%:40%:40%) is plotted into the lower ternary coordinate systems. The dashed black arrows show the projection of both anions and cations into the central prism.*

### 2.3.8 Multivariate analysis and visualisation

Multivariate statistical methods are dimension-reducing techniques used for extracting relevant information from large datasets that contain many parallel measurements (many parameters). These powerful methods are suitable for finding underlying factors affecting many parameters at the same time, factors which may represent an ultimate explanation.

The inability to imagine more than three or four dimensions at the same time may restrict the ability to grasp large datasets of 10 or perhaps 100 dimensions (parameters). In short, multivariate analyses may be seen as methods that explore projections (shadows) of multidimensional objects plotted into coordinate systems of several orthogonal axes, and by studying these two-dimensional projections conclusions may be drawn about the multidimensional object which is hard to visualise in a three-dimensional world. The metaphysical nature of multivariate analysis is a necessary consequence of the difficulties to grasp more than 3–4 dimensions at the same time.

### 2.3.9 Principal component analysis (PCA)

A principal component analysis (PCA) is based on a correlation or covariance matrix and may be seen as a graphical tool to interpret the correlation structure among both variables and observations. In this report all PCA models are based on a standard Pearson correlation matrix using the Simca 5.1 software code /Umetrics 2008/. Due to the explorative character of the analysis this approach with no transformation of data was thought to facilitate the interpretations of the models. PCA does not assume normality among the investigated variables and can be used as a descriptive tool whether the variables are normally distributed or not /Jolliffe 2002/. Frequency distributions and effects of skewed data are further discussed in Section 9.2. The results of the PCA analysis are visualised as loading and score plots:

- In the **loading plot** the relationships among the variables are revealed. Each variable is projected onto the so called principal components, which can be seen as latent factors influencing several variables to a varying degree. If a variable shows a close relationship to a principal component, it is located far from the origin of the loading plot in the direction of that component. Variables that plot close to each other are correlated, whereas variables located on opposite sides of the origin are negatively correlated. Variables located near the origin show little correlation with the selected principal components, and therefore little can be said about the correlation structure among these variables. The principal components may have a real meaning, for example a climatic factor, or may just represent a linear combination of unknown factors.
- The **score plot** reveals relationships among the observations. The score plot is a complement to the loading plot in the sense that observations located in a specific region of the score plot show high values for variables located in the corresponding region of the loading plot.

### 2.3.10 Partial least squares modelling (PLS)

Partial Least Squares Regression modelling (PLS) is a multivariate method closely related to PCA. This technique may be seen as two parallel PCAs, one representing the explanatory parameters, the X space, and one representing the explained parameter(s), the Y space. The principal components in both ‘spaces’ are rotated in order to achieve maximal correlation between these structures. Besides being used for fitting empirical explanatory models, PLS plots may, like PCA plots, be used in explorative analysis of correlation structures among groups of parameters.

### 2.3.11 Coding and labelling in figures

The different object types are consistently marked in all plots throughout the report by a unique symbol and colour according to Table 2-7. Individual observations are also labelled by an identification code to facilitate detailed analysis of the patterns among individual objects and different

**Table 2-7. Different objects are marked by a unique symbol/colour in the plots throughout the report. KBH, KLX, KSH, KAS, KAV = cored boreholes, HBH, HLX, HSH, HAS, HAV = percussion boreholes, SSM = soil tubes, PSM denotes lake water, stream water or sea water samples. Reference samples of different types are shown as a black dot. Cf Section 2.2.3 for an explanation of Idcodes.**

| Object type | IDCODE prefix in Sicada database | Label code | Symbol |
|---|---|---|---|
| Cored borehole | KBH, KLX, KSH, KAS, KAV | KBH, KLX, KSH, KAS, KAV | ● |
| Percussion borehole | HBH, HLX, HSH, HAS, HAV | HBH, HLX, HSH, HAS, HAV | ♦ |
| Soil tube | SSM | S | ■ |
| Private well | PSM | PP | ■x |
| Lake | PSM | PL | ● |
| Stream | PSM | PW | ○ |
| Sea | PSM | PO | ■x |
| Reference | - | - | ● |

depth levels. This code contains a “label code” (cf Table 2-7) of the object type followed by an identification number of the Sicada variable IDCODE, and finally the absolute level expressed in the RHB70 coordinate system. The depth code corresponds to the midpoint of the section (cored boreholes), the main supply level (percussion boreholes), the midpoint of the intake screen (soil tubes – SSM) or the sampling depth (surface water – PSM). A suffix is also added to the surface water samples to indicate whether the sample represents surface (S) or bottom (B) water in the lake or at sea. In private wells, the depth code corresponds to the absolute elevation of the midpoint of the drilled borehole or dug well. The soil tube with IDCODE “SSM000242”, where the midpoint of the intake screen is located at minus 16 metres absolute level below Lake Frisksjön, is for example labelled S242-16 in all figures.

### 2.3.12 Marking of trendlines and scenarios in figures

In many figures, hypothetical trendlines or scenarios have been added to facilitate interpretations and descriptions in the report. It should be kept in mind that these scenarios are more or less probable. The use of non-linear scales on the axes, isotope ratios and parameter transformations, leads to curved mixing lines which are visualised by the hypothetical binary mixing lines. Several types of lines are included in the figures, and they are consequently displayed according to the following:

- Hypothetical trendlines: **bold dashed pink line**.
- Model line: **bold dashed orange line**.
- Mixing lines showing hypothetical binary mixing trends between specific objects: **thin dashed pink line**. These lines are not always probable and the purpose is to explore the borders of the conservative mixing hypothesis and to show the curvature of mixing lines in non-linear plots.
- The flow direction of surface water: **thin dashed green arrow**. These arrows connect surface water objects in the downstream direction in the major catchments.
- Hypothetical depth trend from surface towards depth: **black dotted arrow**.

# 3 Hydrochemical overview of the Laxemar-Simpevarp area

The purpose of this part of the report is to visualise hydrochemical data in order to identify important patterns and to raise relevant questions concerning, for example, the origin and fate of water or dissolved elements, as well as effects of various processes.

## 3.1 Traditional water type classifications

Traditionally, different water bodies are classified into water types based on the (relative) chemical composition of major elements. Different plots are used for this purpose, for example the Ludwig-Langelier diagram and the ternary Piper diagram. The resulting classifications tell which cations and anions dominate in a sample. Trends along flow paths may be identified in the diagrams and conclusions of the evolution of water types may be drawn based on generalised assumptions. However, these assumptions are primarily applicable to larger aquifers and flow systems, and in the case of a small-scale topography characterised by short flow paths, interpretations may entail pitfalls.

### 3.1.1 Ludwig-Langelier plot

Ludwig-Langelier plots visualise the relative proportions of the major cations on the horizontal axes, and proportions of the anions on the vertical axes. Observations located in the lower left corner are dominated by $Ca^{2+}$ and $HCO_3^-$, and can be expected to represent a relatively immature groundwater, i.e. a groundwater strongly influenced by surface water. Observations in the opposite corner are dominated by cations such as $Na^+$ and $K^+$, and anions such as $Cl^-$ and $SO_4^{2-}$, and these observations usually represent an older, mature groundwater, sometimes with possible marine influences (Figure 3-1).

The surface water flow path along the catchment of the Laxemarån River, from the small inlet of Lake Jämsen (PW067) to the outlet into the brackish basin of Borholmsfjärden (PW087), show a typical trend from Ca-$HCO_3$ types at higher topographical levels towards Na-Cl types closer to the Baltic (Figure 3-1). There are however exceptions to this pattern, such as PW071 located in the upper parts of this catchment for which data indicate that there are other sources than leaching from marine relicts that add marine ions to the surface system. Winter road salt has been identified as a major source that adds marine signatures to the dilute water in the upstream parts of the Laxemar-Simpevarp model area (cf Section 7.5).

Most of the shallow groundwater observations from soil tubes follow the main trend of the surface water, marked by the green arrows, indicating that they represent a gradient from undeveloped Ca-$HCO_3^-$ types to brackish Na-Cl types. Most soil tube samples, however, show a less marine composition compared to the major cluster of fresh surface waters. This difference may be attributed to the leaching of road salt into the fresh water system (cf Section 7.5). There are a few soil tubes located below the sea sediments in the brackish basins which show a composition close to modern sea water, indicating a modern or relict marine source of these ions.

A few soil tubes, as well as several observations from the upper parts of the bedrock deviate from the marine trend by showing enrichment of Na+K at the expense of Ca+Mg (e.g. S029-5 and S022-1). This is probably an effect of cation exchange processes. The chemistry of deeper groundwaters in the bedrock, mostly represented by cored boreholes, deviate substantially from the general mixing trend shown by most surface water samples by showing large enrichment of Ca+Mg and Cl+$SO_4^{2-}$.

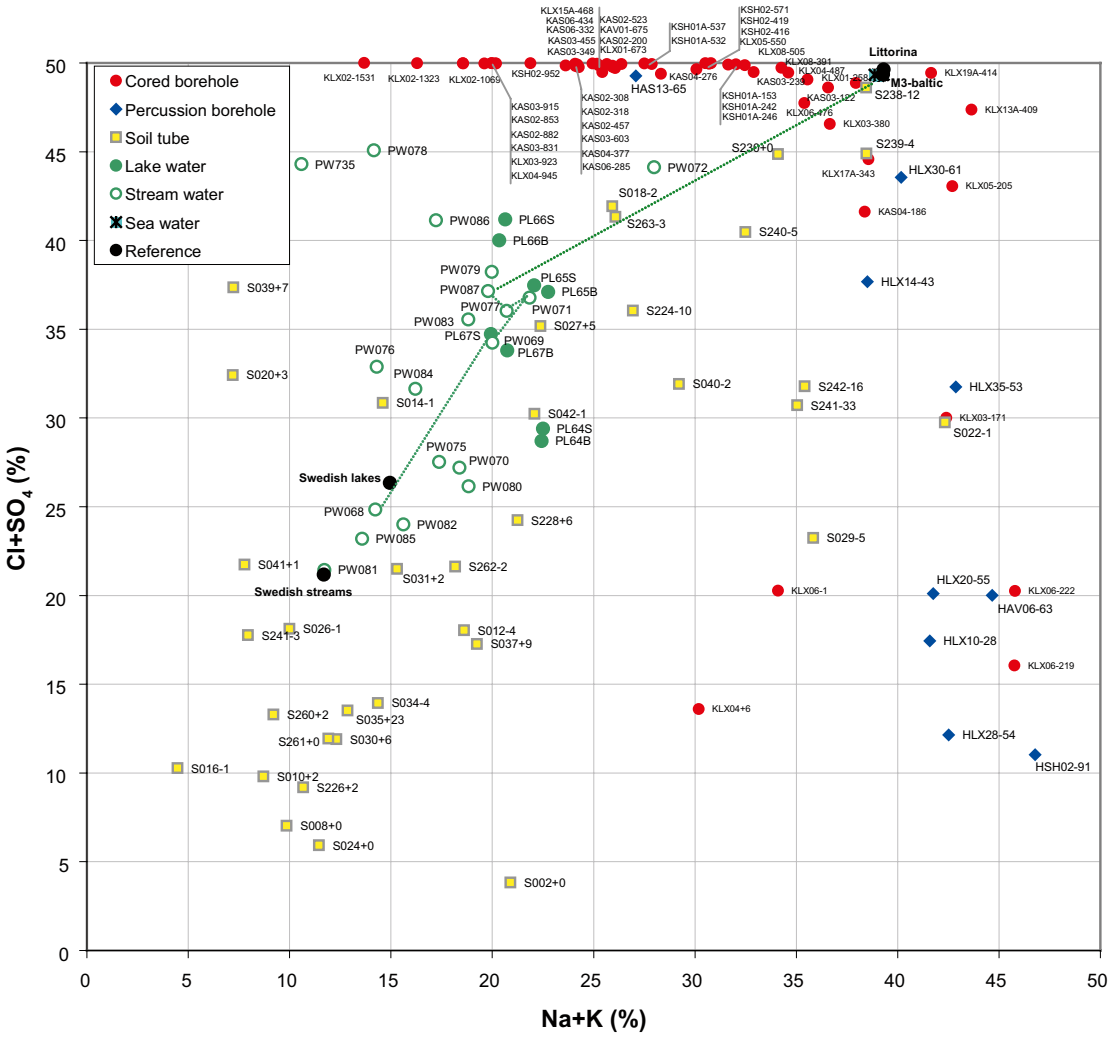


***Figure 3-1.*** *Ludwig-Langelier plot all data from the Laxemar-Simpevarp area based on mean values of data selection C (cf Sections 2.2.4 and 2.2.5). See Sections 2.3.11 and 2.3.12 for an explanation of labels and trendlines in the figure. The relative amounts on the axes are calculated according to the following formulas: Na+K(%)=50*([Na+]+[K+])/([Na+]+[K+]+2[$Mg^{2+}$]+2[$Ca^{2+}$]), Cl+$SO_4^{2-}$(%)=50*([$Cl^-$]+2[$SO_4^{2-}$])/([$Cl^-$]+2[$SO_4^{2-}$]+[$HCO_3^-$]).*

### 3.1.2 Piper plot

A Piper plot is another, slightly more complex tool to visualise the relative fractions of the major ions (Figure 3-2). The lower ternary plots show the relative proportions of cations ($Ca^{2+}$, $Mg^{2+}$, $Na^+$+$K^+$) and anions ($Cl^-$, $HCO_3^-$, $SO_4^{2-}$). The prism, in which the ternary plots are projected, corresponds approximately to the Langelier-Ludwig plot, turned 45 degrees clockwise (cf Section 2.3.5 for an explanation of the Piper plot).

The Piper plot shows that the anomalous composition of the stream sampling sites (PW735 and PW078, marked by a pink oval) may be attributed to $SO_4^{2-}$ rather than $Cl^-$. An additional pattern can be distinguished in the deeper samples of the cored boreholes, with a trend towards the Ca-Cl water type. These samples also show very low relative contents of magnesium and sulphate compared to the general mixing trends in the surface system.

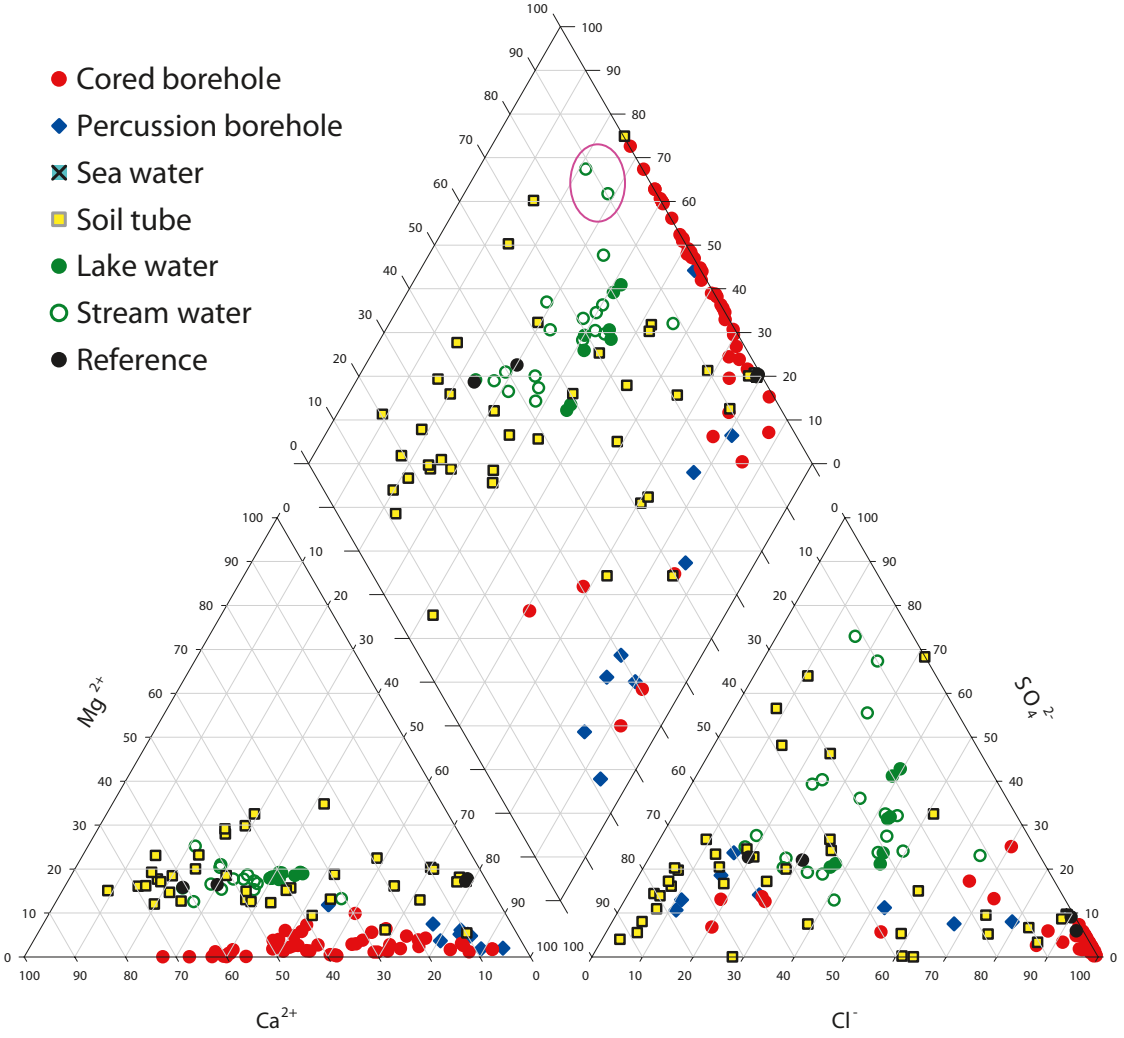


***Figure 3-2.*** *Piper plot of Laxemar-Simpevarp data based on mean values of dataset C (cf Section 2.2.5). See Section 2.3.5 for an explanation of this type of plot.*

## 3.2 Exploring sources of dissolved ions

Dissolved ions in the water are either the product of mixing of different end-members (cf Section 1.1.3), for example sea water or brine, or are formed (or removed) *in situ* as a result of chemical reactions with the rock matrix, fracture-filling minerals, the overburden, organic material or dissolved gases. The residence time of the water determines which processes are dominant within a specific water body.

By a multivariate approach, the main patterns in the chemical composition of surface water and groundwater in the Laxemar-Simpevarp area were explored in a PCA model. Different trends in the model can be interpreted as the influence of different sources of ions which contribute to the observed chemical composition of observations.

The *Ion Source Model* is based on data describing the relative molar quantities of major ions, similar to the previous traditional classification plots. The resulting PCA model can be viewed as a classification model optimised for distinguishing all groundwater types found in the Laxemar-Simpevarp area, in contrast to the previous "classical" classification plots which are less useful for separating groundwater types in the bedrock.

One primary application of the Ion Source Model is to explore similarities between deep groundwater types and observations in shallow groundwater, and thereby possibly detect signatures of deep groundwater discharges into the surface system.

### 3.2.1 Summary of methodology

In order to identify the main hydrochemical variation patterns in the Laxemar-Simpevarp area and to establish a reference model, a common principal components analysis (PCA) was applied to compositional hydrochemical data from data selection B (cf Sections 2.2.4 and 2.2.5 ). The use of relative compositional data cancels dilution effects and results in a model emphasising similarities in relative composition, regardless of dilution by e.g. meteoric or glacial water.

Different data sets were then projected onto the "calibrated" Ion Source Model. For example, projection of data selection C (cf Sections 2.2.4 and 2.2.5), which was used to evaluate similarities and differences in hydrochemical composition between shallow observations and the main variation patterns found in the groundwater in the bedrock. The PCA model was also validated in two steps:

1) A spatial validation where the spatial distribution of the observations, classified into four coarse classes, was explored.
2) A comparison with the results of the multivariate Mixing Model M3 (cf /Laaksoharju et al. 1999/ and further evaluations in /Gómez et al. 2006/).

Finally, the patterns in the model are interpreted in terms of water types and possible ion sources, the latter representing either the hydrochemical composition of end-members or the composition revealed by reactive processes, such as weathering of minerals.

### 3.2.2 Calibration of the Ion Source Model

The Ion Source Model was calibrated to relative compositional data from all water types from the Laxemar-Simpevarp area. Data selection B, which was used for calibration, contains as much data as possible from cored boreholes and percussion boreholes under the conditions of acceptable charge balance (±5%), reasonable accurate depth representation (no tube samplings included), and measurements of flushing water content. For surface water and shallow groundwater included in the calibration dataset, a larger charge balance error of ±15% had to be accepted (cf data selection B described in Sections 2.2.4 and 2.2.5).

Relative chemical composition, expressed as the relative molar abundance, was calculated for cations and anions separately. The calculations were based on the average concentration per object and depth level of all major ions (Na, K, Mg, Ca, Cl, $SO_4^{2-}$, $HCO_3^-$) and a few trace elements (Li, Sr, F, Br). The standard Pearson PCA model based on two principal components comprises about 64% of the total variation in chemical composition among all water types (PC1 41%, PC2 23%). This model condenses the major variation pattern among 11 variables into two latent variables, the principal components. The use of closed compositional data seizes two degrees of freedom, leaving 9 independent variables to the PCA. There may be theoretical objections to the application of a standard PCA to compositional data /e.g. Aitchison and Greenacre 2002/, although this procedure is commonly used in the literature. The use of alternative techniques, for example log-contrasts, to circumvent these possible constraints was, however, rejected in favour of a more transparent approach (cf discussion on uncertainties in Section 9.2 and 9.3.1).

In Figure 3-3 the PCA model is visualised in score and loading plots (cf 2.3.9 for explanation), where calibration data selection B is shown as coloured dots and data selection A, which represents individual samples, is shown as grey marks to give an idea of the total variation in the material. The greatest variation (41%) is shown by the first component (PC1, vertical direction), whereas the second component (PC2, horizontal direction) exhibits a weaker pattern corresponding to 23% of the total variation. The loading plot shows to what extent different variables contribute to the two first principal components. The greatest difference between the observations along the vertical direction (PC1) is exhibited by anions as $Cl^-$ and $HCO_3^-$, whereas the cations $Ca^{2+}$ and $Na^+$ represent the largest differences in the horizontal direction (PC2).

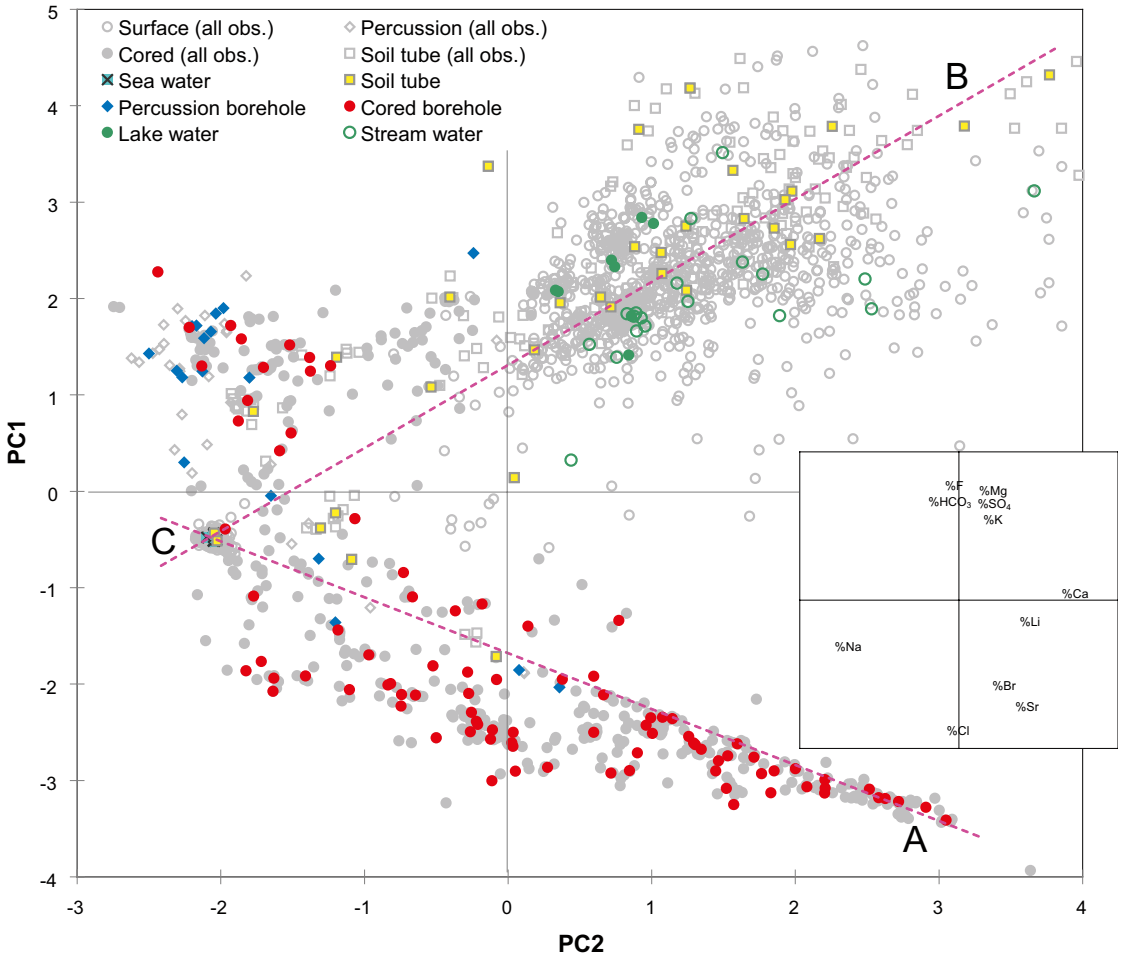


***Figure 3-3.*** *The "score plot" (cf Section 2.3.9) of the calibration dataset of the Ion Source Model. The coloured dots represent calibration data selection B (mean values per object and depth level), while the grey marks show all individual samples of selection A (cf Sections 2.2.4 and 2.2.5. Dashed pink lines mark two major trends in the material: C-A connects modern sea water (C) with deep saline groundwater (A) and C-B connects modern sea water and dilute groundwaters of the surface system (B).*

### 3.2.3 Spatial visualisation of the Ion Source Model

To assess whether the main pattern and interpretation of the PCA model corresponds to a plausible spatial distribution in three dimensions, the observations were roughly classified into five groups according to Figure 3-4.

The spatial distribution of the different classes is visualised as coloured dots in Figure 3-5. All observations of class 5 are located close to the ground surface. Class 4, roughly corresponding to *altered meteoric water* (cf Figure 3-9), reaches slightly deeper levels. Class 3, roughly corresponding to waters with marine influence, is located at depths ranging from 0 to 200 metres. Almost all observations belonging to class 2 are located at vertical depths between 0 and 600 metres, whereas class 1 extends from approximately 200–300 metres to a maximum depth of 1,500 metres. In conclusion: the five different water type classes show a plausible spatial distribution, indicating that the hydrochemical subdivision into different groups by the Ion Source Model probably reflects large-scale structures in the bedrock and the deposits.

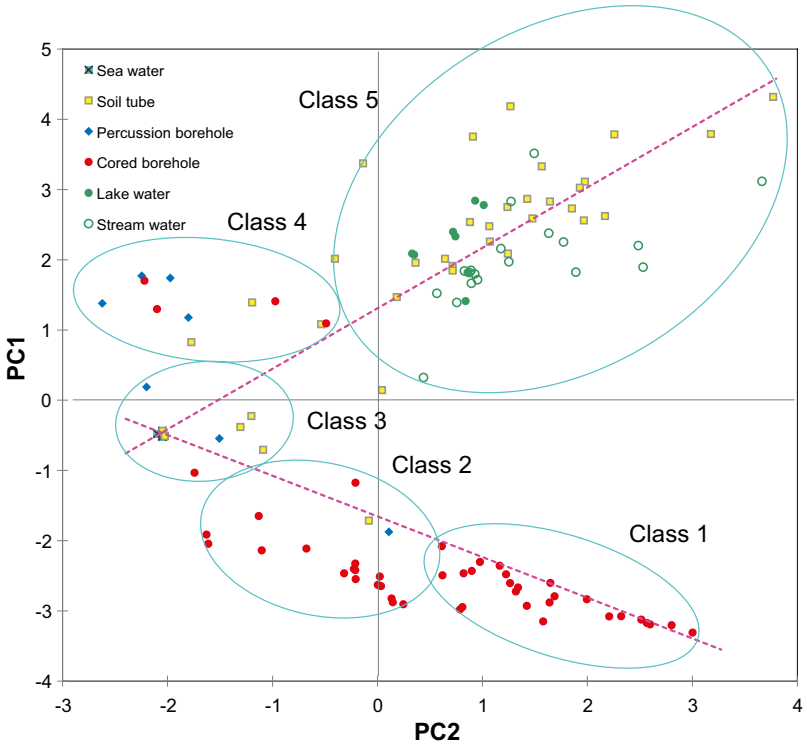


***Figure 3-4.*** *Rough classification of observations in the Ion Source Model into five classes. Observations from data selection C are included in the model (cf Sections 2.2.4 2.2.5).*

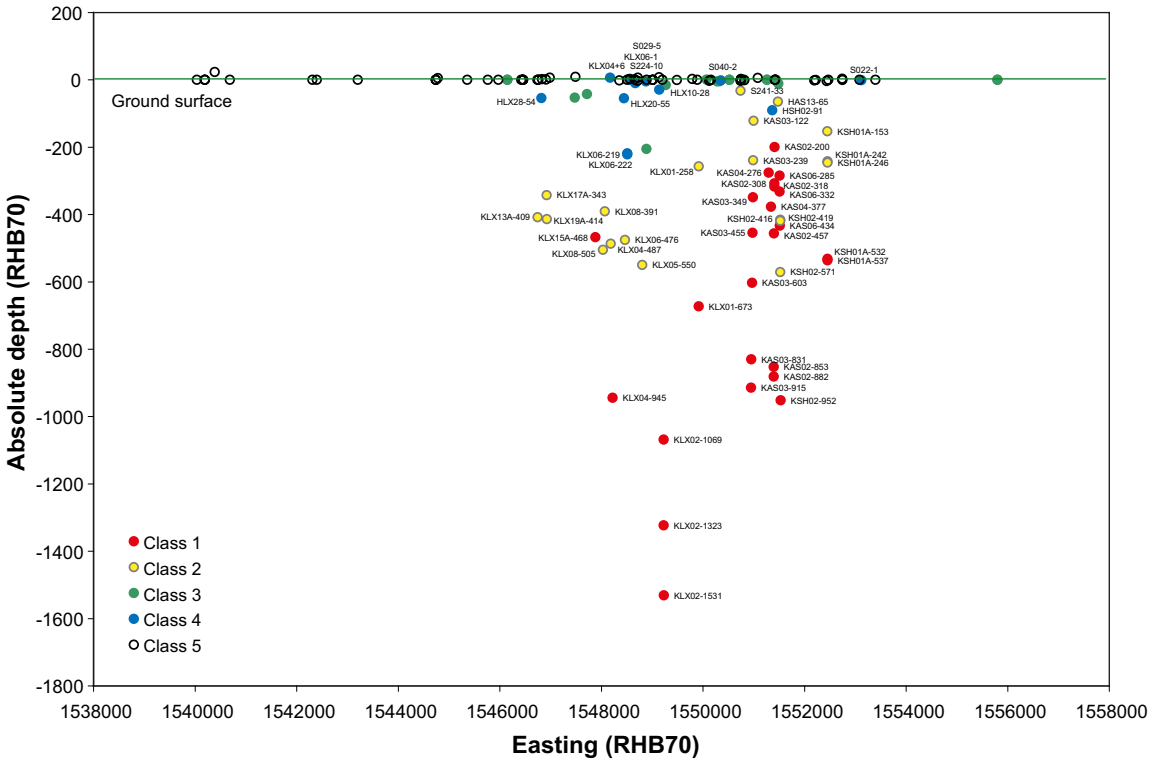


***Figure 3-5.*** *Spatial distribution of the five classes defined in Figure 3-4. The view is from the south with the Laxemar sub-area to the left and the Simpevarp sub-area and the Baltic Sea to the right.*

### 3.2.4 Comparisons with results of the M3-model

In this section, the Ion Source Model is compared with the results of the multivariate model M3, which is used for unmixing calculations of groundwater in the bedrock /Laaksoharju (ed) 2008/. These unmixing calculations reveal the theoretical mixing proportions of the four pre-selected end-members for a sample: *deep saline groundwater* (shield brine), *Littorina Sea water*, *altered meteoric water* and *glacial water*. The M3 model is thoroughly described in /Laaksoharju et al. 1999/ and in /Gómez et al. 2006/ and the results presented here are based on Laxemar 'data freeze' 2.3.

In Figure 3-6, the volumetric mixing proportions of each end-member are projected onto the Ion Source Model for all observations in data selection C. The two models are consistent in the respect that the highest proportion of *deep saline groundwater* according to the M3-model is found in the lower right of the Ion Source Model. The *altered meteoric groundwater* also coincides in the two models (the cluster above "C" in the middle left). According to the M3 model the Littorina end-member contributes only a minor fraction in a few samples from the Laxemar-Simpevarp area, which is in accordance with the Ion Source Model where few observations plot near the marine corner. The glacial end-member is only a minor source of ions and is therefore not explicitly detected as an ion source in the Ion Source Model.

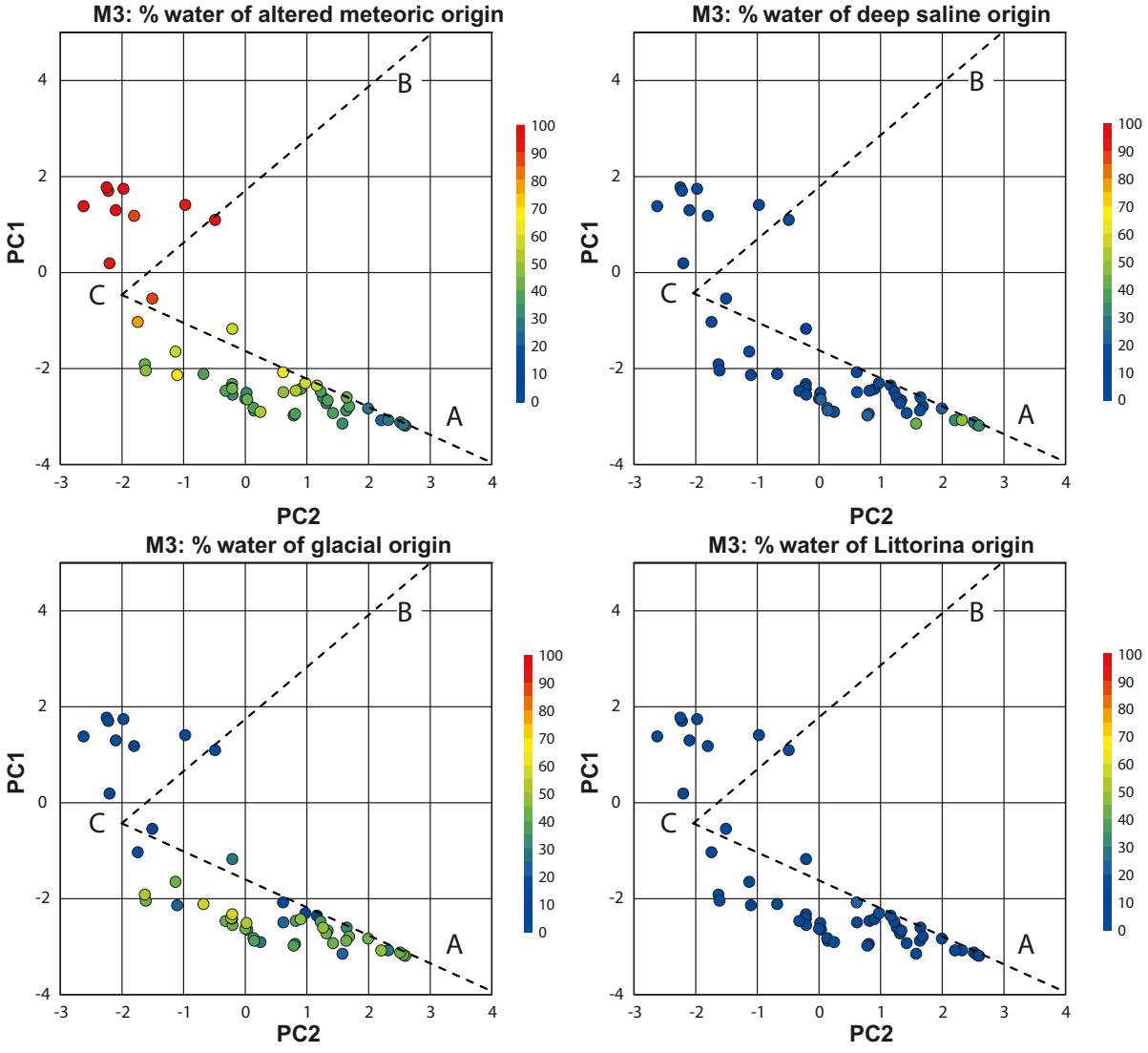


***Figure 3-6.*** *The volumetric mixing proportions of each end-member, calculated by the multivariate Mixing Model M3, projected onto the score plot of the Ion Source Model (cf Section 3.2.5).*

When the fractions of chloride originating from each of the end-members are calculated from the mixing proportions of the M3 model, and the theoretical concentrations of the end-members (cf Table 1-1), the picture is radically changed (Figure 3-7).

According to the proportions calculated by the M3 model, most Cl in the groundwater of the bedrock is of deep saline origin, and the marine fraction only contributes to any significant extent in a few samples. Cl originating from the dilute end-members *altered meteoric* groundwater and *glacial water* contributes only a small fraction in most samples.

It should be noted that this calculation may violate the tolerance of the M3 model and may therefore lead to unreliable results when the volumetric proportion of an end-member falls below 10% /Laaksoharju (ed) 2008/. This is especially the case for deep saline groundwater where the original concentration of the end-member is very high, which could explain the high deep saline proportions indicated in the marked cluster in the upper right panel of Figure 3-7. This cluster is dominated by the dilute *altered meteoric* water type according to the upper left panel in Figure 3-6.

To summarize, there are no obvious contradictions between the Ion Source Model and the results of the M3 model.

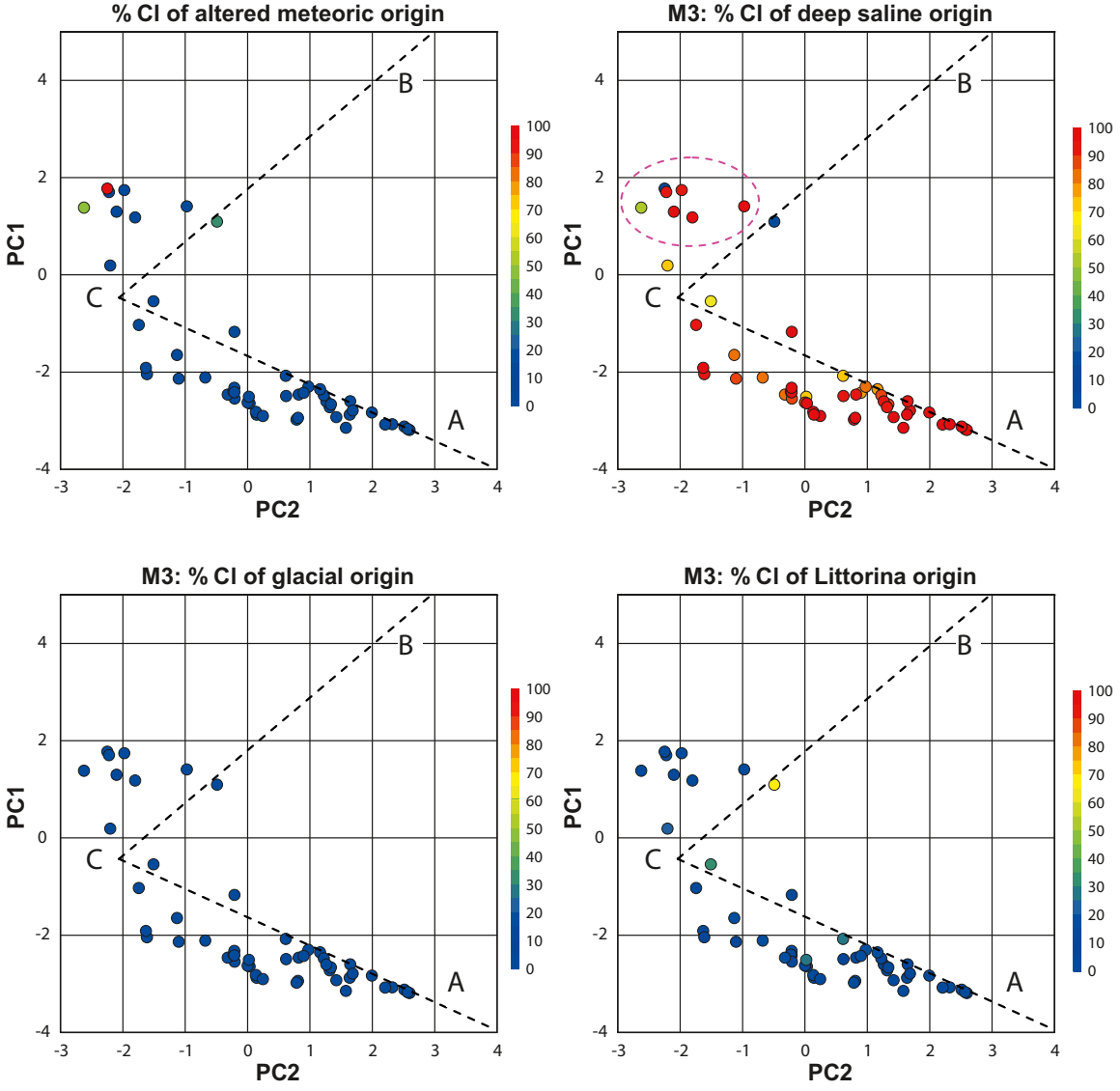


***Figure 3-7.*** *The mass fraction of Cl that originates from each end-member, calculated from the mixing proportions of the multivariate M3 model and the theoretical chloride concentrations of the end-members, projected onto the score plot of the Ion Source Model (cf Section 3.2.5).*

### 3.2.5 Projections onto the Ion Source Model

In Figure 3-8, the representative data selection C (cf Sections 2.2.4 and 2.2.5) has been projected onto the calibrated Ion Source Model. This expert selection – which includes only samples with reasonably correct depth information, low contamination by flushing water and stable hydrochemistry – is assumed to give as unbiased a picture as possible of the hydrochemical conditions in the bedrock. Surface water data (lake, stream and shallow groundwater) are identical in the calibration (selection B) and representative (selection C) datasets (cf 2.2.4).

The main pattern of the calibration dataset in Figure 3-3 is preserved in Figure 3-8. The most obvious difference between the two figures is the total number of objects and depths included in the plots; several percussion boreholes as well as many levels from cored boreholes are excluded in the latter plot. Samples from groundwater in the bedrock in Figure 3-8 are less influenced by artificial mixing and are probably more representative of the depth included in the label of each observation (cf Section 2.3.11).

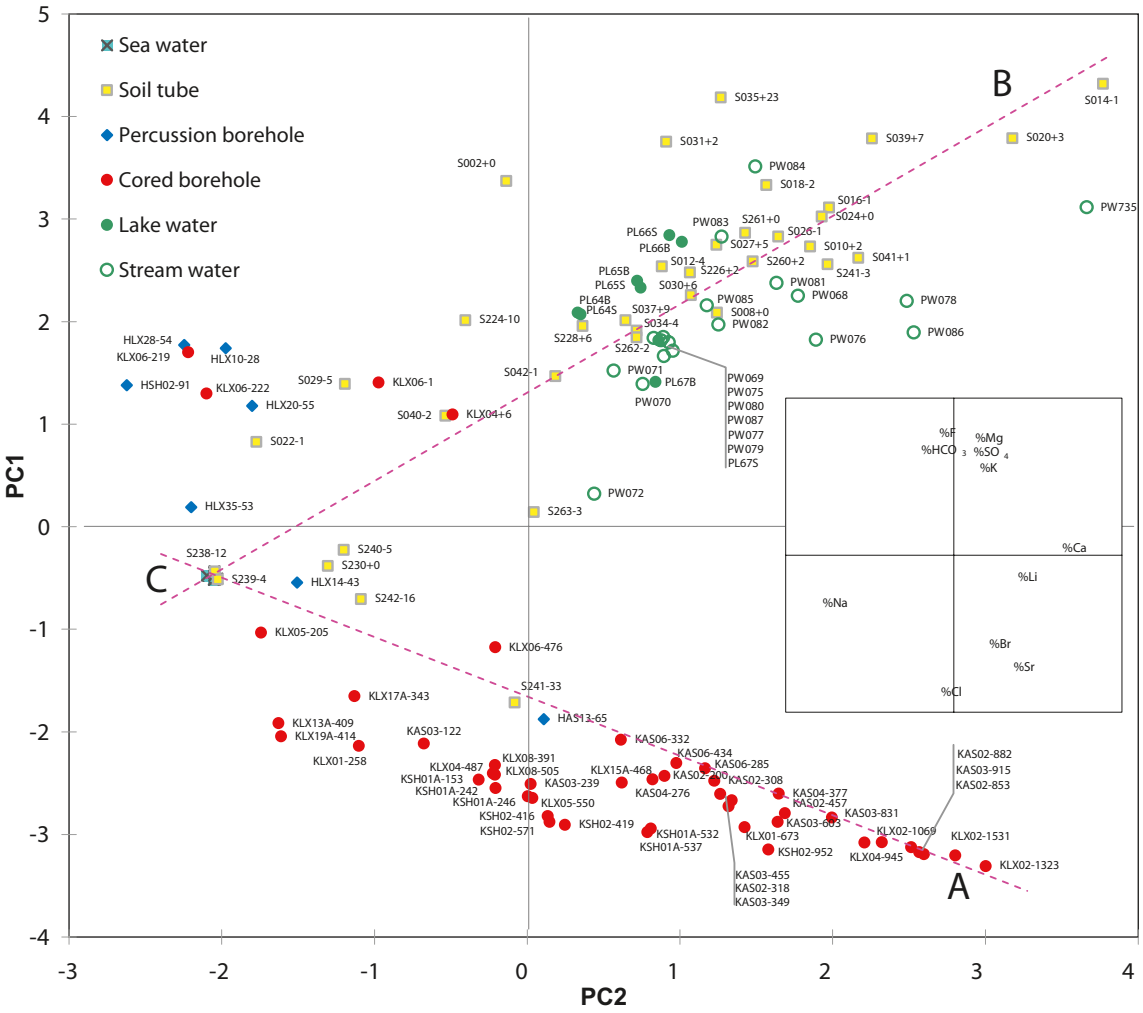


***Figure 3-8.*** *The Ion Source Model. The PCA score plot (cf description in Section 2.3.9) shows how the different groundwater and surface water objects relate to each other regarding the chemical composition of major elements. Labelling of individual objects is explained in Section 2.3.11. See Figure 3-3 for a description of labels A-C.*

Samples located close to each other in the plot show a resemblance with regard to the major elements included in the model. It should, however, be noted that all conclusions regarding similarities and dissimilarities in composition refer to the main variation patterns of the major elements, and sometimes adjacent observations may differ with respect to variation in a direction perpendicular to the paper plane. It should also be noted that a specific composition in the plot may be explained by several combinations of different sources, and therefore not necessarily represent a common origin of the adjacent samples.

Most of the observations from the surface system plot in the upper half of Figure 3-8, whereas samples from the deep system plot in the lower half. This indicates that water in the surface system for the most part differs considerably in composition from the deeper samples in the cored boreholes. Many soil tubes plot along the trendline C-B and therefore show a strong resemblance to the chemical composition of lakes and streams. There are also a few soil tubes that plot near C, indicating similarities with modern sea water. A few soil tubes are associated with the trendline C-A, which may be interpreted as a resemblance to deep saline groundwater.

### 3.2.6 Interpretation of sources and water types in the Ion Source Model

Trends in the observations in the Ion Source Model can be interpreted as influence from different ion sources. Intermediate locations can be interpreted as mixtures of ions from different sources. Groundwater types defined as end-members in the M3 modelling (cf Section 1.1.3) are possible ion sources in mixing processes. The composition of these "water type" sources are plotted in Figure 3-9, together with the theoretical composition of weathering products from selected silicate minerals to kaolinite /Kehew 2001/ (as a simplication, only $H^+$ of biogenic $CO_2$ origin is assumed to drive this process). The compositions of the different salts that are used extensively for road maintenance in the area (NaCl, $CaCl_2$ and $MgCl_2$) are also included in the figure.

To generalise, the three major ion sources affecting the groundwater in the Laxemar-Simpevarp area are A) deep saline groundwater, B) weathering of local minerals driven by $H^+$ of biogenic origin, and C) marine ions, either of modern or relict origin.

The Ion Source Model can also be interpreted in terms of water types, and four encircled groups can be identified in Figure 3-9. It should be noted, however, that any classification is artificial, as most observations belong to continuous gradients between theoretical end-members. The following water types are introduced in order to facilitate the interpretations (cf ChemNet end-members and the definitions of water types listed in Section 1.1.3).

- **Modern sea water or relict marine water (**e.g. Littorina sea water**).**
- **Deep saline groundwater** significantly influenced by shield brine (shield brine is a highly saline groundwater present at great depths in the granitic environment of the Scandinavian shield).
- **Freshwater and dilute shallow groundwater** comprising surface water in lakes and streams, as well as shallow groundwater in deposits showing "immature" ion signatures.
- The fourth group, **Altered meteoric groundwater**, is a rather dilute groundwater of meteoric origin, significantly altered by processes within the Quaternary deposits.
- **Glacial water** is a water type of low ionic strength with water isotope signatures typical of precipitation in a cold climate (cf water origin model in Section 3.3.2). **The old meteoric – glacial** end-member plot in the same point as 'glacial water' which is a consequence of the identical ion composition of these water types.

The most obvious gradient is shown by a large number of observations ranging from *modern sea water* to the *deep saline groundwater* clearly influenced by shield brine. Most of the observations located along this gradient are groundwater samples from the bedrock (percussion boreholes, and cored boreholes). A few shallow observations in soil tubes also plot along this gradient.

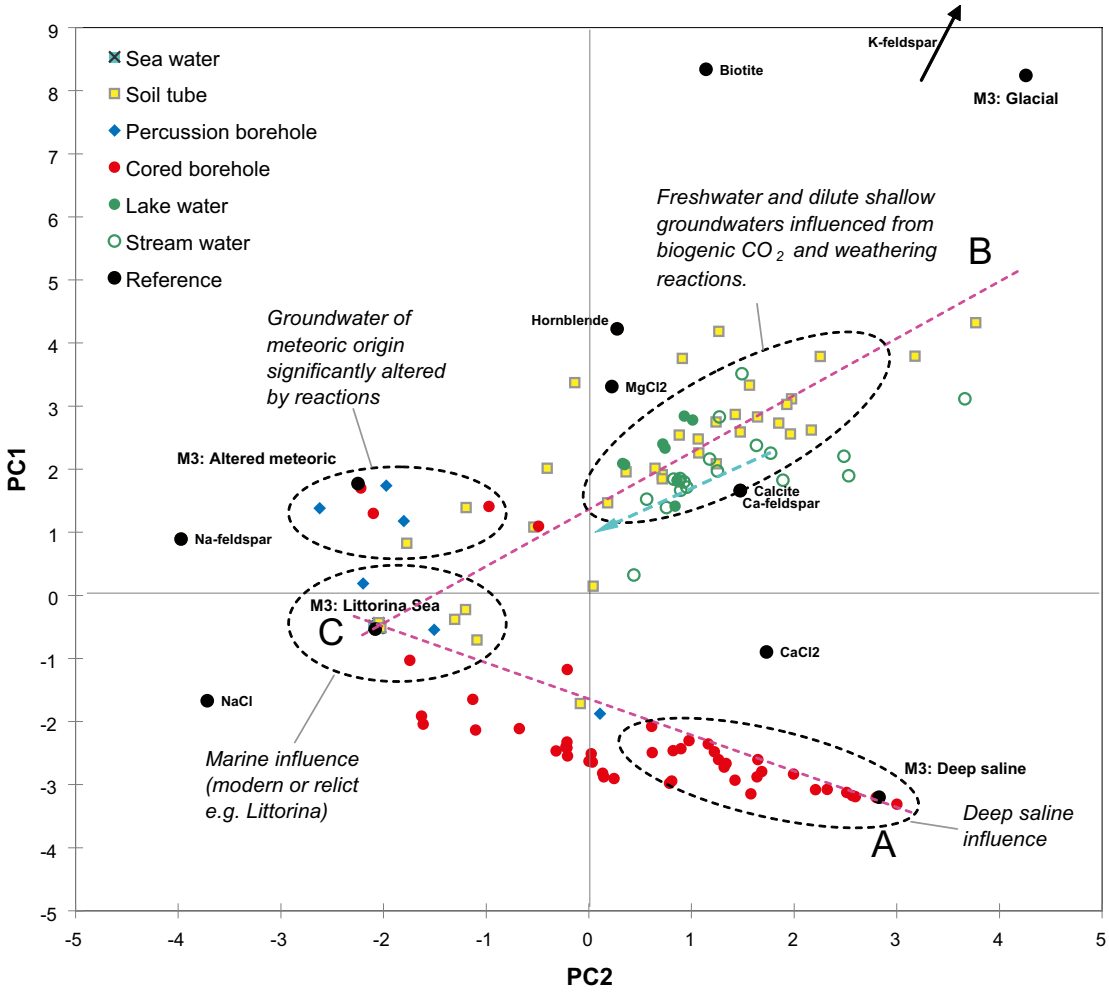


***Figure 3-9.*** *The Ion Source Model, with different possible ion sources marked. The composition of M3 end-members constitute "wet" ion sources, whereas weathering products from selected minerals and from salts used for road maintenance are shown as theoretical compositions. See Figure 3-8 for labels of individual objects and depth levels.*

The marine groundwater type contains all observations from the Baltic Sea and the brackish basins Granholmsfjärden and Borholmsfjärden (hidden under the black symbol for Littorina Sea water end-member), as well as a few observations from the bedrock and deposits. Generally, there are rather few observations of groundwater and shallow groundwater that show significant marine influence (contrary to the Forsmark site where most samples from the bedrock show relict marine influence /Tröjbom et al. 2007/).

The other marked trend connecting C and B contains almost all observations from fresh waters (lakes and streams) and shallow groundwater. These dilute waters have a meteoric origin and are mostly affected by biogenic $CO_2$ and weathering of minerals in the Quaternary deposits. Most theoretical signatures of the few selected minerals plot around this group, indicating possible mineral sources (cf Section 4.2.1). A varying input of marine ions due to deposition and leaching of marine relicts in the deposits causes the trend towards modern sea water. Anthropogenic input of salts used for road maintenance may also contribute to this trend, for example winter road salt (NaCl), where the theoretical shift is marked as a blue-green arrow in the figure (cf Sections 6.2.1 and 4.1.1).

The group *altered meteoric groundwater* probably belongs to the sea water-meteoric trend (C-B), significantly altered by reactions (cf Section 4.2). Many percussion boreholes representing the upper parts of the bedrock plot in this group, along with a few shallow groundwater samples located in the deposits (e.g. SSM000022 located beneath thick sediments on Ävrö, cf Section 7.3).

### 3.2.7 Interpretation of chemical reactions in the Ion Source Model

Deviations from the major mixing patterns in the Ion Source Model may either be caused by mixing with additional sources or be an effect of reactions that have altered the composition of the water. A cation exchange reaction where Ca is replaced by Na shifts the theoretical composition in the plot to the left, as shown by the lilac arrows in Figure 3-10.

The location of the cluster marked “e” can accordingly be explained by alteration of the composition of shallow groundwater in the deposits by Ca-Na cation exchange. Alternatively, the location in the model can be explained by weathering of Na feldspar ($NaAlSi_3O_8$) according to the potential sources shown in Section 3.2.6.

The shift of the cluster marked “d” can also be explained as the net reaction of Ca-Na cation exchange that may have affected groundwater sampled at depths down to 500 metres in the bedrock (this process works in the direction shown by the lilac arrows). A complementary interpretation of the pattern “d” could be mixing between the deep saline source and a pure NaCl source (if this trend is extended towards left it crosses the position of NaCl in Figure 3-9). Discharge of deep saline groundwater of Ca-Cl-type, gradually exchanged with Na derived from wethering reactions in the deposits or the upper parts of the bedrock results in the apparent (hypothetical) mixing with a pure NaCl source (cf Section 4.2.2).

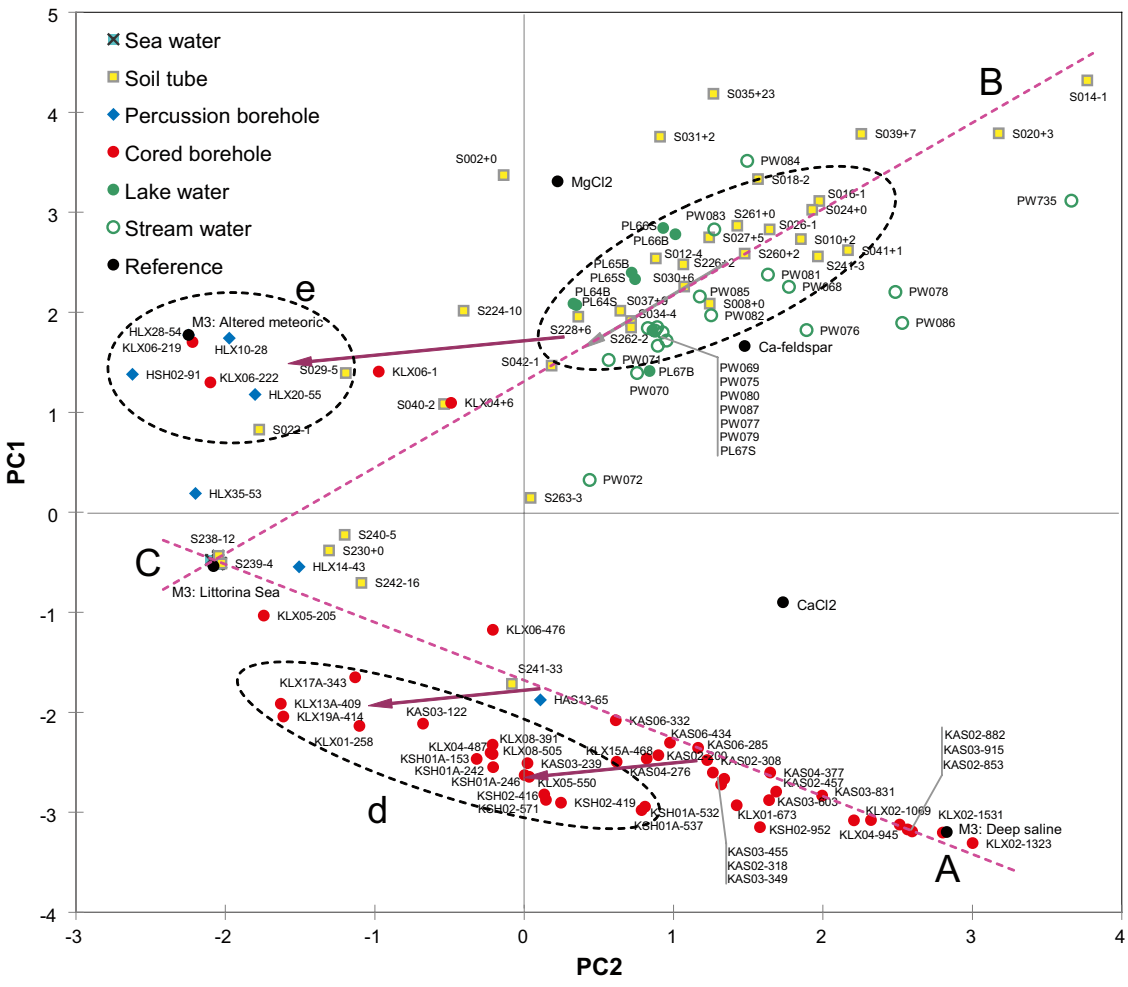


***Figure 3-10.*** *The representative data selection C projected onto the Ion Source Model with possible reactions marked. Lilac arrows denote the theoretical net effect of cation exchange where Ca is replaced by Na. See Figure 3-3 for a description of labels A-C.*

## 3.3 Exploring the origin of water – the solvent

This section deals with the origin of water, the solvent, reflected by the isotopes $^{2}H$ and $^{18}O$, contrary to previous Section 3.2 where the origin of major ions (e.g. Ca, Mg, Na, K, Cl, $SO_4^{2-}$ and $HCO_3^{-}$) was explored. Section 3.4 deals with the situation when ions meet water and form a concentration.

### 3.3.1 Global and local meteoric water lines

The origin of water may be traced from stable or radiogenic isotopes of the elements that comprise the water molecule: hydrogen and oxygen. The ratio between the stable isotopes $^{2}H$ and $^{18}O$ varies depending on different processes influencing the water cycle /Clark and Fritz 1997/. The fraction of $^{2}H$ and $^{18}O$, as well as the activity of the radiogenic $^{3}H$ isotope, are routinely measured in the SKB site investigations.

Globally, the ratio between $^{2}H$ and $^{18}O$ plots along the *global meteoric water line*, GMWL (cf Section 2.3.3). Due to different local conditions, the local precipitation deviates more or less from the global water line. All observations including $^{2}H$ and $^{18}O$ measurements from the Laxemar-Simpevarp area are plotted in Figure 3-11, along with the GMWL.

The local meteoric water line for the Laxemar-Simpevarp area was fitted to the 30 observations in precipitation by least squares regression. LMWL deviates slightly from GMWL by the equation $\delta^{2}H = 7.06\ \delta^{18}O – 1.70$ (cf GMWL in Section 2.3.3).

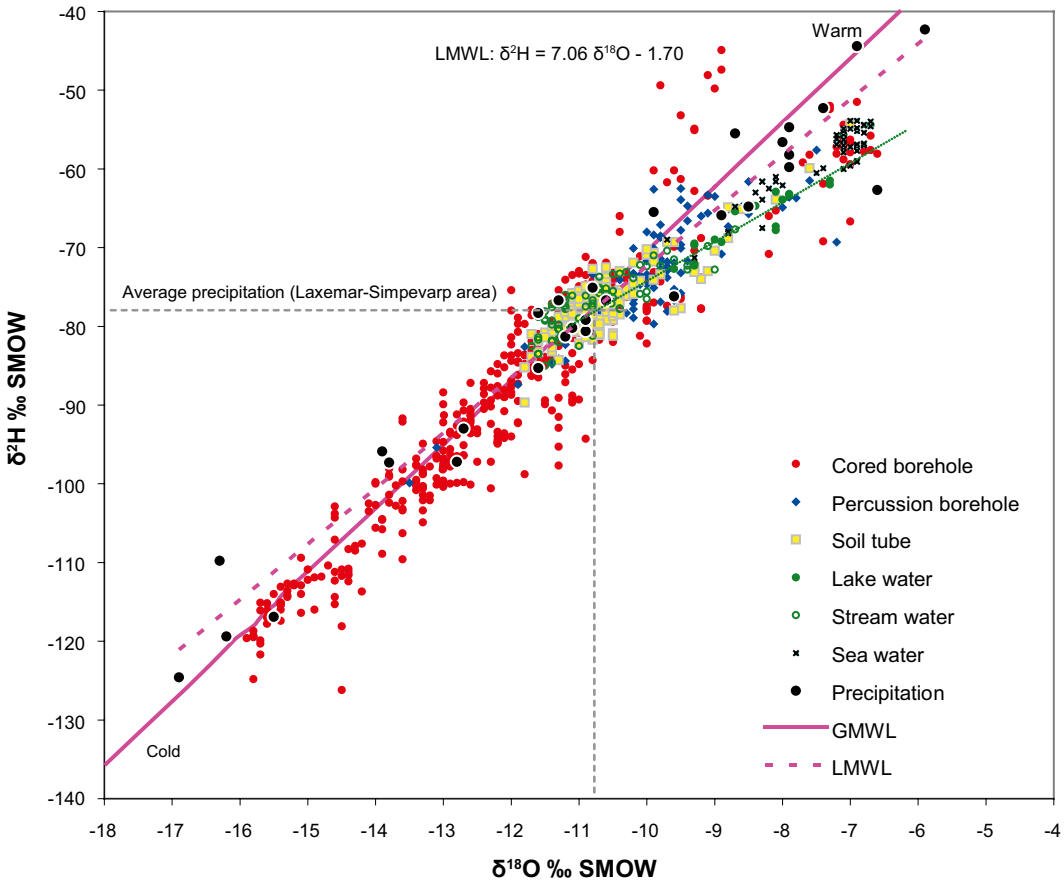


***Figure 3-11.*** *All individual observations including $^{2}H$ and $^{18}O$ measurements from the Laxemar-Simpevarp area, plotted together with the global meteoric water line, GMWL. The local meteoric water line, LMWL, based on all observations in precipitation, is also included. The average composition in precipitation is estimated from the intersection between LMWL and the evaporation trends of the lakes, which coincide with the mean composition of a cluster of soil tubes that are centred on the LMWL.*

Observations from surface waters deviate more or less from the LMWL due to fractionation by evaporation. Observations from Lake Jämsen (PL67) and Lake Frisksjön (PL65) form a trend line, probably originating from a point corresponding to the average composition of precipitation. Observations from sea water show a similar deviation due to evaporation.

The relative location along the evaporation line (based on the average composition of each lake) can be assumed to reflect the water residence time (i.e. the proportion between lake volume and catchment area). Consequently, lakes in the Laxemar-Simpevarp area plot along an evaporation line that deviates from the LMWL, whereas streams with little influence from lakes in the catchments plot close to the LMWL (Figure 3-12). Observations from the larger Lake Götemar (PL66) indicate a rather long residence time compared to the smaller lakes Jämsen (PL67) and Frisksjön (PL65).

Most soil tubes plot in a cluster centred on the LMWL, indicating that the composition of shallow groundwater reflects local average precipitation. A few soil tubes plot along the evaporation trend (e.g. S241-33, S242-16, S239-4 and S238-12), which indicates an influence of either sea water or a fresh surface water component.

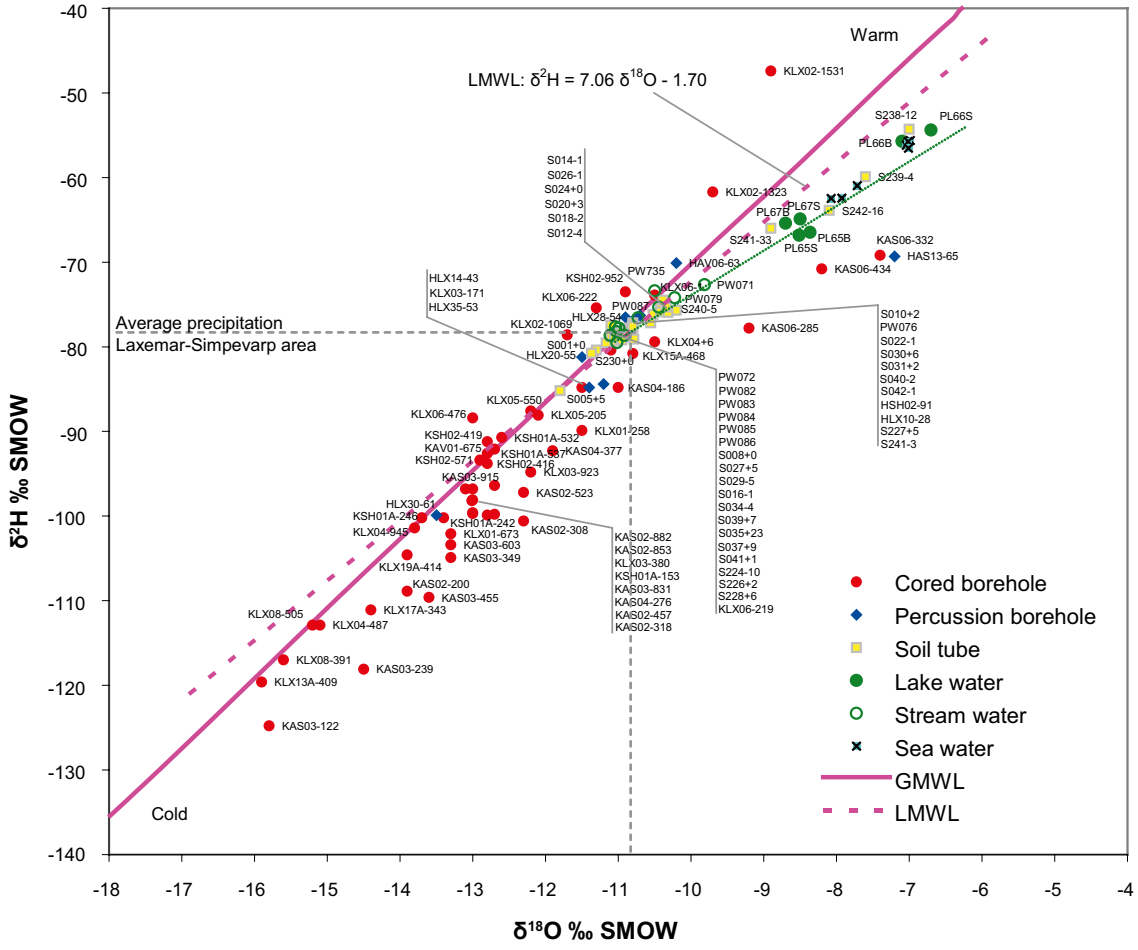


***Figure 3-12.*** *Mean values per object for $^{2}H$ and $^{18}O$, plotted together with the global and local meteoric water lines (GMWL and LMWL, respectively). Only samples from data selection C are included (cf Section 2.2.4 and 2.2.5). The green line indicates the 'evaporation line', based on mean values per lake within the Laxemar-Simpevarp area (Lake Götemar is excluded). Labels are explained in Section 2.3.11.*

Observations from the bedrock show a scattered picture, indicating a varying origin of the water found at deeper levels. Many of the bedrock samples from percussion boreholes as well as from cored boreholes plot in the lower left region of the LMWL, which probably reflects water components originating from a cold climate, e.g. glacial melt water. A few observations from the bedrock plot near the evaporation trend and may thus indicate water components of (relict) marine origin, e.g. Littorina seawater. The fact that some of the soil tubes also plot in this region of the figure indicates that these objects may also be influenced by relict marine seawater. Deviations from the meteoric water lines are further explored in Section 3.3.2.

When $\delta^{18}O$ is plotted against vertical depth the depth dependency is further revealed. Down to depths of approximately 600 metres both depleted and enriched $\delta^{18}O$ values occur. This may be interpreted as if both relict marine water (with enriched $\delta^{18}O$ similar to modern sea water) and glacial water have reached these depths in the bedrock. At greater depths, between 600 to 1,000 metres, the variation is reduced and the $\delta^{18}O$ signature corresponds to either a mixture of glacial and marine signatures or to meteoric recharge in a climate slightly colder than the present. The trend among deep saline samples below approximately 1,000 metres may, if it is not an artefact due to artificial mixing or increased salinity, represent mixing with a deep component enriched in $^{18}O$.

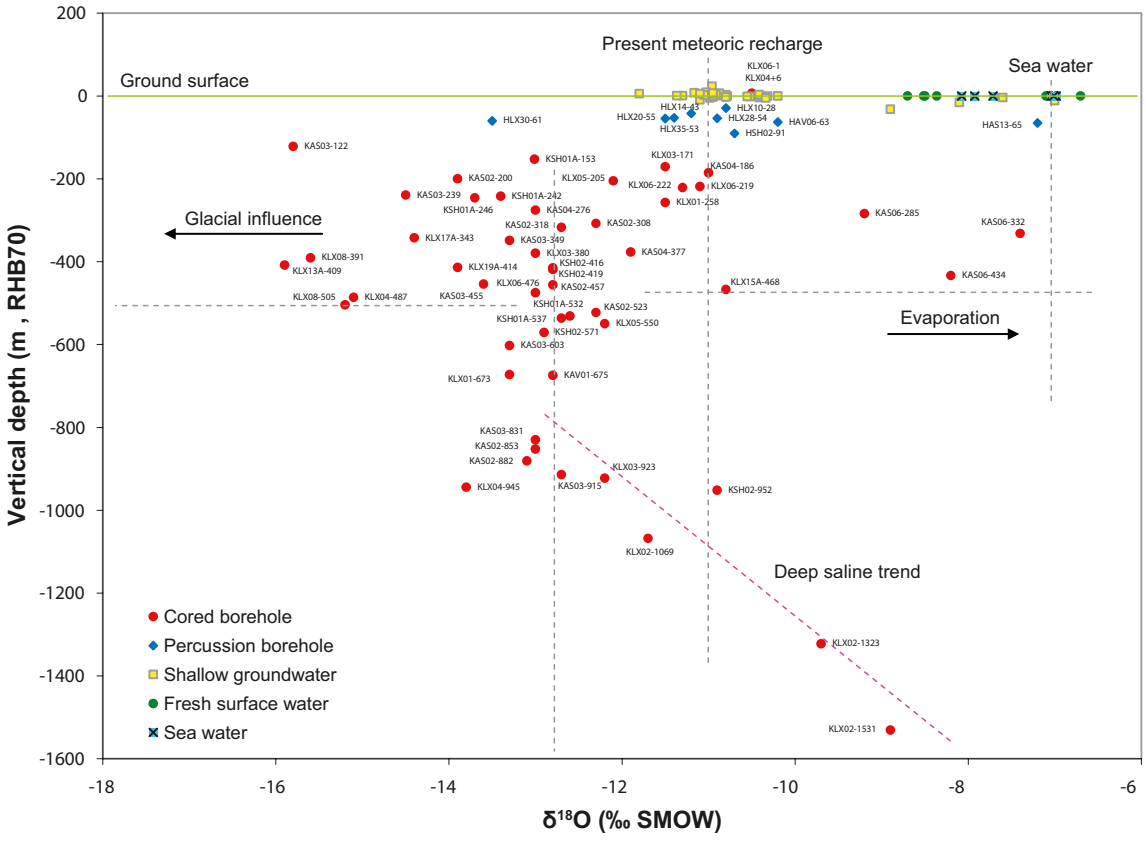


***Figure 3-13.*** *$\delta^{18}O$ against vertical depth. Only samples from data selection C are included (cf Section 2.2.4 and 2.2.5). Labels are explained in Section 2.3.11.*

### 3.3.2 The Water Origin Model

Due to the close correlation between $\delta^{2}H$ and $\delta^{18}O$, most points line up along LMWL. This means that the standard cross plot is less suitable for exploring deviations from the meteoric water lines. In order to make deviations from GMWL more visible, $^{2}H$ and $^{18}O$ may also be transformed and projected onto a coordinate system where one axis coincides with the GMWL and the other represent the perpendicular deviation from the GMWL. This type of plot enlarges the area of interest by rotating the coordinate system displayed by the blue coloured box in Figure 3-14. In this figure is also the literature value of Canadian Shield brine marked /Clark and Fritz 1997/. The transformed GMWL plot, the Water Origin Model, is shown in Figure 3-15.

The upper panel in Figure 3-15 shows mean values per object and depth based on data from the "representative" data selection C, while in the lower panel all available individual samples from data selection A are included as grey marks in the background (cf Sections 2.2.4 and 2.2.5). It should be kept in mind that the lower panel includes samples of varying quality from the bedrock potentially influenced by artificial mixing. However, the main purpose of this plot is to provide an idea of the total variability in the dataset and to support interpretations of major trends among the representative data from the bedrock.

The patterns that appear in the Water Origin Model presented in Figure 3-15 may be subject to a number of uncertainties. The spread around LMWL shown by the soil tubes in the encircled "modern meteoric cluster" may represent a rough estimate of the overall uncertainties attributed to the $^{2}H$ and $^{18}O$ measurements. Contamination by flushing water during drilling, and uncontrolled mixing due to shortcuts through fractures, will also contribute to uncertainties in the model. Adjacent objects in the plots (i.e. objects with a similar composition of $^{2}H$ and $^{18}O$) may belong to completely different water regimes, which hypothetically could be separated by a third parameter into different planes.

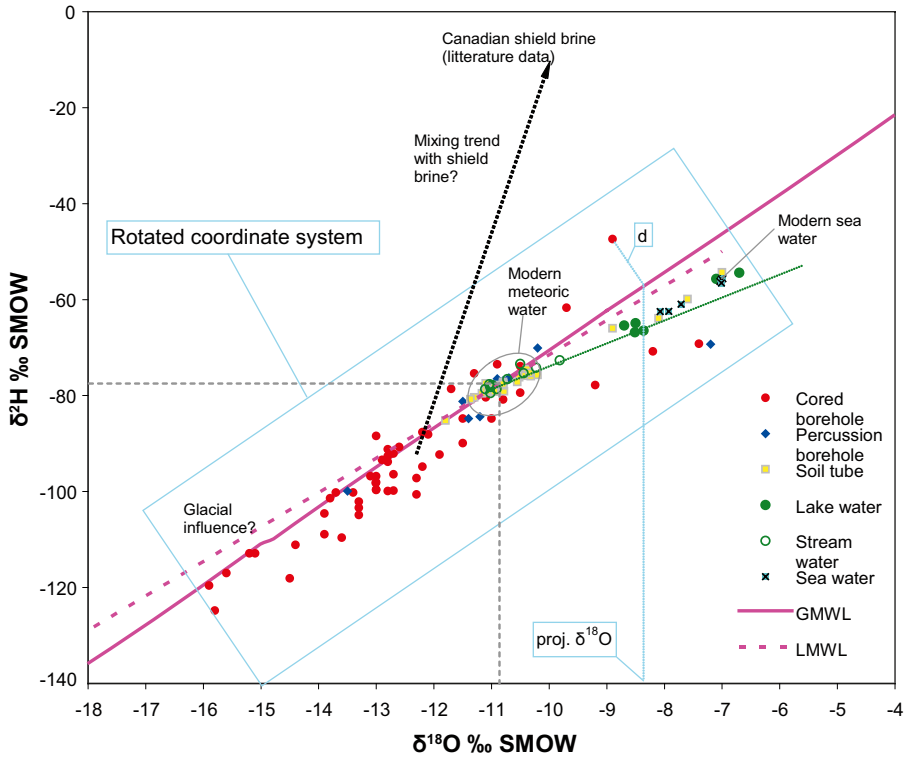


***Figure 3-14.*** *This schematic figure shows the principles behind the rotated coordinate systems used in Figure 3-15. The perpendicular deviation from GMWL is marked by a "d", and the $\delta^{18}O$-value corresponding to a point perpendicularly projected on the GMWL is marked "proj. $\delta^{18}O$". A hypothetical mixing trend towards depth, from meteoric waters to the literature value of Canadian Shield brine (-10;-10), is marked by dashed black lines.*

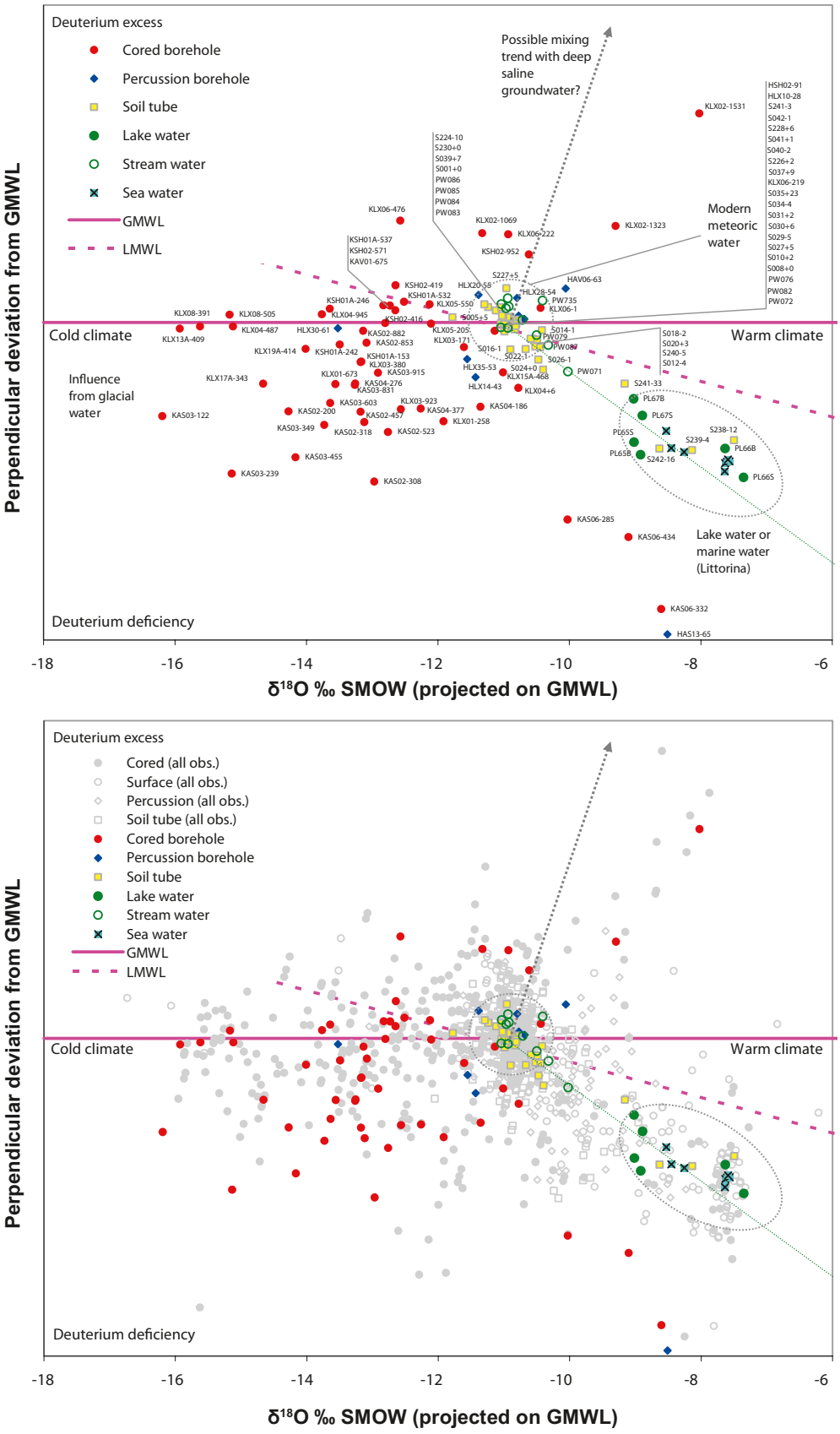


***Figure 3-15.*** *The Water Origin Model (see explanation in Figure 3-14). The upper plot is based on mean values per object and depth of selection C and the lower plot is based on individual samples of selection A (cf Sections 2.2.4 and 2.2.5).*

A few conclusions can be drawn from the patterns in Figure 3-15:

- Most shallow groundwater sampling points in the Quaternary deposits (soil tubes) exhibit a mean isotopic composition which corresponds to the yearly average of modern meteoric water. The seasonal variation in the soil tubes is small compared to the substantial variation in precipitation (cf Figure 3-11), indicating that the seasonally related fluctuations are greatly moderated at the depths of the groundwater sampling.
- Streams in the Laxemar area contain water corresponding to the meteoric composition of precipitation. The short residence time of stream water, in combination with few and small lakes in the Laxemar area, results in almost no isotopic fractionation in this water type. The discharge pattern is the area is also characterised by short peaks with intervening periods of very small discharge (cf Figure 5-11).
- Lake water and brackish water in the basins Granholmsfjärden and Borholmsfjärden, as well as in the open Baltic Sea, show a typical isotopic shift due to evaporative fractionation during the summer. The green dashed line marks this trend, where the slope probably is characteristic for the region and the relative shift along this line from the meteoric composition reflects the water residence time. Four soil tubes located below marine sediments (SSM000238, 239, 241, 242), also show an evaporation signature that indicates a marine origin of the water (modern or relict).
- There is a group of soil tubes located close the Baltic Sea (all but one on Ävrö) that show an isotopic signature indicating some influence of evaporation (SSM000012, 14, 16, 18, 20, 22, 24, 26). As there are no lakes influencing these groundwater sites, this is either a local phenomenon caused by the nearness to the large surfaces of water, or the influence of relict marine groundwater. The latter alternative is least plausible due to low ionic strength at most of these sampling sites /Tröjbom and Söderbäck 2006/ and the absence of marine ion signatures (cf Ion Source Model in Section 3.2.5).
- Most of the observations from the bedrock are shifted towards the cold (left) part of the Water Origin Model, indicating that this water was precipitated during a cold climate and probably represents glacial meltwater injected into the bedrock during the latest glaciation. The strongest glacial signatures are, with a few exceptions, present at 200–500 metres depth in the bedrock.
- At greater depths in the cored boreholes (e.g. KLX02, KLX06 and KSH02), there is a tendency for the glacial signature to be shifted above the GMWL line towards $^{2}H$ excess. This is especially evident for the deepest borehole KLX02, where the deepest samples show significant $^{2}H$ excess according to Figure 3-16. Although this picture is distorted by artificial mixing during sampling and unreliable depth information from so called “tube samplings”, there is a clear shift towards $^{2}H$ excess among several samples. One possible explanation for this pattern could be mixing with deep saline groundwater characterised by very high $^{2}H$ excess according to the hypothetical mixing trend with shield brine (cf literature value of Canadian Shield brine in Figure 3-14). This possible characteristic signature of deep saline groundwater is however not useful for detecting deep discharge in the surface system due to the theoretical dilution constraints (cf Section 4.3.1).

### 3.3.3 Detailed evaluation of two lakes in the Laxemar area

In this section, the isotopic signatures in water from two soil tubes located below lakes are explored in detail. Individual observations in the soil tubes are compared with observations from the overlying surface water, as well as with adjacent streams. The composition of modern sea water is included in all figures as a reference.

Samples from a soil tube located below Lake Frisksjön and one located very close to the shore of Lake Jämsen show rather dissimilar composition in the ratio between $^{2}H$ and $^{18}O$ (cf Figure 3-17). This probably indicates that waters found in these soil tubes have different origins. The periodical samplings in SSM000035 near Lake Jämsen show little variation, indicating rather stable conditions with little influence by the seasonal fluctuations of $^{2}H$ and $^{18}O$. There is at present only one isotope analysis available from the soil tube below Lake Frisksjön

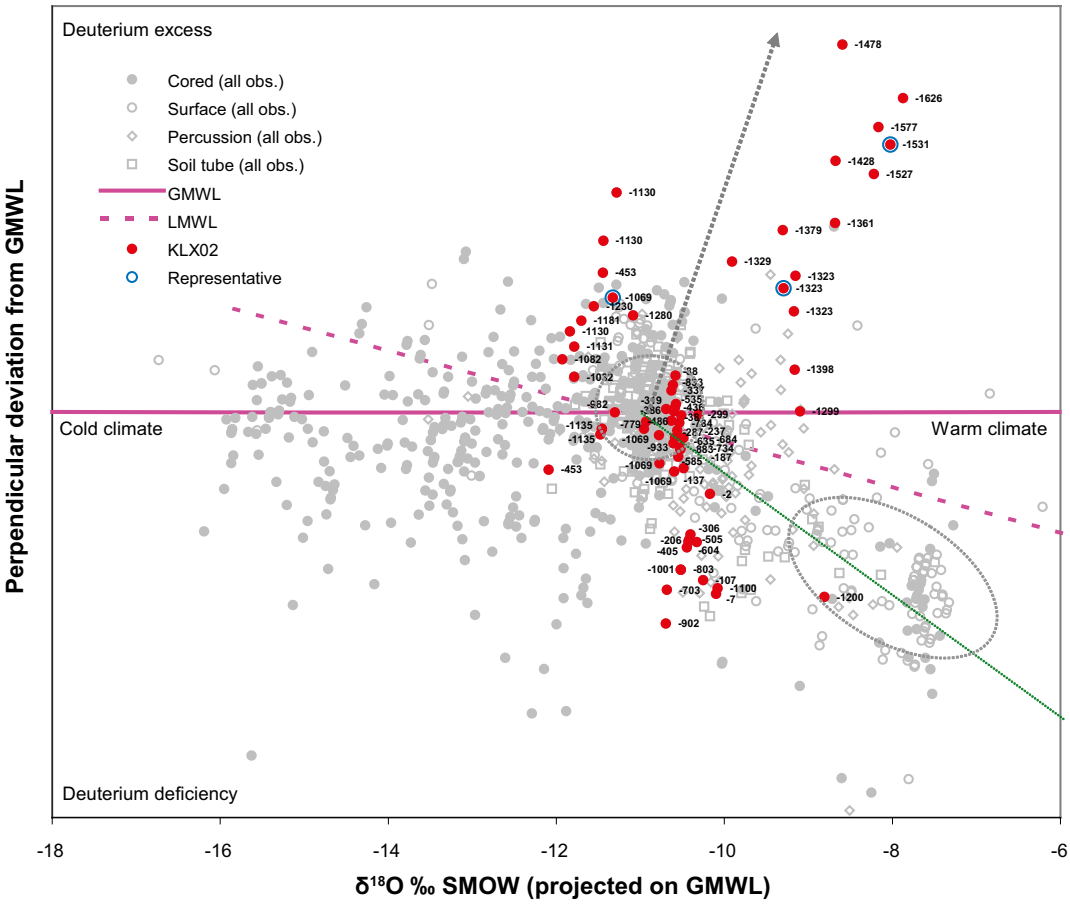


***Figure 3-16.*** *All available samples from the deep cored borehole KLX02, including the so called "tube samplings" which show less accurate depth information. The three samples that have been considered as "representative" (cf data selection C in Section 2.2.5) are encircled in blue. The figures show the vertical depth expressed in the coordinate system RHB70.*

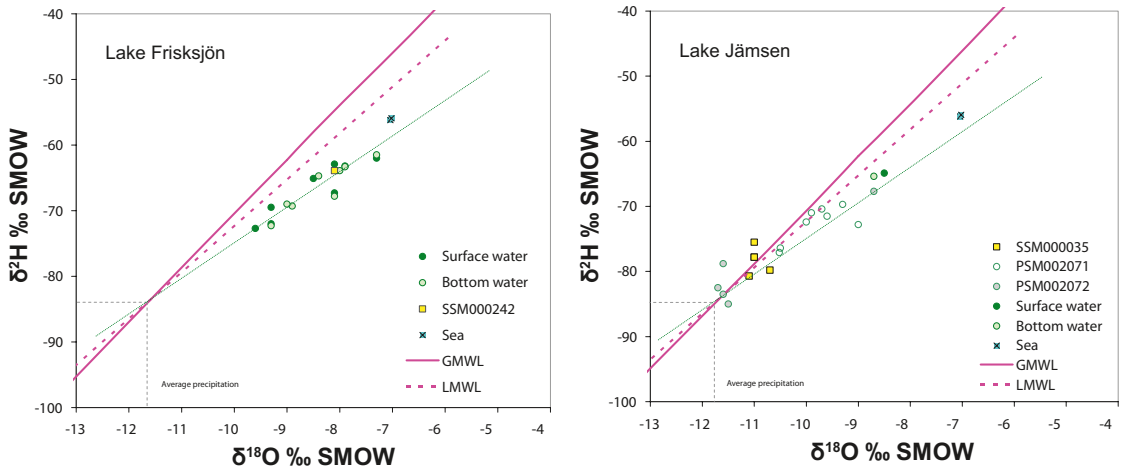


***Figure 3-17.*** *Detailed explorations of the isotopic signatures ($^{2}H$ and $^{18}O$) in lake water and soil tubes beneath Lake Frisksjön and Lake Jämsen.*

(SSM000242) and no variation could be estimated. The thick sediment overlaying the sampling depth suggests stable conditions in this tube as well, however. When evaluating these patterns it should be kept in mind that contamination by surface waters during installation of the soil tubes may influence the measurements.

The evaporation signature in lake water should be more pronounced the longer the residence time. Surface water in both lakes shows deviations from the local meteoric water line (dashed pink line), indicating fractionation due to evaporation, but the deviation is not as pronounced as for samples from the Baltic Sea. The isotopic composition in the stream site PSM002071 downstream of Lake Jämsen varies between average meteoric composition and a composition possibly influenced by evaporation similar to Lake Jämsen.

The soil tube SSM000035 shows an isotopic signature corresponding to the average composition of precipitation, indicating that meteoric discharge is the main source, and that the influence of the lake water is negligible.

The soil tube beneath Lake Frisksjön, on the other hand, shows an isotopic composition similar to the composition of the lake water, which may be an indication that the water in the soil tube originates from the lake, or alternatively is of marine origin. The latter alternative is the most probable as the ion signature according to the Ion Source Model (cf Section 3.2.5) and the absolute Cl level /Tröjbom and Söderbäck 2006/ support a marine origin of the water, rather than recharge from the lake.

## 3.4 Exploring concentration trends and mixtures

A concentration is the amount of dissolved ions (or other compounds) per unit volume (e.g. water). When either ions or water are added (or removed), the concentration is altered. The *Mixing Model* described in this section may be seen as the product of the previous models: the Ion Source Model and the Water Origin Model. The Mixing Model also complements the other models by providing information on absolute concentrations of ions, and may reveal possible mixing trends of different water types. This model was constructed using a similar methodology described for the Ion Source Model in the summary in Section 3.2.1.

### 3.4.1 Calibration of the the Mixing Model

In a procedure similar to that described for the Ion Source Model in Section 3.2, a standard principal component analysis, PCA, (cf Section 2.3.9) was applied to data selection B, but with the difference that the calibration was conducted on absolute concentrations of major elements rather than relative compositional data. The calibration dataset used contains as much data as possible from cored boreholes and percussion boreholes under the conditions of acceptable charge balance (±5%), reasonable accurate depth representation (no tube samplings included), and measurements of flushing water content. For surface water and shallow groundwater included in the calibration dataset, a larger charge balance error of ±15% had to be accepted (cf data selection B described in Sections 2.2.4 and 2.2.5). Two anomalous observations, SSM000241 and SSM000242 were excluded during the calibration phase, but are projected in all visualisations (cf discussion on uncertainties in Section 9.2 and 9.3.1).

In Figure 3-18 the PCA-model is visualised in score and loading plots (see 2.3.9 for an explanation). This plot shows data from selection B, which is used for calibration. Data from selection A, which includes individual samples, is included in the background to give an idea of the total variation in the material. The major variation (60%) is shown by the first component (PC1, vertical direction), whereas the second component (PC2, horizontal direction) reveals a weaker pattern corresponding to 21% of the total variation. The following loading plot shows to what extent different variables contribute to the two first principal components. The major difference between the observations along the vertical direction (PC1) is shown by anions as Cl and $HCO_3$, whereas the cations Mg and K constitute the largest differences in the horizontal direction (PC2).

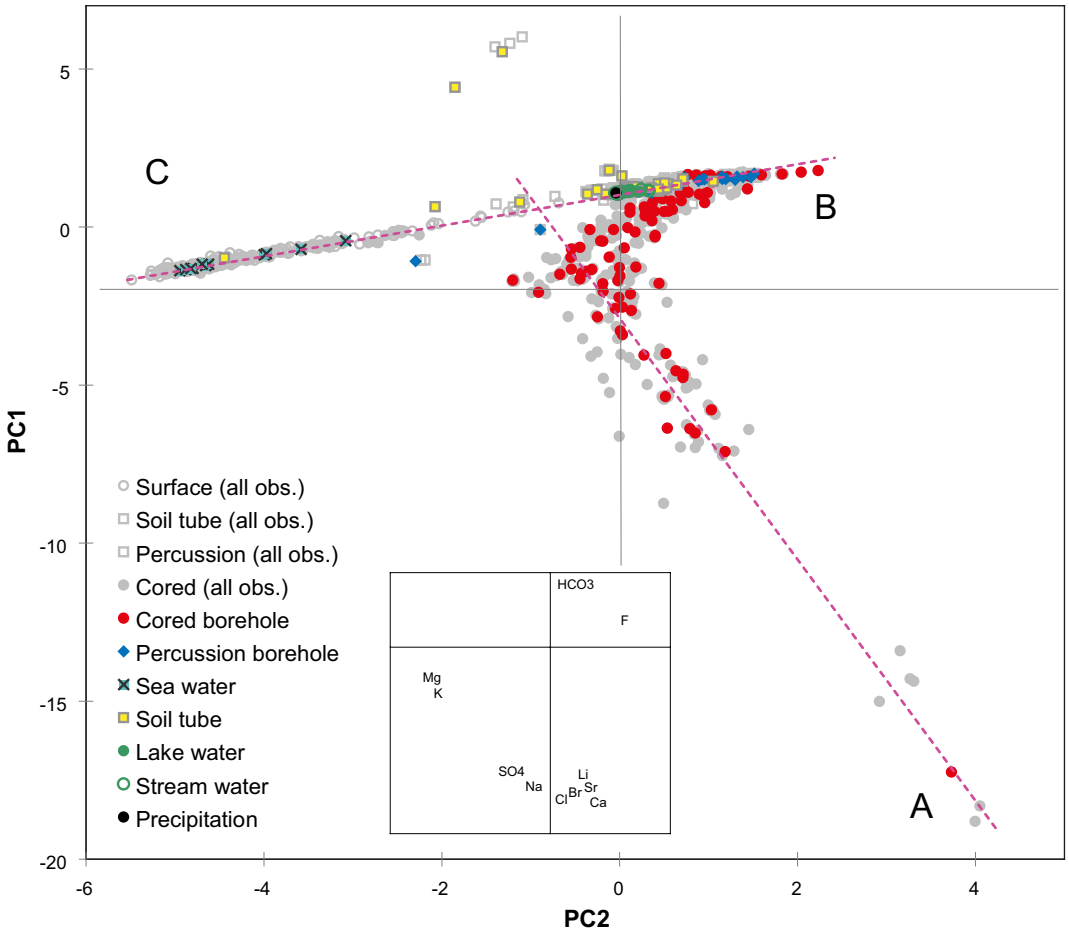


***Figure 3-18.*** *The multivariate Mixing Model reflecting the main variation patterns among concentrations of major ions (Na, K, Mg, Ca, Sr, Li, Cl, $SO_4^{2-}$, $HCO_3^-$, Br, F). This plot includes data selection B used for calibration (coloured marks) and selection A for comparison (grey marks). The first two components comprise 81% of the total variation (PC1 60% and PC2 21%). The major panel is the score plot and the inset is the loading plot (cf Section 2.3.9). Dashed pink lines show hypothetical mixing trends: A marks the mixing trend towards deep saline groundwater and the C-B line connects modern sea water (C) and dilute groundwaters of the surface system (B).*

### 3.4.2 Comparisons between the the Mixing Model and the M3-model

Visualisations based on the Mixing Model may be similar to the outcome from the multivariate M3 model /Gómez et al. 2006/, as the models share data and are based on similar statistical techniques. There are, however, important differences: while the Mixing Model is based exclusively on concentrations, the M3 model also includes isotope data reflecting the origin of water, which may lead to a different appearance of the 2D visualisations depending on the rotation of the principal components in hyperspace and which components are selected.

In Figure 3-20, the Mixing Model can be compared to the end-members identified by the M3 methodology /Laaksoharhju et al. 1999/ and /Gómez et al. 2006/. The marine end-member Littorina Sea water plots on the marine mixing line MX2. The deep saline end-member plots in the extension of the mixing line MX1. End-members of weaker ionic strength, i.e. altered meteoric groundwater and glacial water, plot in the "weak corner", together with most waters from the surface system (soil tubes and fresh surface water).

The relative positions of the end-members from the M3 model and the patterns of the Mixing Model coincide, which is expected as they are based on the same data. The introduction of the M3 end-members can be seen primarily as an orientation of the relationship between the two models.

### 3.4.3 Projections onto the Mixing Model

Different data may be projected onto the calibrated Mixing Model. In Figure 3-19, the representative data selection C (cf Sections 2.2.4 and 2.2.5) has been projected. This expert selection – which includes only samples with reasonably correct depth information, low contamination by flushing water and stable hydrochemistry over time – is thought to provide as unbiased a picture as possible of the hydrochemical conditions in the bedrock. Surface water data (lake, stream and shallow groundwater) are identical in the both the calibration and representative datasets (cf 2.2.4).

The main pattern of the calibration dataset in Figure 3-18 is preserved in Figure 3-19, and the most obvious difference is the total number of objects and depths included in the plots; several percussion boreholes as well as many levels from cored boreholes are excluded in the latter plot. Samples from groundwater in the bedrock in Figure 3-19 are less influenced by artificial mixing and are probably more representative of the depth included in the label of each observation (cf description of labels in Section 2.3.11).

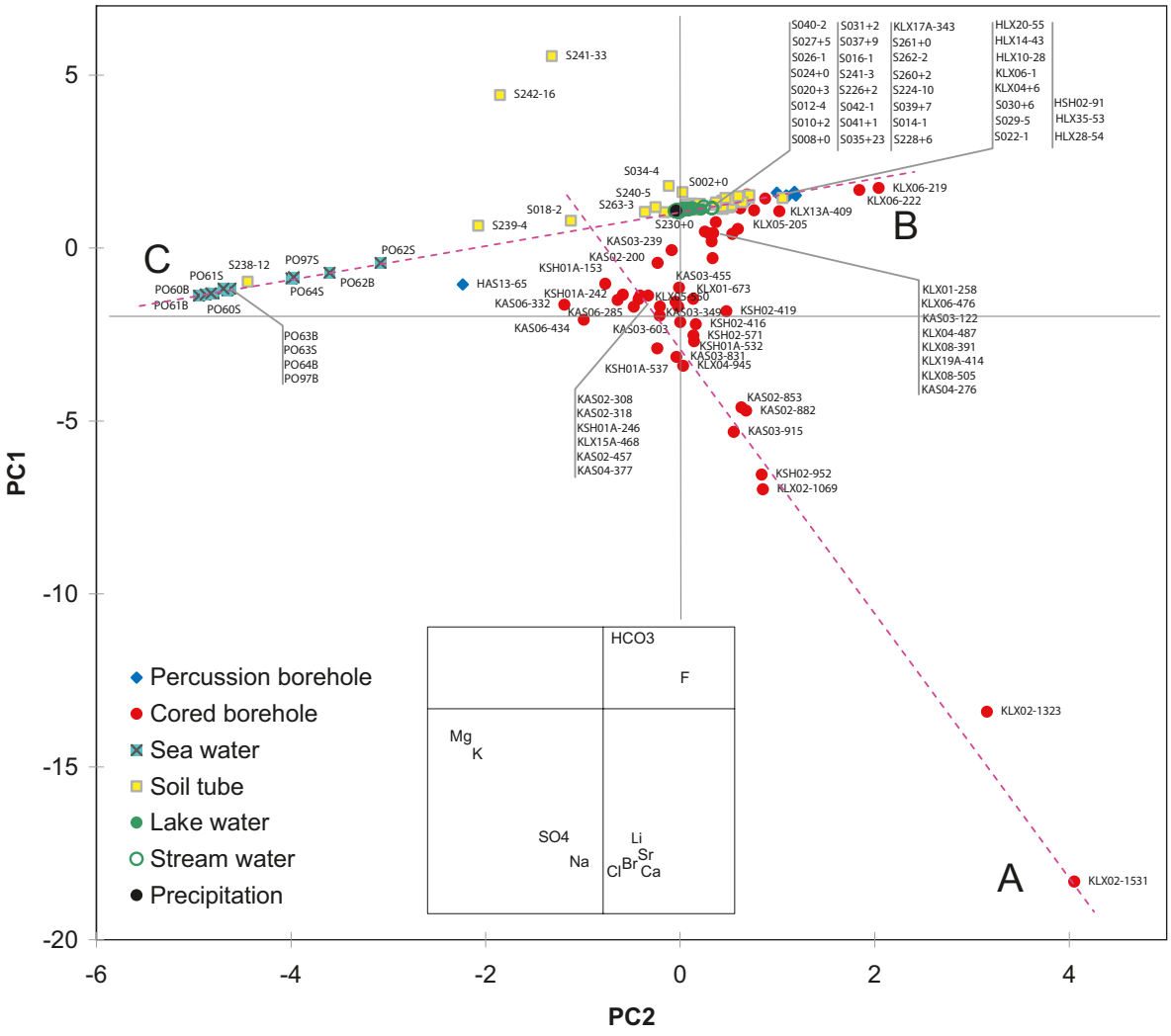


***Figure 3-19.*** *The multivariate Mixing Model reflecting the main variation patterns among concentrations of major elements (Na, K, Mg, Ca, Sr, Li, Cl, $SO_4^{2-}$, $HCO_3^-$, Br, F). This plot shows the projection of representative data selection C. The first two components comprise 81% of the total variation (PC1 60% and PC2 21%). The major panel is the score plot and the inset is the loading plot (cf Section 2.3.9). Dashed pink lines show hypothetical mixing trends. See Section 2.3.11 for a description of labels.*

### 3.4.4 Interpretation of the Mixing Model

An interpretation of the Mixing Model is shown in Figure 3-20. Hypothetical water types and theoretical end-members, also identified in the previous visualisations, are encircled in the figure, along with mixing lines showing hypothetical mixing scenarios. Patterns in the model may also reflect processes which may have altered the water composition, such as ion exchange.

The first component in the Mixing Model (PC1, vertical direction in Figure 3-20) reflects the contrast between Cl and $HCO_3^-$ according to the inset loading plot (cf explanation in Section 2.3.9). Several other elements, e.g. $SO_4^{2-}$, Na, Br, Li, Sr, and Ca, covary with Cl along this gradient, which range from nearly Cl-free, $HCO_3^-$-dominated surface waters, to the Cl-rich deep saline groundwater influenced by shield brine.

The second component (PC2, horizontal direction in Figure 3-20) distinguishes groundwater of marine origin from water originating from the surface system as well as from deeper groundwater types. The strongest influence on this component is shown by marine ions as Mg, K as well as F of terrestrial origin.

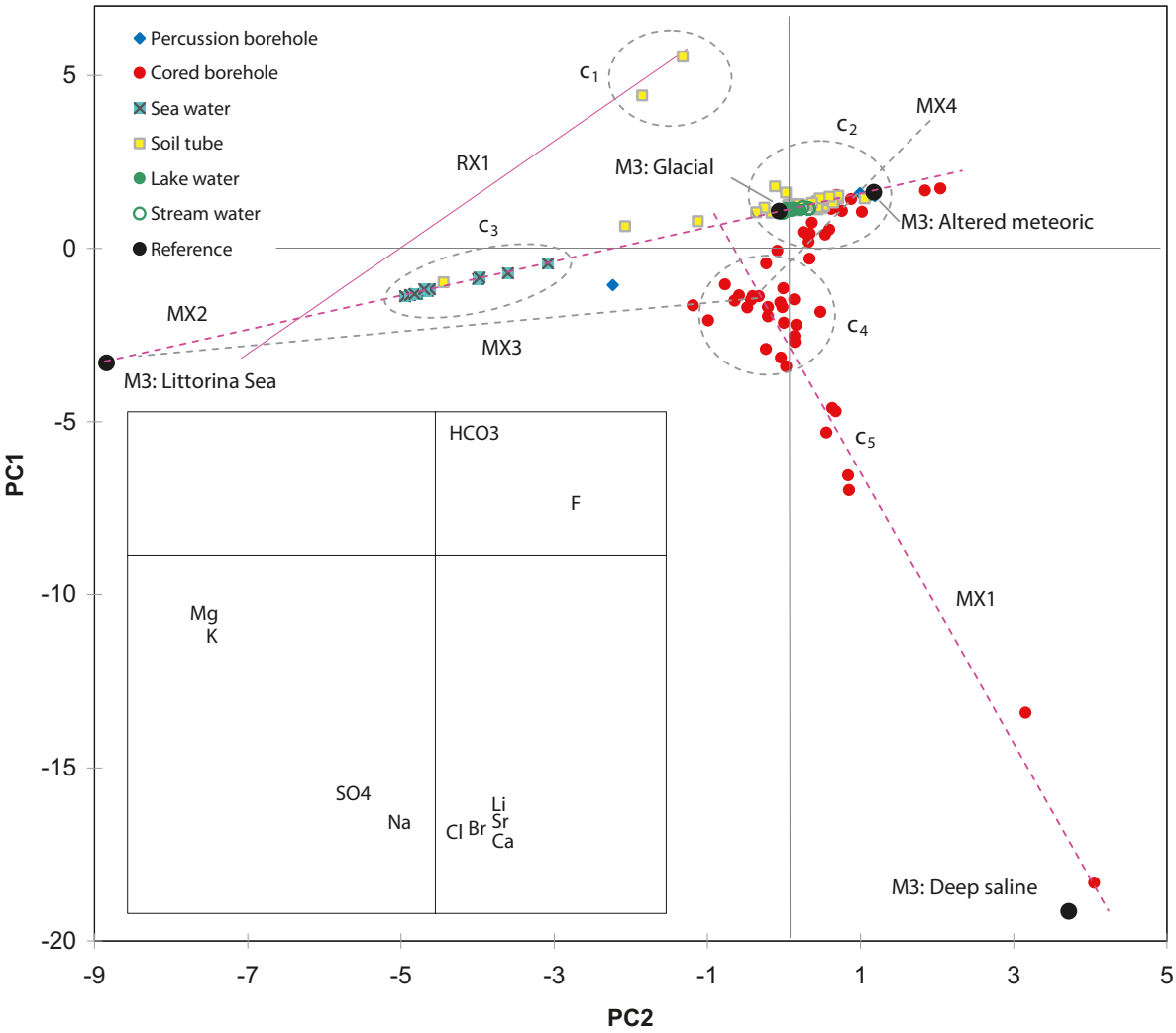


***Figure 3-20.*** *Interpretation of the Mixing Model with representative data selection C included. Hypothetical mixing trends discussed in the text are shown as dashed lines and denoted MX1-MX4. $c_1$ to $c_5$ marks clusters of observations that exhibit similar hydrochemistry. Black dots show the location of the M3 end-members.*

In Figure 3-20, a few hypothetical mixing lines can be distinguished. If mixing is assumed to be the main process forming the hydrochemistry, these mixing lines may reflect different mixing proportions of different water types. Reactions, such as cation exchange, may also affect the composition of water, but Ca versus Na exchange is probably not distinguished in the Mixing Model, as these elements have similar loadings (cf Section 2.3.9) with respect to the principal components. These hypothetical mixing lines, along with a few distinct clusters of observations, are discussed in the bulleted list below:

- MX1 is a hypothetical line connecting deep saline observations influenced by shield brine with the cluster $c_4$, which represents observations from moderate depths in cored boreholes (most observations lie in the range of 400–700 metres vertical depth). There are no observations along the upper left parts of $c_4$ indicating that groundwater at depths above 400 metres has been significantly affected by processes or other mixing events (e.g. glacial flushing, density intrusion or influence from regional recharge/discharge).
- The mixing line MX2 indicates a gradient ranging from fresh surface waters to present sea water in the Laxemar-Simpevarp area. The spread along this trend shown by the sea water sites $c_3$ represents different degrees of dilution by fresh water in the more or less confined brackish basins Granholmsfjärden and Borholmsfjärden. The extension of this *marine trend* plots more saline sea waters, e.g. Littorina. All objects from the surface system (lakes, streams and shallow groundwater) plot along this line, indicating that marine ions are the predominant ion source in the surface system.
- MX3 is a hypothetical mixing line connecting the $c_4$ cluster with the theoretical composition of Littorina sea water. If significant portions of Littorina Sea water were mixed with groundwater corresponding to the composition at $c_4$ in the bedrock these observations should line up along MX3. There are however only a few observations associated with this line, indicating that the marine influences are usually small in the Laxemar-Simpevarp area. The shift of cluster $c_4$ towards the "marine corner", from a hypothetical location on a straight line between $c_2$ and the M3 end-member *deep saline groundwater*, can be explained as a general weak marine influence affecting most observations in the bedrock, perhaps in combination with water-rock interactions corresponding to the net reaction of Ca versus Na ion exchange. As discussed in /Laaksoharju (ed) 2008/, excess of Mg in deeper groundwaters could also be indicating the presence of Littorina remnants in the form of previously exchanged Mg now released back into the groundwater.
- MX4 connects the cluster $c_4$ with the dilute groundwater present in the upper parts of the bedrock, which corresponds to the M3 end-member *altered meteoric groundwater*. Most of the observations that plot along this trend represent groundwater at approximately 200–400 metres depth.
- This cluster $c_2$ contains most fresh water samples from lakes, streams, shallow groundwater and the bedrock. Most percussion boreholes, which represent depths of 100–200 metres, also plot in this region.
- The cluster $c_1$ contain two anomalous observations of shallow groundwater, SSM000241 and SSM000242, which are located in till beneath sea and lake sediments (cf Section 7.2). The Cl concentrations in these soil tubes are almost on a level with the Littorina saline maximum, but the anomalously high $HCO_3^-$ concentrations (about 5,000 $mgL^{-1}$) distort the classification in the Mixing Model. A possible source of $HCO_3^-$ is probably degradation of organic matter, perhaps in combination with calcite dissolution, and if $HCO_3^-$ is removed, the location of SSM000241 moves in the Mixing Model along scenario RX1 towards a point between Littorina and modern sea water.

## 3.5 Age dating and residence time

Groundwater residence time can be estimated from the activity and decay of several radioactive isotopes. Depending on the half-life of the isotope, different timescales are revealed. Examples of radioactive isotopes used for groundwater dating are $^{3}H$, $^{14}C$ and $^{36}Cl$, with half-lives of 12.4, 5,730, and 301,000 years, respectively /Clark and Fritz 1997/.

Groundwater residence time estimates based on $^{3}H$ and $^{14}C$ are problematical due to the difficulties in specifying initial conditions and quantifying the key processes. The abundance of these isotopes in the atmosphere during the fifties and sixties was heavily influenced by nuclear bomb testing, and maximum activities during this period increased by several orders of magnitude compared to normal atmospheric activity. Dilution of $^{14}C$ by $^{14}C$-free carbon derived from calcite dissolution may lead to an overestimation of the groundwater residence time if all dissolved carbon is presumed to originate from the primordial groundwater. Other processes and sources may also complicate $^{14}C$ dating by affecting $^{14}C$ activity, for example matrix diffusion, sulphate reduction, incorporation of geogenic $CO_2$ and methanogenesis /Clark and Fritz 1997/. There is also evidence based on dendrochronological age and U/Th age that $^{14}C$ activity has declined from as much as 140–160 pmC 35,000 years ago to the pre-modern value of about 100 pmC according to /Clark and Fritz 1997/ and references therein. If the initial $^{14}C$ activity is underestimated, the estimated carbon age is also underestimated.

The many unknown factors may consequently lead to many possible interpretations of the observed patterns, and it should also be kept in mind that estimates of groundwater residence time based on $^{14}C$ reflect the age of the dissolved carbon rather than the actual groundwater residence time, whereas estimations based on $^{3}H$ reflect the age of water. Figure 3-21, where $^{3}H$ is plotted versus $^{14}C$, is a clear illustration of the difficulties associated with dating using these isotopes: despite the very different timescales represented by these parameters, where $^{3}H$ refers to years and $^{14}C$ to thousands of years, a quick glance may mistakenly reveal a linear relationship. This pattern probably reflects mixing of different sources of carbon, where artificial mixing during drilling and sampling, as well as calcite dissolution, may play important roles.

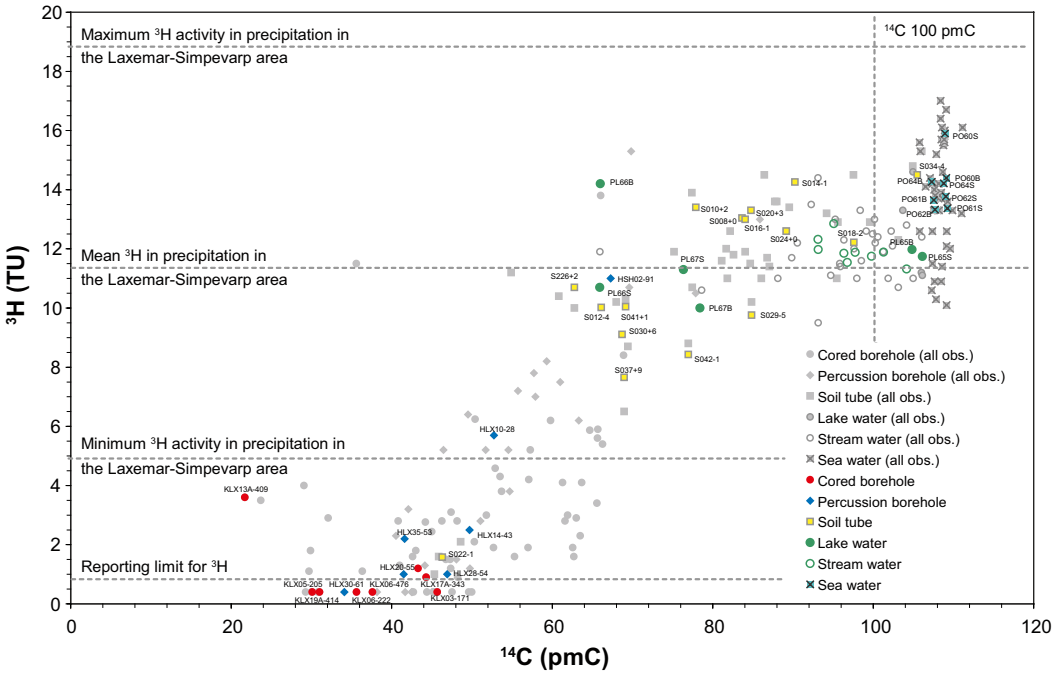


***Figure 3-21.*** *Activities of $^{3}H$ versus $^{14}C$. This picture most of all illustrates the difficulties associated with dating with these isotopes, as the axes represent very different timescales ($^{3}H$ years and $^{14}C$ thousands of years). Coloured marks represent the representative data selection C, while grey marks represent selection A (cf Sections 2.2.4 and 2.2.5 ).*

The varying $^{3}H$-activities observed in many shallow objects may also be an indication of contamination, a complicating fact that must be kept in mind when $^{3}H$ and $^{14}C$ data are interpreted. Nuclear power plants have been known to emit both $^{3}H$ and $^{14}C$ to the surroundings /Clark and Fitz 1997/. The generally higher $^{3}H$ activity measured in sea water from the Laxemar-Simpevarp area compared with the range measured in precipitation may be an indication of emissions from the power plant through cooling water. $^{3}H$ activities up to 100 TU have also been reported in the cooling water outlet from the power plants in Forsmark (A-C Nilsson, pers. comm.).

However, most observations from fresh surface water (lake water, stream water and shallow groundwater) show activities close to the regional background, probably indicating that emissions from the power plant only make a minor contribution to the activities measured in the surface system. When $^{3}H$ measurements in precipitation from the Laxemar-Simpevarp area, as well as from the Forsmark area, are compared to reference measurements from Sjötorp in the central parts of southern Sweden (Figure 3-22), there does not appear to be any significant difference between these stations: the $^{3}H$ activity at the reference station is even higher during the short period where parallel measurements are available.

The tropospheric $CO_2$ background of $^{14}C$ was about 110 pmC around year 2000 (Jeffrey Turner, pers. comm., originally from Cook et al. 2005), which is in accordance with the level measured in sea water in the Laxemar-Simpevarp area. The median $^{14}C$ activity in fresh surface water in the Laxemar-Simpevarp area of 98 pmC during 2003–2007 indicates that there is a significant supply of old carbon in the surface system, originating either from decomposition of peat or from dissolution of calcite (cf Section 4.1.5).

Bearing all these reservations and difficulties in mind, $^{3}H$ and $^{14}C$ are discussed in the following sections in relation to groundwater residence times.

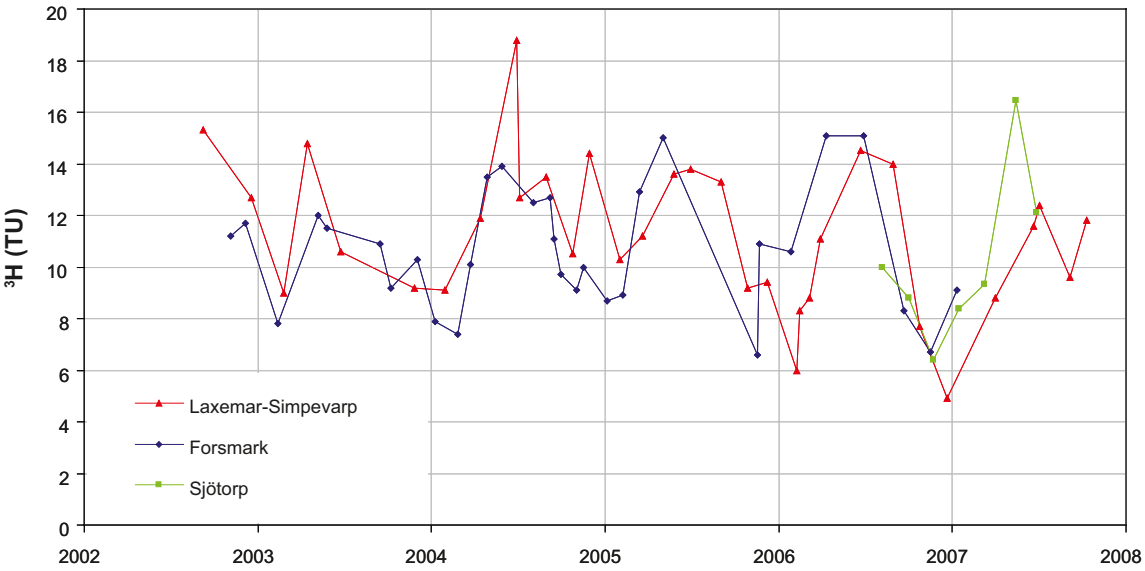


***Figure 3-22.*** *$^{3}H$ activities in precipitation from the Laxemar-Simpevarp area compared with the Forsmark area and the reference area of Sjötorp located in central southern Sweden (Västergötland), at least 200 km from the nearest nuclear power plant.*

### 3.5.1 Age estimations by $^3H$ activity

As a consequence of the half-life of $^3H$ (about 12.4 years) and the detection limit of 0.8 TU (tritium unit), the maximum timespan estimated by decay of natural $^3H$ levels (about 12 TU) is about 50 years. Since the "bomb-peak" is at year 1962, quantitative estimates of groundwater residence time are precluded and only qualitative interpretations can be made, for example as proposed by /Clark and Fritz 1997/ in Table 3-1. This classification may, however, be ambiguous as there are many theoretical combinations of modern, sub-modern and recharge from the sixties that may result in $^3H$ activities in the range between the reporting limit of 0.8 TU and the modern recharge of about 12 TU. $^3H$ is mainly suitable for discriminating between modern and sub-modern groundwater /Laaksoharju (ed) 2008/.

From Figure 3-21 and Figure 3-22 it can be concluded that most of the observations from fresh waters in the surface system show $^3H$ activities between 8 to 15 TU, which reflects the modern origin of these water types. This range is also centred on the average activity measured in precipitation (about 11 TU in the Laxemar-Simpevarp area). Observations in sea water show generally higher $^3H$ activities, ranging between 10 and 18 TU, which probably reflects influence from the nuclear power plant nearby (cf previous section). According to the classification scheme in Table 3-1 only three objects from the surface system contain groundwater of sub-modern origin: SSM000022, SSM000241 and SSM000242 (cf statistical compilation in /Tröjbom and Söderbäck 2006/).

Most deep groundwater samples from cored boreholes should be practically $^3H$-free due to the long residence times normal at great depths in the bedrock. However, $^3H$ data from the bedrock (representative data selection C, cf Section 2.2.5) indicate the influence of modern $^3H$ activities even at great depths according to Figure 3-23. Artificial mixing could explain some of these high values, but the use of reporting limits other than 0.8 TU probably explains most values that line up at 4 and 8 TU, according to the red arrows (these values have probably erroneously not been marked as below the reporting limit in the Sicada database). If the deep samples marked $B_1$ and $B_2$ are excluded, most samples from the bedrock represent groundwater of sub-modern origin.

At shallower levels in the bedrock, represented by percussion boreholes extending to a depth of approximately 100–200 metres, a mixture of sub-modern and modern $^3H$-activities prevail, which may indicate the influence of modern meteoric recharge and may possibly be an indication of relatively short residence times. These conditions may not represent actual conditions in the bedrock at these depths due to disturbances by pumping tests and extensive tapping of flushing water during drilling of cored boreholes.

**Table 3-1. Qualitative estimations of groundwater residence time based on $^3H$ activities. From /Clark and Fritz 1997/. It should be noted that these interpretations could be ambiguous as there are many theoretical combinations of modern, sub-modern and recharge from the sixties that may result in $^3H$ activities in the range between 0.8 TU and 15 TU. Furthermore, activities measured in the Laxemar-Simpevarp area during 2002 to 2007 have also decreasad since the compilation of this table.**

| $^3H$ activity | Estimated groundwater residence time |
|---|---|
| <0.8 TU | Sub-modern – recharged prior to 1952 |
| 0.8 to ~4 | Mixture between sub-modern and recent recharge |
| 5 to 15 | Modern (<5 to 10 yr) |
| 15 to 30 | Some "bomb" $^3H$ present (or contamination from nuclear power plants) |
| >30 | Considerable component of recharge from 1960s or 1970s |

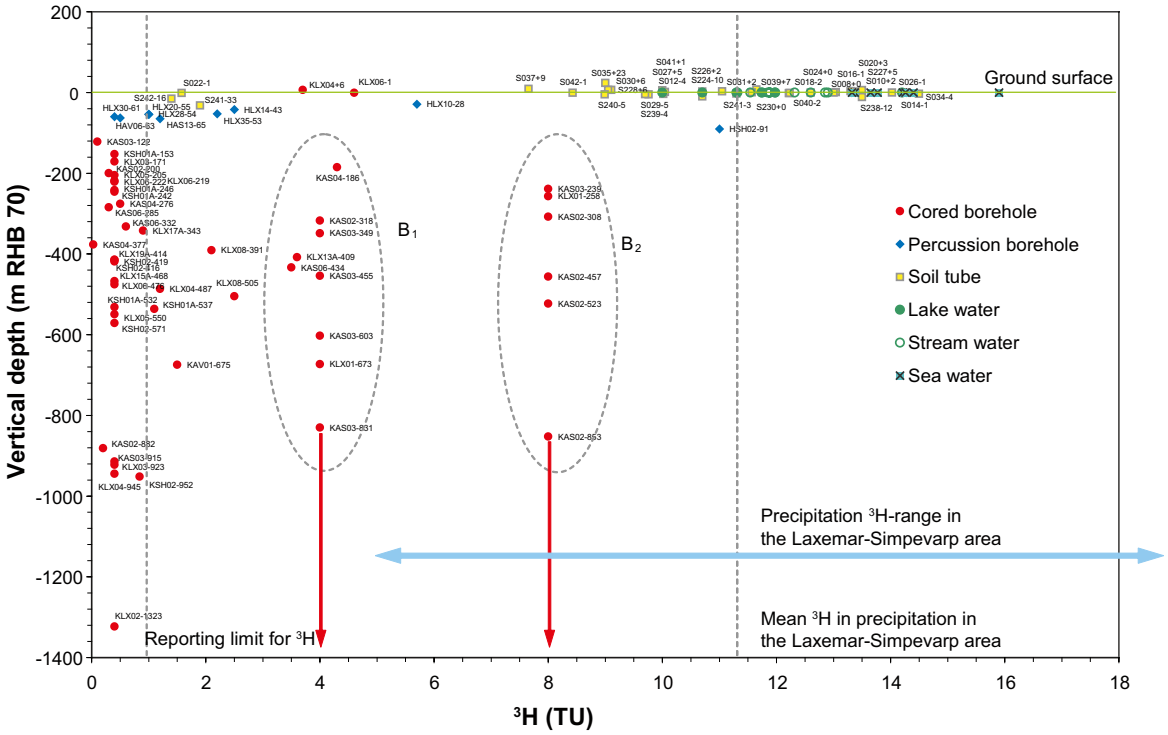


***Figure 3-23.*** *$^{3}H$ activities at different vertical depths in the bedrock and the surface system. This plot includes only data from the representative data selection C (cf Sections 2.2.4 and 2.2.5). The location of observations encircled by $B_1$ and $B_2$ is probably an artefact due to the use of reporting limits other than 0.8 TU, as indicated by the red arrows.*

### 3.5.2 Age estimations by $^{14}C$ activity

Estimates based on $^{14}C$ activity reflect the age of dissolved carbon rather than the actual residence time of the groundwater. Besides the radioactive decay that is used to calculate the elapsed time, several factors may influence the measured $^{14}C$ activities and therefore limit the possibilities making an accurate estimation, for example uncertain initial $^{14}C$ activities and processes influencing the carbon pool, e.g. calcite dissolution (see Section 3.5 for a discussion about uncertainties)

When all objects with $^{13}C$ and $^{14}C$ measurements from the Laxemar-Simpevarp area are plotted in the upper panel of Figure 3-24, few trends are revealed as most samples except from sea water form an extended horizontal cluster. Coloured marks represent mean values of the "representative" data selection C, whereas grey marks represent all individual samples available in data selection A (cf Sections 2.2.4 and 2.2.5). In the lower panel of Figure 3-24 only data from selection C is shown, along with colour coded $^{3}H$ data.

Supportive, generic data are shown by dashed grey lines. Both the $^{14}C$ activity and the $\delta^{13}C$ isotope ratio are assumed to be zero in marine limestone (calcite). $\delta^{13}C$ in air is –7 ‰ PDB, and $\delta^{13}C$ in soil DIC derived from biogenic $CO_2$ (–23 ‰ PDB), is –18.5 ‰ PDB at pH 6.5, and –22 ‰ PDB at pH 5.7 /Clark and Fritz 1997/. In Section 4.1.5 this figure is further interpreted as regards the origin of carbon.

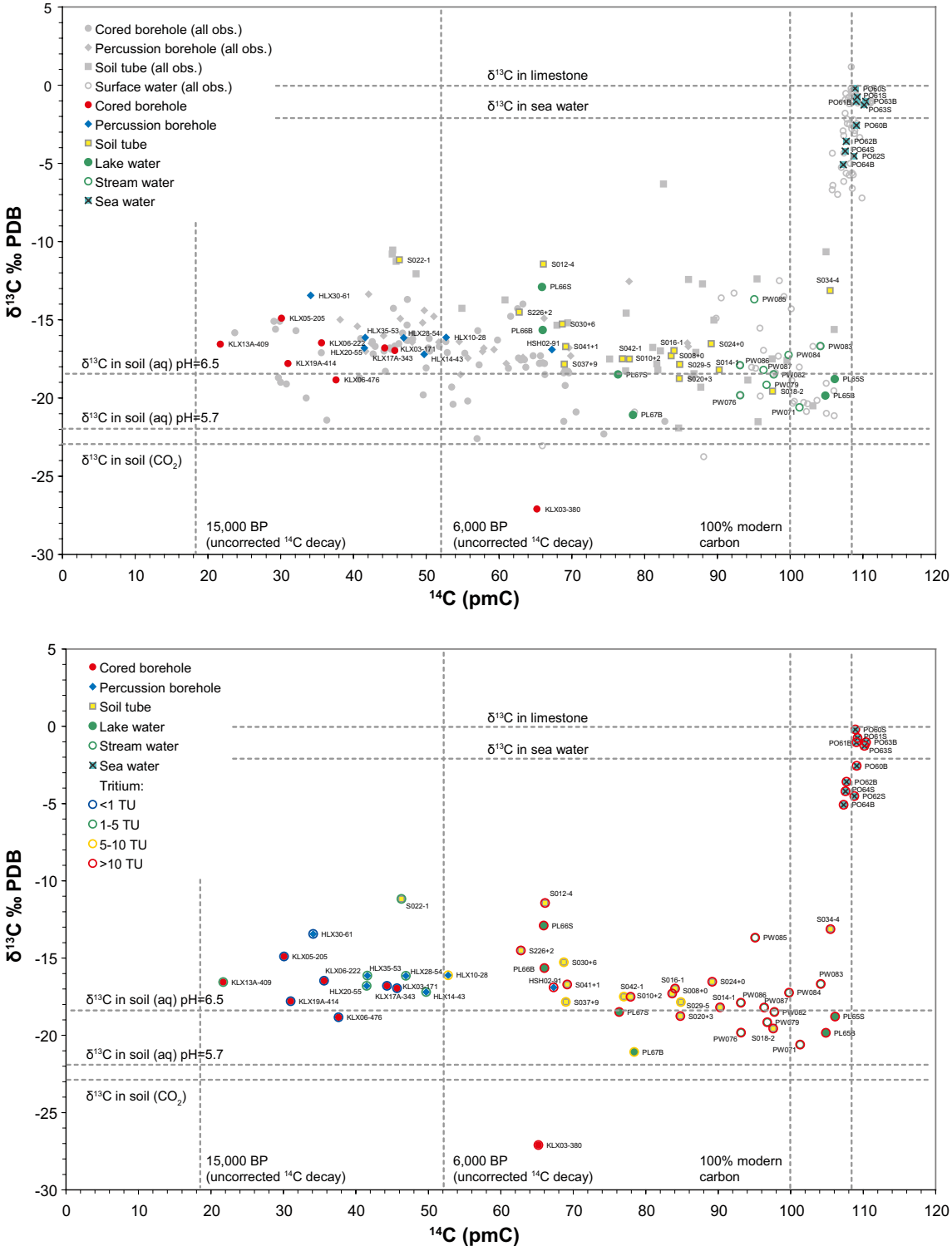


***Figure 3-24.*** *Cross-plots of $\delta^{13}C$ isotope ratio versus $^{14}C$ activity. The upper panel includes observations from both data selections C and X. The matching plot in the lower panel, which is based only on data selection C, is complemented with $^{3}H$ activities shown by a coloured circle ("The age model"). Orange lines are graphical representations of the $^{13}C$ correction models and grey lines represent supportive data. For an explanation of labels, symbols and lines, see Sections 2.3.11. and 2.3.12.*

Conclusions from patterns identified in Figure 3-24 are summarised in the bulleted list below (see further conclusions in Section 4.1.5 dealing with the origin of carbon):

- Most observations from the Laxemar-Simpevarp area form a cluster centred on the $\delta^{13}C$ isotope ratio derived when biogenic $CO_2$ is dissolved at pH 6.5, which is a typical pH value measured in streams and shallow groundwater in the area /Tröjbom and Söderbäck 2006/. This pattern may be interpreted as if biogenic $CO_2$ of different age is a major source of dissolved carbon in the surface system, reflected by $^{14}C$ activities lower than the tropospheric background. $^{14}C$ activities in surface water and shallow groundwater show carbon ages ranging from modern activities to activities corresponding to an uncorrected carbon age up to 2,000–3,000 years. This estimation reflects the mean age of carbon and could not be equated with water residence time in surface water and shallow groundwater (cf origin of carbon in Section 4.1.4).
- Alternatively, low $^{14}C$ activities in the surface system is a result of dilution of zero-activity carbon derived from calcite dissolution. If the calcite present in the regolith is of marine origin ($\delta^{13}C$ = 0‰ PDB, $^{14}C$ = 0 pmC) there should be a simultaneous change in both isotopes if there is a significant carbon input from calcite dissolution. According to Figure 3-24, there is little general correlation between the carbon isotopes, which could be interpreted as if $^{14}C$ dilution effects of calcite of marine origin probably are of less importance. The content of calcite in the regolith is also generally low in the Laxemar-Simpevarp area compared to e.g. the Forsmark area (cf Section 4.1.4). An implication of this interpretation is that the uncorrected carbon age in the surface system probably reflects the biogenic carbon age relatively well. On the other hand, if the calcites in the regolith do not originate from a marine environment, dated biogenic carbon could not be distinguished from carbon derived from calcite dissolution and the biogenic carbon age is likely overestimated.
- Two soil tubes located on Ävrö, SSM000012 and SSM000022, show deviations from the general $\delta^{13}C$ isotope ratio, which together with the lowered $^{14}C$ activity could be explained by calcite dissolution. In the latter soil tube, this shift can additionally be explained by $^{14}C$ decay, and consequently, may indicate an elevated carbon age corresponding to a few thousand years. The $^{3}H$ activity in SSM000022 also indicates influence of sub-modern water.
- At greater depth in the bedrock, uncorrected carbon ages range between 6,000 to 13,000 years among the few samples available from a depth of 50–400 metres. The lack of measurements from greater depths is a consequence of the difficulties in determining the $^{14}C$ activity at low concentrations of dissolved carbon. If biogenic carbon is the main source in the bedrock ($\delta^{13}C$ coincide with the signature of biogenic carbon in the surface system), these carbon age estimates indicate that the groundwater residence time may be several thousand years in the upper parts of the bedrock, and 13,000 thousand years at 400 metres depth. If non-marine calcites contribute with zero-activity carbon with a $\delta^{13}C$ signature similar to the biogenic signature in the surface system, these biogenic carbon ages is probably overestimated and the groundwater residence time may be even shorter. The prescence of glacial signatures at 400 meter in e.g. KLX13A and KLX19A (cf Section 3.3.2) perhaps argue for slightly greater groundwater mean residence times compared to the carbon ages estimated by $^{14}C$.

Generally, there are many difficulties associated with estimating groundwater residence time with the radiogenic isotopes $^{3}H$ and $^{14}C$, as described in the beginning of Section 3.5. Nevertheless, with these difficulties in mind, the estimations presented here may give a range of possible groundwater residence times or average carbon ages which, in combination with other information, can contribute to an understanding of the site.

Most of the shallow groundwater sampling points (soil tubes) probably contain groundwater of recent origin judging by the high $^{3}H$ activities measured. Many of these objects, however, show slightly lowered $^{14}C$ activities, probably not as a consequence of $^{14}C$ decay reflecting high groundwater residence time, but rather due to dated carbon from the decomposition of peat or due to dilution of zero-activity carbon derived from calcite dissolution.

## 3.6 Summary of the four models

The four two-dimensional models presented in this chapter together summarise the hydrochemistry of the Laxemar-Simpevarp area in a total of 8 independent dimensions. The Ion Source Model (Section 3.2), the Water Origin Model (Section 3.3.2), the Mixing Model (Section 3.4) and the "Age Model" (Figure 3-24 in Section 3.5.2) each reflect different aspects of the hydrochemistry of the area. Depending on whether the focus is on dissolved ions, the water (the solvent) or mixtures of water types, the patterns in the models can assume different appearances. The common factor determining the hydrochemistry is however the "container", i.e. the surface water system, the Quaternary deposits and the bedrock, which means that structures and patterns in the models probably have physical explanations, although more or less distorted due to the model focus.

If the four models are put together in Figure 3-25, groups of observations plot in distinct parts of the models. Observations in fresh surface water are encircled in green, sea water in light blue and groundwater from the deepest levels in the bedrock in red. As an example, the location of the soil tube SSM000241 is marked by a black arrow (cf Section 7.2).

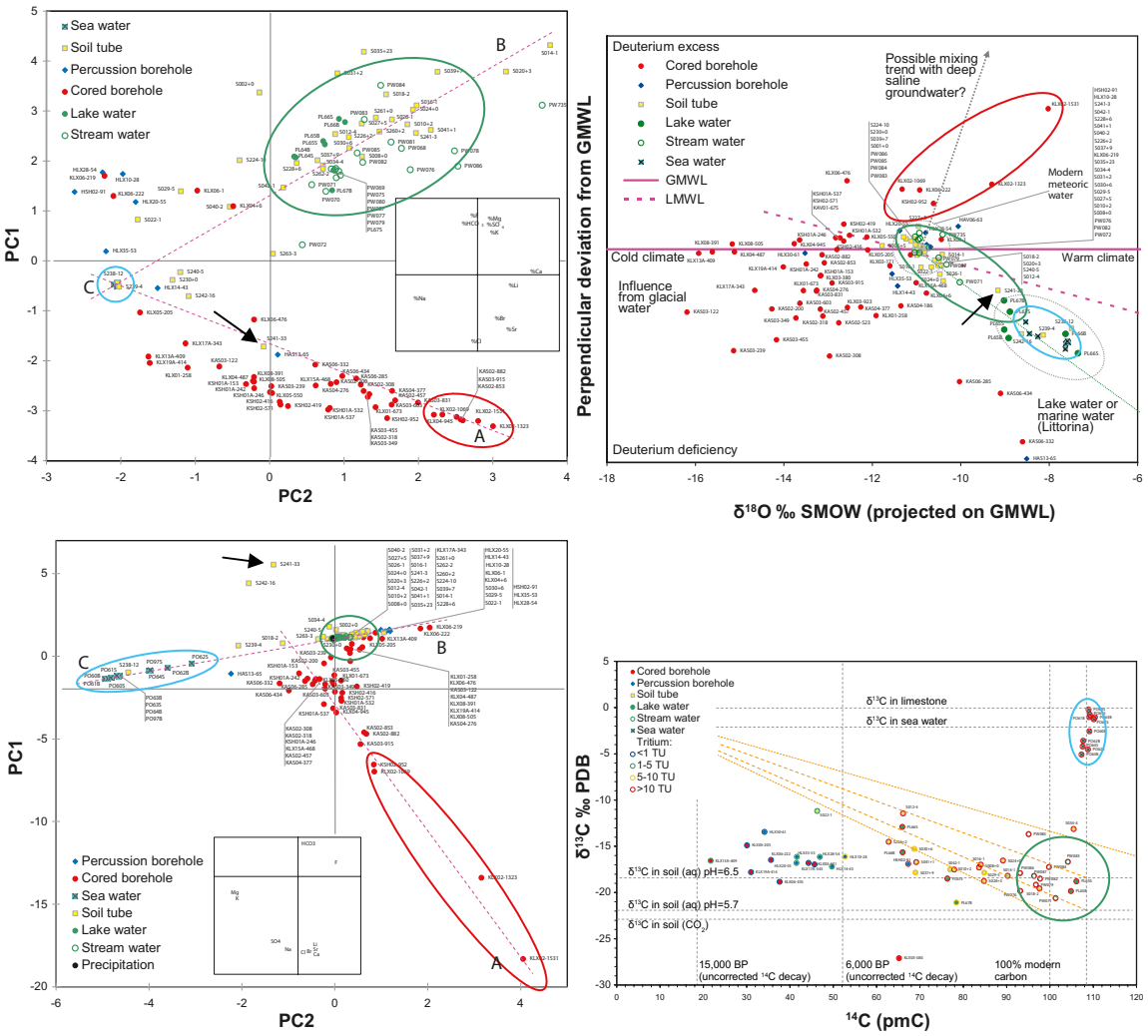


***Figure 3-25.*** *The Ion Source Model (upper left), the Water Origin model (upper right), the Mixing model (lower left) and the "Age model" (lower right) together summarise the hydrochemistry of the Laxemar-Simpevarp area in a total of 8 independent dimensions.*

# 4 Detailed chemical evaluations

The aim of this chapter is to provide detailed visualisations and evaluations that complement the preceding chapter "Hydrochemical overview of the Laxemar-Simpevarp area" for the purpose of answering a number of specific questions concerning the Laxemar-Simpevarp area. The sections deal with the origin and fate of selected elements, tracing of geochemical reactions and, finally, a summary of possible indications of deep groundwater signatures in the shallow system.

## 4.1 Origin and fate of selected elements

Dissolved elements at the Laxemar-Simpevarp site originate from solid or gaseous phases that have either been transformed at the site by reactions or have been transported to the site in dissolved form. Conversely, elements may be lost to the atmosphere or to the geosphere by the formation of solids. In this section, the focus is on marine and deep saline ions as well as on the origin of sulphur, calcium and carbon.

### 4.1.1 Marine influences (Na, Cl, Br)

The recent withdrawal of the Baltic Sea from the Laxemar-Simpevarp area due to isostatic land uplift (shoreline displacement) permits influences by relict marine constituents in areas located at lower altitudes /Söderbäck (ed) 2008/. However, due to the local topography, where higher elevated areas are intersected by steep fissure valleys /Sohlenius and Hedenström 2008/, only a fraction of modern terrestrial areas have been affected since the saline maximum during the Littorina stage at 4000–3000 BC according to Figure 4-1 /Söderbäck (ed) 2008/.

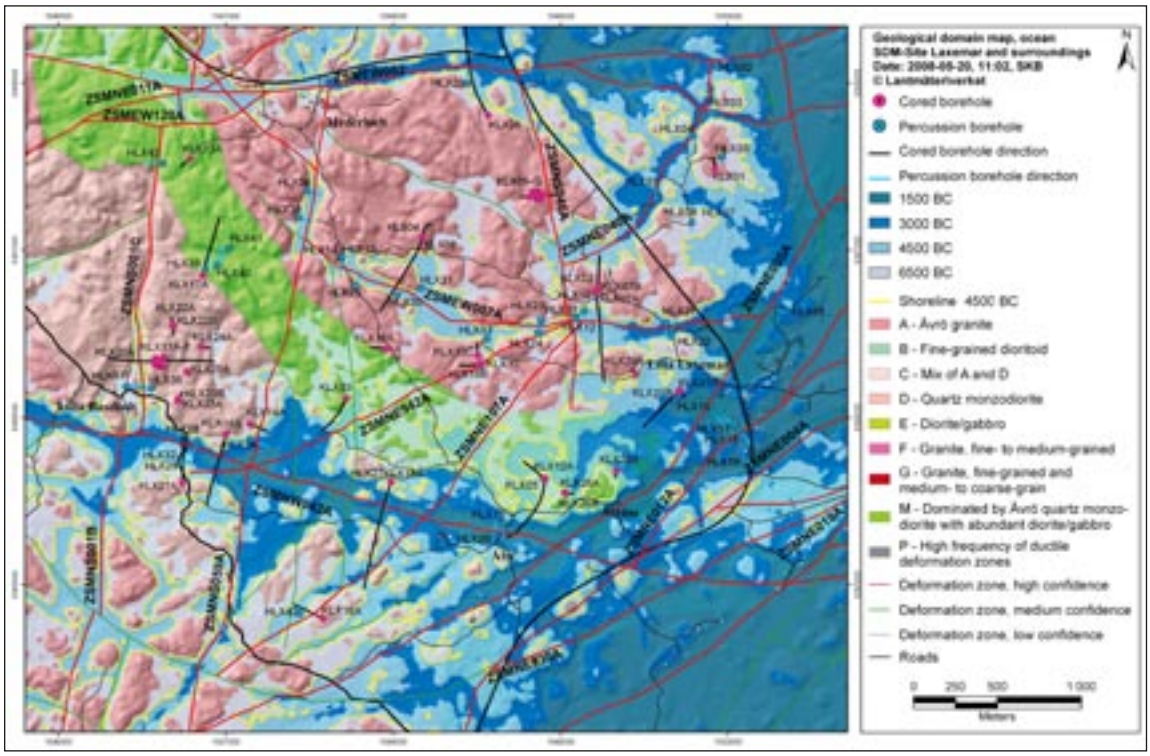


***Figure 4-1.*** *Location of the shoreline at different stages in history (cf Section 8.2).*

The major constituents of sea water, based on molar contributions, are Cl, Na, Mg and $SO_4^{2-}$. In Figure 4-2, the molar composition and concentrations of the major constituents are shown for the sea water sampling site Kråkelund (PSM002060) in the Laxemar-Simpevarp area.

As stated in the water type classification in Section 3.1.1 and in the interpretation of the Ion Source Model in Section 3.2.6, marine influences in the Laxemar-Simpevarp area are relatively weak in both shallow groundwater and fresh surface water, as well as in groundwater in the bedrock /Laaksoharju (ed) 2008/. These conditions contrast with the dominant marine influences on both the surface system and the groundwater in the bedrock at the Forsmark site, where marine relicts are evident at almost all levels /Tröjbom et al. 2007/.

The correlation between Na and Cl is explored in Figure 4-3. In the upper plot there is a clear general trend where Na correlates with Cl, and many points plot along the molar ratio of sea water. Points above (left) this molar ratio trend indicate input of Na, for example by weathering reactions or cation exchange. Deviations below this line may on the other hand indicate input of Cl originating from a deep saline source with a different Na/Cl ratio compared to the marine source. Deviations from the marine trend are emphasised in the plot in the lower panel of Figure 4-3 (Na/Cl versus Cl).

Most surface water samples from lakes and streams cluster just above the marine Na/Cl ratio, which indicates that these ions probably originate from a marine source in combination with input of Na from e.g. weathering processes (cf Section 6.2.2). As described in Section 6.2.1, an important but still artificial marine source dominating the surface system is input of Na and Cl from winter road salt. Sea spray due to nearness to the Baltic Sea may also contribute to the background input along the coast, although the prevailing western winds probably reduce this influence /Werner et al. 2008/.

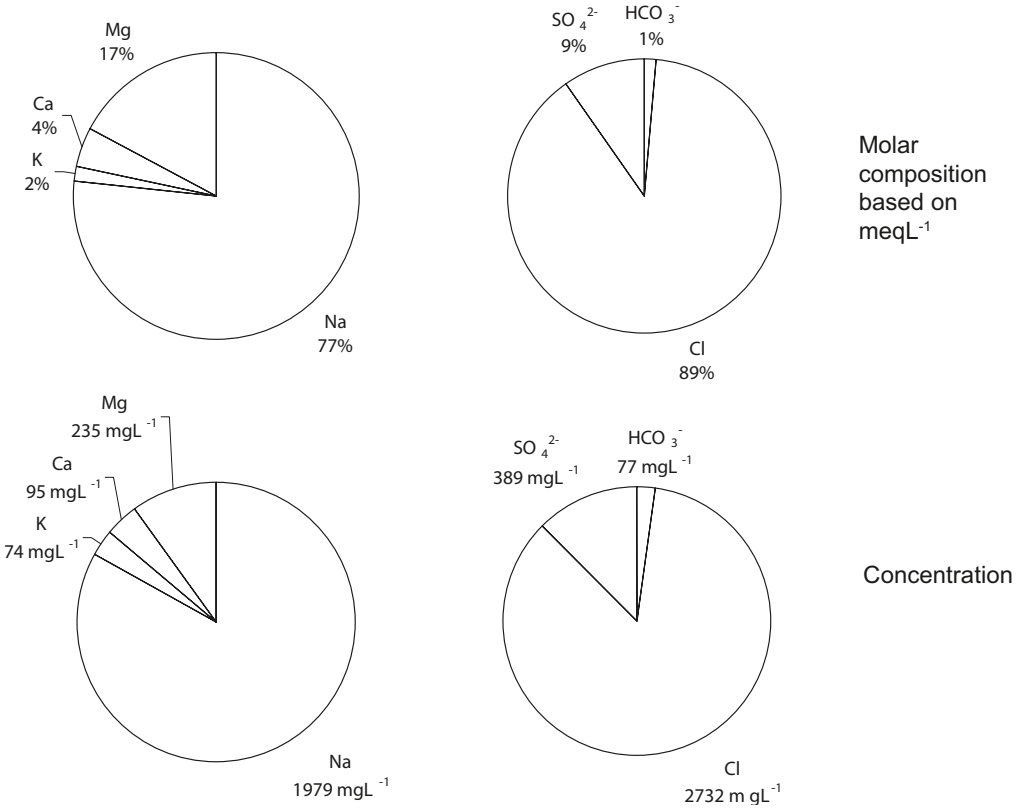


***Figure 4-2.*** *Major ions in sea water measured in surface water at Kråkelund (PSM002060) in the Laxemar-Simpevarp area. Cations to the left and anions to the right. The upper figures represent the molar fractions (based on meqL$^{-1}$) and the lower the concentrations.*

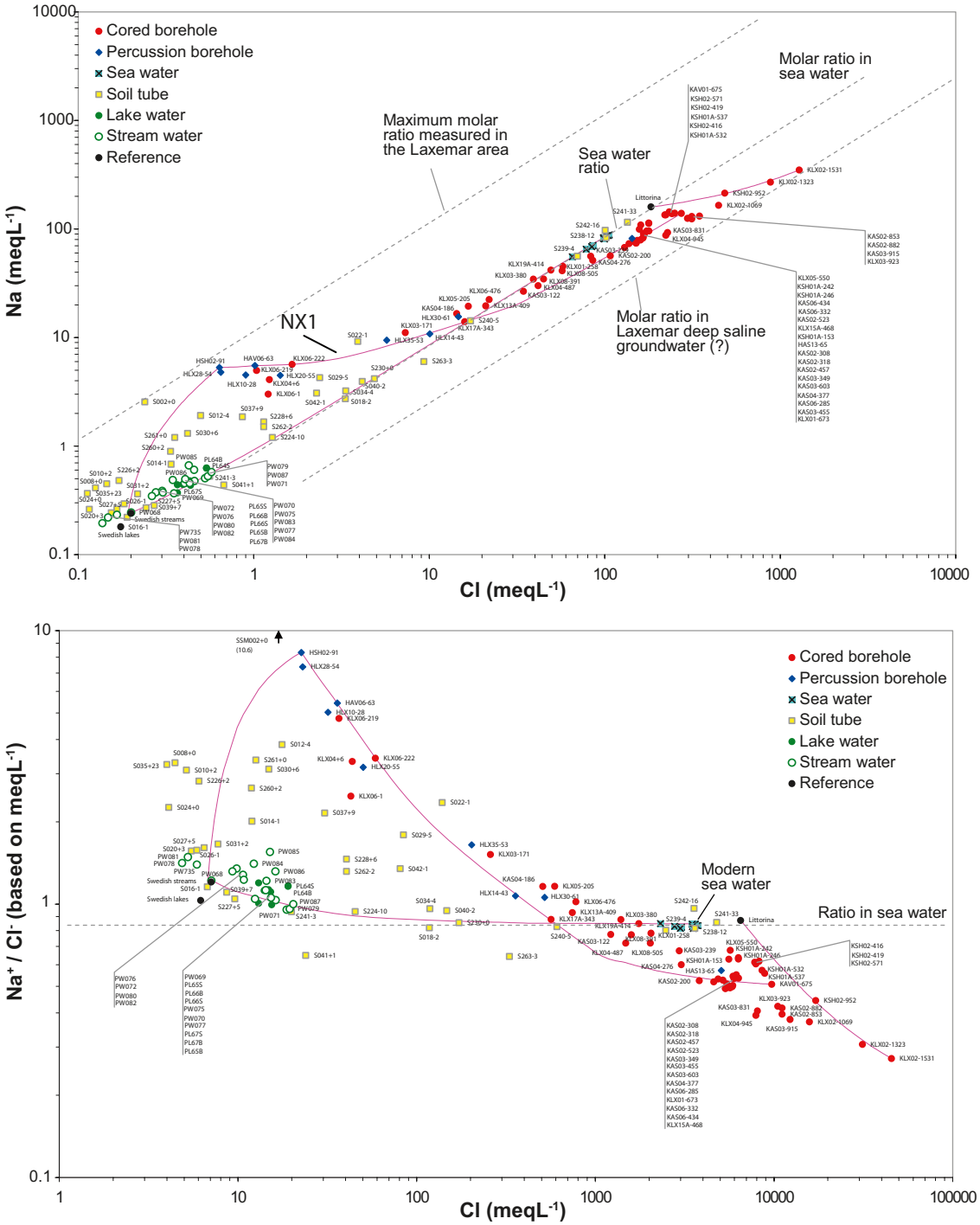


***Figure 4-3.*** *Relationship between Na and Cl in surface water and groundwater in the Laxemar-Simpevarp area. Upper: molar content of Na versus Cl. Lower: Na/Cl ratio (based on meqL$^{-1}$) versus Cl concentration (mgL$^{-1}$). Note that the Cl scales differ between the plots. Dataset C, cf Section 2.2.5. For an explanation of labels, symbols and lines, see Sections 2.3.11 and 2.3.12.*

In Figure 4-3, many shallow groundwater samples in soil tubes follow the hypothetical mixing trend (pink dashed lines) between the dilute freshwater of PW068 (the inlet to Lake Jämsen) to the left and sea water to the right. This indicates that mixing with marine components is probably an important ion source in these objects (e.g. SSM000224, 034, 018, 040, 230 and 263). Five soil tubes located in till beneath lake and sea sediments contain Na and Cl concentrations similar to, or exceeding, sea water (SSM000238, 239, 240, 241, 242, cf Section 7.2). The Ion Source Model (cf Section 3.2.5) and the Li versus Cl plot in the upper panel of Figure 4-7, however, indicate that there are deep saline influences in some of these soil tubes as well. These seemingly contradictory conclusions can be explained by reactions that supply additional Na, for example weathering and cation exchange.

In the upper panel of Figure 4-3 there is an interesting trend, NX1, that follows the hypothetical binary mixing scenario between HSH02-91 and KAV01-675. Both percussion boreholes and cored boreholes from the upper parts of the bedrock (from 50–500 metres vertical depth) form this trend, which corresponds to a gradually increasing Na excess. Possible explanations for this Na excess are weathering of Na-bearing minerals or cation exchange where Na adsorbed onto mineral surfaces is replaced by Ca originating from discharging deep saline groundwater. Many shallow objects in the quaternary deposits are also more ore less associated with this trend, which indicates that weathering reactions and/or cation exchange are important sources of Na in the fresh surface system.

Many deep observations from the bedrock plot below the molar ratio of sea water in the lower panel of Figure 4-3, towards the molar ratio of deep saline groundwater. This deviation below the sea water ratio may in some cases be interpreted as mixing of Na-depleted deep saline groundwater with less depleted marine waters, or mixing with dilute waters showing Na excess (cf Mg in Figure 4-16, which may be an indication of marine influences in the bedrock).

Bromide, like Cl, is usually regarded as a conservative element. In marine influenced ecosystems however, this elements behaves akin to I, rather than Cl, and will not always behave conservatively. This parameter combination may be useful for tracing marine influences, although the reporting limit of Br limits the applicability of this element in very dilute surface waters. The Br versus Cl plot in the upper panel of Figure 4-4 reveals different sources of these elements. In this type of logarithmic plot, samples with similar Br/Cl ratios, but different absolute concentrations, plot along lines with a constant slope. Samples where most of the constituent ions originate from different sources of Br and Cl form parallel lines as marked by the dashed grey lines. There are four possible Br and Cl sources in the Laxemar-Simpevarp area:

- Modern (and probably also relict) sea water is an important common source of Br and Cl.
- Samples of deep saline groundwater indicate another distinct source that differs from the marine source in its Br/Cl ratio.
- Two samples of groundwater from the deposits beneath lake and sea water show a highly elevated Br/Cl ratio, which cannot be explained solely by the marine and deep saline sources. A possible source of the presumably elevated Br concentrations in these samples is degradation of organic matter of marine origin. The blue pigment in e.g. clams is highly enriched in Br (originally of marine origin). A cluster of some dilute shallow groundwater samples denoted "B1" may also be influenced by this Br source, rather than the deep saline source (the Br/Cl ratio in these samples happen to coincide with the ratio of deep saline groundwater).
- A few fresh water observations in streams from a specific area also show an elevated Br/Cl ratio (PW76 and PW86). Since this signature is absent in other similar settings along the coast, a local anthropogenic source of this Br can be suspected. As discussed in 6.2.1, different kinds of road salt contribute most of the Cl in the surface system, and the observed pattern could hypothetically be explained by the use of road salt of different Br/Cl ratios.

When the Br/Cl ratio is plotted against the vertical depth of the observations in the lower panel in Figure 4-4, a distinct pattern appears. Below a vertical depth of about 600 metres only the deep saline prevails, whereas samples at shallower levels constitute mixtures of the marine

and deep saline sources. This pattern can be interpreted as indicating that the sea water in pre-historic time penetrated the bedrock down to 600 metres in the Laxemar-Simpevarp area, and that groundwater at shallower levels in the bedrock constitutes mixtures of ions of marine and deep saline origin. The broad scatter between these sources even at depths below 200 metres indicates that the deep saline contribution is significant even at relatively shallow levels (note the logarithmic scale on the horizontal axis).

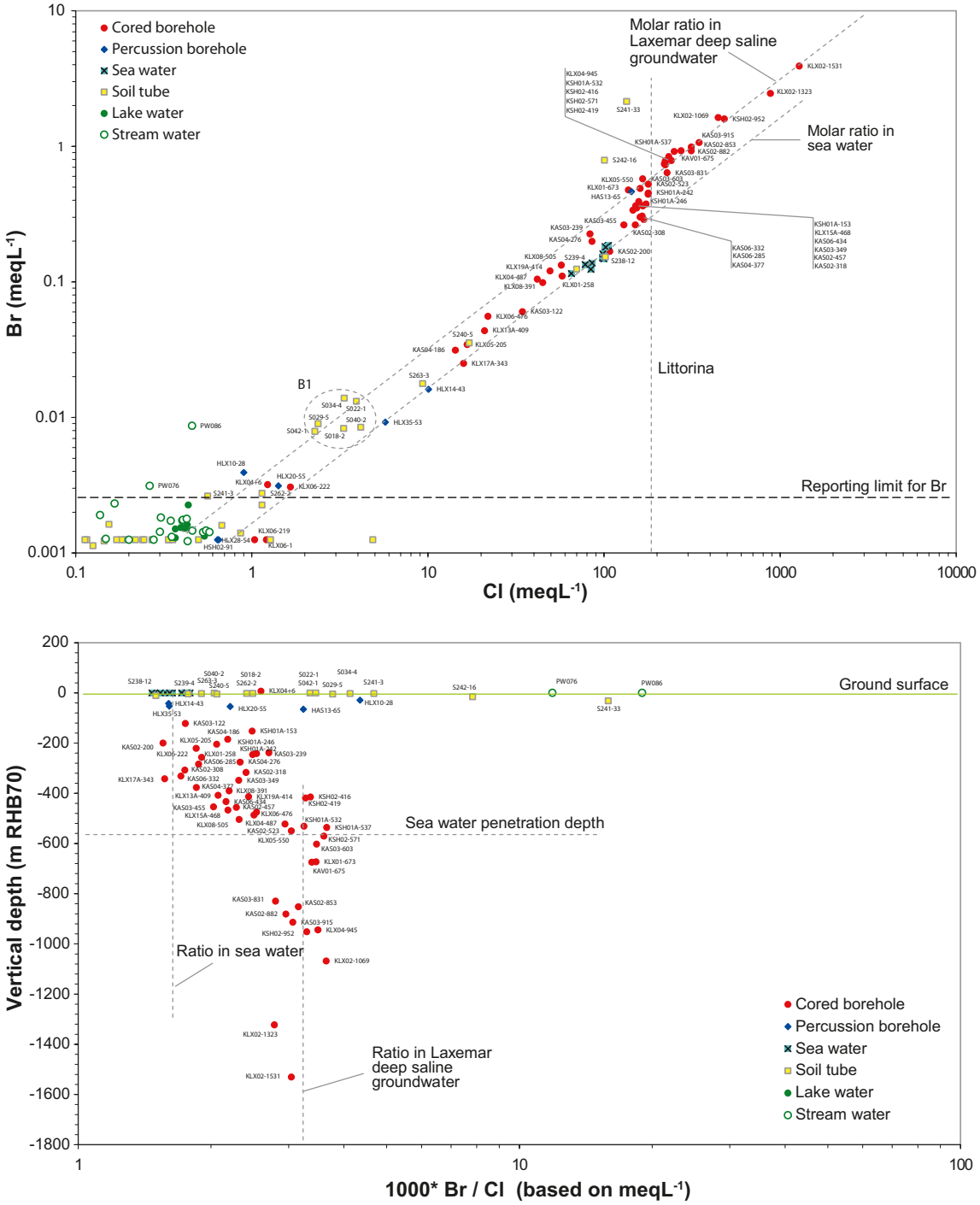


***Figure 4-4.*** *Bromide and Cl in the Laxemar-Simpevarp area expressed in meqL$^{-1}$. Upper panel: Br versus Cl on logarithmic scales, lower panel: vertical depth versus Br/Cl ratio calculated from meqL$^{-1}$. Based on data selection C, cf Section 2.2.5. For an explanation of labels, symbols and lines, see Sections 2.3.11. and 2.3.12. Only observations above the reporting limit are included in the lower plot.*

The major conclusions regarding marine influences are summarised in the bulleted list below:

- The marine contribution is usually weak in the dilute waters of the surface system in the Laxemar-Simpevarp area. Since most parts of the area were located above sea level during the Littorina stage, this can mainly be explained by the topographical conditions and palaeo-hydrological history of the area.
- At lower altitudes close to the coast, especially in the steep fissure valleys that intersect the Laxemar-Simpevarp area, marine relicts in the Quaternary deposits probably contribute marine ions (cf Section 6.2.1).
- Different types of road salt are important sources of Cl and other marine ions in the surface system. As much as 2/3 of the Cl discharge from the area has been estimated to originate from anthropogenic sources such as winter road salt (NaCl) and summer road salt ($MgCl_2$ and $CaCl_2$) according to the estimate in Section 6.2.1. These sources contribute to a marine signature observed in streams and lakes in the area, and in some streams discharging in higher elevated areas located far from the coast this is the major source for marine ions.
- The Na excess (compared to Cl in sea water) evident in most dilute waters probably reflects additional input of Na from weathering and cation exchange reactions. As may be expected, this Na fraction is most pronounced in waters of low ionic strength, and is gradually masked when marine influences increase.
- Several samples from percussion boreholes and cored boreholes show an Na excess similar to many soil tubes, but with significantly higher Na concentrations. A possible explanation for the Na excess in the bedrock may also be weathering and/or cation exchange, perhaps driven by Ca originating from discharging deep groundwater.
- Only a few shallow objects in the Laxemar-Simpevarp area contain marine remnants comparable to the concentrations in modern sea water or relict sea water (e.g. Littorina). Among five soil tubes located in till below lake and sea sediments, two contain modern sea water, one represents meteoric discharge and two contain Cl concentrations exceeding modern sea water. In one of the latter, the Cl concentration is almost on a level with the Littorina saline maximum (cf Section 7.2).
- Marine signatures are generally weak in the groundwater of the bedrock according to e.g. the Ion Source Model in Section 3.2.6, compared to the Forsmark site, which also is located close to the Baltic Sea (the whole Forsmark area was submerged for a considerable time). The Br/Cl ratio, however, indicates that Cl of marine origin may have penetrated down to a depth of 500–600 metres in the bedrock during pre-historic time. On the other hand, the present composition indicates that marine signatures have to a varying extent been flushed away or replaced by deep saline signatures and signatures associated with meteoric recharge (cf Mg in 4.1.4 and $Mn^{2+}$ in 4.2.3).

### 4.1.2 Deep saline influences (Ca, Cl, $^{37}Cl$, Li)

Highly saline solutions are usually found at great depth in granitic environments in the Fennoscandian and Canadian shields. The origin of these so called (shield) brines is unclear, and both *in situ* and allochthonous (e.g. Palaeozoic seawater) origins have been proposed (cf further evaluations of deep groundwater hydrochemistry in /Laaksoharju (ed) 2008/). When samples influenced by deep saline groundwater from Forsmark and the Laxemar-Simpevarp area are compared, they show similar trends towards increasing depth, with increasing concentrations of e.g. Ca, Cl (Figure 4-5), Na, Sr and Br. The presence of dilute waters even at considerable depths in the Laxemar-Simpevarp area according to Figure 4-5 is most certainly an artefact caused by artificial mixing and reflects the difficulties associated with sampling at these depths. If the representative samples in Figure 4-5 (coloured) are compared with samples from the Forsmark site, however, it is evident that dilute waters are present at greater depths in the Laxemar-Simpevarp area.

Deep saline groundwater at both sites shows very similar composition with regard to all major elements, except for $SO_4^{2-}$ where concentrations at great depths are usually higher in the Laxemar-Simpevarp area than in the Forsmark area (Figure 4-10).

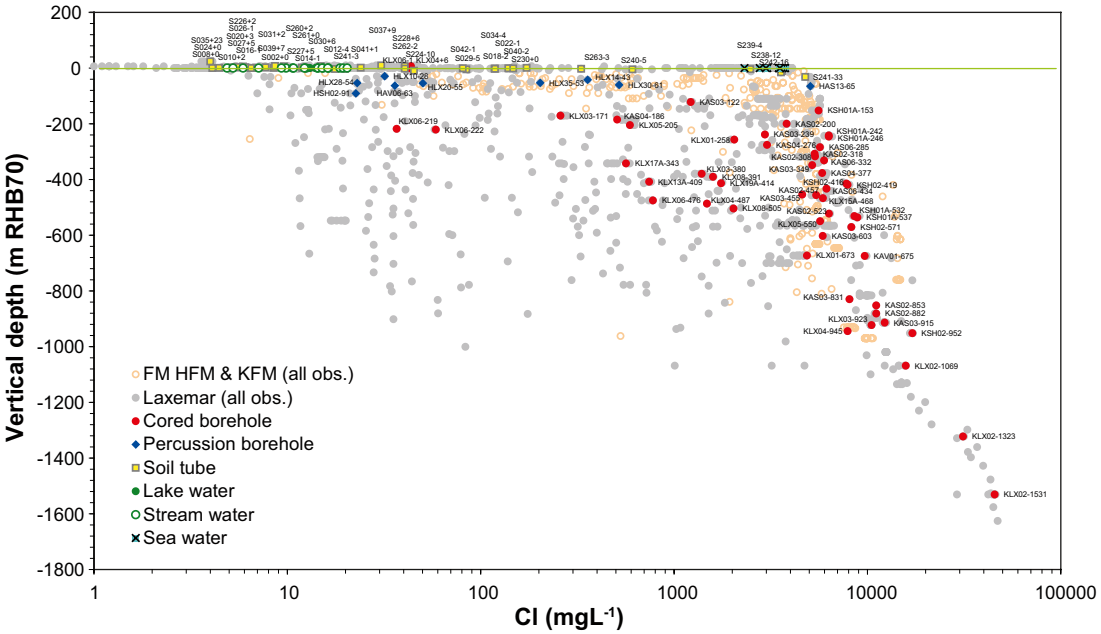


***Figure 4-5.*** *Chloride versus depth in the Laxemar-Simpevarp and Forsmark areas. Coloured marks, which only represent the Laxemar-Simpevarp site, are based on data selection C, cf Section 2.2.5, while grey marks represent individual samples from data selection A. Reference data from Forsmark, marked in light orange, include all available individual samples from the bedrock (percussion boreholes, HFM, and cored boreholes, KFM). For an explanation of labels, symbols and lines, see Sections 2.3.11 and 2.3.12.*

Among trace elements, the difference between the two sites is even more pronounced for lithium. According to Figure 4-6 the Li/Cl ratio differs by a factor of almost 100 when the the deepest samples from the Forsmark and Laxemar-Simpevarp areas are compared. The Li/Cl ratio, which seems converge towards a relatively constant ratio with increasing depth in the Laxemar-Simpevarp deep saline groundwater, indicates that the two elements may have a common source at these levels. The fact that this ratio also differs significantly from the ratio in sea water makes this element a possible tracer for deep saline groundwater in the bedrock in the Laxemar-Simpevarp area. This is especially valid if Li show a conservative behaviour in these environments.

As a complement to the multivariate Ion Source Model in Section 3.2.5 (which includes lithium), the two-dimensional Li versus Cl plot in Figure 4-7 may discriminate between deep saline groundwater and marine influences on assumption that Li behaves rather conservative. Compared with the Na versus Cl and Br versus Cl plots in Figure 4-3 and Figure 4-4, the difference between these water types is enhanced.

Sources of Li and Cl can be explored from the log-log plot in Figure 4-7. In this type of logarithmic plot, samples with the same Li/Cl ratio but with different absolute concentrations plot along lines with a constant slope. Li and Cl originating from different sources form parallel lines as marked by the dashed grey lines. The following sources of Li and Cl can be distinguished:

- Sea water can be distinguished as a source for Li and Cl with a distinct Li/Cl ratio. Modern sea water samples as well as the Littorina M3 end-member and two soil tubes located in till beneath sea sediments show the lowest Li/Cl ratio among all observations in the Laxemar-Simpevarp area.
- Most samples from the bedrock form a cluster that extends along a constant Li/Cl ratio, which is about 10 times higher than the ratio in sea water, indicating that deep saline groundwater contains high concentrations of Li and that this source possibly shows a distinct signature regarding these ions (cf Figure 4-6).

- The scatter of many samples from lakes, streams and shallow groundwater at a level above the deep saline (brine) ratio suggests that there is a Li source in the surface system independent from Cl. Weathering of local minerals is a probable source, and according to analyses of till samples the Li concentrations in the Laxemar-Simpevarp area are slightly elevated compared to the national distribution /Tröjbom and Söderbäck 2006/ and /Sohlenius and Hedenström 2008/.

According to element analyses of till and bedrock, the composition of the till in the area probably reflects the composition of the local bedrock /Sohlenius and Hedenström 2008/. This may suggest that Li present both in the surface system and in the deep saline groundwater may have local Li-bearing minerals as a common origin if the brine is assumed to have been formed *in situ*.

This also suggests that Li and Cl alone are not suitable for detecting deep saline signatures in the dilute surface system, because mixtures between shallow groundwater and sea water may result in a Li/Cl ratio similar to the possible deep saline groundwater source. From the patterns in Figure 4-7 it is, however, clear that Li in combination with Cl can be useful in distinguishing sea water from deep saline sources at higher ionic strengths (cf Section 4.2).

For example, the two soil tubes (SSM000241 and 242) plot along the mixing lines between sea water and the deepest samples from the Laxemar-Simpevarp area, which indicates a potential deep saline influence in these objects provided that Li has a resonably conservative behavior. A similar pattern is also suggested in Figure 4-8, where the Cl isotope composition in SSM000242 also indicates a deep saline influence, whereas the shallower tubes located at similar settings (SSM000238, 239, 240) plot within the sea water range. The single $^{37}Cl$ measurement available from the deepest soil tube SSM000241, however, points in the opposite direction, which makes the interpretation of $^{37}Cl$ unclear (cf Section 7.2). It should be noted that the evaluation of $^{37}Cl$ is ambiguous due to the large measurement uncertainty of 0.2 units and it could not be ruled out that the shift from the marine signature in both SSM000241 and SSM000242 is random.

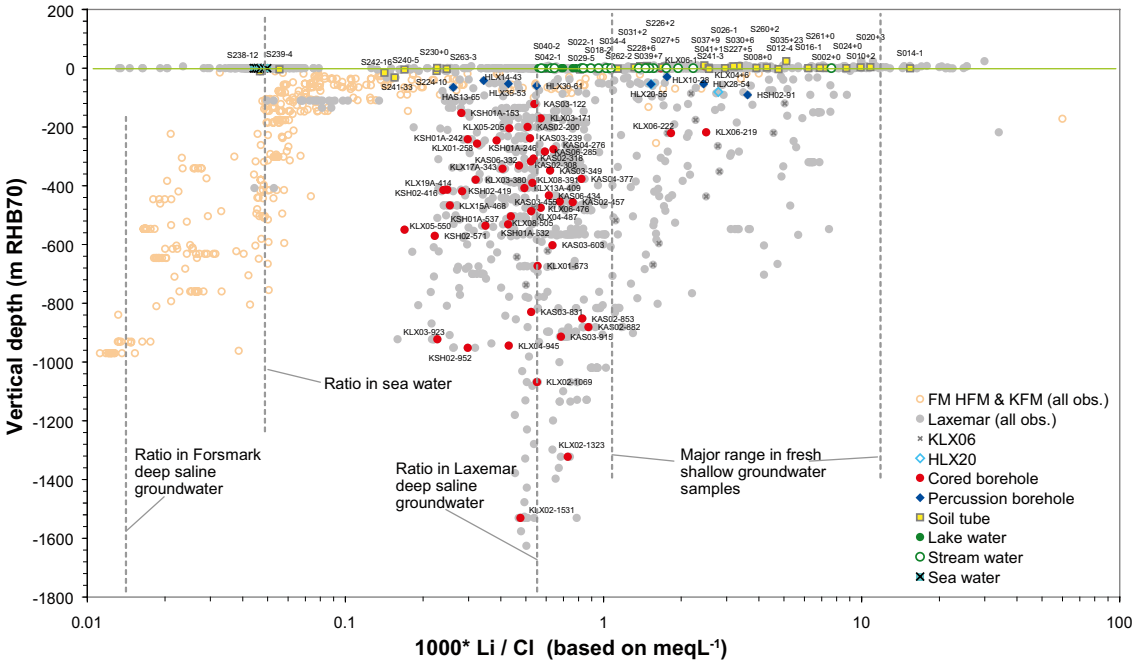


***Figure 4-6.*** *Lithium in the Laxemar-Simpevarp area compared to the Forsmark site. Vertical depth versus Li/Cl ratio calculated from meqL$^{-1}$. Coloured marks are based on data selection C, cf Section 2.2.5, and grey marks represent individual samples from data selection A. Reference data from Forsmark, marked in light orange, include all available individual samples from the bedrock. For an explanation of labels, symbols and lines, see Sections 2.3.11. and 2.3.12.*

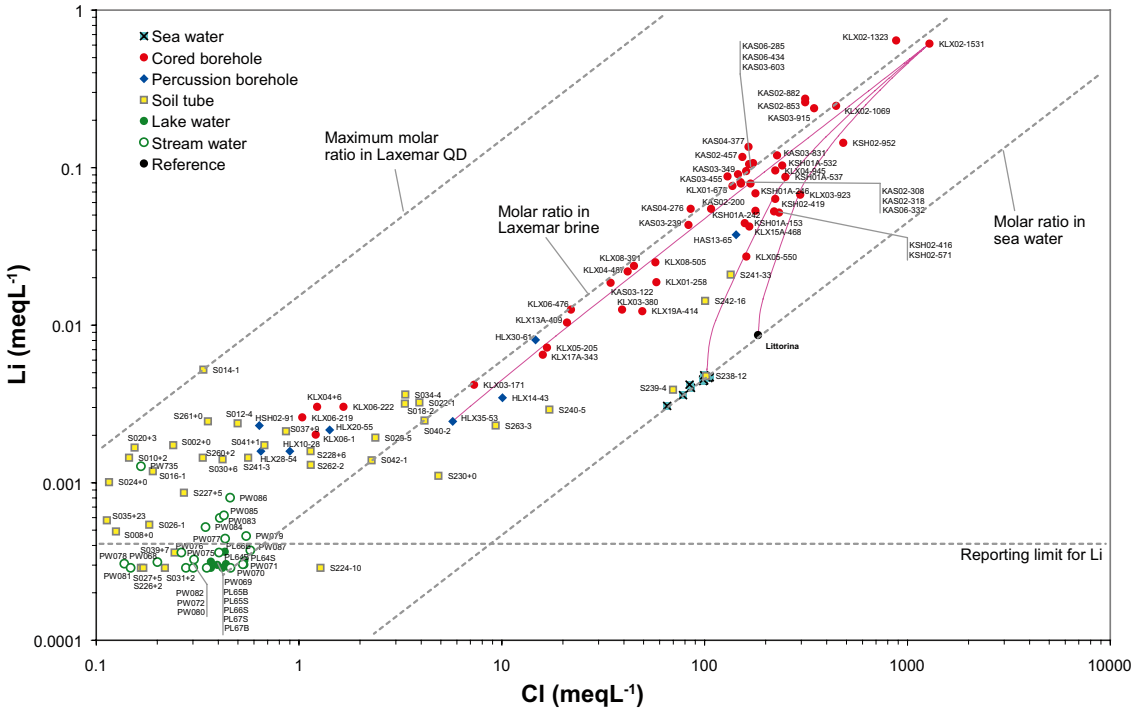


***Figure 4-7.*** *Lithium and Cl in the Laxemar-Simpevarp area expressed in meqL$^{-1}$ on logarithmic scales. Based on data selection C, cf Section 2.2.5. For an explanation of labels, symbols and lines, see Sections 2.3.11. and 2.3.12.*

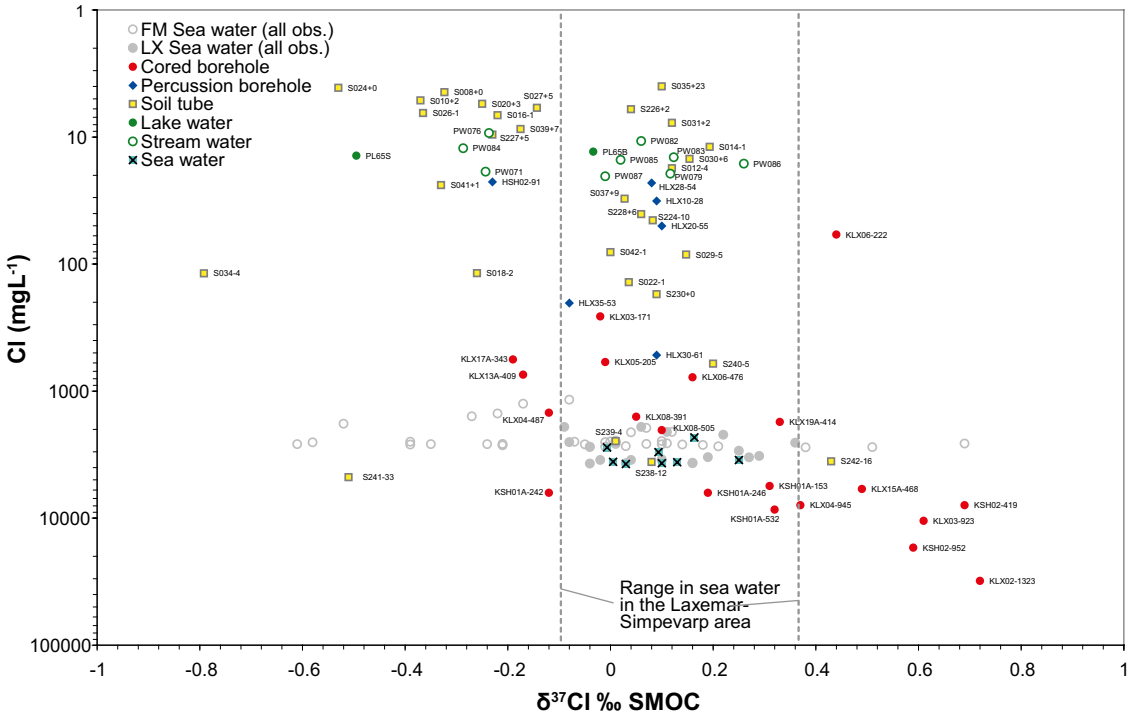


***Figure 4-8.*** *Cl concentration versus the $^{37}$Cl isotope. Coloured marks represent data from the Laxemar-Simpevarp area based on data selection C, cf Section 2.2.5. Closed grey marks represent individual samples from sea water from data selection A, whereas corresponding reference data from Forsmark is marked as open grey dots. For an explanation of labels, symbols and lines, see Sections 2.3.11. and 2.3.12.*

When Na is plotted versus Li in the upper panel of Figure 4-9, the overall pattern is similar to Figure 4-7 (but reversed as Li has changed axis). The most obvious difference is shown by a number of observations from the bedrock that plots along the possible Li/Cl ratio of deep saline groundwater, but deviates from this line in the Na versus Li plot. This can be interpreted as indicating that Na and Li originate from different sources in these samples (for example that excess Na is added at shallower levels in the bedrock).

On the other hand, the molar Na/Li ratio in deep saline samples is similar to the ratio in many shallow groundwater samples (which is most clearly seen in the lower panel of Figure 4-9, where the Na/Li ratio is plotted versus the Cl concentration). This pattern could be interpreted as indicating that there is a common source of both elements (Na and Li) in the surface system as well as in the deep saline groundwater, and that the deviation from this "base line" reflects weak influence of Na from another source, e.g. sea water. A few interesting trends that can be distinguished in Figure 4-9 are summarised in the bulleted list below:

- There is a possible marine mixing trend among deep samples from cored boreholes in the bedrock denoted by CX1 in the lower panel. Two hypothetical mixing lines show mixing with modern sea water and Littorina seawater, respectively.
- The other trend among deep samples (CX2) is towards dilute waters in the deposits, and the extension of this line intersects CX3 at the point Q. The direction of this trend in the Na versus Li plot indicates that the concentration of Na does not decrease as fast as Li during dilution of the deep saline source, if a conservative mixing hypothesis is applied. If Li is considered more conservative than Na, the pattern in the lower plot may be interpreted as indicating that Na comes from a source located at Q (i.e. the zone represented by observations from the lower parts of the regolith or the upper parts of the bedrock).
- The cluster of fresh surface water samples in streams and lakes is slightly shifted along the marine mixing trend CX3, compared to the major cluster of observations from shallow groundwater (soil tubes). This shift may to some extent be attributed to anthropogenic sources of different kinds of road salt, which through ditches affect the surface water discharge to a higher degree than shallow groundwater in the area (e.g. the unaffected inlet to Lake Jämsen PW68 compared to the downstream outlet of the Laxemarån River PW87). As many samples from lakes and streams fall below the reporting limit for Li according to the dashed vertical line in the Na versus Li plot, the vertical shift may in such cases be an artefact caused by the practise of replacing values below the reporting limit with a value corresponding to half the reporting limit.
- Shallow groundwater observations in soil tubes form a cluster in the lower left of the lower panel of Figure 4-9. The location of some tubes coincides with the fresh surface water samples, whereas most show elevated concentrations of both Na and Li, but not of Cl. The latter group of soil tubes follows the hypothetical marine mixing line CX4, and the composition with respect to these ions may be explained by mixing with a marine source. Several observations from the upper 200 metres of the bedrock (percussion boreholes and cored boreholes) also plot along this trend, which indicates that there is a resemblance between shallow groundwater in the deposits and the groundwater in the upper parts of the bedrock.
- Two observations from shallow groundwater in till beneath the sediments of Lake Frisksjön and Granholmsfjärden Basin, SSM000242 and SSM000241, show, like many other plots, an anomalous pattern which may be explained by mixing of a deep saline component with a marine component.

The overall pattern of Figure 4-9 may be interpreted as indicating that the two primordial sources of Na and Li in the Laxemar-Simpevarp area are weathering of local minerals and sea water. The increased Na content relative to Li which is apparent in many samples from both shallow groundwater and groundwater in the bedrock may consequently be attributed primarily to a marine source.

The total lack of observations with a Na/Li ratio above 5,000 (with the exception of SSM000241 and 242 as well as SSM000238 and 239, which resemble sea water), and the disruption of CX2 at Q, indicate that strong marine influences are at present date absent in almost all sampled sites. This disrupted pattern, which also is evident in many plots as well as in the Ion Source Model in Section 3.2.5, could perhaps be explained by meteoric recharge or glacial flushing according to signatures in the Water Origin Model in Section 3.3.2.

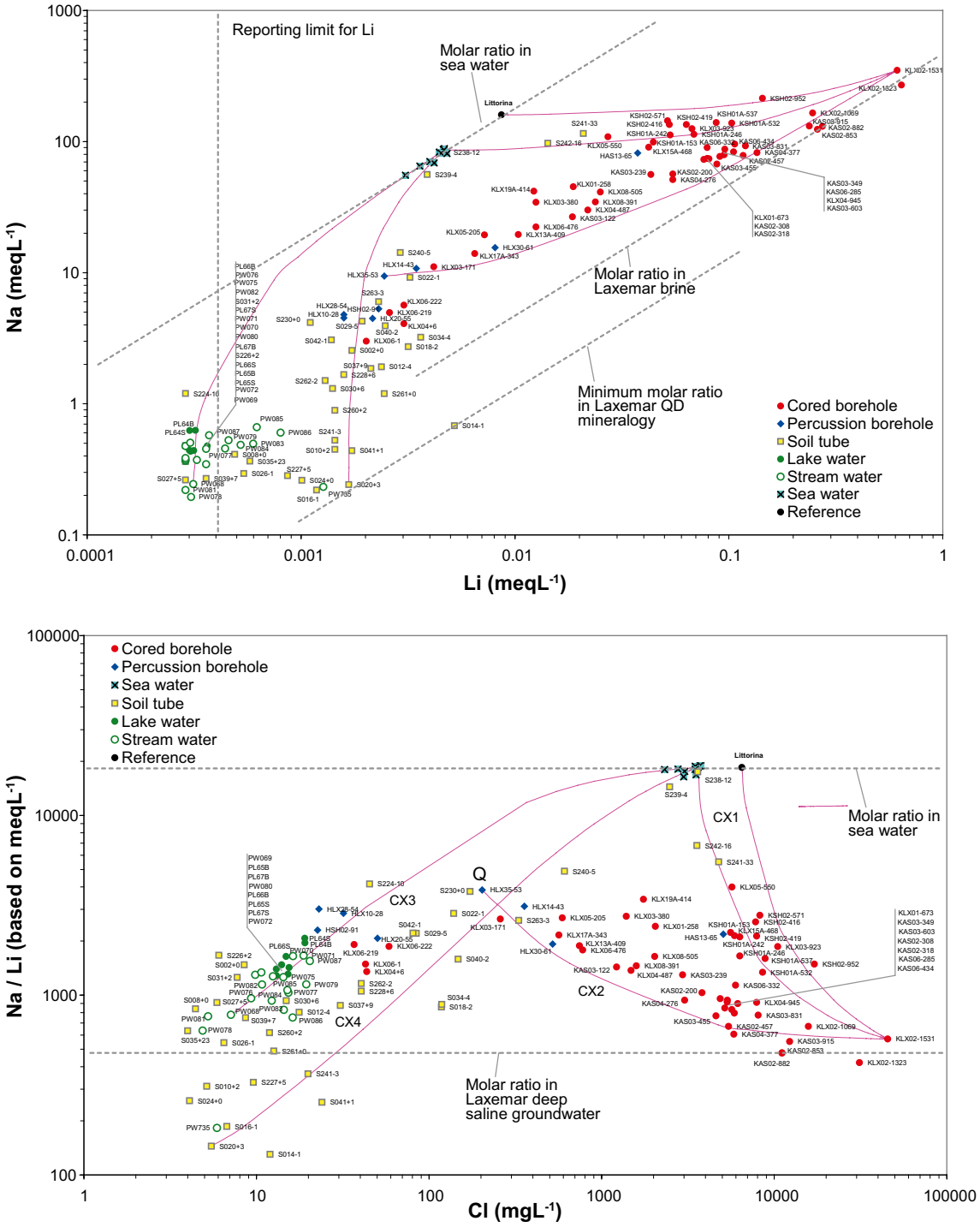


***Figure 4-9.*** *Na, Li and Cl in the Laxemar-Simpevarp area. Upper panel: Na versus Li (both expressed in meqL$^{-1}$), lower panel: Na/Li ratio (calculated from meqL$^{-1}$) versus Cl (mgL$^{-1}$). Note that as the lower plot is based on three parameters, hypothetical mixing lines drawn between adjacent observations do not necessarily follow the same path in this 2-dimensional projection.*

### 4.1.3 On the origin of sulphur

Sulphur in groundwater and surface water may originate from many different sources: relict and modern marine sulphate, sulphur deposition originating from e.g. fossil fuels, and dissolution of sulphur-bearing minerals such as pyrite and gypsum. Moreover, in agricultural areas fertilizers may be a possible sulphur source.

Alternative sulphur sources can be distinguished by the use of sulphur isotopes in combination with other major constituents that covary with sulphur, such as $Cl^-$ from marine sources. Different processes can influence the isotopic composition of sulphur in different directions. Microbial $SO_4^{2-}$ reduction can be traced in the remaining dissolved $SO_4^{2-}$ pool by enrichments in $^{34}S$. The $S^{2-}$ formed is instead depleted in $^{34}S$, and can usually be identified by negative $^{34}S$-values in, for example, precipitated pyrites of biogenic origin.

$SO_4^{2-}$ concentrations in freshwater in the Laxemar-Simpevarp area are slightly elevated compared with most lakes and watercourses in Sweden. As sulphate deposition in this region does not deviate significantly from the rest of southern Sweden, the elevated $SO_4^{2-}$ levels can be attributed to leaching from soils. The vicinity of this coastal area to the Baltic Sea also suggests it as a source of relict marine ions such as $SO_4^{2-}$, and another possible source is direct influence from sea water deposition originating from sea spray /Tröjbom and Söderbäck 2006/. However, the $SO_4^{2-}/Cl^-$ ratio of most fresh waters in the area considerably exceeds the ratio in sea water. This indicates that non-marine sulphate, e.g. large-scale sulphur deposition, is the major sulphur source in the surface system (Figure 4-10).

At deeper levels there is a significant difference between the Laxemar-Simpevarp area and the Forsmark site regarding $SO_4^{2-}$ concentrations. According to Figure 4-10, the $SO_4^{2-}/Cl^-$ ratio at a depth of 1,000 metres is almost an order of magnitude higher in the Laxemar-Simpevarp area, even though the $Cl^-$ concentrations follow a similar trend with depth (cf $Cl^-$ versus depth in Figure 4-5). This deep $SO_4^{2-}$ pattern suggests, together with the corresponding but stronger Li pattern (cf Section 4.1.2), that there are significant differences between deep saline groundwater from the Laxemar-Simpevarp area and the Forsmark area, although the main patterns with regard to other elements (such as Cl and Ca) are similar.

The most compact visualisation of the origin of sulphur is shown in Figure 4-11, where the $SO_4^{2-}/Cl^-$ ratio is plotted against the isotopic composition of $^{34}S$ and $^{32}S$. Complementary plots including $SO_4^{2-}$ concentrations are shown in Figure 4-12.

Modern sea water, marked by dashed grey lines, plots in the middle of both Figure 4-11 and Figure 4-12 (upper panel). Observations that plot above this horizontal line show $SO_4^{2-}$ excess compared with the composition in sea water, and non-marine sources may also be considered. Observations below this line show on the contrary $SO_4^{2-}$ deficiency, due either to removal of $SO_4^{2-}$ or addition of non-marine $Cl^-$ from e.g. a deep saline source (the ratio is lower in the deepest samples from KLX02 according to the upper panel of Figure 4-12).

The isotopic composition, discriminating in the horizontal direction of Figure 4-11, reflects different processes and may reveal different sources of $SO_4^{2-}$. Atmospheric composition /Kendall and McDonnel 2006/, the approximate location of biogenic pyrites /Clark and Fritz 1997/, and the $SO_4^{2-}$ concentration in precipitation /Tröjbom and Söderbäck 2006/ have been marked in the figure. Based on Figure 4-11 and Figure 4-12, the following conclusions concerning the origin of sulphate may be drawn:

- All observations from fresh surface waters in Figure 4-11 plot above the marine composition line, indicating a significant contribution of non-marine $SO_4^{2-}$ in streams and lakes in the Laxemar-Simpevarp area. Possible sources are long-way atmospheric deposition and oxidation of pyrites in the Quaternary deposits. Fertilizers may also contribute, at least in catchments where the proportion of arable land is significant (e.g. PW86). Due to the overlapping hypothetical mixing trends towards modern sea water, it is not possible to distinguish atmospheric from pyritic $SO_4^{2-}$ in the surface waters in Figure 4-11. In the lower panel of Figure 4-12, where $\delta^{34}S$ is plotted versus the $SO_4^{2-}$ concentration, an integrated qualitative

picture of the relative importance of different sulphur sources is provided. The green lines that connect three hypothetical end-members enclose most observations from shallow groundwater and surface water, and the curved shape would be a mixing triangle if plotted in a linear coordinate system. The selected end-members are sea water, atmospheric sulphur in precipitation and pyritic sulphides in SSM000039. The relative location within this shape corresponds to the relative proportion of each end-member in the sample. If isotope selective processes such as microbial sulphate reduction have had significant influence on the measured sulphate, this simplified picture could be somewhat distorted. The location of the surface water cluster almost centred within the green shape indicates that surface waters are influenced to a varying degree by all three sources; atmospheric, pyritic and marine sulphur (cf Section 6.2.7).

- Most observations from shallow groundwater cluster around the surface water samples, but with a greater attraction towards the pyrite corner in the lower right of Figure 4-12 (lower panel). This indicates the larger relative importance of this source in groundwater compared with water in lakes and streams (this is most evident in SSM000039). The high $SO_4^{2-}$ concentrations around 100 $mgL^{-1}$ observed in shallow groundwater probably originates from sulphides (pyrite) in the sediments. Gypsum, which is undersaturated in all surface waters and shallow groundwaters according to thermodynamic calculations in /Laaksoharju (ed) 2008/, is not a probable $SO_4^{2-}$-source in the surface system. There are also some shallow groundwater objects that show stronger marine influences in combination with deviating signatures that could possibly be explained by microbial sulphate reduction (see discussion below).
- In the upper parts of the bedrock, represented by most observations from percussion boreholes, the influence of the deep sulphur source is more or less absent. The pyritic and atmospheric sulphur sources associated with the surface system are probably the main sources in these parts of the bedrock, but the highly enriched $^{34}S$ values suggest the influence of some isotope selective process, for example microbial sulphate reduction.
- Groundwater observations from the deeper parts of the bedrock show an association with sulphur of marine origin and also sulphur of deep saline origin, which may have a different sulphur isotope composition and $SO_4^{2-}/Cl^-$ ratio compared with sea water. The deepest samples available with $^{34}S$ analyses (e.g. KLX04-945) point to a $\delta^{34}S$ of about +10‰ CDT and a $SO_4^{2-}/Cl$ ratio (times 1,000) of about 50. However, the trend in KLX02 (cf depth in the labels in Figure 4-10) suggests that both these values are even lower in deep saline groundwater. Many observations from the bedrock may in such case be explained by mixing between the deep saline and the marine sulphur sources. Deviations from this pattern indicate that processes such as microbial $SO_4^{2-}$ reduction may have altered the composition significantly at levels shallower than 500 metres (see discussion below). According to thermodynamic calculations in /Laaksoharju (ed) 2008/, $SO_4^{2-}$ in deep groundwaters is also controlled by gypsum which is occasionally present in fracture fillings.

There are several indications that reactions such as microbially mediated sulphur reduction have taken place both in shallow groundwater in the deposits and in groundwater in the upper parts of the bedrock (cf /Laaksoharju (ed) 2008/). As microbial sulphate reduction favours uptake of the lighter sulphur isotope, $^{34}S$ is enriched in the remaining $SO_4^{2-}$ pool, which results in an increase in the $\delta^{34}S$ value compared to the original composition. In Figure 4-11 sulphate reduction moves observations in a direction to the right and downwards along the dashed pink lines (i.e. $\delta^{34}S$ increases and the $SO_4^{2-}/Cl^-$ ratio decrease). In the upper panel of Figure 4-12 sulphate reduction shifts observations to the left and downwards, for example as indicated by the sulphate reduction scenario starting at the composition of sea water (i.e. both the $SO_4^{2-}/Cl^-$ ratio and the concentration of $SO_4^{2-}$ decrease). In the lower panel of Figure 4-12 this process instead moves observations to the left and upwards due to the increase in $\delta^{34}S$ and decrease in $SO_4^{2-}$ concentration. The indications of sulphate reduction are summarised and discussed in the list below (see also Section 4.2.4.):

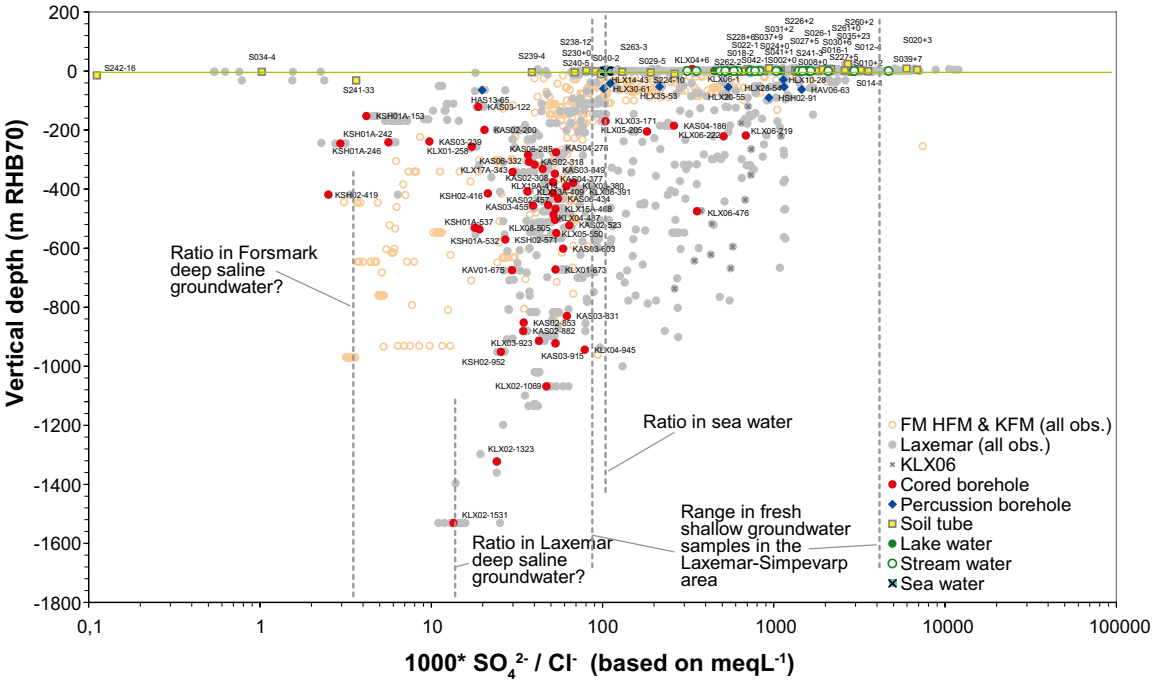


***Figure 4-10.*** *$SO_4^{2-}/Cl^-$ ratio versus depth in the Laxemar-Simpevarp area compared with samples from the bedrock in the Forsmark area. Coloured marks represent data from the Laxemar-Simpevarp area based on data selection C, cf Section 2.2.5. Closed grey marks represent individual samples from data selection A, whereas corresponding reference data from Forsmark is marked as open orange circles. Observations from the cored borehole have been additionally marked by a grey "X". For an explanation of labels, symbols and lines, see Sections 2.3.11. and 2.3.12.*

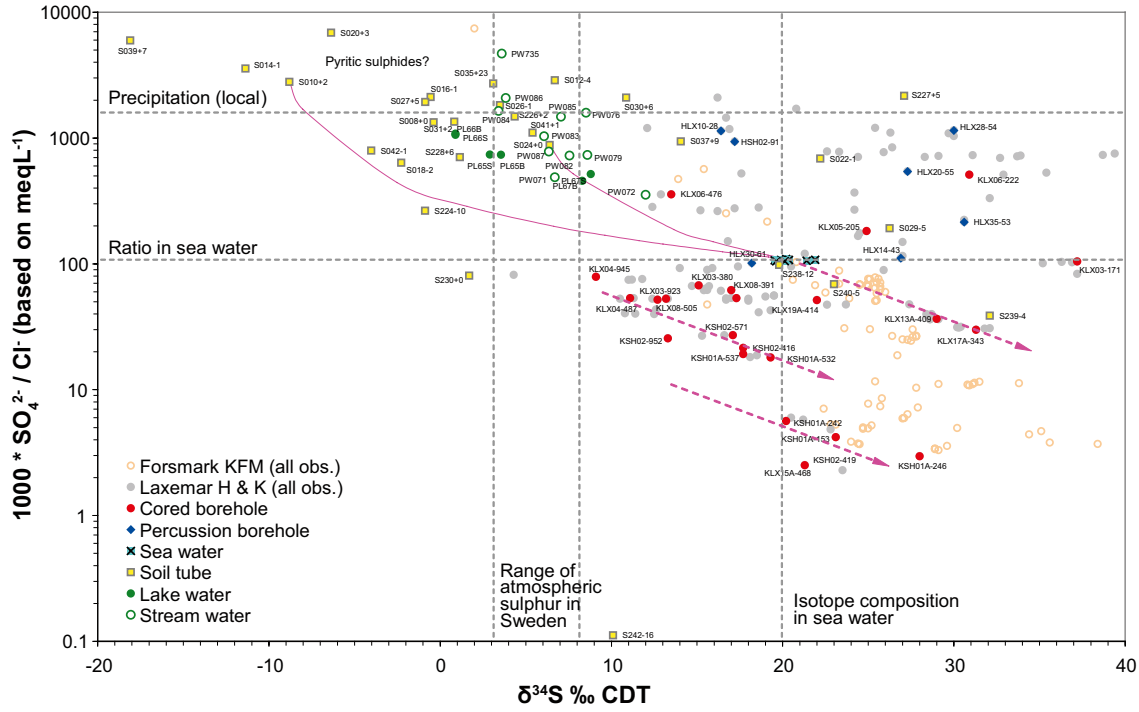


***Figure 4-11.*** *$SO_4^{2-}/Cl^-$ ratio (based on meqL$^{-1}$) versus the isotopic deviation of $^{34}S/^{32}S$ from the international standard (expressed as ‰ deviation from CDT. See Section 2.3.3 for an explanation of the isotope nomenclature). Groundwater data from the bedrock in the Forsmark area are included as reference as orange open circles. Coloured marks in this figure are based on data selection C, cf Section 2.2.5, whereas grey marks represent individual groundwater samples from cored and percussion boreholes from data selection A. For an explanation of labels, symbols and lines, see Sections 2.3.11 and 2.3.12.*

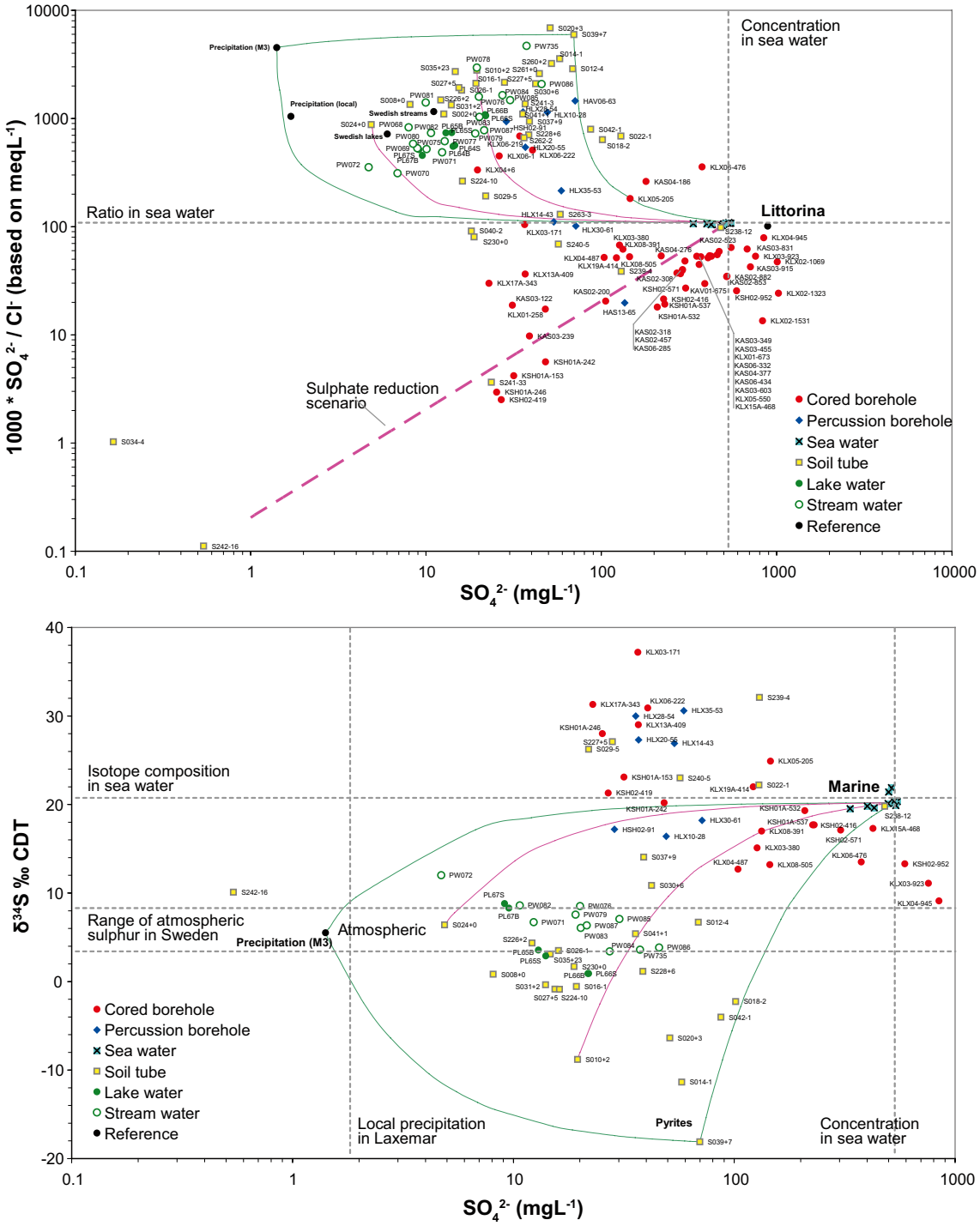


***Figure 4-12.*** *Upper: $SO_4^{2-}/Cl^-$ ratio (based on $meqL^{-1}$) versus $SO_4^{2-}$ concentration ($mgL^{-1}$). Lower: $\delta^{34}S$ (‰CDT) versus $SO_4^{2-}$ concentration. The green coloured line encloses theoretical mixing combinations between three hypothetical end-members. Based on data selection C, cf Section 2.2.5. For an explanation of labels, symbols and lines, see Sections 2.3.11 and 2.3.12.*

- According to the Ion Source Model (cf Section 7.2), two soil tubes located in till beneath sea sediments contain mainly ions of marine origin. This is evident for SSM000238 (denoted S238 in figures) in Figure 4-11, where both the $SO_4^{2-}/Cl^-$ ratio and the $\delta^{34}S$ signature are identical to sea water and consequently show no signs of sulphate reduction. In SSM000239 on the other hand, which is located in a similar setting, the $\delta^{34}S$ signature and the concomitant decrease in the $SO_4^{2-}/Cl^-$ ratio indicate that sulphate reduction may have taken place, starting with a composition similar to sea water. This soil tube also plots along the sulphate reduction scenario in the upper panel of Figure 4-12.
- Like the previously described soil tubes, SSM000241 and SSM000242 are also located in till beneath sediments in a similar setting, but with the difference that these sediments are thicker. Both tubes plot along the sulphate reduction scenario in the upper panel of Figure 4-12, which means that the composition may be explained by withdrawal of $SO_4^{2-}$ from sea water. However, the low $\delta^{34}S$ of +10‰ CDT in SSM000242 ($\delta^{34}S$ is not yet available in S241) indicates that other sources of sulphur may have produced the observed signatures (cf Section 7.2).
- In the upper parts of the bedrock (mainly represented by percussion boreholes) as well as in a few shallow groundwater objects (S022, S029 and S227), positive $\delta^{34}S$ values are noted in these more or less dilute waters. If it is not an artefact due to the low $SO_4^{2-}$ concentrations, this signature may be interpreted as indicating that sulphate reduction has acted on sulphur originating from another source than marine $SO_4^{2-}$ , e.g. pyritic or atmospheric sulphur.
- The composition of several samples from the upper 500 metres of the bedrock can be explained by reduction of sulphate originating from two different sources of $SO_4^{2-}$; marine sulphate and deep saline sulphate. The dashed pink arrows in Figure 4-11 indicate the approximate direction in which observations hypothetically move due to sulphate reduction. The upper arrow, which starts at modern sea water, may explain the composition in e.g. KLX13A-409 and KLX17A-343 as well as in SSM000239, whereas the two lower (more speculative) arrows may explain the composition in several boreholes starting from the composition of a presumed deep saline $SO_4^{2-}$source.

In conclusion: sulphur in the fresh surface system is of atmospheric or local pyritic origin. Sulphur originating from sea water is of minor importance, except for in a few soil tubes where marine relicts or contamination of modern sea water may be significant. In the bedrock, sulphur of deep saline origin is an additional source that mixes with relict marine sulphur. According to thermodynamic calculations in /Laaksoharju (ed) 2008/, equilibrium with gypsum is of minor importance in the surface system, but can have significant influence in deep saline groundwater at greater depths. In the upper parts of the bedrock, which is characterised by meteoric recharge, sulphur of atmospheric or pyritic origin seem to dominate. There are also several indications that reactions such as microbially mediated sulphur reduction have taken place both in shallow groundwater in the deposits and in groundwater of the bedrock.

### 4.1.4 On the origin of calcium, strontium and magnesium (Ca, Sr, Mg)

Calcium concentrations in the surface system in the Laxemar-Simpevarp area are normal compared with the levels usually measured in Sweden /Tröjbom and Söderbäck 2006/. Normal in a Swedish context means ‘low’ due to the sparse occurrence of calcareous bedrock. Calcium may also originate from calcite rich Quaternary deposits, such as in the Forsmark area where the till contains large amounts of calcite originating from the Cambrian and Ordovician sedimentary bedrock on the sea floor in Gävlebukten 100 km north of the site /Tröjbom et al. 2007/.

In the Laxemar-Simpevarp area, the till is mainly of local origin /Sohlenius and Hedenström 2008/ and is usually almost free of calcite. Measurements of 27 till samples contain between 0.1% and 0.6% calcium carbonate per dry weight according to /Tröjbom and Söderbäck 2006/. There are however two till samples in a later study that contained 2.1% and 4.5% of calcium carbonate, respectively. Some gyttja-clay sediments also contain calcium carbonate in the form

of shells (Gustav Sohlenius, pers. comm.). Besides calcite, other minerals such as Ca-bearing silicates may contribute Ca through weathering processes, but usually at a significantly lower rate (cf Section 4.2.1).

Detailed evaluations of the carbonate system in the Laxemar-Simpevarp area has however revealed that calcite probably plays an important role in the dynamics of inorganic carbon as well as Ca in surface system, in spite of the low calcite contents reported in the regolith. The main reason is that carbonate minerals are more reactive and soluble than silicate minerals and they regulate the hydrochemistry of surface waters even if they are present only at trace levels in granitic rocks. Furthermore, fracture filling calcites present in the bedrock is probably an important factor in the evolution of the recharge waters present in the upper parts of the bedrock (see /Laaksoharju (ed) 2008/ for an in depth evaluation of the Ca dynamics in the Laxemar-Simpevarp area.).

The following conclusions about the origin of Ca can be drawn from Figure 4-13:

- The linear relationship between Ca and $HCO_3^-$ close to the 1:1 molar line may indicate that calcite is involved in the dynamics of these elements in surface waters and shallow groundwater. However, this 1:1 relationship may theoretically also be the result of weathering of Ca-bearing silicates such as Ca feldspar.
- Some soil tubes and most of the deeper observations in cored and percussion boreholes plot above the 1:1-line. This pattern is probably attributed to increasing concentrations of Ca originating from deep saline groundwater (shield brine), which is characterised by high contents of Ca and Cl (cf Section 4.1.2). Withdrawal of $HCO_3^-$ by reactions could also contribute to this pattern.
- Most observations from percussion boreholes and some observations from the upper levels of some cored boreholes as well as a few soil tubes plot below the 1:1-line. This indicates a deficiency of Ca if the original Ca source is assumed to be calcite. Ion exchange may be an explanation for this pattern, which is also evident for a number of other parameters (cf cation exchange in Section 4.2.2). Withdrawal of Ca through gypsum precipitation can also contribute to this pattern, but this hypothesis is rejected by thermodynamic calculations in /Laaksoharju (ed) 2008/ indicating that gypsum is undersaturated in all these waters. Moreover, biogenic $HCO_3^-$ may contribute to the observed deviation, although this $HCO_3^-$-source is probably not sufficient to explain more than a fraction of the observed pattern. The lowest located observations in this cluster are hard to explain by this process, which shifts observations horizontally from left to right.
- Two observations from soil tubes located beneath lake and sea sediments (SSM000241 and SSM000242) show anomalously high contents of $HCO_3^-$, which is probably attributable to microbial breakdown of organic matter, perhaps in combination with calcite dissolution (cf Section 7.2).

In order to understand the origin and fate of Ca, the closely related element Sr can be a supportive parameter. As different sources may have differing Ca/Sr ratios, this ratio, possibly in combination with the isotopic composition of Sr, can discriminate among different Ca sources. These bivalent elements, which are able to substitute for each other in mineral lattices, are also slightly differently affected by specific processes as cation exchange, which may reflect changes in the groundwater.

In Figure 4-14, where Ca is plotted versus Sr in a log-log scaled diagram, observations that have the same Ca/Sr ratio plot along diagonal straight lines. This picture could be interpreted as if the surface system is mainly influenced by one Ca source, whereas groundwater in the bedrock is mainly influenced by another source with a differing Ca/Sr ratio:

- The major source in shallow groundwater and in surface water is probably local weathering of minerals in the Quaternary deposits. Ca and Sr concentrations in lake and stream water can be explained by dilution of the slightly more concentrated shallow groundwater which is present in most soil tubes. The median molar Ca/Sr ratio in till samples from the Laxemar-Simpevarp area is about 400 /Tröjbom and Söderbäck 2006/, which can be compared to a

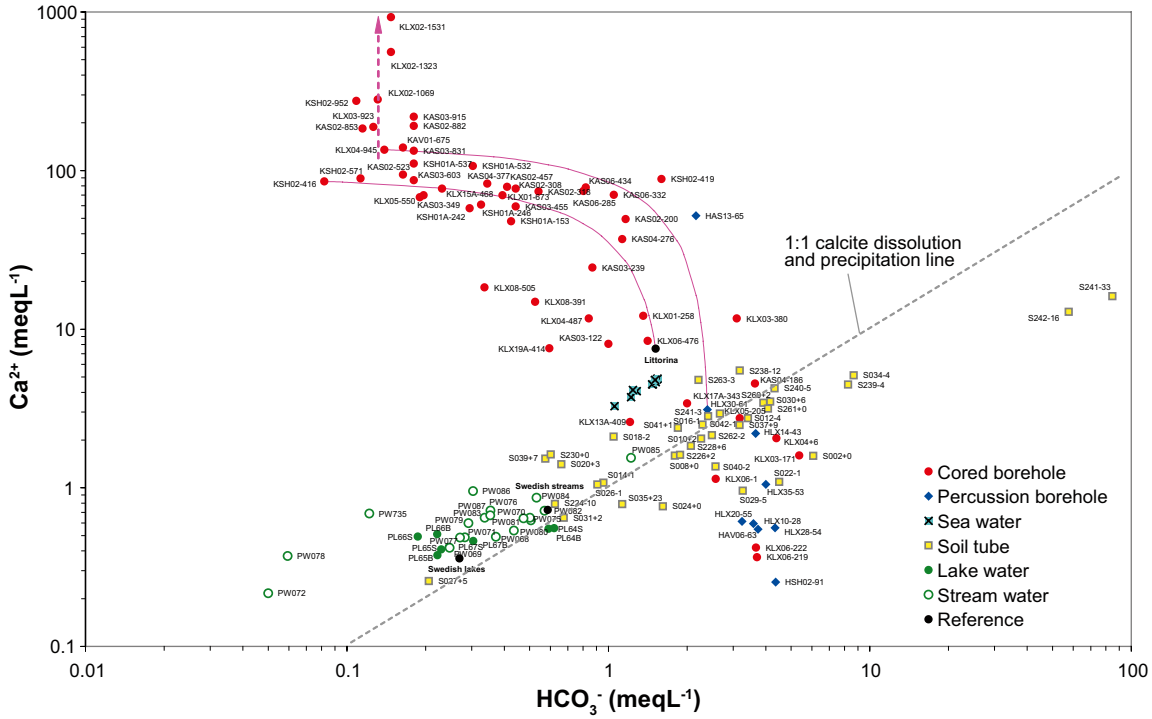


***Figure 4-13.*** *Ca versus $HCO_3^-$ ($meqL^{-1}$). The grey dashed line indicates the 1:1 molar (charge) relationship between Ca and $HCO_3^-$. Based on data selection C, cf Section 2.2.5. For an explanation of labels, symbols and lines, see Sections 2.3.11 and 2.3.12.*

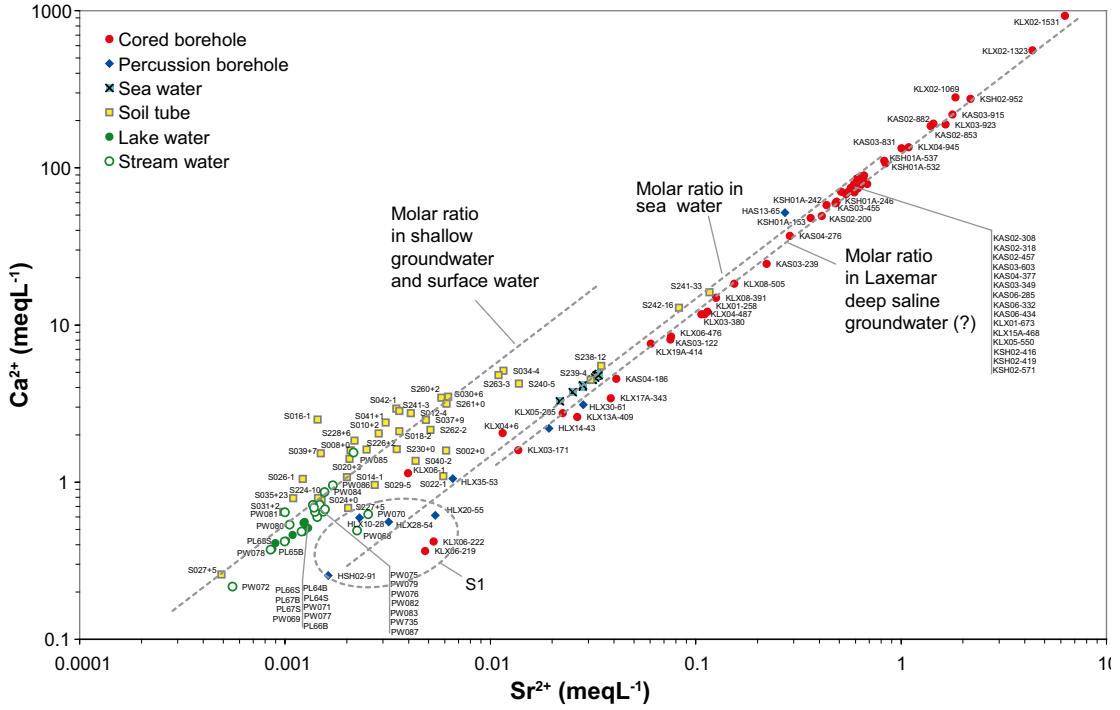


***Figure 4-14.*** *$Ca^{2+}$ versus $Sr^{2+}$ ($meqL^{-1}$). Dashed grey lines in the log-log scaled diagram connect observations of the same Ca/Sr ratio. This figure is based on data selection C, cf Section 2.2.5. An explanation of labels, symbols and lines is given in Sections 2.3.11 and 2.3.12.*

ratio of 500 in fresh surface waters and 100 in deep saline groundwater. Cation exchange reactions, which discriminate slightly differently between $Ca^{2+}$ and $Sr^{2+}$, probably contribute to the spread around the indicated sources.

- Samples from the bedrock (cf Figure 4-14) plot with a constant Ca/Sr ratio, which could be interpreted as indicating that deep saline groundwater (shield brine) is the major source of these elements in groundwater found at deeper levels in the bedrock. The quasi-conservative behaviour of Ca reported by /Laaksoharju (ed) 2008/ also implies that mixing is the main process controlling Ca as well as Sr in the deep groundwater of the bedrock. The marine composition is very close to the deep saline source, which makes the discrimination between the deep saline and marine sources ambiguous with respect to only Ca and Sr.
- A few groundwater observations from percussion boreholes (marked S1), as well as from the upper levels of a few cored boreholes, plot along a Ca/Sr ratio corresponding to deep saline groundwater. The signature of this dilute water may possibly be explained by chemical reactions rather than mixing (dilution) with a deep saline component (see Section 4.2.2 concerning cation exchange).

By using Sr isotopes, further information on the origin of Ca can be revealed. The isotopic ratio $^{87}Sr/^{86}Sr$ has been measured in a subset of samples, and in Figure 4-15 the molar Ca/Sr ratio (corresponding to the straight lines in Figure 4-14) is plotted versus the $^{87}Sr/^{86}Sr$ ratio:

- These three parameters clearly discriminate between the major water types in the Laxemar-Simpevarp area. Most soil tubes and fresh surface waters form a cluster with an elevated Ca/Sr ratio and with $^{87}Sr/^{86}Sr$ values exceeding both marine and deep saline signatures. The Ca/Sr and $^{87}Sr/^{86}Sr$ ratios may be explained by a common source in the surface system characterised by an elevated Ca contents (compared to e.g. the marine source) together with a specific Sr isotope signature of this source. The increase (and horizontal spread) in $^{87}Sr/^{86}Sr$ compared to the marine and deep saline sources may to some extent also be explained by ion-exchange processes with clay minerals in the regolith /Peterman and Wallin 1999/. There is also a large variation in the $^{87}Sr/^{86}Sr$ ratio depending on the minerals involved in the weathering process. In minerals sampled at Äspö, biotite has a $^{87}Sr/^{86}Sr$ ratio of 1.409, microcline = 0.716, plagioclase = 0.705 (Bill Wallin, pers. comm.).
- Observations from percussion and cored boreholes show a very uniform composition with regard to both the Ca/Sr ratio and the $^{87}Sr/^{86}Sr$ isotopic composition, indicating that the deep saline source for Ca and Sr dominates in the groundwater in the bedrock.
- Marine water, which exhibits a Ca/Sr ratio similar to the deep saline source, is clearly discriminated by the lower $^{87}Sr/^{86}Sr$ signature.

Among shallow groundwater samples there are a few examples where marine Ca and Sr are mixed with the superficial source representing weathering of local minerals (SSM000002, 30, 34, and 40 and KSH01A-246). SSM000022 displays a Ca-Sr signature corresponding to the deep saline source (cf Section 7.3), whereas SSM000242 seems to contain a mixture of the marine and deep saline sources of these elements (cf Section 7.2).

Another possible source of Ca (as well as Mg) is congruent dissolution of dolomite ($CaMg(CO_3)_2$), forming equal molar amounts of Ca and Mg. In Figure 4-16 where Ca is plotted versus Mg, straight diagonal lines connect observations with the same Ca/Mg ratio:

- Very few samples plot along the 1:1 molar line for Ca and Mg, which rejects dolomite as a significant source of these elements in the Laxemar-Simpevarp area. This is neither expected due to the generally low contents of carbonates in the overburden.
- Many soil tubes scatter around a constant Ca/Mg ratio which can be interpreted as indicating that there could be a common mineral source for these elements in e.g. the overburden. Different portions of Mg in relation to Ca for these minerals (or differing weathering rates), may contribute to the spread among these samples. Most samples from the surface system are slightly depleted in Ca compared to the general picture in shallow groundwater (they

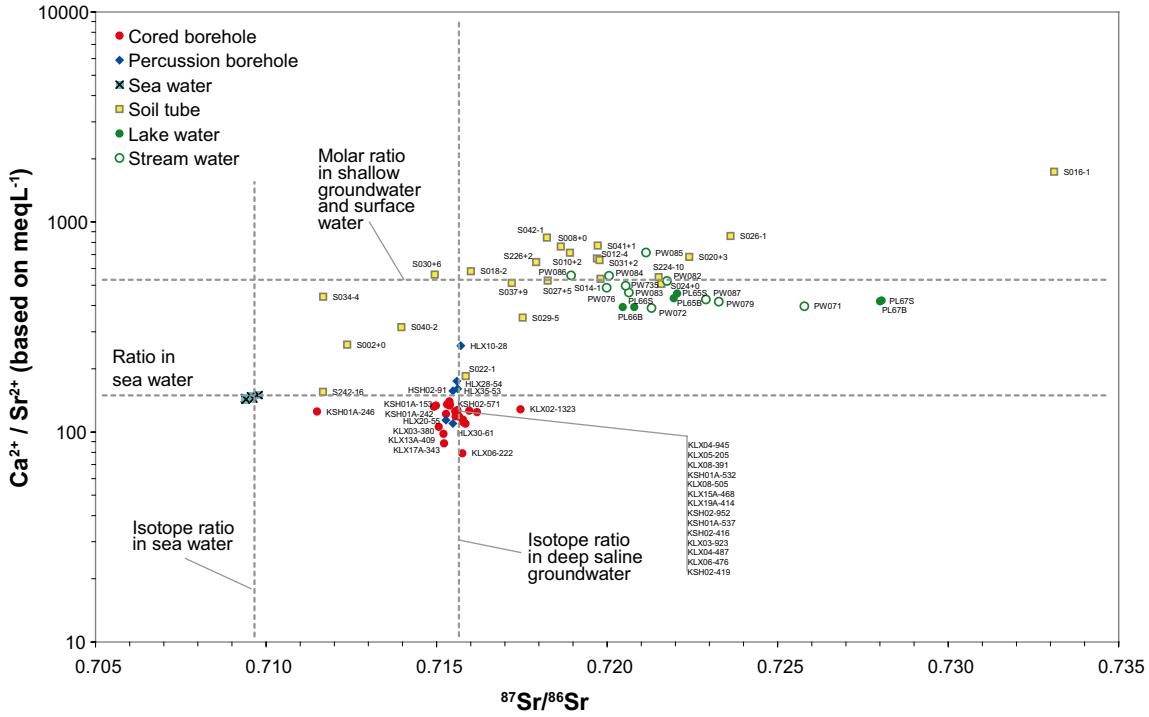


***Figure 4-15.*** *Ca/Sr ratio versus the isotopic ratio of $^{87}Sr/^{86}Sr$. The figure is based on data selection C, cf Section 2.2.5. An explanation of labels, symbols and lines is given in Sections 2.3.11 and 2.3.12.*

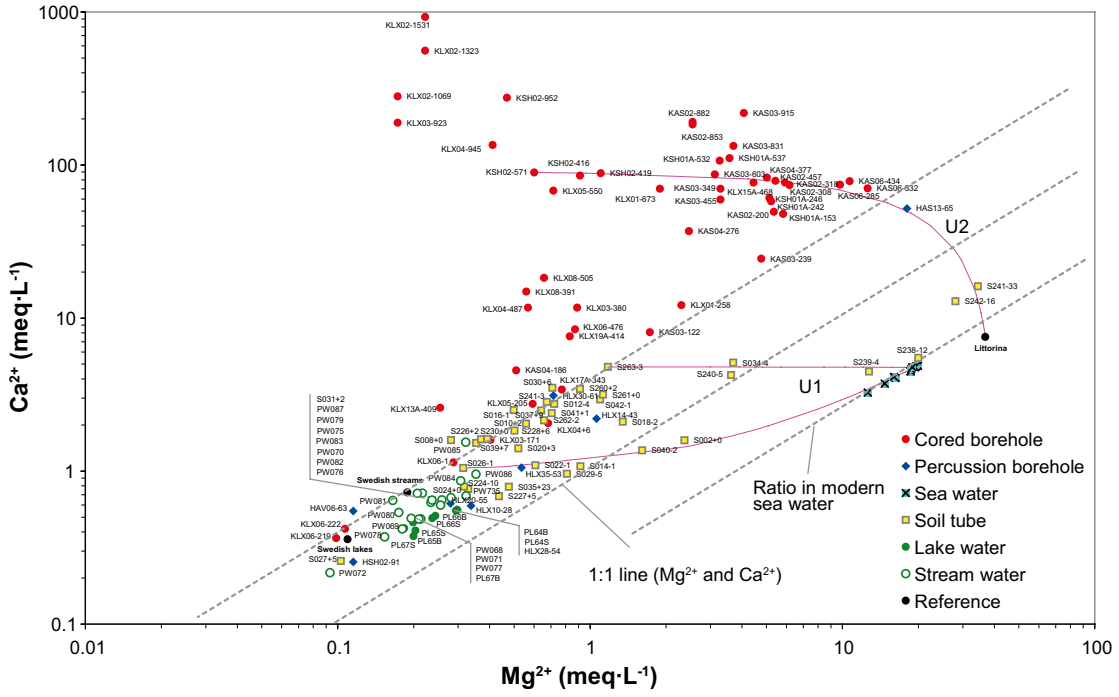


***Figure 4-16.*** *Ca versus Mg (meq·L$^{-1}$). Dashed grey lines in the log-log scaled diagram connect observations with the same Ca/Mg ratio. The figure is based on data selection C, cf Section 2.2.5. For an explanation of labels, symbols and lines see Sections 2.3.11 and 2.3.12.*

are shifted below the dashed grey line that connects many soil tubes). This shift may be attributable to removal of Ca by cation exchange reactions in the deposits, different biological uptake of these ions in plants and algae or calcite precipitation. This shift may also be attributable to the input of summer road salt enriched in Mg (cf Section 6.2.1).

- According to the hypothetical mixing scenario marked U1, the deviations displayed by shallow groundwater in some soil tubes can be explained by mixing with a marine source. Two soil tubes (SSM000241 and 242) and one percussion borehole (HAS13-65) fits the hypothetical mixing scenario with Littorina Sea water marked U2. As Mg is a possible marine indicator, the shift along U2 may possibly be attributable to marine intrusions in the bedrock during pre-historic time, although the scattering of the groundwater samples around these trends implies that Mg probably is also significantly affected by reactions (cf /Laaksoharju (ed) 2008/. Most observations that follow U2 are located in areas near the Baltic Sea, which were covered by the Littorina Sea according to Figure 4-1.
- There is no stable Ca/Mg ratio evident among deep groundwater samples in the upper part of Figure 4-16. Accordingly, there is no indication on a common source for these elements in deep saline groundwater; when Ca increases, Mg seems to be more or less totally depleted.

The major conclusions regarding the origin of calcium, strontium and magnesium are summarised in the bulleted list below:

- In the surface system, the major source of Ca, Sr and Mg seems to be weathering of local minerals in the Quaternary deposits. Although present only in low amounts in the regolith, there are indications that calcite play an important role in the dynamics of Ca in the Laxemar-Simpevarp area /Laaksoharju (ed) 2008/. A few observations indicate that these elements also originate from a marine source, such as relict marine remnants or deposition of sea spray (which is most evident for Mg).
- Ca and Sr of deep saline origin (shield brine) is a significant source of these elements in the groundwater in the bedrock.
- The deep saline groundwater is virtually free of Mg, and the presence of this element at moderate depths could be interpreted as influence from a marine source (for example sea water of Littorina origin). The supposed non-conservative behaviour of Mg in the deep groundwater however makes conclusions based on this parameter less reliable /Laaksoharju (ed) 2008/.

### 4.1.5 On the origin of carbon, nitrogen and phosphorus (C, N, P)

Carbon in groundwater and surface water originates from the atmospheric carbon pool, from carbonates in the rock and overburden, and from microbial reactions involving fossil organic carbon relicts at the site. Moreover, geogenic carbon may also contribute at deeper levels.

Different reactions may act as sinks for carbon. Organic carbon is originally formed during photosynthesis and $CO_2$ assimilation from the atmosphere by plants and algae. This fixed carbon is gradually returned to the atmosphere as $CO_2$ during respiration by animals and bacteria. In soil, biogenic degradation of organic matter (respiration) often causes very high partial pressures of $CO_2$, which lead to high concentrations of dissolved inorganic carbon. Precipitation of carbonates may transfer carbon to the geosphere, whereas for example biogenic processes such as methanogenesis and respiration transfer carbon to the atmospheric pool.

In water, carbon occurs in inorganic or organic compounds. Inorganic carbon involves the carbonic acid dissociation series, ranging from dissolved $CO_{2(aq)}$, to hydrated carbon dioxide ($H_2CO_3$ – carbonic acid), bicarbonate ions ($HCO_3^-$) and carbonate ions ($CO_3^{2-}$). The equilibrium between these species is determined by pH, and at the neutral to slightly acid conditions that prevail in the Laxemar-Simpevarp area, most dissolved inorganic carbon (DIC) occur as $HCO_3^-$. Most organic carbon enters the groundwater as dissolved organic carbon (DOC) and may be transported to deeper levels by the recharging meteoric water. In the presence of oxygen, DOC is oxidized by aerobic bacteria, forming $CO_2$ which contributes to DIC. When all oxygen is

consumed, anaerobic bacteria consume DOC using electron acceptors such as $NO_3^-$, Fe(III)-oxihydroxides or $SO_4^{2-}$. Ultimately, methane is formed by bacteria when all other electron acceptors are depleted.

The distribution of dissolved carbon in different water types in the Laxemar-Simpevarp area is outlined in Figure 4-17. The upper left panel shows that $HCO_3^-$ constitutes most dissolved inorganic carbon (DIC) in surface waters (although the systematic shift above the 1:1 line indicates that there is a slight discrepancy between these independent measurements as the contents of $HCO_3^-$-C should be equal to or lower than the total DIC). In the upper right panel, it is evident that dissolved organic carbon (DOC) constitutes most total organic carbon (TOC) in all water types. The slight shift of TOC above the 1:1 line is attributed to particulate organic carbon, e.g. algae or organic debris. When inorganic carbon (here represented by $HCO_3^-$-C) is plotted versus the concentration of dissolved organic carbon (which is equal to total organic carbon), the following conclusions can be drawn:

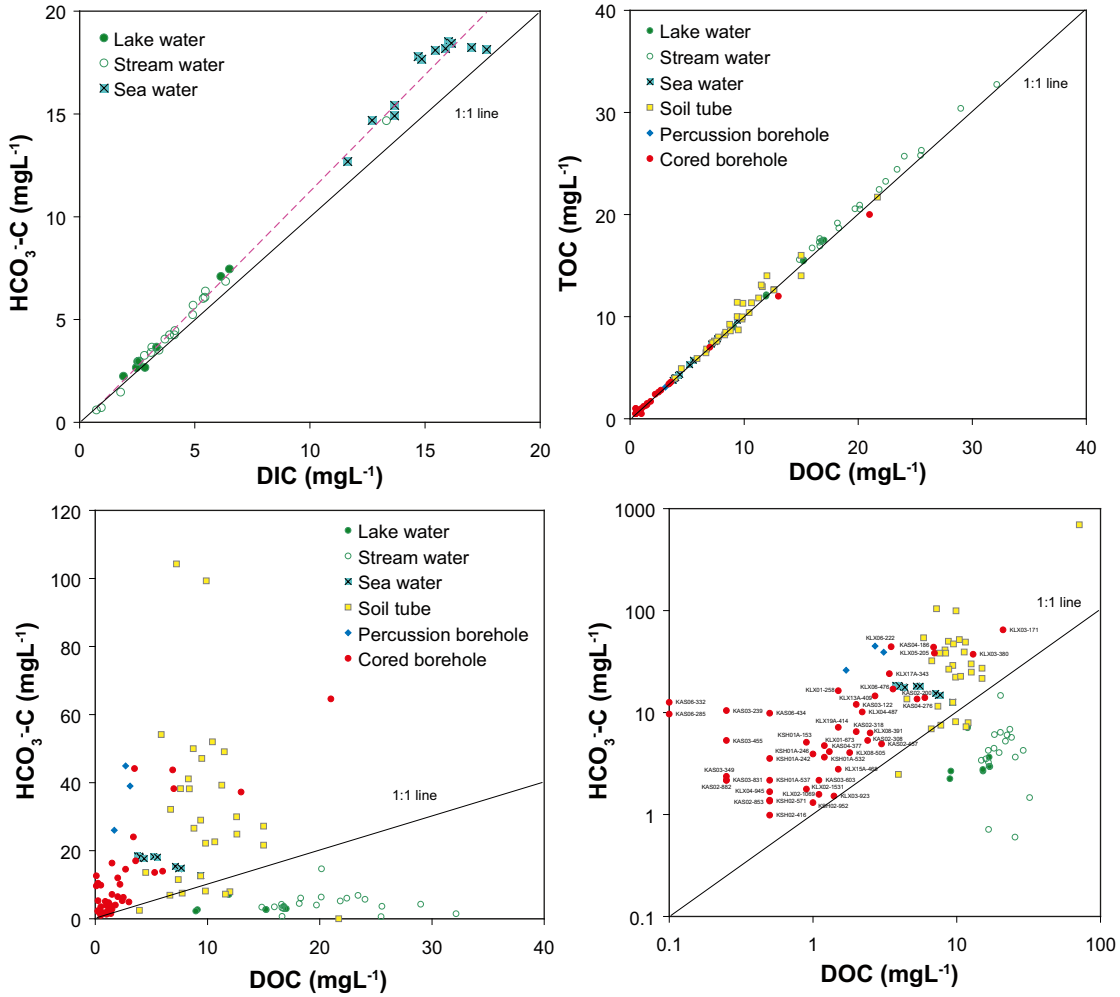


***Figure 4-17.*** *Comparisons of different carbon parameters that reflect inorganic and organic carbon in the Laxemar-Simpevarp area. These figures are based on data selection C, cf Section 2.2.5. The lower panels show the same plot in linear and logarithmic scales.*

- Lake and stream water often contain high concentrations of dissolved organic carbon, and the organic fraction largely predominates over the dissolved inorganic carbon in these water types.
- Shallow groundwater usually contains both organic and inorganic carbon. The inorganic fraction normally predominates and is on the average three times larger than the organic carbon content.
- In the upper parts of the bedrock, represented by percussion boreholes and upper sections of cored boreholes, organic carbon is present at lower concentrations compared to shallow groundwater, whereas the level of inorganic carbon is comparable to that in shallow groundwater.
- At deeper levels in the bedrock both organic carbon and inorganic carbon decrease towards greater depth according to the logarithmic graph in the lower right. At great depths the concentration of organic carbon is very low, whereas concentrations of dissolved inorganic carbon are usually slightly higher.

Different carbon sources often show typical carbon-isotope signatures which reflect the involved reactions. Radiogenic $^{14}C$, which is naturally formed in the upper atmosphere and present in all living matter at very low concentrations, can discriminate between modern carbon and different sources of relict carbon due to the half-life of 5,730 years (cf Section 3.5.2 dealing with dating by $^{14}C$). Reactions mediated by bacteria are usually accompanied by isotope fractionations that clearly shift the proportions of the stable carbon isotopes $^{12}C$ and $^{13}C$. In groundwater in the bedrock the ratio between the stable isotopes $^{13}C/^{12}C$ mainly reflects inorganic carbon, whereas measurements of lake and stream water mainly reflect organic carbon (cf lower panels of Figure 4-17). In shallow groundwater, the isotope measurements reflect a mixture of organic and inorganic carbon. The relative deviation of this ratio from the international $^{13}C$ standard PDB is expressed per mille and denoted $\delta^{13}C$ (cf Section 2.3.3). Atmospheric $\delta^{13}C$ is currently decreasing from originally around –6.4‰, due to the extensive burning of fossil carbon depleted in $^{13}C$.

When $\delta^{13}C$ versus $HCO_3^-$ is examined in Figure 4-18, most observations in surface water and shallow groundwater can be seen to plot within a $\delta^{13}C$ span bounded at the lower end by dissolved $HCO_{3\,(aq)}^-$ ($\delta^{13}C$ –22‰ PDB at pH 5.7) and at the upper end by $\delta^{13}C$ of –10‰ PDB. At pH 6.5, a typical value in shallow groundwater in the Laxemar-Simpevarp area /Tröjbom and Söderbäck 2006/, dissolved $HCO_{3\,(aq)}^-$ derived from biogenic $CO_{2(g)}$ ($\delta^{13}C$ –23‰ PDB) shows a theoretical $\delta^{13}C$ value of about –18.5‰ at 25°C due to fractionation during hydration of $CO_{2(aq)}$ /Clark and Fritz 1997/. Carbon originating from dissolution of marine limestone usually has a $\delta^{13}C$ enrichment of about 0‰ /Clark and Fritz 1997/, whereas Baltic Sea water in the Laxemar-Simpevarp area usually shows $\delta^{13}C$ values between –3 and 0‰ PDB.

The following conclusions regarding the origin of carbon can be drawn from Figure 4-18:

- Most samples from the surface system are centred on the theoretical $\delta^{13}C$ value –18.5‰ PDB, which is derived when biogenic carbon is dissolved in the soil solution at pH 6.5. This may be interpreted as if both organic and inorganic carbon at this level mainly originate from biogenic sources. Microbial degradation (respiration) of organic matter emits $CO_2$, which is dissolved in the soil solution and when hydrolysed inorganic $HCO_3^-$ is formed.
- Observations from the bedrock also plot close to, or slightly above, the biogenic source, which means that carbon at these levels theoretically could be of biogenic origin. Another explanation to this pattern is carbon derived from dissolution of calcite of non-marine origin (in such case $\delta^{13}C$ coincide with the biogenic signature).
- Two soil tubes, SSM000022 and SSM000012, both located on Ävrö, show enriched $\delta^{13}C$ values, which could be explained by calcite dissolution according the scenario marked by the dashed pink line. The addition of carbon enriched in $^{13}C$ from calcite dissolution shifts the original $\delta^{13}C$ values towards more positive values, and if all $H^+$ ions that drive the calcite dissolution are derived from dissolved biogenic $CO_2$, the theoretical maximum $\delta^{13}C$ value is –7.5‰ PDB (50% carbon from calcite, 50% from biogenic $CO_2$ according to the formula in Figure 4-18). Low $^{14}C$ activities in the two soil tubes may further support the contention that much of the carbon is derived from calcite dissolution (cf Figure 4-19).

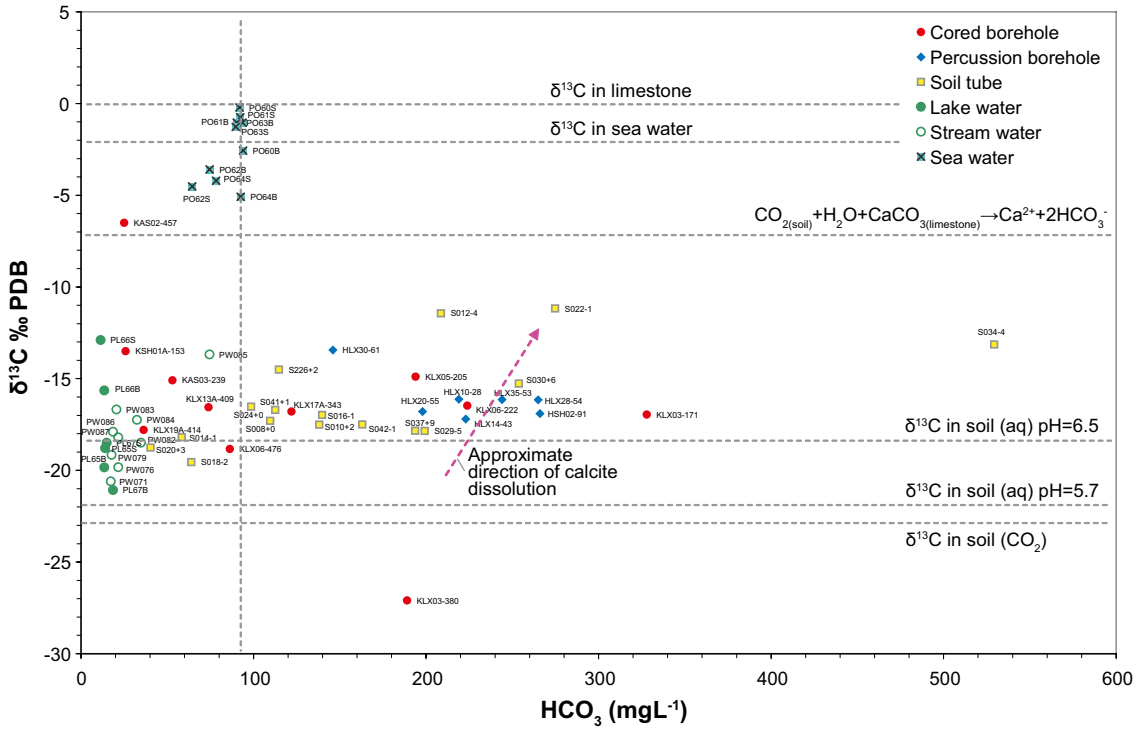


***Figure 4-18.*** *$^{13}C$ expressed as the ‰ deviation from the international standard PDB versus $HCO_3$ ($mgL^{-1}$). This figure is based on data selection C, cf Section 2.2.5. An explanation of labels, symbols and lines is given in Sections 2.3.11 and 2.3.12.*

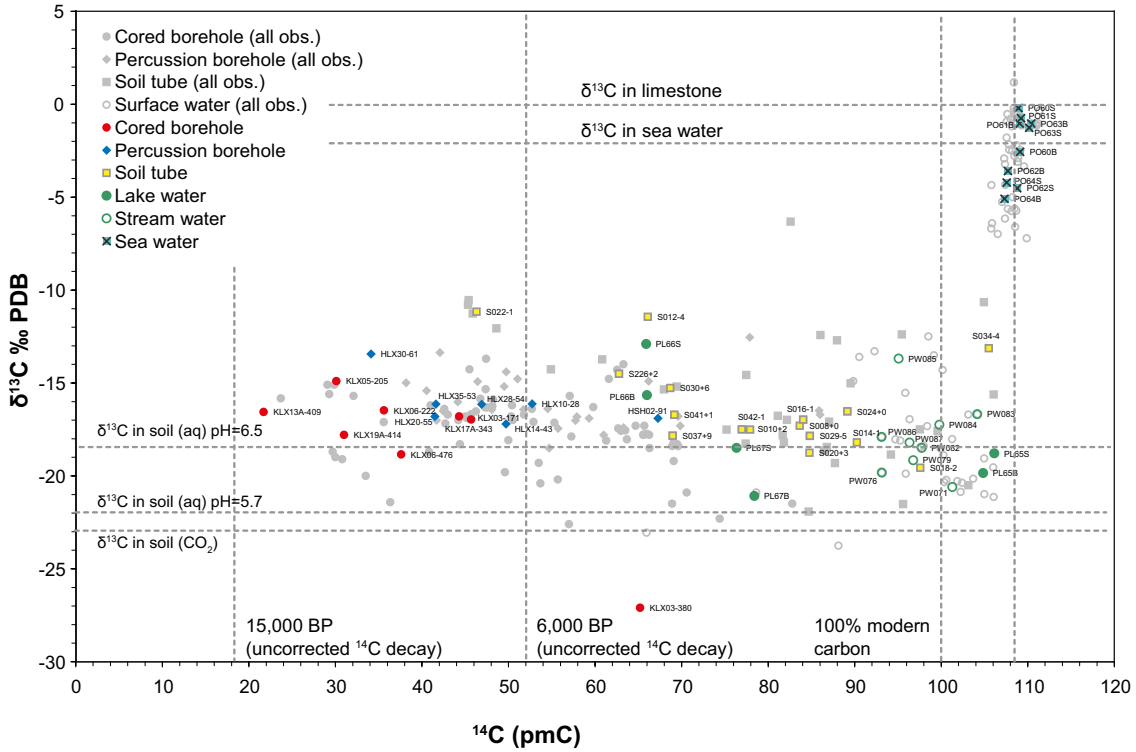


***Figure 4-19.*** *$^{13}C$ expressed, as deviation from the international standard PDB, versus $^{14}C$ activity, expressed as percent modern carbon (pmC). This figure is based on data selection C, cf Section 2.2.5. Individual samples from data selection A are included as grey marks to give an idea of the spread. An explanation of labels, symbols and lines is given in Sections 2.3.11 and 2.3.12.*

The radiogenic isotope $^{14}C$ can, in combination with $\delta^{13}C$, provide further information on the origin of carbon. In Figure 4-19, $\delta^{13}C$ is plotted versus $^{14}C$ activity expressed as percent modern carbon. This plot is also used in Section 3.5.2 dealing with dating and estimates of groundwater residence time with $^{14}C$ and $^{3}H$.

Figure 4-19 gives a similar picture as Figure 4-18, but with the addition of age information due to $^{14}C$ decay instead of the $HCO_3^-$ concentration. As discussed in Section 3.5 age estimations of $^{14}C$ are ambiguous and it should be held in mind that estimations apply to the average carbon-age rather than actual water residence times. Radioactive decay decreases the $^{14}C$ activity with time with a half-live of 5,730 years, whereas addition of carbon derived from calcite dissolution leads to a dilution of carbon with zero $^{14}C$ activity. Depending on the source of the calcite, carbon input from calcite dissolution makes different imprints in the visualisations: If the calcite present in the regolith is of marine origin ($\delta^{13}C$ = 0‰ PDB, $^{14}C$ = 0 pmC) there should be a simultaneous change in both isotopes if there is a significant carbon input from calcite dissolution. According to Figure 4-19, there is little general correlation between the carbon isotopes, which could be interpreted as if $^{14}C$ dilution effects of calcite of marine origin probably are of less importance (cf Sections 4.1.2 and 3.5.2). An implication of this interpretation is that the carbon ages in the surface system mainly reflects the age of biogenic carbon. On the other hand, if the calcites in the regolith do not originate from a marine environment, dated biogenic carbon could not be distinguished from carbon derived from calcite dissolution and the biogenic carbon age is likely overestimated.

Depending on the carbon species present in the sample, the carbon age reflects either the organic or inorganic species, or a mixture of both types:

- Many samples from stream water show $^{14}C$ activities lower that the present day activity of approximately 110 pmC. Since these waters mainly contain organic carbon (cf Figure 4-17), this shift may indicate that the organic carbon source has an average age of several hundred or thousand years (cf Section 3.5.2). A possible source of this carbon could be decomposition of peat.
- If they are not an analytical artefact, samples from Lake Jämsen (PL67) and Lake Götemar (PL66) show even higher average carbon ages. At least in the case of Lake Jämsen this shift can probably not be explained by the input of carbon derived from dissolution of calcite of marine origin according to the $\delta^{13}C$ signature (which corresponds to $\delta^{13}C$ of biogenic origin with no shift towards the marine $\delta^{13}C$ signature at 0 ‰ PDB). A possible explanation in the case of Lake Jämsen is input of aged organic carbon from e.g. peat, whereas the signatures of Lake Götemar may be attributable to calcites.
- Like surface waters, shallow groundwater exhibits low $^{14}C$ activities, which is probably attributable to old organic carbon from e.g. peat. SSM000022 may constitute an exception as this low activity, in combination with an elevated $\delta^{13}C$ signature that to some extent could be explained by dissolution of calcite of marine origin. A marine origin of this calcite is perhaps contradicted by the non-marine Sr isotope signature in Figure 4-15. Another exception is SSM000034, where the elevated $\delta^{13}C$ signature can be explained by mixing with modern marine $HCO_3^-$, or alternatively, as a result of bacterial methanogenesis /Hallbeck 2009./.
- In groundwater in the upper parts of the bedrock, very low $^{14}C$ activities, in combination with biogenic $\delta^{13}C$ signatures, can be interpreted as indicating that the inorganic carbon predominating at these depths originates from an organic carbon source. Alternatively, this signature is a result of carbon input derived from dissolution of non-marine calcite with a $\delta^{13}C$ signature similar to biogenic carbon in the surface system. The age estimations in Section 3.5.2 implies that the carbon input from the surface system must have occurred after the latest glaciation.

The dynamics of nitrogen (N) and phosphorus (P) is closely coupled to the dynamics of organic carbon (C), as these elements are the major constituents of organic matter (the C:N:P stoichiometry of plants is relatively constant at 106:16:1 on a molar basis and 40%:7.2%:1% on dry weight basis /Sterner and Elser 2002/). Like carbon, nitrogen originates from the atmospheric pool, whereas phosphorus mainly originates from mineral sources (weathering or fertilizer input) and is not included in atmospheric cycles (some usually marginal atmospheric phosphate deposition occur).

In the upper panel of Figure 4-20, where the concentration of total nitrogen is plotted against total phosphorus, the content of total organic carbon is displayed as coloured dots. In the lower panel of this plot, individual objects can be identified from object type and Idcode. There are no nitrogen or phosphorus analyses available from groundwater in the bedrock. It can be concluded from Figure 4-20 that:

- The highest TOC concentrations in the Laxemar-Simpevarp area are measured in the fresh surface waters. The concentration of TOC is clearly coupled to N and P according to the increasing gradient along the N/P ratio of 30.
- According to the Swedish environmental water quality criteria /Naturvårdsverket 2000/, most fresh surface waters in the Laxemar-Simpevarp area show a slight N excess, and primary production is probably limited by P (which is the normal situation in fresh waters).
- In brackish water samples from the coastal area, C and N concentrations are generally lower than in fresh water. The N/P ratio indicates equilibrium between these elements or slight N deficiency. The sea water sampling site PSM002060, which is least influenced by discharging surface water, show slight N deficiency, which is in accordance with the normal situation in sea water.
- In shallow groundwater, C and N concentrations are in general lower than in fresh surface water, whereas P concentrations are at the same level or higher. There are however many exceptions in which both N and P are elevated, in combination with moderate C concentrations (e.g. SSM000238, 239, 230 and 261). Microbial degradation of organic matter is the probable source for N and P, which in combination with consumption of organic carbon leads to relatively lower concentrations of TOC (some of this carbon may still be present as inorganic carbon in the form of dissolved $HCO_3^-$, or as methane, $CH_4$). The N/P ratio in these objects is comparable to the theoretical mass ratio in organic matter of 7.
- Two soil tubes located in till beneath sea and lake sediments, SM000241 and 242, show extremely high N and P concentrations, in combination with relatively high concentrations of organic carbon. The N/P ratio of 10 is close to the theoretical ratio of organic matter, which indicates that N and P in this shallow groundwater originate from decomposition of organic matter (cf discussion in Section 7.2).

The major conclusions regarding carbon are summarised in the bulleted list below:

- Dissolved inorganic carbon (DIC), of which $HCO_3^-$ is the main constituent, occurs at normal levels in both surface water and shallow groundwater, compared with the conditions normally measured in the region, as well as in Sweden in general /Tröjbom and Söderbäck 2006/.
- The concentration of organic carbon in the surface system in the Laxemar-Simpevarp area is ‘very high’ according to the Swedish environmental water quality criteria /Naturvårdsverket 2000/.
- According to carbon isotope signatures, inorganic carbon in water samples from the surface system can be interpreted as mainly of biogenic origin. Other carbon sources such as dissolution of calcite or $HCO_3^-$- of marine origin seem to have less influence. In the upper parts of the bedrock similar signatures indicate that biogenic carbon could be an important source at these levels as well.
- According to isotope measurements, decomposition of organic matter, e.g. peat, probably adds organic carbon to the surface waters as well as to shallow groundwater in the area. The $^{14}C$ activities measured in the surface system correspond to average carbon ages of several hundred or thousand years.
- In a few soil tubes (e.g. SSM000241 and 242), microbial decomposition of organic matter present in the Quaternary deposits beneath sea and lake sediments leads to an extreme hydrochemistry. This is for example manifested as very high concentrations of dissolved $HCO_3^-$.

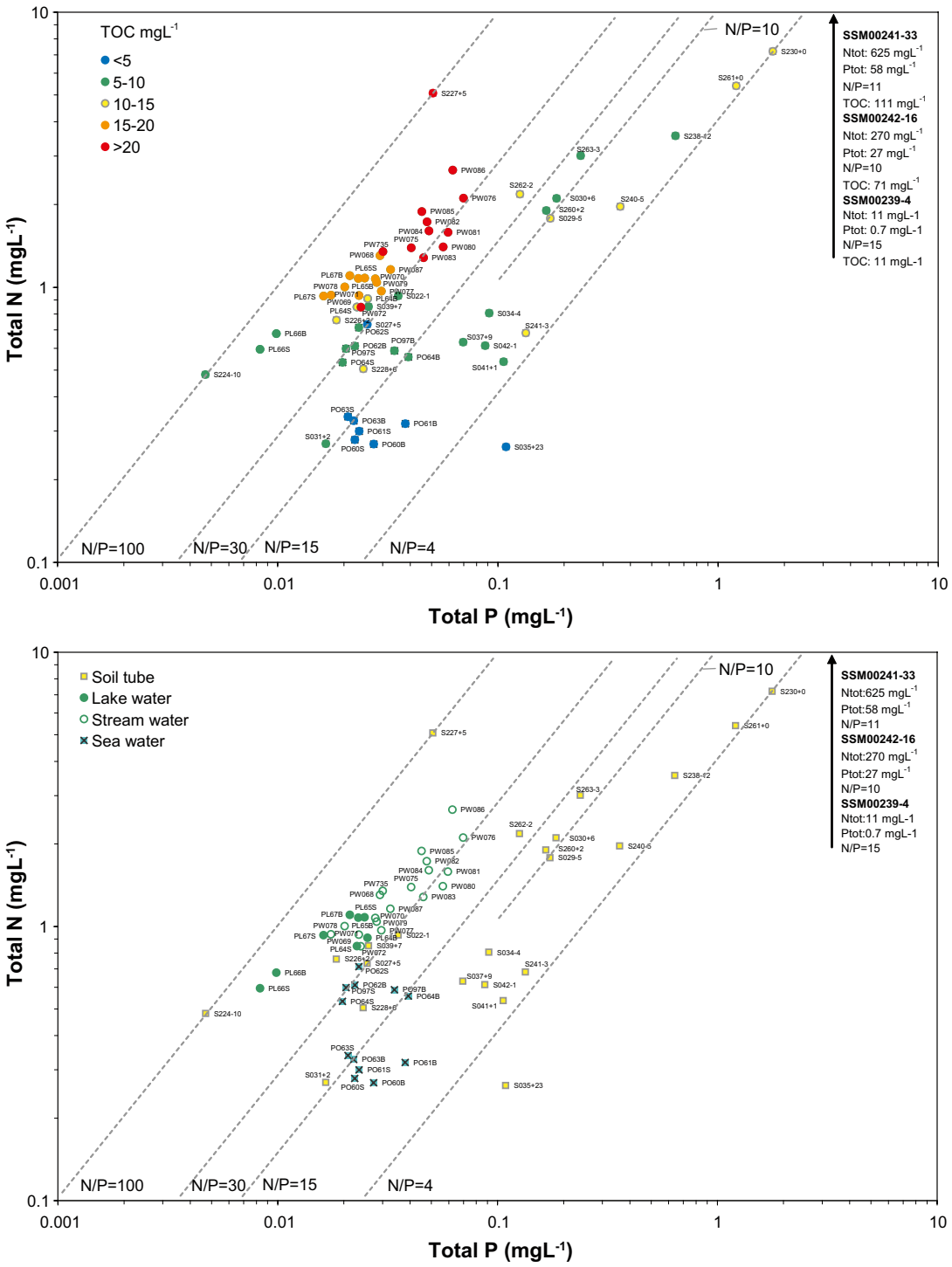


***Figure 4-20.*** *Organic carbon, nitrogen and phosphorus in surface water and shallow groundwater in the Laxemar-Simpevarp area. Total concentrations of nitrogen and phosphorus are plotted on the logarithmic axes, and total content of dissolved organic carbon (TOC) is shown as a colour code per object. Surface water samples are based only on data from June to September. Dashed grey lines connect points with the same N/P mass ratio. Observations in shallow groundwater represent mean values of all available samples.*

## 4.2 Chemical reactions and processes

Besides mixing of different end-members, a large number of previous or ongoing chemical reactions and processes contribute to the present composition of surface water and groundwater. This section focuses on indications of a few important processes that alter the water composition, such as weathering of minerals, ion exchange and in redox reactions. Chemical speices may also be withdrawn from the solution by precipitation. Thermodynamic calculations and solubility control of minerals with focus on groundwater in the bedrock, e.g. calcite and gypsum, are discussed in thoroughly in /Laaksoharju (ed) 2008/. As many reactions are facilitated by bacteria, traces of these reactions are briefly explored.

### 4.2.1 Weathering of minerals

Weak acids of biogenic origin (e.g. carbonic acid and organic acids such as acetic, oxalic and malic acid), as well as strong acids of either natural (e.g. oxidation of sulphides in gyttja-clay sediments used for agriculture) or anthropogenic origin (e.g. sulphur acid of pyritic origin or sulphur deposition originating from fossil fuels) drive weathering processes that dissolve minerals in the Quaternary deposits and in the bedrock. Different minerals are dissolved at different rates and contribute to a varying degree to dissolved ions in groundwater present in the deposits or in surface water due to groundwater discharge. Weathering reactions are reflected in the relative abundance of major ions, and may be used to trace which minerals have been dissolved. Isotopes, such as $^{87}Sr$, may also provide supportive information on weathering reactions (cf Section 4.1.4 and Figure 4-15).

When present, calcite is dissolved at a fast rate, resulting in high concentrations of dissolved $Ca^{2+}$ and $HCO_3^-$, which is evident in all water types in the surface system of the Forsmark area where the Quaternary deposits contain large amounts of calcite /Tröjbom et al. 2007/. In the Laxemar-Simpevarp area, the calcite content in the deposits is almost negligible, which results in a quite different hydrochemistry of the surface system compared to the Forsmark site.

In the Ion Source Model in Section 3.2, the major patterns in the relative composition of major ions are outlined. In this model, the theoretical composition of minerals and salts as well as the element composition of till samples could be projected to explore different mineral sources in relation to hydrochemistry.

In Figure 4-21 a large number of regolith samples from till, clay, sea- and lake sediments are projected onto the Ion Source Model (cf Figure 2-9 and Section 2.2.7), together with the theoretical proportions of ions resulting from carbonic acid weathering of various silicate minerals to kaolinite. Regolith chemistry is further evaluated in /Sohlenius and Hedenström 2008/. The theoretical proportions formed when different kinds of road salt dissolve are also shown for comparison (NaCl, $MgCl_2$ and $CaCl_2$). From this picture it can be concluded that:

- All regolith samples plot in the approximate extension of the trend C-B, in the sector which has been attributed to weathering sources in Section 3.2.6. The discrepancy between the major trend among hydrochemical samples and samples reflecting regolith composition is probably explained by total dissolution by strong acids at preparation and analysis of regolith samples, whereas dissolution by weak acids such as carbonic acid is most important in the groundwater. This picture, however, supports the conclusion that observations which plot in this sector are mostly influenced by ions derived from dissolution of local minerals in the deposits.
- The composition of some regolith samples may not be explained by the selected mineral end-members. This shows that there probably are other minerals or weathering processes present (a complete set of end-members will encompass all samples which constitute mixtures of these end-members).
- There is a systematic difference between till and clay samples on one hand, and sediment samples from sea and lakes on the other hand in that sediments plot more close to the groundwater composition in the deposits. There are also large differences in composition

within different categories, especially among sediments sampled in lakes. For example, samples from the upper sediment levels in Lake Frisksjön (coded 6571_[depth]), deviate from the composition of former marine sediments sampled at greater depth in profiles from this lake. These deeper sediment layers are accordingly more similar to present marine sediments sampled in the brackish basins.

- There are only a few regolith and water samples clustering around the calcite composition, which agrees with the lack of calcite in the Quaternary deposits.

This brief evaluation shows that the hydrochemistry is related to the chemical composition in the Quaternary deposits, as can be expected. Weathering is further discussed in previous sections dealing with the origin of Ca, C and S (cf Section 4.1).

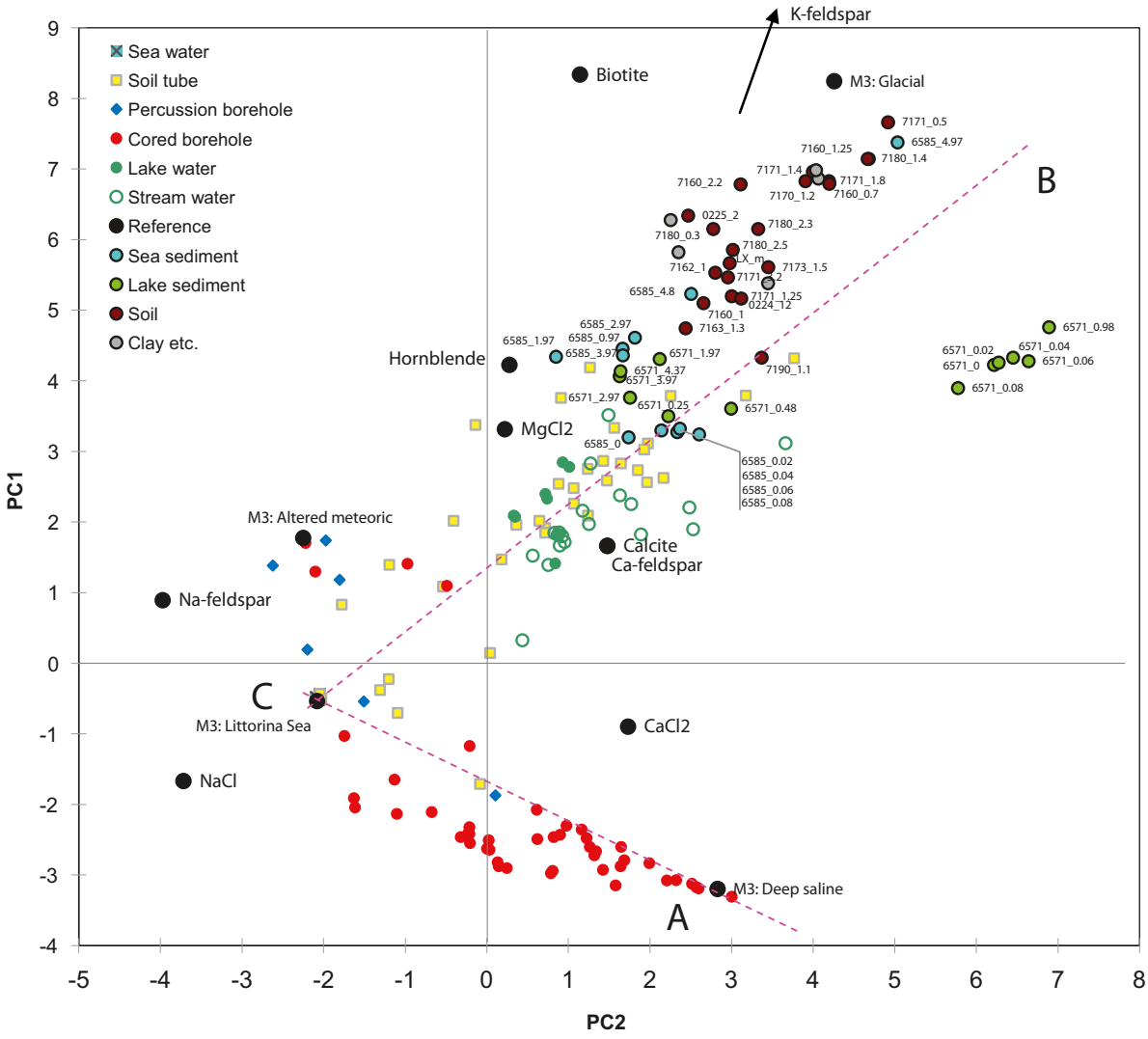


***Figure 4-21.*** *The relative element composition of mineral samples projected onto the Ion Source Model, cf Section 3.2.6. Black marks represent reference theoretical proportions of ions resulting from carbonic acid weathering of various silicate minerals to kaolinite, the composition of salt used for road maintenance and the M3 end-members (in italics). Coloured round marks other than red represent the composition of regolith samples hypothetically balanced with $HCO_3^-$ to achieve zero charge balance error.*

### 4.2.2 Cation exchange in the Quaternary deposits

When aqueous solutions come into contact with rock and regolith, dissolved elements and compounds may interact with mineral surfaces through sorption processes. During ion exchange reactions, dissolved ions switch position with ions of similar charge, adsorbed on e.g. mineral surfaces. One example is cation exchange where one $Ca^{2+}$ ion is adsorbed onto the surface and two $Na^{+}$ ions are released to the solution.

A prerequisite for cation exchange is the movement of dissolved ions through a matrix containing exchangeable ions. For example, $Ca^{2+}$ ions derived from weathering reactions or a deep saline source may function as a driving force for cation exchange that takes place in the overburden or in the fractures of the bedrock. Weathering of minerals in the overburden or an influx of marine ions may load the matrix with exchangeable ions as $Na^{+}$, which is gradually exchanged with $Ca^{2+}$ and released to the solution. The ultimate driving force of this chain is $H^{+}$ derived from dissolved biogenic $CO_2$ (cf Section 4.1.5), and perhaps also to some extent from strong acids derived from oxidation of sulphides in the Quaternary deposits (cf Section 4.1.3) or atmospheric deposition. If calcite is the source of $Ca^{2+}$, the coupled reactions driven by $H^{+}$ of biogenic origin may be written as in Equation 4-1.

*Equation 4-1. Summary of reactions that may take place in the sediments. "X" in the formulas denotes clay or mineral surfaces to which ions are adsorbed. The net reaction shows how a groundwater of Na–$HCO_3$ type may be formed.*

$$CO_2 + H_2O \leftrightarrow HCO_3^- + H^+ \quad (\mathrm{H^+ of\ biogenic\ CO_2\ origin})$$

$$CaCO_3 + H^+ \leftrightarrow Ca^{2+} + HCO_3^- \quad \text{(calcite dissolution)}$$

$$2NaX + Ca^{2+} \leftrightarrow CaX_2 + 2Na^+ \quad \text{(cation exchange)}$$

Net reaction:

$$CaCO_3 + CO_2 + H_2O + 2NaX \leftrightarrow CaX_2 + 2Na^+ + 2HCO_3^-$$

Figure 4-22 and Figure 4-23, may show the effect of $Ca^{2+}$ versus $Na^{+}$ cation exchange reactions. These reactions may also be identified in the Ion Source Model as discussed in Section 3.2.7. The following conclusions can be drawn about cation exchange reactions from these visualisations as well as other element combinations in the report:

- In Figure 4-3, many observations show Na excess compared to the Na/Cl ratio of marine sources. This is especially evident for a group of soil tubes and percussion boreholes that plot along the trendline marked NX1. These samples contain a relatively fresh groundwater with no or very weak marine signatures. A possible source of this Na may be weathering in combination with cation exchange.
- Observations that plot along NX1 also mark out in the Ca versus Na plot in Figure 4-22, as well as the plot of the Ca/Na-ratio versus Cl in Figure 4-23. The composition of this cluster, marked by a dashed grey oval in the lower region of both plots, may be explained by simple $Ca^{2+} \leftrightarrow 2Na^{+}$ exchange according to the modelling scenario that emanates from a typical groundwater composition in the upper part of the overburden.
- In Figure 4-13, the above-mentioned cluster is distinguished by plotting below the 1:1 line, i.e. $Ca^{2+}$ occurs in deficit relative to $HCO_3^-$ in comparison with the normal composition in the recharging shallow groundwater.
- In Figure 4-14 as well, which shows Ca plotted against Sr, the same observations form a deviating cluster in the lower left part of the figure. This pattern can be interpreted as indicating that Ca and Sr are discriminated differently by an ion exchange process, e.g. during infiltration through the sediments, which results in an altered Ca/Sr ratio. As these observations plot below the mixing line with sea water, this pattern cannot solely be explained by mixing with a marine-influenced groundwater component.

- The cluster of observations from the upper parts of the bedrock that are remarked upon in the bulleted points above are also noticeable in the Ion Source Model in Section 3.2.7. According to the cation exchange scenario (lilac arrow in Figure 3-10), the composition of these objects can be explained by Ca-Na exchange of recharging groundwater with a composition similar to the composition in most soil tubes in the Quaternary deposits.
- In the Ion Source Model in Figure 3-10, the composition of a large number of dilute samples in the upper 500 metres of the bedrock (marked "d") can be explained by a net reaction corresponding to Ca versus Na cation exchange, according to the scenario marked by lilac arrows in Figure 3-10. The original composition prior to the exchange alteration according to this scenario was a marine/deep saline ion mixture. The shift below this marine/deep saline mixing trend cannot be explained solely by mixing of the marine and deep saline sources, and this indicates potential influence of reactions. A possible explanation for this pattern is cation exchange reactions driven by discharging $Ca^{2+}$ ions of deep saline origin. $Ca^{2+}$ ions exchanges with $Na^{+}$ derived from weathering in the deposits or in the fractures in the bedrock. $H^{+}$ originating from the surface system is probably an important driving force for these weathering reactions.

In conclusion:

- There are indications that cation exchange reactions affect the groundwater composition in the upper parts of the bedrock and probably also in the Quaternary deposit from which this recharging groundwater originates. In several visualisations, a group of percussion boreholes show an unambiguous pattern that can be explained by the net result of Ca versus Na cation exchange. The evolution of the groundwater in these boreholes probably represents a dilute meteoric recharge evolved from Ca-$HCO_3^-$ types to the Na- $HCO_3^-$ type in the deposits and/or due to percolation in the bedrock (cf Piper classification in Figure 3-2).
- Cation exchange reactions may also have affected groundwater sampled at depths down to 500 metres in the bedrock. A possible explanation for this pattern is cation exchange reactions driven by discharging $Ca^{2+}$ ions of deep saline origin, where $Ca^{2+}$ ions exchanges with $Na^{+}$ derived from weathering in the deposits or in the fractures in the bedrock. $H^{+}$ originating from the surface system is probably an important driving force for these weathering reactions.

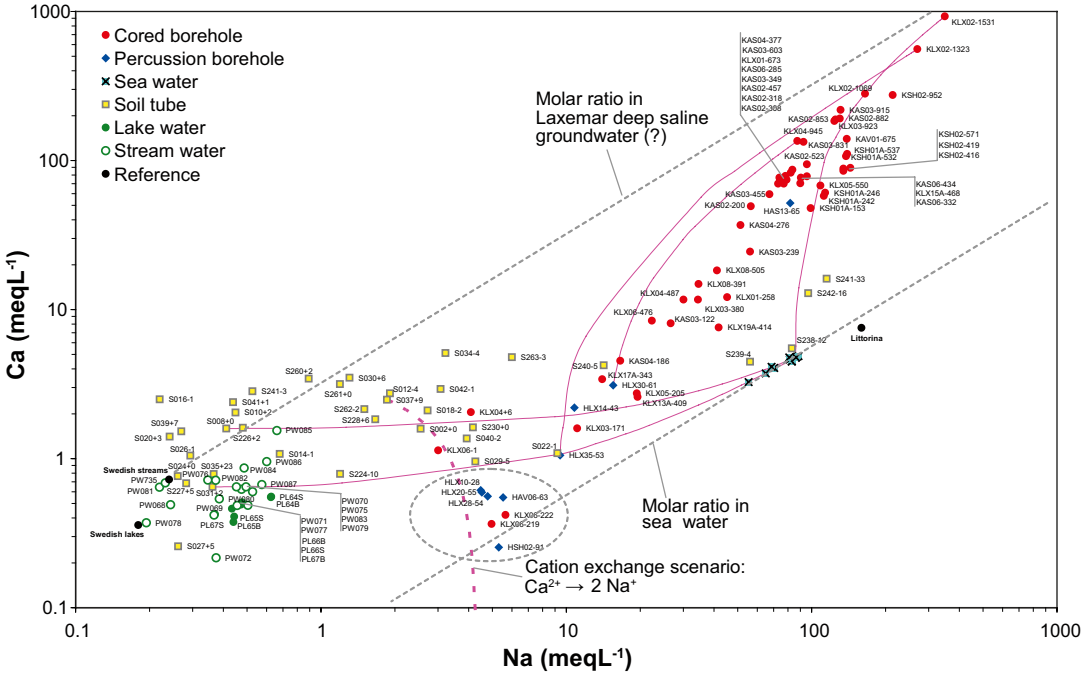


***Figure 4-22.*** *Ca versus Na (meqL$^{-1}$). Dashed grey lines in the log-log scaled diagram connect observations with the same Ca/Mg ratio. This figure is based on data selection C, cf Section 2.2.5. Explanations of labels, symbols and lines are given in Sections 2.3.11 and 2.3.12.*

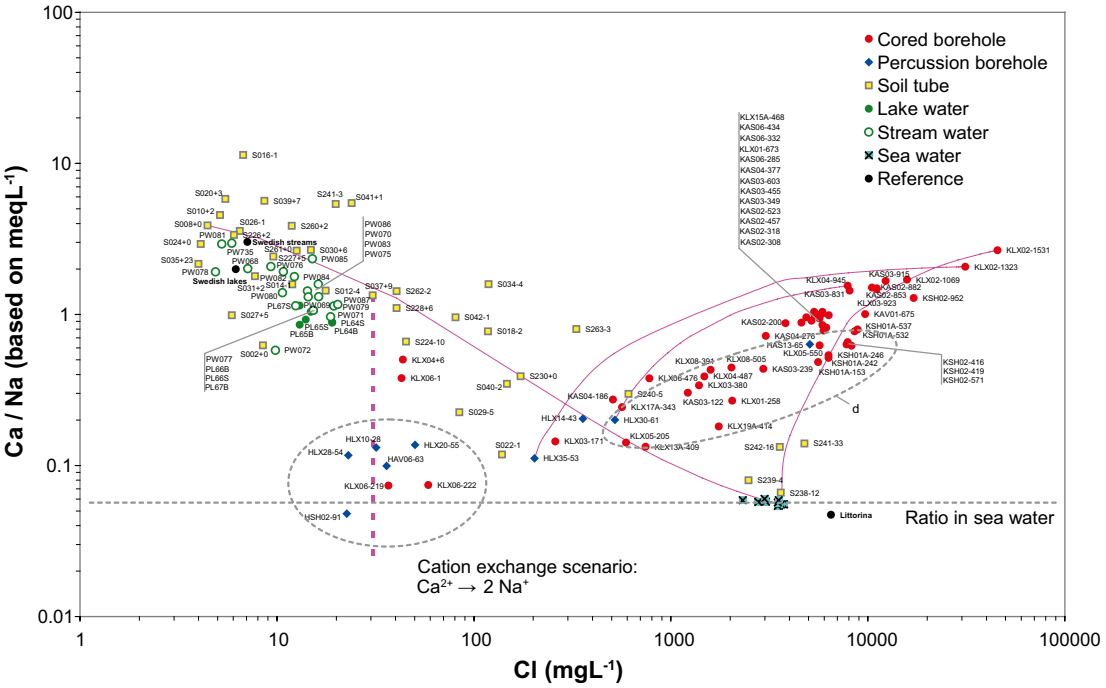


***Figure 4-23.*** *Ca/Na (based on meqL$^{-1}$) versus Cl (mgL$^{-1}$) in water samples from the Laxemar-Simpevarp area. Note the logarithmic scales on both axes. The figure is based on data selection C, cf Section 2.2.5. Explanations of labels, symbols and lines are given in Sections 2.3.11 and 2.3.12. Note: as this two dimensional plot is based on three parameters (three degrees of freedom), hypothetical mixing lines drawn between adjacent observations do not necessarily have to follow the same path in this 2-dimensional projection.*

### 4.2.3 Redox processes

Redox processes involve reactions that transfer electrons between reactants and products, in other words reduction and oxidation reactions. Redox conditions in groundwater are controlled by the abundance of electron donors such as organic carbon and $NH_4^+$ and electron acceptors such as $O_2$, $NO_3^-$, $MnO_2$, $Fe_2O_3$, and $SO_4^{2-}$. As long as there are electron donors available, electron acceptors are depleted according to the above sequence until they are consumed. If sufficient organic carbon remains in the system after all $SO_4^{2-}$ is depleted, methanogenesis may take place, reducing $CO_2$ to methane ($CH_4$).

The gradual utilization of different electron acceptors is accompanied by a gradual decrease in redox potential, measured in the field as Eh, which in the case of groundwater may reflect the distance and travel time from the recharge area. Eh is, however, only a relative measure, as the potential is controlled both by the abundance of electron donors, and by the availability of different electron acceptors in the system. All redox reactions in groundwater are also facilitated by different types of bacteria.

The redox state may be qualitatively estimated from the abundance of dissolved ions. As long as free $O_{2(aq)}$, $NO_3^-$ and $SO_4^{2-}$ are present, the redox potential is *oxic*. In the *suboxic* range, concentrations of dissolved $Mn^{2+}$ and $Fe^{2+}$ rise and $NO_3^-$ falls to very low levels. If the supplies of reactive $MnO_2$ and $Fe_2O_3$ are consumed, $SO_4^{2-}$ is utilized as an electron acceptor by the formation of $H_2S$ gas under *reducing* conditions. Concurrent with the decline in $SO_4^{2-}$, $Fe^{2+}$ concentrations may decrease due to precipitation of metal sulphides. Methanogenesis gives rise to methane, and $Fe^{2+}$ may increase again due to the absence of $H_2S$. It should be noted that this is a simplified, theoretical description of the redox reactions occurring in groundwater systems and the boundaries between the sets of reactions tend to overlap.

High levels of organic carbon in surface water and shallow groundwater in the Laxemar-Simpevarp area (cf Section 4.1.5) provide the prerequisites for low redox potentials even at shallow depths. In Figure 4-24, a selection of parameters reflecting redox conditions are projected onto the Ion Source Model, which separates the observations into different groundwater types according to the relative composition of the major elements (cf Section 3.2.5 for further explanation of this multivariate PCA model).

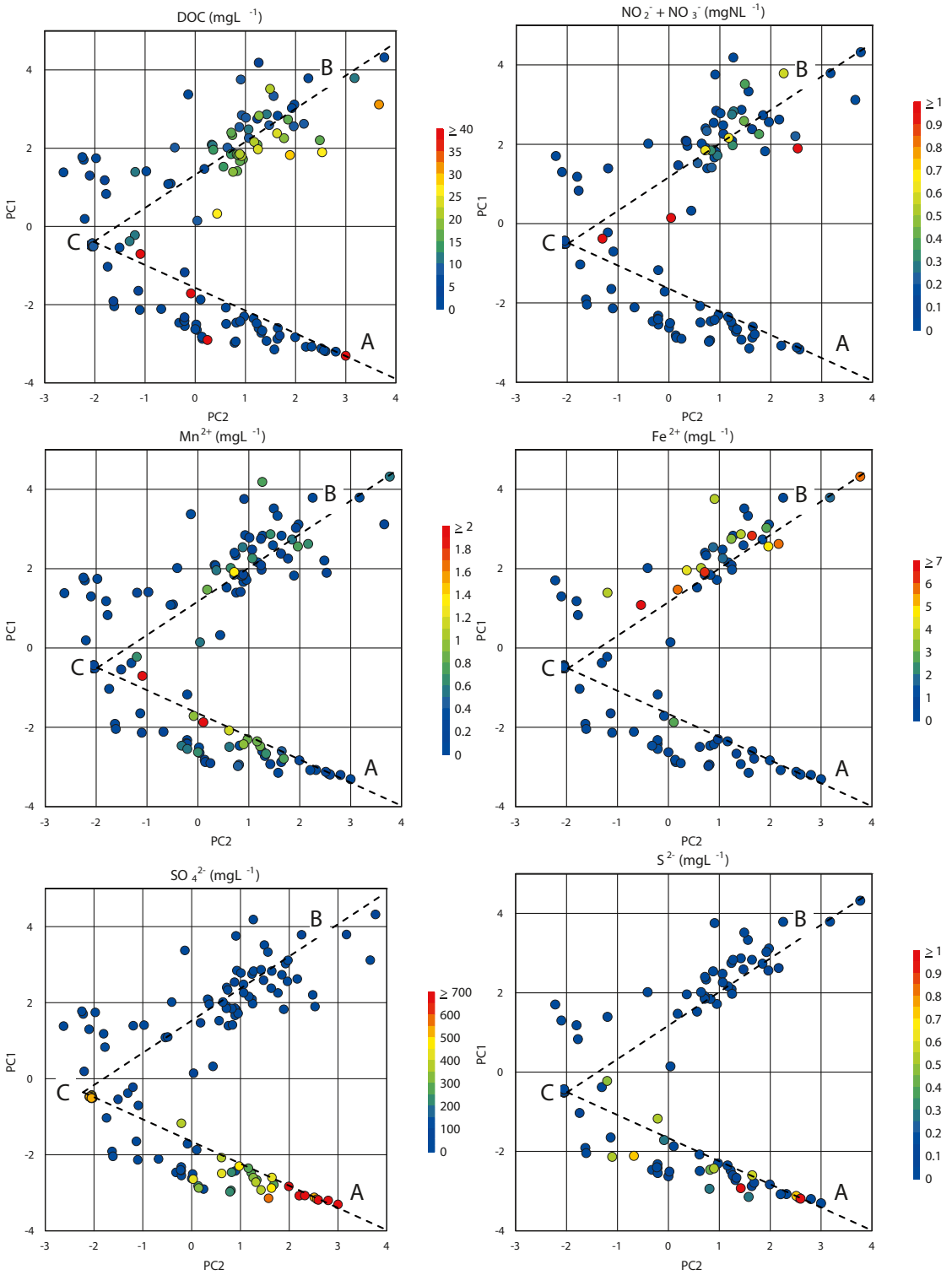


***Figure 4-24.*** *A selection of parameters that reflect redox conditions in groundwater in the Laxemar-Simpevarp area. Concentrations ($mgL^{-1}$) of dissolved organic carbon (DOC), nitrate ($NO_3^-$), manganese ($Mn^{2+}$), iron ($Fe^{2+}$), sulphate ($SO_4^{2-}$, and sulphide ($S^{2-}$) are projected onto the Ion Source Model (cf Section 3.2.5). These figures are based on data selection C, cf Section 2.2.5.*

When projected onto the Ion Source Model, the selected redox-sensitive parameters show considerable and mostly expected variation among different groupings in the model:

- Generally, DOC and $NO_3^-$ are detected in the surface water and shallow groundwater, often at relatively high concentrations, whereas deeper observations in the bedrock generally show very low concentrations. This trend is in concordance with a higher Eh in the surface system compared to deep groundwater in the bedrock. The few exceptions for DOC which plot along the deep saline trend may be artefacts due to e.g. contamination.
- In the surface system, both $Fe^{2+}$ and $Mn^{2+}$ occur at detectable levels in shallow groundwater, indicating lowered Eh and reducing conditions. In contrast to $Fe^{2+}$ in the bedrock, $Mn^{2+}$ is elevated within the group of samples which show the highest Littorina proportions according to the M3 model (cf Figure 3-6), as well as according to the Ion Source Model. This deep pattern, which is similar to but weaker than the corresponding pattern in the Forsmark area /Tröjbom et al. 2007/, may be an indication of the previous Littorina Sea Water intrusion (cf Section 8.2).
- $SO_4^{2-}$ increases in observations significantly influenced by deep saline groundwater, whereas elevated $S^{2-}$ levels are found only in a few samples (according to preliminary evaluations, $S^{2-}$ varies considerably between sampling occasions (Bill Wallin pers. comm.).

### 4.2.4 Microbially mediated processes

Many chemical reactions in water are mediated by different types of bacteria. In the presence of oxygen, aerobic bacteria degrade organic matter, forming $CO_2$. When oxygen is depleted bacteria can use alternative e-acceptors according to the sequence described in 4.2.3. In absence of other electron acceptors, for example $CO_2$ is fermented into methane ($CH_4$) by methanogenic bacteria. The abundance of different types of bacteria has been screened in the cored boreholes in the Laxemar-Simpevarp area, and the results and interpretations of these analyses are presented in /SKB 2004, SKB 2006a and Laaksoharju (ed) 2008/. Further interpretations of microbial activities in shallow groundwater are found in /Hallbeck 2008/.

Bacterial activities have an impact on the hydrochemical parameters measured in groundwater and surface water. In the Laxemar-Simpevarp area, most $HCO_3^-$ in both the surface system and in the bedrock is of biogenic origin according to the $\delta^{13}C$ signatures (cf Section 4.1.5). Bacterial degradation of organic matter in soil leads to very high partial pressure of $CO_{2(g)}$, a prerequisite for the elevated $HCO_3^-$ concentrations in the shallow groundwater compared to surface water (cf Section 4.1.5).

Elevated $\delta^{13}C$ values may be an indication of bacterial fermentation that shift $\delta^{13}C$ in the remaining DIC pool (which is measured as $HCO_3^-$) towards enriched (more positive) values. This process favours the light isotope, which leads to highly negative $\delta^{13}C$ values in the gaseous methane formed. According to $\delta^{13}C$ in the left-hand panel in Figure 4-25 all observations except for one range between –19 and 0. This suggests that the signatures can be explained by either biogenic or marine carbon. Shifts due to microbial fractionation of carbon could however be masked within this range. The slightly enriched signature in SSM000034 could for example be explained by microbial activities /Hallbeck 2008/ (cf Section 4.1.5). One observation from the bedrock (KSH02-419) shows highly enriched $\delta^{13}C$ values, which, if not an analysis artefact, may be an indication of microbial fermentation.

In analogy with carbon as described above, sulphate-reducing bacteria favour the lighter sulphur isotope, which leads to positive, enriched $\delta^{34}S$ values in the remaining $SO_4^{2-}$ pool. The resultant $H_2S$, or precipitated sulphide minerals, are consequently depleted in $^{34}S$, which leads to highly negative $\delta^{34}S$ values in these sulphur pools (cf Section 4.1.3).

In Figure 4-25 there are no general patterns that clearly indicate signatures of sulphate-reducing bacteria. Mixtures of different sources could, however, mask microbially mediated isotope enrichments. The detailed evaluation of sulphur in Section 4.1.3 shows that some patterns in

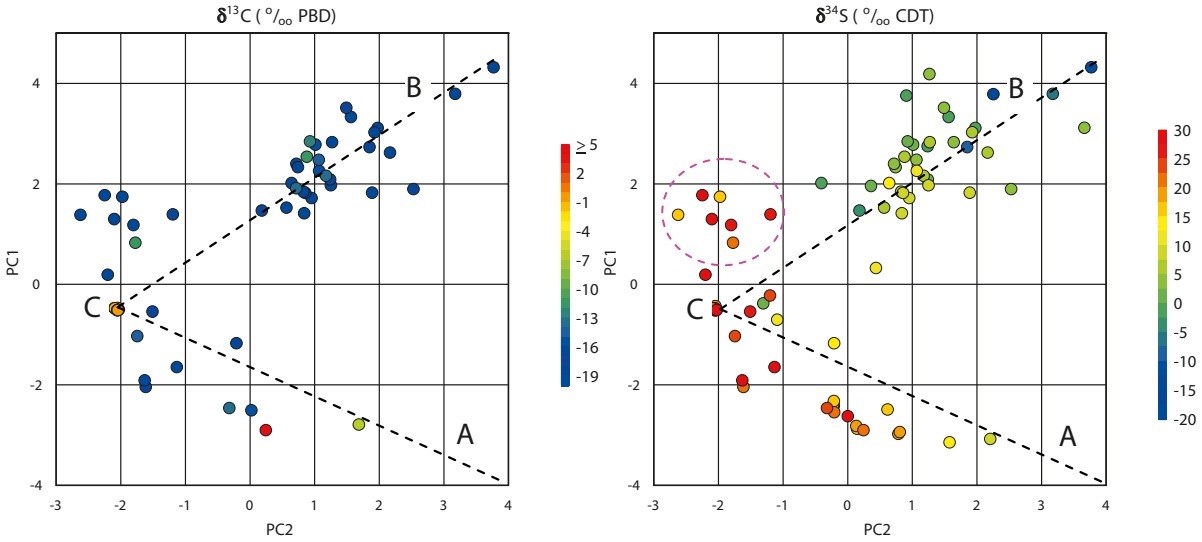


***Figure 4-25.*** *Carbon and sulphur isotopes which are influenced by bacterial fractionation, projected onto the Ion Source Model (this model separates observations regarding the origin of major ion sources, cf Section 3.2.5). Isotope ratios are expressed as the ‰ deviation from international standards: $\delta^{13}C$ ‰ PDB and $\delta^{34}S$ ‰ CDT. Based on data selection C, cf Section 2.2.5.*

for example Figure 4-11, which also includes Cl, may be explained by reduction of sulphate originating from a deep saline sulphur source. Microbial analyses have shown that sulphate reducing bacteria (SRB) are present down to at least 920 meters depth in KLX03A /Laaksoharju (ed) 2008/.

Correspondingly, the cluster marked by a dashed pink ellipse in the right-hand panel of Figure 4-25 could, according to the interpretation of Figure 4-11, be explained by microbial alteration of $SO_4^{2-}$. This $SO_4^{2-}$ probably originates from atmospheric or pyritic sources rather than a marine source, although the $\delta^{34}S$ signature alone could be interpreted as an indication of the marine alternative.

In two shallow groundwater objects (SSM000241 and SSM000242) there are indications that extensive microbial activities have altered the composition of the groundwater. Very high contents of organic carbon, N and P, together with low $SO_4^{2-}$ and high $Mn^{2+}$ characterise this groundwater. At present date there are no isotope measurements available to support these observations. These soil tubes are further evaluated in Section 7.2.

## 4.3 Deep signatures in the shallow system

Possible indications of discharging deep groundwater signatures detected in the shallow groundwater system are summarised in this section. Several visualisations throughout the report are interpreted in the light of deep signatures in order to find support for or reject the hypothesis of discharging deep groundwater components.

The deep saline groundwater in the Laxemar-Simpevarp area is characterised by very high contents of dissolved ions and a specific ion composition enriched in e.g. Ca, Li and Br compared to the concentrations of Cl in sea water. The possibility of detecting dilute deep groundwater signatures discharging into the surface system is restricted by the relative concentration difference between the ion sources, as well as by the reporting limits of the elements. Many trace elements are in that respect not suitable as tracers, as only minor dilution of the deep source of interest will reduce concentrations below the reporting limit.

### 4.3.1 Reporting limits and dilution constraints

When discussing the possible presence of deep groundwater signatures in the surface system, an important factor is the theoretical maximum dilution that is possible to detect according to the difference in concentrations and to the reporting limits for the analysis technique used. In practice, the limited number of available samples also restricts the possibility of detecting very small changes on statistical grounds. Uncertainties regarding factors governing the local hydrochemistry also limit the possibility of identifying objects used for reference.

The dilution factors compiled in Table 4-1 give an indication of the maximum dilution of deep groundwater types that is possible to detect on theoretical grounds for different elements. There is great variation in dilution factors between elements, primarily due to differences in concentrations between deeper groundwater types and fresh surface water (the accuracy of the analysis method is probably selected to reflect the variation within each water type, and is accordingly a consequence of the observed concentration range).

According to Table 4-1, dilution in the magnitude of 1,000–10,000 times is possible to detect for several of the major constituents, whereas many trace elements have a maximum dilution range of 10–100 times. Consequently, concentrations and relative composition of major ions are probably best suited for detecting deep groundwater discharge, whereas most trace elements are inadequate in that respect. There are, however, a few trace elements that do not follow this pattern and therefore may be theoretical candidates for detecting deep signatures: Br, Sr, Ba and Li as well as Rb and Mo. Besides these theoretical constraints, elements suitable for detection of deep discharge must discriminate from other important sources, e.g. marine signatures, and must also show reasonably conservative behaviour on the transition from depth.

Isotopes are also candidates for detecting deep signatures. In practice, the limited analytical precision of e.g. $^{37}Cl$ limits the possibility of detecting significant deviations in dilute water, although this parameter has a distinct signature in deep saline groundwater (cf Figure 4-8). Isotopes such as $^{2}H$ and $^{18}O$, which reflect water origin, also deviate in samples influenced by deep saline groundwater by showing a clear $^{2}H$ excess (cf Section 3.3.2). However, due to the limited measurement precision, in combination with mixing with waters of various origins (which contain these isotopes as well), these parameters are not useful for detecting weak deep signatures.

### 4.3.2 Summary of possible deep signatures in shallow objects

The first question that arises when trying to detect deep signatures in shallow objects is what characterises a deep groundwater? At very deep levels of the Fennoscandian Shield, a deep saline source influences the groundwater composition. At Laxemar-Simpevarp this results in a typical ion signature containing excess Ca, Br and Li and very low Mg in relation to Cl, when compared to the composition of sea water.

The most powerful tool within this report for detecting deviations in relative composition among elements in the surface system, attributed to discharging groundwater with deep saline signatures, is probably the Ion Source Model (cf Section 3.2.5). This model can also discriminate deep saline sources from marine sources. The conclusions listed below are mainly based on the patterns identified in the Ion Source Model, and when available these conclusions are supported by the other models in Chapter 3 and multi-element plots from Chapter 4:

- The most obvious deep signature in the surface system is found in SSM000241 (abbreviated S241-33 in all visualisations, cf Section 2.3.11), located in till beneath thick sea sediments in Granholmsfjärden Basin. This soil tube is located near a major deformation zone and has been pointed out as a candidate area for discharge of deep groundwater into the surface system. As discussed in 7.2, the groundwater chemistry in this object is affected by degrada-

**Table 4-1. Compilation of reporting limits in fresh surface water and the maximal dilution that is possible to detect for two typical deep groundwater samples. Both KSH01A-242 and KLX02-1323 represent groundwater from the bedrock at different depths. The former is selected due to the complete characterisation of trace elements, whereas KLX02-1323 represents the deepest borehole in the area. For comparison, this factor was also calculated for typical dilute surface water in the outlet of the Laxemarån River and for sea water. The dilution factor shown in the four rightmost columns is calculated as the observed mean concentration for the object in question, divided by the reporting limit for the element in fresh surface water.**

| | Reporting limit in fresh water | Unit | Surface water PSM002087 | Sea Water PSM002060 | Groundwater KSH01A-242 | Deep saline GW KLX02-1323 |
|---|---|---|---|---|---|---|
| **Na** | 0.1 | $mgL^{-1}$ | 132 | 19,786 | 25,800 | 62,100 |
| **K** | 0.4 | $mgL^{-1}$ | 5 | 186 | 30 | 45 |
| **Ca** | 0.1 | $mgL^{-1}$ | 134 | 953 | 11,600 | 112,000 |
| **Mg** | 0.09 | $mgL^{-1}$ | 38 | 2,619 | 694 | 30 |
| **$HCO_3^-$** | 1 | $mgL^{-1}$ | 22 | 92 | 20 | 9 |
| **Cl** | 1 | $mgL^{-1}$ | 20 | 3,626 | 6,320 | 31,230 |
| **$SO_4^{2-}$** | 0.5 | $mgL^{-1}$ | 43 | 1,057 | 51 | 2,048 |
| **Br** | 0.2 | $mgL^{-1}$ | 1 | 72 | 177 | 980 |
| **F** | 0.1 | $mgL^{-1}$ | 83 | 3 | 5 | 31 |
| **Si** | 0.03 | $mgL^{-1}$ | 40 | 0 | 116 | 165 |
| **Fe** | 0.4 | $mgL^{-1}$ | | | 3 | 1 |
| **Mn** | 0.03 | $mgL^{-1}$ | 0 | 1 | 18 | 3 |
| **Li** | 0.004 | $mgL^{-1}$ | 17 | 360 | 92 | 1,113 |
| **Sr** | 0.002 | $mgL^{-1}$ | 3,260 | 3,968 | 9,500 | 95,500 |
| **I** | 0.001 | $mgL^{-1}$ | 305 | 777 | 194 | - |
| **U** | 0.001 | $\mu gL^{-1}$ | 109 | 100 | 157 | - |
| **Th** | 0.05 | $\mu gL^{-1}$ | 8,262 | 20 | 2 | - |
| **Al** | 0.2 | $\mu gL^{-1}$ | 2 | 3 | 2 | - |
| **Ars** | 0.01 | $\mu gL^{-1}$ | 13 | 25 | 50 | - |
| **Sc** | 0.05 | $\mu gL^{-1}$ | 1 | 0 | 5 | 11 |
| **Cd** | 0.002 | $\mu gL^{-1}$ | 345 | 25 | 13 | - |
| **Cr** | 0.01 | $\mu gL^{-1}$ | 278 | 50 | 22 | - |
| **Cu** | 0.1 | $\mu gL^{-1}$ | 8 | 0 | 3 | - |
| **Co** | 0.005 | $\mu gL^{-1}$ | 1 | 0 | 33 | - |
| **Hg** | 0.002 | $\mu gL^{-1}$ | 1,531 | 312 | 1 | - |
| **Ni** | 0.05 | $\mu gL^{-1}$ | 238 | 51 | 24 | - |
| **Zn** | 0.2 | $\mu gL^{-1}$ | 1 | 0 | 316 | - |
| **Pb** | 0.01 | $\mu gL^{-1}$ | 81 | 18 | 15 | - |
| **V** | 0.005 | $\mu gL^{-1}$ | 701 | 4,380 | 73 | - |
| **Rb** | 0.025 | $\mu gL^{-1}$ | 115 | 1 | 1,220 | 5,520 |
| **Y** | 0.005 | $\mu gL^{-1}$ | 172 | 60 | 62 | 256 |
| **Zr** | 0.025 | $\mu gL^{-1}$ | 18 | 78 | 94 | - |
| **Mo** | 0.01 | $\mu gL^{-1}$ | 3 | 25 | 1,010 | - |
| **In** | 0.05 | $\mu gL^{-1}$ | 1 | 2 | 5 | 1 |
| **Sb** | 0.025 | $\mu gL^{-1}$ | 1 | 6 | 5 | - |
| **Cs** | 0.025 | $\mu gL^{-1}$ | 1,405 | 732 | 54 | 584 |
| **Ba** | 0.01 | $\mu gL^{-1}$ | 310 | 3 | 142,000 | 20,500 |
| **La** | 0.005 | $\mu gL^{-1}$ | 6 | 5 | 99 | 5 |
| **Hf** | 0.005 | $\mu gL^{-1}$ | 3 | 30 | 89 | - |
| **Tl** | 0.025 | $\mu gL^{-1}$ | 215 | 1 | 6 | 0 |
| **Eu** | 0.005 | $\mu gL^{-1}$ | 98 | 5 | 24 | 1 |

tion of organic matter. The location in the Ion Source Model between the marine and deep saline sources, with a substantial deviation towards the deep saline composition, is most probably attributed to the influence of deep saline groundwater. This conclusion is also supported by other visualisations, e.g. the Na and Li versus Cl plots (Figure 4-9 and Figure 4-7), where this soil tube also plots between the marine and deep saline compositions. In addition to the mixing between meteoric and marine water signatures according to the Water Origin Model in Section 3.3.2, this observation point located below sea water probably contains meteoric discharge from the surrounding higher elevated areas (cf further discussions about SSM000241 in Section 7.2).

- SSM000242 (abbreviated S242-16 in all visualisations, cf Section 2.3.11), located in till beneath sediments in Lake Frisksjön, shows in many respects similar chemical characteristics to SSM000241. The two objects are also located in similar physical settings. According to the Ion Source Model, the deep saline signature is stronger in S241-33 than in S242-16, whereas the latter displays a stronger marine signature, with regard to both the ion composition and the isotope signature of water. The Na and Li versus Cl plots, however, provide a concordant picture of deep saline signatures. There are two $^{37}Cl$ isotope measurements available from S242-16 (cf Figure 4-8), and this signature (although uncertain) points towards the influence of Cl of deep saline origin. The single $^{37}Cl$ measurement available from S241-33 points in the opposite direction, which makes the interpretation of this parameter ambiguous (cf further discussions about SSM000242 in Section 7.2 and uncertainties regarding $^{37}Cl$ in Section 9.3.2).
- SSM000022 (abbreviated S022-1 in all visualisations, cf Section 2.3.11, located on Ävrö, has previously been singled out as a candidate for deep discharge. According to the evaluation in Section 7.3, deep groundwater discharge is less probable, although there are some contradictory indications. There are also no indications of any significant presence of a deep saline component in the surface water discharge from this area.

From observations of major elements and environmental isotopes in shallow groundwater, it can be concluded that deep groundwater signatures are probably present in the Quaternary deposits in potential deep discharge areas, e.g. in the sediments of Lake Frisksjön and the brackish basins near the coast. On land there are no deep signatures detected either in surface water or in shallow groundwater. This indicates that shallow meteoric recharge/discharge patterns dominate or that any potential regional deep discharge into the surface system is too diluted to be detectable in surface water.

# 5 Integrated evaluation of hydrochemical and hydrological data in the surface system

Connections between hydrochemical and hydrological data in shallow groundwater and surface systems are explored in this section. A hydrological field classification of soil tubes, according to recharge and discharge characteristics, is compared to the hydrochemical measurements in shallow groundwater in order to explore possible correlations. Discharge measurements in streams are further compared to the hydrochemical composition of stream water, and possible correlations between water flow and measured concentrations are explored. Finally, discharge measurements are used in combination with hydrochemical data in order to estimate transport of elements in watercourses in the Laxemar-Simpevarp area. These transport estimations are the basis for the catchment modelling described in Section 6.

## 5.1 Evaluation of observed hydrochemistry in relation to hydrological recharge/discharge characteristics

Here, the observed hydrochemistry in shallow groundwater is evaluated in relation to a qualitative, hydrological field classification of soil tubes in the Laxemar-Simpevarp area. The purpose of this evaluation is to explore whether chemical parameters can support field estimations of recharge and discharge characteristics. A matrix where the hydrological characteristics of soil tubes are compiled can be found in Appendix A, and further explanations and hydrological evaluations are found in /Werner et al. 2008/.

The correlation structure among a selection of hydrochemical parameters, representing either the variability or mean values, was studied in relation to the semi-quantitative recharge/discharge parameter. Parameters included in the analysis are listed in Section 2.2.1, along with an explanation of the recharge-discharge parameter (RD). The complete chemical data matrix is found in Appendix A.

### 5.1.1 Hydrological classification compared to traditional hydrochemical classification

The subjective hydrological field classification is probably the best way to reflect the recharge-discharge properties of the soil tubes, and is therefore used as reference when other classifications are evaluated. A thorough description of the prerequisites of this field classification is given in /Werner et al. 2008/. It should, however, be kept in mind that the field classification is solely based on surface characteristics, while measurements in soil tubes may reflect conditions at a depth of several metres where the intake screen is located.

The hydrological recharge-discharge classification is projected onto a traditional hydrochemical classification plot (Piper plot, cf Sections 2.3.5 and 3.1.2) in Figure 5-1. In large groundwater systems, recharging groundwater is often assumed to correspond to the Ca-$HCO_3^-$ type (which plots in the left part of the prism), whereas groundwaters of Na-$HCO_3^-$ to Na-Cl types is assumed to correspond to discharging groundwater. The evolution of groundwater from meteoric recharge to discharge consequently follows the pink arrow according to this simplified picture.

It is evident from Figure 5-1 that there is little agreement between the hydrological classification and the generalised interpretation of the hydrochemical composition in terms of recharge and discharge. Many observations that are classified as hydrological discharge plot in the area of the Ca-$HCO_3^-$ (recharging) groundwater type, whereas the three available soil tubes that are classified as hydrological recharge on the contrary plot to the right where discharging groundwater types are expected. From this example it is clear that there is no agreement between the hydrological field classification and the simplified hydrochemical classification based on a Piper plot.

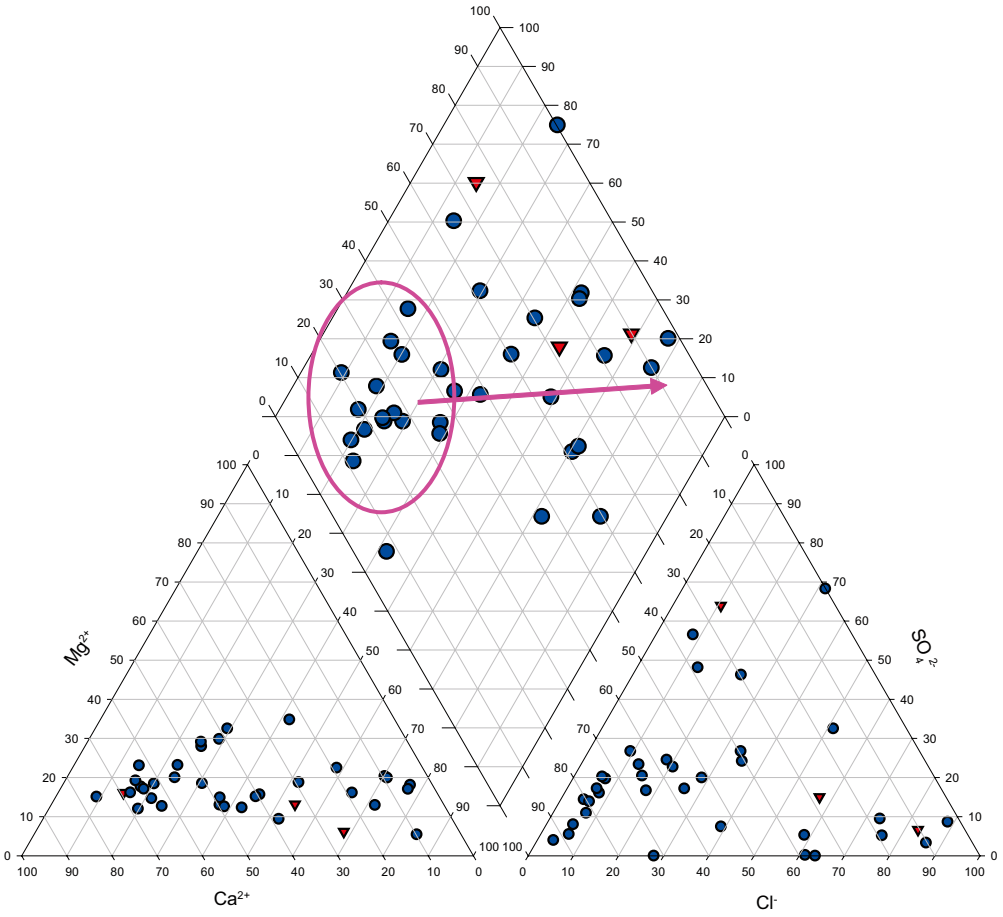


***Figure 5-1.*** *Traditional water type classification Piper plot (cf Section 2.3.5) based on mean values, used for the hydrochemical recharge-discharge classification of shallow groundwater in the Laxemar-Simpevarp area. Encircled points are assumed to represent recharging groundwater. Red triangles correspond to hydrological recharge characteristics and blue dots discharge characteristics according to the hydrological field characterisation.*

### 5.1.2 Exploration by Principal Component Analysis

A standard principal component analysis (PCA, cf Section 2.3.9 for explanation), based on a Pearson correlation matrix, is used to visualise the correlation structure among the selected hydrochemical parameters and the recharge-discharge parameter RD (Figure 5-2). The strongest correlations identified in the PCA are visualised in scatter plots in Figure 5-3, to provide an idea of the strength (or weakness) of the relationships.

When the selected hydrochemical parameters are analysed together with the hydrological RD-parameter, the patterns in Figure 5-2 describes 45% of the total variation in data from these soil tubes. In the score plot in the lower panel, the first principal component discriminate the observations along a concentration gradient which mainly reflects ionic strength (soil tubes with high conductivity and high Cl concentrations plot to the right). The second principal component discriminates the soil tubes in two diffuse groups which differ mainly with respect to the isotopes $^{2}H$ (denoted D) and $^{18}O$ (denoted O18). The following conclusions can be drawn from this analysis:

- The first (horizontal) component describes a concentration gradient which seems to be independent of the hydrological recharge-discharge classification. This gradient is negatively correlated with the variability of $^{2}H$ (D_sd) and $^{18}O$ (18O_sd) and the concentration of $^{3}H$ (Tr in the figure) and DOC. A similar pattern could theoretically be expected if recharging groundwater is compared to discharging groundwater; the seasonal variability in precipitation should be more pronounced in recharging groundwater, in combination with higher concentrations of DOC and $^{3}H$.
- The pattern captured by the second (vertical) component is probably a seasonal effect. Both $^{2}H$ and $^{18}O$ vary systematically over the season and the absolute values of these isotopes reflects the time of the year when the groundwater was recharged. Soil tubes in the lower cluster, which includes the three soil tubes classified as hydrological recharge encircled in red, contain a higher proportion of winter precipitation compared to the upper group. An explanation for this pattern could consequently be a seasonal bias due to the distribution of the sampling occasions over the year.
- The recharge-discharge parameter shows a weak relationship with both components. The limited body of data with only three hydrological recharge tubes could be one explanation for the weak and ambiguous pattern for RD according to Figure 5-3. On the other hand, the distinct gradient along the first principal component could be an indication that the hydrological recharge-discharge classification, which relates to the surface, is not representative of conditions at screen depth.

### 5.1.3 Conclusions – recharge/discharge characteristics

- The traditional water type classification in a Piper plot shows no resemblance to the hydrological field classification as regards recharge-discharge characteristics. This means that the generalised interpretation that Ca-$HCO_3^-$ groundwater type represents recharging groundwater and Na-$HCO_3^-$ to Na-Cl types correspond to discharging groundwater is not valid in the shallow groundwater in the Laxemar-Simpevarp area (providing that the hydrological field classification is assumed to be correct). This interpretation assumes rather unrealistic that any discharge is coming from great depth, when in practice, short and local groundwater flow systems should give premises for discharge of Ca-$HCO_3^-$ water types.
- There are also few clear, straightforward relationships between the hydrological field classification (the recharge/discharge parameter) and the selected chemical parameters according to the multivariate correlation study (this is also manifested in the relatively low explanatory power of the two first principal components in the PCA). A non-representative selection of hydrological settings may explain some of this lack of correlation, as only 3 out of 24 tubes are classified as hydrological recharge.
- The major pattern captured by the first component in the PCA indicates, however, that there is a systematic relationship between the hydrochemical parameters. This could be associated with some hydrological property such as recharge-discharge characteristics, length of flow path, or residence time. High variability in $^{2}H$ and $^{18}O$, together with high concentrations of DOC and $^{3}H$ (which may be indications of recharge conditions), are inversely correlated with possible discharge characteristics, e.g. high concentrations of Cl, $HCO_3^-$ and $SO_4^{2-}$. The weak correlation of the hydrological recharge-discharge parameter RD with this pattern could possibly be an indication that the hydrological classification, which relates to the surface, is not representative of conditions at screen depth.
- The overall conclusion is that the surface hydrochemistry of the Laxemar-Simpevarp area is difficult to understand from a recharge/discharge point of view based on the hydrological field classification of soil tubes.

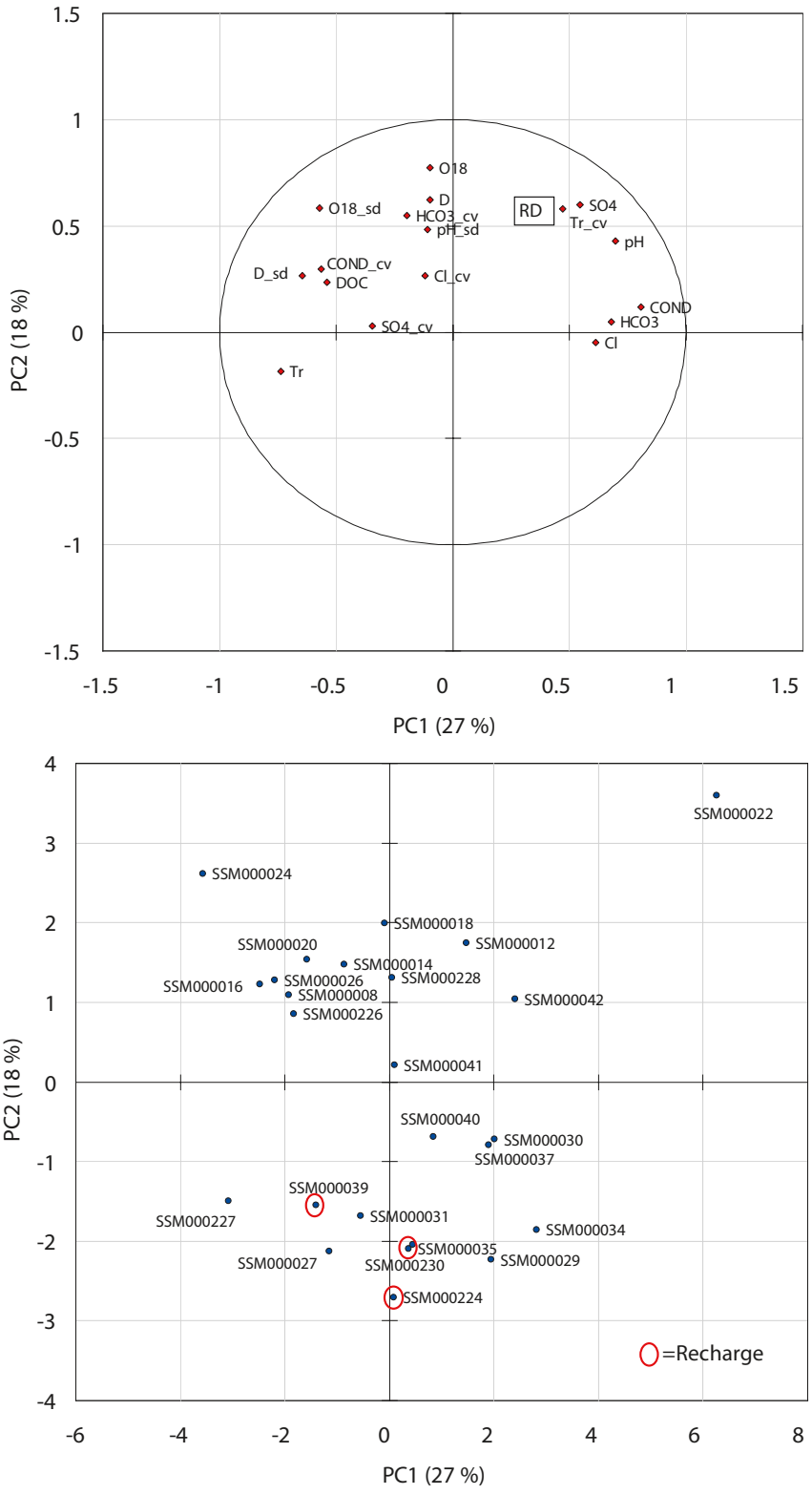


***Figure 5-2.*** *Principal Component Analysis (PCA) of all data from soil tubes with more than 2 observations. Loading plot of parameters (upper) and score plot of observations (lower). See Section 2.3.9 for an explanation of multivariate plots. The recharge-discharge parameter that represents the hydrological field classification is denoted RD and high values of RD corresponds to discharge. The three soil tubes that were classified as recharge are marked by a red circle.*

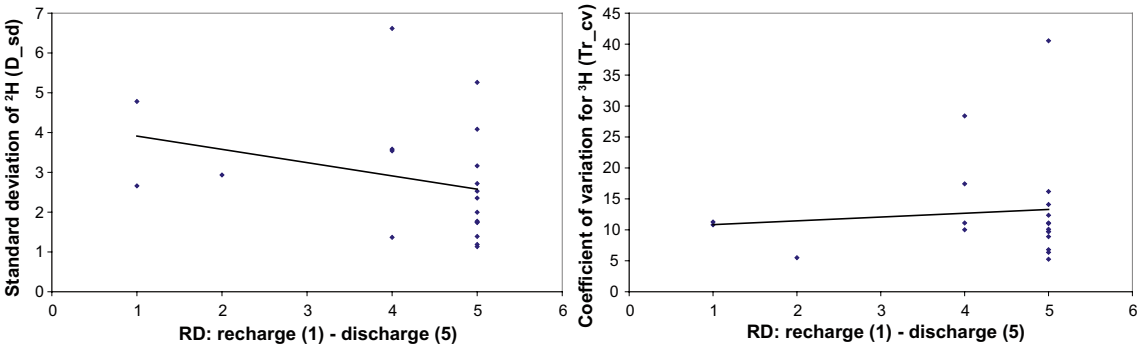


***Figure 5-3.*** *Scatter-plot showing the strongest relationships that were identified in the principal component analysis in Figure 5-2. Data from all soil tubes with more than 2 observations are included in the plots. The trendlines in the figures are adapted by least squares regression.*

## 5.2 Evaluation of concentrations and water flow

Concentrations measured in streams and lakes show variations depending on many different factors, and the influence of water flow on the concentrations of a large number of parameters is explored in this section. Depending on the nature of the underlying processes and pathways that bring different elements to the streams, different responses to variations in water flow can be expected.

The most obvious response to an influx of, for example, meteoric water containing small amounts of dissolved ions or compounds is dilution and reduced concentrations. However, episodes of high flow rates may also lead to release and transport of elements to the surface waters due to erosion and floods, for example particulate matter and ions adsorbed to particles, with increasing concentrations as a consequence. High flow episodes may also lead to more overland discharge, possibly contributing to higher concentrations of organic compounds and elements associated with organic matter. During episodes of lower flow rates, a greater fraction of the surface water usually originates from discharging groundwater, which affects concentrations in different directions depending on the element. Variations in recharge may also influence the chemical environment in soil and regolith, which often results in changed pH or altered redox conditions, which in turn may lead to either release or retention of specific elements.

This simplified but still complex picture should be kept in mind when observed concentrations are correlated with measured discharge in watercourses. In order to facilitate comparisons that involve around two orders of magnitude, concentrations and discharge measurements are displayed in log-log plots. Relationships following power laws (e.g. $y=ax^b$), for example dilution of a point source, form straight lines in this type of plots. However, it should be noted that observations that seem to plot along straight lines in these plots do not necessarily have to be an effect of mechanisms that conform to power laws, as straightness is a necessary but not a sufficient condition for data conforming to a power law relationship.

In Table 5-1, correlation coefficients have been calculated for four years of measured discharge and monthly concentrations of selected elements during the period 1 December 2003 to 31 December 2006 (cf compilations in Table 5-2 and Table 5-3 in Section 5.3). Two observation points located in the Laxemarån River (PSM002079 upstream and PSM002087 near the outlet), and one in the outlet of the Kärrviksån River (PSM002083), are included in the analyses (cf geographical locations in Figure 2-4).

It can be concluded from Table 5-1 that almost all of the studied parameters show significant correlations with water flow in streams at the $p<0.05$ significance level. Among these significant relationships, most parameters are negatively correlated with water flow, which suggests that dilution is a mechanism that influences many parameters at elevated flow rates. It should be kept in mind when calculating the significance of a large number of correlations that about 5% of the relationships are erroneously regarded as significant at the chosen significance level, i.e. about 3 of 64 in Table 5-1.

**Table 5-1. Spearman rank correlation coefficients calculated for the correlation between discharge (Q) and concentrations of selected elements (blue = marine ions, green = elements and compounds associated with organic matter). The correlation versus time is included at top of the table to reveal time trends. Figures in bold face are significant at the p<0.05 level. The analysis is based on a three-year period from 10 December 2003 to 13 December 2006, with a monthly sampling interval at all stations. See Figure 2-4 for the geographical locations of these stations.**

| Time | PSM002079 –0.27 | PSM002083 –0.20 | PSM002087 –0.24 |
|---|---|---|---|
| Na | **–0.86** | **–0.82** | **–0.82** |
| K | **–0.72** | **–0.50** | **–0.69** |
| Ca | **–0.70** | **–0.64** | **–0.67** |
| Mg | **–0.72** | **–0.73** | **–0.69** |
| $HCO_3^-$ | **–0.86** | **–0.79** | **–0.82** |
| $Cl^-$ | **–0.87** | **–0.79** | **–0.81** |
| $SO_4^{2-}$ | 0.13 | **–0.38** | 0.05 |
| $Br^-$ | 0.05 | **–0.38** | **–0.39** |
| $F^-$ | **–0.77** | **–0.78** | **–0.71** |
| $I^-$ | **–0.61** | - | **–0.63** |
| Si | **0.73** | –0.10 | **0.69** |
| Fe | –0.12 | –0.20 | –0.30 |
| Mn | **0.37** | 0.08 | **0.36** |
| Li | 0.04 | **–0.67** | –0.07 |
| Sr | **–0.70** | **–0.62** | **–0.66** |
| pH | **–0.85** | **–0.74** | **–0.78** |
| E. conductivity | **–0.76** | **–0.74** | **–0.70** |
| Tot-N | **0.66** | **0.45** | **0.55** |
| $NO_3^-$-N & $NO_2^-$-N | **0.81** | **0.72** | **0.72** |
| $NH_4^+$-N | 0.15 | **0.42** | 0.03 |
| PON | –0.08 | –0.29 | –0.04 |
| Tot-P | 0.12 | –0.02 | 0.04 |
| $PO_4^{3-}$-P | **0.41** | 0.23 | 0.30 |
| POP | –0.18 | –0.27 | –0.06 |
| DIC | **–0.85** | **–0.76** | **–0.83** |
| TOC | **0.56** | **0.44** | **0.36** |
| DOC | **0.67** | **0.48** | **0.45** |
| POC | –0.09 | **–0.35** | 0.00 |
| **Field measured parameters** | | | |
| Temperature | **–0.62** | **–0.55** | **–0.56** |
| Dissolved $O_2$ | **0.59** | **0.37** | **0.68** |

Parameter groups representing different major sources also show different responses to changes in discharge according to Table 5-1. Among the marine elements, which have been marked in blue in the table, Na, Mg and Cl show strong negative correlations with discharge at all sampling sites. On the other hand, elements and compounds associated with organic matter show positive or no correlation with water flow in streams. This reflects the fact that fundamentally different processes mediate the release and transport of these compounds, compared with ions released by inorganic weathering processes.

Simple dilution may however only partially explain the descending patterns of most major elements. In Figure 5-4, where water flow is plotted versus Cl concentration, two scenarios have been included for comparison. The straight line of scenario 1 represents dilution of a point source assuming an initial Cl concentration of 40 $mg \cdot L^{-1}$ at a discharge of 40 $L \cdot s^{-1}$. This chloride concentration may represent the concentration of the base flow in the catchment of the Laxemarån.

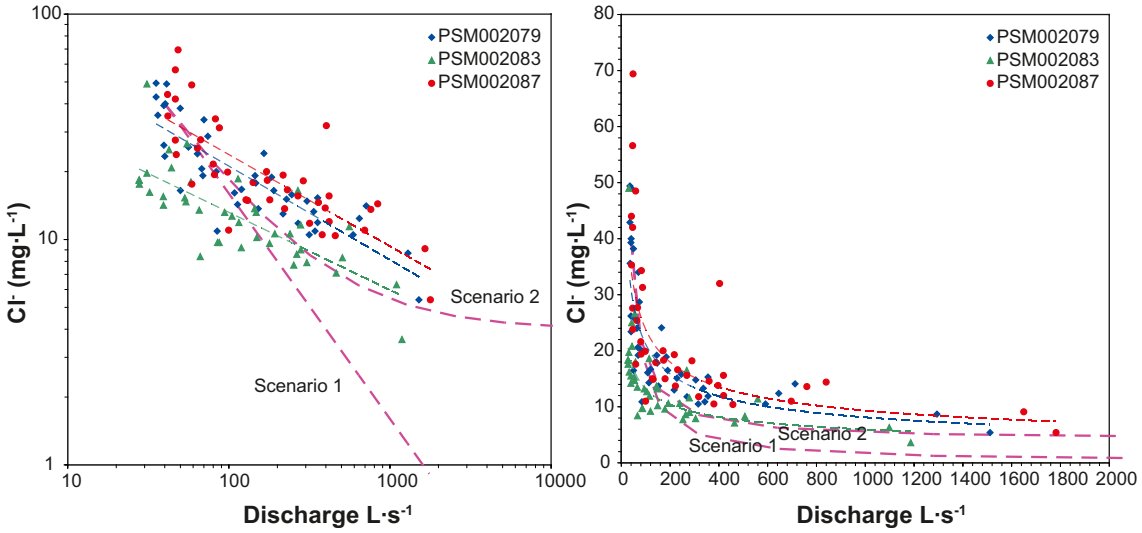


***Figure 5-4.*** *Left-hand panel: log-log plot showing discharge ($L \cdot s^{-1}$) versus Cl ($mg \cdot L^{-1}$) in the Laxemarån (PSM002079 upstream and PSM002087 near the outlet) and the Kärrviksån (PSM002083). Straight lines in the figures are power functions ( y=a·xn) fitted to the observations. Right-hand panel: identical information, but plotted with linear axes for comparison. Two dilution scenarios are shown by dashed pink lines (see text for explanation).*

One interpretation of scenario 1, descending with a steeper slope than the observed patterns, is that additional Cl is provided by discharging groundwater and overland flow, which counteracts the dilution effect. One possible source is input of Cl by atmospheric deposition, which is accounted for in scenario 2. If a Cl concentration corresponding to the observed concentration in precipitation is corrected for the concentrating effects of evapotranspiration by a factor of 3 (according to the approximate relation between evapotranspiration and precipitation in the Laxemar-Simpevarp area /Werner et al. 2008/), a minimum concentration in discharge of about 4 $mg \cdot L^{-1}$ should be the result according to scenario 2. It is evident from Figure 5-4 that atmospheric deposition may not fully explain the observed additional input of Cl, and one probable additional source of Cl is marine relicts in the sediments (cf Section 4.1.1). However, this source is not able to maintain constant concentrations when water flow increases. The observed descending pattern results from increased meteoric dilution of discharging groundwater containing marine ions. However, interpretation of the patterns for Cl is complicated by the fact that a large fraction of Cl in the Laxemarån and the Kärrviksån originates from road salt spread in the upper parts of the catchment (cf Section 6.2.1). Dilution of this point source may be responsible for the decrease along scenario 1 at flow rates below 100 $L \cdot s^{-1}$ in the Laxemarån.

When the response to variations in water flow is compared between the Laxemarån and the Kärrviksån, the overall decrease in Cl concentrations follow straight lines with similar slopes. This suggests that the potential power law relationships have similar exponents which could be interpreted as indicating that common processes regulate Cl concentrations in both catchments. The vertical shift between the Laxemarån and the Kärrviksån probably reflects differences in distributed characteristics within these catchments; the Laxemarån drains a longer stretch of the road salt source E22 and, moreover, it contains a larger proportion of topographically lower-lying areas with a potential supply of relict marine Cl.

Twelve plots, analogous to Figure 5-4, are shown for selected elements in Figure 5-5 and Figure 5-6. Patterns identified in these plots provide information on how concentrations of a number of selected parameters and parameter groups in Table 5-1 respond to variations in estimated water flow in streams. Conclusions and comments are summarised per parameter in the list below, followed by a general conclusion in Section 5.2.1:

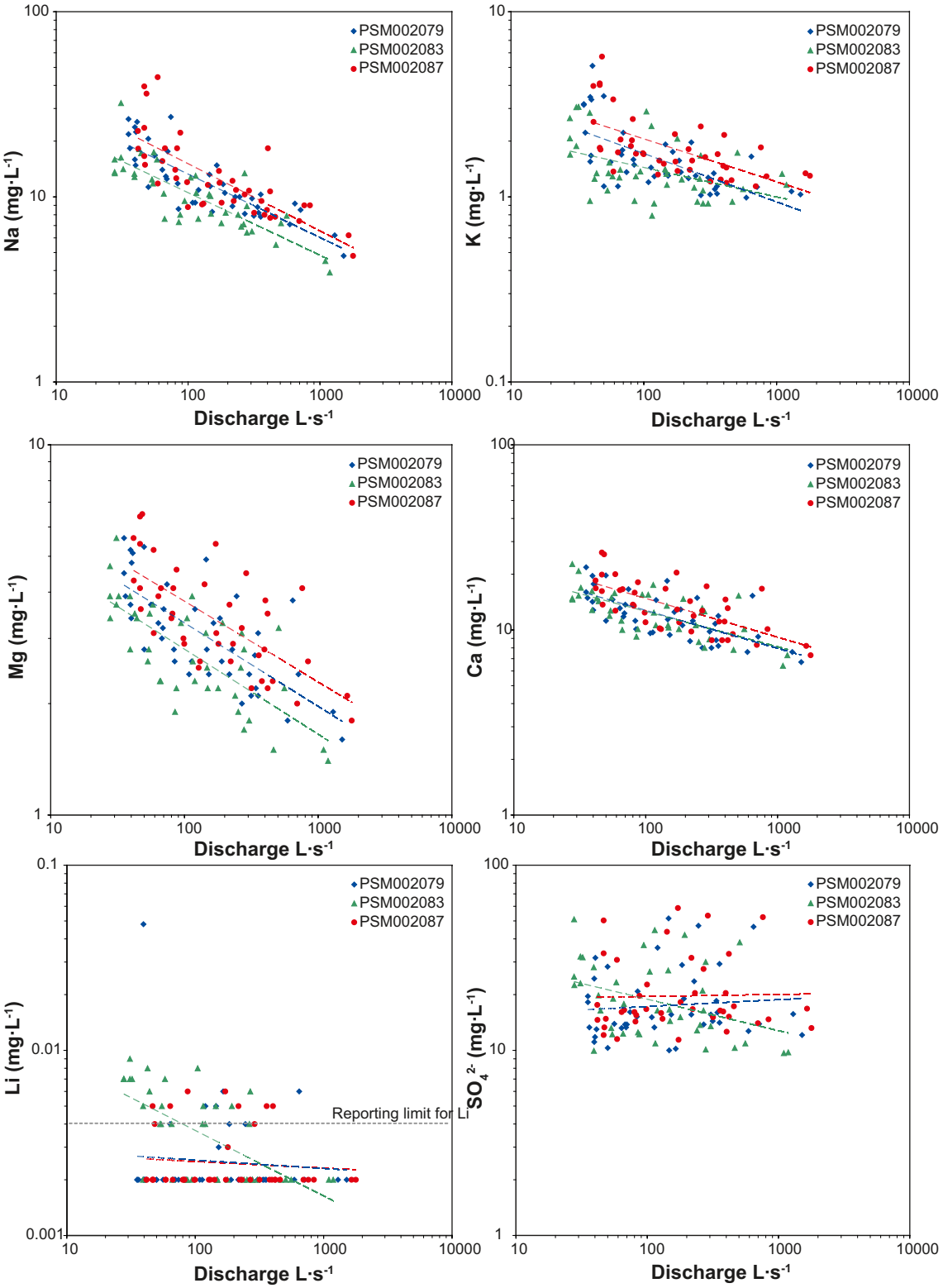


***Figure 5-5.*** *Log-log plots showing discharge ($L \cdot s^{-1}$) versus selected parameters (Na, K, Mg, Ca, Li, and $SO_4^{2-}$) in the Laxemarån (PSM002079 upstream and PSM002087 near the outlet) and the Kärrviksån (PSM002083). Straight lines in the figures are power functions ($y=a \cdot x^n$) fitted to the observations (see explanation in text).*

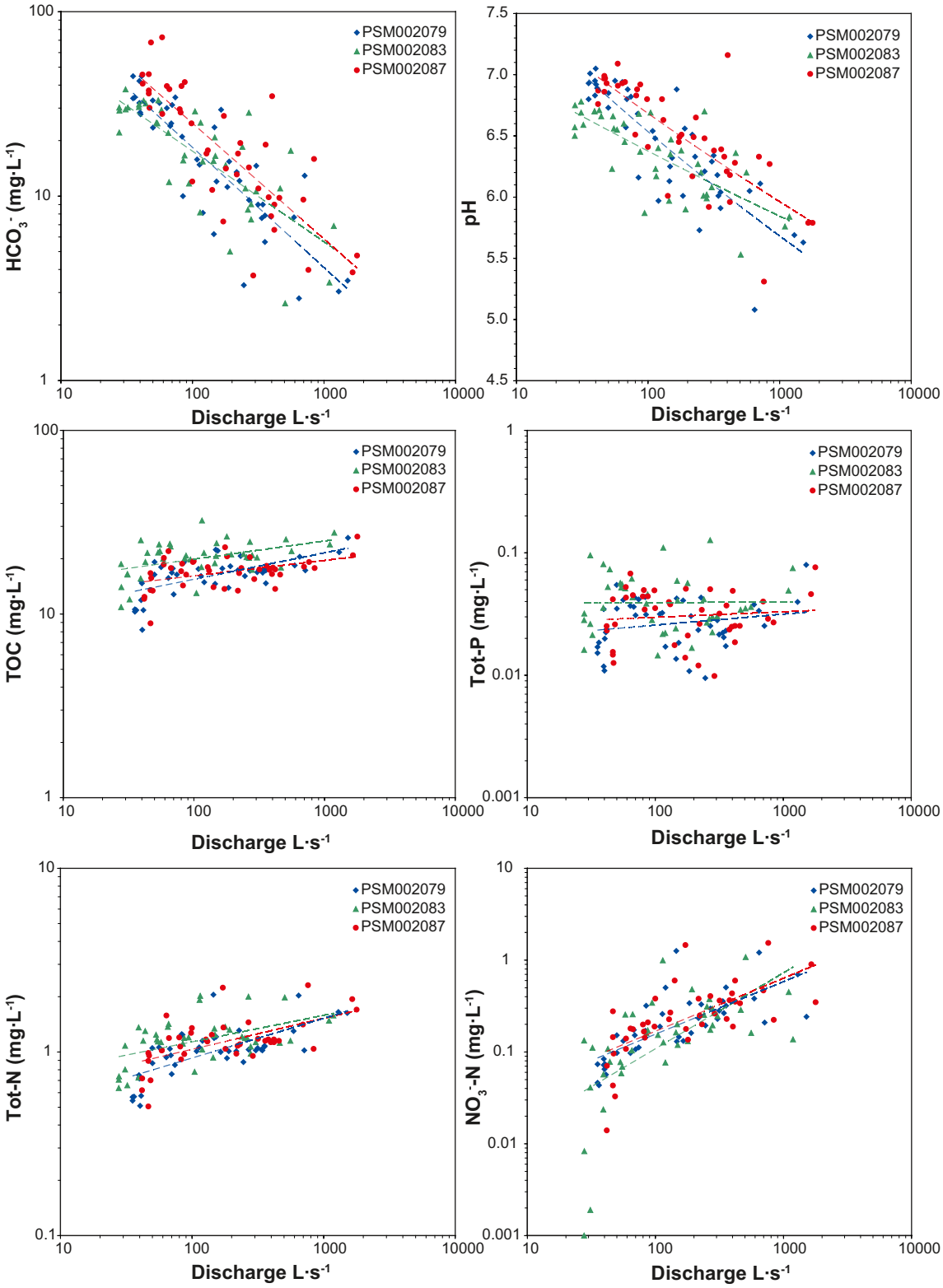


***Figure 5-6.*** *Log-log plots showing discharge ($L \cdot s^{-1}$) versus selected parameters ($HCO_3^-$, pH, TOC, tot-P, tot-N and $NO_3^-$-N) in the Laxemarån (PSM002079 upstream and PSM002087 near the outlet) and the Kärrviksån (PSM002083). Straight lines in the figures are power functions ($y=a \cdot xn$) fitted to the observations (see explanation in text).*

- Cl shows a general negative correlation to discharge in all catchments. The observed pattern is probably mainly attributable to dilution of the road salt sources high upstream in the catchments, in combination with release of marine ions in the lower parts of the Laxemar-Simpevarp area. The power law exponent 'n' varies between –0.42 and –0.34.
- Na shows a pattern very similar to Cl, probably due to the major common source of marine ions. The exponent 'n' ranges between –0.36 and –0.34, which overlaps the exponents for Cl and supports the supposition that there are probably common sources for Na and Cl. The difference in the absolute level of Na between the Laxemarån and the Kärrviksån is, however, less accentuated, which is probably an effect of the lower influence of road salt in relation to mineral weathering sources for Na.
- The correlation of K with discharge differs from that of e.g. Na, indicating that other sources and mechanisms may mediate the distribution of this element. There is still an inverse correlation with water flow, indicated by the correlation analysis in Table 5-1 and by the power law exponents, which range from –0.26 to –0.16. The difference is probably explained by the utilisation of K by biota and the subsequent degradation of organic matter (cf total organic carbon and total nitrogen, which both show positive correlation with water flow in Table 5-1).
- Mg is negatively correlated with discharge, similar to marine ions such as Na and Cl, but with a slightly different response, which is manifested by power exponents ranging from –0.23 to –0.22 (the larger spread in the vertical direction is mainly an effect of the scale chosen). The low variation among the exponents indicates that the same processes mediate the release of Mg in both catchments, and the variation in the vertical direction probably reflects different spatial coverage of these distributed sources.
- Ca shows a response to variations in water flow very similar to Mg, which is manifested as almost identical power exponents (–0.21 to –0.19 for Ca). Most probably, these ions are controlled by similar processes and sources (note that the different scales result in a different appearance in the vertical direction if these elements are compared). As indicated by the mass balance scenarios in Sections 6.2.4 and 6.2.6, the regolith type "Clay" and the associated land use category "Arable land" are distributed factors that are important for the release of both these elements in the Laxemar-Simpevarp area.
- Among the trace elements, Sr shows correlation coefficients very similar to Ca, which is also expected as these elements are often associated (cf Figure 4-14). As most Li observations fall below the reporting limit in surface waters, little can be said about the correlation of Li with water flow. In the Kärrviksån, however, Li concentrations are generally slightly elevated compared to the Laxemarån.This spatial pattern, which is the opposite of that for most other ions, may be an indication that leaching of Li is elevated in the northern part of the Laxemar-Simpevarp area. A possible source of Li is the Götemar granite which originates from the area around Lake Götemar north of the site (cf Section 4.1.2).
- $SO_4^{2-}$ shows, like K, weaker (or no) correlation with water flow. This may be caused by a counteracting process during high flow episodes due to outwash of $SO_4^{2-}$ formed by oxidation of sulphide minerals during the preceding drier period (cf Section 4.1.3). This process, together with atmospheric deposition, counteracts the dilution effect due to meteoric water (cf mass balance for $SO_4^{2-}$ in Section 6.2.7).
- Both pH and $HCO_3^-$, decrease when water flow increases, and this is probably to some extent caused by a common process. When flow increases, pH of stream water normally decreases due to the addition of organic acids in combination with a higher proportion of precipitation with low pH (and much $H^+$). The alkalinity (or buffering capacity, most of which is accounted for by $HCO_3^-$ at the prevailing pH, cf Figure 4-17) is consumed by $H^+$ and this process contributes not only to dilution but also to the decreasing concentrations of $HCO_3^-$ when water flow and supply of $H^+$ increases.

- Total concentrations of elements and compounds associated with organic matter as carbon (TOC) and nitrogen (tot-N) show only minor variations when discharge in streams varies by several orders of magnitude, in contrast to Cl for example. At very low flow rates (below 50 $L \cdot s^{-1}$), there is a tendency towards increasing concentrations of these elements with increasing discharge according to Figure 5-6, which is also seen as positive correlation coefficients in the correlation analysis in Table 5-1. Both the Laxemarån and the Kärrviksån show similar patterns, which suggests that the sources of these major constituents are similar in both these catchments.
- Tot-P, which like N is associated with organic matter but also originates from mineral sources (fertilizer input and a minor atmospheric deposition), shows larger variability compared to N and no clear correlation with variations in water flow. The scattered pattern shown by total phosphorus is most probably an effect of several superimposed processes and sources affecting this element. Leaching of phosphorus is usually associated with particulate matter, and high losses may be recorded during high discharge episodes due to erosion. As P is often a limiting nutrient in fresh water ecosystems, concentrations in water are to a large extent controlled by seasonal biological cycles as shown in Figure 5-7.
- Among the compounds associated with organic matter, $NO_3^-$-N, shows a highly deviating pattern. The $NO_3^-$-N concentrations vary within four orders of magnitude, compared to one or two for the rest of the parameters, and in all catchments $NO_3^-$-N is positively correlated with discharge according to the correlation analysis in Table 5-1. This pattern may be the result of two superimposed mechanisms: during the vegetation period, $NO_3^-$-N is consumed by primary production, especially when the water turnover is low, whereas low $NO_3^-$-N concentrations during the winter may be the result of anoxic conditions when $NH_4^+$-N is formed.

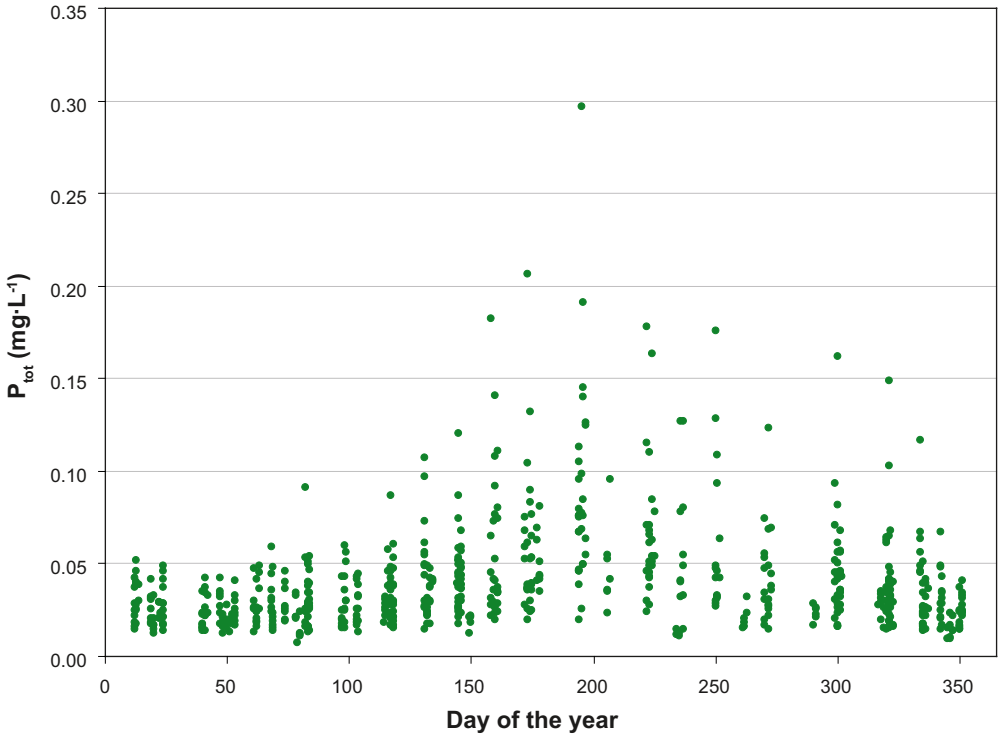


***Figure 5-7.*** *Seasonal variation in total phosphorus during 2003–2007 in all stream water sampling sites in the Laxemar-Simpevarp area.*

### 5.2.1 Conclusions – concentrations and water flow

Investigation of estimated discharge versus measured concentrations of a large number of elements in streams in the Laxemar-Simpevarp area shows that the concentrations of most elements either decrease or stay rather constant when water flow increase:

- Marine ions such as Cl, Na, and Mg show a clear negative correlation with water flow. For Na and Cl, the picture is highly influenced by the input of road salt in the upper parts of the catchments, which together with groundwater discharge contributes Na from mineral weathering and both Na and Cl from marine relicts in the deposits. During episodes of high water flow, these sources are diluted and the negative correlation with discharge emerges.
- $SO_4^{2-}$ and K deviate from the pattern of the other marine ions by showing weak or, in the case of $SO_4^{2-}$, no correlation with variations in water flow. The differing response of K compared to Na is probably attributable to the biological utilisation of this element. An important source of $SO_4^{2-}$ is mineral sulphides in the Quaternary deposits, and the major process behind the $SO_4^{2-}$ pattern is probably outwash of $SO_4^{2-}$ formed by oxidation of sulphide minerals during the preceding drier period. $SO_4^{2-}$ from atmospheric deposition also contributes to maintaining concentrations during episodes of high discharge.
- Concentrations of total organic carbon and total nitrogen, which are elements closely associated with organic matter, decrease or stay rather constant at increasing flow even if measured discharge varies by several orders of magnitude. Total phosphorus, which is also an important constituent of organic matter, deviates slightly from C and N by showing a more scattered picture and no clear correlation with water flow.

## 5.3 Estimation of mass transport in streams in the Laxemar-Simpevarp area

Estimates of mass transport are based on concomitant measurements of concentrations and discharge in streams. Daily transport is calculated by multiplying total daily discharge by a concentration representative of the same period, and these daily estimates are further summarised as monthly and yearly transport.

In the Laxemar-Simpevarp area, daily discharge measurements are available from automatic measurement stations. Unfortunately, these hydrological measurements overlap only partially with the time period when the spatial coverage of hydrochemical data is sufficient (cf compilation in Table 5-2 and Table 5-3). Moreover, there are some uncertainties regarding the level of specific discharge from these hydrological measurements which at present date makes them less suitable for transport estimations /Werner et al. 2008/.

Consequently, there is a need for extrapolation in both time and space in order to make any transport estimates possible. The location of the hydrochemical and hydrological observations points are shown in Figure 5-8. The premises for calculating mass transport are described in the following sections, and the results are compiled in Section 5.3.3.

### 5.3.1 Water discharge measurements used for transport estimates

Due to the lack of reliable surface water discharge measurements with sufficient temporal and spatial overlap with hydrochemical data, discharge was estimated by a combination of data from several sources:

- The temporal variability during the period from 1 December 2003 to 30 November 2004 was estimated by means of a hydrological model (MIKE-SHE) calibrated against discharge measurements from the year 2005 onward. By the use of local meteorological precipitation measurements from 2004, discharge time series were extrapolated back in time in order to cover the time interval selected for transport estimates (Emma Bosson, pers.comm.). The modelled and observed time series can be compared in Figure 5-10, together with the longer time series from Forshultesjön Lake, which is located inland from the Laxemar-Simpevarp area.

**Table 5-2. Available hydrochemical data from the Laxemar-Simpevarp area. Number of observations per month during the period October 2002 to April 2007. Transport was estimated for the time intervals and stations marked in yellow. Blue indicates which observations were used for validation of the mass balance models in Section 6, while green marks observations used in the correlation analysis in Section 5.2, where hydrochemical data are evaluated in relation to water flow.**

| Year | Month | PSM000347 | PSM002068 | PSM002069 | PSM002070 | PSM002071 | PSM002072 | PSM002075 | PSM002076 | PSM002077 | PSM002078 | PSM002079 | PSM002080 | PSM002081 | PSM002082 | PSM002083 | PSM002084 | PSM002085 | PSM002086 | PSM002087 | PSM003715 | PSM003716 | PSM107735 |
|---|---|---|---|---|---|---|---|---|---|---|---|---|---|---|---|---|---|---|---|---|---|---|---|
| 2002 | 10 | | | | | | | | | | | | | | | 1 | 1 | 1 | 1 | 1 | | | |
| 2002 | 11 | | 1 | 1 | | | | 1 | | 1 | 1 | 1 | | 1 | 1 | 1 | 1 | 1 | 1 | 1 | | | |
| 2002 | 12 | | 2 | 2 | 2 | 2 | 2 | 2 | 2 | 2 | 2 | 2 | 2 | 2 | 2 | 2 | 2 | 2 | 2 | 2 | | | |
| 2003 | 1 | | 1 | 1 | 1 | 1 | 1 | 1 | 1 | 1 | 1 | 1 | 1 | 1 | 1 | 1 | 1 | 1 | 1 | 1 | | | |
| 2003 | 2 | | 1 | 1 | 1 | 1 | 1 | 1 | 1 | 1 | 1 | 1 | 1 | 1 | 1 | 1 | 1 | 1 | 1 | 1 | | | |
| 2003 | 3 | | 2 | 2 | 2 | 2 | 2 | 2 | 2 | 2 | 2 | 2 | 2 | 2 | 2 | 2 | 2 | 2 | 2 | 2 | | | |
| 2003 | 4 | | 2 | 2 | 2 | 2 | 2 | 2 | 2 | 2 | 2 | 2 | 2 | 2 | 2 | 2 | 2 | 2 | 2 | 2 | | | |
| 2003 | 5 | | 2 | 2 | 2 | 2 | 2 | 2 | 2 | 2 | 2 | 2 | 2 | 2 | 2 | 2 | 2 | 2 | 2 | 2 | | | |
| 2003 | 6 | | 2 | 2 | 2 | 2 | 2 | 2 | 2 | 2 | 2 | 2 | 2 | 2 | 2 | 2 | 2 | 2 | 2 | 2 | | | |
| 2003 | 7 | | | 1 | 1 | 1 | | 1 | 1 | 1 | 1 | 1 | 1 | 1 | 1 | 1 | 1 | 1 | 1 | 1 | | | |
| 2003 | 8 | | 1 | 1 | 1 | 1 | 1 | 1 | | 1 | | 1 | 1 | 1 | 1 | 1 | 1 | 1 | | 1 | | | |
| 2003 | 9 | | 2 | 2 | 2 | 2 | | 2 | 1 | 2 | 1 | 2 | 2 | | 1 | 1 | 1 | 2 | 1 | 1 | | | |
| 2003 | 10 | | 1 | 1 | 1 | 1 | 1 | 1 | 1 | 1 | | 1 | 1 | 1 | 2 | 2 | 2 | 1 | | 2 | | | |
| 2003 | 11 | | 1 | 1 | | 1 | | | 1 | | 1 | 1 | | 1 | 1 | 1 | 1 | 1 | | 1 | | | |
| 2003 | 12 | | 1 | 1 | | 1 | | | 1 | | 1 | 1 | | | 1 | 1 | 1 | 1 | 1 | 1 | | | 1 |
| 2004 | 1 | | 1 | 1 | | 1 | | | 1 | | 1 | 1 | | 1 | 1 | 1 | 1 | 1 | 1 | 1 | | | 1 |
| 2004 | 2 | | 1 | 1 | | 1 | | | 1 | | 1 | 1 | | 1 | 1 | 1 | 1 | 1 | 1 | 1 | 1 | 1 | 1 |
| 2004 | 3 | | 2 | 2 | | 2 | | | 2 | | 2 | 2 | | 2 | 2 | 2 | 2 | 2 | 2 | 2 | 2 | 2 | 2 |
| 2004 | 4 | | 2 | 2 | | 2 | | | 2 | | 2 | 2 | | 2 | 2 | 2 | 2 | 2 | 2 | 2 | 2 | 2 | 2 |
| 2004 | 5 | | 2 | 2 | | 2 | | | 2 | | 2 | 2 | | 2 | 2 | 2 | 2 | 2 | 2 | 2 | 1 | 2 | 1 |
| 2004 | 6 | | 2 | 2 | | 2 | | | 2 | | | 2 | | 1 | 2 | 2 | 2 | 2 | | 2 | 1 | 2 | |
| 2004 | 7 | | 1 | 1 | | 1 | | | 1 | | 1 | 1 | | 1 | 1 | 1 | 1 | 1 | 1 | 1 | 1 | 1 | 1 |
| 2004 | 8 | | 2 | 2 | | 2 | | | 1 | | | 2 | | 2 | 2 | 2 | 2 | 2 | | 2 | | | |
| 2004 | 9 | | 1 | 1 | | 1 | | | | | | 1 | | | 1 | 1 | 1 | | | 1 | | | |
| 2004 | 10 | | 1 | 1 | | 1 | | | 1 | | 1 | 1 | | 1 | 1 | 1 | 1 | 1 | 1 | 1 | | | 1 |
| 2004 | 11 | | 1 | 1 | | 1 | | | 1 | | 1 | 1 | | 2 | 2 | 2 | 2 | 2 | 2 | 2 | | | 1 |
| 2004 | 12 | | 1 | 1 | | 1 | | | 1 | | 1 | 1 | | | | | | | | | | | 1 |
| 2005 | 1 | 1 | 1 | | | 1 | | | 1 | | | 1 | | | | 1 | | 1 | | 1 | | | |
| 2005 | 2 | 1 | 1 | | | 1 | | | 1 | | | 1 | | | | 1 | | 1 | | 1 | | | |
| 2005 | 3 | 1 | 1 | | | 1 | | | 1 | | | 1 | | | | 1 | | 1 | | 1 | | | |
| 2005 | 4 | 1 | | | | | | | | | | 1 | | | | 1 | | 1 | | 1 | | | |
| 2005 | 5 | 1 | | | | | | | | | | 1 | | | | 1 | | 1 | | 1 | | | |
| 2005 | 6 | 1 | | | | | | | | | | 1 | | | | 1 | | 1 | | 1 | | | |
| 2005 | 7 | | | | | | | | | | | 1 | | | | 1 | | | | 1 | | | |
| 2005 | 8 | | | | | | | | | | | 1 | | | | | | | | 1 | | | |
| 2005 | 9 | | | | | | | | | | | 1 | | | | 1 | | | | 1 | | | |
| 2005 | 10 | | | | | | | | | | | 1 | | | | 1 | | | | 1 | | | |
| 2005 | 11 | | | | | | | | | | | 1 | | | | 1 | | | | 1 | | | |
| 2005 | 12 | | | | | | | | | | | 1 | | | | 1 | | 1 | | 1 | | | |
| 2006 | 1 | 1 | | | | | | | | | | 1 | | | | 1 | | | | 1 | | | |
| 2006 | 2 | 1 | | | | | | | | | | 1 | | | | 1 | | 1 | | 1 | | | |
| 2006 | 3 | 1 | | | | | | | | | | 1 | | | | 1 | | 1 | | 1 | | | |
| 2006 | 4 | 1 | | | | | | | | | | 1 | | | | 1 | | 1 | | 1 | | | |
| 2006 | 5 | 1 | | | | | | | | | | 1 | | | | 1 | | 1 | | 1 | | | |
| 2006 | 6 | | | | | | | | | | | 1 | | | | 1 | | 1 | | 1 | | | |
| 2006 | 7 | | | | | | | | | | | 1 | | | | 1 | | 1 | | 1 | | | |
| 2006 | 8 | | | | | | | | | | | 1 | | | | 1 | | | | 1 | | | |
| 2006 | 9 | | | | | | | | | | | 1 | | | | 1 | 1 | | | | | | |
| 2006 | 10 | | | | | | | | | | | 1 | | | | 1 | | | | 1 | | | |
| 2006 | 11 | 1 | | | | | | | | | | 1 | | | | 1 | | 1 | | 1 | | | |
| 2006 | 12 | 1 | | | | | | | | | | 1 | | | | 1 | | 1 | | 1 | | | |
| 2007 | 1 | 1 | | | | | | | | | | 1 | | | | 1 | | 1 | | 1 | | | |
| 2007 | 2 | 1 | | | | | | | | | | 1 | | | | 1 | | | | 1 | | | |
| 2007 | 3 | | | | | | | | | | | | | | | 1 | | | | | | | |
| 2007 | 4 | | | | | | | | | | | | | | | 1 | | | | | | | |

**Table 5-3. Available hydrological discharge data from the Laxemar-Simpevarp area. The table shows the number of observations from surface water discharge stations during the period March 2004 to April 2007 (the first discharge stations were in operation in March 2004). Yellow colour marks the time interval where enough hydrochemical data for transport calculations are available. Green colour marks the time interval used for evaluation of hydrochemistry in relation to water flow.**

| Year | Month | PSM000341 | PSM000343 | PSM000345 | PSM000347 | PSM000348 | PSM000353 | PSM000364 | PSM000365 | PSM000368 |
|---|---|---|---|---|---|---|---|---|---|---|
| 2004 | 3 | 13 | 13 | 13 | | | | | | |
| 2004 | 4 | 30 | 30 | 30 | | | | | | |
| 2004 | 5 | 31 | 31 | 31 | | | | | | |
| 2004 | 6 | 30 | 30 | 30 | | | | | | |
| 2004 | 7 | 31 | 31 | 31 | | 7 | | | | 7 |
| 2004 | 8 | 31 | 31 | 31 | | 31 | | | | 31 |
| 2004 | 9 | 30 | 30 | 30 | | 30 | 28 | | | 30 |
| 2004 | 10 | 31 | 31 | 31 | | 31 | 31 | | | 31 |
| 2004 | 11 | 30 | 30 | 30 | 0 | 30 | 30 | 6 | | 30 |
| 2004 | 12 | 31 | 31 | 31 | 31 | 31 | 31 | 31 | | 31 |
| 2005 | 1 | 31 | 31 | 31 | 31 | 31 | 31 | 31 | | 31 |
| 2005 | 2 | 28 | 28 | 28 | 28 | 28 | 28 | 28 | 27 | 28 |
| 2005 | 3 | 30 | 30 | 30 | 30 | 30 | 30 | 30 | 30 | 30 |
| 2005 | 4 | 30 | 30 | 30 | 30 | 30 | 30 | 30 | 30 | 30 |
| 2005 | 5 | 31 | 31 | 31 | 31 | 31 | 31 | 31 | 31 | 31 |
| 2005 | 6 | 30 | 30 | 30 | 30 | 30 | 30 | 30 | 30 | 30 |
| 2005 | 7 | 31 | 31 | 31 | 31 | 31 | 31 | 31 | 31 | 31 |
| 2005 | 8 | 31 | 31 | 31 | 31 | 31 | 31 | 31 | 31 | 31 |
| 2005 | 9 | 30 | 30 | 30 | 30 | 30 | 30 | 30 | 30 | 30 |
| 2005 | 10 | 31 | 31 | 31 | 31 | 31 | 31 | 31 | 31 | 31 |
| 2005 | 11 | 30 | 30 | 30 | 30 | 30 | 30 | 30 | 30 | 30 |
| 2005 | 12 | 31 | 31 | 31 | 31 | 31 | 31 | 31 | 31 | 31 |
| 2006 | 1 | 31 | 31 | 31 | 31 | 31 | 31 | 31 | 31 | 31 |
| 2006 | 2 | 28 | 28 | 28 | 28 | 28 | 28 | 28 | 28 | 28 |
| 2006 | 3 | 30 | 30 | 30 | 30 | 30 | 30 | 30 | 30 | 30 |
| 2006 | 4 | 30 | 30 | 30 | 30 | 30 | 30 | 30 | 30 | 30 |
| 2006 | 5 | 31 | 31 | 31 | 31 | 31 | 31 | 31 | 31 | 31 |
| 2006 | 6 | 30 | 30 | 30 | 30 | 30 | 30 | 30 | 30 | 30 |
| 2006 | 7 | 31 | 31 | 31 | 31 | 31 | 31 | 31 | 31 | 31 |
| 2006 | 8 | 31 | 31 | 31 | 31 | 31 | 31 | 31 | 31 | 31 |
| 2006 | 9 | 30 | 30 | 30 | 30 | 30 | 30 | 30 | 30 | 30 |
| 2006 | 10 | 31 | 31 | 31 | 31 | 31 | 31 | 31 | 31 | 31 |
| 2006 | 11 | 30 | 30 | 30 | 30 | 30 | 30 | 30 | 30 | 30 |
| 2006 | 12 | 31 | 31 | 31 | 31 | 31 | 31 | 31 | 31 | 31 |
| 2007 | 1 | 31 | 31 | 31 | 31 | 31 | 31 | 31 | 31 | 31 |
| 2007 | 2 | 28 | 28 | 28 | 28 | 28 | 28 | 28 | 28 | 28 |
| 2007 | 3 | 30 | 30 | 30 | 30 | 30 | 30 | 30 | 30 | 16 |
| 2007 | 4 | 30 | 30 | 30 | 30 | 30 | 30 | 30 | 30 | |


***Figure 5-8.*** *Location of hydrochemical stations in stream water (red) and hydrological observation points (blue) in the Laxemar-Simpevarp area. Among the hydrological observation points PSM000341, 343, 345, 347, 353, 364, 365 and 368 are surface water discharge measurement stations, PSM000342, 344, 348 and 359 are measurements of lake water level and PSM000369, 370 and 371 are observation points for sea water level.*

- It was assumed that the specific discharge is constant throughout the whole Laxemar-Simpevarp area. This assumption is in accordance with the results from the Forsmark area /Johansson et al. 2008/, where hydrological measurements showed a very high level of agreement. The large spatial variation shown by discharge measurements in the Laxemar-Simpevarp area is probably an artefact that can be attributed to difficulties in determining the critical cross-section of the automatic measurement stations, and also the fact that minor streams are occasionally dry (cf Figure 5-9). According to this figure there is relatively good agreement between the two larger catchments of the Laxemarån (PSM000364) and the Kärrviksån (PSM000368), whereas measurements in the smaller catchments sometimes are strongly deviating.
- The specific discharge during the selected time period for transport estimations (2003-12-01 to 2004-11-30) was estimated based on data from the SMHI discharge station Forshultesjön, located outside the Laxemar-Simpevarp area. This catchment includes more lakes than the catchments of the Laxemar-Simpevarp area and the temporal variation is consequently more moderated, as shown in Figure 5-10.
- As a very rough estimate, the specific discharge in the Laxemar-Simpevarp area during the relatively wet year 2004 was approximately 7 $L \cdot s^{-1} \cdot km^{-2}$, based on the information compiled in Table 5-4. The discharge value of 7.6 $L \cdot s^{-1} \cdot km^{-2}$ from Lake Forshultesjön was rounded downwards to one value figure, based on the assumption of generally less precipitation closer to the coast, compared with the inland.
- The water discharge time series for each hydrochemical sampling station was estimated by area proportionalisation. The locally modelled variation (based on local measurements of precipitation) was multiplied with the specific discharge estimated from the SMHI discharge station Forshultesjön for the year 2004. The resulting time series are shown in Figure 5-11. Due to the assumptions presented above, differences between the series are only attributed to variations in catchment size.

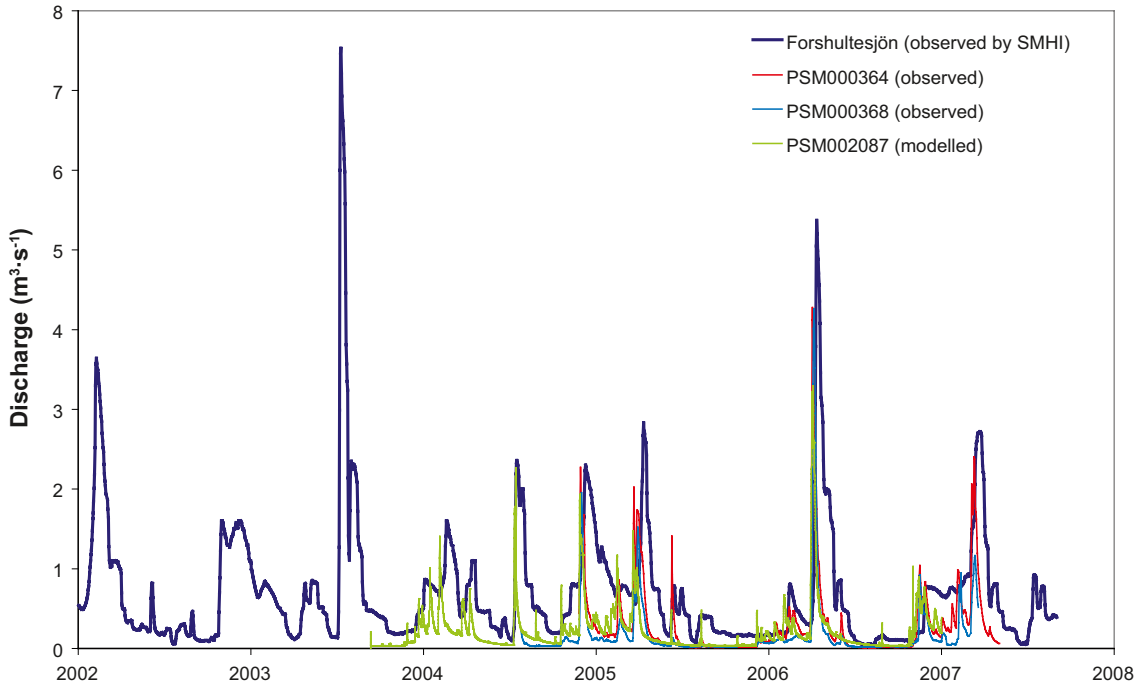


***Figure 5-9.*** *Area-specific discharge in the Laxemar-Simpevarp area. 30-day moving average (centred) plotted on a logarithmic scale during the period March 2005 to March 2007. The small streams PSM000343, 345 and 341 are sometimes dry and fall below 0.001 L·S$^{-1}$·km$^{-2}$.*

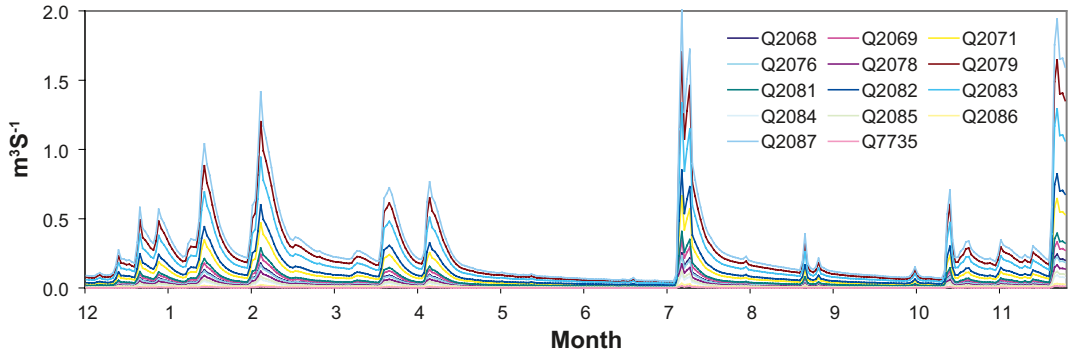


***Figure 5-10.*** *Discharge time series recorded automatically at two discharge stations in the Laxemar-Simpevarp area (PSM000364 and 368), compared to the modelled time series for the hydrochemical sampling station PSM002087 (Laxemarån) and the time series for the SMHI discharge station Forshultesjön.*

**Table 5-4. Observed area-specific discharge (L·s$^{-1}$·km$^{-2}$) for the SMHI discharge station Forshultesjön and the automatic discharge stations in the Kärrviksån and the Laxemarån.**

| | Forshultesjön (SMHI) | Kärrviksån (PSM000368) | Laxemarån (PSM000364) |
|---|---|---|---|
| Catchment size (km²) | 103.2 | 27.2 | 40 |
| **Specific discharge** | | | |
| 2004 | 7.6 | **7 (estimation)** | **7 (estimation)** |
| 2005 | 5.3 | 4.3 | 5.1 |
| 2006 | 5.6 | 7.5 | 7.3 |
| 2005–2006 (average) | 5.5 | 5.9 | 6.2 |

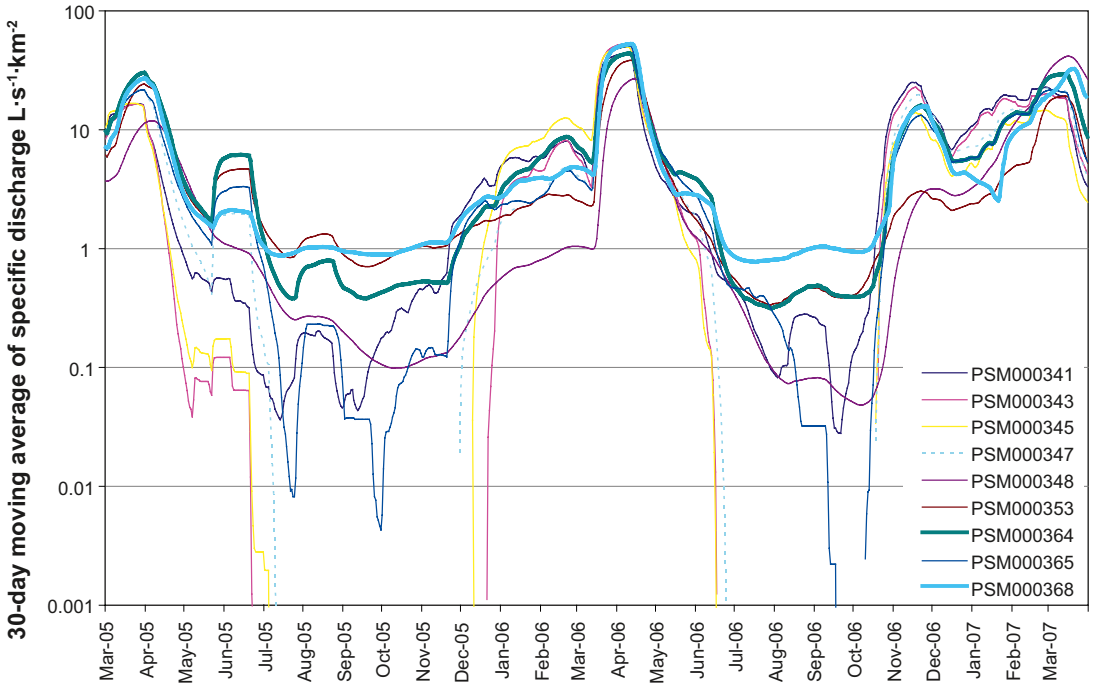


***Figure 5-11.*** *Estimated discharge time series in streams in the Laxemar-Simpevarp area used in the calculation of mass transport. Due to the assumptions (see bullet list above), temporal variation and area-specific discharge are identical between stations, and differences are attributable only to variations in catchment size.*

### 5.3.2 Hydrochemical data used for transport estimates

A major source of uncertainty in the calculations of mass transport in the Laxemar-Simpevarp area is the estimate of representative concentrations. The spatial error regarding concentrations is negligible, since all mass transport are calculated for the specific hydrochemical sampling points, but the temporal resolution is more limited due to the monthly sampling interval.

As mass transport are estimated by multiplication of daily discharge and the concentration representative for this time interval (one day), daily concentrations have to be interpolated (linear) from the monthly measurements according to the calculation technique commonly used. This rough generalisation may of course have a strong impact on the estimated mass transport if concentrations fluctuate between the sampling occasions. However, concentrations usually show much less variation than variations in discharge, which was also concluded in Section 5.2 where the relationship between discharge and concentrations in streams was explored. This error varies depending on the element. Total concentrations of major nutrients and carbon showed a weak correlation with water flow, suggesting that mass calculations for these elements are less affected by variations in water flow. Cl and other marine ions, on the other hand, show a clear negative correlation with discharge, which may lead to overestimated transport of these ions during episodes of high discharge (see Table 5-1 for details on each parameter).

In order to achieve maximum spatial resolution, hydrochemical data from the time period 1 December 2003 to 30 November 2004 were selected for transport estimates in 14 out of 22 available hydrochemical stations according to Table 5-2. For a total of 25 hydrochemical parameters, at least 12 observations were available for the transport estimate according to Figure 5-12: Na, K, Ca, Mg, Sr, Li, $HCO_3^-$, Cl , $SO_4^{2-}$, $SO_4^{2-}$-S, Br, F, Si, $SiO_2$-Si, $NH_4^+$-N, $NO_3^-$-N, $N_{tot}$, $P_{tot}$, $PO_4^{3-}$-P, POP, PON, POC, TOC, DOC and DIC. Br and Li had to be excluded from the estimation as most samples in surface water fall below the detection limit for these elements. A few parameters are more or less duplicates, such as $SO_4^{2-}$ and $SO_4^{2-}$-S, Si and $SiO_2$-Si and to some extent TOC and DOC. This means that transport can be estimated for a total of 20–23 independent parameters.

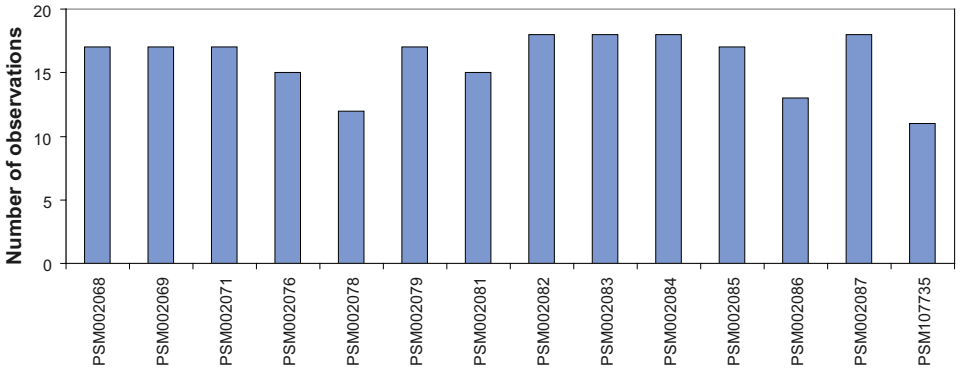


***Figure 5-12.*** *Number of available observations during the period 1 December 2003 to 30 November 2004 for Na, K, Ca, Mg, Sr, Li, $HCO_3^-$, Cl, $SO_4^{2-}$, $SO_4^{2-}$-S, Br, F, Si, $SiO_2$-Si, $NH_4^+$-N, $NO_3^-$-N, $N_{tot}$, $P_{tot}$, $PO_4^{3-}$-P, POP, PON, POC, TOC, DOC and DIC.*

### 5.3.3 Compilation of transport, area-specific transport and flow-weighted concentrations

Daily mass transport was estimated by multiplying daily discharge (cf Section 5.3.1) with the interpolated daily concentrations (cf Section 5.3.2). These transport figures were further summarised to monthly and yearly transport.

Estimated mass transport at stream sampling points may also be presented as area-specific transport (mass transport per unit area and year) or flow-weighted concentrations (total transport divided by total discharge volume). In Table 5-5, mass transports are compiled for one year (1 December 2003 to 30 November 2004). Corresponding compilations for flow-weighted concentrations and for area-specific transport are given in Table 5-6 and Table 5-7, respectively.

**Table 5-5. Estimated mass transport during one year (2003-12-01 to 2004-11-30) in streams in the Laxemar-Simpevarp area (kg·year$^{-1}$). Red figures denote uncertain estimates based on observations where many concentrations fall below reporting limits.**

| Element | PSM002068 | PSM002069 | PSM002071 | PSM002076 | PSM002078 | PSM002079 | PSM002081 | PSM002082 | PSM002083 | PSM002084 | PSM002085 | PSM002086 | PSM002087 | PSM107735 |
|---|---|---|---|---|---|---|---|---|---|---|---|---|---|---|
| Na | 4,677 | 12,748 | 32,224 | 6,841 | 3,127 | 66,997 | 7,674 | 24,740 | 45,124 | 3,645 | 4,027 | 1,739 | 80,929 | 346 |
| K | 963 | 1,986 | 4,241 | 1,217 | 450 | 9,624 | 1,937 | 4,330 | 7,033 | 1,126 | 670 | 459 | 13,397 | 96 |
| Ca | 8,392 | 12,953 | 27,348 | 14,159 | 5,428 | 69,992 | 19,887 | 39,119 | 56,151 | 6,676 | 14,770 | 2,459 | 91,250 | 891 |
| Mg | 2,065 | 3,362 | 7,258 | 2,541 | 1,362 | 17,630 | 3,193 | 6,986 | 12,068 | 1,419 | 1,727 | 545 | 22,872 | 253 |
| Sr | 47 | 67 | 149 | 63 | 28 | 368 | 68 | 158 | 264 | 26 | 41 | 10 | 462 | 4 |
| Li | 2.4 | 3.1 | 6.3 | 2.4 | 1.5 | 16.5 | 3.7 | 7.8 | 15.2 | 1.3 | 1.2 | 0.7 | 19.3 | 0.6 |
| $HCO_3^-$ | 13,957 | 24,124 | 41,716 | 18,598 | 2,170 | 88,932 | 36,840 | 66,476 | 82,591 | 10,575 | 35,566 | 1,997 | 124,056 | 453 |
| Cl | 5,103 | 19,374 | 52,110 | 7,711 | 3,024 | 98,262 | 8,082 | 31,567 | 56,018 | 3,964 | 3,144 | 2,020 | 118,526 | 371 |
| $SO_4^{2-}$ | 8,319 | 13,672 | 40,902 | 19,454 | 14,148 | 116,695 | 17,959 | 40,097 | 79,393 | 11,502 | 11,750 | 5,666 | 151,391 | 2,385 |
| $SO_4^{2-}$-S | 3,174 | 4,974 | 14,190 | 7,328 | 4,878 | 40,337 | 6,746 | 15,172 | 29,242 | 4,000 | 4,137 | 1,936 | 52,773 | 799 |
| Br | 113 | 154 | 299 | 217 | 97 | 904 | 183 | 415 | 674 | 61 | 63 | 92 | 932 | 11 |
| F | 505 | 671 | 926 | 397 | 140 | 2,074 | 541 | 1,191 | 5,473 | 610 | 443 | 86 | 2,551 | 34 |
| Si | 6,056 | 6,491 | 17,820 | 11,552 | 9,028 | 60,298 | 15,692 | 32,564 | 51,770 | 4,185 | 5,894 | 1,913 | 75,657 | 562 |
| $SiO_2$-Si | 6,533 | 6,269 | 18,335 | 11,593 | 9,317 | 61,755 | 15,941 | 33,015 | 52,753 | 4,219 | 5,891 | 1,960 | 77,098 | 579 |
| Tot-N | 1,377 | 1,460 | 3,000 | 2,307 | 858 | 9,141 | 2,390 | 5,217 | 8,035 | 833 | 1,150 | 505 | 12,072 | 91 |
| $NO_3^-$-N[A] | 224 | 248 | 782 | 363 | 233 | 2,159 | 171 | 977 | 1,314 | 292 | 421 | 264 | 3,300 | 13 |
| $NH_4^+$-N | 81 | 47 | 131 | 143 | 14 | 401 | 187 | 283 | 419 | 23 | 30 | 18 | 467 | 6 |
| PON | 135 | 99 | 240 | 260 | 54 | 765 | 253 | 404 | 854 | 60 | 63 | 20 | 1,017 | 8 |
| Tot-P | 29 | 27 | 74 | 73 | 18 | 281 | 86 | 146 | 305 | 24 | 30 | 11 | 369 | 2 |
| $PO_4^{3-}$-P | 3 | 2 | 11 | 14 | 3 | 56 | 18 | 27 | 62 | 6 | 4 | 3 | 75 | 0 |
| POP | 16 | 12 | 38 | 34 | 6 | 119 | 37 | 62 | 148 | 11 | 11 | 4 | 167 | 1 |
| TOC | 25,910 | 27,270 | 47,589 | 32,544 | 14,276 | 147,375 | 44,080 | 91,085 | 136,978 | 9,191 | 11,582 | 4,122 | 173,534 | 2,173 |
| DOC | 24,787 | 25,989 | 45,867 | 30,952 | 14,102 | 142,133 | 42,874 | 88,613 | 132,083 | 8,947 | 11,396 | 4,039 | 169,292 | 2,137 |
| POC | 2,115 | 973 | 3,389 | 3,103 | 564 | 8,855 | 3,370 | 4,901 | 9,824 | 807 | 646 | 215 | 12,530 | 109 |
| DIC | 2,628 | 4,106 | 7,737 | 3,398 | 732 | 15,192 | 6,557 | 12,980 | 14,049 | 1,815 | 6,171 | 418 | 21,713 | 124 |

A: Includes $NO_2^-$-N

**Table 5-6. Estimated flow weighted concentrations during one year (1 December 2003 to 30 November 2004) in streams in the Laxemar-Simpevarp area ($mgL^{-1}$). Red figures denote uncertain estimates based on observations where many concentrations fall below reporting limits.**

| Element | PSM002068 | PSM002069 | PSM002071 | PSM002076 | PSM002078 | PSM002079 | PSM002081 | PSM002082 | PSM002083 | PSM002084 | PSM002085 | PSM002086 | PSM002087 | PSM107735 |
|---|---|---|---|---|---|---|---|---|---|---|---|---|---|---|
| **Q ($m^3 \cdot s^{-1}$)** | 0.036 | 0.049 | 0.094 | 0.033 | 0.024 | 0.242 | 0.058 | 0.121 | 0.190 | 0.013 | 0.017 | 0.005 | 0.285 | 0.002 |
| **Na** | 4.1 | 8.3 | 10.8 | 6.6 | 4.1 | 8.8 | 4.2 | 6.5 | 7.5 | 8.6 | 7.3 | 11.6 | 9.0 | 5.3 |
| **K** | 0.9 | 1.3 | 1.4 | 1.2 | 0.6 | 1.3 | 1.1 | 1.1 | 1.2 | 2.7 | 1.2 | 3.1 | 1.5 | 1.5 |
| **Ca** | 7 | 8 | 9 | 14 | 7 | 9 | 11 | 10 | 9 | 16 | 27 | 16 | 10 | 14 |
| **Mg** | 1.8 | 2.2 | 2.4 | 2.4 | 1.8 | 2.3 | 1.8 | 1.8 | 2.0 | 3.4 | 3.1 | 3.6 | 2.5 | 3.9 |
| **Sr** | 0.04 | 0.04 | 0.05 | 0.06 | 0.04 | 0.05 | 0.04 | 0.04 | 0.04 | 0.06 | 0.07 | 0.07 | 0.05 | 0.06 |
| **Li** | 0.002 | 0.002 | 0.002 | 0.002 | 0.002 | 0.002 | 0.002 | 0.002 | 0.003 | 0.003 | 0.002 | 0.005 | 0.002 | 0.009 |
| **$HCO_3^-$** | 12 | 16 | 14 | 18 | 3 | 12 | 20 | 17 | 14 | 25 | 65 | 13 | 14 | 7 |
| **Cl** | 5 | 13 | 17 | 7 | 4 | 13 | 4 | 8 | 9 | 9 | 6 | 14 | 13 | 6 |
| **$SO_4^{2-}$** | 7 | 9 | 14 | 19 | 18 | 15 | 10 | 11 | 13 | 27 | 21 | 38 | 17 | 36 |
| **$SO_4^{2-}$-S** | 3 | 3 | 5 | 7 | 6 | 5 | 4 | 4 | 5 | 9 | 8 | 13 | 6 | 12 |
| **Br** | 0.1 | 0.1 | 0.1 | 0.2 | 0.1 | 0.1 | 0.1 | 0.1 | 0.1 | 0.1 | 0.1 | 0.6 | 0.1 | 0.2 |
| **F** | 0.4 | 0.4 | 0.3 | 0.4 | 0.2 | 0.3 | 0.3 | 0.3 | 0.9 | 1.4 | 0.8 | 0.6 | 0.3 | 0.5 |
| **Si** | 5.4 | 4.2 | 6.0 | 11.1 | 11.8 | 7.9 | 8.6 | 8.5 | 8.7 | 9.9 | 10.7 | 12.8 | 8.4 | 8.6 |
| **$SiO_2$-Si** | 5.8 | 4.1 | 6.2 | 11.1 | 12.2 | 8.1 | 8.8 | 8.7 | 8.8 | 10.0 | 10.7 | 13.1 | 8.6 | 8.8 |
| **Tot-N** | 1.22 | 0.95 | 1.01 | 2.22 | 1.12 | 1.20 | 1.31 | 1.37 | 1.34 | 1.97 | 2.10 | 3.38 | 1.34 | 1.38 |
| **$NO_3^-$-N[A]** | 0.20 | 0.16 | 0.26 | 0.35 | 0.30 | 0.28 | 0.09 | 0.26 | 0.22 | 0.69 | 0.77 | 1.76 | 0.37 | 0.19 |
| **$NH_4^+$-N** | 0.07 | 0.03 | 0.04 | 0.14 | 0.02 | 0.05 | 0.10 | 0.07 | 0.07 | 0.05 | 0.06 | 0.12 | 0.05 | 0.09 |
| **PON** | 0.12 | 0.06 | 0.08 | 0.25 | 0.07 | 0.10 | 0.14 | 0.11 | 0.14 | 0.14 | 0.11 | 0.14 | 0.11 | 0.11 |
| **Tot-P** | 0.025 | 0.018 | 0.025 | 0.071 | 0.023 | 0.037 | 0.047 | 0.038 | 0.051 | 0.057 | 0.054 | 0.072 | 0.041 | 0.032 |
| **$PO_4^{3-}$-P** | 0.003 | 0.001 | 0.004 | 0.014 | 0.003 | 0.007 | 0.010 | 0.007 | 0.010 | 0.014 | 0.008 | 0.019 | 0.008 | 0.004 |
| **POP** | 0.014 | 0.008 | 0.013 | 0.033 | 0.008 | 0.016 | 0.020 | 0.016 | 0.025 | 0.026 | 0.020 | 0.028 | 0.019 | 0.017 |
| **TOC** | 23.0 | 17.8 | 16.0 | 31.3 | 18.6 | 19.4 | 24.2 | 23.9 | 22.9 | 21.7 | 21.1 | 27.6 | 19.3 | 33.1 |
| **DOC** | 22.0 | 17.0 | 15.4 | 29.7 | 18.4 | 18.7 | 23.5 | 23.3 | 22.1 | 21.2 | 20.8 | 27.0 | 18.9 | 32.6 |
| **POC** | 1.9 | 0.6 | 1.1 | 3.0 | 0.7 | 1.2 | 1.9 | 1.3 | 1.6 | 1.9 | 1.2 | 1.4 | 1.4 | 1.7 |
| **DIC** | 2.3 | 2.7 | 2.6 | 3.3 | 1.0 | 2.0 | 3.6 | 3.4 | 2.4 | 4.3 | 11.2 | 2.8 | 2.4 | 1.9 |

A: Includes $NO_2^-$-N

**Table 5-7. Area specific transport during one year (2003-12-01 to 2004-11-30) in streams in the Laxemar-Simpevarp area (kg·km$^{-2}$·year$^{-1}$). Red figures denote uncertain estimates based on observations where many concentrations fall below reporting limits.**

| Element | PSM002068 | PSM002069 | PSM002071 | PSM002076 | PSM002078 | PSM002079 | PSM002081 | PSM002082 | PSM002083 | PSM002084 | PSM002085 | PSM002086 | PSM002087 | PSM107735 |
|---|---|---|---|---|---|---|---|---|---|---|---|---|---|---|
| **Area (km²)** | 5.1 | 7.0 | 13.5 | 4.7 | 3.5 | 34.6 | 8.3 | 17.3 | 27.2 | 1.9 | 2.5 | 0.7 | 40.8 | 0.3 |
| **Na** | 913 | 1,832 | 2,381 | 1,447 | 898 | 1,937 | 928 | 1,429 | 1,662 | 1,897 | 1,615 | 2,562 | 1,984 | 1,161 |
| **K** | 188 | 285 | 313 | 257 | 129 | 278 | 234 | 250 | 259 | 586 | 269 | 676 | 328 | 322 |
| **Ca** | 1,638 | 1,861 | 2,021 | 2,995 | 1,559 | 2,023 | 2,404 | 2,260 | 2,068 | 3,476 | 5,925 | 3,622 | 2,237 | 2,990 |
| **Mg** | 403 | 483 | 536 | 538 | 391 | 510 | 386 | 404 | 444 | 739 | 693 | 803 | 561 | 848 |
| **Sr** | 9 | 10 | 11 | 13 | 8 | 11 | 8 | 9 | 10 | 14 | 16 | 14 | 11 | 13 |
| **Li** | 0.5 | 0.4 | 0.5 | 0.5 | 0.4 | 0.5 | 0.4 | 0.4 | 0.6 | 0.7 | 0.5 | 1.0 | 0.5 | 1.9 |
| **$HCO_3^-$** | 2,724 | 3,467 | 3,082 | 3,934 | 623 | 2,571 | 4,453 | 3,841 | 3,042 | 5,505 | 14,266 | 2,941 | 3,042 | 1,519 |
| **Cl** | 996 | 2,784 | 3,850 | 1,631 | 869 | 2,840 | 977 | 1,824 | 2,063 | 2,064 | 1,261 | 2,975 | 2,906 | 1,245 |
| **$SO_4^{2-}$** | 1,624 | 1,965 | 3,022 | 4,116 | 4,063 | 3,373 | 2,171 | 2,317 | 2,924 | 5,987 | 4,713 | 8,345 | 3,712 | 8,004 |
| **$SO_4^{2-}$-S** | 619 | 715 | 1,048 | 1,550 | 1,401 | 1,166 | 815 | 877 | 1,077 | 2,082 | 1,660 | 2,851 | 1,294 | 2,681 |
| **Br** | 22 | 22 | 22 | 46 | 28 | 26 | 22 | 24 | 25 | 32 | 25 | 135 | 23 | 38 |
| **F** | 99 | 96 | 68 | 84 | 40 | 60 | 65 | 69 | 202 | 317 | 178 | 127 | 63 | 113 |
| **Si** | 1,182 | 933 | 1,317 | 2,444 | 2,593 | 1,743 | 1,897 | 1,882 | 1,907 | 2,178 | 2,364 | 2,818 | 1,855 | 1,887 |
| **$SiO_2$-Si** | 1,275 | 901 | 1,355 | 2,453 | 2,676 | 1,785 | 1,927 | 1,908 | 1,943 | 2,196 | 2,363 | 2,886 | 1,890 | 1,944 |
| **Tot-N** | 269 | 210 | 222 | 488 | 247 | 264 | 289 | 301 | 296 | 434 | 461 | 744 | 296 | 304 |
| **$NO_3^-$-N[A]** | 44 | 36 | 58 | 77 | 67 | 62 | 21 | 56 | 48 | 152 | 169 | 388 | 81 | 42 |
| **$NH_4^+$-N** | 16 | 7 | 10 | 30 | 4 | 12 | 23 | 16 | 15 | 12 | 12 | 27 | 11 | 21 |
| **PON** | 26 | 14 | 18 | 55 | 15 | 22 | 31 | 23 | 31 | 31 | 25 | 30 | 25 | 25 |
| **Tot-P** | 6 | 4 | 5 | 16 | 5 | 8 | 10 | 8 | 11 | 12 | 12 | 16 | 9 | 7 |
| **$PO_4^{3-}$-P** | 0.7 | 0.3 | 0.8 | 3.0 | 0.8 | 1.6 | 2.2 | 1.5 | 2.3 | 3.0 | 1.7 | 4.3 | 1.8 | 0.9 |
| **POP** | 3.1 | 1.8 | 2.8 | 7.2 | 1.9 | 3.4 | 4.5 | 3.6 | 5.5 | 5.6 | 4.5 | 6.1 | 4.1 | 3.7 |
| **TOC** | 5,057 | 3,919 | 3,516 | 6,885 | 4,100 | 4,260 | 5,328 | 5,263 | 5,044 | 4,785 | 4,646 | 6,070 | 4,255 | 7,292 |
| **DOC** | 4,837 | 3,735 | 3,389 | 6,548 | 4,050 | 4,108 | 5,182 | 5,120 | 4,864 | 4,658 | 4,571 | 5,949 | 4,151 | 7,172 |
| **POC** | 413 | 140 | 250 | 656 | 162 | 256 | 407 | 283 | 362 | 420 | 259 | 317 | 307 | 365 |
| **DIC** | 513 | 590 | 572 | 719 | 210 | 439 | 793 | 750 | 517 | 945 | 2,475 | 616 | 532 | 418 |

A: Includes $NO_2^-$-N

Visualisations of area-specific transport emphasise differences in the underlying sources of the selected parameters by normalisation with the whole catchment area upstream each sampling point. If ions and substances are evenly distributed throughout the Laxemar-Simpevarp area, the bars will be equal in height. Area-specific transport for Cl are shown in Figure 5-13, and in Figure 5-14 the other major constituents (Na, K, Ca, Mg, $SO_4^{2-}$, $HCO_3^-$) are visualised together with Sr and F. Organic substances and nutrients are shown in Figure 5-15, together with total concentrations of Si. Conclusions based on these figures are summarised in the list below:

- The area-specific transport of an element or compound usually varies by a factor of 2-3 among the selected surface sampling sites. The least variation among the major constituents is shown by Mg and Sr, whereas TOC shows the least variation among organic substances and major nutrients in Figure 5-15.
- Na and Cl show similar patterns, and as discussed in Section 7.5 the influx of NaCl in the form of winter road salt adds significantly to the total input of these ions to the Laxemar-Simpevarp area. This is especially evident in PSM002071, which is located close to European highway E22 in the western part of the Laxemar sub-area (cf Figure 5-8).
- Ca shows a pattern similar to Mg, except for the station PSM002085 where the Ca transport is slightly elevated. Transport of $HCO_3^-$ also deviates in this catchment, and as speculated in Section 6.2.8 this is probably due to anthropogenic input, e.g. liming.

- Area-specific transport of K are evenly distributed in the Laxemar-Simpevarp area except for two stations, PSM002084 and PSM002086, which are located in the outlets of the catchments ASM001486b and ASM001518b, respectively (cf Figure 6-1). The deviant behaviour of K compared to Na is probably mainly an effect of the utilisation of K in biota, which is probably also the reason for the flat pattern. Agricultural activities may also contribute K via fertilizers, which could be the reason for the elevated area-specific transport in PSM002084 and 2086 (cf Section 6.2.3).
- F shows elevated area-specific transport in three adjacent catchments in the northern part of the Laxemar area (PSM002083, 2084 and 2085). The fact that there is no elevated F transport in PSM002082 upstream of PSM002083 indicates that leaching of F may be enhanced in the topographically lower-lying areas close to the coast (cf Figure 2-5). According to the analysis in Section 5.2, F concentrations are negatively correlated with water flow, like many cations and Cl. Local F-bearing minerals in deposits in the northern area may be one reason for this pattern rather than marine input (which should have influenced lower-lying areas in the southern part as well).
- The spatial variation in the area-specific transport of organic substances and related ions in Figure 5-15, differs with the exception of K from most "inorganic" ion species in the previous figure. This probably reflects differences in sources of these groups of elements and substances. Agricultural activities and arable land (which in turn is associated with the presence of clay and lower-lying areas) is probably a common source that is responsible for elevated transport of K, as well as of N and P, in PSM002086. PSM002076 nearby shows elevated N and P specific transport, whereas K is on a level with most other observations in the area (cf mass balance for nitrogen in Section 6.2.10).
- Area-specific transport of Si are clearly lower in three stations located downstream of lakes in the western part of the Laxemar sub-area. This is particularly evident in PSM002069, located in the outlet of Lake Jämsen. The explanation for this pattern is probably uptake of Si by diatoms (algae) and sequestration in sediments due to sedimentation (cf Section 6.2.12).

The origin and fate of a selection of these elements are further explored in mass-balance models in Section 6.

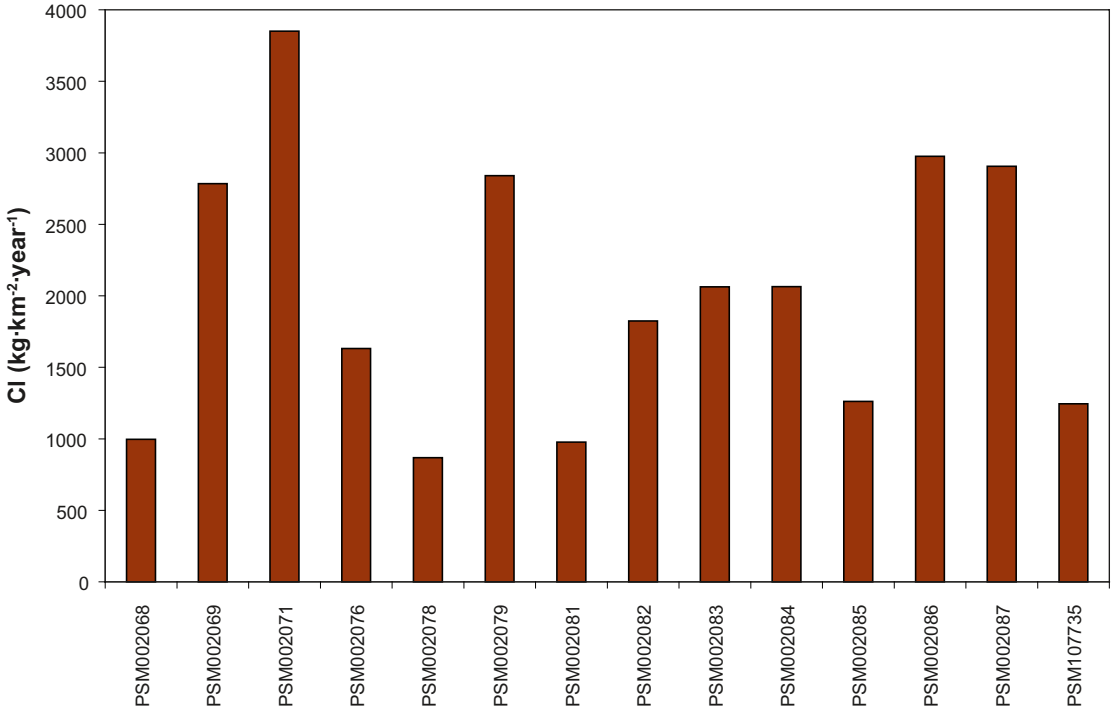


***Figure 5-13.*** *Area-specific Cl transport in the Laxemar-Simpevarp area (kg·km$^{-2}$·year$^{-1}$). The bars in the graph represent specific transport calculated for one year, which corresponds to the period 1 December 2003 to 30 November 2004. See Figure 5-8 for location of sampling points.*

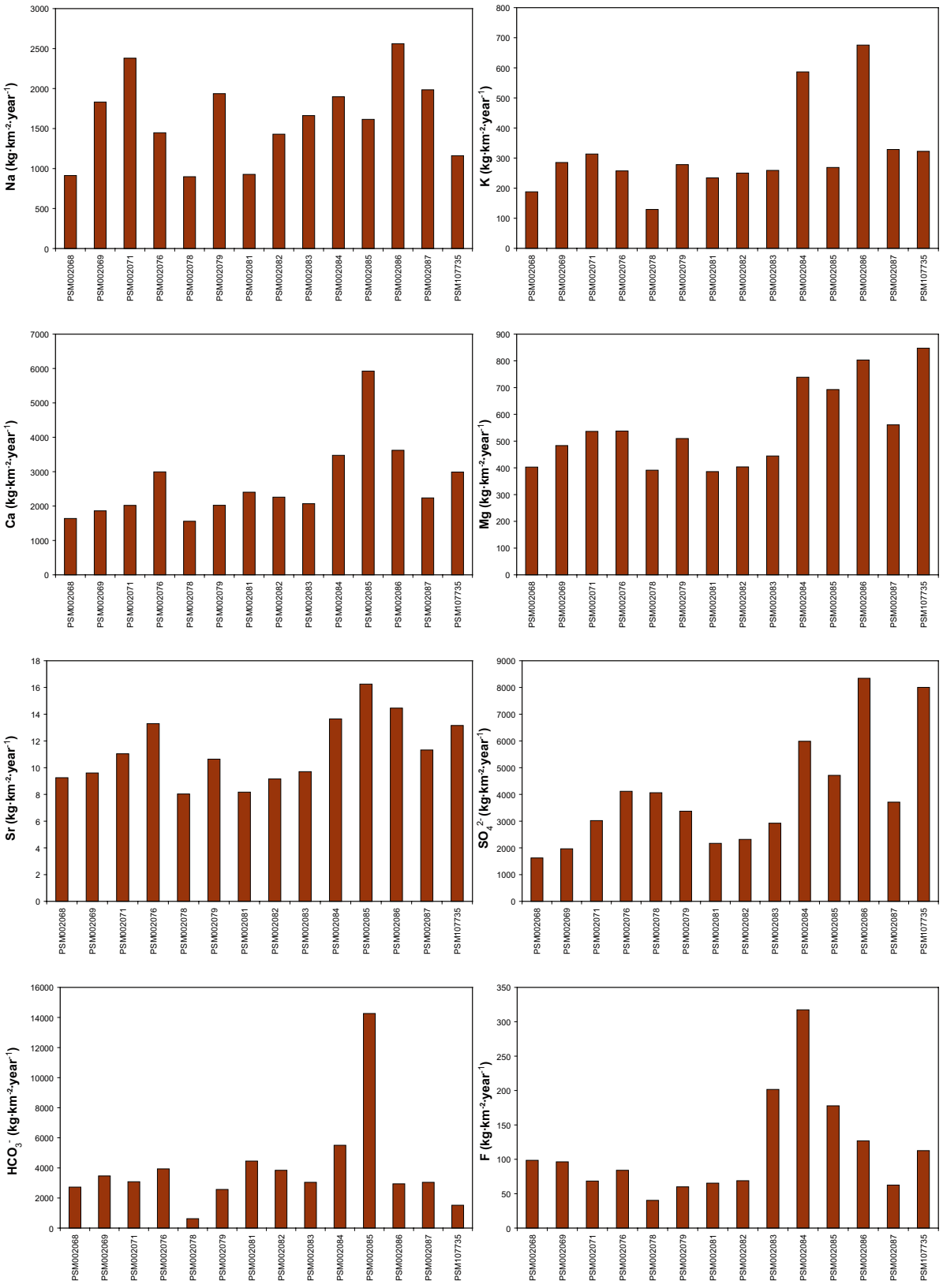


***Figure 5-14.*** *Area-specific transport of Na, K, Ca, Mg, Sr, $SO_4^{2-}$, $HCO_3^-$ and F in the Laxemar-Simpevarp area (kg·km$^{-2}$·year$^{-1}$). See Figure 5-13 for an explanation of the graphs, and Figure 5-8 for location of sampling points.*


***Figure 5-15.*** *Area-specific transport of Tot-N, $NO_3$-N, Tot-P, $NH_4$-N, TOC, $PO_4$-P, POC, and Si in the Laxemar-Simpevarp area (kg·km$^{-2}$·year$^{-1}$). See Figure 5-13 for an explanation to the graphs, and Figure 5-8 for location of sampling points.*

### 5.3.4 Estimated transport of trace elements

Based on the estimated transport of major constituents in Section 5.3.3, and on a correlation analysis of concentrations of a large number of trace elements versus these major constituents, mass transport and area-specific transport were roughly estimated for almost 40 trace elements. The results in the form of mass transport per year and area-specific transport per year are compiled in Table 5-9 and Table 5-10. Four selected trace elements are visualised in Figure 5-16, analogous to previous visualisations of area-specific transport (cf Figure 5-13).

The basis for the selection of which major constituent should be used as a representative for each trace element was a Spearman rank correlation analysis performed on 40 samples from fresh surface water in the Laxemar-Simpevarp area with complete characterisation of trace elements, which is summarised in Table 5-8. The scale factor in the rightmost column represents the ratio between the average concentration of the trace element and the average of the selected major constituents that show the largest significant ($p<0.05$) positive correlation coefficient. This coefficient is multiplied by the previously estimated transport of the current major constituent, thus providing a rough estimate of the transport of the trace element in question. This estimate, which is accordingly based on several assumptions, can mainly be regarded as an estimate of the order (or orders) of magnitude of transport of trace elements in watercourses Laxemar-Simpevarp area. One major souce of error is the non-linear behaviour of many trace elements which is not accounted for by the use of a linear model for the transport estimation.

It should also be noted that errors in transport estimates due to the statistical approach are expected, especially when the correlation coefficients are low or erroneously regarded as significant. When the significance of a large number of correlations is investigated, about 5% of the relationships may erroneously be regarded as significant due to the assumptions of the underlying statistical testing, i.e. 8 out of 155 significant relationships in Table 5-8.

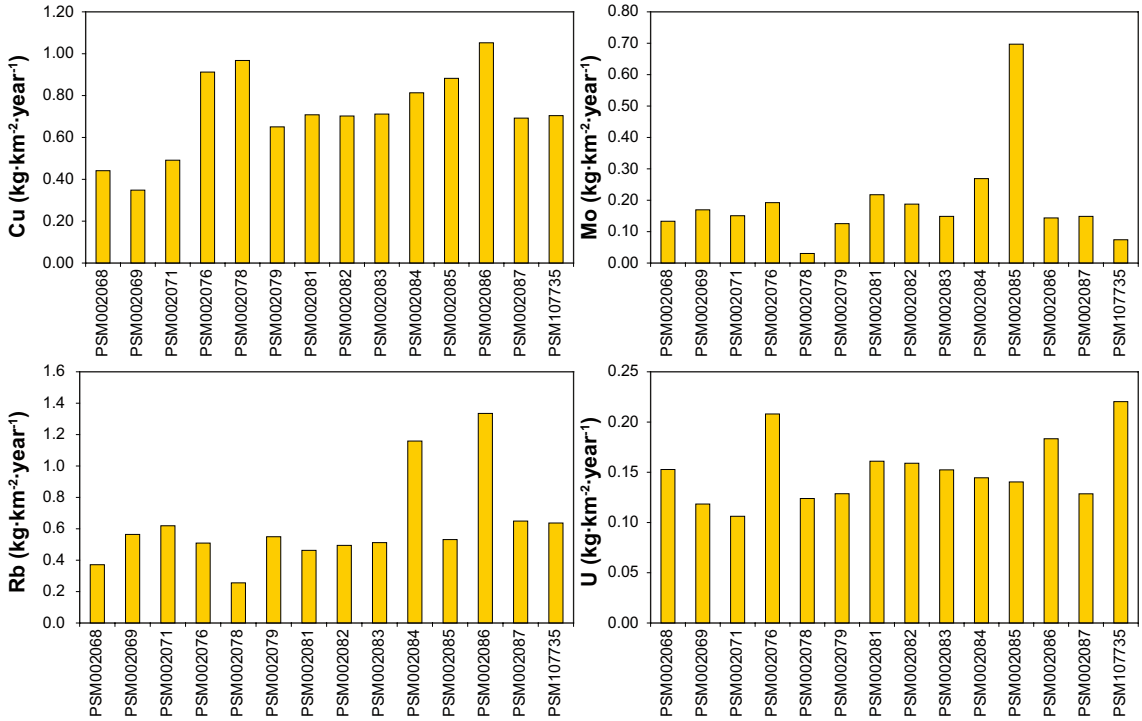


***Figure 5-16.*** *Estimated area-specific transport of Cu, Mo, Rb and U (kg·km$^{-2}$·year$^{-1}$).*

**Table 5-8. Spearman rank correlation coefficients for concentrations in fresh surface water in the Laxemar-Simpevarp area of trace elements and selected major elements for which transport are estimated. The largest significant (p<0.05) correlation coefficient per trace element used for the transport estimate is marked red in the table (other significant coefficients are marked in bold black figures). The scale factor in the rightmost column is the ratio between the average concentration of the trace element and the average concentration of the selected major constituent in freshwaters in the Laxemar-Simpevarp area (only calculated in case of significant correlation).**

| Element | TOC | POC | Tot-P | Na | K | Ca | Mg | $HCO_3^-$ | Cl | $SO_4^{2-}$ | Si | Scale factor |
|---|---|---|---|---|---|---|---|---|---|---|---|---|
| Al | **0.36** | 0.05 | 0.04 | **–0.37** | –0.08 | 0.04 | –0.08 | **–0.62** | –0.20 | **0.33** | **0.57** | 5.2E-02 |
| Ba | 0.08 | –0.30 | –0.30 | 0.17 | 0.18 | **0.63** | **0.68** | –0.12 | **0.35** | **0.79** | **0.70** | 9.5E-04 |
| Cd | 0.28 | –0.17 | –0.11 | –0.10 | 0.06 | **0.52** | **0.44** | –0.27 | 0.11 | **0.77** | **0.83** | 7.3E-06 |
| Ce | –0.06 | –0.31 | **–0.47** | **–0.31** | 0.06 | –0.02 | 0.04 | **–0.68** | 0.07 | **0.54** | **0.51** | 1.6E-04 |
| Co | **0.55** | 0.14 | 0.23 | –0.19 | **–0.34** | 0.27 | 0.11 | **–0.34** | –0.02 | 0.28 | **0.55** | 8.9E-05 |
| Cr | **0.80** | 0.27 | **0.46** | –0.08 | **–0.31** | **0.47** | 0.16 | 0.27 | –0.19 | 0.19 | **0.60** | 5.1E-05 |
| Cs | **–0.35** | –0.22 | –0.10 | **0.34** | **0.44** | 0.10 | 0.22 | 0.18 | **0.33** | 0.16 | –0.13 | 1.7E-05 |
| Cu | **0.53** | –0.05 | 0.16 | –0.16 | –0.13 | **0.53** | **0.37** | 0.13 | –0.05 | **0.52** | **0.74** | 3.7E-04 |
| Dy | –0.01 | –0.25 | **–0.47** | –0.29 | 0.03 | 0.07 | 0.10 | **–0.59** | 0.09 | **0.57** | **0.54** | 1.1E-05 |
| Er | –0.01 | –0.26 | **–0.48** | –0.28 | 0.03 | 0.08 | 0.11 | **–0.59** | 0.08 | **0.59** | **0.56** | 7.1E-06 |
| Eu | –0.03 | –0.30 | **–0.48** | –0.25 | 0.06 | 0.06 | 0.10 | **–0.59** | 0.11 | **0.57** | **0.55** | 2.6E-06 |
| Fe | **0.33** | **0.59** | **0.41** | –0.03 | –0.16 | –0.09 | –0.22 | **0.33** | –0.31 | **–0.58** | **–0.42** | 7.6E-01 |
| Gd | –0.03 | –0.29 | **–0.48** | –0.27 | 0.06 | 0.08 | 0.12 | **–0.60** | 0.10 | **0.58** | **0.55** | 1.4E-05 |
| Hf | **0.59** | **0.37** | **0.77** | –0.10 | **–0.38** | 0.17 | –0.11 | 0.29 | **–0.42** | –0.26 | 0.12 | 2.7E-03 |
| Hg | **0.73** | **0.47** | **0.49** | –0.19 | –0.26 | 0.10 | –0.21 | 0.19 | –0.20 | –0.11 | 0.23 | 1.6E-07 |
| Ho | –0.02 | –0.25 | **–0.48** | –0.28 | 0.04 | 0.08 | 0.11 | **–0.59** | 0.08 | **0.59** | **0.55** | 2.2E-06 |
| I | 0.16 | 0.23 | 0.23 | –0.12 | 0.06 | –0.08 | –0.18 | **0.40** | **–0.32** | **–0.32** | –0.27 | 9.0E-04 |
| La | –0.04 | –0.28 | **–0.50** | –0.28 | 0.06 | 0.04 | 0.09 | **–0.63** | 0.11 | **0.56** | **0.52** | 8.9E-05 |
| Lu | –0.06 | –0.26 | **–0.41** | **–0.32** | 0.05 | 0.04 | 0.08 | **–0.60** | 0.03 | **0.56** | **0.54** | 1.2E-06 |
| Mn | 0.17 | 0.08 | 0.04 | –0.12 | –0.11 | 0.10 | 0.10 | –0.27 | 0.13 | 0.12 | 0.22 | - |
| Mo | 0.15 | –0.14 | 0.13 | 0.12 | 0.08 | 0.25 | 0.20 | **0.51** | –0.01 | 0.10 | 0.16 | 4.9E-05 |
| Nd | –0.02 | –0.28 | **–0.47** | –0.27 | 0.04 | 0.05 | 0.08 | **–0.59** | 0.10 | **0.56** | **0.54** | 9.4E-05 |
| Ni | **0.63** | 0.08 | 0.31 | –0.14 | –0.22 | **0.67** | **0.43** | 0.17 | –0.14 | **0.52** | **0.78** | 4.3E-04 |
| Pb | –0.10 | 0.26 | 0.03 | –0.24 | 0.10 | **–0.68** | **–0.55** | **–0.32** | –0.24 | **–0.52** | **–0.57** | - |
| Pr | –0.02 | –0.29 | **–0.48** | –0.26 | 0.05 | 0.04 | 0.08 | **–0.60** | 0.11 | **0.56** | **0.53** | 2.3E-05 |
| Rb | **–0.58** | –0.19 | **–0.40** | 0.28 | **0.88** | –0.13 | 0.11 | –0.09 | **0.33** | 0.11 | –0.24 | 2.0E-03 |
| Sb | –0.16 | –0.23 | –0.20 | –0.06 | 0.15 | –0.29 | –0.09 | –0.23 | 0.03 | 0.02 | –0.03 | - |
| Sc | –0.02 | **–0.39** | **–0.41** | –0.20 | –0.03 | 0.14 | 0.12 | **–0.42** | 0.15 | **0.60** | **0.59** | 4.7E-06 |
| Sm | –0.02 | –0.27 | **–0.47** | –0.28 | 0.04 | 0.05 | 0.07 | **–0.59** | 0.09 | **0.56** | **0.54** | 1.6E-05 |
| Tb | 0.13 | –0.19 | –0.26 | **–0.45** | –0.19 | 0.01 | –0.01 | **–0.65** | –0.07 | **0.47** | **0.57** | 6.1E-06 |
| Th | 0.00 | –0.23 | **–0.39** | –0.15 | 0.10 | 0.08 | 0.05 | **–0.35** | 0.11 | **0.52** | **0.54** | 1.5E-05 |
| Tl | **0.47** | –0.04 | 0.20 | –0.17 | –0.22 | 0.19 | 0.09 | **–0.34** | –0.04 | 0.24 | **0.45** | 8.6E-07 |
| Tm | –0.03 | –0.29 | **–0.48** | –0.30 | 0.03 | 0.08 | 0.10 | **–0.60** | 0.06 | **0.60** | **0.57** | 1.0E-06 |
| U | **0.68** | 0.16 | **0.48** | –0.23 | –0.27 | **0.42** | 0.12 | 0.30 | **–0.32** | 0.22 | **0.58** | 3.0E-05 |
| V | **0.39** | 0.25 | **0.38** | –0.02 | –0.11 | –0.13 | –0.17 | 0.26 | –0.24 | **–0.37** | –0.16 | 6.3E-05 |
| Y | 0.00 | –0.25 | **–0.46** | –0.28 | 0.04 | 0.11 | 0.14 | **–0.57** | 0.09 | **0.61** | **0.57** | 7.9E-05 |
| Yb | –0.01 | –0.27 | **–0.46** | –0.31 | 0.02 | 0.07 | 0.09 | **–0.59** | 0.04 | **0.59** | **0.56** | 7.3E-06 |
| Zn | 0.18 | –0.14 | –0.19 | –0.22 | 0.08 | 0.15 | 0.14 | **–0.57** | 0.03 | **0.54** | **0.61** | 1.1E-03 |
| Zr | **0.75** | **0.46** | **0.81** | –0.07 | **–0.44** | **0.32** | –0.01 | **0.40** | **–0.39** | –0.18 | 0.26 | 5.7E-02 |

**Table 5-9. Estimated mass transport of trace elements in the Laxemar-Simpevarp area (kg·year$^{-1}$). The calculation, which is based on several uncertain assumptions, can mainly be regarded as an estimate of the order of magnitude of transport of trace elements in watercourses in the Laxemar-Simpevarp area.**

| Element | PSM002068 | PSM002069 | PSM002071 | PSM002076 | PSM002078 | PSM002079 | PSM002081 | PSM002082 | PSM002083 | PSM002084 | PSM002085 | PSM002086 | PSM002087 | PSM107735 |
|---|---|---|---|---|---|---|---|---|---|---|---|---|---|---|
| **Al** | 313 | 335 | 921 | 597 | 467 | 3,116 | 811 | 1,683 | 2,675 | 216 | 305 | 99 | 3,910 | 29 |
| **Ba** | 8 | 13 | 39 | 19 | 13 | 111 | 17 | 38 | 76 | 11 | 11 | 5 | 144 | 2 |
| **Cd** | 0.04 | 0.05 | 0.13 | 0.08 | 0.07 | 0.44 | 0.11 | 0.24 | 0.38 | 0.03 | 0.04 | 0.01 | 0.55 | 0.00 |
| **Ce** | 1.4 | 2.3 | 6.7 | 3.2 | 2.3 | 19.2 | 3.0 | 6.6 | 13.1 | 1.9 | 1.9 | 0.9 | 24.9 | 0.4 |
| **Co** | 0.54 | 0.58 | 1.58 | 1.03 | 0.80 | 5.36 | 1.39 | 2.89 | 4.60 | 0.37 | 0.52 | 0.17 | 6.72 | 0.05 |
| **Cr** | 1.32 | 1.39 | 2.42 | 1.66 | 0.73 | 7.51 | 2.25 | 4.64 | 6.98 | 0.47 | 0.59 | 0.21 | 8.84 | 0.11 |
| **Cs** | 0.02 | 0.03 | 0.07 | 0.02 | 0.01 | 0.16 | 0.03 | 0.07 | 0.12 | 0.02 | 0.01 | 0.01 | 0.22 | 0.00 |
| **Cu** | 2.3 | 2.4 | 6.7 | 4.3 | 3.4 | 22.5 | 5.9 | 12.2 | 19.3 | 1.6 | 2.2 | 0.7 | 28.2 | 0.2 |
| **Dy** | 0.09 | 0.15 | 0.44 | 0.21 | 0.15 | 1.25 | 0.19 | 0.43 | 0.85 | 0.12 | 0.13 | 0.06 | 1.63 | 0.03 |
| **Er** | 0.06 | 0.10 | 0.29 | 0.14 | 0.10 | 0.83 | 0.13 | 0.28 | 0.56 | 0.08 | 0.08 | 0.04 | 1.07 | 0.02 |
| **Eu** | 0.02 | 0.04 | 0.11 | 0.05 | 0.04 | 0.30 | 0.05 | 0.10 | 0.21 | 0.03 | 0.03 | 0.01 | 0.40 | 0.01 |
| **Fe** | 1,600 | 740 | 2,600 | 2,300 | 430 | 6,700 | 2,500 | 3,700 | 7,400 | 610 | 490 | 160 | 9,500 | 82 |
| **Gd** | 0.12 | 0.19 | 0.58 | 0.28 | 0.20 | 1.66 | 0.26 | 0.57 | 1.13 | 0.16 | 0.17 | 0.08 | 2.15 | 0.03 |
| **Hf** | 0.08 | 0.07 | 0.20 | 0.20 | 0.05 | 0.75 | 0.23 | 0.39 | 0.81 | 0.06 | 0.08 | 0.03 | 0.98 | 0.01 |
| **Hg** | 0.004 | 0.004 | 0.008 | 0.005 | 0.002 | 0.023 | 0.007 | 0.014 | 0.022 | 0.001 | 0.002 | 0.001 | 0.028 | 0.000 |
| **Ho** | 0.02 | 0.03 | 0.09 | 0.04 | 0.03 | 0.26 | 0.04 | 0.09 | 0.18 | 0.03 | 0.03 | 0.01 | 0.34 | 0.01 |
| **I** | 13 | 22 | 37 | 17 | 2 | 80 | 33 | 60 | 74 | 10 | 32 | 2 | 110 | 0.4 |
| **La** | 0.7 | 1.2 | 3.6 | 1.7 | 1.3 | 10.4 | 1.6 | 3.6 | 7.1 | 1.0 | 1.0 | 0.5 | 13.4 | 0.2 |
| **Lu** | 0.01 | 0.02 | 0.05 | 0.02 | 0.02 | 0.14 | 0.02 | 0.05 | 0.09 | 0.01 | 0.01 | 0.01 | 0.18 | 0.00 |
| **Mn** | No significant correlation | | | | | | | | | | | | | |
| **Mo** | 0.7 | 1.2 | 2.0 | 0.9 | 0.1 | 4.3 | 1.8 | 3.2 | 4.0 | 0.5 | 1.7 | 0.1 | 6.1 | 0.0 |
| **Nd** | 0.8 | 1.3 | 3.8 | 1.8 | 1.3 | 10.9 | 1.7 | 3.8 | 7.4 | 1.1 | 1.1 | 0.5 | 14.2 | 0.2 |
| **Ni** | 2.6 | 2.8 | 7.6 | 4.9 | 3.9 | 25.8 | 6.7 | 13.9 | 22.2 | 1.8 | 2.5 | 0.8 | 32.4 | 0.2 |
| **Pb** | No significant correlation | | | | | | | | | | | | | |
| **Pr** | 0.2 | 0.3 | 1.0 | 0.5 | 0.3 | 2.7 | 0.4 | 0.9 | 1.9 | 0.3 | 0.3 | 0.1 | 3.5 | 0.1 |
| **Rb** | 1.9 | 3.9 | 8.4 | 2.4 | 0.9 | 19.0 | 3.8 | 8.6 | 13.9 | 2.2 | 1.3 | 0.9 | 26.5 | 0.2 |
| **Sb** | No significant correlation | | | | | | | | | | | | | |
| **Sc** | 0.04 | 0.06 | 0.19 | 0.09 | 0.07 | 0.54 | 0.08 | 0.19 | 0.37 | 0.05 | 0.05 | 0.03 | 0.71 | 0.01 |
| **Sm** | 0.1 | 0.2 | 0.7 | 0.3 | 0.2 | 1.9 | 0.3 | 0.7 | 1.3 | 0.2 | 0.2 | 0.1 | 2.5 | 0.0 |
| **Tb** | 0.04 | 0.04 | 0.11 | 0.07 | 0.05 | 0.37 | 0.10 | 0.20 | 0.31 | 0.03 | 0.04 | 0.01 | 0.46 | 0.00 |
| **Th** | 0.09 | 0.09 | 0.26 | 0.17 | 0.13 | 0.88 | 0.23 | 0.47 | 0.75 | 0.06 | 0.09 | 0.03 | 1.10 | 0.01 |
| **Tl** | 0.02 | 0.02 | 0.04 | 0.03 | 0.01 | 0.13 | 0.04 | 0.08 | 0.12 | 0.01 | 0.01 | 0.00 | 0.15 | 0.00 |
| **Tm** | 0.01 | 0.01 | 0.04 | 0.02 | 0.01 | 0.12 | 0.02 | 0.04 | 0.08 | 0.01 | 0.01 | 0.01 | 0.15 | 0.00 |
| **U** | 0.78 | 0.82 | 1.44 | 0.98 | 0.43 | 4.45 | 1.33 | 2.75 | 4.14 | 0.28 | 0.35 | 0.12 | 5.24 | 0.07 |
| **V** | 1.6 | 1.7 | 3.0 | 2.1 | 0.9 | 9.4 | 2.8 | 5.8 | 8.7 | 0.6 | 0.7 | 0.3 | 11.0 | 0.1 |
| **Y** | 0.7 | 1.1 | 3.2 | 1.5 | 1.1 | 9.2 | 1.4 | 3.2 | 6.2 | 0.9 | 0.9 | 0.4 | 11.9 | 0.2 |
| **Yb** | 0.06 | 0.10 | 0.30 | 0.14 | 0.10 | 0.86 | 0.13 | 0.29 | 0.58 | 0.08 | 0.09 | 0.04 | 1.11 | 0.02 |
| **Zn** | 7 | 7 | 20 | 13 | 10 | 68 | 18 | 37 | 58 | 5 | 7 | 2 | 85 | 1 |
| **Zr** | 1.6 | 1.5 | 4.2 | 4.2 | 1.0 | 15.9 | 4.9 | 8.3 | 17.2 | 1.4 | 1.7 | 0.6 | 20.9 | 0.1 |

**Table 5-10. Estimated area-specific transport of trace elements in the Laxemar-Simpevarp area (kg·km$^{-2}$·year$^{-1}$). The calculation, which is based on several uncertain assumptions, can mainly be regarded as an estimate of the order of magnitude of specific transport of trace elements in the Laxemar-Simpevarp area.**

| Element | PSM002068 | PSM002069 | PSM002071 | PSM002076 | PSM002078 | PSM002079 | PSM002081 | PSM002082 | PSM002083 | PSM002084 | PSM002085 | PSM002086 | PSM002087 | PSM107735 |
|---|---|---|---|---|---|---|---|---|---|---|---|---|---|---|
| **Al** | 61 | 48 | 68 | 126 | 134 | 90 | 98 | 97 | 99 | 113 | 122 | 146 | 96 | 98 |
| **Ba** | 1.5 | 1.9 | 2.9 | 3.9 | 3.9 | 3.2 | 2.1 | 2.2 | 2.8 | 5.7 | 4.5 | 7.9 | 3.5 | 7.6 |
| **Cd** | 0.01 | 0.01 | 0.01 | 0.02 | 0.02 | 0.01 | 0.01 | 0.01 | 0.01 | 0.02 | 0.02 | 0.02 | 0.01 | 0.01 |
| **Ce** | 0.27 | 0.32 | 0.50 | 0.68 | 0.67 | 0.56 | 0.36 | 0.38 | 0.48 | 0.99 | 0.78 | 1.38 | 0.61 | 1.32 |
| **Co** | 0.10 | 0.08 | 0.12 | 0.22 | 0.23 | 0.15 | 0.17 | 0.17 | 0.17 | 0.19 | 0.21 | 0.25 | 0.16 | 0.17 |
| **Cr** | 0.26 | 0.20 | 0.18 | 0.35 | 0.21 | 0.22 | 0.27 | 0.27 | 0.26 | 0.24 | 0.24 | 0.31 | 0.22 | 0.37 |
| **Cs** | 0.003 | 0.005 | 0.005 | 0.004 | 0.002 | 0.005 | 0.004 | 0.004 | 0.004 | 0.010 | 0.004 | 0.011 | 0.005 | 0.005 |
| **Cu** | 0.44 | 0.35 | 0.49 | 0.91 | 0.97 | 0.65 | 0.71 | 0.70 | 0.71 | 0.81 | 0.88 | 1.05 | 0.69 | 0.70 |
| **Dy** | 0.02 | 0.02 | 0.03 | 0.04 | 0.04 | 0.04 | 0.02 | 0.02 | 0.03 | 0.06 | 0.05 | 0.09 | 0.04 | 0.09 |
| **Er** | 0.01 | 0.01 | 0.02 | 0.03 | 0.03 | 0.02 | 0.02 | 0.02 | 0.02 | 0.04 | 0.03 | 0.06 | 0.03 | 0.06 |
| **Eu** | 0.004 | 0.005 | 0.008 | 0.011 | 0.011 | 0.009 | 0.006 | 0.006 | 0.008 | 0.016 | 0.012 | 0.022 | 0.010 | 0.021 |
| **Fe** | 310 | 110 | 190 | 500 | 120 | 190 | 310 | 210 | 270 | 320 | 200 | 240 | 230 | 280 |
| **Gd** | 0.023 | 0.028 | 0.043 | 0.058 | 0.058 | 0.048 | 0.031 | 0.033 | 0.042 | 0.085 | 0.067 | 0.119 | 0.053 | 0.114 |
| **Hf** | 0.015 | 0.010 | 0.015 | 0.041 | 0.013 | 0.022 | 0.028 | 0.022 | 0.030 | 0.033 | 0.032 | 0.042 | 0.024 | 0.019 |
| **Hg** | 0.0,008 | 0.0,006 | 0.0,006 | 0.0,011 | 0.0,007 | 0.0,007 | 0.0,008 | 0.0,008 | 0.0,008 | 0.0,008 | 0.0,007 | 0.0,010 | 0.0,007 | 0.0,012 |
| **Ho** | 0.004 | 0.004 | 0.007 | 0.009 | 0.009 | 0.008 | 0.005 | 0.005 | 0.007 | 0.013 | 0.011 | 0.019 | 0.008 | 0.018 |
| **I** | 2.4 | 3.1 | 2.8 | 3.5 | 0.6 | 2.3 | 4.0 | 3.5 | 2.7 | 4.9 | 13 | 2.6 | 2.7 | 1.4 |
| **La** | 0.144 | 0.175 | 0.268 | 0.366 | 0.361 | 0.300 | 0.193 | 0.206 | 0.260 | 0.532 | 0.419 | 0.741 | 0.330 | 0.711 |
| **Lu** | 0.002 | 0.002 | 0.004 | 0.005 | 0.005 | 0.004 | 0.003 | 0.003 | 0.003 | 0.007 | 0.006 | 0.010 | 0.004 | 0.010 |
| **Mn** | No significant correlation | | | | | | | | | | | | | |
| **Mo** | 0.13 | 0.17 | 0.15 | 0.19 | 0.03 | 0.13 | 0.22 | 0.19 | 0.15 | 0.27 | 0.70 | 0.14 | 0.15 | 0.07 |
| **Nd** | 0.15 | 0.18 | 0.28 | 0.39 | 0.38 | 0.32 | 0.20 | 0.22 | 0.27 | 0.56 | 0.44 | 0.78 | 0.35 | 0.75 |
| **Ni** | 0.51 | 0.40 | 0.56 | 1.05 | 1.11 | 0.75 | 0.81 | 0.81 | 0.82 | 0.93 | 1.01 | 1.21 | 0.79 | 0.81 |
| **Pb** | No significant correlation | | | | | | | | | | | | | |
| **Pr** | 0.038 | 0.046 | 0.071 | 0.096 | 0.095 | 0.079 | 0.051 | 0.054 | 0.068 | 0.140 | 0.110 | 0.195 | 0.087 | 0.187 |
| **Rb** | 0.37 | 0.56 | 0.62 | 0.51 | 0.26 | 0.55 | 0.46 | 0.49 | 0.51 | 1.16 | 0.53 | 1.34 | 0.65 | 0.64 |
| **Sb** | No significant correlation | | | | | | | | | | | | | |
| **Sc** | 0.008 | 0.009 | 0.014 | 0.019 | 0.019 | 0.016 | 0.010 | 0.011 | 0.014 | 0.028 | 0.022 | 0.039 | 0.017 | 0.037 |
| **Sm** | 0.026 | 0.032 | 0.049 | 0.067 | 0.066 | 0.055 | 0.035 | 0.038 | 0.047 | 0.097 | 0.077 | 0.136 | 0.060 | 0.130 |
| **Tb** | 0.007 | 0.006 | 0.008 | 0.015 | 0.016 | 0.011 | 0.011 | 0.011 | 0.012 | 0.013 | 0.014 | 0.017 | 0.011 | 0.011 |
| **Th** | 0.017 | 0.014 | 0.019 | 0.036 | 0.038 | 0.025 | 0.028 | 0.027 | 0.028 | 0.032 | 0.034 | 0.041 | 0.027 | 0.027 |
| **Tl** | 0.004 | 0.003 | 0.003 | 0.006 | 0.004 | 0.004 | 0.005 | 0.005 | 0.004 | 0.004 | 0.004 | 0.005 | 0.004 | 0.006 |
| **Tm** | 0.002 | 0.002 | 0.003 | 0.004 | 0.004 | 0.003 | 0.002 | 0.002 | 0.003 | 0.006 | 0.005 | 0.008 | 0.004 | 0.008 |
| **U** | 0.153 | 0.118 | 0.106 | 0.208 | 0.124 | 0.129 | 0.161 | 0.159 | 0.152 | 0.145 | 0.140 | 0.183 | 0.129 | 0.220 |
| **V** | 0.32 | 0.25 | 0.22 | 0.44 | 0.26 | 0.27 | 0.34 | 0.33 | 0.32 | 0.30 | 0.29 | 0.39 | 0.27 | 0.46 |
| **Y** | 0.13 | 0.15 | 0.24 | 0.32 | 0.32 | 0.27 | 0.17 | 0.18 | 0.23 | 0.47 | 0.37 | 0.66 | 0.29 | 0.63 |
| **Yb** | 0.012 | 0.014 | 0.022 | 0.030 | 0.030 | 0.025 | 0.016 | 0.017 | 0.021 | 0.044 | 0.035 | 0.061 | 0.027 | 0.059 |
| **Zn** | 1.3 | 1.0 | 1.5 | 2.7 | 2.9 | 2.0 | 2.1 | 2.1 | 2.1 | 2.4 | 2.7 | 3.2 | 2.1 | 2.1 |
| **Zr** | 0.32 | 0.22 | 0.31 | 0.88 | 0.29 | 0.46 | 0.59 | 0.48 | 0.63 | 0.70 | 0.67 | 0.90 | 0.51 | 0.40 |

# 6 Evaluation of hydrochemistry on catchment scale

In this section a catchment model is used to evaluate hydrochemistry at the catchment level. The objective of these scenarios is to determine whether the observed hydrochemistry can be explained by spatially distributed factors such as regolith characteristics and land use, and ultimately the causes of the observed variation within the Laxemar-Simpevarp area. The calibrated catchment model is also a tool that may be used to extrapolate observations into areas where no measurements are conducted.

## 6.1 Catchment model VBX-VII.

The catchment model VBX-VII (WaterBoX version VII) couples hydrochemistry in surface water with hydrology and spatial environmental factors such as land use, regolith category, elevation distribution, and vegetation. Retention in lakes and emission from point sources are also handled in the model. Previous model versions are reported in /Naturvårdsverket 2003/ and /Tröjbom and Lindeström 2004/. A similar approach was also used in e.g. /Kvarnäs 1997/). VBX-VII is an empirical and static model, describing the average conditions over a fixed time-period, such as in the Laxemar-Simpevarp case one year from 1 December 2003 to 30 November 2004 (cf Sections 5.3.1 and 5.3.2).

VBX-VII is applied to all elements for which mass transport were estimated in Section 5.3.3 (except for F and Br where many observations fall below the reporting limit in many surface water samples). The outcome of the model should be regarded as one possible solution of the mass balance for a specific element, and it should be noted that there may be other alternative scenarios working as well. In most cases, however, the model converges towards only one stable solution regarding the selected factors (cf Section 6.1.4). As the model is calibrated against the observed transport in the outlets of the catchments, the model consequently describes the net balance per sub-catchment. In other words, in the case of for example organic carbon, only net fixation or loss is included in the model and nothing can be said about total exchange with the atmosphere.

When the catchment model satisfactorily describes the variation within the studied area, the major underlying factors will probably be understood. Deviations in the model may also contribute to the overall understanding of the site by indicating where unknown sources are affecting specific areas. The output of the model is the yearly mass transport or flow weighted concentrations in the outflow of each sub-catchment. If the element in question is subject to retention in lakes, the model provides estimates of this loss (or conversely, the gain if this is the case). The results may also be summarised per source, giving source apportionments at sub-catchment or catchment scales.

### 6.1.1 Hydrological network and water balance

The sub-catchment is the smallest spatial unit in the catchment model, and all information is aggregated and related to this unit. Sub-catchments used in VBX-VII are based on the water divides described in /Brunberg et al. 2004/. These are in a few cases further divided in order to form sub-catchments that intersect the hydrochemical sampling points (these catchments have an additional letter at the end of the idcode in Figure 6-1).

Sub-catchments are related to each other according to the hydrological network formed by streams and lakes in the area. A schematic representation of this network is shown in Figure 6-1 with arrows connecting catchment labels. There are two larger catchments in the Forsmark area that contain a large number of sub-catchments: the catchments of the Kärrviksån (outlet via


***Figure 6-1.*** *Sub-catchments and hydrological network of the Laxemar-Simpevarp area. Grey arrows show how sub-catchments (grey labels) are interconnected and black arrows show discharge to the Baltic Sea. Red labels indicate the locations of the hydrochemical sampling points. Several catchments are further divided into sub-catchments that intersect the hydrochemical sampling points (sub-catchments inherit the idcode from /Brunberg et al. 2004/ with addition of an additional letter at the end of the idcode, e.g. AFM002476a).*

ASM002486a) and the Laxemarån (outlet via ASM002476a). Besides these large catchments, a large number of catchments of varying size discharge either through small streams or directly into the Baltic Sea.

This hydrological network is implemented in VBX-VII in a spreadsheet according to the mathematical model structure described in Section 6.1.2. Additional information such as land use and other premises are also included in this spreadsheet (see Section 6.1.3), where diffuse sources and point sources are summarised downstream along the flow paths. The spreadsheet also includes calibration procedures (cf Section 6.1.4) and visualisation of the results (cf Section 6.2).

Annual discharge from a specific catchment is estimated by multiplying the specific discharge for a catchment by the catchment area. The specific discharge, which is assumed to be constant for the entire Laxemar-Simpevarp area as supported by the analysis in Section 5.3.1, have been estimated to be 7 $Ls^{-1}km^{-2}$ (220 mm $year^{-1}$) during the modelled time period 1 December 2003 to 30 November 2004 (see Sections 5.3.1 and 5.3.2). The estimated discharge in the outlets of the sub-catchments is shown in Figure 6-2. Modelled specific discharge with better spatial resolution was not available at the time of publication of this report.

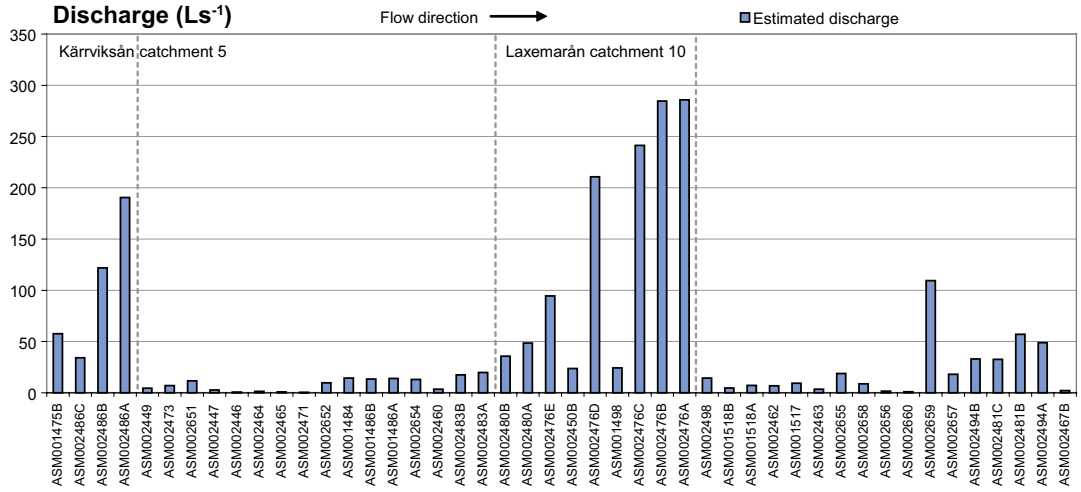


***Figure 6-2.*** *Estimated discharge ($L \cdot s^{-1}$) in outlet of sub-catchments in the Laxemar-Simpevarp area.*

### 6.1.2 Mathematical description of the VBX-VI model

In the catchment model VBX-VII, the average mass balance per sub-catchment is calculated as the sum of all inputs from upstream sub-catchments, as well as the sum of diffuse and point sources, minus retention and output through the outlet of the sub-catchment. Depending on the character of the sources, they may be implemented in the catchment model by three different methods, as shown in Equation 6-1 and in the example in Table 6-1:

- Distributed diffuse sources such as weathering are modelled by a *typical concentration* ($mg \cdot L^{-1}$) per category (e.g. land use) and class (e.g. forest land), multiplied by the discharge from this category/class within each sub-catchment (cf Section 6.1.3 for a list of categories and included classes). When discharge increases, concentrations are assumed to be constant and transport consequently increases proportionally.
- Distributed diffuse sources such as deposition can also be modelled by a *typical area-specific loss* per category and class ($kg \cdot km^{-2} \cdot yr^{-1}$), multiplied by the area of this category (class) in each sub-catchment (cf Section 6.1.3). In this case, concentrations in watercourses decrease when discharge increases, whereas transport stays constant.
- Point sources are modelled as *constant input* of elements ($kg \cdot yr^{-1}$). In this case concentrations decrease due to dilution effects when discharge increases, whereas transport stay constant.

The average flow-weighted concentration in the outlet of the catchment is derived by dividing the annual mass transport in the outlet by the yearly discharge, as shown in the generalised mathematical description for an arbitrary catchment in Equation 6-1. This quantity is compared to the measured concentrations when calibrating the catchment model (cf Section 6.1.4). Parameter abbreviations and units are explained in Table 6-1, where the calculation sequence is exemplified for a hypothetical two-catchment model.

*Equation 6-1. Mathematical formulation of the relationship used for calculating the flow-weighted concentration, $c_a$, in the outlet of catchment "a". The lower equation is the statistical relationship used for retention apportionment describing the proportion that is lost due to retention. Parameters and units are explained in Table 6-1. In the generalised equation below, the typical concentration $c_{typ,i}$ for different diffuse sources is denoted $c_{typ,1}$, $c_{typ,2}$, ... $c_{typ,n}$.*

$$c_a = \left[ \sum_{i=1}^{n} c_{typ,i} A_{a,typ,i} Q + \sum_{j=1}^{n} M_{a,spec,j} A_{a,spec,j} + \sum_{k=1}^{n} m_{pnt,k} + \sum_{l=1}^{n} T_{a,in,l} \right] \cdot \left[ 1 - f(\lambda, V_{a,lake}, q_a) \right] / q_a$$

$$q_a = A_a Q$$

$$f(\lambda, V_{a,lake}, q_a) = 1 - \frac{1}{1 + \lambda \frac{V_{a,lake}}{q_a}}$$

**Table 6-1. Generalised scheme showing the calculation order of different sources for the hypothetical catchments a and b, where catchment a is located upstream of catchment b. Red arrows indicate the direction of summation, blue arrows indicate subtraction due to retention processes, and green arrows denote transfer to catchments downstream. Conversion constants $k_1$ and $k_2$ are used to correct for the different units used in the calculations. $V_{a,lake}$ denotes the total lake volume of catchment a.**

| Catchment | Area | Specific discharge | Discharge | Typical concen-tration | Typical areal loss | Point source | Estimated transport | Comment |
|---|---|---|---|---|---|---|---|---|
| | A | Q | q | $c_{typ}$ | $M_{spec}$ | $m_{pnt}$ | T | Abbreviation |
| | $km^2$ | mm/yr | $m^3$/yr | mg/L | kg/$km^2$,yr | kg/yr | kg/yr | Unit |
| a | $A_{a,typ1}$ | Q | $q_{a,typ1}=k_1*A_{a,typ1}*Q$ | $c_{typ1}$ | | | $T_{a,1}=k_2*c_{typ1}*q_{a,typ1}$ | Diffuse source 1 |
| a | $A_{a,typ2}$ | Q | $q_{a,typ2}=k_1*A_{a,typ2}*Q$ | $c_{typ2}$ | | | $T_{a,2}=k_2*c_{typ2}*q_{a,typ2}$ | Diffuse source 2 |
| a | $A_{a,spec1}$ | Q | | | $M_{spec1}$ | | $T_{a,3}=M_{spec1}*A_{a,spec1}$ | Diffuse source 3 |
| a | | | | | | $m_{point1}$ | $T_{a,4}=m_{pnt1}$ | Point source 1 |
| a | | | | | | | $T_{a,tot}=T_{a,1}+T_{a,2}+T_{a,3}+T_{a,4}$ | Total input, Gross |
| a | $A_{a,lake}$ | | $q_a= k_1*A_a*Q$ | | | | $T_{a,ret}=f(\lambda, V_{a,lake}, q_a)*T_{a,tot}$ | Retention in lakes |
| a | $A_a$ | Q | $q_a= k_1*A_a*Q$ | | | | $T_{a,out}=T_{a,tot}-T_{a,ret}$ | Total output, Net |
| b | | | | | | | $T_{b,in}=T_{a,out}$ | Upstream input |
| b | $A_{b,typ1}$ | Q | $q_{typ1,b}= k_1*A_{typ1,b}*Q$ | $c_{typ1}$ | | | $T_{b,1}=k_2*c_{typ1}*q_{b,typ1}$ | Diffuse source 1 |
| b | $A_{b,typ2}$ | Q | $q_{a,typ2}= k_1*A_{a,typ2}*Q$ | $c_{typ2}$ | | | $T_{b,2}=k_2*c_{typ2}*q_{b,typ2}$ | Diffuse source 2 |
| b | $A_{b,spec1}$ | Q | | | $M_{spec1}$ | | $T_{b,3}=M_{spec1}*A_{b,spec1}$ | Diffuse source 3 |
| b | | | | | | $m_{point2}$ | $T_{b,4}=m_{pnt2}$ | Point source 2 |
| b | | | | | | | $T_{b,tot}=T_{b,in}+T_{b,1}+T_{b,2}+T_{b,3}+T_{b,}$ | Total input, Gross |
| b | $A_{b,lake}$ | | | | | | $T_{b,ret}=f(\lambda, V_{b,lake}, q_b)*T_{b,tot}$ | Retention in lakes |
| b | $A_b$ | Q | $q_b= k_1*A_b*Q$ | | | | $T_{b,out}=T_{b,tot}-T_{b,ret}$ | Total output, Net |

Unit conversion factors: $k_1$=1000, $k_2$=0.001

The total retention in the studied area is distributed among the sub-catchments by a statistical model where a) the total residence time in the lakes and b) a general retention constant (λ) are parameters. This model reflects how the proportion of retention of the specific element increases when the residence time increases, i.e. there is a larger loss in the lake when the residence time is long. In the interval where most sub-catchments in the Laxemar-Simpevarp area are found, this model is approximately linear (Lake Frisksjön 264 days and Lake Jämsen 275 days /Brunberg et al. 2004/), according to the relationships in Figure 6-3. A similar statistical relationship was used by /Grimwall and Stålnacke 1996/ in the MESAW model. If the retention parameter arrives at a negative value during calibration (cf Section 6.1.4), a net gain in the lake instead of a loss is indicated.

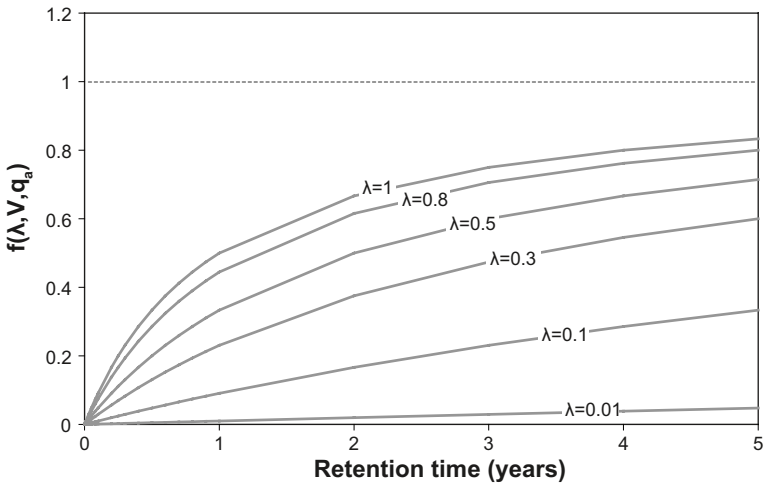


***Figure 6-3.*** *Visualisation of the relationship f(λ,V,q), describing the proportion of an element that is lost by retention as a function of residence time (years) for different values of λ (year–1). See Equation 6-1 for a mathematical description of this function.*

### 6.1.3 Distributed land characteristics and prerequisites for retention

Modelling of emissions from diffuse sources in the catchment model is based on statistical information on the areas of different distributed characteristics within each sub-catchment (cf Section 6.1.2 for a description of the methodology). A compilation and description of original and aggregated classifications used in the VBX-VII model can be found in Appendix B, along with the areas listed per class and catchment. Four major categories, each describing different distributed characteristics, are compiled per sub-catchment and may be implemented in the model:

- **Regolith**: The area of each of six regolith classes within each sub-catchment, based on aggregated classes from the regolith survey /Sohlenius and Hedenström 2008/: Jwater, Jsand, Jpeat, Jrock, Jclay, Jtill.
- **Land use**: The area of each of six land use categories within each sub-catchment, based on the topographical map: Mwater, Mforest, Mclear, Marable, Mopen, Mhard.
- **Vegetation cover**: The areas of eight different vegetation classes from the vegetation map in each sub-catchment /Lundin et al. 2005/: Vwater, Vwet, Vrock, Vforest, Vclear, Varable, Vopen, and Vhard.
- **Elevation distribution**: The topographical elevation distribution per sub-catchment of seven classes was calculated from the digital elevation model /Brydsten and Strömgren 2005/: 0–2m, 2–4m, 4–6m, 6–8m, 8–10m, 10–15m, and >15m.

As the sources of different elements are coupled to different environmental factors, the categories and classes included in the models differ between specific elements as well as between element groups. As indicated in the mathematical description in Section 6.1.2, the same geographical spot may also, be subject to several sources from different environmental categories. Besides the spatial information listed above, the total lake volume per sub-catchment is used as a parameter for the retention model (data derived from /Brunberg et al. 2004/).

### 6.1.4 Model setup, calibration and verification

Model setup and calibration is an iterative process aimed at finding as simple model as possible that satisfactorily describes the spatial variation of element concentrations within the Laxemar-Simpevarp area. There is necessarily a subjective stage in this process, when the governing parameters are selected based on the PLS explorative analysis described below, and on expert knowledge of the behaviour of different elements.

Prior to model setup, a partial least squares regression was performed on the relative areas of the distributed characteristics (cf Section 6.1.3) upstream of the hydrochemical sampling points (see Section 2.3.10 for an explanation of PLS). This analysis provides a rough indication of which factors are most correlated with the observed concentrations of the element in question and are therefore candidates in the initial model setup.

During calibration of the catchment model, general parameters valid for the whole area are varied in order to achieve maximum agreement between modelled and observed concentrations. These parameters include typical concentrations, typical area loss and the retention constant. The automatic calibration procedure uses the relationship in Equation 6-2 to find local minima that represent maximum agreement between modelled and observed concentrations. In most cases, the solver converges towards a stable single solution when a decent initial guess is applied.

*Equation 6-2. Relationship used by the automatic calibration procedure to calculate the total deviation, dev, between modelled and observed concentrations in the catchment model.*

$$dev = \sum ABS(c_{\mathrm{mod}} - c_{obs}) / c_{obs}$$

Calibration was carried out on flow-weighted concentrations estimated for 14 streams, as described in Section 5.3.3, representing average conditions during the period 1 December 2003 to 30 November 2004.

A secondary dataset representing mean values from 18 streams, based on monthly measurements between 1 November 2002 and 30 October 2003, was used for validation (cf Sections 5.3.1 and 5.3.2). This dataset, which includes 4 more stations than the calibration dataset, shows lower confidence than the primary dataset by the use of (non flow-weighted) mean values and because it represents a previous time period. The rationale for using this dataset for validation is the addition of 4 independent sampling points, and the addition of the 14 sampling stations used in the calibration dataset is for use as a reference for comparisons between the years.

In some cases it is convenient to add a hypothetical point source to the model scenario in order to neutralize anomalies, e.g. road salt from roads. These point (or line) sources are quantified in the summary tables, along with sinks such as retention in lakes (when applicable).

As a final validation step, calibrated typical concentrations from different land use classes, regolith or vegetation types are compared to local observations in shallow groundwater (cf /Tröjbom and Söderbäck 2006/) and, when applicable, to distributions of nationwide surveys of streams and lakes, to provide an idea as to whether these values are plausible.

## 6.2 Mass balance scenarios

In this section, mass balance scenarios are shown for a large number of elements. It should be noted that these are just scenarios and that there may be other plausible solutions for the mass balances of the Laxemar-Simpevarp area. In most cases, however, the models converge towards only one stable solution from the selected premises, and in the case of equivalent solutions these are mentioned in the text or shown in alternative presentations.

The results of the mass balance models are presented for each element in the form of bar graphs showing the flow-weighted concentrations and transport in the outlets of the catchments. Modelled values are shown together with observed values from the primary calibration and secondary validation sets of data, described in Section 6.1.4. Model parameters are listed in a table in each section, as well as in the summary in Table 6-15.

As supportive information, the calibrated typical concentrations are plotted into the concentration distributions from the Swedish survey of lakes and stream /IMA 2007/. A partial least squares regression model (PLS) is also included, showing the correlation structure between observed concentrations and the relative area proportion of the different distributed characteristics (cf Section 2.3.10 for a description of PLS), which was used for the initial selection of parameters during model setup.

### 6.2.1 Mass balance for chloride (Cl)

The initial calibration of the Cl mass balance model did not converge to a stable solution, even though many combinations of distributed factors were tested. This, in combination with the lack of systematic patterns in the PLS analysis in Figure 6-4, indicated that unknown sources were affecting the system. A potential source is different kinds of road salt spread on roads in the area:

- Winter road salt (98% NaCl) is spread on larger roads for anti-skid treatment. On motorway E22, approximately 9 tonnes of NaCl (containing 5.5 tonnes of Cl) was spread per km during the winters of 2003/2004 and 2004/2005, if information from /Ojala and Mellqvist 2004/, /Vägverket 2008/ and Figure 6-6 are combined (cf Section 7.5.1).
- Sand with the addition of winter road salt is spread on smaller roads. The magnitude of this source is not known.

- Summer road salt (either $MgCl_2$ of $CaCl_2$) is spread on gravel roads to reduce dusting. During road maintenance approximately 1 tonne of $MgCl_2$ or 1.3 tonnes of $CalCl_2$ may be spread per km /VTI 2008/. The magnitude of this source is not known, but there are clear indications that this source may contribute significantly in the Laxemar-Simpevarp area (cf Section 7.5.2).

In order to model the contribution of road salt, E22 (cf Figure 2-7) was implemented in the mass balance model as a line source. This source was divided between the catchments in relation to the length of the stretch of E22 that passes each catchment, and the total amount from this source was calibrated as a free parameter in the model.

The addition of the road salt source greatly improved the modelling result. Among the distributed characteristics, only the elevation category was able to satisfactorily model the variation pattern for chloride within the Laxemar-Simpevarp area, as shown in Figure 6-5. Model parameters and the contribution from each source are shown in Table 6-2. See Appendix C for detailed model results.

By adjusting the typical concentrations of three parameters ('0–5m' and '5–10m', and 10–15m), together with the road salt source, the variation in Cl concentration is satisfactorily modelled within the Laxemar-Simpevarp area. Compared to the calibration dataset, the greatest overestimate is found in ASM001475B, whereas concentrations are underestimated in ASM001486B and ASM001518B. When the model results are compared to the (more uncertain) validation dataset, discrepancies are (consequently) larger, but the overall concordance is still evident. The average deviation between modelled and observed concentrations is 27% for the primary calibration dataset and 39% for the secondary validation dataset.

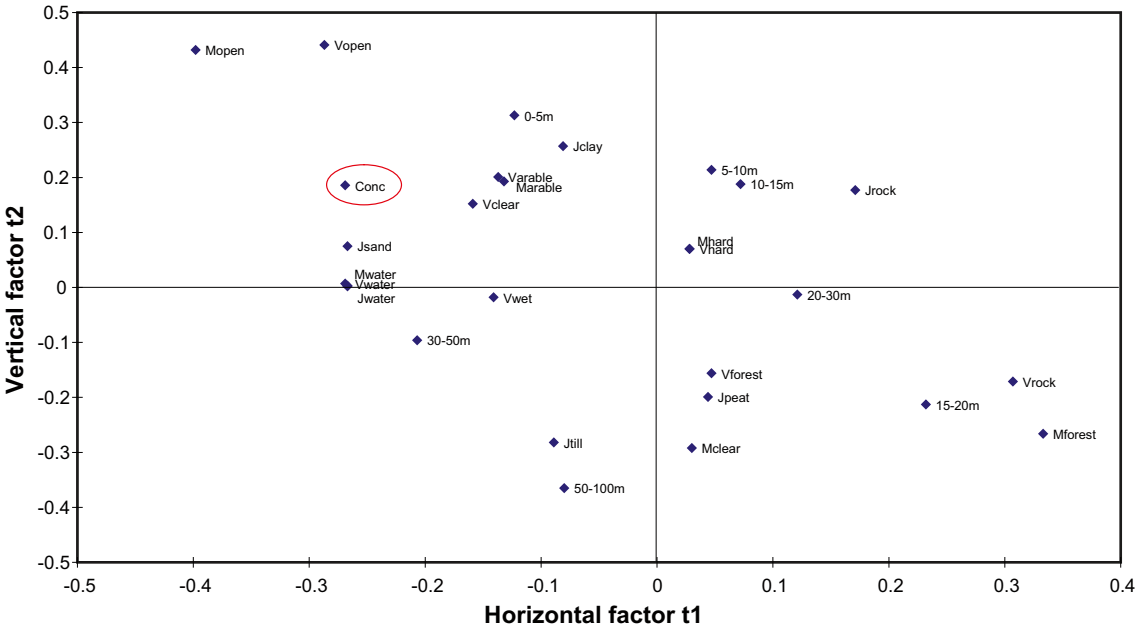


***Figure 6-4.*** *Partial least squares regression model, PLS, (see Section 2.3.10 for an explanation of PLS) showing the correlation structure among distributed catchment characteristics, and the observed Cl concentration (encircled in red). The parameters represent the relative distribution of each regolith, land use, vegetation and elevation class upstream of the hydrochemical sampling point in the outlet of the catchments. Factor t1 describes 29% of the variation among the explanatory variables and t2 24%. 43% of the variance in 'Conc' is described by t1 and 16% by t2.*

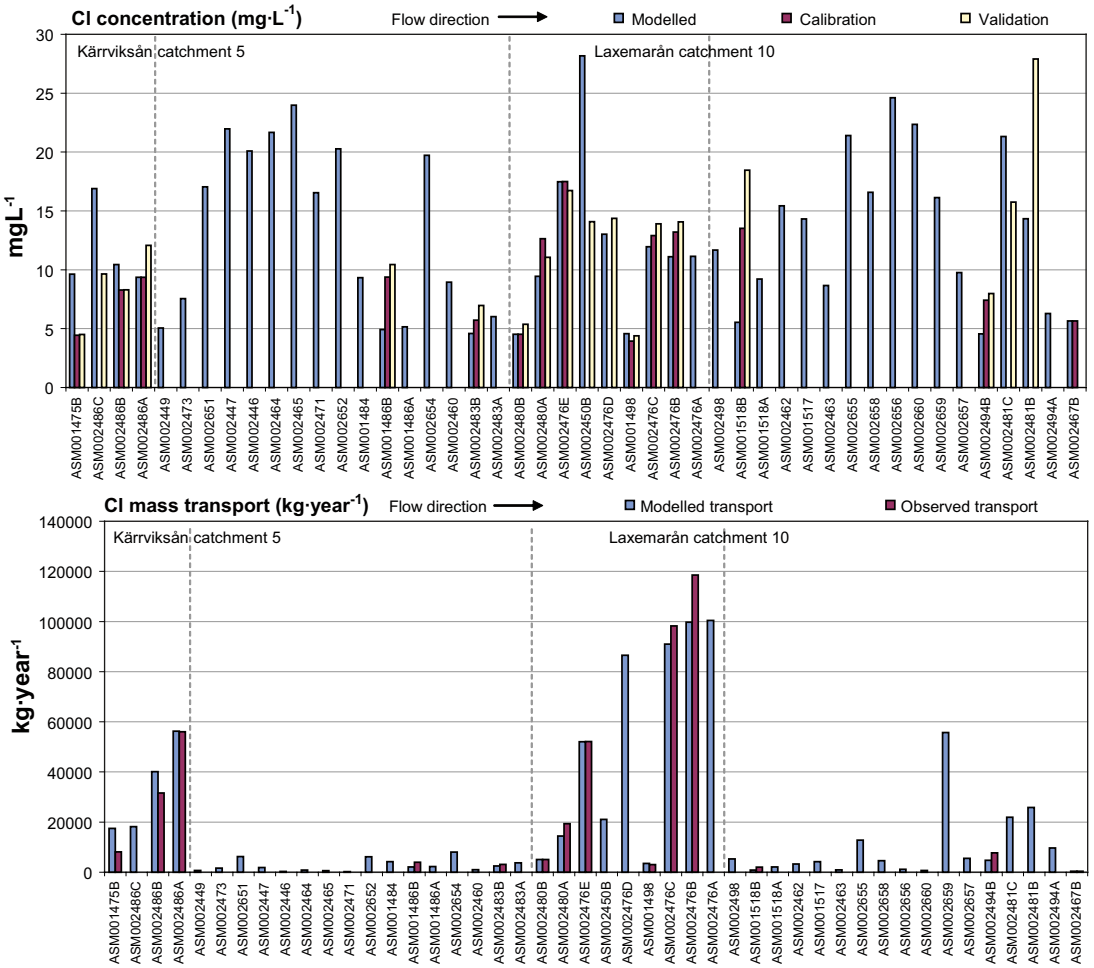


***Figure 6-5.*** *Mass balance scenario for Cl in the Laxemar-Simpevarp area. Flow-weighted concentrations (mg·L$^{-1}$) above, and transport (kg·year$^{-1}$) below, describe the conditions in the outlet of selected catchments.*

**Table 6-2. Compilation of parameters and model results from the Cl mass balance model. Categories not used have been omitted from the table. The total contribution from each category is listed for the entire modelled area and for the catchments of the Laxemarån and the Kärrviksån. The estimated flow-weighted concentration during the period 1 December 2003 to 30 November 2004 is listed at the bottom of the table.**

| | Model parameters | | | Model results | | | | | |
|---|---|---|---|---|---|---|---|---|---|
| **Diffuse sources** | | | | **All catchments** | | **Laxemarån** | | **Kärrviksån** | |
| Category | Class | mg·L$^{-1}$ | kg·ha$^{-1}$·year$^{-1}$ | kg·yr$^{-1}$ | % | kg·yr$^{-1}$ | % | kg·yr$^{-1}$ | % |
| Regolith | - | | | | | | | | |
| Land use | - | | | | | | | | |
| Vegetation | - | | | | | | | | |
| Topography | 0–5m | 28.8 | | 96,002 | 29 | 3,043 | 3 | 6,373 | 11 |
| | 5–10m | 6.1 | | 26,567 | 8 | 3,229 | 3 | 4,718 | 8 |
| | 10–15m | 4.5 | | 22,008 | 7 | 5,813 | 6 | 4,796 | 9 |
| | 15–20m | =10–15m | | 19,891 | 6 | 6,135 | 6 | 6,195 | 11 |
| | 20–30m | =10–15m | | 31,874 | 10 | 12,410 | 12 | 8,589 | 15 |
| | 30–50m | =10–15m | | 20,566 | 6 | 13,245 | 13 | 3,112 | 6 |
| | 50–100m | =10–15m | | 314 | 0 | 314 | 0 | 0 | 0 |
| **Point sources** | | | | | | | | | |
| Road salt from E22 | | | | 118,249 | 35 | 56,275 | 56 | 22,508 | 40 |
| **Total** | | | | | | | | | |
| Gross | | | | 335,470 | 100 | 100,464 | 100 | 56,291 | 100 |
| Retention (λ), yr$^{-1}$ | | | | 0 | 0 | 0 | 0 | 0 | 0 |
| Net | | | | 335,470 | 100 | 100,464 | 100 | 56,291 | 100 |
| **Concentration** (mg·L$^{-1}$) | | | | 12 | | 11 | | 9.4 | |

The following conclusions can be drawn about sources of Cl from the mass balance scenario in Figure 6-5:

- Diffuse sources of Cl are probably related to the topographical elevation distribution, rather than factors such as regolith or land use within the catchments. The catchment model indicates that areas located below an elevation of 5 metres show increased Cl influx (29 $mgL^{-1}$ compared to the background of 4.5 $mgL^{-1}$ prevailing at higher topographical elevations).
- The background level in discharge from higher elevations was calibrated to 4.5 $mgL^{-1}$, which is significantly higher than the concentration in precipitation of about 1.2 $mgL^{-1}$ /Tröjbom and Söderbäck 2006/. The discrepancy may to some extent be explained by loss of water to the atmosphere through evapotranspiration. This should theoretically concentrate the remaining water, which comprises surface discharge into streams and lakes, approximately 3 times. If the concentration due to atmospheric deposition is compared with the estimated flow-weighted concentration from the whole area, approximately 10–30% of the Cl originates from this atmospheric source depending on the influence of evaporation. The background level corresponds to the 85$^{th}$ percentile of the distribution from the Swedish national survey of lakes and streams according to Figure 6-7.
- Road salt is probably a major source of Cl in the Laxemar-Simpevarp area. According to the model results as much as 56% of the total Cl input to the sub-catchments of Laxemarån is attributable to road salt spread on E22.
- The high background level, in combination with the known use of a number of additional potential salt sources listed in Table 6-3, indicate that different types of road salt probably contribute to the Cl concentration to an even higher degree than shown in the model results. These sources are then included in the diffuse sources, thus leading to an elevated background level. Estimates in Table 6-3 indicates that as much as 2/3 of the total Cl input to the Laxemar-Simpevarp area may originate from either winter salt (NaCl) or summer road salt ($MgCl_2$ or $CaCl_2$).
- The large underestimation of Cl in ASM001518B is probably attributable to road salt from road 743, which is not included in the model as a point or line source.
- There are, as presumed, no indications of retention for Cl.

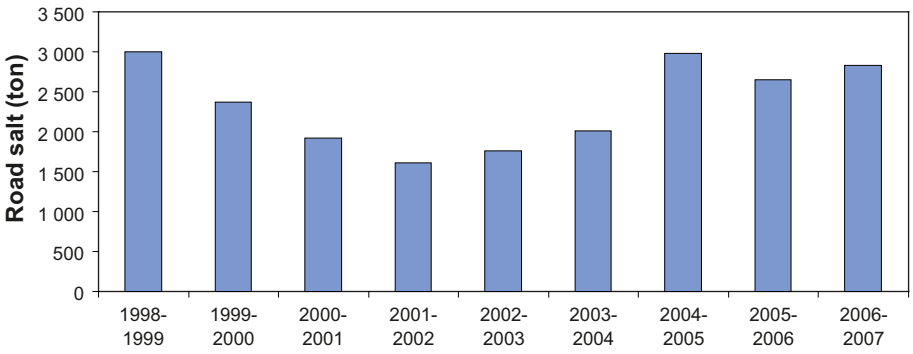


***Figure 6-6.*** *The total amount of road salt spread on public roads around Oskarshamn during the winters of 1998–2007. Based on statistics from (Lotta Olsson, Vägverket, 2008, pers. comm.).*

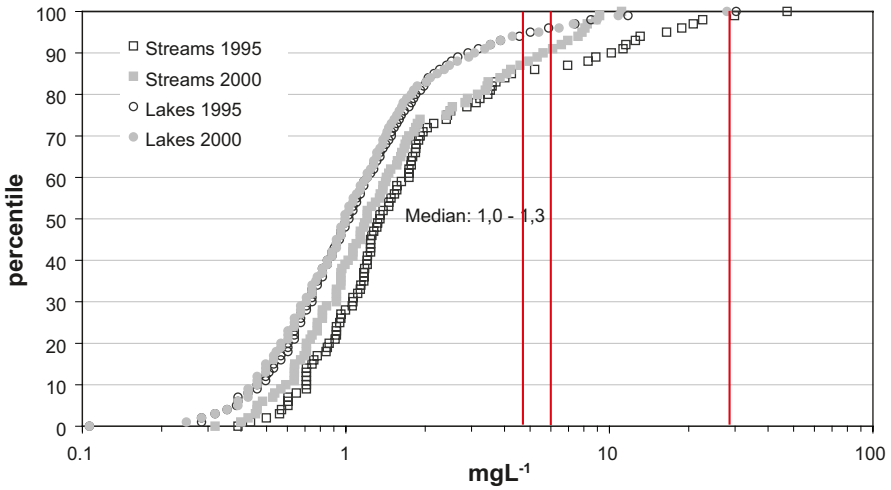


***Figure 6-7.*** *Distribution of Cl concentrations in the Swedish surveys of lakes and streams in 1995 and 2000 /IMA 2007/. Typical concentrations for categories in the Laxemar-Simpevarp area, calibrated within the VBX-VII model, are marked as red lines.*

**Table 6-3. Potential sources of road salt compared to the total discharge from the entire Laxemar-Simpevarp area according to the model results.**

| Source | Salt type | Intensity per km | Total (ton Cl) | Reference |
|---|---|---|---|---|
| E22 | NaCl | 5.5 ton Cl $km^{-1}$ | 126 | Statistics (see text) |
| Road 743 | NaCl | 3 ton Cl $km^{-1}$ | 46 | Statistics (see text) |
| Municipal | NaCl | | 10? | Rough estimate |
| Dust control | $MgCl_2$ or $CaCl_2$ | 1 ton Cl $km^{-1}$ | 10–50? | Rough estimate |
| **Total supply from point sources** | | | **190–230** | **Estimate** |
| **Total discharge from area** | | | **335** | **Measurements** |

### 6.2.2 Mass balance for sodium (Na)

The mass balance for Na is similar to the Cl balance (Section 6.2.1) insofar as road salt is an important Na source in the Laxemar-Simpevarp area. Accordingly, the PLS analysis in Figure 6-8 showed very weak correlations with most distributed factors, which is explained by this anthropogenic source that diminishes natural relationships. The road salt source was handled analogously to Cl. The model results are shown in Figure 6-9, and model parameters are listed in Table 6-4. See Appendix C for detailed model results.

By adjusting the typical concentrations of two regolith parameters (‘’Jtill’ and ‘Jclay’) together with the road salt source, the variation in Na concentration is satisfactorily modelled within the Laxemar-Simpevarp area. Similar to Cl, the largest overestimate compared to the calibration dataset is found for ASM001475B, whereas concentrations are underestimated in ASM001486B and ASM001518B. When the model results are compared to the (more uncertain) validation dataset, discrepancies are consequently larger, but the overall concordance is still evident. The average deviation between modelled and observed concentrations is 18% for the primary calibration dataset and 23% for the secondary validation dataset.

The following conclusions can be drawn about sources of Na from the mass balance scenario:

- Diffuse sources of Na are strongest coupled to regolith class (e.g. till and clay), rather than to topographical elevation as was the case for Cl. The additional weathering source, which is valid for Na but not for Cl, is responsible for the differing patterns.

- The regolith class representing clay (‘Jclay’) shows almost 10 times as high Na concentrations in discharge compared to discharge from e.g. till or sand. This Quaternary deposit is predominantly located at lower located areas, and relict marine Na may partly explain the elevated value. Enhanced weathering in combination with cation exchange may explain this pattern.
- The background level in discharge from other regolith categories than ‘Jclay’ was calibrated to 4 $mgL^{-1}$, which is 4 times higher than the median concentration in precipitation of 1 $mgL^{-1}$ in the Laxemar-Simpevarp area /Tröjbom and Söderbäck 2006/. These levels correspond to the 90$^{th}$ percentile in the distribution from the Swedish national survey of lakes and streams according to Figure 6-10. When the concentration in precipitation is corrected for evapotranspiration, the discrepancy becomes smaller, and roughly half of the background concentration of Na can be attributed to weathering or other terrestrial sources.
- According to the model results, road salt is a significant source of Na as well. About 1/3 of the total influx of Na is estimated to originate from this source. When compared to estimates of the input of Cl from E22, the estimate for Na corresponds to about 75% of the expected value if NaCl is the source. This discrepancy is probably attributable to model uncertainties rather than reflecting actual conditions.
- There are, as expected, no indications of retention for Na.

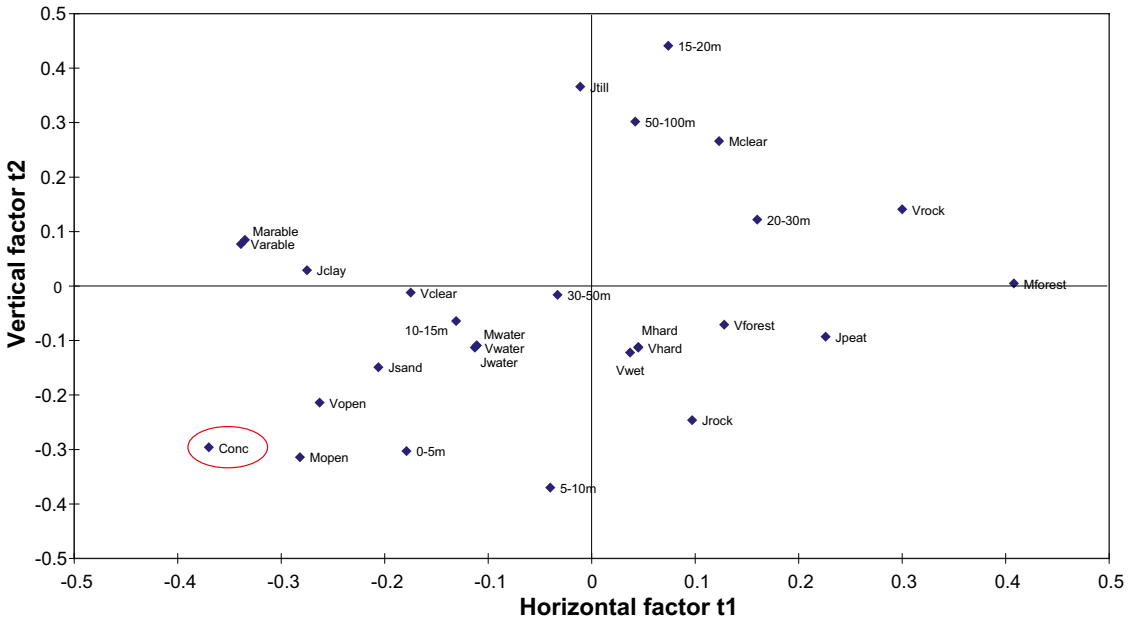


***Figure 6-8.*** *Partial least squares regression model, PLS (see Section 2.3.10 for an explanation of PLS) showing the correlation structure among distributed catchment characteristics, and the observed Na concentration (encircled in red). The parameters represent the relative distribution of each regolith, land use, vegetation and elevation class upstream of the hydrochemical sampling point in the outlet of the catchments. Factor t1 describes 18% of the variation among the explanatory variables and t2 8%. 62% of the variance in ‘Conc’ is described by t1 and 15% by t2.*

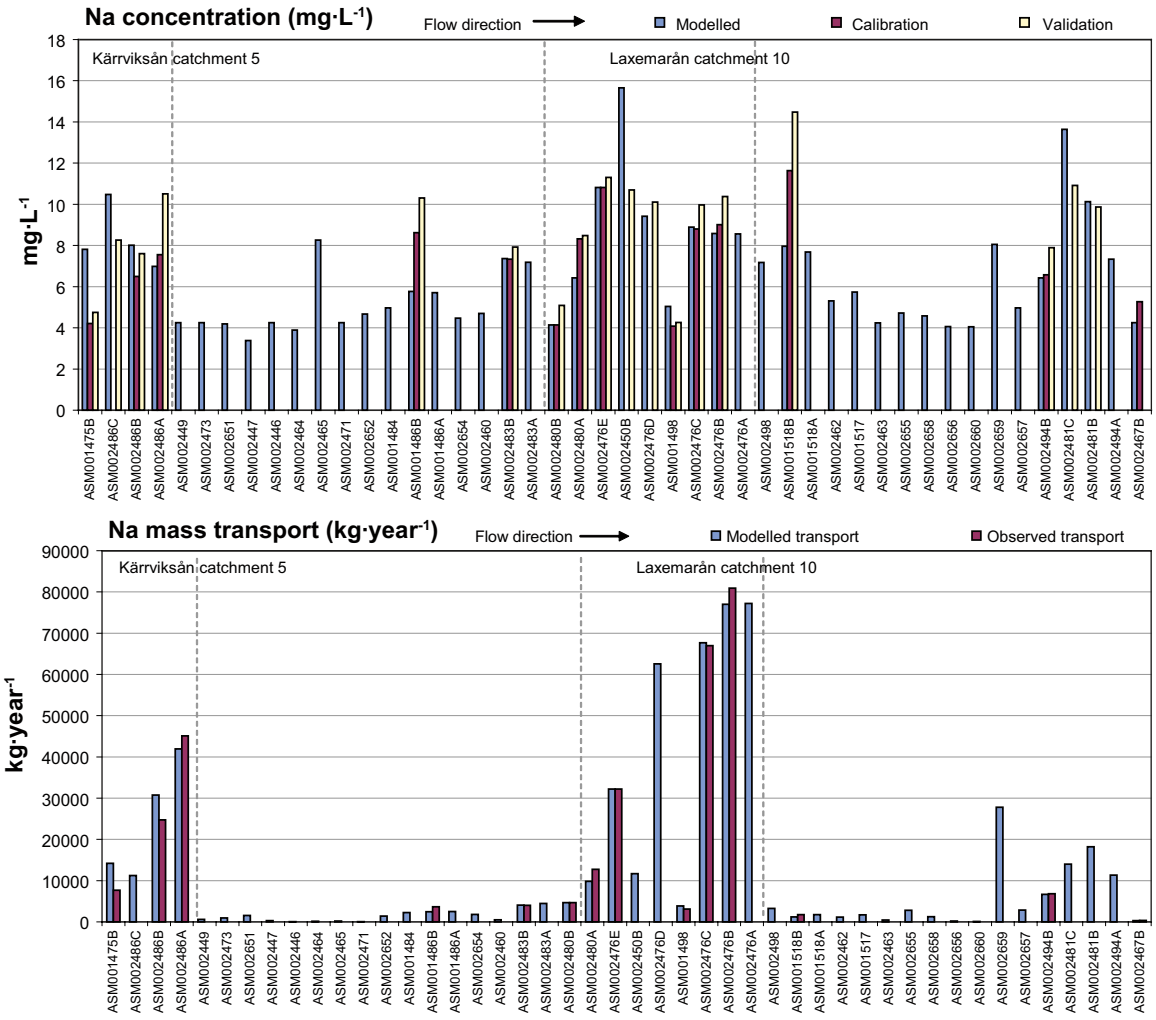


***Figure 6-9.*** *Mass balance for Na in the Laxemar-Simpevarp area. Flow- weighted concentrations (mg·L$^{-1}$) above, and transport (kg·year$^{-1}$) below, describing the conditions in the outlet of each catchment.*

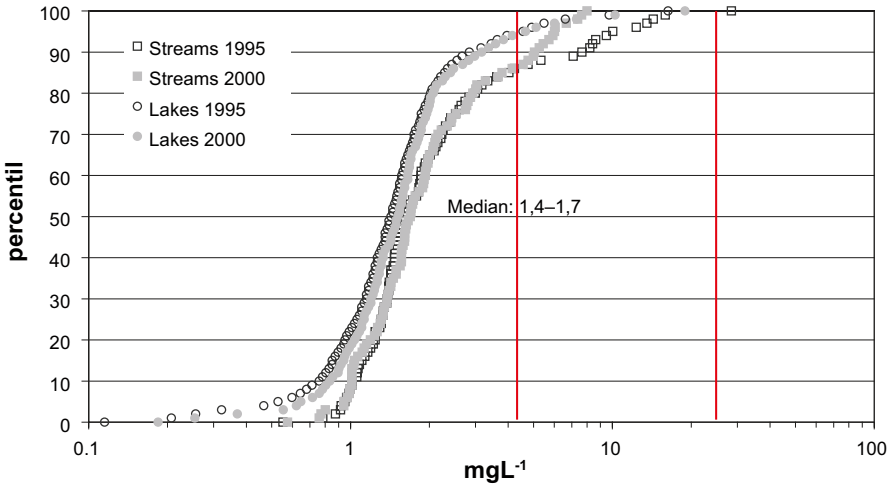


***Figure 6-10.*** *Distribution of Na concentrations in the Swedish surveys of lakes and streams in 1995 and 2000 /IMA 2007/. Typical concentrations for categories in the Laxemar-Simpevarp area, calibrated within the VBX-VII model, are marked as red lines.*

**Table 6-4. Compilation of parameters and model results from the Na mass balance model. Categories not used have been omitted from the table. The total contribution from each category is listed for the entire modelled area and for the catchments of the Laxemarån and the Kärrviksån. The estimated flow-weighted concentration during the period 1 December 2003 to 30 November 2004 is listed at the bottom of the table.**

| Model parameters | | | | Model results | | | | | |
|---|---|---|---|---|---|---|---|---|---|
| **Diffuse sources** | | | kg·ha$^{-1}$·year$^{-1}$ | **All catchments** | | **Laxemarån** | | **Kärrviksån** | |
| Category | Class | mg·L$^{-1}$ | | kg·yr$^{-1}$ | % | kg·yr$^{-1}$ | % | kg·yr$^{-1}$ | % |
| Regolith | Jwater | - | | | | | | | |
| | Jsand | =Jtill | | 5,264 | 2 | 1,447 | 2 | 1,211 | 3 |
| | Jpeat | =Jtill | | 8,965 | 4 | 3,494 | 5 | 2,282 | 5 |
| | Jrock | =Jtill | | 44,351 | 21 | 11,940 | 15 | 14,002 | 33 |
| | Jclay | 34 | | 42,396 | 20 | 14,994 | 19 | 6,829 | 16 |
| | Jtill | 4.2 | | 56,581 | 27 | 19,121 | 25 | 7,124 | 17 |
| Land use | - | | | | | | | | |
| Vegetation | - | | | | | | | | |
| Topography | - | | | | | | | | |
| **Point sources** | | | | | | | | | |
| Road salt from E22 | | | | 55,041 | 26 | 26,194 | 34 | 10,477 | 25 |
| **Total** | | | | | | | | | |
| Gross | | | | 212,601 | 100 | 77,193 | 100 | 41,928 | 100 |
| Retention (λ), yr$^{-1}$ | | | | 0 | 0 | 0 | 0 | 0 | 0 |
| Net | | | | 212,601 | 100 | 77,193 | 100 | 41,928 | 100 |
| **Concentration (mg·L$^{-1}$)** | | | | 7.4 | | 8.6 | | 7.0 | |

### 6.2.3 Mass balance for potassium (K)

The distribution of K differs from that of Na and Cl by showing lower spatial variability within the Laxemar-Simpevarp area. The correlation analysis shown in Figure 6-11 gives a scattered picture where e.g. arable land show positive correlation to observed K concentrations. Due to the low K variability among the hydrochemical sampling points, the potential for elucidating the factors governing K in surface water is limited. The model results are shown in Figure 6-12, and model parameters are listed in Table 6-5. See Appendix C for detailed model results.

By using a model similar to the Na mass balance where the typical concentrations of two regolith parameters (‘’Jtill’ and ‘Jclay’) are adjusted together with the road salt source, the variation in K concentration is acceptably modelled within the Laxemar-Simpevarp area. Compared to both the calibration and validation datasets, K concentrations are notably underestimated at three stations (ASM001486B, ASM001518B and ASM002467B). This indicates that not all factors behind the K pattern are captured by the model. When the model results are compared to the (more uncertain) validation dataset, the discrepancies are on a level with the discrepancies from the calibration dataset. The average deviation between modelled and observed concentrations is 20% for the primary calibration dataset and 34% for the secondary validation dataset (most of the discrepancies are attributed to the three deviating stations).

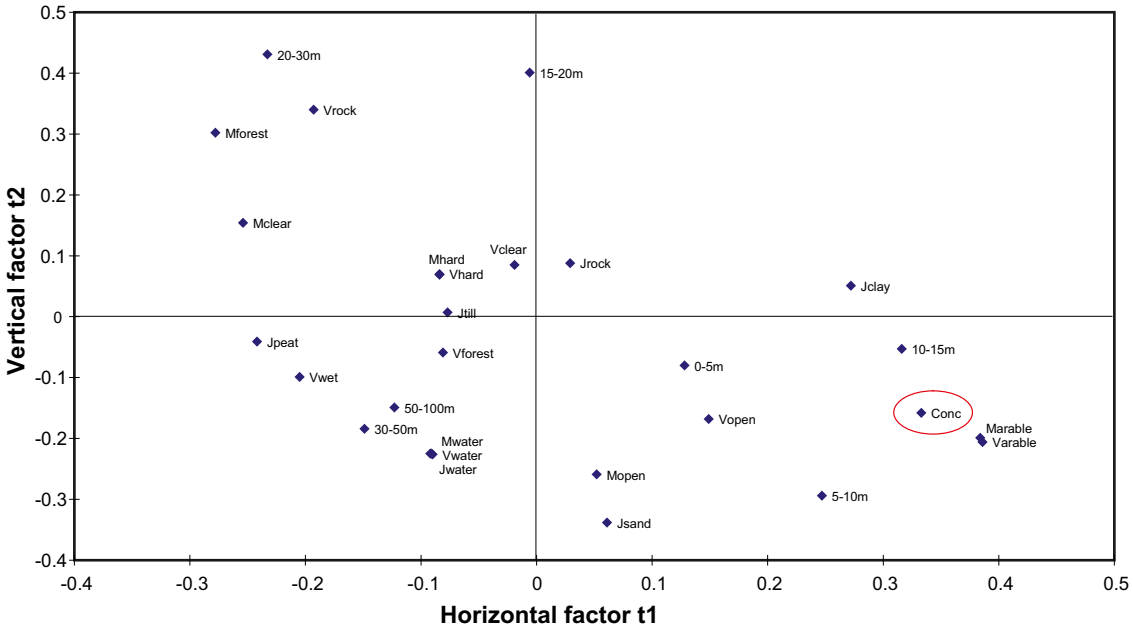


***Figure 6-11.*** *Partial least squares regression model, PLS (see Section 2.3.10 for an explanation of PLS) showing the correlation structure among distributed catchment characteristics, and the observed K concentration (encircled in red). The parameters represent the relative distribution of each regolith, land use, vegetation and elevation class upstream of the hydrochemical sampling point in the outlet of the catchments. Factor t1 describe 27% of the variation among the explanatory variables and t2 27%. 67% of the variance in 'Conc' is described by t1 and 15% by t2.*

**Table 6-5. Parameters and model results from the K mass balance model. Categories not used have been omitted from the table. The total contribution from each category is listed for the entire modelled area and for the catchments of the Laxemarån and the Kärrviksån. The estimated flow-weighted concentration during the period 1 December 2003 to 30 November 2004 is listed at the bottom of the table.**

| Model parameters | | | | Model results | | | | | |
|---|---|---|---|---|---|---|---|---|---|
| **Diffuse sources** | | | kg·ha–1·year$^{-1}$ | **All catchments** | | **Laxemarån** | | **Kärrviksån** | |
| Category | Class | mg·L$^{-1}$ | | kg·yr$^{-1}$ | % | kg·yr$^{-1}$ | % | kg·yr$^{-1}$ | % |
| Regolith | Jwater | - | | | | | | | |
| | Jsand | =Jclay | | 4,626 | 14 | 1,272 | 11 | 1,064 | 16 |
| | Jpeat | =Jtill | | 1,590 | 5 | 619 | 6 | 404 | 6 |
| | Jrock | =Jtill | | 7,866 | 24 | 2,117 | 19 | 2,483 | 37 |
| | Jclay | 3.7 | | 4,656 | 14 | 1,646 | 15 | 750 | 11 |
| | Jtill | 0.75 | | 10,036 | 30 | 3,391 | 31 | 1,263 | 19 |
| Land use | - | | | | | | | | |
| Vegetation | - | | | | | | | | |
| Topography | - | | | | | | | | |
| **Point sources** | | | | | | | | | |
| Road salt from E22? | | | | 4,313 | 13 | 2,053 | 18 | 821 | 12 |
| **Total** | | | | | | | | | |
| Gross | | | | 33,089 | 100 | 11,101 | 100 | 6,788 | 100 |
| Retention (λ), yr$^{-1}$ | | | | 0 | 0 | 0 | 0 | 0 | 0 |
| Net | | | | 33,089 | 100 | 11,101 | 100 | 6,788 | 100 |
| **Concentration (mg·L$^{-1}$)** | | | | 1.2 | | 1.2 | | 1.1 | |

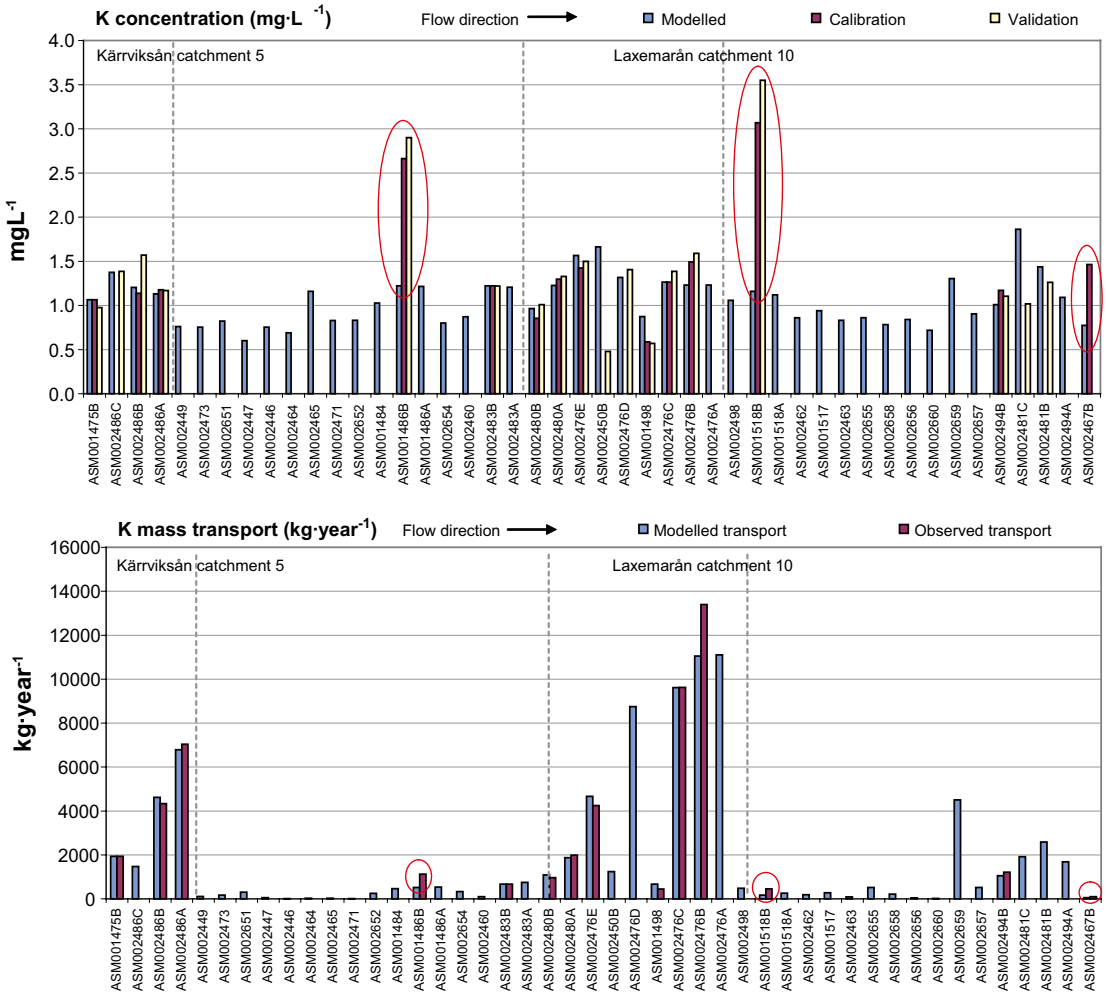


***Figure 6-12.*** *Mass balance for K in the Laxemar-Simpevarp area. Flow-weighted concentrations (mg·L$^{-1}$) above, and transport (kg·year$^{-1}$) below, describing the conditions in the outlet of each catchment.*

The following conclusions about sources of K can be drawn from the mass balance scenario:

- Diffuse sources of K are more uniformly distributed over the Laxemar-Simpevarp area compared with e.g. marine ions such as Cl and Na. The potential for identifying governing factors for K is more limited due to the low K variability among the hydrochemical sampling points.
- As with Na, elevated K concentrations are associated with the regolith types clay and sand. These deposits are predominantly distributed in the valleys that cut through higher elevated areas with usually thin regolith cover. A probable source of K in areas with clay and sand may be weathering in the deposits, whereas uptake in plants may serve as a sink (K is an important nutrient in plants and uptake of this element in biota be one factor governing the spatial pattern in K concentrations).
- Large discrepancies between modelled and observed concentrations for ASM001486B, ASM001518B and ASM002467B indicate that the factors governing K are not fully understood. This may be interpreted as indicating that there are sources of K that are not reflected by the tested categories. None of the distributed properties – such as topographical elevation, land use or vegetation cover – seems to have any important influence when these factors are tested. An anthropogenic point source could be a potential supply of K, probably associated with agricultural activities of some kind (such as use of fertilizers or leaching from manure). ASM001486B (with the chemical sampling station PSM002084 in the outlet) and ASM1518B (PSM002086) are both small catchments that contain high proportions of arable land with farms upstream of the chemical sampling point.

- The calibrated background level of about 0.75 $mgL^{-1}$ in discharge from the most widespread regolith categories in the Laxemar-Simpevarp area is on a level with the mean concentration in precipitation of 0.58 $mgL^{-1}$ /Tröjbom and Söderbäck 2006/ and corresponds to the 80$^{th}$ percentile of the national distribution. If this value is corrected for concentration effects due to evapotranspiration, the discrepancy becomes smaller or even negative. This situation may be interpreted as indicating that the amount of K released into surface waters by local weathering is small compared to the input from atmospheric deposition. However, weathering of the regolith is usually regarded as the major input source for K and the observed pattern may be an artefact, perhaps due to uncertainties related to the large uptake and recycling of K in biota.
- Likely, the uptake and recycling of K in biota strongly affects the overall pattern of K and these processes may hide variations due to distributed environmental factors. The seasonal influence is evident in Figure 6-14, where catchments with high proportions of arable and/or forest land show elevated K concentrations during autumn when biota is degraded.
- The K mass balance is further improved if a road salt source along E22 is added, although K is usually not reported as a major constituent of road salt. The relative influence of this source is, however, weaker for K compared to Na. The amount of K in relation to Na is 8%, compared with the sea water mass ratio of 4% in the Baltic Sea (cf Figure 4-2). Depending on the composition and origin of the source of the road salt, it is not excluded that K could be added to the surface system via this source.
- There are no indications of significant retention of K in the lakes.

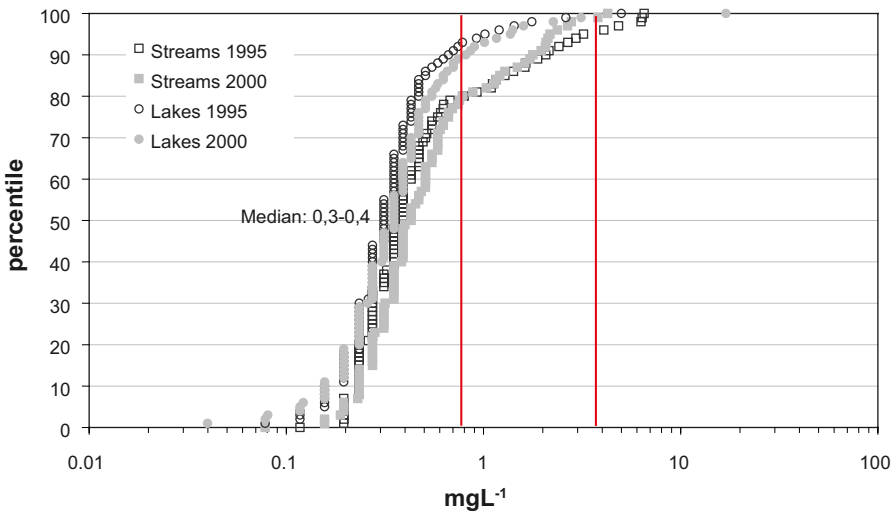


***Figure 6-13.*** *Distribution of K concentrations in the Swedish surveys of lakes and streams in 1995 and 2000 /IMA 2007/. Typical concentrations for categories calibrated within the VBX-VII model are marked as red lines.*

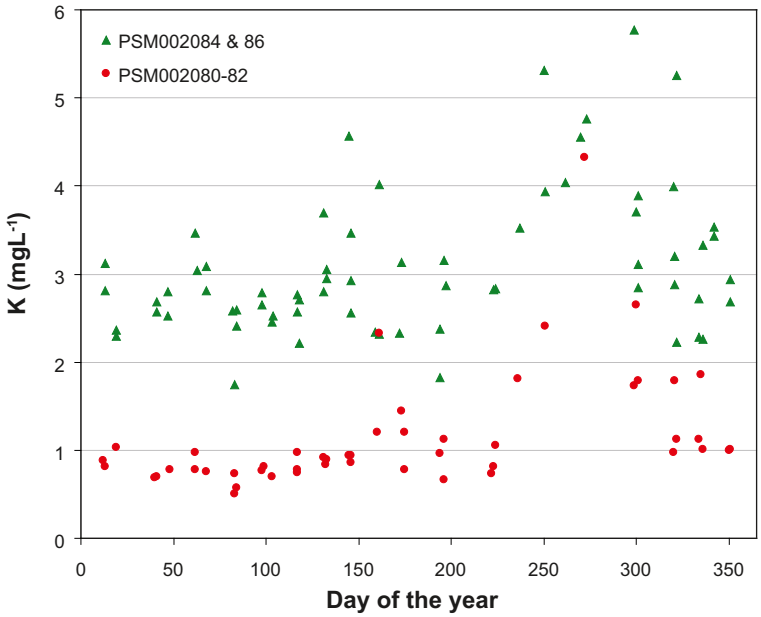


***Figure 6-14.*** *Seasonal variation in K concentration for two catchments containing large proportions of arable land (PSM002084 and PSM002086), and two catchments dominated by forest (PSM002080 and PSM002081). Observations represent the period 2002–2006.*

### 6.2.4 Mass balance for calcium (Ca)

According to the PLS analysis in Figure 6-15, the spatial variability of Ca is closely correlated with the presence of clay and arable land. These properties are inter-correlated due to the fact that arable land usually is located on soils which contain clay, e.g. previous sea and lake sediments. As a validation of previous Na and K models, a line source representing E22 was also included in the Ca mass balance to test whether this source increased the explanatory power of the model. The model results are shown in Figure 6-16, and model parameters are shown in Table 6-6. See Appendix C for detailed model results.

The spatial variation is acceptably modelled within the Laxemar-Simpevarp area by means of two calibrated typical concentrations that represent concentrations in discharge from the regolith class ‘Jclay’ and a concentration common for the remaining regolith classes. Compared with both the calibration and validation datasets, Ca concentrations are slightly overestimated in the downstream parts of the Laxemarån, whereas concentrations are greatly underestimated in ASM002483B. The average deviation between modelled and observed concentrations is 11% for the primary calibration dataset and 19% for the secondary validation dataset.

The following conclusions about sources of Ca can be drawn from the mass balance scenario:

- Among the distributed sources, the occurrence of clay (or arable land, which usually overlap) is an important factor that increases the discharge of Ca. According to the model results, the typical concentration in discharge from the regolith class ‘Jclay’ is elevated by a factor of about 10 compared with discharge from other types of regolith.
- The background concentration of 7.6 $mgL^{-1}$ for regolith classes other than ‘Jclay’ corresponds to the $80^{th}$ percentile of the Swedish distribution in Figure 6-17, and is elevated by a factor of approximately 10 compared with the concentration measured in precipitation. This implies (as expected) that weathering is the main source of Ca and that Ca from weathering is elevated compared with the normal situation in Sweden. The deposits probably contain other Ca-bearing minerals than calcite, as the till in the area is almost free of calcite /Tröjbom and Söderbäck 2006/.

- The large underestimate in ASM002483B is accompanied by a similar underestimate of $HCO_3^-$. This may be an indication that a specific source of these ions is located in the catchment. There are, however, no obvious deviations in regolith composition or a deviating land use that could explain the discrepancy for these elements in this catchment. A hypothetical source of both these ions could be lime added to soils or directly in the watercourses for agricultural or environmental management purposes. Summer road salt ($CaCl_2$), which is spread on gravel roads for dust control (cf Section 7.5), could also be a potential source of Ca.
- There are no indications of Ca retention in the lakes. The few and small lakes in the area provide low potential for retention, although this is evident for Si (cf Section 6.2.12).
- The calibration of a line source representing road salt from E22 (cf Section 6.2.1) resulted in a very low contribution from this source. According to the model, only 1% is attributable to this potential source. This estimate, which is probably an artefact below the accuracy of the model, can nevertheless be regarded as an indication that winter road salt does not add Ca to the surface system (cf Section 7.5.2).

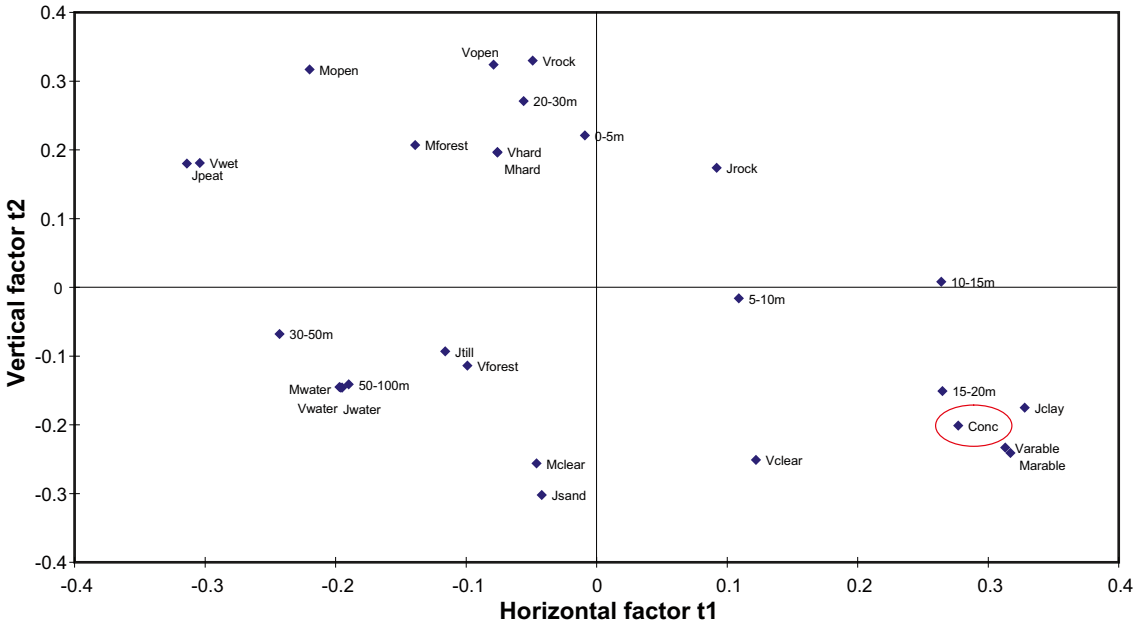


***Figure 6-15.*** *Partial least squares regression model, PLS (see Section 2.3.10 for an explanation of PLS) showing the correlation structure among distributed catchment characteristics, and the observed Ca concentration (encircled in red). The parameters represent the relative distribution of each regolith, land use, vegetation and elevation class upstream of the hydrochemical sampling point in the outlet of the catchments. Factor t1 describe 34% of the variation among the explanatory variables and t2 20%. 61% of the variance in 'Conc' is described by t1 and 17% by t2.*

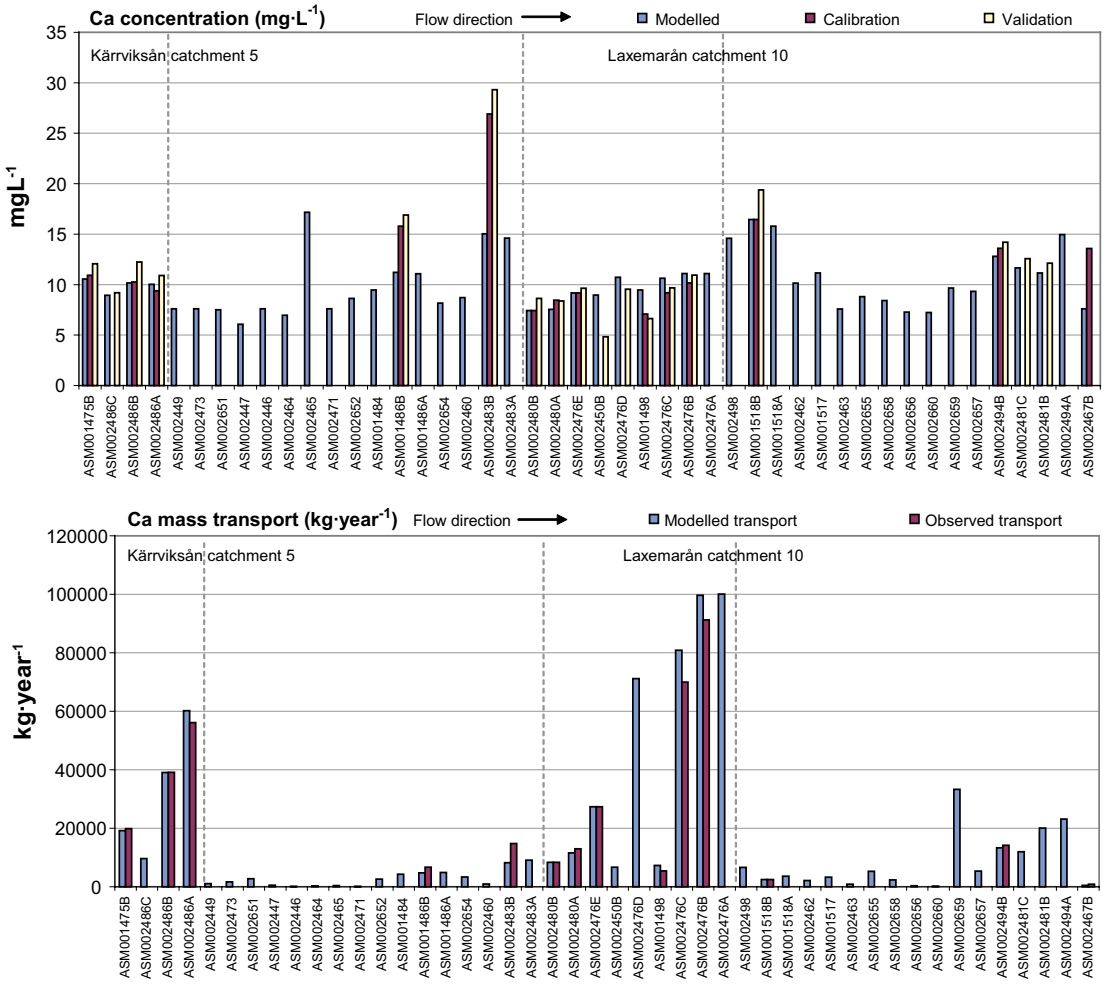


***Figure 6-16.*** *Mass balance for Ca in the Laxemar-Simpevarp area. Flow-weighted concentrations (mg·L$^{-1}$) above, and transport (kg·year$^{-1}$) below, describing the conditions in the outlet of each catchment.*

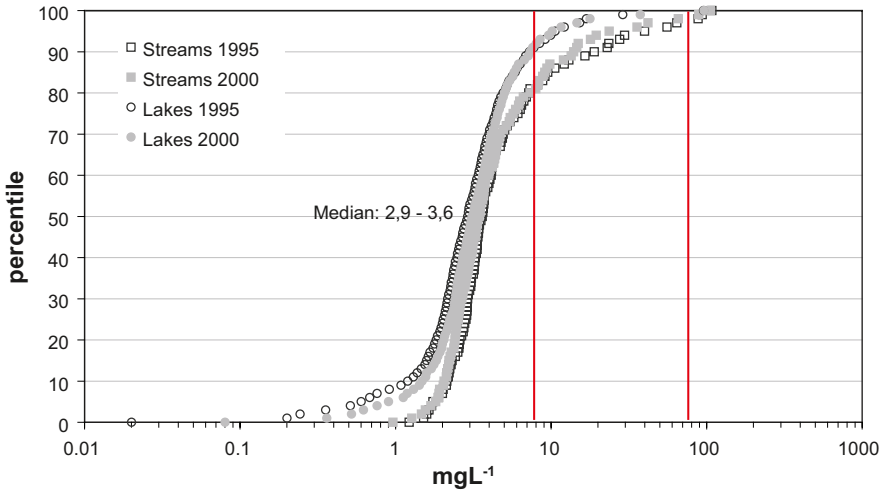


***Figure 6-17.*** *Distribution of Ca concentrations in the Swedish surveys of lakes and streams in 1995 and 2000 /IMA 2007/. Typical concentrations for categories calibrated within the VBX-VII model are marked as a red line.*

**Table 6-6. Parameters and model results from the Ca mass balance model. Categories not used have been omitted from the table. The total contribution from each category is listed for the entire modelled area and for the catchments of the Laxemarån and the Kärrviksån. The estimated flow-weighted concentration during the period 1 December 2003 to 30 November 2004 is listed at the bottom of the table.**

| Model parameters | | | | Model results | | | | | |
|---|---|---|---|---|---|---|---|---|---|
| **Diffuse sources** | | | | **All catchments** | | **Laxemarån** | | **Kärrviksån** | |
| Category | Class | mg·L$^{-1}$ | kg·ha$^{-1}$·year$^{-1}$ | kg·yr$^{-1}$ | % | kg·yr$^{-1}$ | % | kg·yr$^{-1}$ | % |
| Regolith | Jwater | - | | | | | | | |
| | Jsand | =Jtill | | 9,423 | 3 | 2,591 | 3 | 2,169 | 4 |
| | Jpeat | =Jtill | | 16,050 | 5 | 6,255 | 6 | 4,086 | 7 |
| | Jrock | =Jtill | | 79,395 | 26 | 21,374 | 21 | 25,067 | 42 |
| | Jclay | 78 | | 97,871 | 32 | 34,615 | 35 | 15,765 | 26 |
| | Jtill | 7.6 | | 101,288 | 33 | 34,230 | 34 | 12,753 | 21 |
| Land use | | | | | | | | | |
| Vegetation | | | | | | | | | |
| Topography | | | | | | | | | |
| **Point sources** | | | | | | | | | |
| Road salt from E22? | | | | 2,059 | 1 | 980 | 1 | 392 | 1 |
| **Total** | | | | | | | | | |
| Gross | | | | 306,089 | 100 | 100,048 | 100 | 60,234 | 100 |
| Retention | | | | 0 | 0 | 0 | 0 | 0 | 0 |
| Net | | | | 306,089 | 100 | 100,048 | 100 | 60,234 | 100 |
| **Concentration (mg·L$^{-1}$)** | | | | 11 | | 11 | | 10 | |

## 6.2.5 Mass balance for strontium (Sr)

The occurrence of strontium is often closely linked to the occurrence of calcium. According to Figure 4-14, many observations from the surface system plot along a specific Ca/Sr ratio, which reflects a common source of these elements. This ratio, together with the $^{87}Sr$ isotope composition in Figure 4-15, indicates that Sr of marine origin probably has a minor role in the surface system. The correlation analysis in Figure 6-18 also indicates that the spatial pattern of Sr (and consequently the distribution of sources) is similar to that of Ca (cf Figure 6-15). The model results are shown in Figure 6-19, and model parameters are listed in Table 6-7. See Appendix C for detailed model results.

The outcome of the Sr mass balance model is very similar to that of the Ca model. By adjusting two parameters, Jclay and Jtill, the Sr concentrations within the Laxemar-Simpevarp area are satisfactorily modelled. The average model deviation between modelled and observed concentrations in the calibration dataset is 13%, and the validation dataset shows a mean deviation of 22%. The following conclusions about sources of Sr can be drawn from the mass balance scenario:

- All conclusions from the Ca model are applicable to the Sr model, except for the deviating catchments ASM001486B and ASM002483B, which showed anomalously high concentrations of Ca and $HCO_3^-$. There is also a slight underestimate of Sr in the Sr model for these catchments, although much less pronounced. This suggests that the proposed anthropogenic Ca and $HCO_3^-$ source in these catchments probably does not contain very much Sr.
- The ratio between the regolith classes ‘Jclay’ and ‘Jtill’ is 5 for Sr, whereas the same ratio for Ca is 10. This discrepancy may, if significant, suggest that there is a slight difference between Ca and Sr regarding either the origin of these elements in the Laxemar-Simpevarp area, or alterations by reactions such as cation exchange.

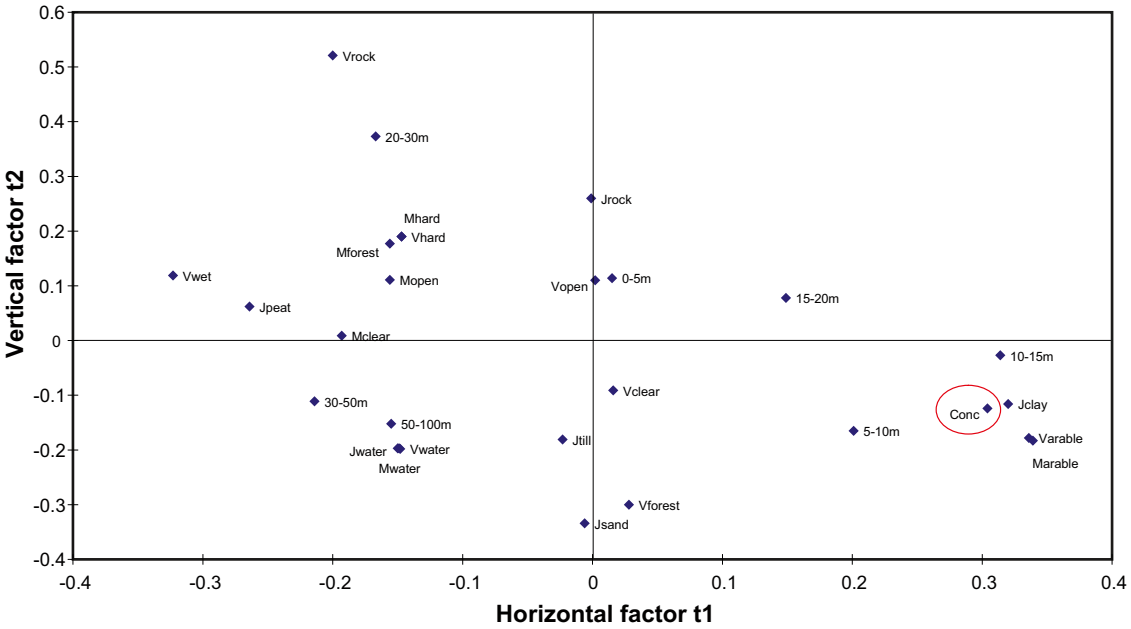


***Figure 6-18.*** *Partial least squares regression model, PLS (cf Section 6.5.3 for an explanation of PLS) showing the correlation structure among distributed catchment characteristics, and the observed Sr concentration (encircled in red). The parameters represent the relative distribution of each regolith, land use, vegetation and elevation class upstream of the hydrochemical sampling point in the outlet of the catchments. Factor t1 describe 29% of the variation among the explanatory variables and t2 27%. 65% of the variance in 'Conc' is described by t1 and 10% by t2.*

**Table 6-7 Parameters and model results from the Sr mass balance model. Categories not used have been omitted from the table. The total contribution from each category is listed for the entire modelled area and for the catchments of the Laxemarån and the Kärrviksån. The estimated flow-weighted concentration during the period 1 December 2003 to 30 November 2004 is listed at the bottom of the table.**

| Model parameters | | | | Model results | | | | | |
|---|---|---|---|---|---|---|---|---|---|
| **Difuse sources** | | | kg·ha$^{-1}$·year$^{-1}$ | **All catchments** | | **Laxemarån** | | **Kärrviksån** | |
| Category | Class | mg·L$^{-1}$ | | kg·yr$^{-1}$ | % | kg·yr$^{-1}$ | % | kg·yr$^{-1}$ | % |
| Regolith | Jwater | - | | 0 | 0 | 0 | 0 | 0 | 0 |
| | Jsand | =Jtill | | 53 | 4 | 14 | 3 | 12 | 4 |
| | Jpeat | =Jtill | | 90 | 6 | 35 | 8 | 23 | 8 |
| | Jrock | =Jtill | | 449 | 31 | 120 | 26 | 141 | 48 |
| | Jclay | 0.22 | | 279 | 19 | 98 | 21 | 45 | 15 |
| | Jtill | 0.04 | | 573 | 40 | 193 | 42 | 72 | 25 |
| Landuse | | | | | | | | | |
| Vegetation | | | | | | | | | |
| Topography | | | | | | | | | |
| **Point sources** | | | | | | | | | |
| No point sources included | | | | | | | | | |
| **Total** | | | | | | | | | |
| Gross | | | | 1,446 | 100 | 464 | 100 | 294 | 100 |
| Retention | | | | 0 | 0 | 0 | 0 | 0 | 0 |
| Net | | | | 1,446 | 100 | 464 | 100 | 294 | 100 |
| **Concentration (mg·L$^{-1}$)** | | | | 0.05 | | 0.05 | | 0.05 | |

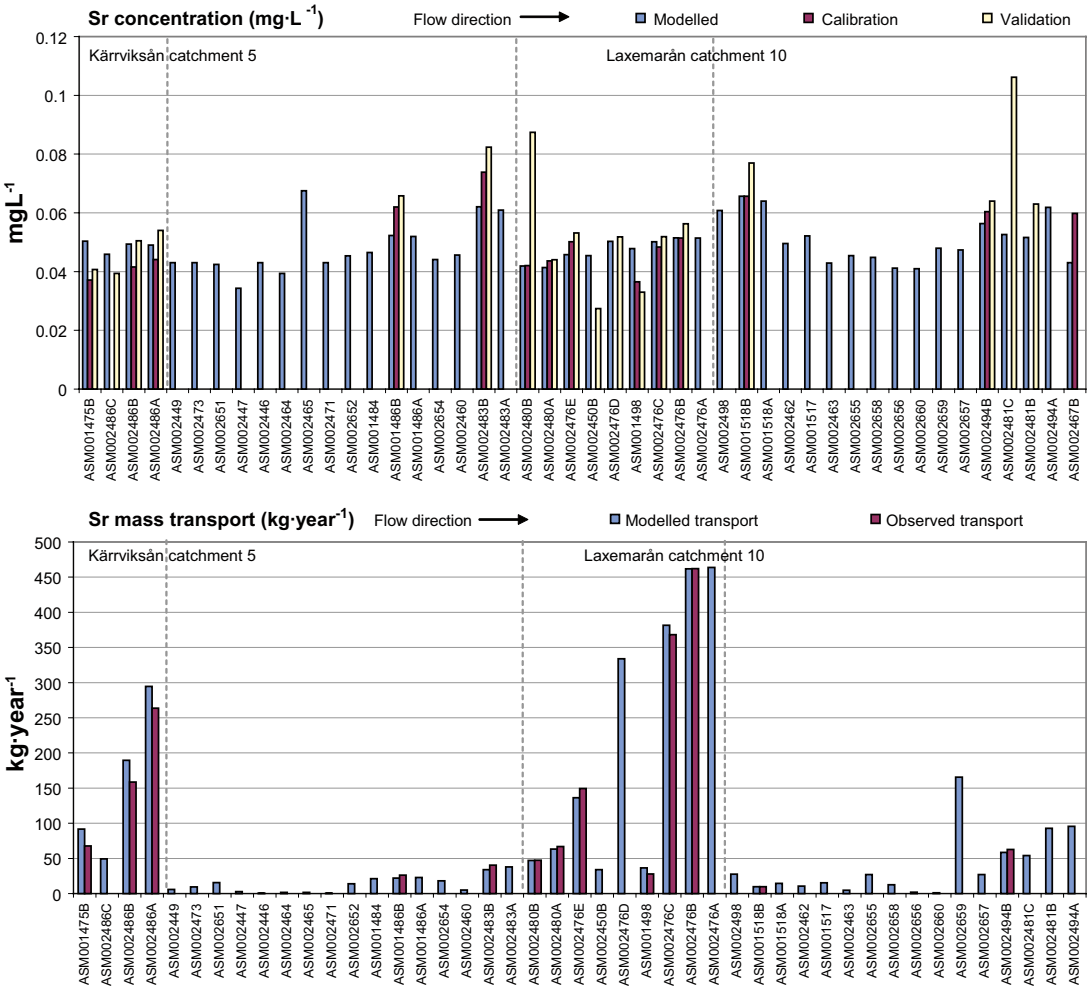


***Figure 6-19.*** *Mass balance for Sr in the Laxemar-Simpevarp area. Flow-weighted concentrations (mg·L$^{-1}$) above, and transport (kg·year$^{-1}$) below, describing the conditions in the outlet of each catchment.*

### 6.2.6 Mass balance for magnesium (Mg)

Mg shows a pattern similar to Ca. According to the PLS analysis in Figure 6-20, the spatial variability of Mg shows a close correlation with the topographical elevation and presence of arable land and clay. These properties are intercorrelated due to the fact that arable land is often located at low elevations in the valleys, usually on soils which contain clay, e.g. previous sea and lake sediments. The model results are shown in Figure 6-21, and model parameters are shown in Table 6-8. See Appendix C for detailed model results.

The calibration of the Mg mass balance model showed that several scenarios can give similar results, and a common factor for these scenarios was elevated typical concentrations from lower-lying areas and land used for agriculture. These properties are, as described above, correlated in the Laxemar-Simpevarp area. The simplest model with the least number of free parameters in combination with acceptable agreement between modelled and observed concentration was achieved when the land use classes were used as parameters. The spatial variation is acceptably modelled within the Laxemar-Simpevarp area by means of two calibrated typical concentrations that represent concentrations in discharge from the land use class ‘Marable’ and a concentration common for the remaining land use classes. Compared to both the calibration and validation datasets, Mg concentrations are slightly underestimated in the catchment of the Laxemarån. The average deviation between modelled and observed concentrations is 12% for the primary calibration dataset and 16% for the secondary validation dataset.

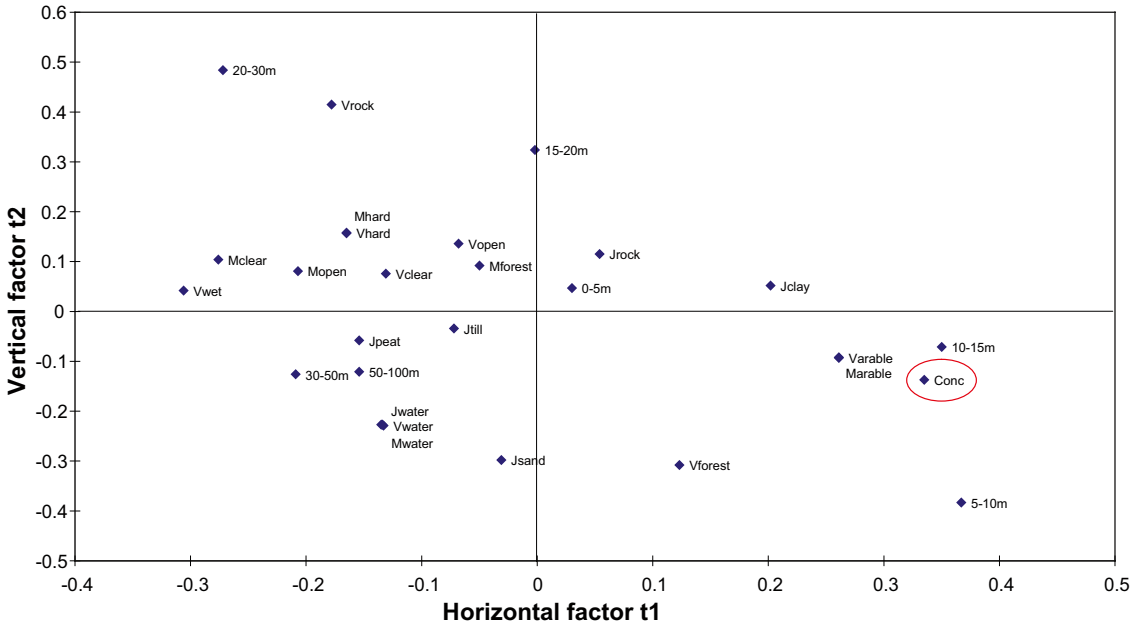


***Figure 6-20.*** *Partial least squares regression model, PLS (see Section 2.3.10 for an explanation of PLS) showing the correlation structure among distributed catchment characteristics, and the observed Mg concentration (encircled in red). The parameters represent the relative distribution of each regolith, land use, vegetation and elevation class upstream of the hydrochemical sampling point in the outlet of the catchments. Factor t1 describe 28% of the variation among the explanatory variables and t2 28%. 71% of the variance in 'Conc' is described by t1 and 12% by t2.*

**Table 6-8. Compilation of parameters and model results from the Mg mass balance model. Categories not used have been omitted from the table. The total contribution from each category is listed for the entire modelled area and for the catchments of the Laxemarån and the Kärrviksån. The estimated flow weighted concentration during the period 1 December 2003 to 30 November 2004 is listed at the bottom of the table.**

| Model parameters | | | | Model results | | | | | |
|---|---|---|---|---|---|---|---|---|---|
| **Diffuse sources** | | | kg·ha$^{-1}$· | **All catchments** | | **Laxemarån** | | **Kärrviksån** | |
| Category | Class | mg·L$^{-1}$ | year$^{-1}$ | kg·yr$^{-1}$ | % | kg·yr$^{-1}$ | % | kg·yr$^{-1}$ | % |
| Regolith | | | | | | | | | |
| Land use | Mwater | - | | | | | | | |
| | Mforest | 1.6 | | 38,080 | 63 | 12,138 | 63 | 8,234 | 68 |
| | Mclear | 1.6 | | 581 | 1 | 316 | 2 | 145 | 1 |
| | Marable | 14 | | 18,197 | 30 | 6,007 | 31 | 3,141 | 26 |
| | Mopen | 1.6 | | 3,157 | 5 | 751 | 4 | 550 | 5 |
| | Mhard | 1.6 | | 340 | 1 | 0 | 0 | 54 | 0 |
| Vegetation | | | | | | | | | |
| Topography | | | | | | | | | |
| **Point sources** | | | | | | | | | |
| No point sources included | | | | | | | | | |
| **Total** | | | | | | | | | |
| Gross | | | | 60,358 | 100 | 19,214 | 100 | 12,127 | 100 |
| Retention | | | | 0 | 0 | 0 | 0 | 0 | 0 |
| Net | | | | 60,358 | 100 | 19,214 | 100 | 12,127 | 100 |
| **Concentration (mg·L$^{-1}$)** | | | | 2.1 | | 2.1 | | 2.0 | |

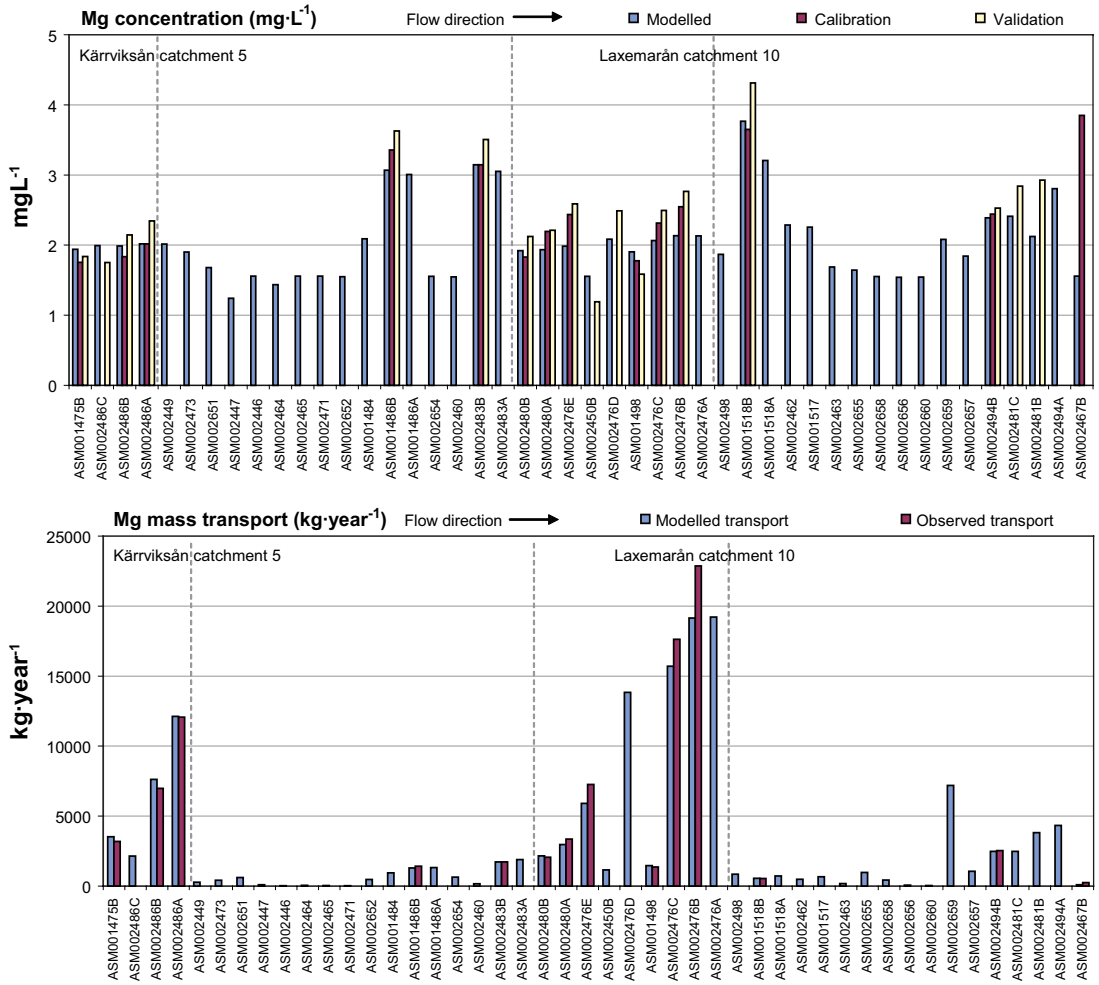


***Figure 6-21.*** *Mass balance for Mg in the Laxemar-Simpevarp area. Flow-weighted concentrations ($mg \cdot L^{-1}$) above, and transport ($kg \cdot year^{-1}$) below, describing the conditions in the outlet of each catchment.*

The following conclusions about sources of Mg can be drawn from the mass balance scenario:

- Among the distributed sources, the occurrence of arable land is an important factor that enhances discharge of Mg. This factor is, however, closely correlated with both topographical elevation and presence of clay in soils, and the exact dependencies could not be elucidated in the present model version. According to the model results, the typical concentration in discharge from the land use class 'Marable' is elevated by a factor of nearly 10 compared with discharge from e.g. forest land. Underlying factors responsible for the enhanced concentrations from arable land could be agricultural activities (cultivation, draining and fertilization), in combination with enhanced weathering of the usually thick and fine-grained regolith. Outwash of marine relicts could also be a potential source in these lower-lying areas, but the resolution in the model and the location of the hydrochemical observation points used for calibration do not permit separation of these sources. The strong correlation with the elevation gradient (at least to the '5–10m' and '10–15m' classes) in Figure 6-20 may be an indication that marine relicts is an important source, similar to the situation for Cl. The weak correlation with the '0–5m' class may be explained by the low proportion of this elevation category upstream of the available hydrochemical sampling points (cf Figure 2-5).
- The background concentration of 1.8 $mgL^{-1}$ for land use classes other than 'Marable' corresponds to the 80$^{th}$ percentile of the Swedish distribution in Figure 6-22, and is elevated by a factor of more than 10 compared with the concentration measured in precipitation.

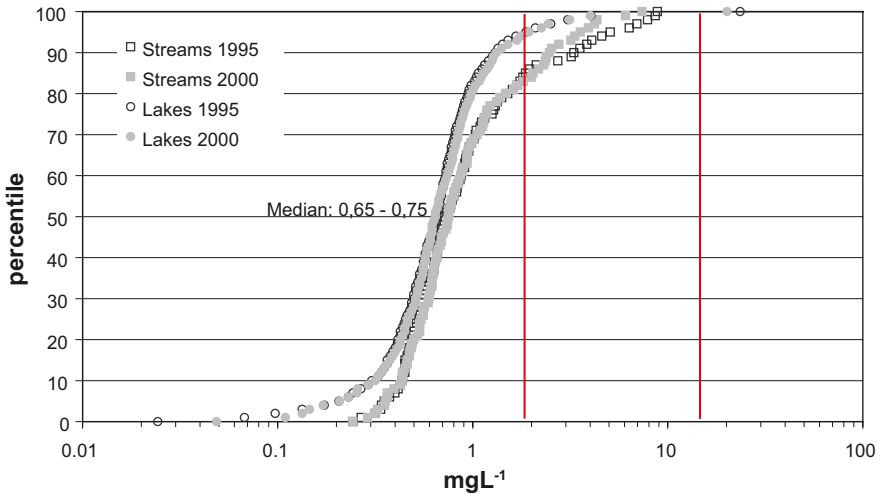


***Figure 6-22.*** *Distribution of Mg concentrations in the Swedish surveys of lakes and streams in 1995 and 2000 /IMA 2007/. Typical concentrations for categories calibrated within the VBX-VII model are marked as red lines.*

- Besides a minor underestimate in the Laxemarån catchment, the concentration in the very small stream on Ävrö (Catchment ASM002467B and the hydrochemical sampling point PSM107735) is strongly underestimated, similar to the situation for several other elements such as K and Ca. Uncertainties attributed to sampling in a very small watercourse which is sometimes completely dry may to an unknown extent explain these discrepancies. The possibility cannot, however, be ruled out that there is a natural factor behind this pattern, for example a deviating local mineralogy in the deposits.
- Another source that may affect the Mg model is summer road salt ($MgCl_2$). There is no possibility to quantify this source, but qualitative indications from Lake Frisksjön show that this is a potential source in the area (cf Section 7.5.2). If this is the case, this source probably contributes to the uncertainties in the model and may be responsible for local deviations due to the use of summer road salt in the catchment.
- There are no indications of significant retention of Mg in the lakes.

### 6.2.7 Mass balance for sulphate ($SO_4^{2-}$)

$SO_4^{2-}$ in surface water originates from three major sources according to the qualitative analysis in Section 4.1.3, where the origin of sulphur is explored. These sources are atmospheric deposition and marine relicts in the form of either sulphide minerals or sulphate. According to the correlation analysis in Figure 6-23, the topographical elevation and the land-use category 'Marable' are positively correlated with the $SO_4^{2-}$ concentration, similar to the pattern for Mg. A possible candidate is the Quaternary deposits, which may contain large amounts of sulphide minerals of marine origin from the period when the Laxemar-Simpevarp area was submerged by lake or sea water. The model results are shown in Figure 6-24, and model parameters are listed in Table 6-9. See Appendix C for detailed model results.

By adjusting two parameters that represent typical concentrations in discharging water from two elevation categories, the $SO_4^{2-}$-concentration within the Laxemar-Simpevarp area is satisfactorily modelled. $SO_4^{2-}$-concentrations are generally overestimated in the catchment of the Kärrviksån, whereas there is a slight underestimate in the catchment of Laxemarån. The average deviation between modelled and observed concentrations is 16% for the primary calibration dataset and 14% for the secondary validation dataset.

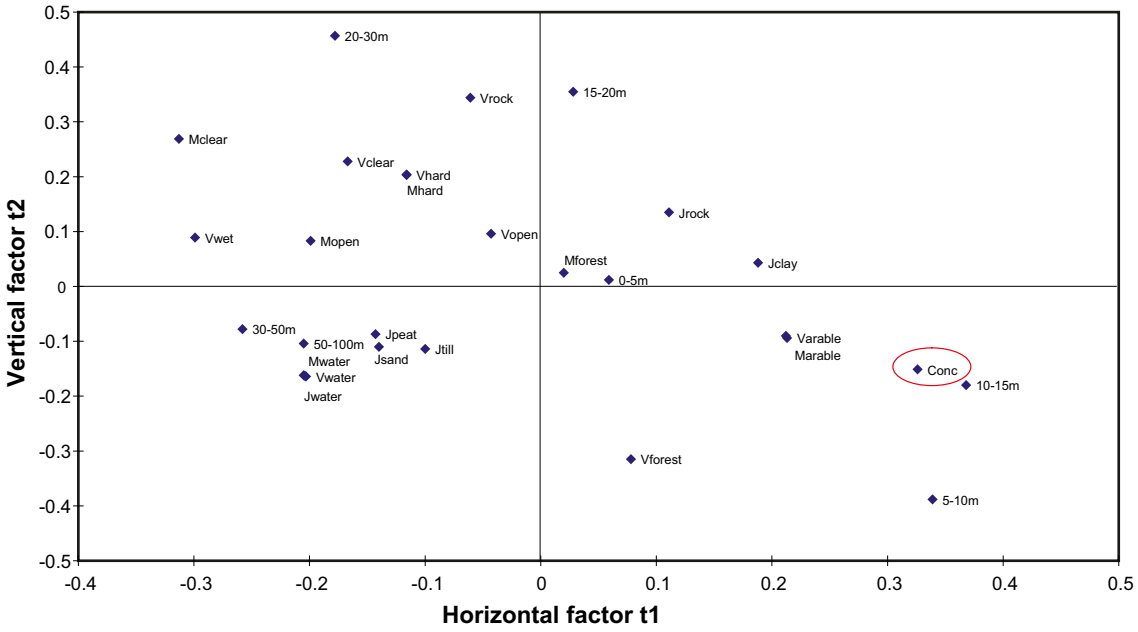


***Figure 6-23.*** *Partial least squares regression model, PLS (see Section 6.5.3 for an explanation of PLS) showing the correlation structure among distributed catchment characteristics, and the observed $SO_4^{2-}$ concentration (encircled in red). The parameters represent the relative distribution of each regolith, land use, vegetation and elevation class upstream of the hydrochemical sampling point in the outlet of the catchments. Factor t1 describe 32% of the variation among the explanatory variables and t2 24%. 81% of the variance in 'Conc' is described by t1 and 14% by t2.*

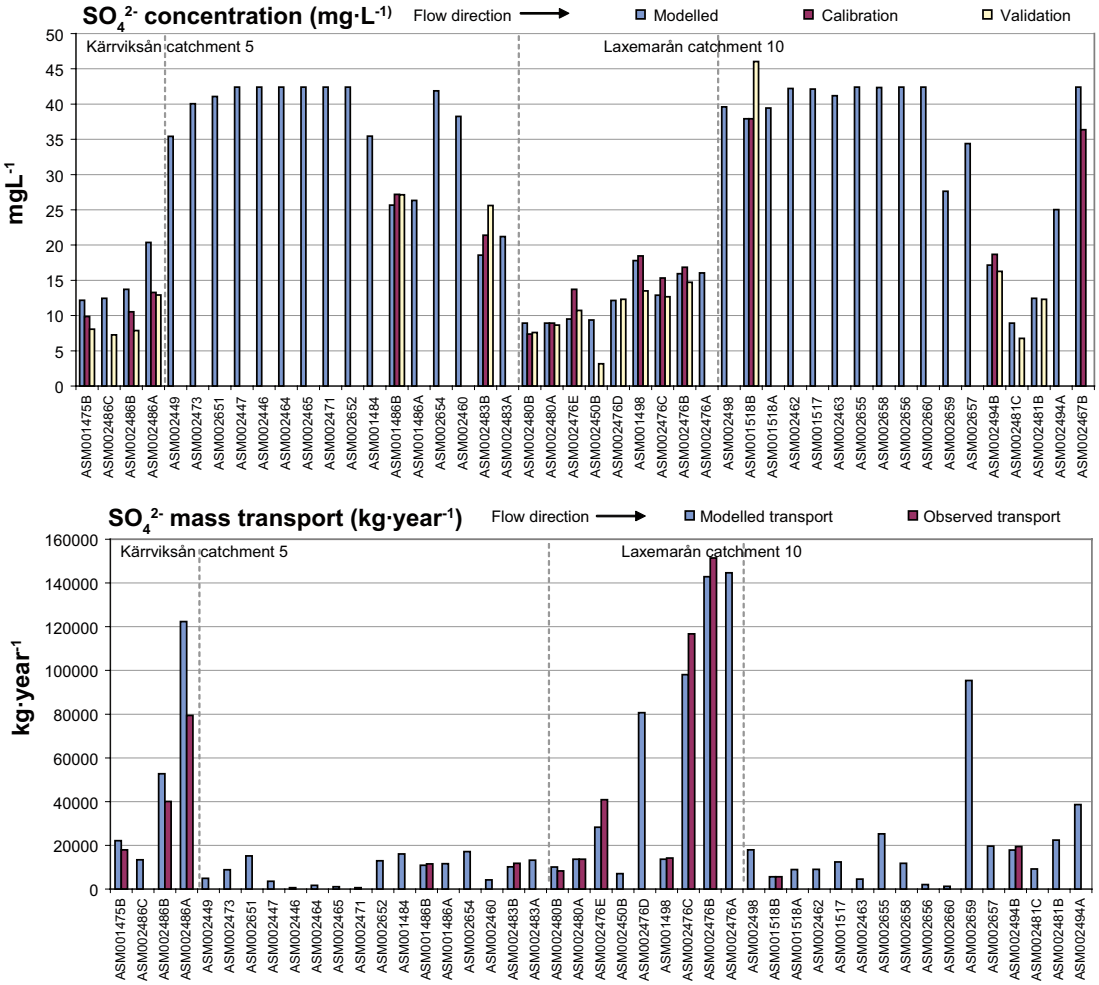


***Figure 6-24.*** *Mass balance for $SO_4^{2-}$ in the Laxemar-Simpevarp area. Flow-weighted concentrations ($mg \cdot L^{-1}$) above, and transport ($kg \cdot year^{-1}$) below, describing the conditions in the outlet of each catchment.*

**Table 6-9. Parameters and results from the $SO_4^{2-}$ mass balance model. Categories not used have been omitted from the table. The total contribution from each category is listed for the entire modelled area and for the catchments of the Laxemarån and the Kärrviksån. The estimated flow-weighted concentration during the period 1 December 2003 to 30 November 2004 is listed at the bottom of the table.**

| Model parameters | | | | Model results | | | | | |
|---|---|---|---|---|---|---|---|---|---|
| **Diffuse sources** | | | kg·ha$^{-1}$· | **All catchments** | | **Laxemarån** | | **Kärrviksån** | |
| Category | Class | mg·L$^{-1}$ | year$^{-1}$ | kg·yr$^{-1}$ | % | kg·yr$^{-1}$ | % | kg·yr$^{-1}$ | % |
| Regolith | | | | | | | | | |
| Land use | | | | | | | | | |
| Vegetation | | | | | | | | | |
| Topography | 0–5m | 42 | | 141,590 | 21 | 4,488 | 3 | 9,399 | 8 |
| | 5–10m | =0–5m | | 183,716 | 27 | 22,331 | 15 | 32,623 | 27 |
| | 10–15m | =0–5m | | 206,359 | 31 | 54,503 | 38 | 44,968 | 37 |
| | 15–20m | 8.9 | | 39,242 | 6 | 12,104 | 8 | 12,222 | 10 |
| | 20–30m | =15–20m | | 62,883 | 9 | 24,484 | 17 | 16,945 | 14 |
| | 30–50m | =15–20m | | 40,573 | 6 | 26,130 | 18 | 6,140 | 5 |
| | 50–100m | =15–20m | | 619 | 0 | 619 | 0 | 0 | 0 |
| **Point sources** | | | | | | | | | |
| No point sources included | | | | | | | | | |
| **Total** | | | | | | | | | |
| Gross | | | | 674,982 | 100 | 144,659 | 100 | 122,298 | 100 |
| Retention | | | | 0 | 0 | 0 | 0 | 0 | 0 |
| Net | | | | 674,982 | 100 | 144,659 | 100 | 122,298 | 100 |
| **Concentration (mg·L$^{-1}$)** | | | | 24 | | 16 | | 20 | |

The following conclusions about sources of $SO_4^{2-}$ can be drawn from the mass balance scenario:

- Among the distributed factors, the topographical elevation is an important factor that enhances discharge of $SO_4^{2-}$. This factor is, however, closely correlated with both the presence of arable land and clay in soils, and the exact dependencies could not be elucidated in the present model version. According to the model results, the typical concentration in discharge from areas located below 15m is nearly 5 times higher than in discharge from higher areas.
- Oxidation of sulphide minerals in the deposits is a potential source of $SO_4^{2-}$, especially in the lower-lying areas which contain fine grained regolith deposited as sea or lake sediments. Aeration of these soils enhances leaching of $SO_4^{2-}$, due to agricultural activities as cultivation or drainage. Input of sulphur via fertilizers is another potential source.
- The calibrated background $SO_4^{2-}$ level of 8.9 mgL$^{-1}$ in discharge from higher areas is about 6 times higher than the median $SO_4^{2-}$-concentration in precipitation of 1.7 mgL$^{-1}$ /Tröjbom and Söderbäck 2006/. If these values are corrected for evapotranspiration, the discrepancy in relation to the background level is less than 2 times, corresponding to a concentration of 5 mgL$^{-1}$ (evapotranspiration was assumed to constitute about two thirds of total precipitation, which leads to an increase in concentration by a factor of 3, cf /Werner et al. 2008/). One interpretation of this result is that deposition may be a major source contributing to the background level in the Laxemar-Simpevarp area.
- If the estimated concentration in precipitation is compared with the average concentration in discharge from the catchment of Laxemarån (16 mgL$^{-1}$), approximately one third of the $SO_4^{2-}$ that reaches the sea originates from deposition. Of this airborne fraction, only about 10% originates from sea spray, if the marine part is estimated from local Cl measurements in precipitation, and the rest originates from regional sulphur deposition, i.e. 4.5 mgL$^{-1}$. Compared with the national distribution, this background level corresponds to the 80–90$^{th}$ percentile in lakes and streams (Figure 6-25). The measurements of $SO_4^{2-}$ in precipitation,

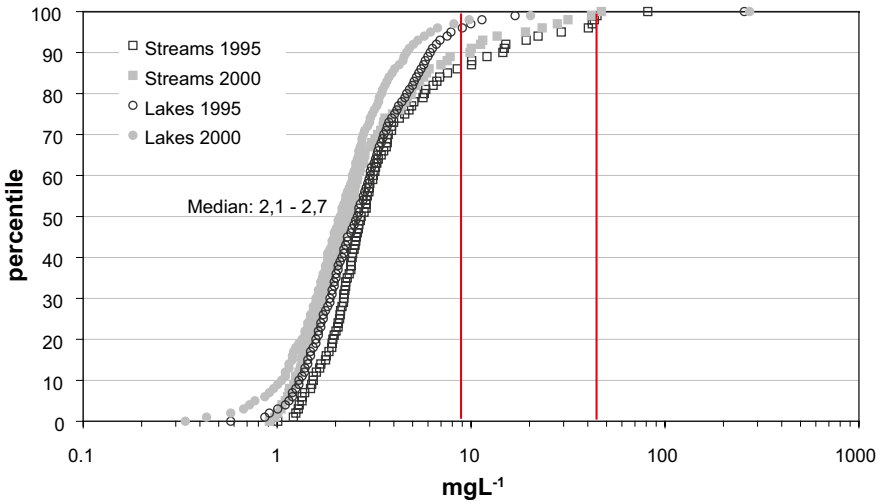


***Figure 6-25.*** *Distribution of $SO_4^{2-}$ concentrations in the Swedish surveys of lakes and streams in 1995 and 2000 /IMA 2007/. Typical concentrations for categories calibrated within the VBX-VII model are marked as red lines.*

which is sampled in a container located in an open field, may to some extent discriminate the additional input from dry deposition. According to measurements, this fraction may contribute a further 50–100% compared with observed wet deposition (P.O. Johansson, pers. comm.), which means that the total background $SO_4^{2-}$ level of 8.9 $mgL^{-1}$ could be explained by atmospheric deposition. In that case, approximately 2/3 of the sulphur that reaches the sea may originate from regional sulphur deposition.

- The remaining portion, corresponding to between 1/3 and 2/3 of the total $SO_4^{2-}$ discharge, is probably of marine origin, where oxidation of sulphide minerals is probably mainly reponsible, according to isotope measurements (cf Section 4.1.3).
- There are no indications of significant retention of $SO_4^{2-}$ in the lakes.

### 6.2.8 Mass balance for bicarbonate ($HCO_3^-$)

The mass balance for $HCO_3^-$ did not converge to a stable solution for any combination of the included distributed factors. The correlation analysis in Figure 6-26 indicates that arable land, clear-cuts and clay are distributed factors that potentially affect the $HCO_3^-$ concentrations, but none of these factors resulted in a stable model. This suggests that the spatial variation of $HCO_3^-$ in the Laxemar-Simpevarp area cannot be explained by a linear combination of sources linked to distributed properties in the catchments. This contrasts to the situation in the Forsmark area, where the spatial variation in $HCO_3^-$ was satisfactorily modelled in a manner similar to Ca /Tröjbom et al. 2007/. For comparison, a basic scenario based on only one typical concentration is shown in Figure 6-27 and in Table 6-10. See Appendix C for detailed model results. This scenario corresponds to a constant concentration in discharge from all land categories and the variation in mass transport only reflects the size of the catchments.

One important reason for the poor modelling result is probably the fact that sinks are not included into the model structure; in surface waters $HCO_3^-$ is the main constituent comprising the alkalinity or buffering capacity that is consumed during neutralisation of $H^+$ from acid waters. $H^+$ is derived either from weak acids from biogenic sources originating from degradation of organic matter, or from strong acids as sulphuric acid, which is derived from atmospheric deposition or oxidation of sulphides in the deposits. Comparisons between the simple constant concentration scenario and observed concentrations may, however, reveal information that helps to explain the origin and fate of $HCO_3^-$. The following conclusions regarding the origin and fate of $HCO_3^-$ can be drawn:

- Within the catchment of the Laxemarån, observed $HCO_3^-$ concentrations are almost constant and total transport can consequently be explained by this simple scenario. ASM001498 shows considerably lower observed concentrations of $HCO_3^-$ compared with the rest of the catchment of the Laxemarån. This may hypothetically be explained by for example unusual land use or regolith distribution in this part of the catchment. According to the land use map in Figure 2-6, this sub-catchment contains mainly forest land.
- The observed $HCO_3^-$ concentration tend to decrease along the Kärrviksån. This may be explained either by mixing with water with lower concentrations in the downstream parts of the catchment, or by influx of $H^+$ that reduces alkalinity and consumes $HCO_3^-$. A potential source of $H^+$ could be oxidation of sulphides in the deposits. According to the sulphur mass balance in Figure 6-24, the $SO_4^{2-}$ concentration also increases along the Kärrviksån, which could be an indication of sulphur input from sulphides. When the isotopic composition is compared between PSM002083 at the outlet of the Kärrviksån and PSM002082 upstream, the former shows a slightly more negative $\delta^{34}S$ value. This may be an indication of influx of sulphur of pyritic origin in the downstream parts of the catchment (cf Figure 4-12). Mineral sulphides are usually depleted in the heavier $^{34}S$ isotope, thus having a more negative $\delta^{34}S$ value.
- In one catchment, ASM002483B (and to some extent in ASM001486B), $HCO_3^-$ concentrations are underestimated compared with the average value in the Laxemar-Simpevarp area. A similar deviation is also observed for Ca (cf Figure 6-16), which indicates that there may be an unknown source of these elements in the catchment. A hypothetical source of both of these ions could be anthropogenic addition of lime to soils or directly in the watercourses for agricultural or environmental management purposes.
- There are no indications of significant retention of $HCO_3^-$ in the lakes.
- The poor modelling result and the difficulties in finding distributed factors that describe the variation in $HCO_3^-$ concentrations within the Laxemar-Simpevarp area probably reflects the fact that important sinks are not modelled. The alkalinity (or the buffering capacity, most of which is accounted for by $HCO_3^-$) is consumed by neutralisation of $H^+$. Sources of weak or strong acids, which could be perceived as $HCO_3^-$ sinks, in combination with sources of $HCO_3^-$, constitute the observed spatial pattern for $HCO_3^-$. Possible $H^+$ sources are weak acids of biogenic origin, sulphur deposition or oxidation of sulphides in the deposits.

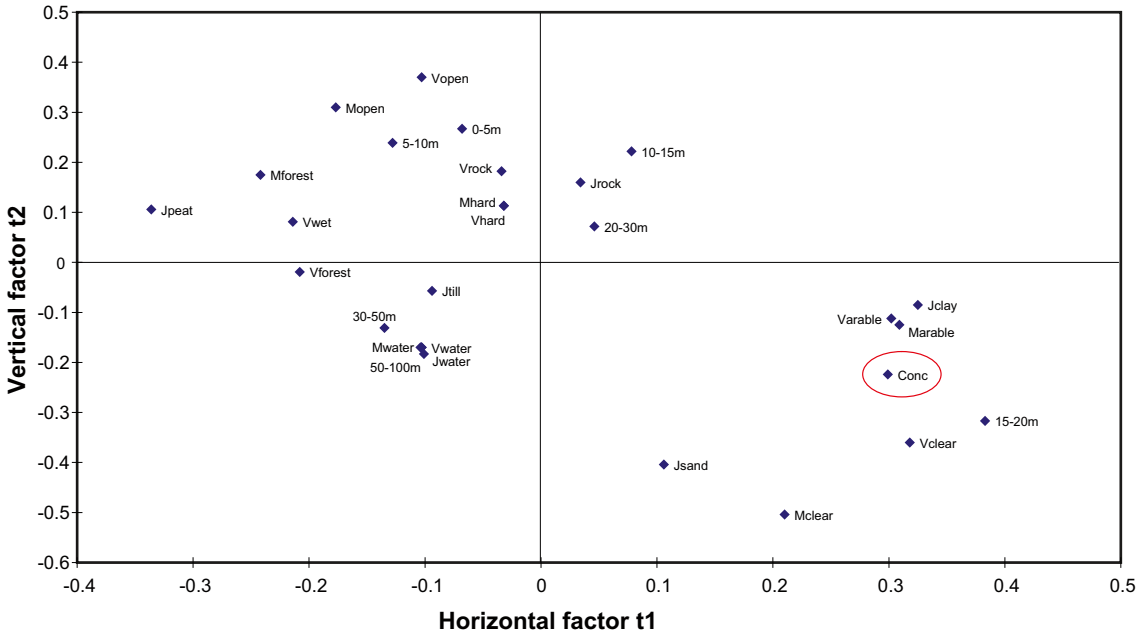


***Figure 6-26.*** *Partial least squares regression model, PLS (see Section 6.5.3 for an explanation of PLS) showing the correlation structure among distributed catchment characteristics, and the observed $HCO_3^-$ concentration (encircled in red). The parameters represent the relative distribution of each regolith, land use, vegetation and elevation class upstream of the hydrochemical sampling point in the outlet of the catchments. Factor t1 describe 28% of the variation among the explanatory variables and t2 23%. 49% of the variance in 'Conc' is described by t1 and 22% by t2.*

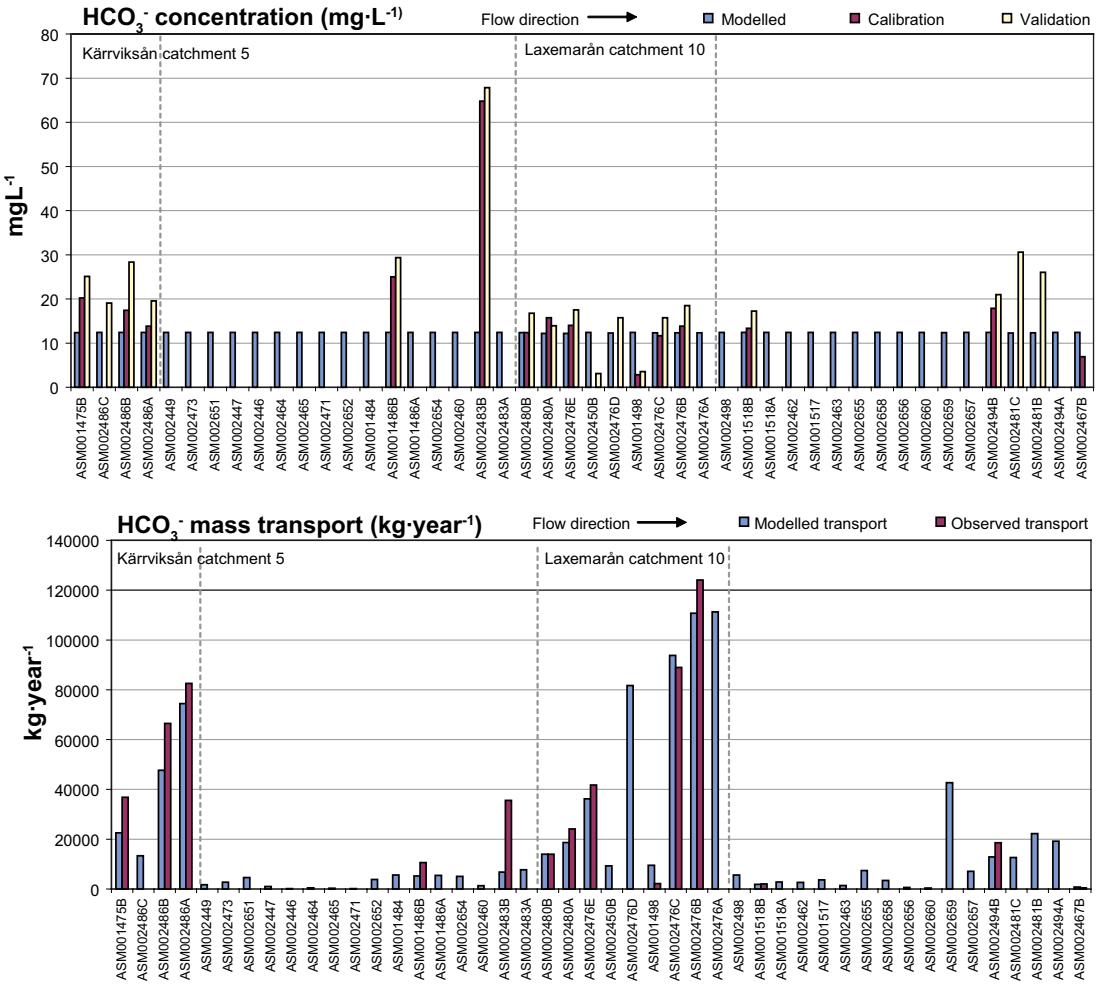


***Figure 6-27.*** *Mass balance for HCO3– in the Laxemar-Simpevarp area. Note that the HCO3–-model did not converge to any stable solution based on the included distributed factors. Only one typical concentration is thus included representing an average for all categories. This scenario describes the hypothesis of a constant concentration in discharge from all categories, and variations in mass transport consequently only reflect the size of the catchments. Flow-weighted concentrations (mg·L$^{-1}$) above, and transport (kg·year$^{-1}$) below, describing the conditions in the outlet of each catchment.*

**Table 6-10. Compilation of parameters and results from the $HCO_3^-$ mass balance model. Categories not used have been omitted from the table. The total contribution from each category is listed for the entire modelled area and for the catchments of the Laxemarån and the Kärrviksån. The estimated flow-weighted concentration during the period 1 December 2003 to 30 November 2004 is listed at the bottom of the table.**

| Model parameters | | | | Model results | | | | | |
|---|---|---|---|---|---|---|---|---|---|
| **Diffuse sources** | | | kg·ha$^{-1}$·year$^{-1}$ | **All catchments** | | **Laxemarån** | | **Kärrviksån** | |
| Category | Class | mg·L$^{-1}$ | | kg·yr$^{-1}$ | % | kg·yr$^{-1}$ | % | kg·yr$^{-1}$ | % |
| Regolith | - | | | | | | | | |
| Land use | - | | | | | | | | |
| Vegetation | Vwater | =Vforest | | 3,245 | 1 | 1,287 | 1 | 152 | 0 |
| | Vwet | =Vforest | | 10,175 | 3 | 2,475 | 2 | 3,075 | 4 |
| | Vrock | =Vforest | | 37,489 | 11 | 8,812 | 8 | 12,570 | 17 |
| | Vforest | 12.4 | | 254,846 | 72 | 84,069 | 76 | 49,126 | 66 |
| | Vclear | =Vforest | | 12,756 | 4 | 4,701 | 4 | 4,050 | 5 |
| | Varable | =Vforest | | 16,625 | 5 | 5,464 | 5 | 2,887 | 4 |
| | Vopen | =Vforest | | 15,501 | 4 | 4,431 | 4 | 2,157 | 3 |
| | Vhard | =Vforest | | 3,271 | 1 | 0 | 0 | 437 | 1 |
| Topography | - | | | | | | | | |
| **Point sources** | | | | | | | | | |
| No point sources included | | | | | | | | | |
| **Total** | | | | | | | | | |
| Gross | | | | 353,911 | 100 | 111,244 | 100 | 74,457 | 100 |
| Retention | | | | 0 | 0 | 0 | 0 | 0 | 0 |
| Net | | | | 353,911 | 100 | 111,244 | 100 | 74,457 | 100 |
| **Concentration (mg·L$^{-1}$)** | | | | 12 | | 12 | | 12 | |

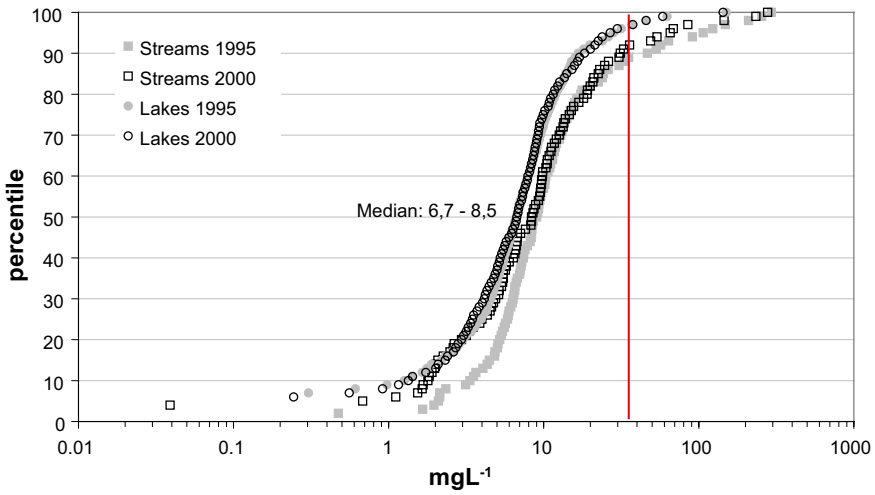


***Figure 6-28.*** *Distribution of HCO3– concentrations in the Swedish surveys of lakes and streams in 1995 and 2000 /IMA 2007/. The typical concentration for categories calibrated within the VBX-VII model is marked as a red line.*

### 6.2.9 Mass balance for total organic carbon (TOC)

Due to the limited spatial variation in concentrations of total organic carbon (TOC), the prospects of finding governing factors are poor. The correlation analysis in Figure 6-29 also gives a scattered picture with weak relationships between observed concentrations and distributed characteristics in the catchments. The TOC model comprises a very basic scenario with only one typical concentration in discharge from all vegetation types in combination with retention in lakes. The model results are shown in Figure 6-30, and model parameters are listed in Table 6-11. See Appendix C for detailed model results.

No combination of the available parameters could satisfactorily reproduce the spatial pattern of TOC in the Laxemar-Simpevarp area. The modelled spatial variation of the concentrations (upper panel) in the basic scenario shown in Figure 6-30 is mainly attributable to varying lake area in proportion to the catchment area. The variation displayed by mass transport in the lower panel mainly reflects the size of the catchments. According to the estimates in Table 6-11, retention has a very small impact on the overall transport (retention loss constitutes only 2% of the total transport). This is mainly an effect of the few and small lakes in the area.

The limited variation in TOC leads to small relative deviations between modelled and observed concentrations. The average deviation between modelled and observed concentrations is only 13% for the primary calibration dataset and 11% for the secondary validation dataset, which is low compared to most other elements. Although governing factors are not distinguished, the small variation suggests that estimated transport in the watercourses is probably more or less correct. The following conclusions about sources of TOC can be drawn from the mass balance scenario:

- The very small catchment at Ävrö (ASM00002467B) shows large deviations for TOC, as well as many other parameters. The main reason for the large discrepancy is probably increased uncertainties due to the small size of the catchment.
- ASM002494B and ASM001518B also display elevated TOC concentrations, which may indicate point sources or an unusual land use in the vicinity. Both of these catchments are located in the same area close to farms and large areas of agricultural land, which could be a source of organic carbon.
- There are indications of retention in the lakes. These estimates are of course uncertain due to the small number of lakes in the area. In Lake Jämsen and Lake Frisksjön the TOC retention was estimated to be about 10%, whereas the total retention in the whole catchment is less than 2% according to this TOC scenario.
- The low observed variation in the Laxemar-Simpevarp area leads to difficulties in identifying governing factors for TOC. The low variability, however, suggests that the estimated transport in the watercourses is more or less correct and mainly controlled by discharge and, ultimately, catchment size.

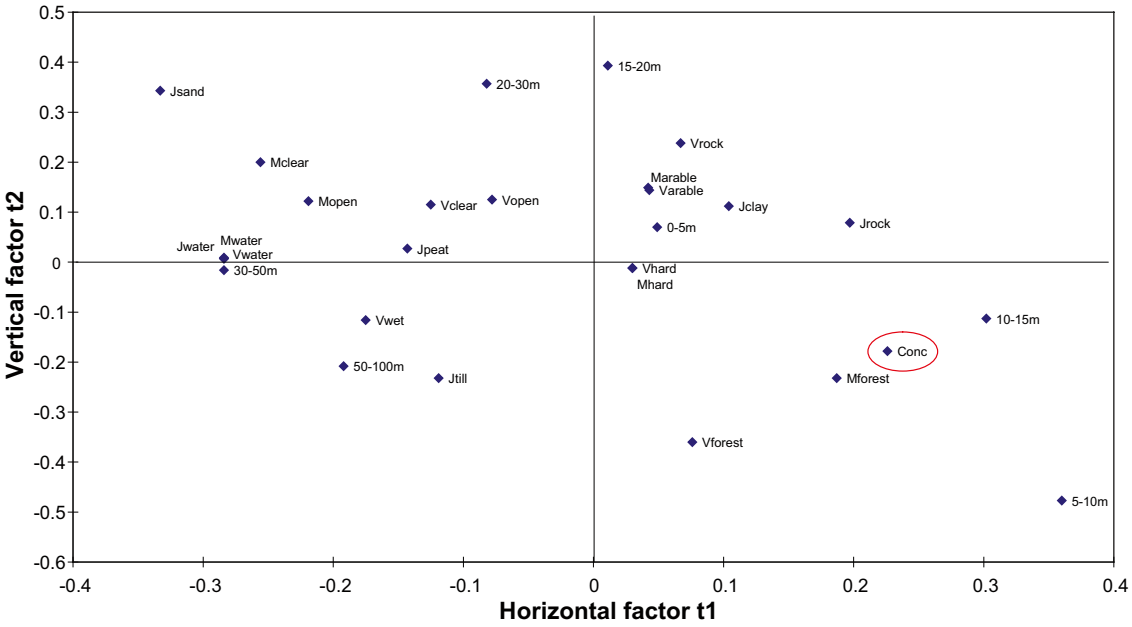


***Figure 6-29.*** *Partial least squares regression model, PLS (see Section 6.5.3 for an explanation of PLS) showing the correlation structure among distributed catchment characteristics, and the observed TOC concentration (encircled in red). The parameters represent the relative distribution of each regolith, land use, vegetation and elevation class upstream of the hydrochemical sampling point in the outlet of the catchments. Factor t1 describe 34% of the variation among the explanatory variables and t2 20%. 42% of the variance in 'Conc' is described by t1 and 12% by t2.*

**Table 6-11. Parameters and results from the TOC mass balance model. Categories not used have been omitted from the table. The total contribution from each category is listed for the entire modelled area and for the catchments of the Laxemarån and the Kärrviksån. The estimated flow-weighted concentration during the period 1 December 2003 to 30 November 2004 is listed at the bottom of the table.**

| Model parameters | | | | Model results | | | | | |
|---|---|---|---|---|---|---|---|---|---|
| **Diffuse sources** | | | kg·ha$^{-1}$·year$^{-1}$ | **All catchments** | | **Laxemarån** | | **Kärrviksån** | |
| Category | Class | mg·L$^{-1}$ | | kg·yr$^{-1}$ | % | kg·yr$^{-1}$ | % | kg·yr$^{-1}$ | % |
| Regolith | - | | | | | | | | |
| Landuse | - | | | | | | | | |
| Vegetation | Vwater | - | | | | | | | |
| | Vwet | 22 | | 17,810 | 3 | 4,333 | 2 | 5,383 | 4 |
| | Vrock | =Vwet | | 65,620 | 11 | 15,425 | 8 | 22,003 | 17 |
| | Vforest | =Vwet | | 446,077 | 73 | 147,154 | 76 | 85,990 | 67 |
| | Vclear | =Vwet | | 22,328 | 4 | 8,229 | 4 | 7,089 | 5 |
| | Varable | =Vwet | | 29,100 | 5 | 9,565 | 5 | 5,053 | 4 |
| | Vopen | =Vwet | | 27,134 | 4 | 7,757 | 4 | 3,776 | 3 |
| | Vhard | - | | | | | | | |
| Topography | | | | | | | | | |
| **Point sources** | | | | | | | | | |
| No point sources included | | | | | | | | | |
| **Total** | | | | | | | | | |
| Gross | | | | 608,071 | 100 | 192,466 | 100 | 129,296 | 100 |
| Retention (λ=0.5, yr$^{-1}$) | | | | 10,388 | 2 | 4,500 | 2 | 620 | 0 |
| Net | | | | 597,683 | 98 | 187,966 | 98 | 128,676 | 100 |
| **Concentration (mg·L$^{-1}$)** | | | | 21 | | 21 | | 21 | |

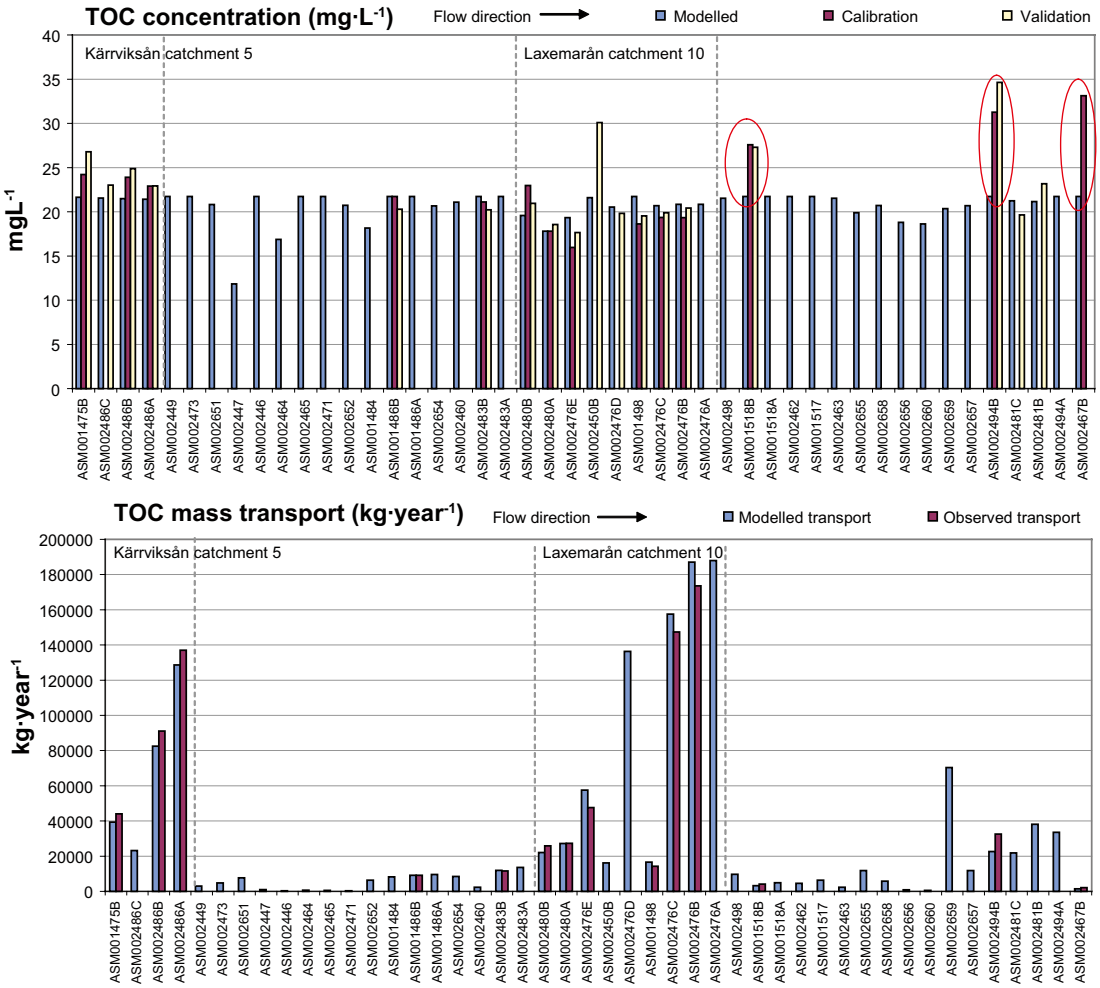


***Figure 6-30.*** *Mass balance for TOC in the Laxemar-Simpevarp area. Flo- weighted concentrations (mg·L$^{-1}$) above, and transport (kg·year$^{-1}$) below, describing the conditions in the outlet of each catchment.*

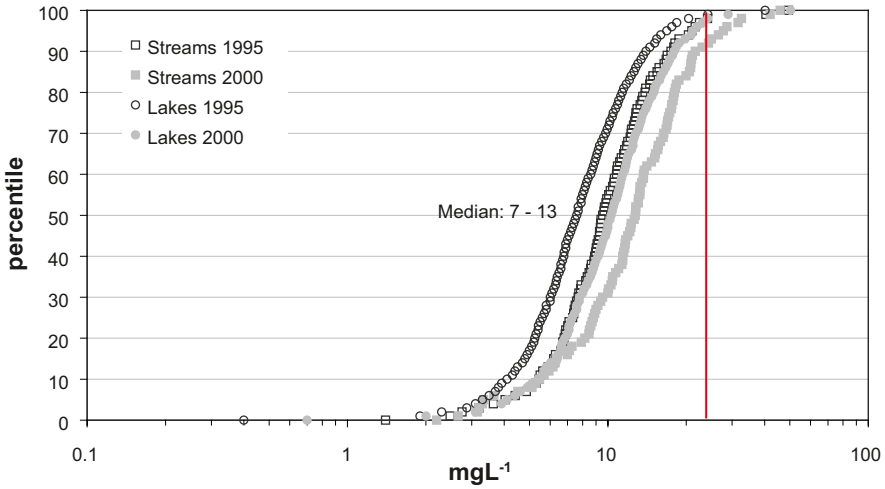


***Figure 6-31.*** *Distribution of TOC concentrations in the Swedish surveys of lakes and streams in 1995 and 2000 /IMA 2007/. Typical concentrations for categories calibrated within the VBX-VII model are marked as red lines.*

### 6.2.10 Mass balance for total nitrogen (Tot-N)

The mass balance model for total nitrogen, tot-N, differs from the previous TOC model by showing a clear correlation with characteristics related to arable land, for example clay and lower-lying areas, according to the correlation analysis in Figure 6-32. As in the case of Mg, a very simple mass balance model is applied to total nitrogen as shown in Figure 6-33. Model details are shown in Table 6-12. See Appendix C for detailed model results.

The spatial variation is acceptably modelled within the Laxemar-Simpevarp area by means of two calibrated typical concentrations that represent concentrations in discharge from the land use class 'Varable' and a concentration common for the remaining land use classes. If a retention parameter is included, the model result is only slightly improved but the total N loss through retention is marginal, which indicates that retention in lakes has a minor impact in the Laxemar-Simpevarp area. The average deviation between modelled and observed concentrations is 9% for the primary calibration dataset and 15% for the secondary validation dataset.

The following conclusions about sources of tot-N can be drawn from the mass balance scenario:

- In the Laxemar-Simpevarp area, total nitrogen concentrations are significantly higher in areas that contain arable land. This indicates that agricultural activities are important factors increasing N leaching from this land use category. The fact that arable land is predominantly located on clayey soils in low-lying areas leads to a correlation between these characteristics and total nitrogen as well.
- The typical total nitrogen concentration in discharge from arable land is elevated by a factor of 8 compared with the concentration in discharge from other vegetation types. At the specific water discharge, this corresponds to an annual area loss from arable land of approximately 1,300 $kg \cdot km^{-2} \cdot year^{-1}$. This is on a level with the area-specific loss of 1,000 $kg \cdot km^{-2} \cdot year^{-1}$ that was estimated for the adjacent coastal area (TRK identity 068074) /TRK 2008/. The corresponding area loss from forest land and vegetation types other than arable land is approximately 150 $kg \cdot km^{-2} \cdot year^{-1}$.
- The calibrated value of 1.1 $mg \cdot L^{-1}$ from all vegetation types except for arable land corresponds to the 90$^{th}$ percentile of the Swedish distribution. This indicates that N leaching may be elevated in the Laxemar-Simpevarp area compared with the normal situation in Sweden (cf Tröjbom and Söderbäck 2006/. The typical N concentration in discharge from forest land for the parts of southern Sweden that discharge into the Baltic is 0.62 $mg \cdot L^{-1}$ according to /TRK 2008/. The value from the Laxemar-Simpevarp area is almost twice this. The discrepancy may to some extent be explained by variation between years, as the calibrated value of 1.1 $mg \cdot L^{-1}$ represents 2004, whereas the TRK value represents the average for a longer time period.
- Atmospheric deposition of N contributes approximately 600 $kg \cdot km^{-2} \cdot year^{-1}$ in the coastal region including the Laxemar-Simpevarp area, according to /TRK 2008/. When this input (which is automatically included in the typical concentrations in discharge) is compared with the calibrated background discharge from all vegetation types except for arable land (150 $kg \cdot km^{-2} \cdot year^{-1}$), it is evident that atmospheric deposition is an important source of N, and that only a fraction of this N reaches the sea (less than 25%). Additionally, biological nitrogen fixation contributes an unknown input of N to the surface system, which further reduces this fraction.
- The overall effect of N retention in lakes in the Laxemar-Simpevarp area is marginal and only 3% of the total discharge from land is lost in the lakes according to this scenario. Of the N that reaches specific lakes, between 16% and 27% is lost due to retention in Lake Jämsen and Lake Frisksjön, respectively. When these fractions are compared with the above figures, it is evident that significant N retention must take place before the discharging water reaches larger streams and lakes, i.e. in the soil and in wetlands and small ditches.

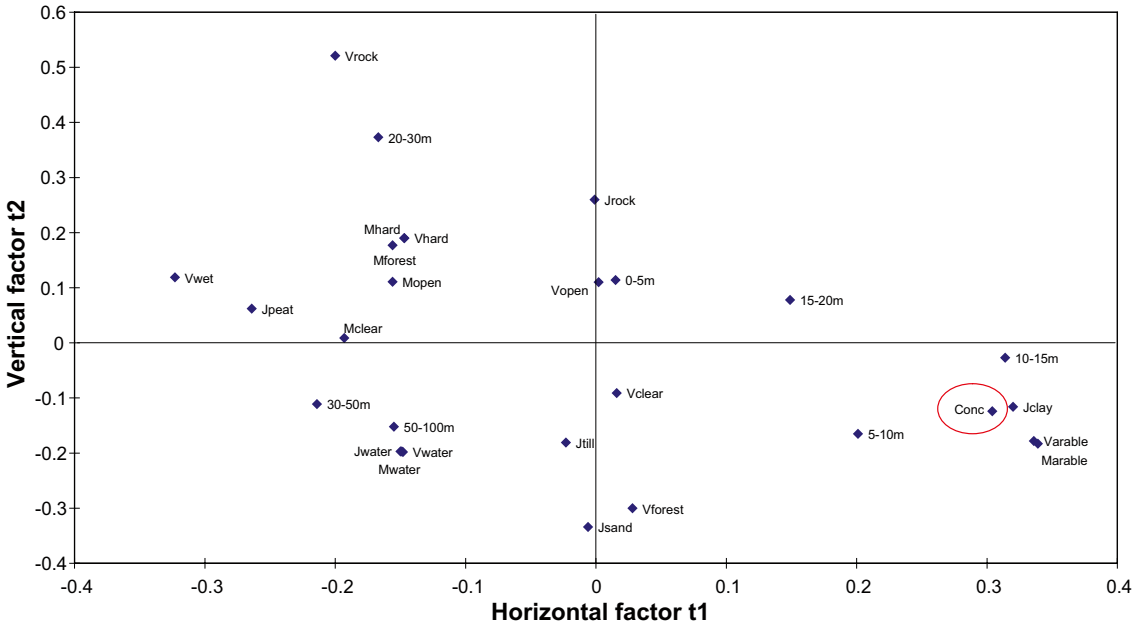


***Figure 6-32.*** *Partial least squares regression model, PLS (see Section 6.5.3 for an explanation of PLS) showing the correlation structure among distributed catchment characteristics, and the observed tot-N concentration (encircled in red). The parameters represent the relative distribution of each regolith, land use, vegetation and elevation class upstream of the hydrochemical sampling point in the outlet of the catchments. Factor t1 describe 29% of the variation among the explanatory variables and t2 27%. 65% of the variance in 'Conc' is described by t1 and 10% by t2.*

**Table 6-12. Parameters and results from the Tot-N mass balance model. Categories not used have been omitted from the table. The total contribution from each category is listed for the entire modelled area and for the catchments of the Laxemarån and the Kärrviksån. The estimated flow-weighted concentration during the period 1 December 2003 to 30 November 2004 is listed at the bottom of the table.**

| Model parameters | | | | Model results | | | | | |
|---|---|---|---|---|---|---|---|---|---|
| **Diffuse sources** | | | kg·ha$^{-1}$·year$^{-1}$ | **All catchments** | | **Laxemarån** | | **Kärrviksån** | |
| Category | Class | mg·L$^{-1}$ | | kg·yr$^{-1}$ | % | kg·yr$^{-1}$ | % | kg·yr$^{-1}$ | % |
| Regolith | - | | | | | | | | |
| Land use | - | | | | | | | | |
| Vegetation | Vwater | - | | | | | | | |
| | Vwet | =Vforest | | 865 | 2 | 210 | 2 | 261 | 3 |
| | Vrock | =Vforest | | 3,188 | 8 | 749 | 6 | 1,069 | 13 |
| | Vforest | 1.1 | | 21,673 | 54 | 7,149 | 56 | 4,178 | 51 |
| | Vclear | =Vforest | | 1,084 | 3 | 399 | 3 | 344 | 4 |
| | Varable | 9.0 | | 12,000 | 30 | 3,944 | 31 | 208 | 26 |
| | Vopen | =Vforest | | 1,318 | 3 | 376 | 3 | 183 | 2 |
| | Vhard | =Vforest | | 278 | 1 | 0 | 0 | 37 | 0 |
| Topography | - | | | | | | | | |
| **Point sources** | | | | | | | | | |
| No point sources included | | | | | | | | | |
| **Total** | | | | | | | | | |
| Gross | | | | 40,409 | 100 | 12,831 | 100 | 8,158 | 100 |
| Retention (λ=1.3 yr$^{-1}$) | | | | 1,364 | 3 | 614 | 5 | 82 | 1 |
| Net | | | | 39,045 | 97 | 12,217 | 95 | 8,075 | 99 |
| **Concentration (mg·L$^{-1}$)** | | | | 1.4 | | 1.4 | | 1.3 | |

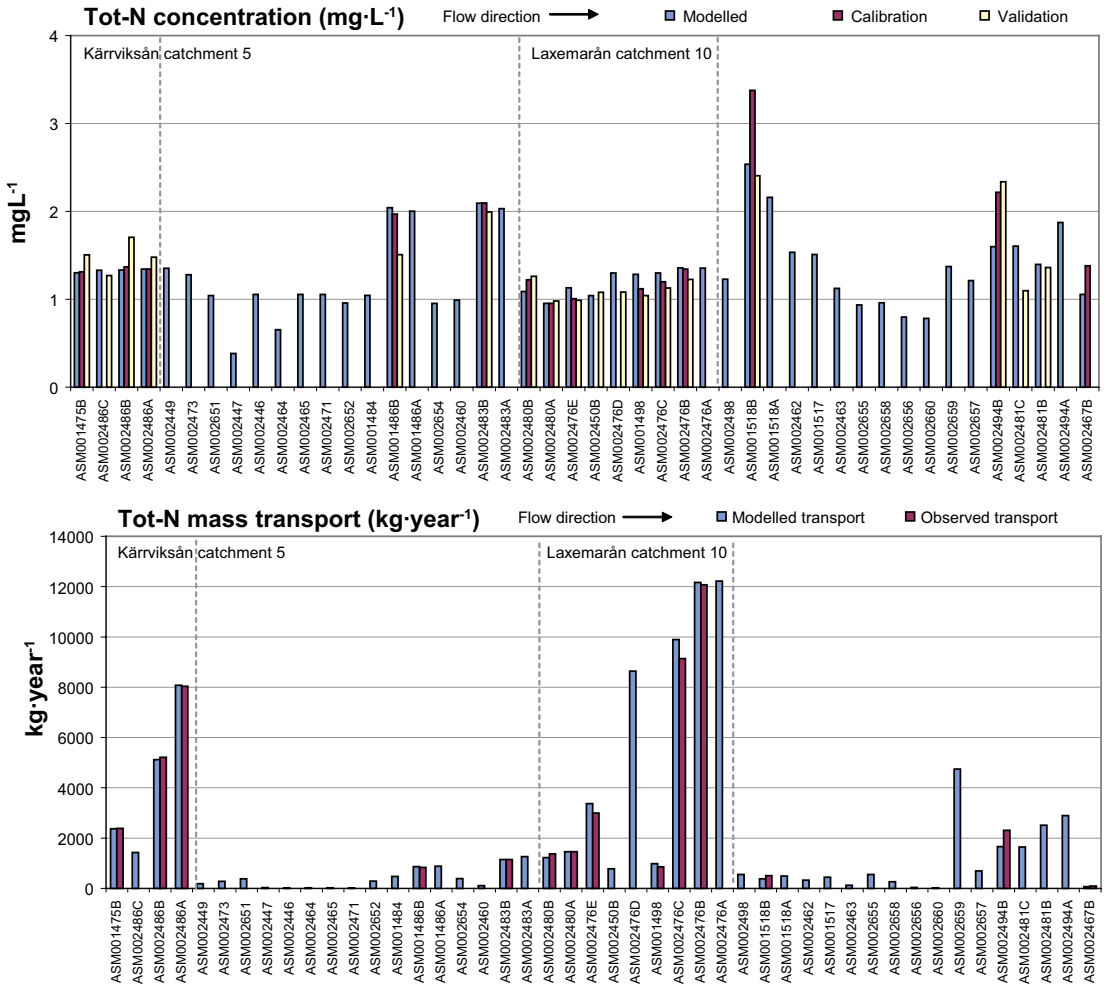


***Figure 6-33.*** *Mass balance for Tot-N in the Laxemar-Simpevarp area. Flow-weighted concentrations (mg·L$^{-1}$) above, and transport (kg·year$^{-1}$) below, describing the conditions in the outlet of each catchment.*

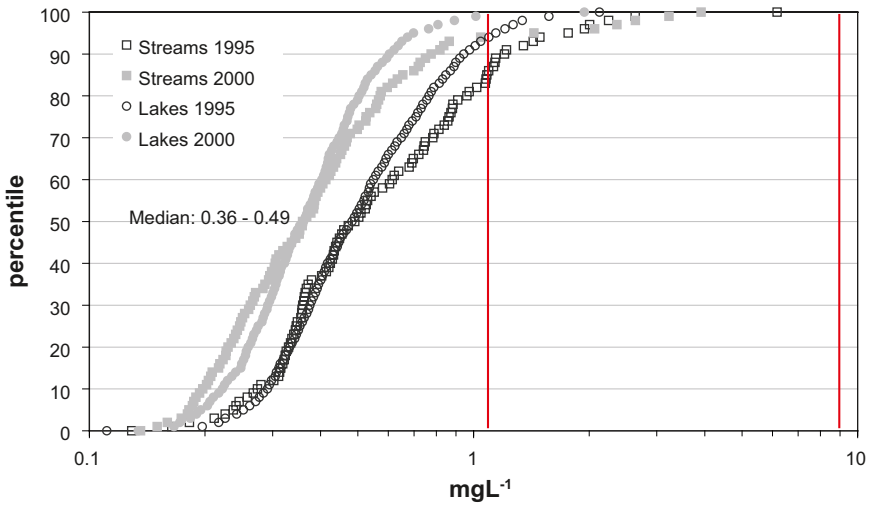


***Figure 6-34.*** *Distribution of Tot-N concentrations in the Swedish surveys of lakes and streams in 1995 and 2000 /IMA 2007/. Typical concentrations for categories calibrated within the VBX-VII model are marked as red lines.*

### 6.2.11 Mass balance for total phosphorus (Tot-P)

The overall spatial pattern for total phosphorus is in many respects very similar to the pattern for total nitrogen in Section 6.2.10, although there are fundamental differences in the sources of these elements: nitrogen is derived from the atmosphere whereas phosphorus is released by weathering of minerals (some atmospheric deposition of phosphorus may also occur). According to the correlation analysis in Figure 6-35 high tot-P concentrations are, in the case of tot-N, correlated with the land use category arable land and the regolith class 'Jclay'. Both N and P are intimately linked to organic matter (cf Section 4.1.5). The common sources of these elements related to arable land are the use of fertilizers, degradation of organic matter and manure. As in the case of tot-N, a very simple mass balance model is applied to total phosphorus as shown in Figure 6-36. Model details are compiled in Table 6-13. See Appendix C for detailed model results.

The spatial variation is acceptably modelled within the Laxemar-Simpevarp area by means of two calibrated typical concentrations that represent concentrations in discharge from the land use class 'Varable' and a concentration common for the remaining land use classes If a retention parameter is included, the model result is only slightly improved but the total P loss through retention is small, which indicates that retention in lakes has a minor impact in the Laxemar-Simpevarp area. The average deviation between modelled and observed concentrations is 13% for the primary calibration dataset and 19% for the secondary validation dataset.

The following conclusions about sources of tot-P can be drawn from the mass balance scenario:

- In the Laxemar-Simpevarp area, total phosphorus concentrations are, as in the case of tot-N, significantly higher in areas that contain arable land. This indicates that agricultural activities are probably important factors enhancing P loss. The fact that arable land is predominantly located on clayey soils in low-lying areas leads to a correlation between these characteristics and total phosphorus as well.
- The typical total phosphorus concentration in discharge from arable land is elevated by a factor of 8 compared with the concentration in discharge from other vegetation types (the same ratio as for tot-N). At the specific water discharge, this corresponds to an annual area loss from arable land of approximately 37 $kg \cdot km^{-2} \cdot year^{-1}$. This is on a level with the area specific loss of 35 $kg \cdot km^{-2} \cdot year^{-1}$ which was estimated for the coastal area (TRK identity 068074) /TRK 2008/. The corresponding area loss from forest land and vegetation types other than arable land is approximately 5 $kg \cdot km^{-2} \cdot year^{-1}$.
- The calibrated value of 0.03 $mg \cdot L^{-1}$ from all vegetation types except for arable land corresponds to the 90$^{th}$ percentile of the Swedish distribution. This indicates that P leaching may be elevated in the Laxemar-Simpevarp area compared with the normal situation in Sweden (cf Tröjbom and Söderbäck 2006/. Compared with the typical concentration in discharge from forest land (0.012 $mg \cdot L^{-1}$) according to /TRK 2008/ for the parts of southern Sweden that discharge into the Baltic, the value from the Laxemar-Simpevarp area is almost three times higher. The discrepancy may to some extent be explained by variation between years, as the calibrated value of 0.03 $mg \cdot L^{-1}$ represents 2004, whereas the TRK value represents the average for a longer time period.
- Atmospheric deposition of P is usually considered negligible and the main factor behind the background level from all vegetation types other than arable land is probably weathering of minerals. Any atmospheric phosphorus deposition is lumped into the land-use categories and the model is probably not sensitive enough to distinguish the effect of this source in the small lakes in the Laxemar-Simpevarp area (theoretically, phosphorus retention in lakes could mask this atmospheric input to the lake surface). As P is an important nutrient for plants, usually limiting primary production in both in terrestrial and aquatic systems, most of the mobile P pool is incorporated in organic matter. Phosphorus fluxes within the biosphere are considerably larger than the flux leaving the system. If the system is in a steady state, the P leaving the system through discharge and long-term sequestration in the sediments should be approximately balanced by input from weathering of minerals, i.e. 5 $kg \cdot km^{-2} \cdot year^{-1}$.
- The overall effect of P retention in lakes in the Laxemar-Simpevarp area is small. Only 10% of the total discharge from land is lost in the lakes as long-term sequestration according to this scenario. This is mainly an effect of the small number of (usually small) lakes in the Laxemar-Simpevarp area. Of the P that reaches specific lakes, up to 60% is lost through retention (37% in Lake Jämsen and 54% in Lake Frisksjön). From these figures it is evident that significant P retention takes place in the lakes. This contrasts to the pattern for N, for which most of the retention seems to take place before the discharging water reaches larger streams and lakes.

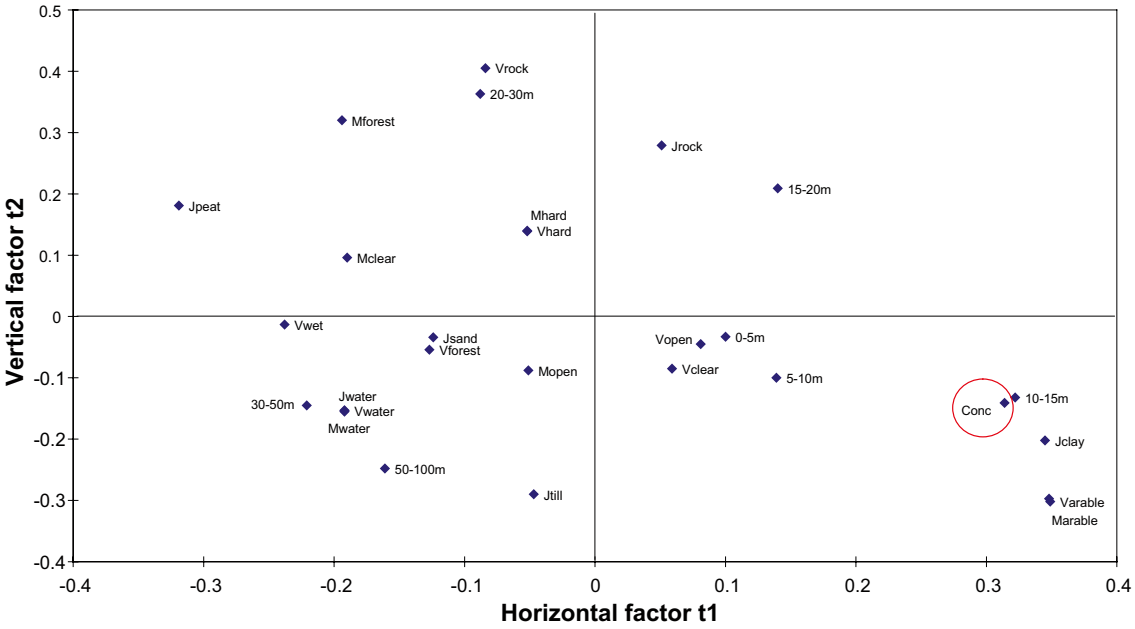


***Figure 6-35.*** *Partial least squares regression model, PLS (see Section 6.5.3 for an explanation of PLS) showing the correlation structure among distributed catchment characteristics, and the observed tot-P concentration (encircled in red). The parameters represent the relative distribution of each regolith, land use, vegetation and elevation class upstream of the hydrochemical sampling point in the outlet of the catchments. Factor t1 describe 33% of the variation among the explanatory variables and t2 24%. 80% of the variance in 'Conc' is described by t1 and 12% by t2.*

**Table 6-13. Parameters and results from the Tot-P mass balance model. Categories not used have been omitted from the table. The total contribution from each category is listed for the entire modelled area and for the catchments of the Laxemarån and the Kärrviksån. The estimated flow-weighted concentration during 1 December 2003 to 30 November 2004 is listed at the bottom of the table.**

| Model parameters | | | | Model results | | | | | |
|---|---|---|---|---|---|---|---|---|---|
| **Diffuse sources** | | | kg·ha$^{-1}$·year$^{-1}$ | **All catchments** | | **Laxemarån** | | **Kärrviksån** | |
| Category | Class | mg·L$^{-1}$ | | kg·yr$^{-1}$ | % | kg·yr$^{-1}$ | % | kg·yr$^{-1}$ | % |
| Regolith | - | | | | | | | | |
| Landuse | - | | | | | | | | |
| Vegetation | Vwater | - | | | | | | | |
| | Vwet | =Vforest | | 26 | 2 | 6 | 2 | 7 | 3 |
| | Vrock | =Vforest | | 96 | 8 | 22 | 6 | 32 | 13 |
| | Vforest | 0.03 | | 656 | 55 | 216 | 57 | 126 | 52 |
| | Vclear | =Vforest | | 32 | 3 | 12 | 3 | 10 | 4 |
| | Varable | 0.25 | | 331 | 28 | 109 | 29 | 57 | 24 |
| | Vopen | =Vforest | | 39 | 3 | 11 | 3 | 5. | 2 |
| | Vhard | =Vforest | | 8 | 1 | 0 | 0 | 1. | 0 |
| Topography | - | | | | | | | | |
| **Point sources** | | | | | | | | | |
| No point sources included | | | | | | | | | |
| **Total** | | | | | | | | | |
| Gross | | | | 1,193 | 100 | 378 | 100 | 242 | 100 |
| Retention (λ=3.9 yr$^{-1}$) | | | | 90 | 8 | 38 | 10 | 6 | 2 |
| Net | | | | 1,103 | 92 | 340 | 90 | 236 | 98 |
| **Concentration (mg·L$^{-1}$)** | | | | 0.039 | | 0.038 | | 0.039 | |

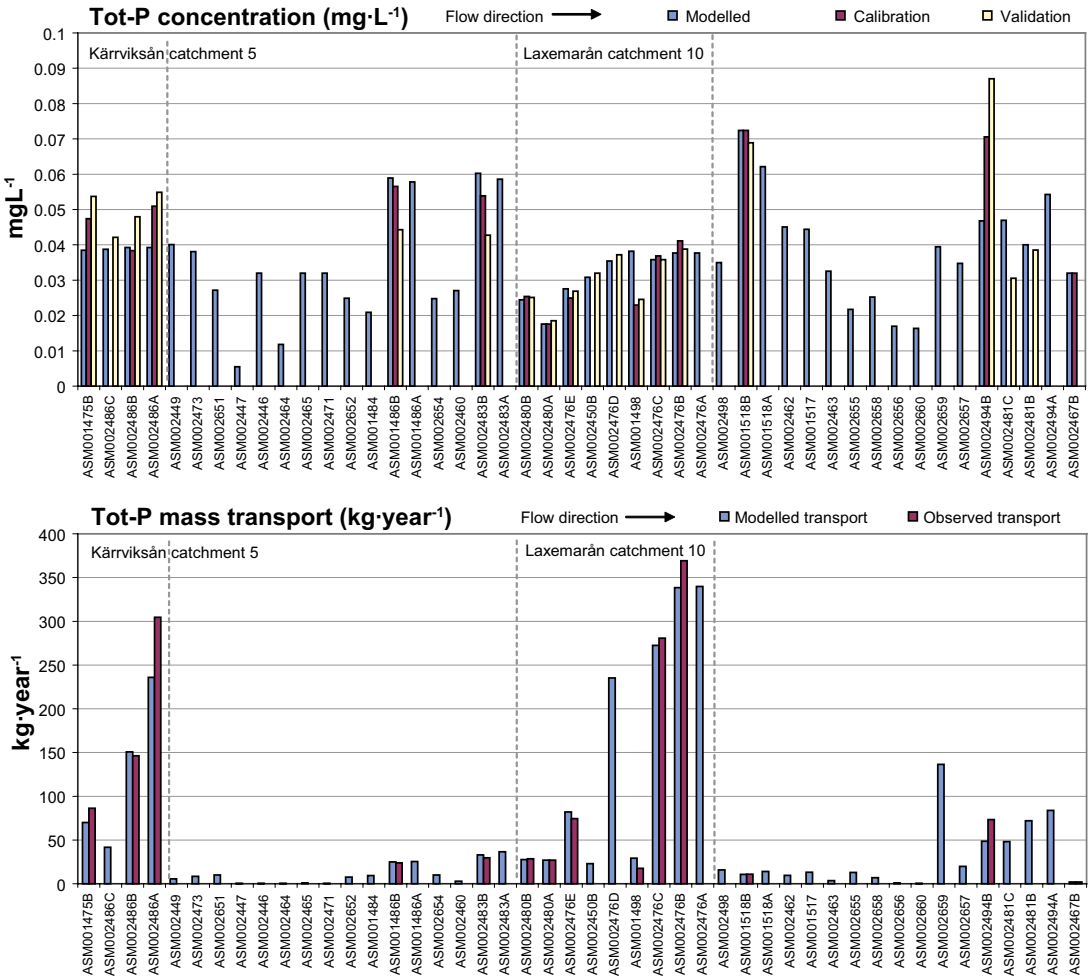


***Figure 6-36.*** *Mass balance for Tot-P in the Laxemar-Simpevarp area. Flow-weighted concentrations (mg·L$^{-1}$) above, and transport kg·year$^{-1}$) below, describing the conditions in the outlet of each catchment.*

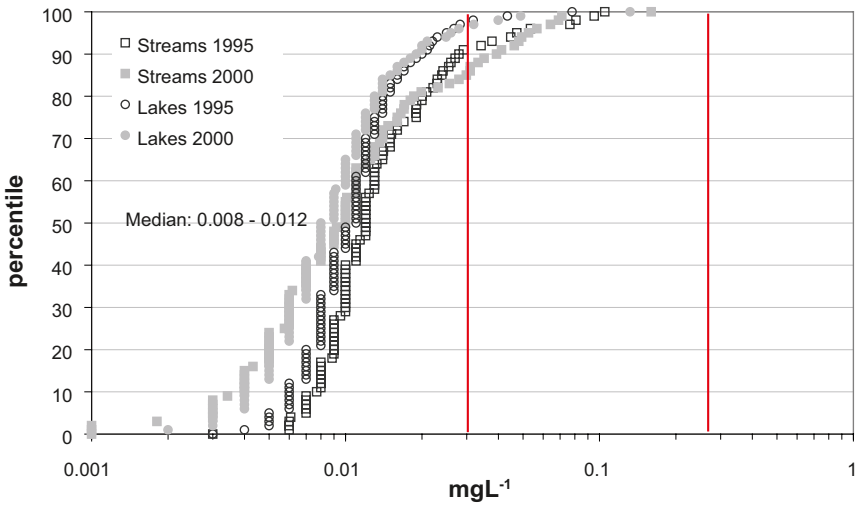


***Figure 6-37.*** *Distribution of Tot-P concentrations in the Swedish surveys of lakes and streams 1995 and 2000 /IMA 2007/. Typical concentrations for categories calibrated within the VBX-VII model are marked as red lines.*

### 6.2.12 Mass balance for total silicon (Si)

The spatial variability of Si in the Laxemar-Simpevarp area is clearly influenced by retention processes, such as precipitation in lakes (concentrations in the outlets of lakes are significantly lower than expected from the typical concentrations in the discharge from land). The correlation structure in Figure 6-38 shows that higher concentrations of Si are correlated with the presence of fine-grained regolith such as clay. As these soil types are usually used for agriculture, there is automatically a correlation with the land use class 'Marable'. The model results are shown in Figure 6-39, and model parameters are listed in Table 6-14. See Appendix C for detailed model results.

The spatial variation within the Laxemar-Simpevarp area is satisfactorily modelled by means of two calibrated typical concentrations that represent the concentration in discharge from the regolith class clay and one concentration common for till, sand and rock. If a retention parameter is included the model result is further improved. The total Si loss through retention is only 6% indicating that retention in lakes in the Laxemar-Simpevarp area has a minor impact on the overall balance. This is mainly a consequence of the few and small lakes in the area. The average deviation between modelled and observed concentrations is 6% for the primary calibration dataset and 12% for the secondary validation dataset.

The following conclusions about sources of Si can be drawn from the mass balance scenario:

- The typical concentration in the discharge from the regolith class 'jTill' is calibrated to 8.9 $mg \cdot L^{-1}$, which is on a level with the median of shallow groundwater in the Laxemar-Simpevarp area of 11 $mg \cdot L^{-1}$ /Tröjbom and Söderbäck 2006/. The typical concentration for 'Jclay' of 31 $mg \cdot L^{-1}$ is on a level with the highest observed Si concentrations in the range of 30 to 34 $mg \cdot L^{-1}$ in SSM000035, 41 and 42. Both typical concentrations are accordingly reasonable compared to observed levels in shallow groundwater.
- With the exception of the fine-grained regolith class 'Jclay', the variation in typical Si concentration in discharge among the remaining regolith types seem to be rather small ('Jtill', 'Jrock' and 'Jsand'). This conclusion is based on the fact that the spatial variation in the area is satisfactorily modelled by means of only two typical concentrations representing clay and all other regolith types as one lumped typical concentration, despite the clear gradient ranging from 'Jrock' in the north to 'Jtill' in the south /Rudmark et al. 2005/. If there is a significant difference in Si concentration in discharge from these regolith classes, this should have become evident as systematic bias in the model. Alternatively, the concentration of Si is not mainly controlled by the regolith type in the catchment, but instead by a limitation in the input of $H^+$ that drives the weathering reactions that in turn release Si to the discharging surface water.
- The Si loss from areas containing clay is elevated by a factor of 3 compared with other regolith categories. This pattern is similar (but more or less pronounced) for several major cations as well as for nutrients such as N and P. Agricultural activities are most probably the common factor that enhances loss of several elements from arable land consisting predominantly of clayey soils; Nutrients such as N and P, and to some extent also Ca and $HCO_3^-$, probably originate from direct input via fertilizers, whereas elevated concentrations of several cations are an indirect effect of enhanced weathering in these areas. The predominant regolith type clay, the release of $H^+$ from intensively grown crops and farming practices such as draining and cultivation may be responsible for the elevated area loss of Si from this land use category.
- There is substantial retention of Si in lakes during the growth season due to biological uptake in diatoms, followed by sedimentation and sequestration in lake sediments. The chemical composition of the gyttja-clay sediments and the rich contents of diatoms observed suggest that this mechanism may be an important sink for Si in lakes (Gustav Sohlenius, pers.comm). As much as 46% of the Si input to Lake Frisksjön is lost through retention and the corresponding figure for Lake Jämsen is 30% according to the mass balance model. The overall effect of Si retention in lakes is limited due to the few and small lakes in the Laxemar-Simpevarp area and only 6% of the total input to the surface waters are lost in lakes.

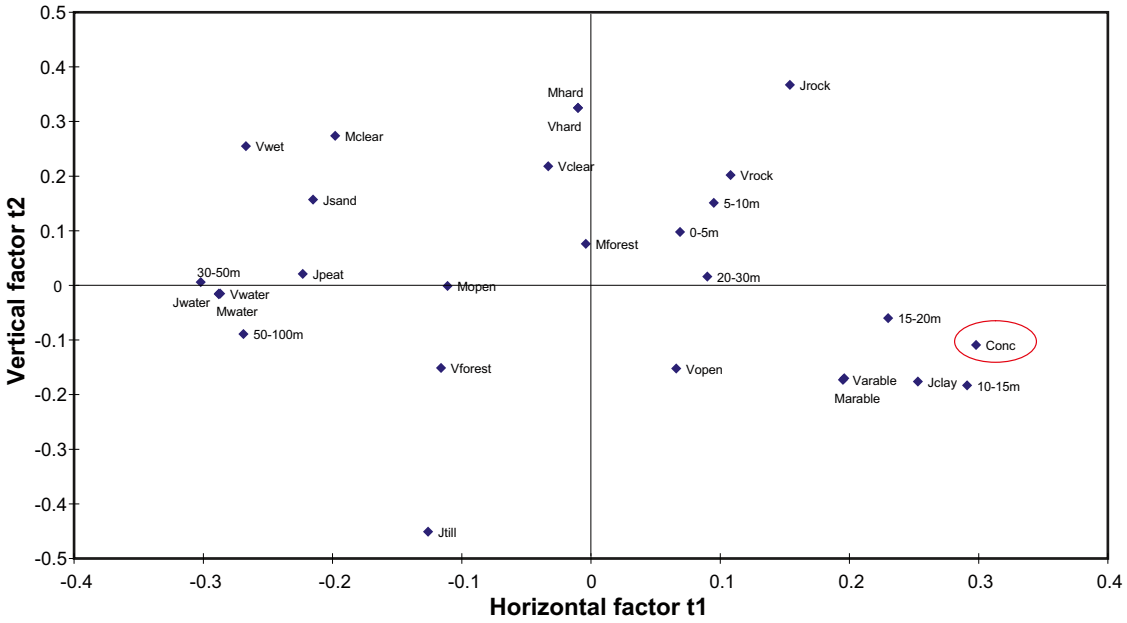


***Figure 6-38.*** *Partial least squares regression model, PLS (see Section 6.5.3 for an explanation of PLS) showing the correlation structure among distributed catchment characteristics, and the observed total Si concentration (encircled in red). The parameters represent the relative distribution of each regolith, land use, vegetation and elevation class upstream of the hydrochemical sampling point in the outlet of the catchments. Factor t1 describe 37% of the variation among the explanatory variables and t2 18%. 88% of the variance in 'Conc' is described by t1 and 5% by t2.*

**Table 6-14. Parameters and results from the Si mass balance model. Categories not used have been omitted from the table. The total contribution from each category is listed for the entire modelled area and for the catchments of the Laxemarån and the Kärrviksån. The estimated flow-weighted concentration during the period 1 December 2003 to 30 November 2004 is listed at the bottom of the table.**

| Model parameters | | | | Model results | | | | | |
|---|---|---|---|---|---|---|---|---|---|
| **Diffuse sources** | | | kg·ha$^{-1}$· | **All catchments** | | **Laxemarån** | | **Kärrviksån** | |
| Category | Class | mg·L$^{-1}$ | year$^{-1}$ | kg·yr$^{-1}$ | % | kg·yr$^{-1}$ | % | kg·yr$^{-1}$ | % |
| Regolith | Jwater | - | | 0 | 0 | 0 | 0 | 0 | 0 |
| | Jsand | =Jtill | | 11,032 | 4 | 3,033 | 4 | 2,539 | 5 |
| | Jpeat | - | | 0 | 0 | 0 | 0 | 0 | 0 |
| | Jrock | =Jtill | | 92,946 | 36 | 25,022 | 31 | 29,345 | 55 |
| | Jclay | 31 | | 38,585 | 15 | 13,647 | 17 | 6,215 | 12 |
| | Jtill | 8.9 | | 118,576 | 45 | 40,072 | 49 | 14,930 | 28 |
| Landuse | - | | | | | | | | |
| Vegetation | - | | | | | | | | |
| Topography | - | | | | | | | | |
| **Point sources** | | | | | | | | | |
| No point sources included | | | | | | | | | |
| **Total** | | | | | | | | | |
| Gross | | | | 261,140 | 100 | 81,776 | 100 | 53,030 | 100 |
| Retention λ=2.9 yr–1 | | | | 16,632 | 6 | 6,686 | 8 | 1,008 | 2 |
| Net | | | | 244,508 | 94 | 75,090 | 92 | 52,023 | 98 |
| **Concentration (mg·L$^{-1}$)** | | | | 8.6 | | 8.3 | | 8.7 | |

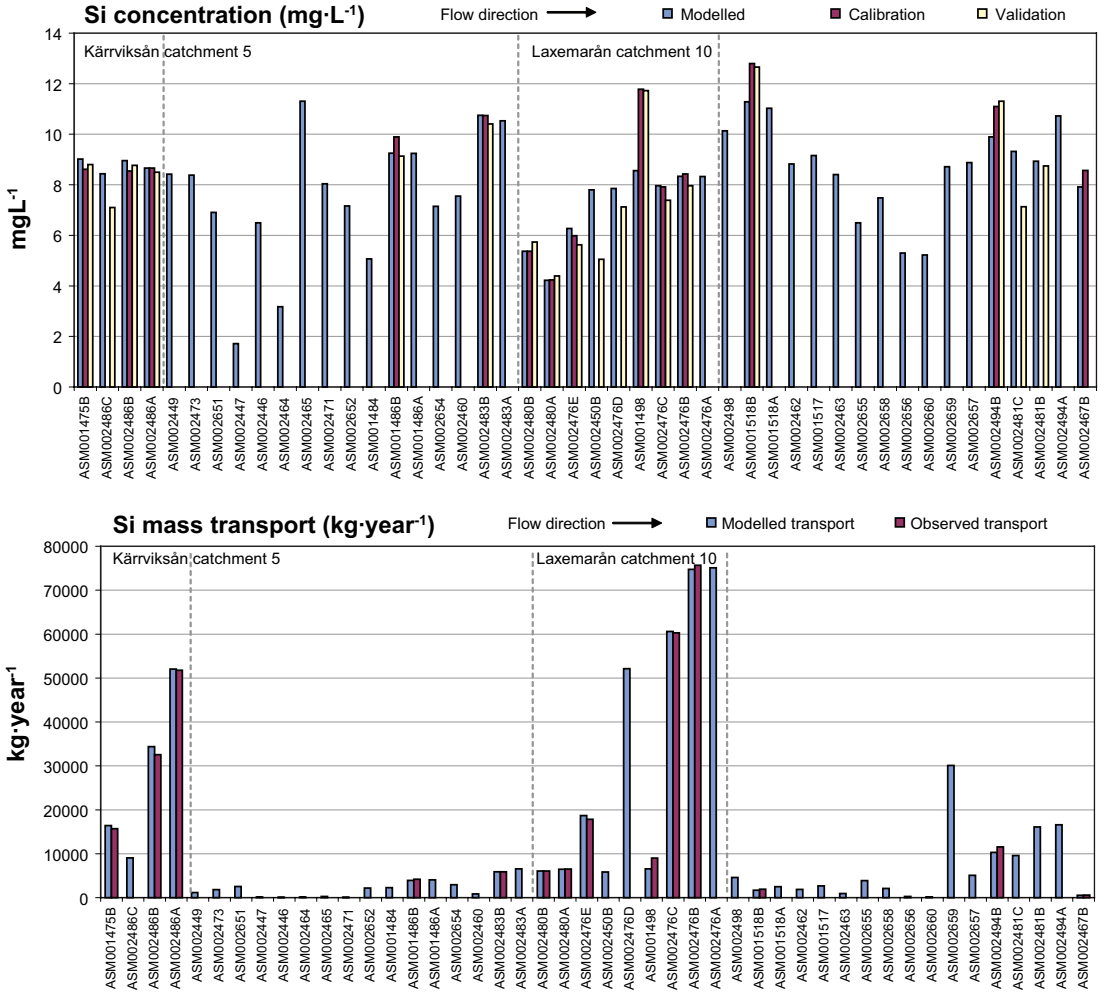


***Figure 6-39.*** *Mass balance for Si in the Laxemar-Simpevarp area. Flow-weighted concentrations (mg·L$^{-1}$) above, and transport (kg·year$^{-1}$) below, describing the conditions in the outlet of each catchment.*

## 6.3 Summary and conclusions of catchment modelling

The catchment model is a formalised method that combines distributed spatial information about the catchment with water balance data and observed concentrations in watercourses and lakes into an integrated model. The model results in a scenario that describes the overall mass balance of an element. It should, however, be noted that the models presented are just scenarios representing one probable solution of the mass balance of a given element, and that there are usually other possible solutions as well. The construction and calibration of each model have followed identical schemes, with the overall objective of finding as simple a model as possible that satisfactorily describes the observed variation in element concentrations in the Laxemar-Simpevarp area. In most cases, the calibration of the model converges towards a single, stable, probable solution for the selected set of parameters, but the subjective element involved in selecting the governing parameters cannot be circumvented. However, the use of an initial PLS correlation analysis provides an objective picture of the correlation structure among the parameters and may provide an indication of which parameters may be fruitful to include in the model.

In all models, retention has been tested as an initial scenario, but only a few elements show clear indications of retention loss in lakes. There is always a possibility that retention takes place at a local level, in riparian zones, in wetlands or in small streams that are not distinguished in the model. In this case the catchment model to some extent describes net transport and net concentrations in surface waters rather than representing the actual typical concentration from a specific regolith type or land use category. According to Table 6-15, which shows all model parameters,

**Table 6-15. Overview of model parameters and calibration results. Typical concentrations ($mg \cdot L^{-1}$) per category (see Section 6.1.3 for descriptions of categories), included point sources expressed as portion of total input (Point %) and total retention in the Laxemar-Simpevarp area (Ret %). The calibration result, expressed as the mean deviation between modelled and observed concentrations, is shown in the Dev % columns (calculated for the calibration and validation datasets, see Section 6.1.4).**

| | | | | | | | | | Point | Ret | Dev % | |
|---|---|---|---|---|---|---|---|---|---|---|---|---|
| **Elevation categories** | **0–5m** | **5–10m** | **10–15m** | **15–20m** | **20–30m** | **30–50m** | **50–100m** | | **%** | **%** | **Calib.** | **Valid.** |
| Cl | 29 | 6.1 | 4.5 | 4.5 | 4.5 | 4.5 | 4.5 | | 35 | - | 27 | 39 |
| $SO_4^{2-}$ | 42 | 42 | 42 | 8.9 | 8.9 | 8.9 | 8.9 | | - | - | 16 | 14 |
| **Regolith categories** | **Water** | **Sand** | **Peat** | **Rock** | **Clay** | **Till** | | | | | | |
| Na | - | 4.2 | 4.2 | 4.2 | 34 | 4.2 | | | 26 | - | 18 | 23 |
| K | - | 0.75 | 0.75 | 0.75 | 3.7 | 0.75 | | | 13 | - | 20 | 34 |
| Ca | - | 7.6 | 7.6 | 7.6 | 78 | 7.6 | | | 1 | - | 11 | 19 |
| Sr | - | 0.04 | 0.04 | 0.04 | 0.22 | 0.04 | | | - | - | 13 | 22 |
| Si | - | 8.9 | 8.9 | 8.9 | 31 | 8.9 | | | - | 6 | 6 | 12 |
| **Land use categories** | **Water** | **Forest** | **Clear-cuts** | **Arable** | **Open land** | **Hard surface** | | | | | | |
| Mg | - | 1.6 | 1.6 | 14 | 1.6 | 1.6 | | | - | - | 12 | 16 |
| **Vegetation categories** | **Water** | **Wetland** | **Rock** | **Forest** | **Clear-cuts** | **Arable** | **Open land** | **Hard surface** | | | | |
| $HCO_3^-$ | 12 | 12 | 12 | 12 | 12 | 12 | 12 | 12 | - | - | 49 | 65 |
| TOC | - | 22 | 22 | 22 | 22 | 22 | 22 | 22 | - | 2 | 13 | 11 |
| Tot-N | - | 1.1 | 1.1 | 1.1 | 1.1 | 9 | 1.1 | 1.1 | - | 3 | 9 | 15 |
| Tot-P | - | 0.03 | 0.03 | 0.03 | 0.03 | 0.25 | 0.03 | 0.03 | - | 8 | 13 | 19 |

Si and tot-P show significant retention in lakes. The prospects of detecting retention are however small in the Laxemar-Simpevarp area due to the few and small lakes, and the possibility cannot be ruled out that these results are to some extent a consequence of limited precision in the model.

Model parameters and calibration results are shown in Table 6-15 below in order to facilitate comparisons between elements. Depending on the particular element, different categories of distributed characteristics have been used and the calibrated typical concentrations used for each category are listed in the table (see Section 6.1.3 for explanations of these categories). If point sources are included in the model, the total extent of these sources compared to the total input is shown in the column headed 'Point' (expressed as % of total input). In the case of retention in lakes, the estimate of the total retention in the entire Laxemar-Simpevarp area (expressed as % of total input) is shown in the 'Ret' column. The calibration result, expressed as the average deviation (%) between modelled and observed concentrations, is calculated for the calibration and validation datasets (cf Section 6.1.4).

The main conclusions per element are summarised in the bulleted list below:

- Diffuse sources of **chloride** (Cl) are probably related to the topographical elevation distribution rather than factors as regolith or land use within the catchments, which indicates that relict marine Cl in the deposits is a probable source. Deposition of Cl originating from e.g. sea spray constitutes approximately 10–30% of the total Cl input to the surface system. Road salt is probably a major source of Cl in the Laxemar-Simpevarp area. As much as 56% of the total Cl input to the sub-catchments of the Laxemarån is attributable to road salt spread on E22 according to the model results. Estimates indicate that different types of road salt (winter road salt used for anti-skid treatment and summer road salt used for dust control on gravel roads) may make an even greater contribution than shown by the model results. There are, as presumed, no indications of retention for Cl.

- Diffuse sources of **sodium** (Na) are mainly related to regolith class (e.g. till and clay) rather than topographical elevation as was the case for Cl. The additional weathering source for Na, which is not valid for Cl, is responsible for the different patterns. Areas that contain clay show almost 10 times higher Na concentrations in discharge compared to other regolith categories. This regolith type is predominantly located in lower-lying areas, and relict marine Na, in combination with enhanced weathering, may partly explain the elevated value (perhaps due to agricultural activities and cation exchange reactions). According to the model results, road salt is also a significant source of Na in the surface system. About 1/3 of the total supply of Na is estimated to originate from this source. There are, as presumed, no indications of retention for Na.
- Diffuse sources of **potassium** (K) are more uniformly distributed over the Laxemar-Simpevarp area compared with marine ions as Cl and Na. The prospects for identifying governing factors for K are more limited due to low K variability among the hydrochemical sampling points. As with Na, elevated K concentrations are associated with the regolith types clay and sand that are predominant in the valleys. A probable source of K in areas with clay and sand may be weathering of the deposits. Uptake and recycling of K in biota is probably a factor that strongly affects the overall pattern of K and diminishes variations due to distributed environmental factors. The K mass balance is further improved if a road salt source along E22 is added, although K is usually not reported as a major constituent of road salt. The relative influence of this source is, however, weaker for K compared with Na. There are no indications of significant retention of K in the lakes.
- Among the distributed sources, the occurrence of clay (or arable land, which usually overlap) is an important factor that enhance leaching of **calcium** (Ca). According to the model results, discharge from clay is about 10 times greater than discharge from other regolith categories. When the background concentration from these regolith types (other than clay) is compared with the concentration in precipitation, it is evident that weathering is the main source of Ca. Summer road salt (the $CaCl_2$ type), which is spread on gravel roads for dust control, could also be a potential source of Ca in the Laxemar-Simpevarp area. There are indications in Lake Frisksjön that Ca (as well as Mg and Cl) originates from this source, but the total magnitude of this potential source in the Laxemar-Simpevarp area is not known. There are no indications of any substantial Ca retention in the lakes.
- Most conclusions for Ca are applicable to **strontium** (Sr), as these elements are closely associated in the surface system in the Laxemar-Simpevarp area. The evaluation of Ca and Sr signatures in Section 4.1.4, however, indicates that these elements originate from at least three different sources and that reactions may affect the composition selectively.
- Among the distributed sources, the occurrence of arable land is an important factor that enhances discharge of **magnesium** (Mg). This factor is, however, closely correlated with both topographical elevation and presence of clay, and the exact dependencies could not be elucidated in the present model version. According to the model results, the typical concentration in discharge from the land use class ‘Marable’ is nearly 10 times greater than discharge from e.g. forest land. Underlying factors responsible for the enhanced concentrations from arable land may be agricultural activities (cultivation, drainage and fertilization), in combination with enhanced weathering on the usually thick and fine-grained regolith. Outwash of marine relicts could also be a potential source in these lower-lying areas, but the resolution in the model and the location of the hydrochemical observation points used for calibration do not permit separation of these sources. Another source that may affect the Mg model is summer road salt (the $MgCl_2$ type). It is not possible to quantify this source, but qualitative indications from Lake Frisksjön show that this is a potential source in the area. If this is the case, this source probably contributes to the uncertainties in the model and may be responsible for local variations depending on the use of summer road salt in the catchment. There are no indications of significant retention of Mg in the lakes.
- Among the distributed factors, topographical elevation is an important factor that enhances discharge of **sulphate** ($SO_4^{2-}$). This factor is, however, closely correlated with both arable land and presence of clay, and the exact dependencies could not be elucidated in the present

model version. As much as 1/3–2/3 of the sulphur input may originate from sulphur deposition. Of this airborne fraction, only about 10% originates from sea spray, if the marine part is estimated from local Cl measurements in precipitation, while the rest originates from regional or global sulphur sources. The remaining portion, between 1/3–2/3 of the total $SO_4^{2-}$ discharge, is probably of marine origin, and most probably comes from oxidation of sulphide minerals according to isotope measurements (cf Section 4.1.3). There are no indications of significant retention of $SO_4^{2-}$in the lakes.

- The difficulties in finding a mass balance model based on distributed factors that describe the variation in **bicarbonate** ($HCO_3^-$) concentrations in the Laxemar-Simpevarp area probably reflects the fact that important sinks are not included. The alkalinity (or the buffering capacity, most of which is accounted for by $HCO_3^-$) is consumed during neutralisation of $H^+$. Sources of weak or strong acids, which could be perceived as $HCO_3^-$ sinks, in combination with sources of $HCO_3^-$ constitute the observed spatial pattern for $HCO_3^-$. Within the catchment of the Laxemarån, observed $HCO_3^-$ concentrations are almost constant and total transport may consequently be explained by a simple scenario with only one typical concentration for $HCO_3^-$. There are also examples of potential point sources for $HCO_3^-$ in the catchment of the Ekerumsån (catchment ASM002483B and hydrochemical sampling station PSM002085). A similar deviation is also displayed by Ca, and a hypothetical source of both of these ions could be lime added to soils or directly in the watercourses for agricultural or environmental management purposes. There are no indications of significant retention of $HCO_3^-$ in the lakes.
- The low variation of **total organic carbon** (TOC) in the Laxemar-Simpevarp area causes difficulties in identifying governing factors. However, this low variability suggests that the estimated transport in the watercourses is more or less correct and mainly controlled by discharge and, ultimately, catchment size. There are however indications of additional sources of TOC in two adjacent catchments (ASM002494B and ASM001518B), which are located close to farms and contain a great deal of agricultural land. Unusual land use practices or direct discharges to surface water are potential sources of organic carbon (leaching of K is also elevated in these catchments). There are indications of TOC retention loss in the lakes. The TOC loss in Lake Jämsen and Lake Frisksjön has been estimated to be about 10%, whereas the total loss in the whole catchment is less than 2%.
- **Total nitrogen** (tot-N) concentrations in the Laxemar-Simpevarp area are significantly higher in areas that contain arable land, indicating that agricultural activities are probably important factors enhancing N loss. Atmospheric deposition of N contributes approximately 600 $kg \cdot km^{-2} \cdot year^{-1}$ in the coastal region, which includes the Laxemar-Simpevarp area according to /TRK 2008/. When this input is compared with the calibrated background discharge from all vegetation types except for arable land, it is evident that atmospheric deposition is an important source of N. From these figures it is evident that only a fraction of this atmospheric N reaches the sea (less than 25%). The overall effect of N retention in lakes is marginal in the Laxemar-Simpevarp area and only 3% of the total discharge from land is lost in the lakes according to this scenario. Of the N that reaches specific lakes, between 16% and 27% is lost through retention in Lake Jämsen and Lake Frisksjön, respectively. When these fractions are compared with the above figures, it is evident that a significant N retention must take place before the discharging water reaches larger streams and lakes, i.e. in the soil and in wetlands and small ditches.
- In the Laxemar-Simpevarp area, **total phosphorus** (tot-P) concentrations are higher in areas containing arable land. This indicates that agricultural activities are probably important factors enhancing P loss. Atmospheric deposition of P is usually considered negligible, and the major source behind the background level from all vegetation types other than arable land is probably mainly attributable to weathering of minerals. As P is an important nutrient for plants, usually limiting primary production both in terrestrial and aquatic systems, most of the mobile P pool is incorporated into organic matter. Phosphorus fluxes in the lake or stream ecosystem are considerably larger than the flux leaving the system. If the system is in a steady state, the P leaving the system through discharge and long-term sequestration in

the sediments should be approximately balanced by input from weathering of minerals, i.e. 5 $kg \cdot km^{-2} \cdot year^{-1}$. The overall effect of P retention in lakes in the Laxemar-Simpevarp area is small. Only 10% of the total discharge from land is lost in the lakes as long-term sequestration according to this scenario. This is mainly an effect of the small number of (usually small) lakes in the Laxemar-Simpevarp area. Of the P that reaches specific lakes, up to 60% of the P is lost through retention (37% in Lake Jämsen and 54% in Lake Frisksjön). From these figures it is evident that a significant P retention takes place in the lakes, which contrasts with N retention where a significant fraction seems to take place before the discharging water reaches larger streams and lakes.

- The loss of **silicon** (Si) from areas that contain clay is greater by a factor of three than from other regolith categories. This pattern is similar (but more or less pronounced) for several major cations, as well as for nutrients as N and P. Agricultural activities are probably the common factor that enhances loss of several elements from arable land consisting predominantly of clayey soils. Nutrients such as N and P, and to some extent also Ca and $HCO_3^-$, probably originate from direct input via fertilizers, whereas elevated concentrations of several cations and Si are an indirect effect of enhanced weathering in these areas. The predominating regolith type clay, the release of $H^+$ from intensively grown crops and farming practices such as drainage and cultivation, may be responsible for the elevated area loss of Si from this land use category. There is a substantial retention of Si in lakes during the growing season due to biological uptake in diatoms followed by sedimentation and sequestration in the lake sediments. As much as 46% of the Si input to Lake Frisksjön is lost through retention, and the corresponding figure for Lake Jämsen is 30% according to the mass balance model. The overall effect of Si retention in lakes is limited due to the few and small lakes in the Laxemar-Simpevarp area, and only 6% of the total input to the surface waters is lost in lakes.

As stated in the beginning of this section, the models presented should be regarded as scenarios that represent possible solutions of the mass balances of selected elements. Despite the many uncertainties regarding water balance, representativeness of hydrochemical samples, and classification and aggregation of different regolith, land use and vegetation types, most models converge towards more or less stable solutions, although there are a few exceptions. The overall uncertainties of the models are discussed in Chapter 9.

Due to the limited number of hydrochemical sampling points available, true validation of the models is not possible. Another problem is that the validation dataset contains only four stations independent of the calibration dataset, and that the validation dataset represents mean values from the previous year, 2003. The calibration dataset represents flow-weighted concentrations that take into account variations in concentration in relation to water flow.

# 7 Integrated hydrochemical evaluation of selected objects and sub-areas

With a focus on specific objects and sub-areas of particular interest, the integrated evaluation in this section attempts to explain the observed hydrochemical patterns by combining information from previous chapters. As a complement, additional visualisations based on the model of regolith layers /Nyman et al. 2008/, interpolated ground water levels (Emma Bosson pers. comm.) and topography, are shown in order to visualise hydrochemical conditions and physical/ hydrological prerequisites in the sub-areas presented (cf Section 2.3.7).

## 7.1 Identification of objects and sub-areas of special interest

A number of sampling points in shallow groundwater and surface water show deviant characteristics in many visualisations throughout this report. These objects, many of which are soil tubes located in till beneath lakes and the Baltic Sea, were the basis upon which the profiles shown in Figure 7-1 were selected.


***Figure 7-1.*** *Dotted red lines denote the location of profiles, including cross sections of regolith layers, groundwater levels and boreholes in the vicinity of these transects (profiles start at the end marked with a black dot). Soil tubes are labelled with the last three figures of the idcode, e.g. SSM000022. See map in Figure 2-8 for the locations of groundwater sampling points in the bedrock.*

Each sub-area or group of objects is briefly characterised in the bulleted list below, and hydrochemical conditions and potentially important prerequisites are compiled per sub-area in the following sections.

- **Five soil tubes located in till beneath lake and sea sediments** show both similarities and dissimilarities in hydrochemistry, despite comparable physical conditions. The evolution of the groundwater in these shallow groundwater objects is discussed in Section 7.2. These sampling sites are located in the vicinity of major deformation zones that may be potentially groundwater discharge areas with possible exit points for deep discharge.
- **SSM000022**, which is a soil tube located on the Island of Ävrö, displays deviant hydrochemistry. Previous evaluations have suggested that the hydrochemical composition of water in this soil tube is an indication of potential deep discharge /Tröjbom and Söderbäck 2006/. The hydrochemical signatures are to some extent contradictory, but the influence of deep groundwater is less probable, as discussed in Section 7.3.
- Elevated concentrations of Ca and $HCO_3^-$ have been recorded in the catchment of the **Ekerumsån**. Presumed anthropogenic sources are discussed in Section 7.4.
- There are also several indications that the surface system in the **central catchment of Laxemarån**, as well as in some other parts of the Laxemar-Simpevarp area, receives significant amounts of salts from an anthropogenic source. Different kinds of road salt and SKB drilling activities are potential sources, and the contribution of these sources is evaluated in Section 7.5.

## 7.2 Shallow groundwater beneath lakes and the Baltic Sea

Four soil tubes are located in the sea sediments beneath the brackish water basins of Granholmsfjärden and Borholmsfjärden, and one is located in similar sediments in Lake Frisksjön nearby (cf locations of soil tubes Figure 2-7 and explanation of the names in Figure 2-4). The rationale for selecting these sampling sites is their vicinity to major deformation zones that are potential groundwater discharge areas with possible exit points for deep groundwater discharge. Despite the similar setting of these tubes, there is considerable variation in hydrochemical composition among these five shallow groundwater sampling points. A description of the installation of theses tubes is provided in /Johansson et al. 2006/.

The regolith depths range between 3 and 16 metres between the five locations (cf profiles in Figure 7-2). The composition of the regolith at most locations is gyttja underlain by sand, clay, silt and till / Johansson et al. 2006/. The composition of the till is mostly sandy. However, in SSM000240 the stratigraphy is slightly different, with a gyttja layer directly underlain by gravelly sand on the bedrock (see Table 7-1). Hydrological conductivity tests (slug tests) also indicate very different hydraulic conductivities in the five soil tubes /Johansson et al. 2006/.

- The measurements in SSM000238 showed very fast recovery and consequently very high hydraulic conductivity to the aquifer.
- SSM000239 had recovery periods of about 200 seconds
- SSM000240 also showed very fast recovery and consequently very high hydraulic conductivity to the aquifer.
- In SSM000241, there was a slow response with a recovery time 19 of minutes.
- In SSM000242, the time for complete recovery was 4 hours and 15 minutes, which indicates low conductivity to the aquifer.

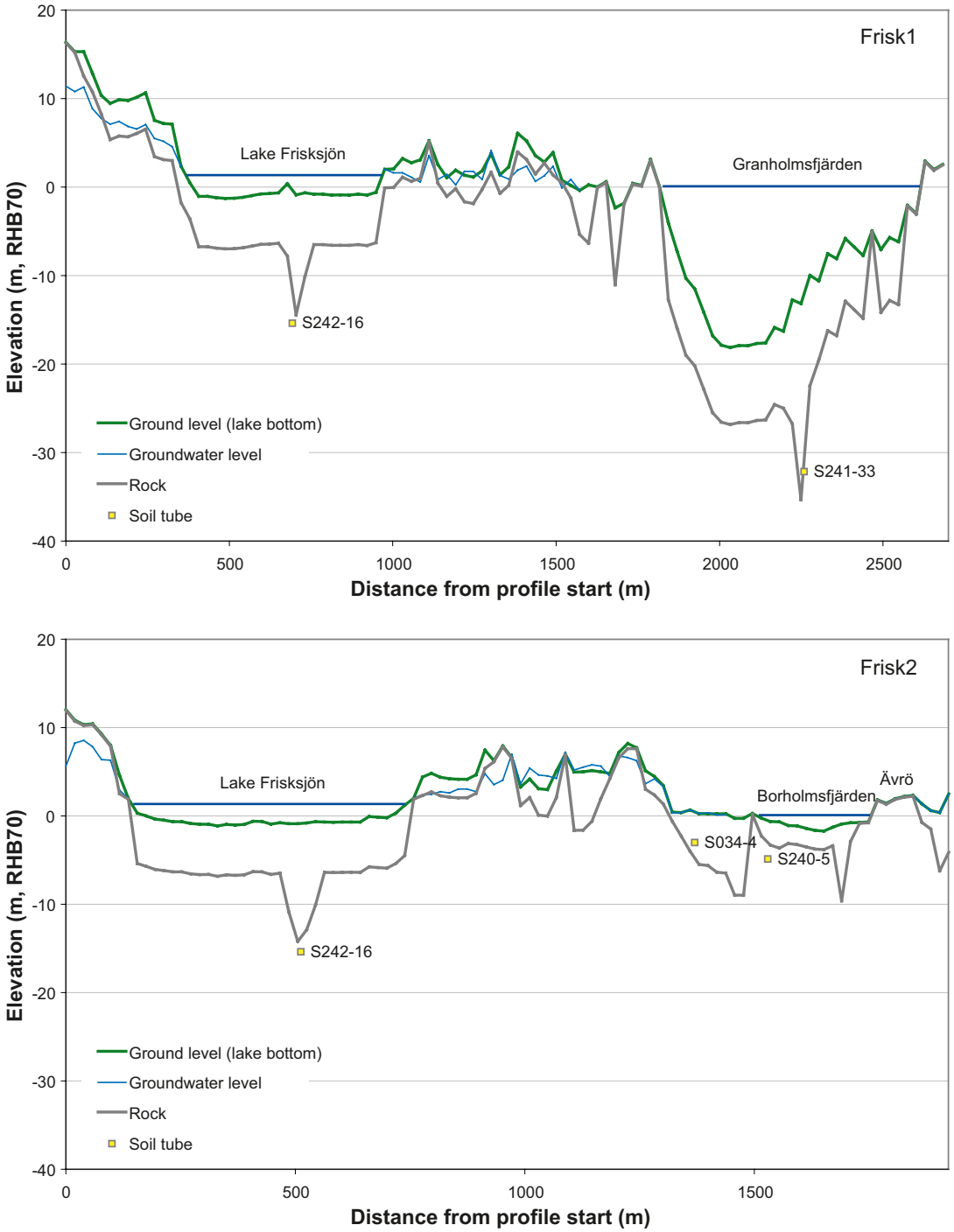


***Figure 7-2.*** *Profiles showing ground level and the upper part of the rock, together with soil tube samples in the vicinity of the transect and the average groundwater level. See Figure 7-1 for a description of the location of the profiles.*

**Table 7-1. Stratigraphy in the five selected soil tubes. From /Johansson et al. 2006/.**

| Site | ID-code | From (m) | To (m) | Layer/Quaternary deposit |
|---|---|---|---|---|
| Borholmsfjärden | **SSM000238** | 0.00 | 4.40 | Water |
| | | 4.40 | 8.40 | Gyttja |
| | | 8.40 | 9.80 | Clay |
| | | 9.80 | 11.50 | Silty till |
| | | 11.50 | 11.60 | Bedrock |
| Norrefjärd south | **SSM000239** | 0.00 | 1.40 | Water |
| | | 1.40 | 3.20 | Gyttja |
| | | 3.20 | 4.20 | Silty till |
| | | 4.20 | 4.40 | Bedrock |
| Norrefjärd north | **SSM000240** | 0.00 | 0.80 | Water |
| | | 0.80 | 3.10 | Gyttja+plant remains |
| | | 3.10 | 3.30 | Gravelly sand |
| | | 3.30 | 3.70 | Sandy gravelly clay |
| | | 3.70 | 5.00 | Sandy till |
| | | 5.00 | 5.40 | Bedrock |
| Granholmsfjärden | **SSM000241** | 0.0 | 14.60 | Water |
| | | 14.60 | 21.00 | Gyttja |
| | | 21.00 | 22.00 | Clay |
| | | 22.00 | 22.80 | Sand |
| | | 22.80 | 31.20 | Clay |
| | | 31.20 | 32.60 | Sand/Till |
| Lake Frisksjön | **SSM000242** | 0.0 | 2.90 | Water |
| | | 2.90 | 13.00 | Gyttja |
| | | 13.00 | 17.80 | Clay |
| | | 17.80 | 18.00 | Till/Bedrock |

### 7.2.1 Major elements and environmental isotopes ($^{2}H$ and $^{18}O$)

If the five soil tubes are compared with respect to the hydrochemistry among the major elements in the Ion Source Model in Section 3.2.6, the overall patterns can be summarised as follows:

- SSM000238-12 and SSM000239-4 contain ion signatures identical to modern sea water.
- SSM0000240-5 shows signatures similar to most shallow groundwater samples.
- SSM000241 (at –33 metres beneath Granholmsfjärden Basin) shows both marine influence and the clear influence of deep saline groundwater corresponding to the signature seen in many cored borehole samples at depths of several hundred metres.
- SSM000242-16 shows a clear marine influence.

The Water Origin Model, which is based on the isotopes $^{2}H$ and $^{18}O$, may give indications of the origin of the water – the solvent (cf Section 3.3.2). Surface water subject to evaporation takes on a typical isotope signature, for example lake water or sea water. The signature of meteoric water differs depending on the season, but always plots along the local meteoric water line (pink dashed line in Figure 3-15). The isotope signature of most soil tubes (shallow groundwater) corresponds to the average composition of meteoric recharge. The five soil tubes in question deviate more or less from this average composition, indicating the origin of the groundwater. The following conclusions regarding the origin of the groundwater in these five tubes can be drawn from this model:

- The isotope composition in SSM000238-12 and SSM000239-4 corresponds to the signature of modern seawater (PO62S = Borholmsfjärden Basin, PO64S = Granholmsfjärden Basin in Figure 3-15).
- SSM000240-5 contains meteoric water with only a minor influence by sea water or lake water, despite its location in deposits beneath brackish water.
- SSM000241-33 shows a signature influenced by evaporation, but also an influence by a clear meteoric signature. This soil tube may contain a mixture between meteoric water and sea water (either Littorina Sea water or modern sea water).
- The signature in SSM000242-16 also shows a typical evaporation signature corresponding to modern sea water or water from Lake Frisksjön above (PL65S&B).

Major concentration trends among the major elements are revealed in the multivariate Mixing Model in Section 3.4.3. The resolution is low in this model for most dilute waters in the surface system, although most of the five soil tubes in question are distinguished by elevated salinities:

1. The concentrations in SSM000238-12 and SSM000239-4 correspond to modern sea water.
2. SSM000240-5 contains a rather dilute groundwater with only slight marine influence. This agrees with the results of the Ion Source Model, which indicate ions originating mainly from weathering, as well as with the results of the Water Origin Model, which indicate water of meteoric origin.
3. SSM000242-16 and SSM000241-33 contain water more similar to Littorina sea water with Cl concentrations of 3,570 $mgL^{-1}$ and 4,770 $mgL^{-1}$, respectively. The location of these objects in the Mixing Model is probably strongly affected by the anomalous high $HCO_3^-$ content (see discussion below). If $HCO_3^-$ is withdrawn according to scenario RX1 in Figure 3-20, this trend intersects the marine mixing trend at a concentration more saline than present Baltic Sea water. That composition is probably closer to the original composition of this groundwater than the composition observed today. In the Ion Source model (cf Section 3.2.5) there are also indications of deep saline influences in SSM0000241 and to some extent in SSM000242. As an alternative hypothesis the high salinity in these soil tubes, which exceeds the salinity of the present Baltic Sea, could have been formed by evaporation in isolated bodies of water rather than representing remnants of the Littorna Sea.

### 7.2.2 Comparisons among trace elements and isotopes

Among the trace elements, Li is a parameter that, together with Cl, discriminates well between sea water and deep saline groundwater (cf Section 4.1.2). If these elements are regarded as conservative they may in such case provide an unbiased picture of the origin of the groundwater in Figure 7-3 as a result of mixing of groundwater types. A plot of Li versus Cl reveals that:

- The composition of SSM000238-12 and SSM000239-4 corresponds to modern sea water.
- SSM000240-5 is mainly associated with fresh water samples, indicating an ion mixture of shallow groundwater and modern sea water.
- Both SSM000241-33 and SSM000242-16 contain a mixture of ions originating from sea water (modern or relict) and deep saline groundwater.

At this point in time, few isotope measurements are available from the five soil tubes of interest that could support the interpretations based on major elements (e.g. $^{13}C$, $^{14}C$ and $^{34}S$). $^{37}Cl$ data available from SSM000238, 239, 240 and 242 do not reject the conclusions based on Li and Cl (cf Figure 4-8); the first three tubes contain Cl mainly of marine origin, whereas the slight shift of SSM00242 towards the deep $^{37}Cl$ signature may be interpreted as influence of Cl of deep saline origin. It should be held in mind that these conclusions based on $^{37}Cl$ are ambiguous due to the large measurement uncertainty of this parameter (cf Section 9.3.2). The single $^{37}Cl$ measurement available from SSM000241 points in the opposite direction compared to SSM000242 and the interpretation of this result is ambiguous. According to the composition of major elements, this soil tube is supposed to show even more pronounced deep saline influence regarding $^{37}Cl$ (a more positive value compared to SSM000242). This is however not the case according to the single negative measurement from SSM000241. It should be noted that interpretations based on $^{37}Cl$ is limited by the high analytical uncertainty of this parameter (cf Section 9.3.2).

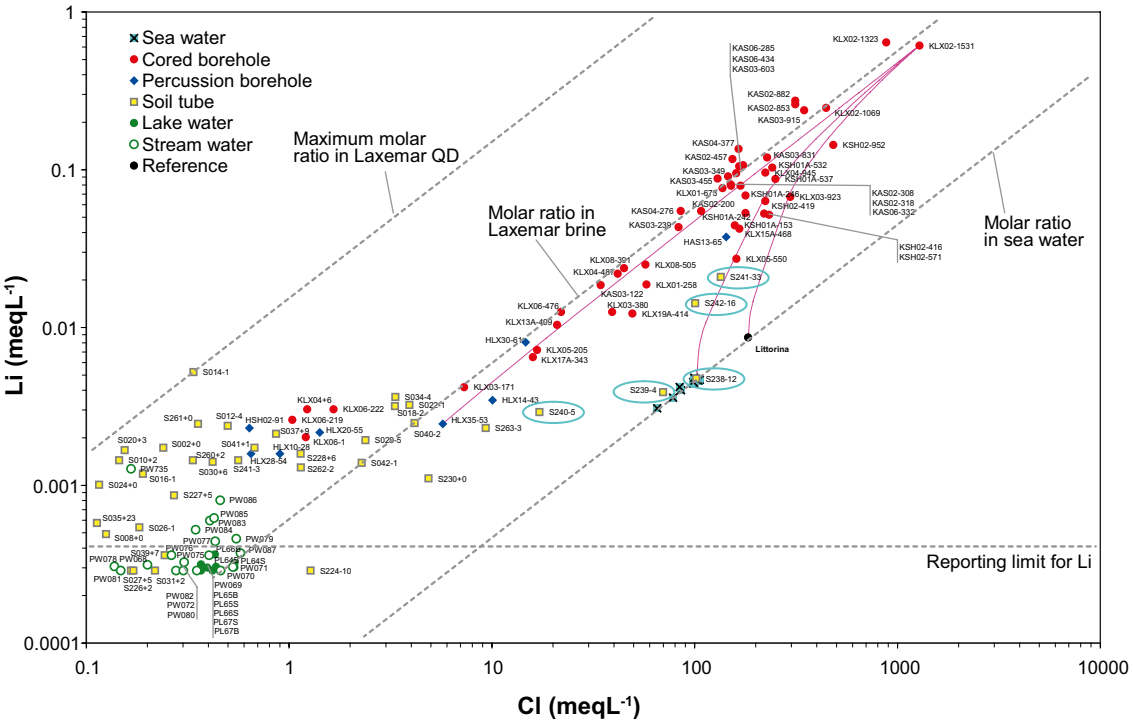


***Figure 7-3.*** *Lithium and Cl in the Laxemar-Simpevarp area expressed in meqL$^{-1}$. The five soil tubes of interest are marked by blue-green circles. Based on data selection C, see Section 2.2.5. For an explanation of labels, symbols and lines, see Sections 2.3.11. and 2.3.12.*

### 7.2.3 The highly deviant hydrochemistry in SSM000241 and SSM000242

SSM000241 (beneath Granholmsfjärden) and SSM000242 (beneath Lake Frisksjön) show highly deviant hydrochemistry compared with all other objects in the Laxemar-Simpevarp area. These two tubes are located beneath the thickest sediments (17 and 15 metres thick, respectively) of all soil tubes in the Laxemar-Simpevarp area, cf Figure 7-2 and Table 7-1.

Extremely high $HCO_3^-$ concentrations, in combination with very high concentrations of nitrogen, organic carbon, phosphorus and bromide, are the most notable hydrochemical characteristics of these two soil tubes, according to Table 7-2. Some of these ions are included in the multivariate models and may, to a varying extent, disturb the hydrochemical interpretations of the Ion Source Model and the Mixing Model. This is most evident in the latter model, whereas the Ion Source Model seems to be more robust (cf Sections 3.2 and 3.4). Conclusions based on the conservative parameters Li and Cl also support the interpretations of the Ion Source Model.

A possible explanation for the deviant hydrochemistry observed in SSM000241 and SSM000242 is microbial degradation of organic matter, which for some unknown reason is strongly enhanced (c. 10 times) compared with the other 3 soil tubes. The degradation of organic matter consumes organic carbon (TOC) with concomitant release of the nutrients N and P. The N/P ratio of about 10 indicates that these elements originate from organic matter that theoretically has a N/P mass ratio of 7 /Chapra 1997/. Dissolved $CO_2$ formed by this process contributes to the high $HCO_3^-$ concentrations measured and possibly also to the lowered pH. The anaerobic environment is evident from the low concentrations of $NO_3^-$ and the presence of dissolved $Fe^{2+}$ and $Mn^{2+}$ ions and sulphide ($S^{2-}$). The lowered $SO_4^{2-}$ concentrations compared with sea water (or SSM000238) may be an indication of ongoing sulphate reduction; sulphate-reducing bacteria consume organic matter and form $CO_2$ by using $SO_4^{2-}$ as an electron acceptor. The presence of dissolved $Fe^{2+}$ and $Mn^{2+}$ also indicates the presence of IRB (ion-reducing bacteria) and MRB (manganese-reducing bacteria), and it is also possible that some methanogenesis take place /Hallbeck 2009/.

**Table 7-2. Mean values of selected parameters in five soil tubes located beneath lake and sea sediments. One single observation from the upper parts of SSM000241 is also included in the table for comparison (shown in italics; extreme values are shown in bold face).**

| IDCODE | | SSM000238 | SSM000239 | SSM000240 | SSM000241 | SSM000241 | SSM000242 |
|---|---|---|---|---|---|---|---|
| **Elevation** | m (RHB70) | –11 | –4 | –5 | –3 | –32 | –15 |
| **$HCO_3^-$** | $mgL^{-1}$ | 194 | 504 | 264 | 147 | 5,170 | 3,520 |
| **pH** | | 7.11 | 7.31 | 7.37 | 6.68 | 6.69 | 6.74 |
| **$N_{tot}$** | $mgL^{-1}$ | 4 | 11 | 2 | 1 | 625 | 270 |
| **$NH_4^+$-N** | $mgL^{-1}$ | 3 | 11 | 2 | 0 | 626 | 269 |
| **$NO_3^-$-N** | $mgL^{-1}$ | 0.001 | 0.001 | 0.001 | 0.020 | 0.003 | 0.003 |
| **$P_{tot}$** | $mgL^{-1}$ | 0.6 | 0.7 | 0.4 | 0.1 | 58 | 27 |
| **$PO_4^-$-P** | $mgL^{-1}$ | 0.4 | 0.6 | 0.5 | 0.0 | 31 | 11 |
| **$N_{tot}/P_{tot}$** | ratio | 6 | 16 | 5 | 5 | 11 | 10 |
| **TOC** | $mgL^{-1}$ | 7.6 | 11 | 10 | 11 | 111 | 71 |
| **DOC** | $mgL^{-1}$ | 7.6 | 9.9 | 10 | 9.4 | 106 | 71 |
| **Fe** | $mgL^{-1}$ | 0.6 | 1.1 | 1.2 | 8.2 | 2.3 | 6.7 |
| **Mn** | $mgL^{-1}$ | 0.3 | 0.3 | 0.7 | 0.7 | 0.9 | 2.0 |
| **$SO_4^{2-}$** | $mgL^{-1}$ | 480 | 130 | 57 | 37 | 24 | 0.5 |
| **$S^{2-}$** | $mgL^{-1}$ | | | 0.46 | 0.07 | 0.29 | |

The bromide concentrations in the two soil tubes are also highly elevated; Br concentrations are almost 10 times higher than in modern sea water. According to the Br/Cl ratio in Figure 4-4, Br comes from a possible third source other than the deep saline groundwater and sea water (these unmistakeable sources form straight diagonal lines of constant ratio in the log-log plot). A third possible Br source is bacterially degraded organic matter of marine origin present in the sediments, e.g. bivalves or plant material. According to the Ca versus $HCO_3^-$ plot, calcite dissolution driven by $H^+$ originating from $CO_2$ of biogenic origin may have contributed to the high $HCO_3^-$concentrations (cf scenario R1 in Figure 4-13). A possible source of calcite could be clamshells. According to what is discussed above, a speculative explanation for the deviant hydrochemistry in SSM000241 and SSM000242 might be that mussel beds have been buried by sediments.

### 7.2.4 Conclusions

The major conclusions regarding the five soil tubes located in till beneath lake and sea sediments are summarised in the bulleted list below:

- The five soil tubes located beneath sea and lake water in the Laxemar-Simpevarp area probably contribute important information for an understanding of the site.
- Two of the soil tubes, SSM000238 and SSM000239, probably contain groundwater of mainly (modern?) sea water origin. However, the possibility of an anthropogenic sampling artefact due to mixing of different waters during pumping could not be excluded at these sites.
- The soil tube SSM000240, located beneath sea sediments near coast, probably represents discharging groundwater of mainly local meteoric origin. This soil tubes probably provide an example of the local discharge that is supposed to take place in lakes and along the coast.
- The deep saline signatures evident in SSM000241 (and to some extent in SSM000242) support the hypothesis of discharging deep groundwater in the main fracture zones in the area. Deep ion signatures in combination with meteoric isotope signatures in SSM000241 may be an indication of regional discharge at these sites.
- The anomalous hydrochemistry of the soil tubes SSM000241 and SSM000242 can be explained by microbial degradation of organic matter. However, the question of how this organic source got into these depths in the sediments remains unanswered.

## 7.3 The soil tube SSM000022 located on Ävrö

The hydrochemistry in the soil tube **SSM000022** located on Ävrö displays deviant hydrochemistry compared with most other soil tubes on Ävrö. Previous evaluations have noted the hydrochemical composition in this soil tube as an indication of potential deep discharge. The signatures in this object are to some extent contradictory, but the influence of deep groundwater is however less probable if all pieces are put together. Interpretations based on different models and parameter combinations are summarised in the list below:

- According to the Ion Source Model in Section 3.2.5, the signature is similar to many observations from the upper parts of the bedrock represented by percussion boreholes. Deep saline signatures are weak according to this model, and the composition could be explained by reactive alterations (e.g. cation exchange) of a mixture of ions derived from weathering and a marine source (cf Section 3.2.7.
- The Water Origin Model in Section 3.3.2 indicates meteoric recharge with some influence by evaporation (there is a slight attraction along the evaporation line towards lake and sea water samples). Also other soilt tubes located on Ävrö show a similar isotopic shift which perhaps could be explained by local conditions on an island surrounded by water.
- The Mixing Model in Section 3.4.3 reveals little information, other than that SSM000022 contains rather dilute groundwater (the Cl concentration is 139 $mg \cdot L^{-1}$) far from marine composition.
- According to measurements of carbon isotopes and $^{3}H$ in Section 3.5.2, the groundwater residence time in SSM000022 may be a few thousand years (corrected for calcite dissolution). There are indications of calcite dissolution in SSM000022 according to the carbon isotope signatures (cf Section 4.1.5).
- The Ca/Sr ratio and $^{87}Sr$ isotope signature in Figure 4-15 indicate similarities with the deep saline source with respect to Ca and Sr.
- The Li/Cl ratio in Figure 7-3 and the Br/Cl ratio in Figure 4-4 coincide with the ratio for deep saline groundwater. These compositions could also be explained by mixtures of shallow groundwater and marine ions. $^{37}Cl$ measurements in Figure 4-7 indicate Cl of mainly marine origin (the uncertainties are however great for $^{37}Cl$).

It is clear from the different indications above that meteoric recharge and reactions in the deposits have important influence on the hydrochemical composition in SSM00022. At present marine influence is weak in SSM000022, although there are traces of Cl of marine origin according to several parameters (see last bullet above). The attraction in the Ion Source Model towards the marine pole can perhaps to some extent be explained by reactive alterations, such as Ca versus Na cation exchange in this rather stagnant groundwater (according to the estimated groundwater residence time). According to carbon isotope signatures, $Ca^{2+}$ ions derived from calcite dissolution could be a driving force for this exchange reaction. This reaction theoretically shifts the observation towards the left in the Ion source Model, which could explain the location of SSM000022 near the cluster of observations from the upper parts of the bedrock (many percussion boreholes plot in this area).

A possible scenario for the observed pattern in SSM000022 could be far gone meteoric flushing of stagnant marine remnants in the deposits. The long groundwater residence time gives requisites for significant alterations of the groundwater composition by chemical reactions. Possible deep signatures indicated by Ca and Sr may be explained by a specific calcite source, rather than ongoing deep discharge. Furthermore, there are no indications of any significant discharge of a deep saline component in the surface water discharge from the area (the hydrochemical sampling station PSM107735, which is labelled PW735 in all figures). The location of SSM000022 within a cross-section of Ävrö is shown in Figure 7-4. A hypothetical groundwater flow regime at the depth of the intake of SSM000022 is marked by blue arrows. According to this scenario groundwater flow has mainly a downward or horizontal direction at the depth of the intake of SSM000022.

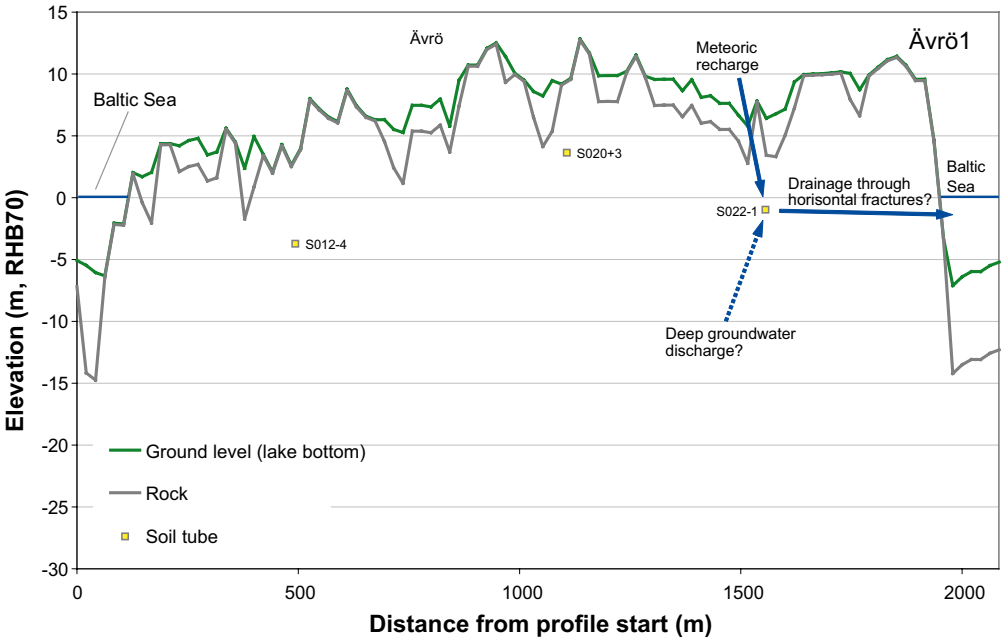


***Figure 7-4.*** *Profile showing cross section of Ävrö. See Figure 7-1 for the location of this profile. Arrows show the hypothetical groundwater flow described in text.*

## 7.4 Elevated concentrations of Ca and $HCO_3^-$ in Ekerumsån

Several visualisations and models reveal that the catchment of the Ekerumsån River exhibits deviant characteristics with respect to Ca and $HCO_3^-$. Some conclusions about this catchment are summarised in the list below:

- The mass balance calculations in Sections 6.2.4 and 6.2.8 indicate that the area-specific transport of these elements is elevated in this catchment. The underestimate in the model, which could be a rough estimate of the unknown source, corresponds to 6,500 kg Ca during 2004.
- Data from a preliminary study conducted in 1998 also show similarly elevated concentrations of Ca at two stream sampling sites in the upstream parts of the catchment /Tröjbom and Söderbäck 2006/.
- If the time series for Ca in the Ekerumsån is compared to the time series for the adjacent catchment in Figure 7-5, fluctuations are correlated and Ca concentrations in the Ekerumsån River are almost double compared with the Mederhultsån River. This indicates that the release of Ca is controlled by common climatic factors.
- According to the Ca versus $HCO_3^-$ plot in Figure 4-13, measurements in the stream site PSM002085 near the outlet of Ekerumsån show elevated concentrations of both elements. This site plots on the calcite dissolution line, which suggests that carbonate is the source of both elements.
- The slightly elevated $\delta^{13}C$ signatures in PSM002085 suggests that calcite of marine origin is the source for $HCO_3^-$ in this catchment (cf Figure 4-19). $^{14}C$ is also slightly lowered in this catchment, which further supports the theory of carbon from calcite (there are however other stream sampling sites that show slightly lowered $^{14}C$ activities as well, probably due to the influx of old carbon from decomposition of peat, cf Section 4.1.5).
- Strontium is usually closely associated with Ca. In Figure 4-14 and Figure 4-15 it is evident that neither the Ca/Sr ratio nor the isotope signature of $^{87}Sr$ deviates from other streams in the area. However, this does not exclude the possibility that some of the Ca, Sr, and $CO_3^{2-}$ originate from an anthropogenic source.

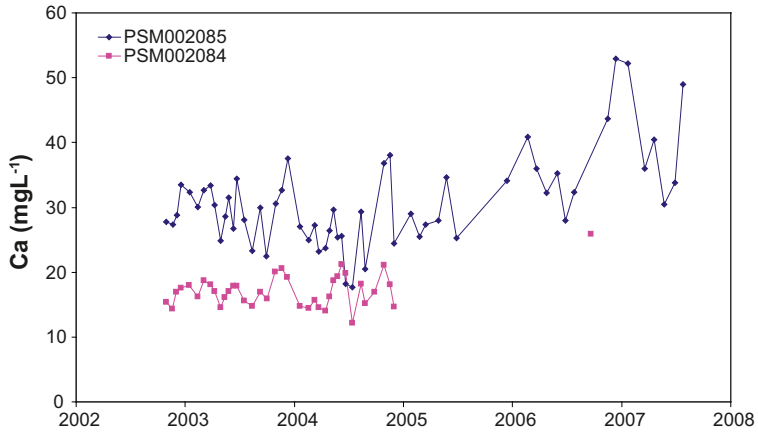


***Figure 7-5.*** *Calcium concentrations in the Ekerumsån (PSM002085) and the adjacent catchment of the Mederhultsån (PSM002084).*

A possible source of both of these ions could be the spreading of lime ($CaCO_3$) on soils for agricultural management purposes. Summer road salt ($CaCl_2$), which is spread on gravel roads for dust control (cf Sections 6.2.1 and 7.5), could also be a potential source of Ca, but there are no indications of an input of the counter-ion Cl to this catchment.

Alternatively, locally elevated weathering rates could lead to a similar pattern, but the lack of calcite in the deposits in the Laxemar-Simpevarp area contradicts this explanation. Neither is there any obvious natural explanation among physical factors such as regolith distribution or land use within the catchment of the Ekerumsån compared to adjacent catchments, e.g. the catchment of the Mederhultsån.

## 7.5 Anthropogenic sources of salts (Cl)

As discussed in Section 6.2.1, winter road salt may contribute significant input of Cl and Na to the surface system. Summer road salt ($CaCl_2$ or $MgCl_2$) may also contribute to the anthropogenic input to an unknown extent. Water released into streams or infiltrated into soil during drilling and pumping of cored boreholes may also contribute large amounts of salts from saline groundwater in the bedrock. These sources are, however, usually limited in time, which reduces the possible impact on mean values used in mass balance calculations and visualisations.

### 7.5.1 Winter road salt

Winter road salt, which is spread for anti-skid treatment, normally contains 98% percent NaCl. Motorway E22 as well as highway 743 from E22 to the nuclear power plant are salted in the winter, and a large portion of this salt drains into the catchment of the Laxemarån River, according to the mass balance model in Section 6.2.1.

According to the model results, as much as 56% of the total Cl input to the sub-catchments of the Laxemarån is attributable to road salt spread on E22 (56 of 100 tonnes). The mass balance for Na in Section 6.2.2 also indicates that a large portion of this element originates from that source. The contribution of Na from road salt to the total transport in the Laxemarån is 33%, which is lower than for Cl due to the existence of other Na sources, such as weathering of minerals. If the estimated amounts of Na and K from road salt that enter the Laxemarån (26 and 2 tonnes, respectively) are compared with the amount of Cl (56 tonnes), approximately 75% of the Cl is balanced by these cations based on molar masses. This discrepancy probably reflects uncertainties in the mass balance model rather than the actual situation (cf Section 9.3.4).

See Section 6.2.1 for further discussion of the influence of winter road salt.

### 7.5.2 Summer road salt

Summer road salt ($CaCl_2$ or $MgCl_2$) spread on gravel roads for dust control is a potential source of Cl, Mg and Ca in the surface system. Approximately 1 tonne of $MgCl_2$ or 1.3 tonnes of $CaCl_2$ may be spread per km /VTI 2008/. The total magnitude of this source in the Laxemar-Simpevarp area is not known. Since 2004, since SKB assumed responsibility for road maintenance in the area, approximately 0.7 tonne of $CaCl_2$ $km^{-1}$ has been spread per year (Alf Engdahl, Medins, pers.comm.). There are clear indications that this source may contribute significantly in the Laxemar-Simpevarp area; in Lake Frisksjön the Cl concentration has increased significantly since 2004, according to the upper panel in Figure 7-6. In the southern part of the catchment there are a few km of gravel roads that drain into Lake Frisksjön according to the map in Figure 7-7.

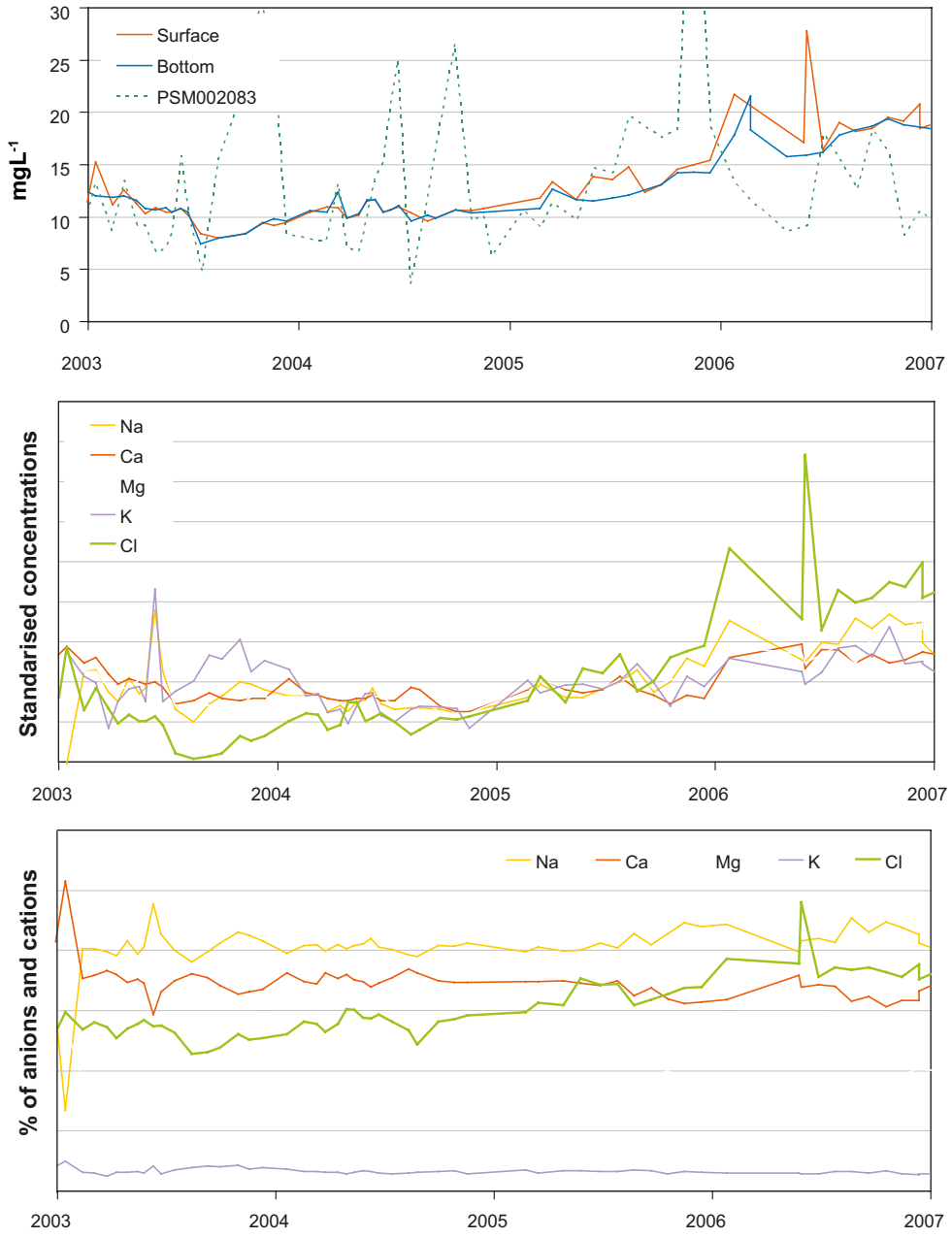


***Figure 7-6.*** *Upper panel: chloride concentrations in surface and bottom water of Lake Frisksjön (PSM002065) compared with Kärrviksån (PSM002083). Middle panel: standardised concentrations in surface water of Na, Ca, Mg, and K, compared with Cl. Lower panel: percentage of each element expressed in meq·$L^{-1}$ of cations and anions, respectively.*


***Figure 7-7.*** *Close-up of the catchments of Lake Frisksjön (PSM002065) and the Ekerumsån River (PSM002085). Discharge points of flushing water from drilling of cored boreholes have also been marked in the map.*

The possibility that the source is SKB's drilling activities and discharge of possibly saline flushing water is less likely, as there are no flushing water discharge points within the catchment of Lake Frisksjön according to Figure 7-7. A similar increasing pattern is also evident among several cations according to the middle panel in Figure 7-6. If the relative proportions of the cations are studied during this time period, when the Cl proportion increases among anions, the relative contribution of each cation to the increasing amounts is more or less constant, i.e. a specific element cannot be linked to the increase in Cl. A possible explanation for this pattern is that either Cl comes from several sources (for example both summer and winter salt) and/or cation ion exchange reactions that diminish the original signatures of summer road salt when Ca is exchanged for Na as the water percolates through the deposits.

An independent indication that the source of Cl is summer road salt is the $^{37}Cl$ measurements in Figure 4-8, where the observation from Lake Frisksjön shows a negative value. This could be an indication that Cl in Frisksjön is mainly of an evaporative origin, e.g. from $CaCl_2$ or $MgCl_2$ in summer road salt, whereas the $^{37}Cl$ signature winter road salt should be slightly positive. It should however in this context be noted that the analytical uncertainties are large for this parameter (cf Section 9.3.2).

In conclusion, the factors behind the increasing Cl concentrations in Lake Frisksjön are complex. There are, however, indications that summer road salt may at least to some extent explain the pattern, perhaps in combination with cations exchange reactions in the deposits. The possibility cannot be excluded that variations in supply of winter road salt on the larger road that intersects the catchment of Lake Frisksjön also contributes to the Cl pattern (cf the upper panel in Figure 7-6 where Cl concentrations in the road-salt-influenced Kärrviksån are shown). A similar baseline shift is also evident in the Ekerumsån in Figure 7-8, but in this case the influence of drilling activities could not be excluded according to Figure 7-7.

### 7.5.3 Salt emissions from SKB drilling of cored boreholes.

There are no comprehensive compilations of salt emissions to the surface system from SKB drilling activities. Based on information of measured flushing water volumes and a few assumptions, a very rough estimate based on data for the catchment of the Laxemarån during 2004 is summarised below:

- Total discharge of drilling water during drilling of KLX03 and KLX05 in 2004: 3,460 $m^3$. Drilling water was infiltrated into the soil within the catchment of the Laxemarån /Ask et al. 2007/.
- KLX03: Assumed Cl concentration in flushing water well HLX14: 357 $mg \cdot L^{-1}$ (cf Table 2-5 and Appendix E).
- KLX05: Assumed Cl concentration in flushing water well HLX10: 32 $mg \cdot L^{-1}$ (cf Table 2-5 and Appendix E).
- Estimated average Cl concentration in water pumped from both cored boreholes: 5,000 $mg \cdot L^{-1}$ (cf Figure 4-5).
- Assumed proportion of flushing water in discharged drilling water 75%.
- Calculated total Cl discharge in the catchment of the Laxemarån during 2004: 1,821 kg (KLX03) and 2,879 kg (KLX05). Total estimated discharge of Cl: 4,700 kg.

The total estimated discharge to the catchment of Laxemarån during drilling of KLX03 and KLX05 the year 2004 is estimated to be approximately 5 tonnes of Cl. This amount constitutes approximately 5% of the total discharge of 100 tonnes Cl in the outlet of Laxemarån 2004 according to the mass balance estimate in Section 6.2.1. Besides emissions of salts during drilling of cored boreholes, hydrological tests may contribute unknown amounts.

From this example it can be concluded that salt emissions from SKB's drilling activities are probably of minor importance on the catchment scale over longer time periods. On the local scale, however, salt emissions during drilling activities may increase Cl concentrations several times in the streams (cf Figure 7-8). This Cl peak coincides with the drilling of KLX18A and KLX13A within the catchment of the Ekerumsån /Ask et al. 2007/ (cf Figure 7-7). A fact that further complicates the interpretation of the possible impact of SKB's drilling activities is the practise of infiltrating drilling water into the soil, which delays discharge into surface water due to the groundwater residence time.

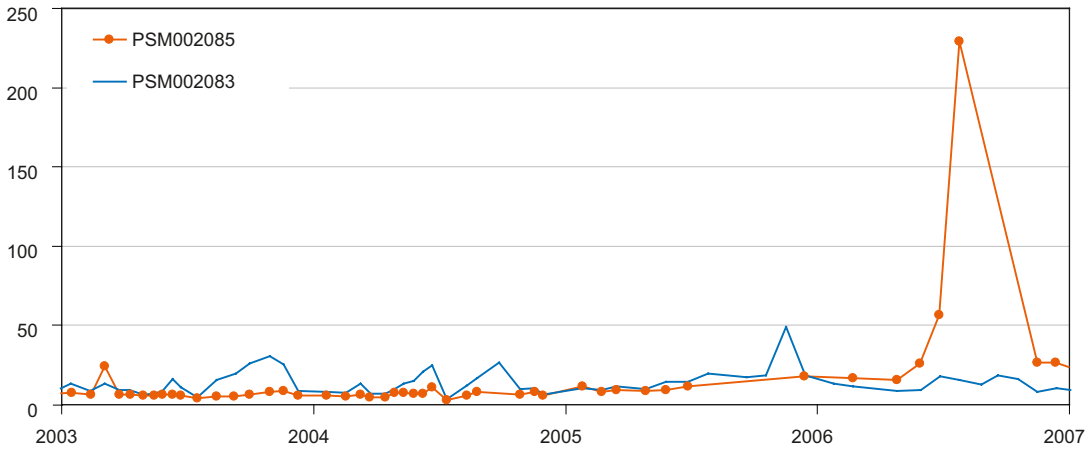


***Figure 7-8.*** *Chloride concentrations in the Ekerumsån (PSM002085) compared to the Kärrviksån (PSM002083). The peak during 2006 may possibly be caused by emissions from SKB's drilling activities within the catchment.*

### 7.5.4 Anthropogenic influence on shallow groundwater

Road salt has been shown to contaminate groundwater wells located close to salted roads /Ojala and Mellqvist 2004/. Groundwater in the Laxemar-Simpevarp area is probably locally affected by winter road salt (NaCl), but these possible anthropogenic influences are difficult to separate from possible marine influences. In Figure 7-9, elevated Cl concentrations in SSM000042 and SSM000263 are probably attributable to marine relicts rather than to road salt from nearby highway 743 (cf Figure 7-1). The influence of summer road salt on shallow groundwater is theoretically detectable due to a deviant $^{37}Cl$ signature. The cluster of soil tubes showing negative $^{37}Cl$ values in Figure 4-8 can be explained by this source, but due to the large analytical uncertainties, no certain conclusions can be drawn about specific objects. The overall pattern is probably not random and may reflect an anthropogenic influence, although the spatial relationships cannot be revealed at present.

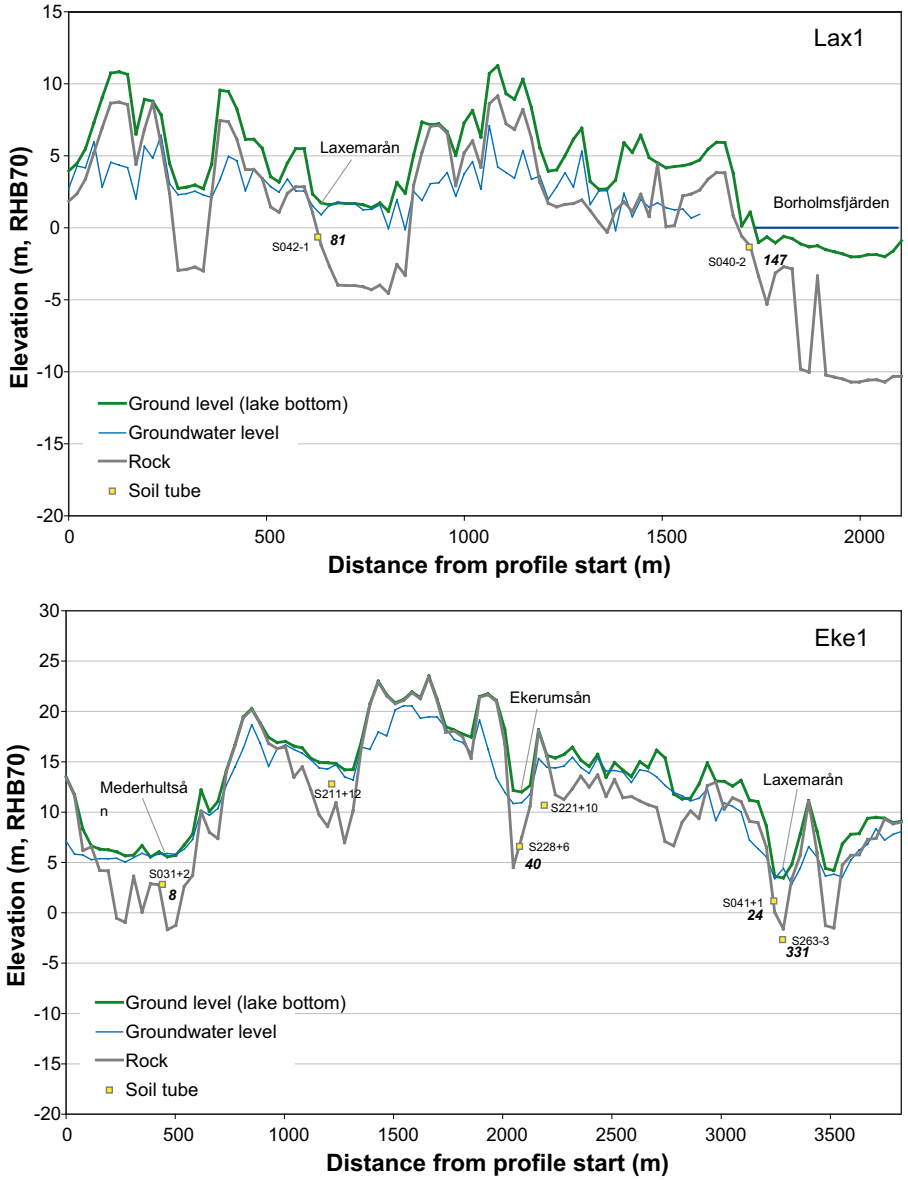


***Figure 7-9.*** *Profiles showing ground level and the upper part of the rock, together with soil tube samples in the vicinity of the transect and the average groundwater level. See Figure 7-1 for a description of the profiles. Cl concentrations (mg·L$^{-1}$) are shown in italics.*

# 8 A conceptual model for the hydrochemistry in surface systems in the Laxemar-Simpevarp area

In this report, a large number of visualisations and models of differing complexity that reflect the hydrochemistry of the Laxemar-Simpevarp area are presented for the purpose of providing an understanding of important processes and factors that affect the hydrochemistry of the surface systems. In order to broaden the perspective, all data, including observations from different levels of the bedrock as well as hydrological measurements and characterisations of the Quaternary deposits, have been included in the analyses. The purpose of this report is to provide a detailed understanding of the site and to explain observed overall patterns as well as anomalies, and ultimately to present a conceptual model that explains the present hydrochemistry in the light of the past. Together with the conceptual model presented in this section, supportive references are included that refer back to the report.

## 8.1 Important factors for the hydrochemistry of the surface systems

The topography in the Laxemar-Simpevarp area is characterised by higher elevated areas covered by thin or no Quaternary deposits, intersected by deep fissure valleys filled with thick sediments. This topography, in combination with the withdrawal of the Baltic Sea due to isostatic land uplift (shoreline displacement), are two important factors determining the hydrochemistry of the Laxemar-Simpevarp area /Söderbäck and Lindborg (eds) 2009/. Marine relicts in the Quaternary deposits influence the hydrochemistry in low-lying areas close to the coast, whereas higher areas are mainly influenced by atmospheric deposition and weathering processes.

Glacial remnants in the form of till were deposited during the Weichselian glaciation and de-glaciation /Fredén (ed) 2002/. When the ice sheet retreated about 12000 BC, the whole area was covered by water and the deposits were exposed on the sea floor. The deep fissure valleys that often coincide with the major deformation zones in the bedrock are now filled with thick sediment layers of glacial and post-glacial origin /Sohlenius and Hedenström 2008/. The gradual isolation of these former brackish bays has resulted in an evolution from brackish water to freshwater lakes followed by wetlands (in the Laxemar-Simpevarp area there was usually no lake stage). In modern time, fertile wetlands have often been converted into agricultural land by ditching and drainage, further altering the hydrochemical conditions in the area /Söderbäck (ed) 2008/.

The growth of vegetation and development of a soil layer on the emerging land had a profound impact on the hydrochemistry of the surface system, for example due to input of $H^+$ of biogenic origin (cf Section 4.1.5). The distribution and fate of elements utilised by the biosphere, such as nutrients and essential trace elements, is profoundly affected by biochemical cycles and retention processes.

In Section 8.2 the evolution of the hydrochemistry of the bedrock is briefly summarised from a palaeohydrological perspective. This section forms a basis for the conceptual model for the hydrochemistry of the surface system, as presented in Section 8.3.

## 8.2 Evolution of the groundwater in the bedrock

This brief account summarises the evolution of the groundwater in the bedrock in order to provide a basis for the interpretations of the hydrochemistry of the surface system in Section 8.3. When applicable, general conclusions refer to visualisations within this report and for further information see /Laaksoharju (ed) 2008/.

In a geological perspective, the conditions underlying the hydrology and hydrochemistry of the Laxemar-Simpevarp area have undergone dramatic changes. Recurring glaciations covering the area with several kilometres of ice have been interrupted by interglacials when the area was covered by sea water or, as at present, by thin soils.

Since the latest deglaciation around 12000 BC, land uplift in combination with water level changes have resulted in gradual withdrawal of the sea and establishment of the present coast line. During the most saline part of the Littorina Sea period in 4000–3000 BC, sea water with a salinity almost two times higher than in the present Baltic Sea covered significant parts of the Laxemar sub-area and all of the Simpevarp sub-area (cf /Söderbäck (ed) 2008/.). In Figure 8-1, the light blue colour roughly corresponds to the area covered by Littorina Sea water in 6000 BC (cf Figure 4-1), whereas the darker blue colour, which represents elevations of 5–10 metres, corresponds to the situation in 4000 BC.

During the last glaciation, the Quaternary deposits as well as the bedrock were infiltrated with glacial meltwater down to a depth of at least 500 metres according to the $\delta^{18}O$ versus depth plot in Figure 3-13. Nowadays, this glacial water has to a varying extent been replaced by sea water due to density intrusion, and at a later stage by meteoric recharge in areas raised above sea level. It is evident from Figure 8-1 that premises for penetration of Littorina Sea water into the bedrock due to density intrusion should have been good, at least in the low altitude near-coastal areas in the Laxemar sub-area. The former "Laxemar peninsula" was partly covered by sea water during the Littorina saline maximum at 4000–3000 BC and was almost surrounded by sea water for several thousands years, until the valleys ultimately were cut off from the Baltic Sea. The following indications support a general marine influence in the very active mixing zone in the upper 500 metres of the bedrock in the Laxemar and Simpevarp sub-areas:

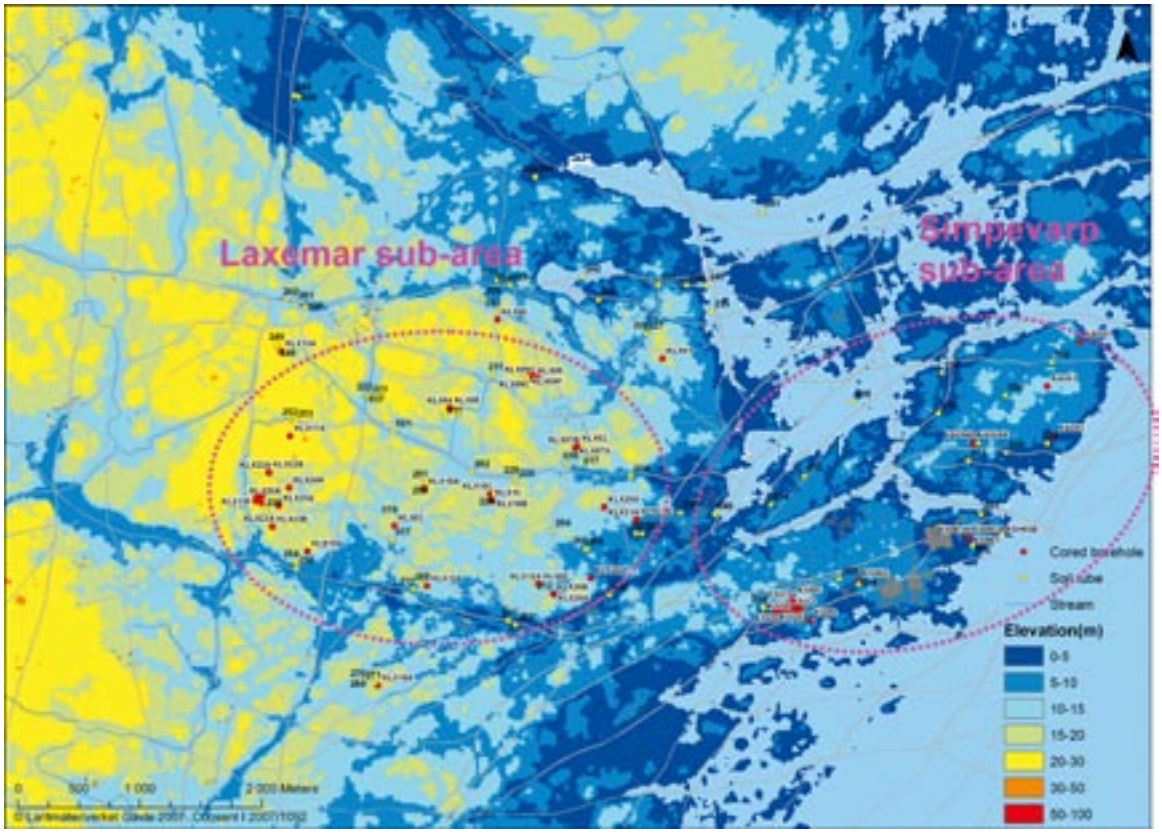


***Figure 8-1.*** *The distribution of different elevation categories in the present land areas in the Laxemar-Simpevarp area. Major deformation zones of high – medium – low confidence according to the Laxemar 1.2 evaluation have been marked in grey of descending width. Cored boreholes and soil tubes have also been marked in the map.*

- The Br/Cl ratio in Figure 4-4 shows that Cl of marine origin occurs down to depths of 500–600 metres in the bedrock. The presence of marine signatures in e.g. KLX17A, KLX04 and KLX08, located in the higher elevated parts of the Laxemar sub-area, may be an indication that sea water may have reached considerable depths even at these sites. At present date, Cl concentrations in the range of 600–2,000 $mg \cdot L^{-1}$ (cf Figure 4-5) prevail at these sites and levels, probably due to dilution by meteoric recharge.
- $^{37}Cl$ isotope signatures in Figure 4-8 support the conclusions based on the Br/Cl ratio. Due to limited analytical precision, conclusions based on this parameter are more uncertain. The marine origin of many samples from cored boreholes (e.g. KLX17A-343 and KLX04-487) is evident as Cl of deep saline origin shows enriched $^{37}Cl$ values.
- Mg, which has been regarded as an important marine indicator in the Forsmark area, is probably a less useful indicator in the dilute groundwater that characterises the Laxemar-Simpevarp area, due to the possible non-conservative behaviour of this element /Laaksoharju (ed) 2008/. Large scale patterns in the Mg versus Ca plot in Figure 4-16 may however be interpreted as a general marine influence according to the hypothetical mixing scenario U2 with Littorina sea water (e.g. HAS13-65).
- Similar to the situation in the Forsmark area, $Mn^{2+}$ concentrations are elevated within the group of samples in Figure 4-24 which show the highest Littorina proportions according to the M3 model (cf Figure 3-6), as well as according to the Ion Source Model in Section 3.2.5. This $Mn^{2+}$ anomaly in the groundwater from the bedrock may reflect a process that influenced the infiltrating Littorina sea water in connection with density intrusion (cf conceptual model for the Forsmark area in / Tröjbom et al. 2007/ and further discussions in /SKB 2006a/).

The spread between the marine and deep saline sources in the Br/Cl plot in Figure 4-4 may also be interpreted as if deep saline influences occur at relatively shallow depths in the seemingly very active mixing zone in the upper parts of the bedrock. This could be an indication that regional groundwater discharge is an important mechanism influencing the composition of the groundwater in the upper parts of the bedrock and potentially also some parts of the the surface system. Indications of deep saline influences in the upper 600 meters of the bedrock of the Laxemar-Simpevarp area can be summarised as follows:

- The Li/Cl plot in Figure 4-7 suggests that deep saline influences occur at relatively shallow depths in the bedrock. Many observations from cored boreholes plot along the presumed deep saline ratio, with varying influence of the sea water source.
- Ca and Sr are important constituents of deep saline groundwater, and these elements show specific signatures in this groundwater type (cf Section 4.1.2). In Figure 4-15, where the Ca/Sr ratio is plotted versus the $^{87}Sr$ isotope ratio, observations from the bedrock form a distinct cluster. The composition of this cluster differs significantly from other Ca and Sr sources, such as sea water and weathering minerals in the surface system. This pattern could be interpreted as indicating that Ca in the groundwater of the bedrock to a significant extent originates from the deep saline source. Ca show a quasi-conservative behaviour at these depths according to evaluations in /Laaksoharju (ed) 2008/.
- In the interpretation of the Ion Source Model in Section 3.2.7, many observations from the bedrock seem to be shifted to the left from the mixing line between the deep saline and the marine sources. A possible explanation for this pattern is cation exchange reactions driven by discharging $Ca^{2+}$ ions of deep saline origin. $Ca^{2+}$ ions exchanges with $Na^{+}$ derived from weathering in the deposits or in the fractures in the bedrock. $H^{+}$ originating from the surface system could probably be an important driving force for these weathering reactions.

Carbon isotope measurements may also provide an indication of the origin of carbon in the groundwater of the upper parts of the bedrock, as well as of the mean carbon age (cf Section 3.5.2). In Figure 3-24, $^{13}C$ and $^{14}C$ measurements in the groundwater from the bedrock show very low $^{14}C$ activities in combination with $\delta^{13}C$ signatures that coincide with biogenic signatures present in the surface system. This may be interpreted as indicating that the inorganic

carbon that predominates at these depths originates from organic carbon in the surface system. According to the decay rate of $^{14}C$, this organic carbon may have an average age of between 6,000 and 14,000 years, which suggests that most of the carbon input from the surface system must have occurred after the latest glaciation. Alternatively, if some of this carbon is derived from non-marine calcites with a $\delta^{13}C$ signature similar to biogenic carbon, this implicates that the biogenic carbon age is overestimated and that the input must have occurred even later. The major conclusion of these speculations is that the surface system probably has had an impact even at depths of several hundred metres in the bedrock since the latest glaciation.

If the evolution of the groundwater in the bedrock is summarised in a palaeohydrological perspective, the major hydrological factors influencing the hydrochemistry are:

- At deeper levels, or in stagnant parts of the bedrock, hydrochemical groundwater signatures probably reflect an integrated picture of hydrological regimes from several glaciations and interglacials during the last million years, cf /Söderbäck (ed) 2008/. The deep saline groundwater, which is present at depths below 600 meters, is characterised by a very high density due to high concentrations of especially Cl and Ca.
- During the latest glaciation, which ended in the Laxemar-Simpevarp area in 12000 BC, glacial meltwater was infiltrated into fractures in the bedrock to a depth of approximately 500 metres. Quaternary deposits should also have been filled with this type of water.
- After the withdrawal of the ice sheet, the Laxemar-Simpevarp area was covered by fresh water, the Ancylus Lake (c 9000–7500 BC). During this stage there was no hydrological driving force in the vertical direction, and there were probably only minor alterations in the hydrochemistry of the bedrock.
- When parts of the Laxemar-Simpevarp area were covered by the brackish Littorina Sea with increasing salinity (c 7500–3000 BC), the difference in density between Littorina Sea water and the groundwater in the bedrock created the conditions for a density intrusion. This hydrological driving force may have infiltrated sea water through the bottom sediments and the minerogenic Quaternary deposits into the fractured bedrock to a depth of approximately 500–600 metres. There is at present no information available regarding how fast this shift took place, or to what extent the Littorina Sea water actually passed the Quaternary deposits, or whether the inflow penetrated uncovered fractures directly. A similar scenario may also have occurred during earlier brackish periods, such as the Yoldia Sea stage (9500–8800 BC).
- In the parts of the Laxemar-Simpevarp area that were still covered by Baltic Sea water after the Littorina salinity maximum (from c 3000 BC), there was no driving force transporting ions and water from the less saline sea water to the heavier, more saline groundwater in the bedrock. On the contrary, there was a possible discharge of groundwater from the fractured bedrock upwards through the Quaternary deposits, driven by the topographical gradient near the coast due to both local and regional discharge flow patterns.
- From the Littorina salinity maximum until the present, when parts of the Laxemar-Simpevarp area have successively emerged from the sea due to isostatic uplift, hydrological conditions in the Quaternary deposits have significantly changed. Recharge of meteoric water has led to a completely new flow pattern, compared with the conditions prevailing when the area was submerged under sea water. This new situation has resulted in local discharge in streams and lakes, as well as recharge through the Quaternary deposits down to the upper parts of the fractured bedrock. This creates conditions for a meteoric influence on the upper parts of the bedrock and the formation of an active mixing zone that seem to extend down to approximately 600 meters. Meteoric recharge into the bedrock also gives premises for regional groundwater flow patterns and potential discharge in the surface system of groundwater of deeper origin. Meteoric recharge influences the groundwater in the bedrock, which leads to alterations of the hydrochemistry due to dilution and reactive processes.

## 8.3 Conceptual model for the hydrochemistry of the surface system

The present situation in the surface system is a consequence of the palaeohydrological past, as described in the previous section. In higher areas, meteoric recharge has a great influence on the observed hydrochemistry, which is usually characterised by dilute fresh waters of low ionic strength. In lower-lying areas near the coast, there are indications of ongoing flushing of marine relicts since the area was covered by sea water. At most locations in the Laxemar-Simpevarp area, this flushing is more or less complete and the observed concentrations of marine ions can be explained by deposition and anthropogenic sources such as road salt.

The establishment of a vegetation cover on previously uncovered Quaternary deposits has also greatly affected the hydrochemistry of the surface system. Degradation of biogenic carbon generates large amounts of $H^+$, which drives weathering processes in the Quaternary deposits as well as in the bedrock. According to isotope measurements, carbon in the upper 400 metres of the bedrock may to some extent originate from a biogenic source, probably from meteoric recharge. The distribution of other elements associated with organic matter, such as N, P, K and Si, is also affected by uptake and cycling in the biosphere.

### 8.3.1 Regional model

On a regional scale, meteoric recharge and the subsequent flushing of ions creates the large-scale hydrochemistry of the area, according to the conceptual model in Figure 8-3. Marine relicts, in combination with regional groundwater flow patterns, may explain the observed anomalous composition of shallow groundwater in sampling points in till beneath lake and sea sediments. These sites are predominantly located close to major facture zones, which are potential deep groundwater discharge points (cf Figure 8-1).

The profile in Figure 8-3, which consists of four segments marked by violet dashed lines, starts in the higher-lying area of the Mederhultsån River, passes Lake Frisksjön and ends close to the northern coast of Granholmsfjärden as shown in Figure 8-2.


***Figure 8-2.*** *Map showing the location of the transect (denoted CPT1) in Figure 8-3 in relation to soil tubes, percussion boreholes and cored boreholes. The profile starts at the black dot at the left, and the three turns between the four sections are marked in Figure 8-3. See Figure 2-6 for a description of land use categories in the background map.*

Cl concentrations measured in shallow groundwater are included in the upper panel of Figure 8-3, whereas deuterium excess is included in the lower panel (see definition of deuterium excess in the explanation to the figure). Measurements in the bedrock are represented by two percussion boreholes located close to the transect: HLX20 and HAS02, of which only the latter is included in data selection A (cf Section 2.2.5). The blue representation of these boreholes corresponds to the vertical extent of the sampled borehole sections.

The spatial distribution of Cl in the upper panel of Figure 8-3 clearly indicates that very low concentrations prevail in the higher-lying areas. Concentrations in the range 8–15 $mg \cdot L^{-1}$ are 2–3 times higher than the estimated background concentration from higher-lying areas (cf catchment model in Section 6.2.1). This may indicate that flushing due to meteoric recharge has gone relatively far, and only traces of Cl occur in the Quaternary deposits. In lower located areas closer to Granholmsfjärden, Cl concentrations are considerably higher in similar settings. In SSM000031 and SSM000240 are Cl concentrations in the range of 100–600 $mg \cdot L^{-1}$ measured, which, if the water isotope signatures also are concerned (see below), may indicate ongoing outwash of marine relicts

In two soil tubes located in till below lake and sea sediments (SSM000242 and SSM000241, respectively), Cl concentrations exceeding the concentrations in present Baltic Sea are measured (cf Figure 4-2). According to the Ion Source Model in Section 3.2.5, the signatures in at least SSM000241 suggests a mixture of relict marine and deep saline ions. In the Li versus Cl plot in Figure 4-7 this interpretation is further supported for both soil tubes. As an alternative hypothesis the high salinity in these soil tubes, which exceeds the salinity of the present Baltic Sea, could have been formed by evaporation in isolated bodies of water rather than representing remnants of the Littorna Sea.

The origin of water is explored in the lower plot of Figure 8-3, where the deuterium excess is shown within the boxes. This parameter is a measure of the deviation from the Global Meteoric Water Line, GMWL (cf Section 3.3.1). Values around 0 indicate meteoric origin whereas negative values indicate influence from evaporation, e.g. in lakes or sea water. From the lower panel in Figure 8-3 can be concluded that all samples which show low Cl concentrations (below 1,000 $mg \cdot L^{-1}$) also show $D_{excess}$ values around 0. This indicates that meteoric recharge is the major source of the water in both shallow groundwater and the upper parts of the bedrock (HLX20) in the higher elevated areas. In the bedrock close to Granholmsfjärden Basin (HAS02), as well as in the deposits below Lake Frisksjön (SSM000242), negative values of the $D_{excess}$ parameter implies that lake water or sea water is the origin of water. In SSM000241 the isotope signature points towards a mixed meteoric and sea water origin.

If all parts are combined, the following conceptual model can explain the area's hydrochemistry on a regional scale:

- In the lower-lying areas near the coast, relict marine water prevails in the deeper parts of the deposits and in the upper parts of the bedrock. The high salinity, compared with the present Baltic Sea, in combination with negative $D_{excess}$, indicates that this sea water is probably a remnant from the Littorina stage when sea water with a Cl concentration of approximately 6,500 $mg \cdot L^{-1}$ infiltrated the deposits and the bedrock (cf Table 1-1 and Section 8.2). The spatial extent where this water type has significant influence is marked by grey dashed lines in Figure 8-3. As an alternative hypothesis the high salinity in these soil tubes could have been formed by evaporation in isolated bodies of water rather than representing remnants of the Littorna Sea.
- In the deposits closer to the surface, intermediate Cl concentrations in combination with meteoric isotope signatures indicate ongoing flushing of relict marine remnants of Littorina or of younger age. This is exemplified by the shallow groundwater sampling points SSM000034 and SSM000240, which are located at different positions within the salinity gradient, ranging from relict Littorina salinities to dilute meteoric recharge.
- In slightly higher located areas, which also should have been covered by sea water after the latest glaciation (cf Section 8.2), meteoric isotope signatures and low Cl concentrations indi-

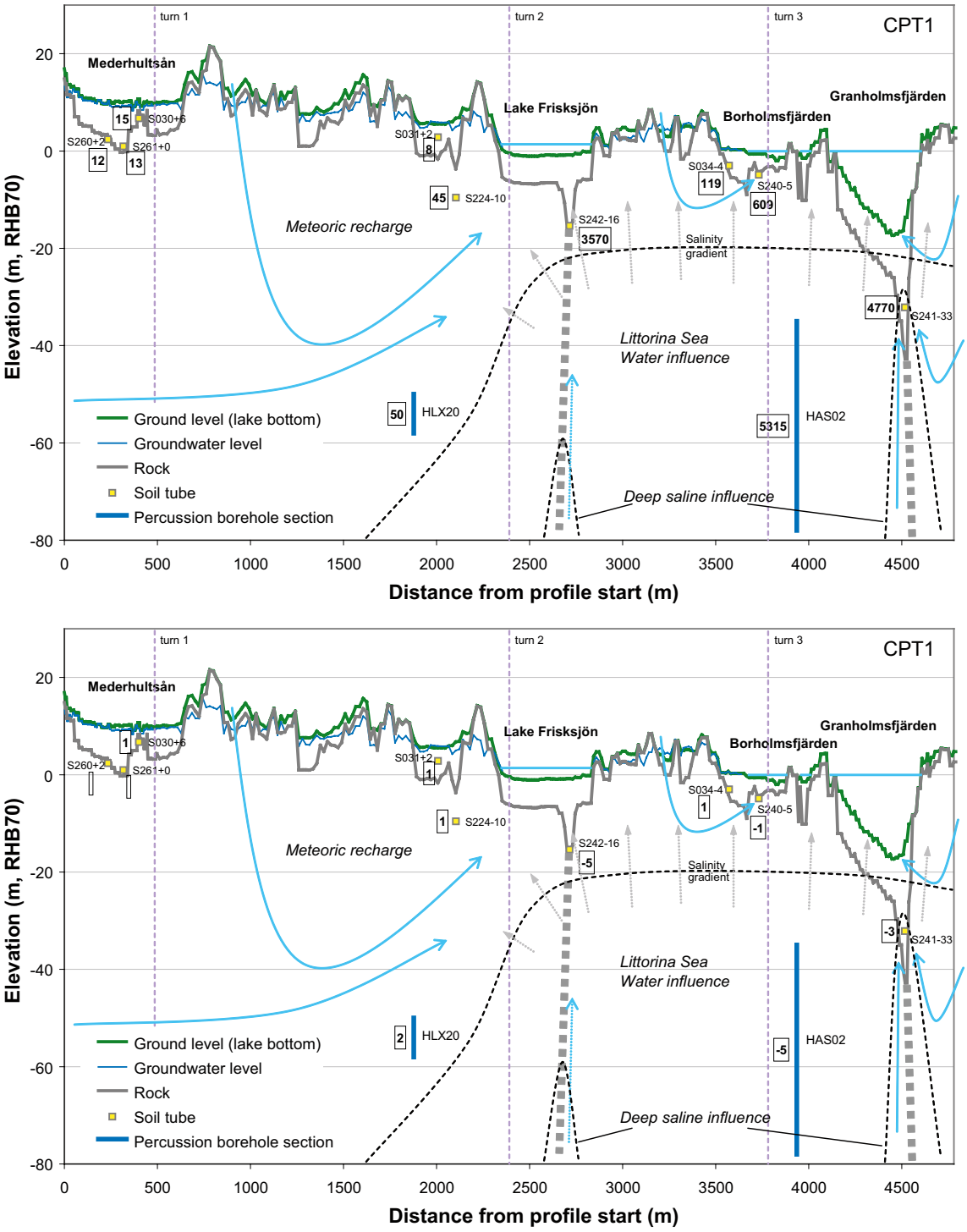


***Figure 8-3.*** *A profile covering a transect of the Laxemar-Simpevarp area (see Figure 8-2 for location). The profile shows ground level and the upper part of the rock, together with soil tubes and percussion boreholes in the vicinity of the transect and the average groundwater level. Thick dotted grey lines represent the approximate location of major fracture zones (cf Figure 8-1). A selection of hypothetical groundwater flow lines are shown by blue-green arrows. Figures within the boxes represent in the upper plot Cl concentrations (mg·L$^{-1}$), whereas corresponding figures in the lower plot represent the deuterium excess ($D_{excess}=\delta^2H-7.06\cdot\delta^{18}O+1.7$ ‰ SMOW).*

cate that any marine relicts have been washed out due to the meteoric recharge. This process has also affected the groundwater in the upper parts of the bedrock, resulting in signatures similar to the shallow groundwater even at a few hundred metres depth.

- In areas located above the highest coastline of the Littorina Sea, relict marine remnants are probably almost absent, which also is reflected by the topographical gradient described in Section 6.2.1. Cl concentrations may in these areas be fully explained by deposition and point sources as road salt. The maximal elevation for Littorina Sea was 17 m, whereas the preceding brackish Yoldia Sea ranged from 57 m (9500 BC) to 20 m (8800 BC) /Söderbäck (ed) 2008/ (the saline Yoldia and Littorina stages were interrupted by the fresh Ancylus lake and hypothetically could the short Yoldia Sea stage also have contributed to relict remnants in higher elevated areas).
- Deep saline signatures present in SSM000241 and SSM000242 (cf Section 7.2) can be explained by the influence of deep groundwater discharge. Both of these sites are located in the vicinity of major fracture zones, which have been proposed as potential areas for deep groundwater discharge. However, the differing water isotope signatures between these two sites indicates that SSM000241 is attributable to regional or local meteoric discharge originating from the higher-lying area in the north (cf Figure 8-1), whereas SSM000242 probably reflects a more stagnant relict marine groundwater less influenced by ongoing meteoric recharge.

# 9 Evaluation of uncertainities

This report comprises an evaluation of a vast amount of hydrochemical data from the Laxemar-Simpevarp area, combined with geological and hydrological supportive data. All these data, as well as the different models that have been constructed, are associated with uncertainties. In the evaluation and interpretation of results, uncertainties at several levels have to be considered:

- Uncertainties associated with analytical precision
- Uncertainties associated with sampling methodology
- Representativity of the sample with respect to disturbances during drilling/installation of boreholes, as well as hydrological testing and sampling. Induced chemical reactions may have a profound impact on the observed hydrochemistry.
- Spatial representativity of the sample due to variation in the environment.
- Temporal representativity due to seasonal fluctuation as well as between-year variation.
- Uncertainties associated with supportive data used in models, e.g. land use characterisations or hydrological measurements, further contributes to the overall uncertainty of the final conclusions.

## 9.1 Selection and representativity of data

Data used in this report have undergone several quality checks in order to identify erroneous values in the data sets. Moreover, the data used in visualisations and models are further selected according to different criteria in Sections 2.2.5 and 2.2.6. For example, only samples with charge balance errors less than ±15% are accepted for surface water and shallow groundwater. For groundwater samples used in visualisations throughout the report (cf data selection C in Section 2.2.6), the criteria for acceptance are charge balance errors less than ±5%, low flushing water content and stable hydrochemistry over time.

In all evaluations the arithmetic mean is used to provide a single value representing all samples from a specific object or depth level. Depending on the shape of the distribution, this measure is more or less influenced from extreme observations. Natural concentrations are often log-normally distributed which means that the distribution is positively skewed with a ‘tail’ towards higher values. The use of the median instead of the arithmetic mean may reduce influence from extreme values, but at the same time it may imply loss of important information. In this evaluation, extreme values are regarded important, e.g. concerning the question of possible deep groundwater discharge in the surface system, and therefore we have chosen to use the arithmetic mean.

## 9.2 Statistical testing and significance

The analyses in this report are mainly explorative for the purpose of objectively identifying and visualising patterns that may be important for the understanding of the hydrochemistry of the surface system. Due to the heterogenic nature of the vast database that contains almost 100 parameters sampled in precipitation, sea water, fresh surface water, shallow groundwater and groundwater from the bedrock, statistical significance testing is in many cases not meaningful to carry out. Experimental design is one way to achieve conditions that meet these criteria, but the available data are usually not optimally organised in this manner.

In scientific contexts, uncertainties are often related to different significance levels that correspond to a 0.1%, 1% or 5% chance that the relationship in question is random rather than an actual relationship. The number of observations, in combination with the variation between repeated observations, are factors that determine the probability that a relationship is the result of chance. All statistical testing is based on theoretical assumptions regarding the nature of the variability, and if these assumptions are violated the testing may not be valid. Relationships and patterns identified in this explorative analysis sometimes correspond to considerably larger probabilities (although not quantified). The rationale for presenting conclusions that consequently may be random at the level of 50% chance, is that the purpose of the explorative analysis to detect possible relationships for further evaluation. A strict application of significance criteria could make it more difficult to find the pieces to build a descriptive model with an acceptable overall level of confidence.

In statistical testing, several assumptions usually have to be satisfied in order to make the tests valid. For example, parametric statistical tests require that data is approximately normally distributed. The multivariate statistical technique principal component analysis (PCA, cf Section 2.3.9), which is used as a descriptive tool in this report, does not assume normality among the investigated variables and can be used for this purpose, no matter if the variables are normally distributed or not /Jolliffe 2002/. If a PCA is applied on approximately normally distributed data, the resulting model describes the variation among the majority of the samples. If the distribution of the data is positively skewed, e.g. follows a log-normal distribution, the resulting model focuses on observations in the 'tail' of the distribution. If these observations in the 'tail' are of specific interest, e.g. if they represent end-members among several water types, the resulting model may adequately describe the variability with respect to these water types (cf the methodology used in the M3 model described by /Laaksoharju et al. 1999/.

The Ion Source Model and the Mixing Model presented in Section 3 are applied on a dataset that includes observations from several water types. Parameter distribution within each water type may follow an approximate normal or a log-normal distribution, whereas the the distributions in the total dataset most probably are not normally distributed. In Table 9-1, skewness and kurtosis coefficients indicate that most variables in the Ion Source Model, which use data on the relative composition, are approximately normally distributed (K and Li deviate most from a normal distribution). The Mixing Model which is based on concentrations, is on the other hand more skewed according to the positive skewness coefficients. The use of non-transformed data in this model results in a linear descriptive model with an appearance similar to that of the M3 model /Laaksoharju et al. 1999/, where focus is laid on marine and deep saline water types (cf M3 end-members in Section 1.1.3).

**Table 9-1. Statistics describing the frequency distribution of the variables included in the multivariate models in Chapter 3. Skewness close to 0 indicates that the distribution is symmetrical, whereas positive values indicate a 'tail' towards higher values, e.g. a log-normal distribution. Kurtosis is a measure of the 'peakedness' of the distribution where values significantly greater than 0 indicates a "narrow" distribution.**

| | Ion Source Model | | Mixing Model | |
|---|---|---|---|---|
| | Skewness | Kurtosis | Skewness | Kurtosis |
| Na | –0.2 | –1.1 | 2.4 | 8.2 |
| K | 3.0 | 15 | 2.7 | 6.0 |
| Ca | 0.1 | –1.1 | 6.0 | 46 |
| Mg | 0.6 | –0.5 | 2.4 | 4.5 |
| Li | 2.6 | 12 | 4.4 | 23 |
| Sr | 1.2 | 0.4 | 5.4 | 37 |
| $HCO_3$ | 0.6 | –1.0 | 0.9 | 0.6 |
| Cl | –0.2 | –1.7 | 4.8 | 31 |
| $SO_4$ | 2.1 | 5.5 | 1.7 | 2.2 |
| Br | 1.9 | 8.1 | 4.8 | 30 |
| F | 1.3 | 1.7 | 0.7 | –0.04 |

## 9.3 Uncertainties associated with specific chapters

A discussion of uncertainties associated with specific chapters in the report follows in the sections below, and when possible these uncertainties are quantified. For quantification of analytical and methodological uncertainties concerning hydrochemistry, see the background reports, cf Table 2-1. For a discussion on the representativity of groundwater samples in the bedrock see Section 2.2.5 and references therein.

### 9.3.1 Uncertainties in Chapter 3

The multivariate models in Chapter 3 are based on mean values per object and depth level. Due to the heterogeneity of the data, different objects in the plots are based on different numbers of observations, and thus show different levels of confidence. To give an idea of the variation among the large number of individual samples, all available data from data selection A (cf Sections 2.2.4 and 2.2.5) are projected onto the models:

- The Ion Source Model in Figure 3-3.
- The Water Origin Model in Figure 3-15.
- The Mixing Model in Figure 3-18.
- The "age model" in Figure 3-24.

It can be concluded from these figures that the distribution of the mean values in the models usually coincides with the distribution of the individual samples. If there is a large spread among individual samples, this may be an indication that there is considerable variation in the material and that conclusions based on mean values may be more uncertain (i.e. the standard deviation is large). In the Ion Source Model, dilute surface water samples show a larger spread among individual samples compared to the variation observed among groundwater samples. This is probably an effect of larger seasonal fluctuations in the surface system as well as greater influence from analytical uncertainties in dilute fresh waters.

To give an idea of the representativeness of different observations, all samples from KLX02 have been projected onto the Water Origin Model in Figure 3-16. This figure shows that the few samples that were regarded as representative (cf expert selection of groundwater data in Section 2.2.5) do not represent all available water types observed in this borehole; the cluster of samples in the lower part represent water influenced by evaporation, e.g. relict marine groundwater. Furthermore, the labels, which represent the absolute level of the sampled section, show that the accuracy of the depth determination is probably low in some samples, possibly due to artificial mixing and the use of less accurate sampling techniques such as "tube sampling".

Among the objects in the surface system, three stream sampling stations and one shallow groundwater object are evaluated in detail in Figure 9-1:

- SSM000241 has been singled out as particularly important due to its possible deep saline groundwater influence and its very deviant hydrochemistry with respect to several elements (cf Section 7.2). The four available analyses from this soil tube, three of which were discarded due to charge balance errors exceeding 15%, show marginal spread in the Ion Source Model.
- The stream sampling site PSM002072 (labelled PW072 in the figure) has a deviant hydrochemistry compared to most other stream sites. This discrepancy is attributable to anthropogenic spreading of road salt (cf Section 6.2.1) and most observations from this station were discarded when the mean value for this stream station was calculated due to large charge balance errors. This is mostly an effect of the very dilute waters at this site, which leads to large relative analytical errors and consequently large relative charge balance errors.
- Observations in the major catchment of the Laxemarån (PSM002087, labelled PW087), plot along the hypothetical marine mixing line "B", which is an indication that this spread mainly reflects seasonal fluctuations in road salt application (cf Section 6.2.1 and variations in water flow (cf Section 5.2).
- The third stream sampling site PSM002086 (labelled PW086), along with adjacent streams (PSM002076 and PSM002078), exhibits deviant hydrochemical characteristics, which may be attributed to the influence of an unidentified point source. Agricultural activities may be a potential source in this area.

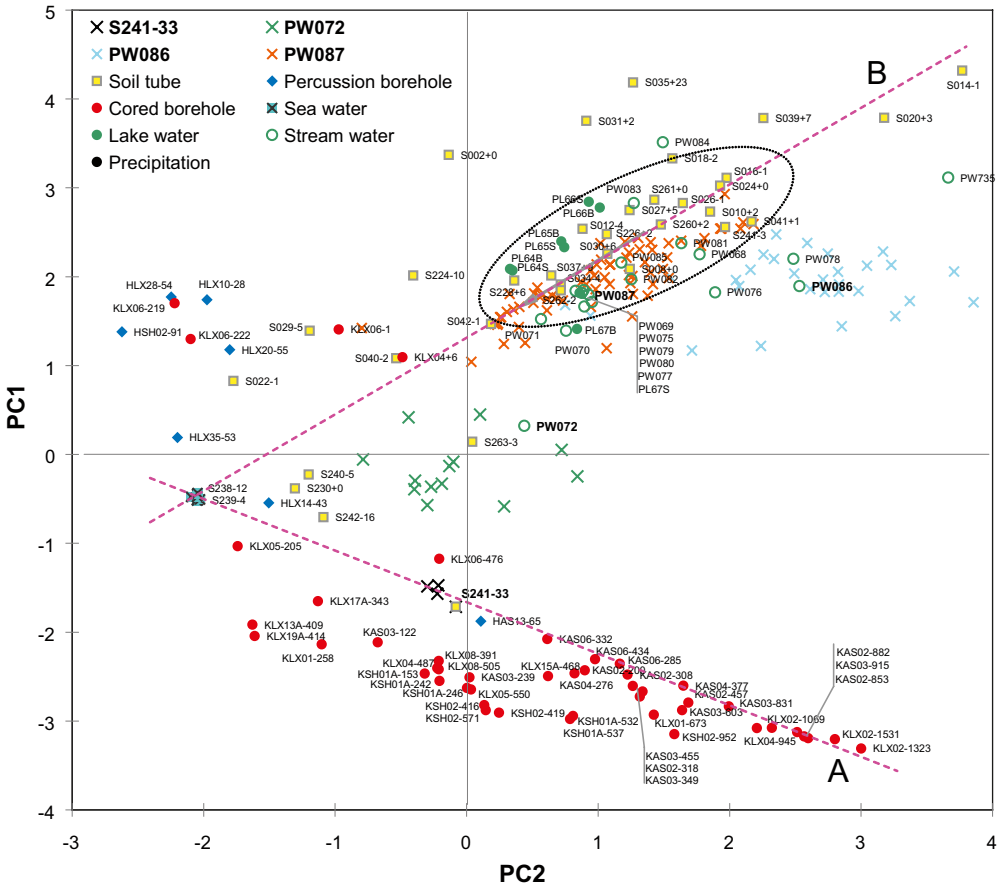


***Figure 9-1.*** *Individual observations of four objects highlighted in the Ion Source model (cf Section 3.2.5). The corresponding mean values (shown with bold labels) are not necessarily based on all these samples due to the selection criteria described in Sections 2.2.4 and 2.2.5.*

### 9.3.2 Uncertainties in Chapter 4

The visualisations in Chapter 4 are based on the same data as the models in Chapter 3. This suggests that the same conclusions regarding mean values apply to these plots as well. In several plots, all data have been included in the background as grey marks to give an idea of the spread and uncertainties in the material.

One parameter that may provide valuable information on deep saline influences is the $^{37}Cl$ isotope. However, the large analytical uncertainty in this parameter of ±0.2 units limits its usefulness, as this uncertainty is comparable to differences between major water types in the Laxemar-Simpevarp area. Theoretically significant discrepancies in time or space could be statistically detected if several recurring observations were available (this is not the case). However, there is a clear pattern evident in Figure 4-8 which seems to differentiate the observations into three categories: deep saline, marine and evaporative origin of Cl. This pattern is most probably not random and reflects the varying origin of Cl. Due to the analytical uncertainty, a single observation may thus not be classified with confidence, despite the significant overall pattern.

### 9.3.3 Uncertainties in Chapter 5

In Chapter 5, the use of hydrological data introduces uncertainties in addition to those associated with hydrochemical data discussed in previous sections:

- The hydrological field classification that is used to evaluate correlations between groundwater flow and hydrochemistry is based on a subjective estimate rather than physical

measurements. The varying depth of the intake screen also means that conditions at ground level, which determine the classification, are not necessarily reflected by the observed hydrochemical conditions.

- The hydrochemical parameters that reflect the variability in the correlation analysis between hydrochemistry and hydrological field classification are sometimes based on as few as three observations. This means that the standard deviation may not be correctly estimated, which leads to further uncertainties for these parameters.
- The estimate of water flow is based on several rough assumptions, which may entail considerable uncertainties. There are probably local deviations in specific discharge, which is assumed to be constant for the whole Laxemar-Simpevarp area. The temporal variation pattern, which is in turn based on a hydrological model with further built-in uncertainties and assumptions, is probably not exactly the same over the whole area.
- The total uncertainties associated with the estimation of water flow make it more difficult to identify correlations between hydrochemistry and water flow and affect mass transport estimates (which are the product of concentration and water flow). Accordingly, the uncertainties in mass transport estimates are relatively large.
- Transport estimates for trace elements entail additional uncertainties compared with transport estimates for major elements. This is due to the use of scale factors that relate a certain trace element to a major element for which transport estimates have been made. The orders of magnitude of these estimates are probably correct, but these figures should be used with caution, for example in comparisons between sites. The trace element and the correlated major element most probably differ with respect to response to e.g. biochemical processes and retention. These drawbacks are particularly problematic when the correlation with the major element is weak.

### 9.3.4 Uncertainties in Chapter 6

Mass balance models in chapter 6 are based on mass transport from Chapter 5, and the difficulties and uncertainties discussed in Section 9.3.3 also apply to this section.

- Besides uncertainties associated with the mass transport estimates, the use of a static model to describe phenomena that may have considerable seasonal dynamics can entail errors. The transport of some elements, such as phosphorus, are associated with episodes of high water flow, and these transport peaks may be underestimated if no measurements are made during these high flow events.
- Limitations inherent in the model structure may also restrict the possibility of modelling the spatial variation of an element, for example if considerable retention occurs before the water reaches the lakes, which may lead to poorer model results and greater uncertainties in the conclusions. This type of limitation is clearly demonstrated in the bad modelling result of the $HCO_3^-$ model in Section 6.2.8, where the sink due to neutralisation of $H^+$ is not accounted for in the model structure. In the Forsmark area, $HCO_3^-$ was satisfactorily modelled due to the plentiful supply of this ion from the calcite in the deposits and the marginal effect due to neutralisation of $H^+$ /Tröjbom et al. 2007/.
- The model set-up is also dependent on the subjective selection of governing factors. A correlation model is used to support this selection to formalise the process. Nevertheless, the partly subjective selection process introduces uncertainties.
- In most cases the selected factors lead to the convergence of the model towards only one stable solution. The calibration of the model may be perceived as solving an equation for local minima (minima in the respect that the discrepancy between modelled and observed concentrations is minimised). Theoretically, this equation with one, two, three or sometimes four free parameters may have several local minima as possible solutions for the mass balance in question.

- The accuracy of the mass balance models can be estimated via the estimates of road salt input from the line source road E22. As road salt mainly contains Na and Cl, independent estimates of the amounts of these elements may provide an indication of the accuracy of the models. If the estimated amounts of Na and K from road salt in the Laxemarån (26 and 2 tonnes, respectively) are compared with the amount of Cl (56 tonnes), approximately 75% of the Cl is balanced based on molar charge amounts. This discrepancy probably reflects uncertainties in the mass balance model rather than the actual situation (cf Section 7.5.1).

### 9.3.5 Uncertainties in Chapter 7

Uncertainties in Chapter 7 are mostly associated with the cross sections in the visualisations. There are uncertainties in the regolith depth model used to visualise profiles of different regolith types. The actual depth of boreholes may, for example, differ from the regolith depth model due to interpolation effects in the regolith depth model (measured points do not necessarily coincide with the layers in the regolith depth model). See /Nyman et al. 2008/ for further discussion of uncertainties associated with the regolith depth model. The interpolated mean groundwater table is also subject to uncertainties, as discussed in /Werner et al. 2008/.

# 10 References


**Aitchison J, Greenacre M, 2002.** Biplots for compositional data. Applied Statistics 51 (4), 375–392.

**Ask H, Tiberg L, Morosini M, 2007.** Summary of water pumping and release. Hydraulic disturbances from drilling and investigations during the site investigation in Oskarshamn, sub-areas Simpevarp and Laxemar, 2002–2007. SKB P-07-174, Svensk Kärnbränslehantering AB.

**Bosson M, 2006.** Near-surface hydrogeological model of Laxemar. Open repository – Laxemar 1.2. SKB R-06-66, Svensk Kärnbränslehantering AB.

**Brunberg A-K, Carlsson T, Brydsten L, Strömgren M, 2004.** Oskarshamn site investigation – Identification of catchments, lake-related drainage parameters and lake habitats. SKB P-04-242, Svensk Kärnbränslehantering AB.

**Brydsten L, Strömgren M, 2005.** Digital elevation models for site investigation programme in Oskarshamn. Site description version 1.2. SKB R-05-38, Svensk Kärnbränslehantering AB.

**Clark I D and Fritz P, 1997.** Environmental Isotopes in Hydrogeology. Boca Raton, FL: CRC Press.

**Chapra S, 1997.** Surface water-quality modelling. Boston, McGraw-Hill.

**Ericsson U, 2004.** Sampling of precipitation at Äspö 2003. Oskarshamn site investigation. SKB P-04-14, Svensk Kärnbränslehantering AB.

**Ericsson U, 2005.** Sampling of precipitation at Simpevarp 2004. Oskarshamn site investigation. SKB P-05-175, Svensk Kärnbränslehantering AB.

**Ericsson U, Engdahl A, 2004a.** Surface water sampling at Simpevarp 2002–2003. SKB P-04-13, Svensk Kärnbränslehantering AB.

**Ericsson U, Engdahl A, 2004b.** Surface water sampling in Oskarshamn October 2003 to February 2004. SKB P-04-75, Svensk Kärnbränslehantering AB.

**Ericsson U, Engdahl A, 2005.** Surface water sampling at Simpevarp 2004. SKB P-05-118, Svensk Kärnbränslehantering AB.

**Ericsson U, Engdahl A, 2007a.** Surface water sampling at Simpevarp 2005. Oskarshamn site investigation. SKB P-06-155, Svensk Kärnbränslehantering AB.

**Ericsson U, Engdahl A, 2007b.** Sampling and analysis of precipitation at Simpevarp 2005. Oskarshamn site investigation. SKB P-06-324, Svensk Kärnbränslehantering AB.

**Ericsson U, Engdahl A, 2007c.** Sampling and analysis of shallow groundwater at Simpevarp 2005. Oskarshamn site investigation. SKB P-06-325, Svensk Kärnbränslehantering AB.

**Fredén C (ed), 2002.** Berg och jord. Sveriges nationalatlas. Tredje utgåvan. 208 pp.

**Grimwall U, Stålnacke P, 1996.** Statistical methods for source apportionment of riverine loads of pollutants. Environmentrics 7:201–213.

**Gómez J B, Laaksoharju M, Skårman E, Gurban I, 2006.** M3 version 3.0: Concepts, methods, and mathematical formulation. SKB TR-06-27, Svensk Kärnbränslehantering AB.

**Hallbeck L, 2008.** Explorative analyses of microbes, colloids, and gases together with microbial modelling. SKB R-08-109, Svensk Kärnbränslehantering AB.

**Hallbeck L, 2009.** Evaluating hydrochemical data from shallow groundwater in Laxemar from a microbiological perspective. SKB R-09-02, Svensk Kärnbränslehantering AB.

**Johansson T, Göransson M, Zetterlund M, Jenkins K, Rönnback K, 2006.** Hydrogeological characterization in bogs, lakes and sea bays. SKB P-06-248, Svensk Kärnbränslehantering AB.

**Johansson P-O, Bosson E, Berglund S, Öhman J, Gustafsson L-G, Sassner M, Marelius F, Stenström P, Tröjbom M, Juston J, Follin S and Holgersson B, 2008.** Description of surface hydrology and near-surface hydrogeology. Site descriptive modelling, SDM-Site Forsmark, SKB R-08-08, Svensk Kärnbränslehantering AB, Stockholm, Sweden.

**Jolliffe, I T, 2002.** Principal component Analysis. Springer-Verlag, New York.

**Kehew A, 2001.** Applied chemical hydrogeology. Prentice Hall, New Jersey.

**Kendall C, McDonnell J, 2006.** Isotope tracers in catchment hydrology. Amsterdam, Elsevier**.**

**Kvarnäs H, 1997.** Modellering av näringsämnen i Vätterns tillrinningsområde – Källfördelning och retention. Vätternvårdsförbundet, Rapport nr 46 (in Swedish).

**Laaksoharju M, Skårman C, Skårman E, 1999.** Multivariate Mixing and Mass-balance (M3) calculations, a new tool for decoding hydrogeochemical information. Applied Geochemistry Vol. 14, #7, 1999, Elsevier Science Ltd, pp 861–871.

**Laaksoharju M (ed), 2008.** Bedrock Hydrogeochemistry Laxemar, Site descriptive modelling, SDM-Site Laxemar. SKB R-08-93, Svensk Kärnbränslehantering AB.

**Lindborg T (ed), 2005.** Description of surface systems. Preliminary site description Simpevarp subarea – version 1.2. SKB R-05-01, Svensk Kärnbränslehantering AB.

**Lindborg T (ed), 2006.** Description of surface systems. Preliminary site description Laxemar subarea – version 1.2. SKB R-06-11, Svensk Kärnbränslehantering AB.

**Lundin L, Lode Elve, Stendahl J, Björkvald L and Hansson J, 2005.** Soils and site types in the Oskarshamn area. Oskarshamn site investigation. SKB R-05-15, Svensk Kärnbränslehantering AB.

**Löfgren A, Lindborg T, 2003.** A descriptive ecosystem model – a strategy for model development during site investigations. SKB R-03-06. Svensk Kärnbränslehantering AB.

**Morosini M, Hultgren H, 2003.** Inventering av privata brunnar i Simpevarpsområdet, 2001–2002. SKB P-03-05, Svensk Kärnbränslehantering AB.

**Naturvårdsverket, 2000.** Environmental Quality Criteria – Lakes and water courses. Swedish Environmental Protections Agency Report 5050.

**Naturvårdsverket, 2003.** Åtgärder och kostnader för minskade fosforutsläpp från enskilda avlopp, industrier m.m. till sjön Glan: underlagsrapport (2) till Miljökvalitetsnormer för fosfor i sjöar – redovisning av ett regeringsuppdrag. NV rapport 5288 (in Swedish).

**Nyman H, 2005.** Depth and stratigraphy of Quaternary deposits. Preliminary site description Laxemar subarea – version 1.2. SKB R-05-54, Svensk Kärnbränslehantering AB.

**Nyman H, Sohlenius G, Strömgren M, Brydsten L, 2008.** Depth and stratigraphy of regolith, Site descriptive modelling, SDM-Site Laxemar. SKB R-08-06, Svensk Kärnbränslehantering AB.

**Ojala L, Mellqvist E, 2004.** Vägsalt – användning och påverkan på grundvattnet. SGU-rapport 2004:13.

**Peterman, Z and Wallin, B. 1999**. Synopsis of strontium isotope variations in groundwater at Äspö Hard Rock Laboratory, Southern Sweden. Applied Geochemistry, vol. 14:7, pp 953–962.

**Rozanski K, Araguás-Araguás L, Gonfiantini R, 1993.** Isotopic patterns in modern global precipitation. In: Continental Isotope Indicators of climate, American Geophysical Union Monograph.

**Rudmark L, Malmberg-Persson K, Mikko H, 2005.** Oskarshamn site investigation: Investigation of Quaternary deposits 2003–2004. SKB P-05-49. Svensk Kärnbränslehantering AB.

**SKB, 2001.** Site investigations. Investigation methods and general execution programme. SKB TR-01-29. Svensk Kärnbränslehantering AB.

**SKB, 2004.** Hydrogeochemical evaluation for Simpevarp model version 1.2. Preliminary site description of the Simpevarp area. SKB R-04-74, Svensk Kärnbränslehantering AB.

**SKB, 2005.** Preliminary site description. Simpevarp subarea – version 1.2. SKB R-05-08, Svensk Kärnbränslehantering AB.

**SKB, 2006a.** Hydrogeochemical evaluation. Preliminary site description Laxemar subarea – version 1.2. SKB R-06-12, Svensk Kärnbränslehantering AB.

**SKB, 2006b.** Preliminary site description. Laxemar subarea – version 1.2. SKB R-06-10, Svensk Kärnbränslehantering AB.

**SKB, 2006c.** Preliminary site description Laxemar stage 2.1. Feedback for completion of the site investigation including input from safety assessment and repository engineering.

**Sohlenius G, Hedenström A, 2008.** Description of the regolith at Laxemar, SDM-Site Laxemar. Site descriptive modelling, SDM-Site Laxemar. SKB R-08-05, Svensk Kärnbränslehantering AB.

**Sterner RW, Elser JJ, 2002.** Ecological stoichiometry. The biology of elements from molecules to the biosphere. Princeton University Press, Oxfordshire, U.K. 439 p.

**Söderbäck B (ed), 2008.** Geological evolution, palaeoclimate and historical development of the Forsmark and Laxemar-Simpevarp areas. Site descriptive modelling, SDM-Site. SKB R-08-19, Svensk Kärnbränslehantering AB.

**Söderbäck B, Lindborg T (eds), 2009.** Surface system Laxemar. Site descriptive modelling, SDM-Site Laxemar. SKB R-09-01, Svensk Kärnbränslehantering AB**.**

**Tröjbom M, Lindeström L, 2004.** Ämnestransporter i Dalälven 1990–2003. Länsstyrelsen i Dalarna rapport 2004:22 (in Swedish).

**Tröjbom M, Söderbäck B, 2006.** Chemical characteristics of surface systems in the Simpevarp area. Visualisation and statistical evaluation of data from surface water, shallow groundwater, precipitation and regolith. SKB R-06-18, Svensk Kärnbränslehantering AB.

**Tröjbom M, Söderbäck B, Johansson P-O, 2007.** Hydrochemistry in surface water and shallow groundwater. Site descriptive modelling SDM-Site Forsmark. SKB R-07-55, Svensk Kärnbränslehantering AB.

**Wahlgren C-H, Curtis P, Hermanson J, Forssberg O, Öhman J, Fox A, LaPointe P, Drake H, Triumf C-A, Mattsson H, Thunehed H, Juhlin C, 2008.** Geology Laxemar. Site descriptive modelling, SDM-Site Laxemar. SKB R-08-54, Svensk Kärnbränslehantering AB.

**Werner K, Bosson E, Berglund S, 2005a.** Description of climate, surface hydrology, and near-surface hydrogeology. Simpevarp 1.2. SKB R-05-04, Svensk Kärnbränslehantering AB.

**Werner K, Bosson E, Berglund S, 2005b.** Laxemar 1.2 – Description of meteorology, surface hydrology, and near-surface hydrogeology. SKB R-05-61, Svensk Kärnbränslehantering AB.

**Werner K, Öhman J, Holgersson B, Rönnback K, Marelius F, 2008.** Meteorological, hydrological and hydrogeological monitoring data and near-surface hydrogeological properties data from Laxemar. Site descriptive modelling, SDM-Site Laxemar, SKB R-08-71, Svensk Kärnbränslehantering AB.

**Web based references**

**ESRI, 2007.** EZ profiler for Arcmap 9.1 (Multi-layers & profile line version). Profiler 91.zip at http://arcscripts.esri.com/details.asp?dbid=13688. Accessed 2008-02-20.

**IMA, 2007.** The National survey of Lakes and Streams at http://info1.ma.slu.se/db.html. Accessed 2007-12-01.

**TRK, 2008.** http://www-nrciws.slu.se/TRK/. Accessed 2008-02-01.

**VTI, 2008.** http://www.vti.se/epibrowser/Webbdokument/Transportforum/TP-f%C3%B6redrag%202008/49%20F%C3%A4ltstudie%20av%20effektiviteten%20Edvardsson.pdf. Accessed 2008-02-01.

**Vägverket, 2008.** www.vv.se. Accessed 2008-02-01.

**Umetrics, 2008.** http://www.umetrics.com. Accessed 2008-02-01.

# Appendix A

1. Compilation of hydrochemical data from shallow groundwater used in the correlation study with hydrological parameters in Chapter 5.
2. Compilation of hydrological characteristics of soil tubes in the Laxemar-Simpevarp area.

| IDCODE | $HCO_3^-$ | | | Cl | | | $^2H$ | | | DOC | | | $^{18}O$ | | | pH | | | COND | | | $SO_4^{2-}$ | | | $^3H$ | | |
|---|---|---|---|---|---|---|---|---|---|---|---|---|---|---|---|---|---|---|---|---|---|---|---|---|---|---|---|
| | Count | Mean | Stddev | Count | Mean | CV | Count | Mean | Stddev | Count | Mean | CV | Count | Mean | Stddev | Count | Mean | Stddev | Count | Mean | CV | Count | Mean | CV | Count | Mean | CV |
| SSM000008 | 5 | 110 | 38 | 5 | 4 | 27 | 5 | -78 | 5 | 1 | 15 | | 5 | -10.9 | 0.8 | 5 | 6.8 | 0.2 | 5 | 22 | 22 | 5 | 8 | 20 | 5 | 13 | 19 |
| SSM000010 | 6 | 138 | 40 | 6 | 5 | 19 | 6 | -77 | 4 | 1 | 15 | | 6 | -10.8 | 0.7 | 6 | 6.9 | 0.4 | 6 | 28 | 25 | 5 | 20 | 34 | 6 | 13 | 14 |
| SSM000012 | 6 | 209 | 11 | 6 | 18 | 38 | 6 | -75 | 3 | 1 | 8 | | 6 | -10.4 | 0.6 | 6 | 7.5 | 0.1 | 6 | 53 | 12 | 6 | 69 | 21 | 6 | 10 | 15 |
| SSM000014 | 6 | 55 | 27 | 6 | 12 | 22 | 6 | -74 | 3 | 1 | 7 | | 6 | -10.4 | 0.6 | 6 | 6.3 | 0.2 | 6 | 28 | 18 | 6 | 61 | 16 | 6 | 14 | 12 |
| SSM000016 | 6 | 139 | 66 | 6 | 6 | 24 | 6 | -79 | 7 | 1 | 7 | | 6 | -10.8 | 1.0 | 6 | 6.6 | 0.2 | 6 | 29 | 38 | 6 | 20 | 41 | 6 | 13 | 10 |
| SSM000018 | 5 | 64 | 15 | 5 | 118 | 42 | 5 | -76 | 4 | 1 | 9 | | 5 | -10.5 | 0.8 | 5 | 6.2 | 0.2 | 5 | 80 | 26 | 5 | 102 | 53 | 5 | 12 | 14 |
| SSM000020 | 6 | 40 | 17 | 6 | 5 | 21 | 6 | -76 | 4 | 1 | 12 | | 6 | -10.4 | 0.8 | 6 | 6.1 | 0.2 | 6 | 22 | 22 | 6 | 54 | 28 | 6 | 13 | 17 |
| SSM000022 | 15 | 267 | 33 | 15 | 135 | 14 | 15 | -77 | 2 | 10 | 6 | 13 | 15 | -10.6 | 0.3 | 15 | 7.8 | 0.3 | 15 | 116 | 8 | 15 | 127 | 10 | 15 | 2 | 41 |
| SSM000024 | 5 | 68 | 30 | 5 | 7 | 32 | 5 | -76 | 5 | 1 | 19 | | 5 | -10.2 | 0.9 | 5 | 6.5 | 0.4 | 5 | 17 | 30 | 5 | 11 | 61 | 5 | 13 | 6 |
| SSM000026 | 6 | 57 | 27 | 6 | 6 | 16 | 6 | -76 | 4 | 1 | 13 | | 6 | -10.3 | 0.8 | 6 | 6.4 | 0.2 | 6 | 18 | 22 | 6 | 17 | 33 | 6 | 14 | 11 |
| SSM000027 | 6 | 10 | 7 | 6 | 5 | 26 | 6 | -79 | 3 | 4 | 4 | 11 | 6 | -11.0 | 0.2 | 6 | 5.6 | 0.3 | 6 | 9 | 23 | 6 | 14 | 36 | 6 | 10 | 8 |
| SSM000029 | 6 | 198 | 4 | 6 | 85 | 4 | 6 | -79 | 1 | 5 | 11 | 4 | 6 | -11.0 | 0.1 | 6 | 6.7 | 0.1 | 6 | 67 | 2 | 6 | 22 | 7 | 6 | 10 | 7 |
| SSM000030 | 12 | 254 | 6 | 12 | 15 | 18 | 12 | -78 | 2 | 10 | 9 | 5 | 12 | -10.9 | 0.1 | 12 | 7.1 | 0.1 | 12 | 52 | 7 | 12 | 42 | 13 | 12 | 9 | 12 |
| SSM000031 | 8 | 43 | 8 | 8 | 7 | 24 | 8 | -78 | 2 | 5 | 10 | 8 | 8 | -10.9 | 0.3 | 8 | 6.3 | 0.1 | 8 | 15 | 10 | 8 | 13 | 20 | 8 | 11 | 9 |
| SSM000034 | 6 | 529 | 16 | 6 | 119 | 14 | 6 | -78 | 1 | 5 | 7 | 4 | 6 | -11.0 | 0.1 | 6 | 6.9 | 0.1 | 6 | 119 | 3 | 6 | 0 | 69 | 6 | 14 | 10 |
| SSM000035 | 5 | 67 | 6 | 5 | 4 | 6 | 5 | -78 | 2 | 4 | 5 | 17 | 5 | -11.0 | 0.2 | 5 | 6.5 | 0.1 | 5 | 17 | 9 | 5 | 14 | 8 | 5 | 11 | 9 |
| SSM000037 | 12 | 196 | 20 | 12 | 29 | 40 | 12 | -79 | 1 | 10 | 8 | 50 | 12 | -11.0 | 0.1 | 12 | 6.9 | 0.2 | 12 | 49 | 8 | 12 | 38 | 35 | 12 | 8 | 16 |
| SSM000039 | 6 | 40 | 14 | 6 | 7 | 31 | 6 | -80 | 3 | 3 | 6 | 28 | 6 | -11.2 | 0.5 | 6 | 6.2 | 0.1 | 6 | 19 | 35 | 6 | 33 | 94 | 6 | 12 | 11 |
| SSM000040 | 5 | 157 | 19 | 5 | 147 | 25 | 5 | -78 | 3 | 0 | | | 5 | -10.8 | 0.2 | 5 | 6.7 | 0.2 | 5 | 94 | 33 | 5 | 18 | 42 | 3 | 12 | 5 |
| SSM000041 | 7 | 111 | 56 | 7 | 22 | 45 | 7 | -79 | 2 | 6 | 10 | 7 | 7 | -10.9 | 0.2 | 7 | 6.5 | 0.4 | 7 | 34 | 10 | 7 | 36 | 36 | 7 | 10 | 11 |
| SSM000042 | 12 | 171 | 33 | 12 | 85 | 26 | 12 | -77 | 2 | 9 | 7 | 12 | 12 | -10.8 | 0.2 | 12 | 6.9 | 0.4 | 12 | 77 | 19 | 12 | 92 | 18 | 12 | 8 | 11 |
| SSM000224 | 4 | 38 | 5 | 4 | 45 | 12 | 4 | -79 | 3 | 4 | 8 | 5 | 4 | -11.1 | 0.2 | 4 | 6.2 | 0.0 | 4 | 28 | 4 | 4 | 16 | 6 | 4 | 11 | 6 |
| SSM000226 | 4 | 91 | 73 | 4 | 6 | 45 | 4 | -79 | 3 | 4 | 14 | 29 | 4 | -11.1 | 0.3 | 4 | 6.7 | 0.4 | 4 | 22 | 53 | 4 | 10 | 33 | 4 | 11 | 10 |
| SSM000227 | 2 | 5 | 4 | 3 | 7 | 39 | 3 | -77 | 3 | 3 | 18 | 27 | 3 | -11.1 | 0.3 | 3 | 5.1 | 0.1 | 3 | 11 | 40 | 3 | 19 | 44 | 3 | 13 | 10 |
| SSM000228 | 8 | 126 | 28 | 8 | 37 | 164 | 8 | -79 | 1 | 8 | 13 | 5 | 8 | -11.0 | 0.3 | 8 | 6.6 | 0.2 | 8 | 42 | 59 | 8 | 37 | 28 | 8 | 10 | 28 |
| SSM000230 | 3 | 37 | 3 | 3 | 173 | 15 | 3 | -81 | 5 | 3 | 12 | 19 | 3 | -11.4 | 0.5 | 3 | 6.4 | 0.2 | 3 | 76 | 14 | 3 | 19 | 11 | 3 | 12 | 11 |
| SSM000240 | 5 | 264 | 13 | 5 | 609 | 21 | 5 | -75 | 1 | 5 | 10 | 2 | 5 | -10.3 | 0.2 | 5 | 7.4 | 0.1 | 5 | 242 | 17 | 5 | 57 | 16 | 5 | 9 | 10 |
| SSM000241 | 5 | 4223 | 2280 | 5 | 3964 | 56 | 5 | -68 | 6 | 5 | 68 | 52 | 5 | -9.3 | 1.0 | 5 | 6.8 | 0.3 | 5 | 1587 | 55 | 5 | 18 | 67 | 5 | 3 | 130 |

| Well no. | Location | Monitoring started | Ground elevation or mean surface water level (RHB70) | Mean sceen elevation (RHB70) | Mean screen depth (m below ground or mean water level) | Mean groundwater elevation (RHB70) | Mean groundwater depth below ground (m) | Min groundwater elevation | Max groundwater depth below ground (m) | Max groundwater elevation | Min groundwater depth below ground (m) | Groundwater level amplitude (m) | Local topography (100 x 100 m) | Local topography (100 x 100 m) (numerical) | Local topography (20 x 20 m) | Local topography (20 x 20 m) (numerical) | Location influence by surface water | If influence by surface water distance m | Soil depth | Soil at screen depth | Soil at screen depth (numerical) | Aquifer type | Aquifer type (numerical) | Forest % (100 x 100 m) | Forest % (20 x 20 m) | Open land (100 x 100 m) % | Open land (20 x 20 m) % | Water (%) (100 x 100 m) | Water (%) (20 x 20 m) | Built up area (%) (100 x 100 m) | Built up area (%) (20 x 20 m) | Tree layer (>30 %) (100 x 100 m) | Tree layer (>30 %) (20 x 20 m) | Shrub layer (<30 %) (100 x 100 m) | Shrub layer (>30 %) (20 x 20 m) | Water (%) (100 x 100 m) | Water (%) (20 x 20 m) | Built up area (%) (100 x 100 m) | Built up area (%) (20 x 20 m) | Site hydrology | Site hydrology (numerical) | Recharge/Discharge area | Recharge/Discharge area (numerical) | Recharge/discharge areas according to Molinero et al. |
|---|---|---|---|---|---|---|---|---|---|---|---|---|---|---|---|---|---|---|---|---|---|---|---|---|---|---|---|---|---|---|---|---|---|---|---|---|---|---|---|---|---|---|---|
| | | | GEL | MSE | MSD | MGE | MGD | MGE | MaGD | MaGE | MiGD | GLA | | LT100 | | LT20 | | SWD | SOD | | SCD | | AQT | F%100 | F%20 | O%100 | O%20 | W%100 | W%20 | B%100 | B%20 | | | | | | | | | | Shyd | | RD | |
| SSM000001 | Simpevarp | 04-06-30 | 2.79 | 0.81 | 1.98 | 1.31 | 1.48 | -0.2 | 2.99 | 1.93 | 0.86 | 2.13 | P | 9 | P | 9 | SEA | 30 | 2.20 | 1,2-1,3 Clay and silt<br>1,3-2,2 Moraine with silt and clay | | Confined? | | 80 | 10 | 0 | 0 | 20 | 0 | 0 | 0 | | | | | | | | | M=moist | 4 | D=discharge | 5 | |
| SSM000005 | | | 6.33 | 5.59 | 0.74 | | | | | | | | | | | | | | 1.50 | 0,15-1,50 Sand, mull | | | | | | | | | | | | | | | | | | | | | | | |
| SSM000008 | CLAB | 04-09-02 | 4.64 | 0.61 | 4.03 | 3.24 | 1.40 | 2.57 | 2.07 | 4.79 | -0.15 | 2.22 | | | | | | | 4.60 | Morän | 3 | Confined | | | | | | | | | | | | | | | | | | | | | |
| SSM000009 | Laxemar | | 14.92 | 11.82 | 3.10 | | | | | | | | SLL | 7 | F | 6 | B | 2 | 4.10 | 2,0-3,0 Siltig sandig morän<br>3,0-4,10 Morän med block | | | | 40 | 60 | 60 | 40 | 0 | 0 | 0 | 0 | | | | | | | | | D | 1 | R | 1 | |
| SSM000011 | Laxemar | 04-04-05 | 16.50 | 14.47 | 2.03 | 14.71 | 1.79 | 13.62 | 2.88 | 16.04 | 0.46 | 2.42 | SLM | 4 | SLM | 4 | - | - | 2.80 | 0,8-2,0 Grusig sand med block<br>2,0-2,8 Siltig sandig morän | | Unconfined | | | | | | | | | | | | | | | | | | D | 1 | D | 5 | |
| SSM000012 | Ävrö | 04-08-27 | 1.77 | -3.75 | 5.52 | 0.10 | 1.67 | -0.60 | 2.37 | 0.49 | 1.28 | 1.09 | | | | | | | 6.10 | Siltig, sandig morän | 2 | Confined | | | | | | | | | | | | | | | | | | | | | |
| SSM000014 | Hålö | 04-09-14 | 1.64 | -0.89 | 2.53 | 0.04 | 1.60 | -0.32 | 1.96 | 0.53 | 1.11 | 0.85 | | | | | | | 2.40 | Sandig grusig morän | 2 | Confined | | | | | | | | | | | | | | | | | | | | | |
| SSM000016 | Ävrö | | 1.87 | -0.13 | 2.00 | | | | | | | | CH | 8 | F | 6 | SEA | 75 | 2.80 | 0,25-1,8 Grusig sand med sten<br>1,8-2,6 Morän med block | | | | 70 | 20 | 30 | 80 | 0 | 0 | 0 | 0 | | | | | | | | | F | 2 | PD | 4 | |
| SSM000018 | Ävrö | 04-08-27 | 0.78 | -1.75 | 2.53 | -0.78 | 1.56 | -2.37 | 3.15 | -0.05 | 0.83 | 2.32 | Ch=channel | 8 | F | 6 | B | 15 | 3.10 | 1,8-2,0 Blockig sandmorän<br>2,0-2,8 Sandmorän | 2 | Confined | | 20 | 5 | 80 | 95 | 0 | 0 | 0 | 0 | | | | | | | | | M | 4 | D | 5 | |
| SSM000020 | Ävrö | | 5.62 | 3.63 | 1.99 | | | | | | | | SLL | 7 | F | 6 | - | - | 2.30 | 0,6-2,0 Lera<br>2,0-2,3 Grusig sandig morän | | | | 90 | 90 | 10 | 10 | 0 | 0 | 0 | 0 | | | | | | | | | F | 2 | PD | 4 | |
| SSM000021 | Laxemar | 04-09-02 tom 05-04-0 | 12.83 | 9.10 | 3.53 | 11.06 | 1.57 | 10.70 | 1.93 | 11.83 | 0.80 | 1.13 | Ch=channel | 8 | F | 6 | B | 3 | När ej till berg | Friktionsmaterial | | Semiconfined? | | 5 | 0 | 95 | 100 | 0 | 0 | 0 | 0 | | | | | | | | | F | 2 | D | 5 | |
| SSM000022 | Ävrö | 04-09-02 | 5.03 | -1.00 | 6.03 | 3.64 | 1.39 | 3.12 | 1.91 | 4.02 | 1.01 | 0.90 | Ch=channel | 8 | F | 6 | B | 15 | 8.60 | 4,6-4,8 Siltig lerig<br>4,8-5,4 Siltig sandig morän<br>5,4-6,6 Blockig morän | | Confined | | 100 | 100 | 0 | 0 | 0 | 0 | 0 | 0 | | | | | | | | | M | 4 | D | 5 | |
| SSM000024 | Ävrö | | 2.36 | 0.11 | 2.24 | | | | | | | | SLL | 7 | SLL | 7 | W | 20 | 4.20 | 1,0-1,6 Lerig, grusig sand<br>1,6-4,2 Sandig morän | | | | 100 | 100 | 0 | 0 | 0 | 0 | 0 | 0 | | | | | | | | | F | 2 | D | 5 | |
| SSM000026 | Ävrö | | 2.47 | -0.33 | 2.80 | | | | | | | | F | 6 | F | 6 | - | - | 4.20 | 1,7-4,2 Sandig morän | | | | 70 | 70 | 30 | 30 | 0 | 0 | 0 | 0 | | | | | | | | | F | 2 | PD | 4 | |
| SSM000027 | Laxemar | 05-07-01 | 9.21 | 5.18 | 4.03 | 6.61 | 2.60 | 6.53 | 2.68 | 6.73 | 2.48 | 0.20 | | | | 6 | | | När ej till berg | 2,8-4,0 Siltig sand<br>4,0-4,8 Sand | 1 | Unconfined? (gyttja) | | | | | | | | | | | | | | | | | | | | | |
| SSM000028 | Laxemar | 05-06-14 | 4.09 | 1.56 | 2.53 | 2.36 | 1.73 | 1.53 | 2.56 | 2.53 | 1.56 | 1.00 | F | 6 | F | 6 | W | 0 | När ej till berg | Torv med gyttja | | Unconfined? | | 10 | 0 | 90 | 100 | 0 | 0 | 0 | 0 | | | | | | | | | W | 5 | D | 5 | |
| SSM000029 | Laxemar | 05-06-14 | 1.26 | -4.77 | 6.03 | 2.31 | -1.05 | 2.12 | -0.86 | 2.50 | -1.24 | 0.38 | SLL | 7 | F | 6 | W | 0 | När ej till berg | Siltig finsand | 1 | Unconfined? (gyttja) | | 10 | 0 | 90 | 100 | 0 | 0 | 0 | 0 | | | | | | | | | M | 4 | D | 5 | |
| SSM000030 | Laxemar | 05-04-18 | 11.19 | 6.67 | 4.52 | 9.61 | 1.58 | 9.20 | 1.99 | 9.83 | 1.36 | 0.63 | Ch=channel | 8 | F | 6 | B | 1 | 3.90 | 2,8-3,0 Gyttja<br>3,0-3,8 Grusig sandig morän | | Confined? | | 30 | 0 | 70 | 100 | 0 | 0 | 0 | 0 | | | | | | | | | FM | 3 | D | 5 | |
| SSM000031 | Laxemar | 05-04-08 | 6.32 | 2.79 | 3.53 | 4.74 | 1.58 | 4.49 | 1.83 | 5.10 | 1.22 | 0.61 | Ch=channel | 8 | F | 6 | B | 1 | När ej till berg | 2,4-2,5 Siltig sandig morän<br>2,5-3,4 Grusig sandig morän | | Unconfined? | | 15 | 5 | 90 | 85 | 0 | 10 | 0 | 0 | | | | | | | | | F | 2 | D | 5 | |
| SSM000032 | Laxemar | 05-04-18 | 2.81 | -0.72 | 3.53 | 1.73 | 1.08 | -0.90 | 3.71 | 1.94 | 0.87 | 2.84 | Ch=channel | 8 | F | 6 | - | - | När ej till berg | Gyttja | | Unconfined? | | 100 | 100 | 0 | 0 | 0 | 0 | 0 | 0 | | | | | | | | | M | 4 | D | 5 | |
| SSM000033 | Laxemar | 05-04-18 | 5.82 | 4.28 | 1.53 | 4.78 | 1.04 | 4.37 | 1.45 | 5.06 | 0.76 | 0.69 | SLL | 7 | SLL | 7 | W | 0 | När ej till berg | 0,3-1,0 Sandig lera<br>1,0-1,3 Lerig sandig morän | | Confined? | | 100 | 100 | 0 | 0 | 0 | 5 | 0 | 0 | | | | | | | | | W | 5 | D | 5 | |
| SSM000034 | Laxemar | 05-04-18 | 0.48 | -3.06 | 3.54 | -0.07 | 0.55 | -3.20 | 3.68 | 0.17 | 0.31 | 3.37 | SLL | 7 | F | 6 | W | 0 | När ej till berg | 2,8-3,5 Finsand | | Confined? | | 50 | 0 | 50 | 100 | 0 | 0 | 0 | 0 | | | | | | | | | W | 5 | D | 5 | |
| SSM000035 | Laxemar | 05-06-15 | 27.11 | 23.60 | 3.51 | 25.51 | 1.60 | 25.16 | 1.95 | 25.86 | 1.25 | 0.70 | | | | | | | När ej till berg | Sandig siltig morän | 2 | Confined? | | | | | | | | | | | | | | | | | | | | | |
| SSM000037 | Laxemar | 05-04-08 | 12.70 | 9.17 | 3.53 | 10.55 | 2.15 | 10.42 | 2.28 | 10.90 | 1.80 | 0.48 | Ch=channel | 8 | F | 6 | B | 2 | 3.80 | Sandig grusig morän | 2 | Unconfined | | 5 | 10 | 95 | 80 | 0 | 10 | 0 | 0 | | | | | | | | | F | 2 | D | 5 | |
| SSM000039 | Laxemar | 05-07-01 | 11.70 | 7.68 | 4.02 | 7.20 | 4.50 | 6.52 | 5.18 | 7.56 | 4.14 | 1.04 | SLL | 7 | F | 6 | B | 70 | När ej till berg | Sandig morän | 2 | Unconfined | | 5 | 0 | 95 | 100 | 0 | 0 | 0 | 0 | | | | | | | | | F | 2 | R | 1 | |
| SSM000040 | Laxemar | 05-07-01 | 1.16 | -1.38 | 2.53 | -0.23 | 1.39 | -0.61 | 1.77 | 0.09 | 1.07 | 0.70 | SLL | 7 | F | 6 | SEA | 5 | När ej till berg | 1,1-1,6 Torv<br>1,6-2,1 Siltig sandig morän | | Confined | | 30 | 10 | 30 | 85 | 40 | 5 | 0 | 0 | | | | | | | | | M | 4 | D | 5 | |
| SSM000041 | Laxemar | 05-07-01 | 4.15 | 1.14 | 3.01 | 1.93 | 2.22 | 1.83 | 2.32 | 2.11 | 2.04 | 0.28 | S | | F | 6 | B | 5 | När ej till berg | 1,2-3,0 Sandig lerig silt<br>3,0-3,2 Sandig siltig morän | | Unconfined | | 30 | 20 | 70 | 75 | 0 | 5 | 0 | 0 | | | | | | | | | F | 2 | D | 5 | |
| SSM000042 | Laxemar | 05-06-15 | 3.35 | -0.83 | 4.18 | 1.23 | 2.12 | -1.27 | 4.62 | 1.77 | 1.58 | 3.04 | F | 6 | F | 6 | B | 5 | När ej till berg | 2,5-3,0 Grusig sand<br>3,0-3,5 Siltig sandig morän<br>3,5-4,2 Berg eller block | | Unconfined | | 10 | 0 | 90 | 100 | 0 | 0 | 0 | 0 | | | | | | | | | FM | 3 | D | 5 | |
| SSM000212 | Laxemar | | 13.28 | 12.08 | 1.20 | | | | | | | | SLM | 4 | SLM | 4 | - | - | 3.80 | 0,2-1,0 Grusig sand (svallad morän?)<br>1,0-1,8 Stenig, grusig, sandig morän | | | | 0 | 0 | 100 | 100 | 0 | 0 | 0 | 0 | | | | | | | | | D | 1 | PD | 4 | |
| SSM000213 | Laxemar | | 11.66 | 10.36 | 1.30 | | | | | | | | F | 6 | F | 6 | - | - | 1.50 | 0,0-0,5 Lerig gyttja<br>0,5-1,1 Sandig lera<br>1,1-1,5 Morän<br>1,5-1,8 Berg | | | | 0 | 0 | 100 | 100 | 0 | 0 | 0 | 0 | | | | | | | | | M | 4 | PD | 4 | |
| SSM000218 | Laxemar | 05-06-29 | | 16.40 | | 17.06 | -17.06 | 15.91 | -15.91 | 18.56 | -18.56 | 2.65 | SLM | 4 | SLM | 4 | B | 5 | 2.90 | Info saknas | | | | 50 | 30 | 50 | 70 | 0 | 0 | 0 | 0 | | | | | | | | | D | 1 | R | 1 | |
| SSM000219 | Laxemar | 05-06-29 | 16.27 | 11.74 | 4.53 | 14.74 | 1.53 | 13.90 | 2.37 | 15.43 | 0.84 | 1.53 | Ch=channel | 8 | F | 6 | B | 7 | 4.70 | Siltig sandmorän | 2 | Confined | | 80 | 70 | 20 | 30 | 0 | 0 | 0 | 0 | | | | | | | | | M | 4 | D | 5 | |
| SSM000220 | Laxemar | 05-06-15 | 13.13 | 10.60 | 2.53 | 12.57 | 0.56 | 10.10 | 3.03 | 12.80 | 0.33 | 2.70 | SLL | 7 | SLL | 7 | - | - | 2.80 | 1,7-2,0 Sandig morän<br>2,0-2,7 Blockig grusig sandmorän | | Confined | | 80 | 80 | 20 | 20 | 0 | 0 | 0 | 0 | | | | | | | | | M | 4 | D | 5 | |
| SSM000221 | Laxemar | 05-06-15 | 13.17 | 10.64 | 2.53 | 12.71 | 0.46 | 11.85 | 1.32 | 12.81 | 0.36 | 0.96 | Ch=channel | 8 | F | 6 | - | - | 2.80 | Blockig siltig sandmorän | | Unconfined | | 80 | 90 | 20 | 10 | 0 | 0 | 0 | 0 | | | | | | | | | FM | 3 | D | 5 | |
| SSM000222 | Laxemar | 05-11-24 | 12.79 | 8.25 | 4.53 | 11.27 | 1.52 | 11.20 | 1.59 | 11.39 | 1.40 | 0.19 | Ch=channel | 8 | F | 6 | B | 2 | 4.90 | 3,8-4,5 sandig morän,enstaka block<br>4,5-4,8 berg | | Unconfined? | | 5 | 10 | 95 | 90 | 0 | 10 | 0 | 0 | | | | | | | | | F | 2 | D | 5 | |
| SSM000223 | Laxemar | 05-11-24 | 13.69 | 6.67 | 7.03 | 10.86 | 2.83 | 10.75 | 2.94 | 10.97 | 2.72 | 0.22 | SLL | 7 | F | 6 | B | 35 | 7.80 | Blockig sandig morän | 2 | Unconfined? | | 40 | 50 | 60 | 50 | 0 | 0 | 0 | 0 | | | | | | | | | F | 2 | PD | 4 | |
| SSM000224 | Laxemar | 05-11-24 | 6.90 | -9.63 | 16.53 | 5.04 | 1.86 | 4.89 | 2.01 | 5.14 | 1.76 | 0.25 | Ch=channel | 8 | F | 6 | - | - | 16.80 | Grusig sand | 1 | Confined | | 40 | | 60 | | 0 | 0 | 0 | 0 | | | | | | | | | D | 1 | PR | 2 | |
| SSM000225 | Laxemar | 05-11-24 | 6.94 | -2.59 | 9.53 | 5.04 | 1.90 | 4.88 | 2.06 | 5.14 | 1.80 | 0.26 | Ch=channel | 8 | F | 6 | - | - | 9.80 | 8,7-8,8 Grusig sand<br>8,8-9,7 Stenigt sandigt grus | 1 | Confined | | 40 | 25 | 60 | 75 | 0 | 0 | 0 | 0 | | | | | | | | | D | 1 | PR | 2 | |
| SSM000226 | Laxemar | 05-11-24 | 6.97 | 2.44 | 4.53 | 6.18 | 0.79 | 5.75 | 1.22 | 6.81 | 0.16 | 1.06 | Ch=channel | 8 | SLL | 7 | B | 9 | 4.90 | Siltig grusig morän | | Confined | | 10 | 0 | 90 | 100 | 0 | 0 | 0 | 0 | | | | | | | | | FM | 3 | D | 5 | |
| SSM000227 | Laxemar | 05-11-24 | 7.28 | 5.75 | 1.53 | 5.94 | 1.34 | 5.50 | 1.78 | 6.41 | 0.87 | 0.91 | Ch=channel | 8 | SLL | 7 | B | 9 | 1.40 | 0,3-0,6 Multhaltig torv<br>0,6-0,9 Sitt<br>0,9-1,3 Siltig grusig sand | | Confined? | | 10 | 0 | 90 | 100 | 0 | 0 | 0 | 0 | | | | | | | | | FM | 3 | D | 5 | |
| SSM000228 | Laxemar | 05-11-24 | 13.09 | 6.56 | 6.53 | 10.16 | 2.93 | 10.07 | 3.02 | 10.24 | 2.85 | 0.17 | Ch=channel | 8 | F | 6 | B | 10 | 8.70 | 5,0-5,8 Sandig morän<br>5,8-6,0 Sandig siltig morän | 2 | Unconfined? | | 70 | 20 | 30 | 80 | 0 | 0 | 0 | 0 | | | | | | | | | F | 2 | PD | 4 | |
| SSM000229 | Laxemar | 05-11-24 | 13.68 | 10.14 | 3.53 | 11.18 | 2.50 | 10.61 | 3.07 | 11.63 | 2.05 | 1.02 | SLM | 4 | SLM | 4 | B | 40 | 3.80 | Grusig sandig morän | 2 | Unconfined | | 90 | 100 | 10 | 0 | 0 | 0 | 0 | 0 | | | | | | | | | F | 2 | PR | 2 | |
| SSM000230 | Laxemar | 05-11-24 | 5.10 | 0.57 | 4.53 | 0.65 | 4.45 | 0.52 | 4.58 | 0.75 | 4.35 | 0.23 | F | 6 | F | 6 | B | 100 | 4.70 | Blockig grusig sand | 1 | Unconfined | | 0 | 0 | 100 | 100 | 0 | 0 | 25 | 0 | | | | | | | | | F | 2 | R | 1 | |
| SSM000236 | Laxemar | | 15.67 | 13.87 | 1.80 | | | | | | | | CH | 8 | CH | 8 | - | - | 2.40 | 0,9-1,4 Lera<br>1,4-1,7 Lerig sandig silt<br>1,7-2,2 Sandig siltig morän<br>2,2-5,2 Berg | | | | 100 | 100 | 0 | 0 | 0 | 0 | 0 | 0 | | | | | | | | | M | 4 | D | 5 | |
| SSM000237 | Laxemar | 05-12-01 | 15.93 | 13.40 | 2.53 | 15.17 | 0.76 | 13.38 | 2.55 | 15.41 | 0.52 | 2.03 | Ch=channel | 8 | F | 6 | - | - | 2.80 | 1,7-1,9 Siltig lera med sandskikt<br>1,9-2,4 Sandig siltig morän<br>2,4-2,7 Berg | | Confined | | 100 | 100 | 0 | 0 | 0 | 0 | 0 | 0 | | | | | | | | | M | 4 | D | 5 | |
| SSM000244 | Laxemar | | 0.91 | -9.59 | 10.50 | | | | | | | | F | 6 | F | 6 | W | 0 | 11.10 | 9,60-11,00 Sandig morän | | | | 5 | 0 | 95 | 100 | 0 | 0 | 0 | 0 | | | | | | | | | M | 4 | D | 5 | |
| SSM000249 | Laxemar | 06-02-11 | 22.08 | 19.54 | 2.53 | Finns ej i SICADA | | | | | | | P | 9 | P | 9 | W | 0 | 2.50 | 1,4-2,2 Grusig sand<br>2,2-2,4 Berg | | Unconfined? (torv) | | 80 | 10 | 0 | 0 | 20 | 90 | 0 | 0 | | | | | | | | | W | 5 | D | 5 | |
| SSM000250 | Laxemar | 06-02-11 | 16.84 | 13.80 | 3.03 | Finns ej i SICADA | | | | | | | SLM | 4 | F | 6 | - | - | 3.20 | 1,1-1,2 Block<br>1,2-2,0 Siltig sandig morän<br>2,0-3,1 Grusig sandig morän | | Unconfined? (torv) | | 50 | 5 | 50 | 95 | 0 | 0 | 0 | 0 | | | | | | | | | FM | 3 | PR | 2 | |
| | | | | | | | | | | | | | Pe=peak | Pe=peak=1 | Pe=peak | Pe=peak=1 | | | | | Sand, gravel, stone=1 | Unconfined | Unconfined=1 | | | | | | | | | | | | | | C=coniferous | C=coniferous | C=coniferous | C=coniferous | | | | D=dry | D=dry=1 | D=discharge | Recharge area =1 | D=discharge |
| | | | | | | | | | | | | | R=ridge | R=ridge=2 | R=ridge | R=ridge=2 | Bl=brook<br>L=lake<br>S=sea<br>W=wetland<br>N=no | | | | Coarse till= sandy and gravelly till=2 | Semiconfined | Semiconfined=2 | Area centered around the well 100x100 m | Area centered around the well 20x20 m | Area centered around the well 100x100 m | Area centered around the well 20x20 m | Area centered around the well 100x100 m | Area centered around the well 20x20 m | Area centered around the well 100x100 m | Area centered around the well 20x20 m | M=mixed | M=mixed | M=mixed | M=mixed | | | | F=fresh | F=fresh=2 | R=recharge | Probable recharge area =2 | R=recharge |
| | | | | | | | | | | | | | Pa=pass | Pa=pass=5 | Pa=pass | Pa=pass=5 | | | | | Till unspecified=3 | Confined | Confined=3 | | | | | | | | | | | | | | D=decidous | D=decidous | D=decidous | D=decidous | | | | FM=fresh/moist | FM=fresh/moist =3 | I=varying | Varying=3 | |
| | | | | | | | | | | | | | Slope:<br>Slu=upper, Slm=mid, Sll=low, F=Flat | Slope:<br>Slu=upper=3, Slm=mid=4, Sll=low=7, F=Flat=6 | Slope:<br>Slu=upper, Slm=mid, Sll=low, F=Flat | Slope:<br>Slu=upper=3, Slm=mid=4, Sll=low=7, F=Flat=6 | | | | | Silty till=4 | | | | | | | | | | | | | | N< = 30 % | N= < 30 % | N= < 30 % | N= < 30 % | | | | M=moist | M=moist=4 | ( ) probable | Probable discharge area=4 | |
| | | | | | | | | | | | | | Ch=channel | Ch=channel=8 | Ch=channel | Ch=channel=8 | | | | | Clayey till=5 | | | | | | | | | | | | | | | | | | | | | W=wet | W=wet=5 | | Discharge area = 5 | |
| | | | | | | | | | | | | | Pit | Pit=9 | Pit | Pit=9 | | | | | | | | | | | | | | | | | | | | | | | | | | | | Oppet vatten=6 | | | |
| | | | | | | | | | | | | | Open water | Open water=10 | Open water | Open water=10 | | | | | | | | | | | | | | | | | | | | | | | | | | | | | | | |

# Appendix B

1. Compilation of original and lumped categories used in the VBX-II modelling.
2. Compilation of areas per catchment for each category included in the VBX-II model (land-use, topography, vegetation and regolith).

| VBX-VII class | Original code | Description |
|---|---|---|
| jClay | J6 | Gyttja |
| jClay | J16 | Lergyttja--gyttjelera |
| jClay | J17 | Postglacial lera, ospecificerad |
| jClay | J40 | Glacial lera, ospecificerad |
| jClay | J416 | Lergyttja--gyttjelera med tunt ytlager av torv |
| jClay | J440 | Glacial lera, ospecificerad med tunt ytlager av torv |
| jClay | J9401 | Glacial lera, ospecificerad med tunt ytlager av svallsediment, sand |
| jClay | J9402 | Glacial lera, ospecificerad med tunt ytlager av svallsediment, grus |
| jClay | J9405 | Glacial lera, ospecificerad med tunt ytlager av postglacialt sediment, lergyttja--gyttjelera |
| jClay | J9406 | Postglacial lera, ospecificerad med tunt ytlager av postglacialt sediment, lergyttja--gyttjelera |
| jPeat | J1 | Torv; mosse |
| jPeat | J5 | Torv; kärr |
| jRock | J890 | Urberg |
| jRock | J4111 | Urberg; med tunt ytlager av morän, sandig |
| jRock | J4112 | Urberg; med tunt ytlager av torv |
| jRock | J4113 | Urberg; med tunt ytlager av svallsediment, sand |
| jSand | J29 | Postglacial mellansand--grovsand |
| jSand | J30 | Svallsediment, sand |
| jSand | J32 | Postglacialt grus |
| jSand | J33 | Svallsediment, grus |
| jSand | J34 | Svallsediment, sten--block (klapper) |
| jSand | J92 | Sten--block (glacial och postglacial) |
| jSand | J290 | Fyllning på okänt underlag |
| jSand | J429 | Postglacial mellansand--grovsand med tunt ytlager av torv |
| jSand | J430 | Svallsediment, sand med tunt ytlager av torv |
| jSand | J432 | Postglacialt grus med tunt ytlager av torv |
| jSand | J433 | Svallsediment, grus med tunt ytlager av torv |
| jSand | J9403 | Svallsediment, sand med tunt ytlager av postglacialt sediment, lergyttja--gyttjelera |
| jTill | J50 | Isälvssediment, grovsilt--block |
| jTill | J59 | Morän på isälvssediment, grovsilt--block |
| jTill | J94 | Morän, lerig sandig |
| jTill | J95 | Morän, sandig |
| jTill | J96 | Morän, lerig sandig-siltig |
| jTill | J495 | Morän, sandig; med tunt ytlager av torv |
| jTill | J496 | Morän, lerig sandig-siltig; med tunt ytlager av torv |
| jTill | J9487 | Morän, lerig sandig-siltig; med tunt ytlager av svallsediment, sand |
| jTill | J9489 | Morän, sandig; med tunt ytlager av svallsediment, sand |
| jTill | J9490 | Morän, sandig; med tunt ytlager av postglacialt sediment, lergyttja--gyttjelera |
| jTill | J9491 | Morän, sandig; med tunt ytlager av glacial lera, ospecificerad |
| jWater | J91 | Vatten |
| mArable | Ma4 | Åker |
| mClear | Ma6 | Hygge |
| mForest | Ma2 | Skog, barr- och blandskog |
| mForest | Ma19 | Lövskog |
| mHard | Ma14 | Låghusbebyggelse |
| mHard | Ma15 | Industriområde |
| mOpen | Ma5 | Annan öppen mark |
| mOpen | Ma17 | Annan öppen mark utan skogskontur |
| mWater | Ma1 | Vattenyta |
|  | Veg0 | Information saknas |
|  | Veg1 | Oklassificerad |
| vClear | Veg45 | Äldre hyggen, sly/ängsartat frodigt |
| vClear | Veg46 | Äldre hyggen, ringa återväxt/block, stenar |
| vClear | Veg50 | Nya hyggen ej hygge -89 |
| vForest | Veg11 | Äldre gran, frisk-fuktig |
| vForest | Veg12 | Yngre gran, frisk-fuktig |
| vForest | Veg13 | Äldre tall, frisk-fuktig |
| vForest | Veg14 | Yngre tall, frisk-fuktig |
| vForest | Veg21 | Björkdominerad skog |
| vForest | Veg26 | Askdominerad skog |
| vForest | Veg30 | Blandskog barr-löv |
| vForest | Veg41 | Granungskog |
| vForest | Veg42 | Tallungskog |
| vForest | Veg43 | Ospecificerad barrungskog |
| vForest | Veg44 | Sly på hygge huvudsakl. björk |
| vHard | Veg92 | Industri |
| vHard | Veg93 | Låghus |
| vHard | Veg96 | Övriga hårda ytor/grus etc |
| vOpen | Veg81 | Odlad mark enligt topokarta |
| vOpen | Veg82 | Övrig öppen mark |
| vRock | Veg15 | Hällmarkstallskog |
| vRock | Veg83 | Kustklippor |
| vWater | Veg100 | Vatten |
| vWet | Veg61 | Grandominerad sankmark |
| vWet | Veg62 | Talldominerad sankmark |
| vWet | Veg63 | Björkdominerad sankmark |
| vWet | Veg64 | Hygge på myr |
| vWet | Veg72 | Frodig blöt myr |
| vWet | Veg74 | Frodig fastmattemyr |
| vWet | Veg75 | Frodig fastmattemyr med viden |
| vWet | Veg76 | Frodig fastmattemyr med björk |
| vWet | Veg77 | Vassdominerad torrare myr |
| vWet | Veg78 | Vass/frodigare, ev. buskar |
| vWet | Veg79 | Vassdominerad blötare myr |

| Idcode | Name | Area | Regolith classes | | | | | | Topographical elevation classes | | | | | | |
|---|---|---|---|---|---|---|---|---|---|---|---|---|---|---|---|
| | | | Jwater | Jsand | Jpeat | Jrock | Jclay | Jtill | 0-5m | 5-10m | 10-15m | 15-20m | 20-30m | 30-50m | 50-100m |
| | | km$^2$ | km$^2$ | km$^2$ | km$^2$ | km$^2$ | km$^2$ | km$^2$ | km$^2$ | km$^2$ | km$^2$ | km$^2$ | km$^2$ | km$^2$ | km$^2$ |
| ASM002474 | Kärrviksån | 0.117 | 0.000 | 0.005 | 0.000 | 0.111 | 0.000 | 0.001 | 0.000 | 0.000 | 0.000 | 0.003 | 0.104 | 0.010 | 0.000 |
| ASM002493 | Kärrviksån | 0.837 | 0.000 | 0.185 | 0.039 | 0.441 | 0.028 | 0.145 | 0.000 | 0.000 | 0.053 | 0.251 | 0.530 | 0.003 | 0.000 |
| ASM001483 | Kärrviksån | 0.151 | 0.000 | 0.061 | 0.000 | 0.053 | 0.024 | 0.013 | 0.000 | 0.000 | 0.001 | 0.080 | 0.071 | 0.000 | 0.000 |
| ASM002492 | Kärrviksån | 1.109 | 0.000 | 0.246 | 0.013 | 0.738 | 0.084 | 0.028 | 0.000 | 0.000 | 0.053 | 0.341 | 0.670 | 0.045 | 0.000 |
| ASM002491 | Kärrviksån | 1.872 | 0.001 | 0.047 | 0.066 | 1.147 | 0.057 | 0.555 | 0.000 | 0.082 | 0.380 | 0.508 | 0.763 | 0.139 | 0.000 |
| ASM001474 | Kärrviksån | 0.450 | 0.000 | 0.000 | 0.029 | 0.321 | 0.019 | 0.080 | 0.000 | 0.017 | 0.152 | 0.167 | 0.109 | 0.005 | 0.000 |
| ASM002487 | Kärrviksån | 1.200 | 0.000 | 0.000 | 0.044 | 0.818 | 0.097 | 0.240 | 0.000 | 0.138 | 0.218 | 0.298 | 0.453 | 0.093 | 0.000 |
| ASM001472 | Kärrviksån | 1.104 | 0.052 | 0.046 | 0.165 | 0.611 | 0.000 | 0.230 | 0.058 | 0.256 | 0.305 | 0.370 | 0.116 | 0.000 | 0.000 |
| ASM001470 | Kärrviksån | 0.398 | 0.000 | 0.006 | 0.028 | 0.154 | 0.008 | 0.202 | 0.032 | 0.094 | 0.161 | 0.094 | 0.017 | 0.000 | 0.000 |
| ASM001469 | Kärrviksån | 0.968 | 0.000 | 0.036 | 0.146 | 0.427 | 0.027 | 0.331 | 0.007 | 0.398 | 0.480 | 0.081 | 0.002 | 0.000 | 0.000 |
| ASM001471 | Kärrviksån | 2.794 | 0.000 | 0.039 | 0.493 | 1.453 | 0.068 | 0.741 | 0.387 | 0.706 | 0.926 | 0.675 | 0.100 | 0.000 | 0.000 |
| ASM001479 | Kärrviksån | 0.647 | 0.000 | 0.000 | 0.029 | 0.224 | 0.000 | 0.394 | 0.000 | 0.000 | 0.000 | 0.000 | 0.000 | 0.647 | 0.000 |
| ASM001480 | Kärrviksån | 0.103 | 0.000 | 0.000 | 0.003 | 0.074 | 0.003 | 0.023 | 0.000 | 0.000 | 0.000 | 0.000 | 0.004 | 0.099 | 0.000 |
| ASM002490 | Kärrviksån | 0.836 | 0.005 | 0.000 | 0.074 | 0.499 | 0.021 | 0.237 | 0.000 | 0.000 | 0.000 | 0.018 | 0.190 | 0.628 | 0.000 |
| ASM001478 | Kärrviksån | 0.493 | 0.000 | 0.000 | 0.067 | 0.348 | 0.000 | 0.078 | 0.000 | 0.000 | 0.000 | 0.002 | 0.410 | 0.081 | 0.000 |
| ASM002489 | Kärrviksån | 1.198 | 0.000 | 0.008 | 0.137 | 0.611 | 0.009 | 0.433 | 0.000 | 0.000 | 0.000 | 0.192 | 0.960 | 0.046 | 0.000 |
| ASM001476 | Kärrviksån | 3.619 | 0.000 | 0.004 | 0.235 | 1.611 | 0.288 | 1.480 | 0.000 | 0.112 | 0.581 | 1.467 | 1.448 | 0.011 | 0.000 |
| ASM001475B | Kärrviksån | 1.377 | 0.000 | 0.000 | 0.117 | 0.953 | 0.014 | 0.293 | 0.000 | 0.021 | 0.087 | 0.327 | 0.786 | 0.157 | 0.000 |
| ASM001475A | Kärrviksån | 0.044 | 0.000 | 0.000 | 0.015 | 0.025 | 0.000 | 0.006 | 0.000 | 0.024 | 0.011 | 0.009 | 0.000 | 0.000 | 0.000 |
| ASM002479 | Kärrviksån | 1.180 | 0.000 | 0.000 | 0.126 | 0.909 | 0.016 | 0.129 | 0.000 | 0.023 | 0.177 | 0.468 | 0.503 | 0.009 | 0.000 |
| ASM002486C | Kärrviksån | 2.748 | 0.007 | 0.011 | 0.192 | 1.932 | 0.034 | 0.572 | 0.000 | 0.027 | 0.234 | 0.304 | 1.032 | 1.152 | 0.000 |
| ASM002486B | Kärrviksån | 1.127 | 0.000 | 0.213 | 0.122 | 0.417 | 0.027 | 0.351 | 0.000 | 0.336 | 0.299 | 0.261 | 0.229 | 0.003 | 0.000 |
| ASM002486A | Kärrviksån | 2.933 | 0.001 | 0.390 | 0.301 | 1.098 | 0.087 | 1.059 | 0.523 | 1.262 | 0.701 | 0.310 | 0.136 | 0.000 | 0.000 |
| ASM002449 | Bjurhidebäcken | 0.632 | 0.000 | 0.001 | 0.035 | 0.244 | 0.000 | 0.352 | 0.008 | 0.090 | 0.402 | 0.132 | 0.000 | 0.000 | 0.000 |
| ASM002472 | Sörviksån | 0.470 | 0.000 | 0.000 | 0.032 | 0.255 | 0.000 | 0.184 | 0.025 | 0.156 | 0.221 | 0.067 | 0.000 | 0.000 | 0.000 |
| ASM002473 | Sörviksån | 0.530 | 0.000 | 0.000 | 0.027 | 0.394 | 0.000 | 0.110 | 0.067 | 0.339 | 0.120 | 0.004 | 0.000 | 0.000 | 0.000 |
| ASM002651 | Coastal area | 1.674 | 0.023 | 0.045 | 0.120 | 1.085 | 0.000 | 0.401 | 0.831 | 0.511 | 0.266 | 0.066 | 0.000 | 0.000 | 0.000 |
| ASM002447 | Bodvikebäcken | 0.380 | 0.077 | 0.000 | 0.036 | 0.178 | 0.000 | 0.088 | 0.267 | 0.103 | 0.010 | 0.000 | 0.000 | 0.000 | 0.000 |
| ASM002446 | Långbonäsbäcken | 0.070 | 0.000 | 0.000 | 0.019 | 0.038 | 0.000 | 0.013 | 0.043 | 0.027 | 0.000 | 0.000 | 0.000 | 0.000 | 0.000 |
| ASM002464 | Flakvarpebäcken | 0.184 | 0.016 | 0.000 | 0.031 | 0.021 | 0.000 | 0.117 | 0.127 | 0.055 | 0.003 | 0.000 | 0.000 | 0.000 | 0.000 |
| ASM002465 | Jössesbäcken | 0.111 | 0.000 | 0.000 | 0.007 | 0.022 | 0.015 | 0.067 | 0.088 | 0.023 | 0.000 | 0.000 | 0.000 | 0.000 | 0.000 |
| ASM002471 | Äspöbäcken | 0.063 | 0.000 | 0.002 | 0.006 | 0.032 | 0.000 | 0.023 | 0.029 | 0.033 | 0.001 | 0.000 | 0.000 | 0.000 | 0.000 |
| ASM002652 | Coastal area | 1.387 | 0.021 | 0.019 | 0.090 | 0.835 | 0.022 | 0.401 | 0.871 | 0.461 | 0.055 | 0.001 | 0.000 | 0.000 | 0.000 |
| ASM001445 | Frisksjön | 1.848 | 0.119 | 0.151 | 0.078 | 0.894 | 0.067 | 0.539 | 0.277 | 0.480 | 0.664 | 0.378 | 0.050 | 0.000 | 0.000 |
| ASM001484 | Kåreviksån | 0.213 | 0.000 | 0.000 | 0.030 | 0.091 | 0.000 | 0.092 | 0.093 | 0.092 | 0.027 | 0.001 | 0.000 | 0.000 | 0.000 |
| ASM001486B | Mederhultsån | 1.921 | 0.000 | 0.204 | 0.168 | 0.637 | 0.098 | 0.815 | 0.004 | 0.412 | 0.545 | 0.611 | 0.348 | 0.001 | 0.000 |
| ASM001486A | Mederhultsån | 0.082 | 0.000 | 0.008 | 0.000 | 0.063 | 0.000 | 0.011 | 0.019 | 0.033 | 0.029 | 0.002 | 0.000 | 0.000 | 0.000 |
| ASM002654 | Coastal area | 1.861 | 0.028 | 0.019 | 0.090 | 0.964 | 0.017 | 0.743 | 1.130 | 0.555 | 0.147 | 0.029 | 0.000 | 0.000 | 0.000 |
| ASM002460 | Pistlanbäcken | 0.499 | 0.005 | 0.013 | 0.038 | 0.307 | 0.008 | 0.127 | 0.080 | 0.167 | 0.190 | 0.060 | 0.002 | 0.000 | 0.000 |
| ASM001490 | Ekerumsån | 0.222 | 0.000 | 0.002 | 0.010 | 0.061 | 0.035 | 0.115 | 0.000 | 0.000 | 0.053 | 0.084 | 0.085 | 0.000 | 0.000 |
| ASM001489 | Ekerumsån | 0.767 | 0.000 | 0.020 | 0.008 | 0.347 | 0.153 | 0.239 | 0.000 | 0.000 | 0.157 | 0.382 | 0.228 | 0.000 | 0.000 |
| ASM002483B | Ekerumsån | 1.504 | 0.000 | 0.108 | 0.113 | 0.529 | 0.073 | 0.680 | 0.002 | 0.064 | 0.443 | 0.677 | 0.318 | 0.000 | 0.000 |
| ASM002483A | Ekerumsån | 0.341 | 0.000 | 0.020 | 0.044 | 0.116 | 0.019 | 0.141 | 0.161 | 0.113 | 0.047 | 0.019 | 0.001 | 0.000 | 0.000 |
| ASM002478 | Laxemarån | 0.023 | 0.000 | 0.000 | 0.000 | 0.000 | 0.000 | 0.023 | 0.000 | 0.000 | 0.000 | 0.000 | 0.000 | 0.023 | 0.000 |
| ASM002482 | Laxemarån | 0.867 | 0.000 | 0.118 | 0.106 | 0.007 | 0.000 | 0.636 | 0.000 | 0.000 | 0.000 | 0.000 | 0.014 | 0.853 | 0.000 |
| ASM002480B | Laxemarån | 4.234 | 0.162 | 0.279 | 0.512 | 0.388 | 0.005 | 2.888 | 0.000 | 0.000 | 0.000 | 0.000 | 0.028 | 3.896 | 0.310 |
| ASM002480A | Jämsen | 1.834 | 0.225 | 0.354 | 0.064 | 0.025 | 0.022 | 1.145 | 0.000 | 0.000 | 0.000 | 0.000 | 0.463 | 1.366 | 0.005 |
| ASM001516 | Laxemarån | 0.533 | 0.000 | 0.000 | 0.040 | 0.180 | 0.028 | 0.285 | 0.000 | 0.000 | 0.002 | 0.012 | 0.061 | 0.458 | 0.000 |
| ASM001515 | Laxemarån | 0.337 | 0.000 | 0.107 | 0.046 | 0.061 | 0.032 | 0.091 | 0.000 | 0.000 | 0.014 | 0.029 | 0.238 | 0.056 | 0.000 |
| ASM001514 | Laxemarån | 0.487 | 0.000 | 0.000 | 0.007 | 0.182 | 0.072 | 0.226 | 0.000 | 0.000 | 0.014 | 0.031 | 0.237 | 0.204 | 0.000 |
| ASM001446 | Plittorpsgöl | 0.678 | 0.034 | 0.007 | 0.037 | 0.481 | 0.007 | 0.114 | 0.000 | 0.000 | 0.000 | 0.000 | 0.079 | 0.599 | 0.000 |
| ASM002459 | Laxemarån | 0.099 | 0.000 | 0.000 | 0.009 | 0.042 | 0.000 | 0.048 | 0.000 | 0.000 | 0.011 | 0.007 | 0.054 | 0.027 | 0.000 |
| ASM001512 | Laxemarån | 0.494 | 0.000 | 0.000 | 0.052 | 0.221 | 0.007 | 0.214 | 0.000 | 0.000 | 0.004 | 0.013 | 0.167 | 0.310 | 0.000 |
| ASM002476E | Laxemarån | 3.949 | 0.003 | 0.478 | 0.533 | 1.112 | 0.129 | 1.694 | 0.000 | 0.000 | 0.189 | 0.457 | 1.299 | 2.004 | 0.000 |
| ASM001510 | Laxemarån | 0.562 | 0.000 | 0.004 | 0.082 | 0.371 | 0.002 | 0.103 | 0.000 | 0.000 | 0.000 | 0.000 | 0.418 | 0.144 | 0.000 |
| ASM002453 | Laxemarån | 0.445 | 0.001 | 0.000 | 0.025 | 0.300 | 0.002 | 0.116 | 0.000 | 0.000 | 0.004 | 0.013 | 0.322 | 0.106 | 0.000 |
| ASM002450B | Laxemarån | 2.392 | 0.005 | 0.004 | 0.345 | 1.581 | 0.042 | 0.415 | 0.000 | 0.000 | 0.041 | 0.126 | 1.455 | 0.769 | 0.000 |
| ASM002450A | Laxemarån | 0.187 | 0.000 | 0.000 | 0.073 | 0.037 | 0.003 | 0.074 | 0.000 | 0.032 | 0.121 | 0.031 | 0.002 | 0.000 | 0.000 |
| ASM001511 | Laxemarån | 0.740 | 0.000 | 0.000 | 0.105 | 0.370 | 0.006 | 0.260 | 0.000 | 0.000 | 0.027 | 0.074 | 0.398 | 0.241 | 0.000 |
| ASM001448 | Grangöl | 0.495 | 0.027 | 0.000 | 0.022 | 0.136 | 0.011 | 0.300 | 0.000 | 0.000 | 0.000 | 0.000 | 0.148 | 0.347 | 0.000 |
| ASM002499 | Laxemarån | 0.058 | 0.000 | 0.000 | 0.000 | 0.004 | 0.011 | 0.043 | 0.000 | 0.000 | 0.000 | 0.000 | 0.049 | 0.009 | 0.000 |
| ASM001506 | Laxemarån | 0.398 | 0.000 | 0.000 | 0.000 | 0.062 | 0.036 | 0.299 | 0.000 | 0.000 | 0.000 | 0.012 | 0.308 | 0.078 | 0.000 |
| ASM001447 | Fjällgöl | 0.295 | 0.021 | 0.008 | 0.024 | 0.103 | 0.000 | 0.140 | 0.000 | 0.000 | 0.000 | 0.000 | 0.179 | 0.116 | 0.000 |
| ASM002451 | Laxemarån | 0.325 | 0.000 | 0.000 | 0.000 | 0.079 | 0.036 | 0.210 | 0.000 | 0.000 | 0.001 | 0.066 | 0.248 | 0.010 | 0.000 |
| ASM002452 | Laxemarån | 2.375 | 0.002 | 0.000 | 0.100 | 0.731 | 0.179 | 1.364 | 0.000 | 0.026 | 0.020 | 0.085 | 1.021 | 1.223 | 0.000 |
| ASM001503 | Laxemarån | 0.416 | 0.000 | 0.000 | 0.002 | 0.159 | 0.055 | 0.199 | 0.000 | 0.050 | 0.151 | 0.165 | 0.050 | 0.000 | 0.000 |
| ASM002454 | Laxemarån | 0.808 | 0.000 | 0.000 | 0.102 | 0.312 | 0.107 | 0.286 | 0.000 | 0.039 | 0.468 | 0.231 | 0.068 | 0.002 | 0.000 |
| ASM001501 | Laxemarån | 0.806 | 0.000 | 0.000 | 0.052 | 0.302 | 0.082 | 0.369 | 0.000 | 0.000 | 0.091 | 0.277 | 0.435 | 0.002 | 0.000 |
| ASM002457 | Laxemarån | 1.389 | 0.000 | 0.001 | 0.028 | 0.305 | 0.262 | 0.794 | 0.000 | 0.016 | 0.316 | 0.661 | 0.396 | 0.000 | 0.000 |
| ASM002476D | Laxemarån | 4.963 | 0.000 | 0.024 | 0.636 | 2.113 | 0.177 | 2.015 | 0.000 | 0.434 | 0.831 | 1.124 | 2.259 | 0.314 | 0.000 |
| ASM001499 | Laxemarån | 0.711 | 0.000 | 0.003 | 0.053 | 0.310 | 0.022 | 0.322 | 0.000 | 0.009 | 0.207 | 0.282 | 0.213 | 0.000 | 0.000 |
| ASM001498 | Laxemarån | 2.771 | 0.000 | 0.045 | 0.310 | 0.882 | 0.069 | 1.465 | 0.000 | 0.090 | 0.615 | 0.731 | 1.188 | 0.146 | 0.000 |
| ASM001497 | Laxemarån | 0.609 | 0.000 | 0.003 | 0.045 | 0.307 | 0.044 | 0.210 | 0.000 | 0.005 | 0.059 | 0.157 | 0.387 | 0.001 | 0.000 |
| ASM002476C | Laxemarån | 0.315 | 0.001 | 0.008 | 0.046 | 0.064 | 0.012 | 0.194 | 0.000 | 0.088 | 0.113 | 0.086 | 0.028 | 0.000 | 0.000 |
| ASM001494 | Laxemarån | 1.001 | 0.000 | 0.006 | 0.026 | 0.316 | 0.152 | 0.501 | 0.002 | 0.199 | 0.473 | 0.315 | 0.013 | 0.000 | 0.000 |
| ASM001493 | Laxemarån | 0.319 | 0.000 | 0.000 | 0.008 | 0.122 | 0.026 | 0.162 | 0.004 | 0.066 | 0.181 | 0.068 | 0.001 | 0.000 | 0.000 |
| ASM001492 | Laxemarån | 0.460 | 0.000 | 0.002 | 0.009 | 0.209 | 0.054 | 0.186 | 0.047 | 0.182 | 0.203 | 0.028 | 0.000 | 0.000 | 0.000 |
| ASM001496 | Laxemarån | 0.890 | 0.000 | 0.011 | 0.034 | 0.264 | 0.067 | 0.514 | 0.004 | 0.095 | 0.187 | 0.399 | 0.203 | 0.001 | 0.000 |
| ASM001495 | Laxemarån | 0.290 | 0.000 | 0.001 | 0.016 | 0.020 | 0.005 | 0.248 | 0.000 | 0.045 | 0.124 | 0.115 | 0.006 | 0.000 | 0.000 |
| ASM002476B | Laxemarån | 3.231 | 0.004 | 0.055 | 0.158 | 0.584 | 0.234 | 2.202 | 0.326 | 0.949 | 1.350 | 0.570 | 0.035 | 0.000 | 0.000 |
| ASM002476A | Laxemarån | 0.188 | 0.000 | 0.031 | 0.032 | 0.029 | 0.004 | 0.096 | 0.098 | 0.069 | 0.021 | 0.000 | 0.000 | 0.000 | 0.000 |

| | | | | | | | | | | | | | | | | |
|---|---|---|---|---|---|---|---|---|---|---|---|---|---|---|---|---|
| ASM002495 | Glostadsbäcken | 0.126 | 0.000 | 0.001 | 0.016 | 0.068 | 0.001 | 0.040 | 0.040 | 0.061 | 0.025 | 0.000 | 0.000 | 0.000 | 0.000 |
| ASM002485 | Glostadsbäcken | 0.331 | 0.000 | 0.000 | 0.000 | 0.061 | 0.032 | 0.238 | 0.080 | 0.189 | 0.054 | 0.008 | 0.000 | 0.000 | 0.000 |
| ASM002498 | Glostadsbäcken | 1.597 | 0.008 | 0.008 | 0.071 | 0.543 | 0.170 | 0.797 | 0.440 | 0.428 | 0.565 | 0.162 | 0.002 | 0.000 | 0.000 |
| ASM001518B | Stålglobäcken | 0.679 | 0.000 | 0.008 | 0.028 | 0.257 | 0.085 | 0.302 | 0.012 | 0.250 | 0.326 | 0.091 | 0.000 | 0.000 | 0.000 |
| ASM001518A | Stålglobäcken | 0.354 | 0.000 | 0.000 | 0.021 | 0.074 | 0.034 | 0.225 | 0.161 | 0.156 | 0.036 | 0.000 | 0.000 | 0.000 | 0.000 |
| ASM002462 | Uvöbäcken | 0.967 | 0.000 | 0.000 | 0.094 | 0.216 | 0.035 | 0.622 | 0.410 | 0.380 | 0.172 | 0.006 | 0.000 | 0.000 | 0.000 |
| ASM002497 | Stekebäcken | 0.435 | 0.000 | 0.000 | 0.022 | 0.193 | 0.039 | 0.181 | 0.064 | 0.233 | 0.127 | 0.011 | 0.000 | 0.000 | 0.000 |
| ASM001517 | Stekebäcken | 0.903 | 0.000 | 0.017 | 0.107 | 0.270 | 0.027 | 0.482 | 0.433 | 0.431 | 0.040 | 0.000 | 0.000 | 0.000 | 0.000 |
| ASM002463 | Svartebäck | 0.504 | 0.002 | 0.014 | 0.007 | 0.103 | 0.000 | 0.378 | 0.067 | 0.282 | 0.136 | 0.019 | 0.000 | 0.000 | 0.000 |
| ASM002655 | Coastal area | 2.711 | 0.078 | 0.062 | 0.047 | 0.693 | 0.054 | 1.777 | 1.842 | 0.680 | 0.188 | 0.001 | 0.000 | 0.000 | 0.000 |
| ASM002658 | Coastal area | 1.261 | 0.017 | 0.000 | 0.037 | 0.421 | 0.016 | 0.770 | 0.595 | 0.486 | 0.176 | 0.003 | 0.000 | 0.000 | 0.000 |
| ASM002656 | Coastal area | 0.220 | 0.010 | 0.009 | 0.004 | 0.143 | 0.000 | 0.054 | 0.180 | 0.039 | 0.001 | 0.000 | 0.000 | 0.000 | 0.000 |
| ASM002660 | Coastal area | 0.138 | 0.007 | 0.000 | 0.000 | 0.099 | 0.000 | 0.033 | 0.099 | 0.034 | 0.005 | 0.000 | 0.000 | 0.000 | 0.000 |
| ASM002659 | Coastal area | 15.699 | 0.036 | 1.237 | 0.914 | 5.237 | 0.432 | 7.843 | 3.141 | 3.235 | 2.388 | 1.734 | 3.532 | 1.668 | 0.000 |
| ASM002657 | Coastal area | 2.597 | 0.009 | 0.070 | 0.041 | 0.341 | 0.064 | 2.072 | 0.520 | 0.623 | 0.832 | 0.557 | 0.065 | 0.000 | 0.000 |
| ASM001522 | Uthammarsån | 0.571 | 0.000 | 0.000 | 0.047 | 0.152 | 0.032 | 0.340 | 0.000 | 0.032 | 0.239 | 0.234 | 0.067 | 0.000 | 0.000 |
| ASM001523 | Uthammarsån | 0.958 | 0.000 | 0.051 | 0.028 | 0.229 | 0.092 | 0.559 | 0.000 | 0.006 | 0.283 | 0.284 | 0.353 | 0.032 | 0.000 |
| ASM001521 | Uthammarsån | 0.204 | 0.000 | 0.000 | 0.008 | 0.069 | 0.031 | 0.095 | 0.000 | 0.008 | 0.143 | 0.052 | 0.000 | 0.000 | 0.000 |
| ASM001520 | Uthammarsån | 0.081 | 0.000 | 0.000 | 0.000 | 0.027 | 0.017 | 0.038 | 0.000 | 0.009 | 0.065 | 0.007 | 0.000 | 0.000 | 0.000 |
| ASM002494B | Uthammarsån | 2.913 | 0.000 | 0.009 | 0.248 | 0.535 | 0.175 | 1.946 | 0.000 | 0.036 | 0.339 | 0.897 | 1.599 | 0.042 | 0.000 |
| ASM001533 | Uthammarsån | 0.512 | 0.000 | 0.003 | 0.021 | 0.175 | 0.078 | 0.236 | 0.000 | 0.143 | 0.309 | 0.060 | 0.000 | 0.000 | 0.000 |
| ASM002494A | Uthammarsån | 1.781 | 0.001 | 0.000 | 0.001 | 0.451 | 0.305 | 1.023 | 0.444 | 0.763 | 0.555 | 0.019 | 0.000 | 0.000 | 0.000 |
| ASM001528 | Släthultebäcken | 0.320 | 0.000 | 0.000 | 0.011 | 0.113 | 0.000 | 0.196 | 0.000 | 0.000 | 0.000 | 0.000 | 0.223 | 0.097 | 0.000 |
| ASM002477 | Släthultebäcken | 0.659 | 0.023 | 0.000 | 0.052 | 0.192 | 0.000 | 0.391 | 0.000 | 0.000 | 0.000 | 0.001 | 0.532 | 0.126 | 0.000 |
| ASM001531 | Släthultebäcken | 0.302 | 0.000 | 0.000 | 0.000 | 0.028 | 0.000 | 0.274 | 0.000 | 0.000 | 0.000 | 0.000 | 0.278 | 0.024 | 0.000 |
| ASM001532 | Släthultebäcken | 0.111 | 0.000 | 0.001 | 0.000 | 0.033 | 0.029 | 0.049 | 0.000 | 0.000 | 0.000 | 0.000 | 0.073 | 0.038 | 0.000 |
| ASM002455 | Släthultebäcken | 0.761 | 0.000 | 0.000 | 0.031 | 0.175 | 0.099 | 0.456 | 0.000 | 0.000 | 0.000 | 0.000 | 0.565 | 0.195 | 0.000 |
| ASM002475 | Släthultebäcken | 1.055 | 0.000 | 0.000 | 0.127 | 0.159 | 0.000 | 0.769 | 0.000 | 0.000 | 0.000 | 0.048 | 0.520 | 0.486 | 0.000 |
| ASM001526 | Släthultebäcken | 0.401 | 0.001 | 0.000 | 0.037 | 0.003 | 0.000 | 0.360 | 0.010 | 0.127 | 0.115 | 0.106 | 0.044 | 0.000 | 0.000 |
| ASM002481C | Släthultebäcken | 2.441 | 0.000 | 0.530 | 0.235 | 0.148 | 0.118 | 1.408 | 0.000 | 0.000 | 0.000 | 0.052 | 0.940 | 1.450 | 0.000 |
| ASM002481B | Släthultebäcken | 2.133 | 0.009 | 0.000 | 0.092 | 0.196 | 0.146 | 1.693 | 0.049 | 0.182 | 0.375 | 0.442 | 1.016 | 0.070 | 0.000 |
| ASM001525 | Släthultebäcken | 0.771 | 0.000 | 0.000 | 0.000 | 0.061 | 0.106 | 0.604 | 0.004 | 0.108 | 0.284 | 0.291 | 0.084 | 0.000 | 0.000 |
| ASM002481A | Släthultebäcken | 0.001 | 0.000 | 0.000 | 0.000 | 0.000 | 0.000 | 0.000 | 0.000 | 0.000 | 0.000 | 0.000 | 0.000 | 0.000 | 0.000 |
| ASM001444 | Söråmagasinet | 0.523 | 0.093 | 0.100 | 0.007 | 0.098 | 0.000 | 0.225 | 0.221 | 0.251 | 0.051 | 0.000 | 0.000 | 0.000 | 0.000 |
| ASM002466 | Stekflagebäcken | 0.359 | 0.025 | 0.006 | 0.033 | 0.158 | 0.000 | 0.136 | 0.215 | 0.109 | 0.035 | 0.000 | 0.000 | 0.000 | 0.000 |
| ASM002653 | Coastal area | 0.759 | 0.010 | 0.005 | 0.006 | 0.454 | 0.005 | 0.279 | 0.387 | 0.300 | 0.071 | 0.001 | 0.000 | 0.000 | 0.000 |
| ASM002470 | Skölkebäcken | 0.165 | 0.000 | 0.021 | 0.002 | 0.093 | 0.003 | 0.046 | 0.063 | 0.092 | 0.010 | 0.000 | 0.000 | 0.000 | 0.000 |
| ASM002469 | Gloebäcken | 0.131 | 0.000 | 0.018 | 0.001 | 0.068 | 0.002 | 0.043 | 0.022 | 0.088 | 0.021 | 0.000 | 0.000 | 0.000 | 0.000 |
| ASM002468 | Lindströmmebäcken | 0.192 | 0.000 | 0.001 | 0.002 | 0.085 | 0.014 | 0.090 | 0.063 | 0.114 | 0.014 | 0.000 | 0.000 | 0.000 | 0.000 |
| ASM002467B | Vadvikebäcken | 0.298 | 0.000 | 0.002 | 0.033 | 0.153 | 0.000 | 0.110 | 0.000 | 0.203 | 0.094 | 0.000 | 0.000 | 0.000 | 0.000 |
| ASM002467A | Vadvikebäcken | 0.009 | 0.000 | 0.001 | 0.000 | 0.003 | 0.000 | 0.005 | 0.002 | 0.007 | 0.000 | 0.000 | 0.000 | 0.000 | 0.000 |

| | | | Landuse classes | | | | | | Vegetation classes | | | | | | | |
|---|---|---|---|---|---|---|---|---|---|---|---|---|---|---|---|---|
| **Idcode** | **Name** | Area | Mwater | Mforest | Mclear | Marable | Mopen | Mhard | Vwater | Vwet | Vrock | Vforest | Vclear | Varable | Vopen | Vhard |
| | | km² | km² | km² | km² | km² | km² | km² | km² | km² | km² | km² | km² | km² | km² | km² |
| ASM002474 | Kärrviksån | 0.117 | 0.000 | 0.081 | 0.000 | 0.027 | 0.009 | 0.000 | 0.000 | 0.000 | 0.003 | 0.078 | 0.000 | 0.027 | 0.009 | 0.000 |
| ASM002493 | Kärrviksån | 0.837 | 0.000 | 0.672 | 0.000 | 0.138 | 0.027 | 0.000 | 0.000 | 0.010 | 0.053 | 0.585 | 0.026 | 0.140 | 0.023 | 0.000 |
| ASM001483 | Kärrviksån | 0.151 | 0.000 | 0.099 | 0.000 | 0.012 | 0.040 | 0.000 | 0.000 | 0.000 | 0.005 | 0.094 | 0.000 | 0.012 | 0.040 | 0.000 |
| ASM002492 | Kärrviksån | 1.109 | 0.000 | 0.815 | 0.000 | 0.145 | 0.148 | 0.001 | 0.000 | 0.054 | 0.181 | 0.604 | 0.000 | 0.148 | 0.122 | 0.001 |
| ASM002491 | Kärrviksån | 1.872 | 0.001 | 1.791 | 0.000 | 0.012 | 0.043 | 0.025 | 0.001 | 0.072 | 0.375 | 1.124 | 0.231 | 0.012 | 0.033 | 0.025 |
| ASM001474 | Kärrviksån | 0.450 | 0.000 | 0.432 | 0.000 | 0.000 | 0.018 | 0.000 | 0.000 | 0.007 | 0.021 | 0.401 | 0.010 | 0.000 | 0.000 | 0.000 |
| ASM002487 | Kärrviksån | 1.200 | 0.000 | 1.189 | 0.000 | 0.000 | 0.011 | 0.000 | 0.000 | 0.017 | 0.185 | 0.984 | 0.011 | 0.000 | 0.003 | 0.000 |
| ASM001472 | Kärrviksån | 1.104 | 0.043 | 0.943 | 0.000 | 0.022 | 0.096 | 0.000 | 0.043 | 0.068 | 0.111 | 0.770 | 0.043 | 0.022 | 0.000 | 0.000 |
| ASM001470 | Kärrviksån | 0.398 | 0.000 | 0.357 | 0.000 | 0.041 | 0.000 | 0.000 | 0.000 | 0.000 | 0.130 | 0.221 | 0.006 | 0.041 | 0.000 | 0.000 |
| ASM001469 | Kärrviksån | 0.968 | 0.000 | 0.950 | 0.000 | 0.013 | 0.005 | 0.000 | 0.000 | 0.005 | 0.105 | 0.838 | 0.001 | 0.013 | 0.005 | 0.000 |
| ASM001471 | Kärrviksån | 2.794 | 0.000 | 2.396 | 0.000 | 0.036 | 0.362 | 0.000 | 0.000 | 0.347 | 0.360 | 1.821 | 0.193 | 0.036 | 0.037 | 0.000 |
| ASM001479 | Kärrviksån | 0.647 | 0.000 | 0.640 | 0.000 | 0.000 | 0.007 | 0.000 | 0.000 | 0.015 | 0.120 | 0.355 | 0.157 | 0.000 | 0.000 | 0.000 |
| ASM001480 | Kärrviksån | 0.103 | 0.000 | 0.097 | 0.000 | 0.002 | 0.004 | 0.000 | 0.000 | 0.002 | 0.006 | 0.072 | 0.018 | 0.001 | 0.004 | 0.000 |
| ASM002490 | Kärrviksån | 0.836 | 0.004 | 0.771 | 0.014 | 0.005 | 0.041 | 0.000 | 0.004 | 0.026 | 0.234 | 0.409 | 0.137 | 0.005 | 0.021 | 0.000 |
| ASM001478 | Kärrviksån | 0.493 | 0.000 | 0.486 | 0.000 | 0.000 | 0.007 | 0.000 | 0.000 | 0.022 | 0.204 | 0.266 | 0.000 | 0.000 | 0.000 | 0.000 |
| ASM002489 | Kärrviksån | 1.198 | 0.000 | 1.160 | 0.000 | 0.012 | 0.026 | 0.000 | 0.000 | 0.031 | 0.381 | 0.737 | 0.031 | 0.012 | 0.006 | 0.000 |
| ASM001476 | Kärrviksån | 3.619 | 0.000 | 2.935 | 0.314 | 0.214 | 0.155 | 0.000 | 0.000 | 0.062 | 0.149 | 2.871 | 0.191 | 0.218 | 0.128 | 0.000 |
| ASM001475B | Kärrviksån | 1.377 | 0.000 | 1.277 | 0.000 | 0.028 | 0.072 | 0.000 | 0.000 | 0.048 | 0.389 | 0.832 | 0.022 | 0.029 | 0.037 | 0.000 |
| ASM001475A | Kärrviksån | 0.044 | 0.000 | 0.033 | 0.000 | 0.000 | 0.011 | 0.000 | 0.000 | 0.007 | 0.000 | 0.056 | 0.000 | 0.000 | 0.002 | 0.000 |
| ASM002479 | Kärrviksån | 1.180 | 0.000 | 1.156 | 0.000 | 0.000 | 0.024 | 0.000 | 0.000 | 0.041 | 0.375 | 0.739 | 0.020 | 0.000 | 0.004 | 0.000 |
| ASM002486C | Kärrviksån | 2.748 | 0.007 | 2.516 | 0.095 | 0.010 | 0.102 | 0.017 | 0.007 | 0.114 | 0.603 | 1.594 | 0.335 | 0.010 | 0.066 | 0.017 |
| ASM002486B | Kärrviksån | 1.127 | 0.000 | 0.799 | 0.000 | 0.010 | 0.201 | 0.116 | 0.000 | 0.067 | 0.083 | 0.705 | 0.001 | 0.012 | 0.144 | 0.117 |
| ASM002486A | Kärrviksån | 2.933 | 0.000 | 2.420 | 0.000 | 0.313 | 0.198 | 0.000 | 0.000 | 0.111 | 0.530 | 1.827 | 0.051 | 0.319 | 0.106 | 0.001 |
| ASM002449 | Bjurhidebäcken | 0.632 | 0.000 | 0.600 | 0.000 | 0.024 | 0.008 | 0.000 | 0.000 | 0.007 | 0.248 | 0.348 | 0.000 | 0.024 | 0.005 | 0.000 |
| ASM002472 | Sörviksån | 0.470 | 0.000 | 0.449 | 0.000 | 0.021 | 0.001 | 0.000 | 0.000 | 0.010 | 0.230 | 0.210 | 0.000 | 0.020 | 0.001 | 0.000 |
| ASM002473 | Sörviksån | 0.530 | 0.000 | 0.510 | 0.000 | 0.008 | 0.013 | 0.000 | 0.000 | 0.003 | 0.282 | 0.226 | 0.000 | 0.008 | 0.012 | 0.000 |
| ASM002651 | Coastal area | 1.674 | 0.004 | 1.467 | 0.000 | 0.017 | 0.185 | 0.000 | 0.019 | 0.099 | 0.537 | 0.934 | 0.006 | 0.018 | 0.061 | 0.000 |
| ASM002447 | Bodvikebäcken | 0.380 | 0.077 | 0.300 | 0.000 | 0.000 | 0.003 | 0.000 | 0.077 | 0.007 | 0.081 | 0.215 | 0.000 | 0.000 | 0.000 | 0.000 |
| ASM002446 | Långbonäsbäcken | 0.070 | 0.000 | 0.070 | 0.000 | 0.000 | 0.000 | 0.000 | 0.000 | 0.013 | 0.011 | 0.046 | 0.000 | 0.000 | 0.000 | 0.000 |
| ASM002464 | Flakvarpebäcken | 0.184 | 0.015 | 0.142 | 0.000 | 0.000 | 0.027 | 0.000 | 0.014 | 0.029 | 0.011 | 0.130 | 0.000 | 0.000 | 0.000 | 0.000 |
| ASM002465 | Jössesbäcken | 0.111 | 0.000 | 0.092 | 0.000 | 0.000 | 0.019 | 0.000 | 0.000 | 0.000 | 0.003 | 0.089 | 0.000 | 0.000 | 0.019 | 0.000 |
| ASM002471 | Åspöbäcken | 0.063 | 0.000 | 0.063 | 0.000 | 0.000 | 0.000 | 0.000 | 0.000 | 0.005 | 0.017 | 0.041 | 0.000 | 0.000 | 0.000 | 0.000 |
| ASM002652 | Coastal area | 1.387 | 0.008 | 1.230 | 0.000 | 0.000 | 0.149 | 0.000 | 0.020 | 0.089 | 0.506 | 0.733 | 0.000 | 0.000 | 0.039 | 0.000 |
| ASM001445 | Frisksjön | 1.848 | 0.117 | 1.584 | 0.000 | 0.105 | 0.042 | 0.000 | 0.118 | 0.016 | 0.192 | 1.332 | 0.049 | 0.105 | 0.036 | 0.000 |
| ASM001484 | Kåreviksån | 0.213 | 0.000 | 0.202 | 0.000 | 0.000 | 0.011 | 0.000 | 0.000 | 0.012 | 0.014 | 0.185 | 0.002 | 0.000 | 0.000 | 0.000 |
| ASM001486B | Mederhultsån | 1.921 | 0.000 | 1.587 | 0.000 | 0.238 | 0.096 | 0.000 | 0.000 | 0.002 | 0.124 | 1.429 | 0.030 | 0.240 | 0.096 | 0.000 |
| ASM001486A | Mederhultsån | 0.082 | 0.000 | 0.078 | 0.000 | 0.000 | 0.004 | 0.000 | 0.000 | 0.000 | 0.022 | 0.057 | 0.000 | 0.000 | 0.004 | 0.000 |
| ASM002654 | Coastal area | 1.861 | 0.005 | 1.660 | 0.000 | 0.000 | 0.196 | 0.000 | 0.031 | 0.099 | 0.360 | 1.311 | 0.012 | 0.000 | 0.047 | 0.001 |
| ASM002460 | Pistlanbäcken | 0.499 | 0.004 | 0.471 | 0.000 | 0.000 | 0.023 | 0.000 | 0.004 | 0.016 | 0.057 | 0.399 | 0.016 | 0.000 | 0.007 | 0.000 |

| | | | | | | | | | | | | | | | | | |
|---|---|---|---|---|---|---|---|---|---|---|---|---|---|---|---|---|---|
| ASM001490 | Ekerumsån | 0.222 | 0.000 | 0.176 | 0.000 | 0.039 | 0.007 | 0.000 | 0.000 | 0.000 | 0.017 | 0.122 | 0.037 | 0.038 | 0.007 | 0.000 |
| ASM001489 | Ekerumsån | 0.767 | 0.000 | 0.577 | 0.077 | 0.111 | 0.002 | 0.000 | 0.000 | 0.000 | 0.088 | 0.513 | 0.053 | 0.112 | 0.002 | 0.000 |
| ASM002483B | Ekerumsån | 1.504 | 0.000 | 1.312 | 0.000 | 0.176 | 0.016 | 0.000 | 0.000 | 0.001 | 0.112 | 1.102 | 0.097 | 0.177 | 0.014 | 0.000 |
| ASM002483A | Ekerumsån | 0.341 | 0.000 | 0.222 | 0.000 | 0.022 | 0.098 | 0.000 | 0.000 | 0.001 | 0.023 | 0.199 | 0.000 | 0.022 | 0.096 | 0.000 |
| ASM002478 | Laxemarån | 0.023 | 0.000 | 0.023 | 0.000 | 0.000 | 0.000 | 0.000 | 0.000 | 0.000 | 0.000 | 0.023 | 0.000 | 0.000 | 0.000 | 0.000 |
| ASM002482 | Laxemarån | 0.867 | 0.000 | 0.795 | 0.046 | 0.023 | 0.004 | 0.000 | 0.000 | 0.007 | 0.005 | 0.761 | 0.067 | 0.023 | 0.004 | 0.000 |
| ASM002480B | Laxemarån | 4.234 | 0.158 | 3.633 | 0.105 | 0.150 | 0.189 | 0.000 | 0.157 | 0.203 | 0.120 | 3.416 | 0.113 | 0.152 | 0.056 | 0.000 |
| ASM002480A | Jämsen | 1.834 | 0.222 | 1.221 | 0.063 | 0.092 | 0.236 | 0.000 | 0.223 | 0.037 | 0.006 | 1.077 | 0.150 | 0.092 | 0.137 | 0.000 |
| ASM001516 | Laxemarån | 0.533 | 0.000 | 0.494 | 0.000 | 0.011 | 0.028 | 0.000 | 0.000 | 0.000 | 0.035 | 0.398 | 0.060 | 0.011 | 0.028 | 0.000 |
| ASM001515 | Laxemarån | 0.337 | 0.000 | 0.259 | 0.000 | 0.016 | 0.062 | 0.000 | 0.000 | 0.005 | 0.004 | 0.241 | 0.013 | 0.017 | 0.027 | 0.000 |
| ASM001514 | Laxemarån | 0.487 | 0.000 | 0.306 | 0.000 | 0.114 | 0.067 | 0.000 | 0.000 | 0.000 | 0.015 | 0.279 | 0.012 | 0.115 | 0.065 | 0.000 |
| ASM001446 | Plittorpsgöl | 0.678 | 0.033 | 0.640 | 0.000 | 0.004 | 0.000 | 0.000 | 0.033 | 0.000 | 0.059 | 0.474 | 0.107 | 0.004 | 0.000 | 0.000 |
| ASM002459 | Laxemarån | 0.099 | 0.000 | 0.071 | 0.000 | 0.002 | 0.025 | 0.000 | 0.000 | 0.000 | 0.004 | 0.064 | 0.002 | 0.002 | 0.026 | 0.000 |
| ASM001512 | Laxemarån | 0.494 | 0.000 | 0.433 | 0.057 | 0.000 | 0.004 | 0.000 | 0.000 | 0.017 | 0.005 | 0.458 | 0.010 | 0.000 | 0.004 | 0.000 |
| ASM002476E | Laxemarån | 3.949 | 0.000 | 3.584 | 0.015 | 0.114 | 0.236 | 0.000 | 0.000 | 0.154 | 0.064 | 3.096 | 0.276 | 0.115 | 0.139 | 0.000 |
| ASM001510 | Laxemarån | 0.562 | 0.000 | 0.498 | 0.000 | 0.000 | 0.064 | 0.000 | 0.000 | 0.069 | 0.103 | 0.349 | 0.042 | 0.000 | 0.000 | 0.000 |
| ASM002453 | Laxemarån | 0.445 | 0.001 | 0.444 | 0.000 | 0.000 | 0.000 | 0.000 | 0.001 | 0.000 | 0.102 | 0.340 | 0.002 | 0.000 | 0.000 | 0.000 |
| ASM002450B | Laxemarån | 2.392 | 0.005 | 2.192 | 0.096 | 0.000 | 0.099 | 0.000 | 0.005 | 0.202 | 0.751 | 1.399 | 0.019 | 0.000 | 0.017 | 0.000 |
| ASM002450A | Laxemarån | 0.187 | 0.000 | 0.177 | 0.000 | 0.000 | 0.010 | 0.000 | 0.000 | 0.000 | 0.000 | 0.177 | 0.000 | 0.000 | 0.010 | 0.000 |
| ASM001511 | Laxemarån | 0.740 | 0.000 | 0.691 | 0.036 | 0.000 | 0.013 | 0.000 | 0.000 | 0.037 | 0.055 | 0.639 | 0.002 | 0.000 | 0.008 | 0.000 |
| ASM001448 | Grangöl | 0.495 | 0.027 | 0.421 | 0.036 | 0.000 | 0.011 | 0.000 | 0.027 | 0.016 | 0.032 | 0.352 | 0.068 | 0.000 | 0.000 | 0.000 |
| ASM002499 | Laxemarån | 0.058 | 0.000 | 0.051 | 0.000 | 0.003 | 0.003 | 0.000 | 0.000 | 0.000 | 0.000 | 0.051 | 0.000 | 0.003 | 0.003 | 0.000 |
| ASM001506 | Laxemarån | 0.398 | 0.000 | 0.324 | 0.000 | 0.027 | 0.047 | 0.000 | 0.000 | 0.000 | 0.037 | 0.279 | 0.008 | 0.027 | 0.046 | 0.000 |
| ASM001447 | Fjällgöl | 0.295 | 0.021 | 0.261 | 0.000 | 0.007 | 0.007 | 0.000 | 0.021 | 0.001 | 0.051 | 0.206 | 0.004 | 0.007 | 0.005 | 0.000 |
| ASM002451 | Laxemarån | 0.325 | 0.000 | 0.293 | 0.000 | 0.015 | 0.017 | 0.000 | 0.000 | 0.000 | 0.029 | 0.260 | 0.004 | 0.016 | 0.017 | 0.000 |
| ASM002452 | Laxemarån | 2.375 | 0.002 | 2.067 | 0.089 | 0.114 | 0.103 | 0.000 | 0.001 | 0.013 | 0.172 | 1.787 | 0.185 | 0.114 | 0.103 | 0.000 |
| ASM001503 | Laxemarån | 0.416 | 0.000 | 0.278 | 0.000 | 0.045 | 0.093 | 0.000 | 0.000 | 0.004 | 0.013 | 0.261 | 0.004 | 0.045 | 0.089 | 0.000 |
| ASM002454 | Laxemarån | 0.808 | 0.000 | 0.616 | 0.000 | 0.142 | 0.050 | 0.000 | 0.000 | 0.000 | 0.031 | 0.582 | 0.002 | 0.145 | 0.048 | 0.000 |
| ASM001501 | Laxemarån | 0.806 | 0.000 | 0.742 | 0.000 | 0.042 | 0.023 | 0.000 | 0.000 | 0.000 | 0.031 | 0.711 | 0.000 | 0.042 | 0.022 | 0.000 |
| ASM002457 | Laxemarån | 1.389 | 0.000 | 1.190 | 0.000 | 0.171 | 0.028 | 0.000 | 0.000 | 0.000 | 0.027 | 1.147 | 0.014 | 0.173 | 0.028 | 0.000 |
| ASM002476D | Laxemarån | 4.963 | 0.000 | 4.288 | 0.116 | 0.272 | 0.287 | 0.000 | 0.000 | 0.027 | 0.638 | 3.669 | 0.073 | 0.276 | 0.279 | 0.000 |
| ASM001499 | Laxemarån | 0.711 | 0.000 | 0.660 | 0.000 | 0.002 | 0.049 | 0.000 | 0.000 | 0.008 | 0.128 | 0.517 | 0.007 | 0.002 | 0.049 | 0.000 |
| ASM001498 | Laxemarån | 2.771 | 0.000 | 2.609 | 0.018 | 0.097 | 0.047 | 0.000 | 0.000 | 0.013 | 0.430 | 2.161 | 0.023 | 0.098 | 0.046 | 0.000 |
| ASM001497 | Laxemarån | 0.609 | 0.000 | 0.552 | 0.025 | 0.018 | 0.015 | 0.000 | 0.000 | 0.000 | 0.059 | 0.512 | 0.005 | 0.018 | 0.015 | 0.000 |
| ASM002476C | Laxemarån | 0.315 | 0.003 | 0.274 | 0.001 | 0.016 | 0.028 | 0.000 | 0.003 | 0.005 | 0.009 | 0.262 | 0.004 | 0.014 | 0.032 | 0.000 |
| ASM001494 | Laxemarån | 1.001 | 0.000 | 0.817 | 0.000 | 0.145 | 0.039 | 0.000 | 0.000 | 0.007 | 0.065 | 0.702 | 0.042 | 0.146 | 0.039 | 0.000 |
| ASM001493 | Laxemarån | 0.319 | 0.000 | 0.288 | 0.000 | 0.023 | 0.008 | 0.000 | 0.000 | 0.000 | 0.017 | 0.266 | 0.004 | 0.023 | 0.008 | 0.000 |
| ASM001492 | Laxemarån | 0.460 | 0.000 | 0.386 | 0.000 | 0.052 | 0.022 | 0.000 | 0.000 | 0.006 | 0.027 | 0.358 | 0.002 | 0.051 | 0.016 | 0.000 |
| ASM001496 | Laxemarån | 0.890 | 0.000 | 0.779 | 0.051 | 0.032 | 0.028 | 0.000 | 0.000 | 0.003 | 0.028 | 0.747 | 0.051 | 0.032 | 0.028 | 0.000 |
| ASM001495 | Laxemarån | 0.290 | 0.000 | 0.235 | 0.036 | 0.013 | 0.006 | 0.000 | 0.000 | 0.004 | 0.002 | 0.213 | 0.052 | 0.013 | 0.006 | 0.000 |
| ASM002476B | Laxemarån | 3.231 | 0.003 | 2.680 | 0.132 | 0.228 | 0.190 | 0.000 | 0.000 | 0.043 | 0.074 | 2.428 | 0.294 | 0.221 | 0.176 | 0.000 |
| ASM002476A | Laxemarån | 0.188 | 0.000 | 0.133 | 0.002 | 0.000 | 0.054 | 0.000 | 0.000 | 0.024 | 0.000 | 0.116 | 0.000 | 0.002 | 0.048 | 0.000 |
| ASM002495 | Glostadsbäcken | 0.126 | 0.000 | 0.105 | 0.000 | 0.021 | 0.000 | 0.000 | 0.000 | 0.000 | 0.017 | 0.089 | 0.000 | 0.020 | 0.000 | 0.000 |
| ASM002485 | Glostadsbäcken | 0.331 | 0.000 | 0.307 | 0.000 | 0.000 | 0.024 | 0.000 | 0.000 | 0.010 | 0.008 | 0.280 | 0.011 | 0.000 | 0.022 | 0.000 |
| ASM002498 | Glostadsbäcken | 1.597 | 0.000 | 1.413 | 0.000 | 0.032 | 0.152 | 0.000 | 0.000 | 0.111 | 0.085 | 1.279 | 0.047 | 0.032 | 0.043 | 0.000 |
| ASM001518B | Stålglobäcken | 0.679 | 0.000 | 0.527 | 0.000 | 0.123 | 0.029 | 0.000 | 0.000 | 0.005 | 0.028 | 0.460 | 0.037 | 0.127 | 0.023 | 0.000 |
| ASM001518A | Stålglobäcken | 0.354 | 0.000 | 0.285 | 0.016 | 0.017 | 0.036 | 0.000 | 0.000 | 0.007 | 0.004 | 0.294 | 0.003 | 0.017 | 0.028 | 0.000 |
| ASM002462 | Uvöbäcken | 0.967 | 0.000 | 0.708 | 0.000 | 0.058 | 0.201 | 0.000 | 0.000 | 0.083 | 0.077 | 0.622 | 0.008 | 0.059 | 0.117 | 0.000 |
| ASM002497 | Stekebäcken | 0.435 | 0.000 | 0.345 | 0.008 | 0.056 | 0.026 | 0.000 | 0.000 | 0.005 | 0.057 | 0.282 | 0.014 | 0.057 | 0.021 | 0.000 |
| ASM001517 | Stekebäcken | 0.903 | 0.000 | 0.738 | 0.005 | 0.021 | 0.139 | 0.000 | 0.000 | 0.069 | 0.049 | 0.692 | 0.000 | 0.020 | 0.072 | 0.000 |
| ASM002463 | Svartebäck | 0.504 | 0.001 | 0.486 | 0.000 | 0.005 | 0.011 | 0.000 | 0.001 | 0.003 | 0.041 | 0.436 | 0.005 | 0.006 | 0.011 | 0.000 |
| ASM002655 | Coastal area | 2.711 | 0.025 | 2.382 | 0.000 | 0.022 | 0.282 | 0.000 | 0.066 | 0.060 | 0.333 | 2.096 | 0.026 | 0.022 | 0.107 | 0.000 |
| ASM002658 | Coastal area | 1.261 | 0.005 | 1.131 | 0.010 | 0.000 | 0.115 | 0.000 | 0.022 | 0.047 | 0.136 | 1.000 | 0.003 | 0.000 | 0.052 | 0.000 |
| ASM002656 | Coastal area | 0.220 | 0.003 | 0.156 | 0.000 | 0.000 | 0.062 | 0.000 | 0.010 | 0.002 | 0.102 | 0.105 | 0.000 | 0.000 | 0.000 | 0.000 |
| ASM002660 | Coastal area | 0.138 | 0.001 | 0.123 | 0.000 | 0.000 | 0.014 | 0.000 | 0.007 | 0.000 | 0.069 | 0.062 | 0.000 | 0.000 | 0.000 | 0.000 |
| ASM002659 | Coastal area | 15.699 | 0.035 | 12.575 | 0.171 | 0.680 | 1.564 | 0.673 | 0.108 | 0.538 | 0.785 | 11.565 | 0.405 | 0.689 | 0.802 | 0.739 |
| ASM002657 | Coastal area | 2.597 | 0.002 | 1.985 | 0.005 | 0.061 | 0.448 | 0.096 | 0.010 | 0.009 | 0.071 | 1.905 | 0.006 | 0.061 | 0.439 | 0.096 |
| ASM001522 | Uthammarsån | 0.571 | 0.000 | 0.512 | 0.004 | 0.055 | 0.000 | 0.000 | 0.000 | 0.007 | 0.032 | 0.478 | 0.000 | 0.054 | 0.000 | 0.000 |
| ASM001523 | Uthammarsån | 0.958 | 0.000 | 0.801 | 0.000 | 0.094 | 0.063 | 0.000 | 0.000 | 0.000 | 0.104 | 0.639 | 0.058 | 0.095 | 0.062 | 0.000 |
| ASM001521 | Uthammarsån | 0.204 | 0.000 | 0.171 | 0.000 | 0.030 | 0.002 | 0.000 | 0.000 | 0.004 | 0.017 | 0.126 | 0.027 | 0.031 | 0.000 | 0.000 |
| ASM001520 | Uthammarsån | 0.081 | 0.000 | 0.066 | 0.000 | 0.011 | 0.004 | 0.000 | 0.000 | 0.001 | 0.006 | 0.061 | 0.000 | 0.011 | 0.003 | 0.000 |
| ASM002494B | Uthammarsån | 2.913 | 0.000 | 2.560 | 0.015 | 0.133 | 0.205 | 0.000 | 0.000 | 0.027 | 0.130 | 2.299 | 0.118 | 0.133 | 0.204 | 0.000 |
| ASM001533 | Uthammarsån | 0.512 | 0.000 | 0.375 | 0.000 | 0.085 | 0.052 | 0.000 | 0.000 | 0.001 | 0.020 | 0.320 | 0.035 | 0.087 | 0.050 | 0.000 |
| ASM002494A | Uthammarsån | 1.781 | 0.001 | 1.230 | 0.000 | 0.312 | 0.238 | 0.000 | 0.000 | 0.001 | 0.085 | 1.137 | 0.010 | 0.317 | 0.232 | 0.000 |
| ASM001528 | Släthultebäcken | 0.320 | 0.000 | 0.320 | 0.000 | 0.000 | 0.000 | 0.000 | 0.000 | 0.000 | 0.010 | 0.296 | 0.014 | 0.000 | 0.000 | 0.000 |
| ASM002477 | Släthultebäcken | 0.659 | 0.023 | 0.633 | 0.000 | 0.000 | 0.003 | 0.000 | 0.023 | 0.021 | 0.037 | 0.531 | 0.045 | 0.000 | 0.003 | 0.000 |
| ASM001531 | Släthultebäcken | 0.302 | 0.000 | 0.269 | 0.022 | 0.000 | 0.011 | 0.000 | 0.000 | 0.002 | 0.011 | 0.278 | 0.000 | 0.000 | 0.011 | 0.000 |
| ASM001532 | Släthultebäcken | 0.111 | 0.000 | 0.083 | 0.000 | 0.026 | 0.002 | 0.000 | 0.000 | 0.000 | 0.008 | 0.066 | 0.008 | 0.026 | 0.002 | 0.000 |
| ASM002455 | Släthultebäcken | 0.761 | 0.000 | 0.611 | 0.000 | 0.107 | 0.043 | 0.000 | 0.000 | 0.000 | 0.078 | 0.533 | 0.001 | 0.109 | 0.040 | 0.000 |
| ASM002475 | Släthultebäcken | 1.055 | 0.000 | 1.011 | 0.000 | 0.027 | 0.017 | 0.000 | 0.000 | 0.003 | 0.063 | 0.945 | 0.001 | 0.027 | 0.017 | 0.000 |
| ASM001526 | Släthultebäcken | 0.401 | 0.001 | 0.376 | 0.000 | 0.004 | 0.017 | 0.002 | 0.000 | 0.004 | 0.000 | 0.317 | 0.056 | 0.004 | 0.017 | 0.003 |
| ASM002481C | Släthultebäcken | 2.441 | 0.000 | 1.949 | 0.014 | 0.168 | 0.309 | 0.000 | 0.000 | 0.213 | 0.091 | 1.609 | 0.123 | 0.169 | 0.133 | 0.057 |
| ASM002481B | Släthultebäcken | 2.133 | 0.009 | 1.867 | 0.000 | 0.052 | 0.195 | 0.011 | 0.008 | 0.012 | 0.059 | 1.706 | 0.095 | 0.053 | 0.192 | 0.011 |
| ASM001525 | Släthultebäcken | 0.771 | 0.000 | 0.609 | 0.000 | 0.039 | 0.072 | 0.051 | 0.000 | 0.000 | 0.000 | 0.607 | 0.001 | 0.040 | 0.071 | 0.051 |
| ASM002481A | Släthultebäcken | 0.001 | 0.000 | 0.000 | 0.000 | 0.000 | 0.000 | 0.000 | 0.000 | 0.000 | 0.000 | 0.001 | 0.000 | 0.000 | 0.000 | 0.000 |
| ASM001444 | Söråmagasinet | 0.523 | 0.089 | 0.339 | 0.000 | 0.000 | 0.095 | 0.000 | 0.089 | 0.005 | 0.023 | 0.315 | 0.001 | 0.000 | 0.011 | 0.079 |
| ASM002466 | Stekflagebäcken | 0.359 | 0.024 | 0.308 | 0.000 | 0.000 | 0.026 | 0.000 | 0.024 | 0.021 | 0.048 | 0.260 | 0.000 | 0.000 | 0.005 | 0.000 |
| ASM002653 | Coastal area | 0.759 | 0.002 | 0.722 | 0.000 | 0.000 | 0.035 | 0.000 | 0.008 | 0.007 | 0.217 | 0.517 | 0.000 | 0.000 | 0.009 | 0.000 |
| ASM002470 | Skölkebäcken | 0.165 | 0.000 | 0.158 | 0.000 | 0.000 | 0.007 | 0.000 | 0.000 | 0.000 | 0.014 | 0.144 | 0.000 | 0.000 | 0.007 | 0.000 |
| ASM002469 | Gloebäcken | 0.131 | 0.000 | 0.126 | 0.000 | 0.000 | 0.005 | 0.000 | 0.000 | 0.000 | 0.010 | 0.117 | 0.000 | 0.000 | 0.004 | 0.000 |
| ASM002468 | Lindströmmebäcken | 0.192 | 0.000 | 0.185 | 0.000 | 0.000 | 0.007 | 0.000 | 0.000 | 0.000 | 0.008 | 0.172 | 0.005 | 0.000 | 0.007 | 0.000 |
| ASM002467B | Vadvikebäcken | 0.298 | 0.000 | 0.298 | 0.000 | 0.000 | 0.000 | 0.000 | 0.000 | 0.003 | 0.031 | 0.264 | 0.000 | 0.000 | 0.000 | 0.000 |
| ASM002467A | Vadvikebäcken | 0.009 | 0.000 | 0.009 | 0.000 | 0.000 | 0.000 | 0.000 | 0.000 | 0.000 | 0.001 | 0.008 | 0.000 | 0.000 | 0.000 | 0.000 |

# Appendix C

Compilation of detailed results from the VBX-II mass balance models: Total phosphorus, total nitrogen, total organic carbon (TOC), $HCO_3^-$, Mg, Si, Sr, Ca, K, Na, $SO_4^{2-}$ and Cl.

Red figures denote catchments that discharge into the Baltic. Yellow colour marks catchments that have been further divided from the original catchments.

| **Total phosphorus (tot-P)** | | | | Water balance | | | Total per catchment | | | Total including contributions from upstream catchments | | | | | Calibration data | | | |
|---|---|---|---|---|---|---|---|---|---|---|---|---|---|---|---|---|---|---|
| Idcode | Name | ARO | Area | $Q_{catch}$ | $Q_{out}$ | q | Diffuse | Point | Total | Total IN | Retention | | Total OUT | Conc. | Reference | q | Conc. | Deviation |
| | | | $km^2$ | $m^3 \cdot yr^{-1}$ | $m^3 \cdot yr^{-1}$ | $L \cdot s^{-1}$ | $kg \cdot yr^{-1}$ | $kg \cdot yr^{-1}$ | $kg \cdot yr^{-1}$ | $kg \cdot yr^{-1}$ | $kg \cdot yr^{-1}$ | % | $kg \cdot yr^{-1}$ | $mg \cdot L^{-1}$ | | $L \cdot s^{-1}$ | $mg \cdot L^{-1}$ | % |
| ASM002474 | Kärrviksån | 5:20 | 0.12 | 25740 | 25740 | 0.8 | 2.1 | 0.0 | 2.1 | 2.1 | 0.0 | 0 | 2.1 | 0.083 | | | | |
| ASM002493 | Kärrviksån | 5:19 | 0.84 | 184140 | 209880 | 6.7 | 12.5 | 0.0 | 12.5 | 14.7 | 0.0 | 0 | 14.7 | 0.070 | | | | |
| ASM001483 | Kärrviksån | 5:17 | 0.15 | 33220 | 33220 | 1.1 | 1.6 | 0.0 | 1.6 | 1.6 | 0.0 | 0 | 1.6 | 0.049 | | | | |
| ASM002492 | Kärrviksån | 5:16 | 1.11 | 243980 | 277200 | 8.8 | 14.8 | 0.0 | 14.8 | 16.4 | 0.0 | 0 | 16.4 | 0.059 | | | | |
| ASM002491 | Kärrviksån | 5:15 | 1.87 | 411840 | 689040 | 21.8 | 13.7 | 0.0 | 13.7 | 30.2 | 0.2 | 1 | 30.0 | 0.044 | | | | |
| ASM001474 | Kärrviksån | 5:7 | 0.45 | 99000 | 99000 | 3.1 | 3.1 | 0.0 | 3.1 | 3.1 | 0.0 | 0 | 3.1 | 0.031 | | | | |
| ASM002487 | Kärrviksån | 5:6 | 1.20 | 264000 | 363000 | 11.5 | 8.4 | 0.0 | 8.4 | 11.5 | 0.0 | 0 | 11.5 | 0.032 | | | | |
| ASM001472 | Kärrviksån | 5:4 | 1.10 | 242880 | 242880 | 7.7 | 8.2 | 0.0 | 8.2 | 8.2 | 3.7 | 46 | 4.4 | 0.018 | | | | |
| ASM001470 | Kärrviksån | 5:3 | 0.40 | 87560 | 87560 | 2.8 | 4.8 | 0.0 | 4.8 | 4.8 | 0.0 | 0 | 4.8 | 0.054 | | | | |
| ASM001469 | Kärrviksån | 5:2 | 0.97 | 212960 | 212960 | 6.8 | 7.4 | 0.0 | 7.4 | 7.4 | 0.0 | 0 | 7.4 | 0.035 | | | | |
| ASM001471 | Kärrviksån | 5:5 | 2.79 | 614680 | 614680 | 19.5 | 21.4 | 0.0 | 21.4 | 21.4 | 0.0 | 0 | 21.4 | 0.035 | | | | |
| ASM001479 | Kärrviksån | 5:13 | 0.65 | 142340 | 142340 | 4.5 | 4.6 | 0.0 | 4.6 | 4.6 | 0.0 | 0 | 4.6 | 0.032 | | | | |
| ASM001480 | Kärrviksån | 5:14 | 0.10 | 22660 | 22660 | 0.7 | 0.8 | 0.0 | 0.8 | 0.8 | 0.0 | 0 | 0.8 | 0.035 | | | | |
| ASM002490 | Kärrviksån | 5:12 | 0.84 | 183920 | 348920 | 11.1 | 6.1 | 0.0 | 6.1 | 11.5 | 0.6 | 5 | 10.9 | 0.031 | | | | |
| ASM001478 | Kärrviksån | 5:11 | 0.49 | 108460 | 108460 | 3.4 | 3.5 | 0.0 | 3.5 | 3.5 | 0.0 | 0 | 3.5 | 0.032 | | | | |
| ASM002489 | Kärrviksån | 5:10 | 1.20 | 263560 | 372020 | 11.8 | 9.0 | 0.0 | 9.0 | 12.5 | 0.0 | 0 | 12.5 | 0.034 | | | | |
| ASM001476 | Kärrviksån | 5:9 | 3.62 | 796180 | 796180 | 25.2 | 35.8 | 0.0 | 35.8 | 35.8 | 0.0 | 0 | 35.8 | 0.045 | | | | |
| ASM001475B | Kärrviksån | 5:8 | 1.38 | 302940 | 1820060 | 57.7 | 10.9 | 0.0 | 10.9 | 70.1 | 0.0 | 0 | 70.1 | 0.038 | PSM002081 | 0.058 | 0.047 | 19 |
| ASM001475A | Kärrviksån | 5:8 | 0.04 | 9680 | 1829740 | 58.0 | 0.5 | 0.0 | 0.5 | 70.5 | 0.0 | 0 | 70.5 | 0.039 | | | | |
| ASM002479 | Kärrviksån | 5:18 | 1.18 | 259600 | 259600 | 8.2 | 8.3 | 0.0 | 8.3 | 8.3 | 0.0 | 0 | 8.3 | 0.032 | | | | |
| ASM002486C | Kärrviksån | 5:1 | 2.75 | 604560 | 1074040 | 34.1 | 19.8 | 0.0 | 19.8 | 42.7 | 1.1 | 3 | 41.6 | 0.039 | PSM002080 | | | |
| ASM002486B | Kärrviksån | 5:1 | 1.13 | 247940 | 3840760 | 121.8 | 8.5 | 0.0 | 8.5 | 150.7 | 0.0 | 0 | 150.7 | 0.039 | PSM002082 | 0.121 | 0.038 | 2 |
| ASM002486A | Kärrviksån | 5:1 | 2.93 | 645260 | 6007100 | 190.5 | 35.9 | 0.0 | 35.9 | 236.1 | 0.2 | 0 | 235.9 | 0.039 | PSM002083 | 0.190 | 0.051 | 23 |
| ASM002449 | Bjurhidebäcken | 4:1 | 0.63 | 139040 | 139040 | 4.4 | 5.6 | 0.0 | 5.6 | 5.6 | 0.0 | 0 | 5.6 | 0.040 | | | | |
| ASM002472 | Sörviksån | 3:2 | 0.47 | 103400 | 103400 | 3.3 | 4.3 | 0.0 | 4.3 | 4.3 | 0.0 | 0 | 4.3 | 0.041 | | | | |
| ASM002473 | Sörviksån | 3:1 | 0.53 | 116600 | 220000 | 7.0 | 4.1 | 0.0 | 4.1 | 8.4 | 0.0 | 0 | 8.4 | 0.038 | | | | |
| ASM002651 | Coastal area | | 1.67 | 368280 | 368280 | 11.7 | 12.5 | 0.0 | 12.5 | 12.5 | 2.5 | 20 | 10.0 | 0.027 | | | | |
| ASM002447 | Bodvikebäcken | 2:1 | 0.38 | 83600 | 83600 | 2.7 | 2.1 | 0.0 | 2.1 | 2.1 | 1.7 | 78 | 0.5 | 0.005 | | | | |
| ASM002446 | Långbonäsbäcken | 1:1 | 0.07 | 15400 | 15400 | 0.5 | 0.5 | 0.0 | 0.5 | 0.5 | 0.0 | 0 | 0.5 | 0.032 | | | | |
| ASM002464 | Flakvarpebäcken | 19:1 | 0.18 | 40480 | 40480 | 1.3 | 1.2 | 0.0 | 1.2 | 1.2 | 0.7 | 60 | 0.5 | 0.012 | | | | |
| ASM002465 | Jössesbäcken | 20:1 | 0.11 | 24420 | 24420 | 0.8 | 0.8 | 0.0 | 0.8 | 0.8 | 0.0 | 0 | 0.8 | 0.032 | | | | |
| ASM002471 | Åspöbäcken | 21:1 | 0.06 | 13860 | 13860 | 0.4 | 0.4 | 0.0 | 0.4 | 0.4 | 0.0 | 0 | 0.4 | 0.032 | | | | |
| ASM002652 | Coastal area | | 1.39 | 305140 | 305140 | 9.7 | 9.6 | 0.0 | 9.6 | 9.6 | 2.0 | 21 | 7.6 | 0.025 | | | | |
| ASM001445 | Frisksjön | 7:2 | 1.85 | 406560 | 406560 | 12.9 | 17.2 | 0.0 | 17.2 | 17.2 | 9.2 | 54 | 8.0 | 0.020 | | | | |
| ASM001484 | Kåreviksån | 7:1 | 0.21 | 46860 | 453420 | 14.4 | 1.5 | 0.0 | 1.5 | 9.5 | 0.0 | 0 | 9.5 | 0.021 | | | | |
| ASM001486B | Mederhultsån | 6:1 | 1.92 | 422620 | 422620 | 13.4 | 24.9 | 0.0 | 24.9 | 24.9 | 0.0 | 0 | 24.9 | 0.059 | PSM002084 | 0.013 | 0.057 | 4 |
| ASM001486A | Mederhultsån | 6:1 | 0.08 | 18040 | 440660 | 14.0 | 0.6 | 0.0 | 0.6 | 25.5 | 0.0 | 0 | 25.5 | 0.058 | | | | |
| ASM002654 | Coastal area | | 1.86 | 409420 | 409420 | 13.0 | 12.9 | 0.0 | 12.9 | 12.9 | 2.7 | 21 | 10.1 | 0.025 | | | | |
| ASM002460 | Pistlanbäcken | 8:1 | 0.50 | 109780 | 109780 | 3.5 | 3.5 | 0.0 | 3.5 | 3.5 | 0.5 | 15 | 3.0 | 0.027 | | | | |
| ASM001490 | Ekerumsån | 9:3 | 0.22 | 48840 | 48840 | 1.5 | 3.4 | 0.0 | 3.4 | 3.4 | 0.0 | 0 | 3.4 | 0.069 | | | | |
| ASM001489 | Ekerumsån | 9:2 | 0.77 | 168740 | 168740 | 5.4 | 10.7 | 0.0 | 10.7 | 10.7 | 0.0 | 0 | 10.7 | 0.063 | | | | |
| ASM002483B | Ekerumsån | 9:1 | 1.50 | 330880 | 548460 | 17.4 | 19.0 | 0.0 | 19.0 | 33.1 | 0.0 | 0 | 33.1 | 0.060 | PSM002085 | 0.017 | 0.054 | 12 |
| ASM002483A | Ekerumsån | 9:1 | 0.34 | 75020 | 623480 | 19.8 | 3.5 | 0.0 | 3.5 | 36.5 | 0.0 | 0 | 36.5 | 0.059 | | | | |
| ASM002478 | Laxemarån | 10:32 | 0.02 | 5060 | 5060 | 0.2 | 0.2 | 0.0 | 0.2 | 0.2 | 0.0 | 0 | 0.2 | 0.032 | | | | |
| ASM002482 | Laxemarån | 10:31 | 0.87 | 190740 | 195800 | 6.2 | 7.2 | 0.0 | 7.2 | 7.3 | 0.0 | 0 | 7.3 | 0.037 | | | | |
| ASM002480B | Laxemarån | 10:30 | 4.23 | 931480 | 1127280 | 35.7 | 35.8 | 0.0 | 35.8 | 43.1 | 15.6 | 36 | 27.5 | 0.024 | PSM002068 | 0.036 | 0.025 | 4 |
| ASM002480A | Jämsen | 10:30 | 1.83 | 403480 | 1530760 | 48.5 | 14.9 | 0.0 | 14.9 | 42.5 | 15.6 | 37 | 26.9 | 0.018 | PSM002069 | 0.049 | 0.018 | 0 |
| ASM001516 | Laxemarån | 10:29 | 0.53 | 117260 | 117260 | 3.7 | 4.3 | 0.0 | 4.3 | 4.3 | 0.0 | 0 | 4.3 | 0.036 | | | | |
| ASM001515 | Laxemarån | 10:28 | 0.34 | 74140 | 74140 | 2.4 | 2.9 | 0.0 | 2.9 | 2.9 | 0.0 | 0 | 2.9 | 0.040 | | | | |
| ASM001514 | Laxemarån | 10:27 | 0.49 | 107140 | 107140 | 3.4 | 8.9 | 0.0 | 8.9 | 8.9 | 0.0 | 0 | 8.9 | 0.083 | | | | |
| ASM001446 | Plittorpsgöl | 10:26 | 0.68 | 149160 | 149160 | 4.7 | 4.7 | 0.0 | 4.7 | 4.7 | 2.2 | 47 | 2.5 | 0.017 | | | | |
| ASM002459 | Laxemarån | 10:25 | 0.10 | 21780 | 170940 | 5.4 | 0.8 | 0.0 | 0.8 | 3.3 | 0.0 | 0 | 3.3 | 0.019 | | | | |
| ASM001512 | Laxemarån | 10:24 | 0.49 | 108680 | 108680 | 3.4 | 3.5 | 0.0 | 3.5 | 3.5 | 0.0 | 0 | 3.5 | 0.032 | | | | |
| ASM002476E | Laxemarån | 10:1 | 3.95 | 868780 | 2977700 | 94.4 | 32.5 | 0.0 | 32.5 | 82.3 | 0.3 | 0 | 82.1 | 0.028 | PSM002071 | 0.094 | 0.025 | 10 |
| ASM001510 | Laxemarån | 10:22 | 0.56 | 123640 | 123640 | 3.9 | 4.0 | 0.0 | 4.0 | 4.0 | 0.0 | 0 | 4.0 | 0.032 | | | | |
| ASM002453 | Laxemarån | 10:21 | 0.45 | 97900 | 221540 | 7.0 | 3.1 | 0.0 | 3.1 | 7.1 | 0.2 | 2 | 6.9 | 0.031 | | | | |
| ASM002450B | Laxemarån | 10:20 | 2.39 | 526240 | 747780 | 23.7 | 16.8 | 0.0 | 16.8 | 23.7 | 0.7 | 3 | 23.1 | 0.031 | PSM002072 | | | |
| ASM002450A | Laxemarån | 10:20 | 0.19 | 41140 | 788920 | 25.0 | 1.3 | 0.0 | 1.3 | 24.4 | 0.0 | 0 | 24.4 | 0.031 | | | | |
| ASM001511 | Laxemarån | 10:23 | 0.74 | 162800 | 162800 | 5.2 | 5.2 | 0.0 | 5.2 | 5.2 | 0.0 | 0 | 5.2 | 0.032 | | | | |
| ASM001448 | Grangöl | 10:19 | 0.50 | 108900 | 108900 | 3.5 | 3.3 | 0.0 | 3.3 | 3.3 | 1.6 | 49 | 1.7 | 0.015 | | | | |
| ASM002499 | Laxemarån | 10:18 | 0.06 | 12760 | 121660 | 3.9 | 0.6 | 0.0 | 0.6 | 2.2 | 0.0 | 0 | 2.2 | 0.018 | | | | |
| ASM001506 | Laxemarån | 10:17 | 0.40 | 87560 | 87560 | 2.8 | 4.1 | 0.0 | 4.1 | 4.1 | 0.0 | 0 | 4.1 | 0.047 | | | | |
| ASM001447 | Fjällgöl | 10:16 | 0.30 | 64900 | 64900 | 2.1 | 2.3 | 0.0 | 2.3 | 2.3 | 1.3 | 56 | 1.0 | 0.015 | | | | |
| ASM002451 | Laxemarån | 10:15 | 0.33 | 71500 | 136400 | 4.3 | 3.0 | 0.0 | 3.0 | 4.0 | 0.0 | 0 | 4.0 | 0.029 | | | | |
| ASM002452 | Laxemarån | 10:14 | 2.38 | 522500 | 868120 | 27.5 | 22.1 | 0.0 | 22.1 | 32.5 | 0.3 | 1 | 32.2 | 0.037 | | | | |
| ASM001503 | Laxemarån | 10:13 | 0.42 | 91520 | 91520 | 2.9 | 5.1 | 0.0 | 5.1 | 5.1 | 0.0 | 0 | 5.1 | 0.055 | | | | |
| ASM002454 | Laxemarån | 10:12 | 0.81 | 177760 | 269280 | 8.5 | 12.6 | 0.0 | 12.6 | 17.6 | 0.0 | 0 | 17.6 | 0.065 | | | | |
| ASM001501 | Laxemarån | 10:11 | 0.81 | 177320 | 177320 | 5.6 | 7.7 | 0.0 | 7.7 | 7.7 | 0.0 | 0 | 7.7 | 0.043 | | | | |
| ASM002457 | Laxemarån | 10:10 | 1.39 | 305580 | 482900 | 15.3 | 18.0 | 0.0 | 18.0 | 25.6 | 0.0 | 0 | 25.6 | 0.053 | | | | |
| ASM002476D | Laxemarån | 10:1 | 4.96 | 1091860 | 6641580 | 210.6 | 48.0 | 0.0 | 48.0 | 235.2 | 0.0 | 0 | 235.2 | 0.035 | PSM002077 | | | |
| ASM001499 | Laxemarån | 10:9 | 0.71 | 156420 | 156420 | 5.0 | 5.1 | 0.0 | 5.1 | 5.1 | 0.0 | 0 | 5.1 | 0.033 | | | | |
| ASM001498 | Laxemarån | 10:8 | 2.77 | 609620 | 766040 | 24.3 | 24.2 | 0.0 | 24.2 | 29.3 | 0.0 | 0 | 29.3 | 0.038 | PSM002078 | 0.024 | 0.023 | 66 |
| ASM001497 | Laxemarån | 10:7 | 0.61 | 133980 | 133980 | 4.2 | 5.1 | 0.0 | 5.1 | 5.1 | 0.0 | 0 | 5.1 | 0.038 | | | | |
| ASM002476C | Laxemarån | 10:1 | 0.32 | 69300 | 7610900 | 241.3 | 3.0 | 0.0 | 3.0 | 272.5 | 0.1 | 0 | 272.4 | 0.036 | PSM002079 | 0.242 | 0.037 | 3 |
| ASM001494 | Laxemarån | 10:4 | 1.00 | 220220 | 220220 | 7.0 | 14.0 | 0.0 | 14.0 | 14.0 | 0.0 | 0 | 14.0 | 0.064 | | | | |
| ASM001493 | Laxemarån | 10:3 | 0.32 | 70180 | 70180 | 2.2 | 3.4 | 0.0 | 3.4 | 3.4 | 0.0 | 0 | 3.4 | 0.048 | | | | |
| ASM001492 | Laxemarån | 10:2 | 0.46 | 101200 | 101200 | 3.2 | 5.7 | 0.0 | 5.7 | 5.7 | 0.0 | 0 | 5.7 | 0.056 | | | | |
| ASM001496 | Laxemarån | 10:6 | 0.89 | 195800 | 195800 | 6.2 | 7.8 | 0.0 | 7.8 | 7.8 | 0.0 | 0 | 7.8 | 0.040 | | | | |
| ASM001495 | Laxemarån | 10:5 | 0.29 | 63800 | 63800 | 2.0 | 2.6 | 0.0 | 2.6 | 2.6 | 0.0 | 0 | 2.6 | 0.042 | | | | |
| ASM002476B | Laxemarån | 10:1 | 3.23 | 710820 | 8972920 | 284.5 | 33.3 | 0.0 | 33.3 | 339.1 | 0.7 | 0 | 338.5 | 0.038 | PSM002087 | 0.285 | 0.041 | 8 |
| ASM002476A | Laxemarån | 10:1 | 0.19 | 41360 | 9014280 | 285.8 | 1.4 | 0.0 | 1.4 | 339.9 | 0.0 | 0 | 339.9 | 0.038 | | | | |
| ASM002495 | Glostadsbäcken | 12:3 | 0.13 | 27720 | 27720 | 0.9 | 1.9 | 0.0 | 1.9 | 1.9 | 0.0 | 0 | 1.9 | 0.067 | | | | |
| ASM002485 | Glostadsbäcken | 12:2 | 0.33 | 72820 | 72820 | 2.3 | 2.3 | 0.0 | 2.3 | 2.3 | 0.0 | 0 | 2.3 | 0.032 | | | | |
| ASM002498 | Glostadsbäcken | 12:1 | 1.60 | 351340 | 451880 | 14.3 | 12.8 | 0.0 | 12.8 | 16.9 | 1.1 | 7 | 15.8 | 0.035 | | | | |
| ASM001518B | Stålglobäcken | 13:1 | 0.68 | 149380 | 149380 | 4.7 | 10.8 | 0.0 | 10.8 | 10.8 | 0.0 | 0 | 10.8 | 0.072 | PSM002086 | 0.005 | 0.072 | 0 |
| ASM001518A | Stålglobäcken | 13:1 | 0.35 | 77880 | 227260 | 7.2 | 3.3 | 0.0 | 3.3 | 14.1 | 0.0 | 0 | 14.1 | 0.062 | | | | |
| ASM002462 | Uvöbäcken | 15:1 | 0.97 | 212740 | 212740 | 6.7 | 9.6 | 0.0 | 9.6 | 9.6 | 0.0 | 0 | 9.6 | 0.045 | | | | |
| ASM002497 | Stekebäcken | 14:2 | 0.44 | 95700 | 95700 | 3.0 | 5.7 | 0.0 | 5.7 | 5.7 | 0.0 | 0 | 5.7 | 0.060 | | | | |
| ASM001517 | Stekebäcken | 14:1 | 0.90 | 198660 | 294360 | 9.3 | 7.3 | 0.0 | 7.3 | 13.1 | 0.0 | 0 | 13.1 | 0.044 | | | | |
| ASM002463 | Svartebäck | 16:1 | 0.50 | 110880 | 110880 | 3.5 | 3.8 | 0.0 | 3.8 | 3.8 | 0.2 | 5 | 3.6 | 0.033 | | | | |
| ASM002655 | Coastal area | | 2.71 | 596420 | 596420 | 18.9 | 19.7 | 0.0 | 19.7 | 19.7 | 6.7 | 34 | 13.0 | 0.022 | | | | |
| ASM002658 | Coastal area | | 1.26 | 277420 | 277420 | 8.8 | 8.7 | 0.0 | 8.7 | 8.7 | 1.7 | 20 | 7.0 | 0.025 | | | | |
| ASM002656 | Coastal area | | 0.22 | 48400 | 48400 | 1.5 | 1.5 | 0.0 | 1.5 | 1.5 | 0.7 | 44 | 0.8 | 0.017 | | | | |
| ASM002660 | Coastal area | | 0.14 | 30360 | 30360 | 1.0 | 0.9 | 0.0 | 0.9 | 0.9 | 0.4 | 46 | 0.5 | 0.016 | | | | |
| ASM002659 | Coastal area | | 15.70 | 3453780 | 3453780 | 109.5 | 142.0 | 0.0 | 142.0 | 142.0 | 5.6 | 4 | 136.4 | 0.039 | | | | |
| ASM002657 | Coastal area | | 2.60 | 571340 | 571340 | 18.1 | 21.1 | 0.0 | 21.1 | 21.1 | 1.2 | 6 | 19.9 | 0.035 | | | | |
| ASM001522 | Uthammarsån | 17:5 | 0.57 | 125620 | 125620 | 4.0 | 6.6 | 0.0 | 6.6 | 6.6 | 0.0 | 0 | 6.6 | 0.053 | | | | |
| ASM001523 | Uthammarsån | 17:6 | 0.96 | 210760 | 210760 | 6.7 | 11.3 | 0.0 | 11.3 | 11.3 | 0.0 | 0 | 11.3 | 0.053 | | | | |
| ASM001521 | Uthammarsån | 17:4 | 0.20 | 44880 | 44880 | 1.4 | 2.9 | 0.0 | 2.9 | 2.9 | 0.0 | 0 | 2.9 | 0.065 | | | | |
| ASM001520 | Uthammarsån | 17:3 | 0.08 | 17820 | 17820 | 0.6 | 1.1 | 0.0 | 1.1 | 1.1 | 0.0 | 0 | 1.1 | 0.061 | | | | |
| ASM002494B | Uthammarsån | 17:1 | 2.91 | 640860 | 1039940 | 33.0 | 26.8 | 0.0 | 26.8 | 48.7 | 0.0 | 0 | 48.7 | 0.047 | PSM002076 | 0.033 | 0.071 | 34 |
| ASM001533 | Uthammarsån | 17:2 | 0.51 | 112640 | 112640 | 3.6 | 7.8 | 0.0 | 7.8 | 7.8 | 0.0 | 0 | 7.8 | 0.069 | | | | |
| ASM002494A | Uthammarsån | 17:1 | 1.78 | 391820 | 1544400 | 49.0 | 27.6 | 0.0 | 27.6 | 84.0 | 0.2 | 0 | 83.8 | 0.054 | | | | |
| ASM001528 | Släthultebäcken | 18:5 | 0.32 | 70400 | 70400 | 2.2 | 2.3 | 0.0 | 2.3 | 2.3 | 0.0 | 0 | 2.3 | 0.032 | | | | |
| ASM002477 | Släthultebäcken | 18:4 | 0.66 | 144980 | 215380 | 6.8 | 4.5 | 0.0 | 4.5 | 6.7 | 2.0 | 30 | 4.7 | 0.022 | | | | |
| ASM001531 | Släthultebäcken | 18:8 | 0.30 | 66440 | 66440 | 2.1 | 2.1 | 0.0 | 2.1 | 2.1 | 0.0 | 0 | 2.1 | 0.032 | | | | |
| ASM001532 | Släthultebäcken | 18:9 | 0.11 | 24420 | 24420 | 0.8 | 2.0 | 0.0 | 2.0 | 2.0 | 0.0 | 0 | 2.0 | 0.082 | | | | |
| ASM002455 | Släthultebäcken | 18:7 | 0.76 | 167420 | 258280 | 8.2 | 10.5 | 0.0 | 10.5 | 14.7 | 0.0 | 0 | 14.7 | 0.057 | | | | |
| ASM002475 | Släthultebäcken | 18:6 | 1.06 | 232100 | 490380 | 15.5 | 8.7 | 0.0 | 8.7 | 23.4 | 0.0 | 0 | 23.4 | 0.048 | | | | |
| ASM001526 | Släthultebäcken | 18:3 | 0.40 | 88220 | 88220 | 2.8 | 3.0 | 0.0 | 3.0 | 3.0 | 0.1 | 3 | 2.9 | 0.033 | | | | |
| ASM002481C | Släthultebäcken | 18:1 | 2.44 | 537020 | 1027400 | 32.6 | 24.9 | 0.0 | 24.9 | 48.2 | 0.0 | 0 | 48.2 | 0.047 | PSM002070 | | | |
| ASM002481B | Släthultebäcken | 18:1 | 2.13 | 469260 | 1800260 | 57.1 | 17.5 | 0.0 | 17.5 | 73.3 | 1.3 | 2 | 72.0 | 0.040 | PSM002075 | | | |
| ASM001525 | Släthultebäcken | 18:2 | 0.77 | 169620 | 169620 | 5.4 | 7.3 | 0.0 | 7.3 | 7.3 | 0.0 | 0 | 7.3 | 0.043 | | | | |
| ASM002481A | Släthultebäcken | 18:1 | 0.00 | 220 | 1970100 | 62.5 | 0.0 | 0.0 | 0.0 | 79.3 | 0.0 | 0 | 79.3 | 0.040 | | | | |
| ASM001444 | Sörämagasinet | 11:1 | 0.52 | 115060 | 115060 | 3.6 | 3.1 | 0.0 | 3.1 | 3.1 | 2.3 | 76 | 0.7 | 0.006 | | | | |
| ASM002466 | Stekflagebäcken | 22:1 | 0.36 | 78980 | 78980 | 2.5 | 2.4 | 0.0 | 2.4 | 2.4 | 1.3 | 56 | 1.0 | 0.013 | | | | |
| ASM002653 | Coastal area | | 0.76 | 166980 | 166980 | 5.3 | 5.3 | 0.0 | 5.3 | 5.3 | 1.0 | 19 | 4.3 | 0.026 | | | | |
| ASM002470 | Skölkebäcken | 26:1 | 0.17 | 36300 | 36300 | 1.2 | 1.2 | 0.0 | 1.2 | 1.2 | 0.0 | 0 | 1.2 | 0.032 | | | | |
| ASM002469 | Gloebäcken | 25:1 | 0.13 | 28820 | 28820 | 0.9 | 0.9 | 0.0 | 0.9 | 0.9 | 0.0 | 0 | 0.9 | 0.032 | | | | |
| ASM002468 | Lindströmmebäcken | 24:1 | 0.19 | 42240 | 42240 | 1.3 | 1.4 | 0.0 | 1.4 | 1.4 | 0.0 | 0 | 1.4 | 0.032 | | | | |
| ASM002467B | Vadvikebäcken | 23:1 | 0.30 | 65560 | 65560 | 2.1 | 2.1 | 0.0 | 2.1 | 2.1 | 0.0 | 0 | 2.1 | 0.032 | PSM107735 | 0.002 | 0.032 | 0 |
| ASM002467A | Vadvikebäcken | 23:1 | 0.01 | 1980 | 67540 | 2.1 | 0.1 | 0.0 | 0.1 | 2.2 | 0.0 | 0 | 2.2 | 0.032 | | | | |
| | **Kärrviksån** | 5:1-20 | 27.31 | 6007100 | 6007100 | 26.9 | 241.7 | 0.0 | 241.7 | | 5.8 | 2 | 235.9 | 0.039 | | | | |
| | **Laxemarån** | 10:1-32 | 40.97 | 9014280 | 9014280 | 37.5 | 378.4 | 0.0 | 378.4 | | 38.5 | 10 | 339.9 | 0.038 | | | | |
| | **All catchments** | | 129.97 | 28593620 | 28593620 | 22.3 | 1192.8 | 0.0 | 1192.8 | | 89.7 | 8 | 1103.1 | 0.039 | | | | |

| **Total nitrogen (tot-N)** | | | | Water balance | | | Total per catchment | | | Total including contributions from upstream catchments | | | | | Calibration data | | | |
|---|---|---|---|---|---|---|---|---|---|---|---|---|---|---|---|---|---|---|
| Idcode | Name | ARO | Area | $Q_{catch}$ | $Q_{out}$ | q | Diffuse | Point | Total | Total IN | Retention | | Total OUT | Conc. | Reference | q | Conc. | Deviation |
| | | | $km^2$ | $m^3 \cdot yr^{-1}$ | $m^3 \cdot yr^{-1}$ | $L \cdot s^{-1}$ | $kg \cdot yr^{-1}$ | $kg \cdot yr^{-1}$ | $kg \cdot yr^{-1}$ | $kg \cdot yr^{-1}$ | $kg \cdot yr^{-1}$ | % | $kg \cdot yr^{-1}$ | $mg \cdot L^{-1}$ | | $L \cdot s^{-1}$ | $mg \cdot L^{-1}$ | % |
| ASM002474 | Kärrviksån | 5:20 | 0.12 | 25740 | 25740 | 0.8 | 74.9 | 0.0 | 74.9 | 74.9 | 0.0 | 0 | 74.9 | 2.911 | | | | |
| ASM002493 | Kärrviksån | 5:19 | 0.84 | 184140 | 209880 | 6.7 | 437.6 | 0.0 | 437.6 | 512.5 | 0.0 | 0 | 512.5 | 2.442 | | | | |
| ASM001483 | Kärrviksån | 5:17 | 0.15 | 33220 | 33220 | 1.1 | 55.2 | 0.0 | 55.2 | 55.2 | 0.0 | 0 | 55.2 | 1.661 | | | | |
| ASM002492 | Kärrviksån | 5:16 | 1.11 | 243980 | 277200 | 8.8 | 514.8 | 0.0 | 514.8 | 570.0 | 0.0 | 0 | 570.0 | 2.056 | | | | |
| ASM002491 | Kärrviksån | 5:15 | 1.87 | 411840 | 689040 | 21.8 | 455.2 | 0.0 | 455.2 | 1025.2 | 1.8 | 0 | 1023.4 | 1.485 | | | | |
| ASM001474 | Kärrviksån | 5:7 | 0.45 | 99000 | 99000 | 3.1 | 102.0 | 0.0 | 102.0 | 102.0 | 0.0 | 0 | 102.0 | 1.031 | | | | |
| ASM002487 | Kärrviksån | 5:6 | 1.20 | 264000 | 363000 | 11.5 | 278.8 | 0.0 | 278.8 | 380.8 | 0.0 | 0 | 380.8 | 1.049 | | | | |
| ASM001472 | Kärrviksån | 5:4 | 1.10 | 242880 | 242880 | 7.7 | 273.7 | 0.0 | 273.7 | 273.7 | 58.9 | 22 | 214.7 | 0.884 | | | | |
| ASM001470 | Kärrviksån | 5:3 | 0.40 | 87560 | 87560 | 2.8 | 164.2 | 0.0 | 164.2 | 164.2 | 0.0 | 0 | 164.2 | 1.876 | | | | |
| ASM001469 | Kärrviksån | 5:2 | 0.97 | 212960 | 212960 | 6.8 | 247.3 | 0.0 | 247.3 | 247.3 | 0.0 | 0 | 247.3 | 1.161 | | | | |
| ASM001471 | Kärrviksån | 5:5 | 2.79 | 614680 | 614680 | 19.5 | 711.7 | 0.0 | 711.7 | 711.7 | 0.0 | 0 | 711.7 | 1.158 | | | | |
| ASM001479 | Kärrviksån | 5:13 | 0.65 | 142340 | 142340 | 4.5 | 150.3 | 0.0 | 150.3 | 150.3 | 0.0 | 0 | 150.3 | 1.056 | | | | |
| ASM001480 | Kärrviksån | 5:14 | 0.10 | 22660 | 22660 | 0.7 | 26.5 | 0.0 | 26.5 | 26.5 | 0.0 | 0 | 26.5 | 1.170 | | | | |
| ASM002490 | Kärrviksån | 5:12 | 0.84 | 183920 | 348920 | 11.1 | 202.1 | 0.0 | 202.1 | 378.9 | 6.6 | 2 | 372.4 | 1.067 | | | | |
| ASM001478 | Kärrviksån | 5:11 | 0.49 | 108460 | 108460 | 3.4 | 114.5 | 0.0 | 114.5 | 114.5 | 0.0 | 0 | 114.5 | 1.056 | | | | |
| ASM002489 | Kärrviksån | 5:10 | 1.20 | 263560 | 372020 | 11.8 | 299.1 | 0.0 | 299.1 | 413.6 | 0.0 | 0 | 413.6 | 1.112 | | | | |
| ASM001476 | Kärrviksån | 5:9 | 3.62 | 796180 | 796180 | 25.2 | 1218.9 | 0.0 | 1218.9 | 1218.9 | 0.0 | 0 | 1218.9 | 1.531 | | | | |
| ASM001475B | Kärrviksån | 5:8 | 1.38 | 302940 | 1820060 | 57.7 | 365.5 | 0.0 | 365.5 | 2370.3 | 0.0 | 0 | 2370.3 | 1.302 | PSM002081 | 0.058 | 1.312 | 1 |
| ASM001475A | Kärrviksån | 5:8 | 0.04 | 9680 | 1829740 | 58.0 | 15.0 | 0.0 | 15.0 | 2385.3 | 0.0 | 0 | 2385.3 | 1.304 | | | | |
| ASM002479 | Kärrviksån | 5:18 | 1.18 | 259600 | 259600 | 8.2 | 274.1 | 0.0 | 274.1 | 274.1 | 0.0 | 0 | 274.1 | 1.056 | | | | |
| ASM002486C | Kärrviksån | 5:1 | 2.75 | 604560 | 1074040 | 34.1 | 653.9 | 0.0 | 653.9 | 1440.5 | 12.6 | 1 | 1428.0 | 1.330 | PSM002080 | | | |
| ASM002486B | Kärrviksån | 5:1 | 1.13 | 247940 | 3840760 | 121.8 | 284.1 | 0.0 | 284.1 | 5120.7 | 0.0 | 0 | 5120.7 | 1.333 | PSM002082 | 0.121 | 1.369 | 3 |
| ASM002486A | Kärrviksån | 5:1 | 2.93 | 645260 | 6007100 | 190.5 | 1238.5 | 0.0 | 1238.5 | 8077.8 | 2.4 | 0 | 8075.4 | 1.344 | PSM002083 | 0.190 | 1.344 | 0 |
| ASM002449 | Bjurhidebäcken | 4:1 | 0.63 | 139040 | 139040 | 4.4 | 188.0 | 0.0 | 188.0 | 188.0 | 0.0 | 0 | 188.0 | 1.352 | | | | |
| ASM002472 | Sörviksån | 3:2 | 0.47 | 103400 | 103400 | 3.3 | 144.7 | 0.0 | 144.7 | 144.7 | 0.1 | 0 | 144.6 | 1.398 | | | | |
| ASM002473 | Sörviksån | 3:1 | 0.53 | 116600 | 220000 | 7.0 | 136.8 | 0.0 | 136.8 | 281.4 | 0.0 | 0 | 281.4 | 1.279 | | | | |
| ASM002651 | Coastal area | | 1.67 | 368280 | 368280 | 11.7 | 415.1 | 0.0 | 415.1 | 415.1 | 31.1 | 7 | 384.0 | 1.043 | | | | |
| ASM002447 | Bodvikebäcken | 2:1 | 0.38 | 83600 | 83600 | 2.7 | 70.3 | 0.0 | 70.3 | 70.3 | 38.2 | 54 | 32.1 | 0.384 | | | | |
| ASM002446 | Långbonäsbäcken | 1:1 | 0.07 | 15400 | 15400 | 0.5 | 16.3 | 0.0 | 16.3 | 16.3 | 0.0 | 0 | 16.3 | 1.056 | | | | |
| ASM002464 | Flakvarpebäcken | 19:1 | 0.18 | 40480 | 40480 | 1.3 | 39.6 | 0.0 | 39.6 | 39.6 | 13.1 | 33 | 26.5 | 0.653 | | | | |
| ASM002465 | Jössesbäcken | 20:1 | 0.11 | 24420 | 24420 | 0.8 | 25.8 | 0.0 | 25.8 | 25.8 | 0.0 | 0 | 25.8 | 1.056 | | | | |
| ASM002471 | Äspöbäcken | 21:1 | 0.06 | 13860 | 13860 | 0.4 | 14.6 | 0.0 | 14.6 | 14.6 | 0.0 | 0 | 14.6 | 1.056 | | | | |
| ASM002652 | Coastal area | | 1.39 | 305140 | 305140 | 9.7 | 317.6 | 0.0 | 317.6 | 317.6 | 25.5 | 8 | 292.1 | 0.957 | | | | |
| ASM001445 | Frisksjön | 7:2 | 1.85 | 406560 | 406560 | 12.9 | 584.8 | 0.0 | 584.8 | 584.8 | 160.4 | 27 | 424.5 | 1.044 | | | | |
| ASM001484 | Kåreviksån | 7:1 | 0.21 | 46860 | 453420 | 14.4 | 49.5 | 0.0 | 49.5 | 473.9 | 0.0 | 0 | 473.9 | 1.045 | | | | |
| ASM001486B | Mederhultsån | 6:1 | 1.92 | 422620 | 422620 | 13.4 | 863.2 | 0.0 | 863.2 | 863.2 | 0.0 | 0 | 863.2 | 2.043 | PSM002084 | 0.013 | 1.970 | 4 |
| ASM001486A | Mederhultsån | 6:1 | 0.08 | 18040 | 440660 | 14.0 | 19.2 | 0.0 | 19.2 | 882.4 | 0.0 | 0 | 882.4 | 2.003 | | | | |
| ASM002654 | Coastal area | | 1.86 | 409420 | 409420 | 13.0 | 425.2 | 0.0 | 425.2 | 425.2 | 34.6 | 8 | 390.6 | 0.954 | | | | |
| ASM002460 | Pistlanbäcken | 8:1 | 0.50 | 109780 | 109780 | 3.5 | 114.9 | 0.0 | 114.9 | 114.9 | 6.2 | 5 | 108.7 | 0.990 | | | | |
| ASM001490 | Ekerumsån | 9:3 | 0.22 | 48840 | 48840 | 1.5 | 117.9 | 0.0 | 117.9 | 117.9 | 0.0 | 0 | 117.9 | 2.414 | | | | |
| ASM001489 | Ekerumsån | 9:2 | 0.77 | 168740 | 168740 | 5.4 | 372.4 | 0.0 | 372.4 | 372.4 | 0.0 | 0 | 372.4 | 2.207 | | | | |
| ASM002483B | Ekerumsån | 9:1 | 1.50 | 330880 | 548460 | 17.4 | 657.1 | 0.0 | 657.1 | 1147.4 | 0.0 | 0 | 1147.4 | 2.092 | PSM002085 | 0.017 | 2.096 | 0 |
| ASM002483A | Ekerumsån | 9:1 | 0.34 | 75020 | 623480 | 19.8 | 118.4 | 0.0 | 118.4 | 1265.8 | 0.0 | 0 | 1265.8 | 2.030 | | | | |
| ASM002478 | Laxemarån | 10:32 | 0.02 | 5060 | 5060 | 0.2 | 5.3 | 0.0 | 5.3 | 5.3 | 0.0 | 0 | 5.3 | 1.056 | | | | |
| ASM002482 | Laxemarån | 10:31 | 0.87 | 190740 | 195800 | 6.2 | 240.6 | 0.0 | 240.6 | 245.9 | 0.0 | 0 | 245.9 | 1.256 | | | | |
| ASM002480B | Laxemarån | 10:30 | 4.23 | 931480 | 1127280 | 35.7 | 1207.6 | 0.0 | 1207.6 | 1453.6 | 227.3 | 16 | 1226.3 | 1.088 | PSM002068 | 0.036 | 1.221 | 11 |
| ASM002480A | Jämsen | 10:30 | 1.83 | 403480 | 1530760 | 48.5 | 509.0 | 0.0 | 509.0 | 1735.3 | 276.9 | 16 | 1458.3 | 0.953 | PSM002069 | 0.049 | 0.953 | 0 |
| ASM001516 | Laxemarån | 10:29 | 0.53 | 117260 | 117260 | 3.7 | 143.1 | 0.0 | 143.1 | 143.1 | 0.0 | 0 | 143.1 | 1.220 | | | | |
| ASM001515 | Laxemarån | 10:28 | 0.34 | 74140 | 74140 | 2.4 | 100.0 | 0.0 | 100.0 | 100.0 | 0.0 | 0 | 100.0 | 1.349 | | | | |
| ASM001514 | Laxemarån | 10:27 | 0.49 | 107140 | 107140 | 3.4 | 313.3 | 0.0 | 313.3 | 313.3 | 0.0 | 0 | 313.3 | 2.924 | | | | |
| ASM001446 | Plittorpsgöl | 10:26 | 0.68 | 149160 | 149160 | 4.7 | 157.3 | 0.0 | 157.3 | 157.3 | 35.7 | 23 | 121.6 | 0.815 | | | | |
| ASM002459 | Laxemarån | 10:25 | 0.10 | 21780 | 170940 | 5.4 | 27.2 | 0.0 | 27.2 | 148.8 | 0.0 | 0 | 148.8 | 0.870 | | | | |
| ASM001512 | Laxemarån | 10:24 | 0.49 | 108680 | 108680 | 3.4 | 115.5 | 0.0 | 115.5 | 115.5 | 0.0 | 0 | 115.5 | 1.063 | | | | |
| ASM002476E | Laxemarån | 10:1 | 3.95 | 868780 | 2977700 | 94.4 | 1093.0 | 0.0 | 1093.0 | 3372.0 | 3.8 | 0 | 3368.2 | 1.131 | PSM002071 | 0.094 | 1.007 | 12 |
| ASM001510 | Laxemarån | 10:22 | 0.56 | 123640 | 123640 | 3.9 | 130.5 | 0.0 | 130.5 | 130.5 | 0.0 | 0 | 130.5 | 1.056 | | | | |
| ASM002453 | Laxemarån | 10:21 | 0.45 | 97900 | 221540 | 7.0 | 103.1 | 0.0 | 103.1 | 233.6 | 1.9 | 1 | 231.7 | 1.046 | | | | |
| ASM002450B | Laxemarån | 10:20 | 2.39 | 526240 | 747780 | 23.7 | 554.3 | 0.0 | 554.3 | 786.0 | 7.3 | 1 | 778.8 | 1.041 | PSM002072 | | | |
| ASM002450A | Laxemarån | 10:20 | 0.19 | 41140 | 788920 | 25.0 | 43.6 | 0.0 | 43.6 | 822.4 | 0.0 | 0 | 822.4 | 1.042 | | | | |
| ASM001511 | Laxemarån | 10:23 | 0.74 | 162800 | 162800 | 5.2 | 171.9 | 0.0 | 171.9 | 171.9 | 0.0 | 0 | 171.9 | 1.056 | | | | |
| ASM001448 | Grangöl | 10:19 | 0.50 | 108900 | 108900 | 3.5 | 108.7 | 0.0 | 108.7 | 108.7 | 26.4 | 24 | 82.3 | 0.755 | | | | |
| ASM002499 | Laxemarån | 10:18 | 0.06 | 12760 | 121660 | 3.9 | 19.4 | 0.0 | 19.4 | 101.7 | 0.0 | 0 | 101.7 | 0.836 | | | | |
| ASM001506 | Laxemarån | 10:17 | 0.40 | 87560 | 87560 | 2.8 | 140.2 | 0.0 | 140.2 | 140.2 | 0.0 | 0 | 140.2 | 1.601 | | | | |
| ASM001447 | Fjällgöl | 10:16 | 0.30 | 64900 | 64900 | 2.1 | 75.4 | 0.0 | 75.4 | 75.4 | 22.1 | 29 | 53.3 | 0.822 | | | | |
| ASM002451 | Laxemarån | 10:15 | 0.33 | 71500 | 136400 | 4.3 | 102.6 | 0.0 | 102.6 | 155.9 | 0.0 | 0 | 155.9 | 1.143 | | | | |
| ASM002452 | Laxemarån | 10:14 | 2.38 | 522500 | 868120 | 27.5 | 748.8 | 0.0 | 748.8 | 1146.6 | 3.2 | 0 | 1143.4 | 1.317 | | | | |
| ASM001503 | Laxemarån | 10:13 | 0.42 | 91520 | 91520 | 2.9 | 175.3 | 0.0 | 175.3 | 175.3 | 0.0 | 0 | 175.3 | 1.915 | | | | |
| ASM002454 | Laxemarån | 10:12 | 0.81 | 177760 | 269280 | 8.5 | 439.5 | 0.0 | 439.5 | 614.8 | 0.0 | 0 | 614.8 | 2.283 | | | | |
| ASM001501 | Laxemarån | 10:11 | 0.81 | 177320 | 177320 | 5.6 | 260.4 | 0.0 | 260.4 | 260.4 | 0.0 | 0 | 260.4 | 1.469 | | | | |
| ASM002457 | Laxemarån | 10:10 | 1.39 | 305580 | 482900 | 15.3 | 622.9 | 0.0 | 622.9 | 883.3 | 0.0 | 0 | 883.3 | 1.829 | | | | |
| ASM002476D | Laxemarån | 10:1 | 4.96 | 1091860 | 6641580 | 210.6 | 1632.8 | 0.0 | 1632.8 | 8636.7 | 0.0 | 0 | 8636.7 | 1.300 | PSM002077 | | | |
| ASM001499 | Laxemarån | 10:9 | 0.71 | 156420 | 156420 | 5.0 | 168.6 | 0.0 | 168.6 | 168.6 | 0.0 | 0 | 168.6 | 1.078 | | | | |
| ASM001498 | Laxemarån | 10:8 | 2.77 | 609620 | 766040 | 24.3 | 814.3 | 0.0 | 814.3 | 982.9 | 0.0 | 0 | 982.9 | 1.283 | PSM002078 | 0.024 | 1.120 | 15 |
| ASM001497 | Laxemarån | 10:7 | 0.61 | 133980 | 133980 | 4.2 | 172.5 | 0.0 | 172.5 | 172.5 | 0.0 | 0 | 172.5 | 1.288 | | | | |
| ASM002476C | Laxemarån | 10:1 | 0.32 | 69300 | 7610900 | 241.3 | 100.8 | 0.0 | 100.8 | 9892.9 | 1.5 | 0 | 9891.5 | 1.300 | PSM002079 | 0.242 | 1.200 | 8 |
| ASM001494 | Laxemarån | 10:4 | 1.00 | 220220 | 220220 | 7.0 | 487.2 | 0.0 | 487.2 | 487.2 | 0.0 | 0 | 487.2 | 2.212 | | | | |
| ASM001493 | Laxemarån | 10:3 | 0.32 | 70180 | 70180 | 2.2 | 114.9 | 0.0 | 114.9 | 114.9 | 0.0 | 0 | 114.9 | 1.638 | | | | |
| ASM001492 | Laxemarån | 10:2 | 0.46 | 101200 | 101200 | 3.2 | 196.0 | 0.0 | 196.0 | 196.0 | 0.0 | 0 | 196.0 | 1.936 | | | | |
| ASM001496 | Laxemarån | 10:6 | 0.89 | 195800 | 195800 | 6.2 | 262.1 | 0.0 | 262.1 | 262.1 | 0.0 | 0 | 262.1 | 1.339 | | | | |
| ASM001495 | Laxemarån | 10:5 | 0.29 | 63800 | 63800 | 2.0 | 89.6 | 0.0 | 89.6 | 89.6 | 0.0 | 0 | 89.6 | 1.404 | | | | |
| ASM002476B | Laxemarån | 10:1 | 3.23 | 710820 | 8972920 | 284.5 | 1135.8 | 0.0 | 1135.8 | 12177.1 | 7.8 | 0 | 12169.3 | 1.356 | PSM002087 | 0.285 | 1.344 | 1 |
| ASM002476A | Laxemarån | 10:1 | 0.19 | 41360 | 9014280 | 285.8 | 48.0 | 0.0 | 48.0 | 12217.2 | 0.0 | 0 | 12217.2 | 1.355 | | | | |
| ASM002495 | Glostadsbäcken | 12:3 | 0.13 | 27720 | 27720 | 0.9 | 64.8 | 0.0 | 64.8 | 64.8 | 0.0 | 0 | 64.8 | 2.337 | | | | |
| ASM002485 | Glostadsbäcken | 12:2 | 0.33 | 72820 | 72820 | 2.3 | 76.9 | 0.0 | 76.9 | 76.9 | 0.0 | 0 | 76.9 | 1.056 | | | | |
| ASM002498 | Glostadsbäcken | 12:1 | 1.60 | 351340 | 451880 | 14.3 | 426.6 | 0.0 | 426.6 | 568.3 | 13.2 | 2 | 555.1 | 1.228 | | | | |
| ASM001518B | Stålglobäcken | 13:1 | 0.68 | 149380 | 149380 | 4.7 | 378.8 | 0.0 | 378.8 | 378.8 | 0.0 | 0 | 378.8 | 2.536 | PSM002086 | 0.005 | 3.378 | 25 |
| ASM001518A | Stålglobäcken | 13:1 | 0.35 | 77880 | 227260 | 7.2 | 112.1 | 0.0 | 112.1 | 490.9 | 0.0 | 0 | 490.9 | 2.160 | | | | |
| ASM002462 | Uvöbäcken | 15:1 | 0.97 | 212740 | 212740 | 6.7 | 326.6 | 0.0 | 326.6 | 326.6 | 0.0 | 0 | 326.6 | 1.535 | | | | |
| ASM002497 | Stekebäcken | 14:2 | 0.44 | 95700 | 95700 | 3.0 | 199.4 | 0.0 | 199.4 | 199.4 | 0.0 | 0 | 199.4 | 2.084 | | | | |
| ASM001517 | Stekebäcken | 14:1 | 0.90 | 198660 | 294360 | 9.3 | 245.2 | 0.0 | 245.2 | 444.6 | 0.0 | 0 | 444.6 | 1.511 | | | | |
| ASM002463 | Svartebäck | 16:1 | 0.50 | 110880 | 110880 | 3.5 | 126.9 | 0.0 | 126.9 | 126.9 | 2.3 | 2 | 124.6 | 1.123 | | | | |
| ASM002655 | Coastal area | | 2.71 | 596420 | 596420 | 18.9 | 652.5 | 0.0 | 652.5 | 652.5 | 94.6 | 14 | 557.9 | 0.935 | | | | |
| ASM002658 | Coastal area | | 1.26 | 277420 | 277420 | 8.8 | 287.7 | 0.0 | 287.7 | 287.7 | 21.4 | 7 | 266.3 | 0.960 | | | | |
| ASM002656 | Coastal area | | 0.22 | 48400 | 48400 | 1.5 | 48.7 | 0.0 | 48.7 | 48.7 | 10.1 | 21 | 38.6 | 0.798 | | | | |
| ASM002660 | Coastal area | | 0.14 | 30360 | 30360 | 1.0 | 30.5 | 0.0 | 30.5 | 30.5 | 6.7 | 22 | 23.8 | 0.783 | | | | |
| ASM002659 | Coastal area | | 15.70 | 3453780 | 3453780 | 109.5 | 4804.9 | 0.0 | 4804.9 | 4804.9 | 64.0 | 1 | 4741.0 | 1.373 | | | | |
| ASM002657 | Coastal area | | 2.60 | 571340 | 571340 | 18.1 | 707.1 | 0.0 | 707.1 | 707.1 | 14.2 | 2 | 692.9 | 1.213 | | | | |
| ASM001522 | Uthammarsån | 17:5 | 0.57 | 125620 | 125620 | 4.0 | 227.3 | 0.0 | 227.3 | 227.3 | 0.0 | 0 | 227.3 | 1.810 | | | | |
| ASM001523 | Uthammarsån | 17:6 | 0.96 | 210760 | 210760 | 6.7 | 387.7 | 0.0 | 387.7 | 387.7 | 0.0 | 0 | 387.7 | 1.839 | | | | |
| ASM001521 | Uthammarsån | 17:4 | 0.20 | 44880 | 44880 | 1.4 | 101.2 | 0.0 | 101.2 | 101.2 | 0.0 | 0 | 101.2 | 2.254 | | | | |
| ASM001520 | Uthammarsån | 17:3 | 0.08 | 17820 | 17820 | 0.6 | 37.8 | 0.0 | 37.8 | 37.8 | 0.0 | 0 | 37.8 | 2.120 | | | | |
| ASM002494B | Uthammarsån | 17:1 | 2.91 | 640860 | 1039940 | 33.0 | 908.0 | 0.0 | 908.0 | 1662.0 | 0.0 | 0 | 1662.0 | 1.598 | PSM002076 | 0.033 | 2.217 | 28 |
| ASM001533 | Uthammarsån | 17:2 | 0.51 | 112640 | 112640 | 3.6 | 271.1 | 0.0 | 271.1 | 271.1 | 0.0 | 0 | 271.1 | 2.406 | | | | |
| ASM002494A | Uthammarsån | 17:1 | 1.78 | 391820 | 1544400 | 49.0 | 964.5 | 0.0 | 964.5 | 2897.5 | 2.3 | 0 | 2895.2 | 1.875 | | | | |
| ASM001528 | Släthultebäcken | 18:5 | 0.32 | 70400 | 70400 | 2.2 | 74.3 | 0.0 | 74.3 | 74.3 | 0.0 | 0 | 74.3 | 1.056 | | | | |
| ASM002477 | Släthultebäcken | 18:4 | 0.66 | 144980 | 215380 | 6.8 | 147.6 | 0.0 | 147.6 | 222.0 | 27.4 | 12 | 194.6 | 0.904 | | | | |
| ASM001531 | Släthultebäcken | 18:8 | 0.30 | 66440 | 66440 | 2.1 | 70.2 | 0.0 | 70.2 | 70.2 | 0.0 | 0 | 70.2 | 1.057 | | | | |
| ASM001532 | Släthultebäcken | 18:9 | 0.11 | 24420 | 24420 | 0.8 | 70.7 | 0.0 | 70.7 | 70.7 | 0.0 | 0 | 70.7 | 2.896 | | | | |
| ASM002455 | Släthultebäcken | 18:7 | 0.76 | 167420 | 258280 | 8.2 | 366.4 | 0.0 | 366.4 | 507.3 | 0.0 | 0 | 507.3 | 1.964 | | | | |
| ASM002475 | Släthultebäcken | 18:6 | 1.06 | 232100 | 490380 | 15.5 | 291.4 | 0.0 | 291.4 | 798.8 | 0.0 | 0 | 798.8 | 1.629 | | | | |
| ASM001526 | Släthultebäcken | 18:3 | 0.40 | 88220 | 88220 | 2.8 | 100.0 | 0.0 | 100.0 | 100.0 | 1.1 | 1 | 98.9 | 1.121 | | | | |
| ASM002481C | Släthultebäcken | 18:1 | 2.44 | 537020 | 1027400 | 32.6 | 849.4 | 0.0 | 849.4 | 1648.2 | 0.0 | 0 | 1648.2 | 1.604 | PSM002070 | | | |
| ASM002481B | Släthultebäcken | 18:1 | 2.13 | 469260 | 1800260 | 57.1 | 586.6 | 0.0 | 586.6 | 2528.3 | 15.3 | 1 | 2513.0 | 1.396 | PSM002075 | | | |
| ASM001525 | Släthultebäcken | 18:2 | 0.77 | 169620 | 169620 | 5.4 | 248.2 | 0.0 | 248.2 | 248.2 | 0.0 | 0 | 248.2 | 1.463 | | | | |
| ASM002481A | Släthultebäcken | 18:1 | 0.00 | 220 | 1970100 | 62.5 | 0.2 | 0.0 | 0.2 | 2761.4 | 0.0 | 0 | 2761.4 | 1.402 | | | | |
| ASM001444 | Sörämagasinet | 11:1 | 0.52 | 115060 | 115060 | 3.6 | 100.8 | 0.0 | 100.8 | 100.8 | 51.5 | 51 | 49.3 | 0.428 | | | | |
| ASM002466 | Stekflagebäcken | 22:1 | 0.36 | 78980 | 78980 | 2.5 | 77.7 | 0.0 | 77.7 | 77.7 | 22.6 | 29 | 55.1 | 0.698 | | | | |
| ASM002653 | Coastal area | | 0.76 | 166980 | 166980 | 5.3 | 174.4 | 0.0 | 174.4 | 174.4 | 12.4 | 7 | 162.0 | 0.970 | | | | |
| ASM002470 | Skölkebäcken | 26:1 | 0.17 | 36300 | 36300 | 1.2 | 38.3 | 0.0 | 38.3 | 38.3 | 0.0 | 0 | 38.3 | 1.056 | | | | |
| ASM002469 | Gloebäcken | 25:1 | 0.13 | 28820 | 28820 | 0.9 | 30.4 | 0.0 | 30.4 | 30.4 | 0.0 | 0 | 30.4 | 1.056 | | | | |
| ASM002468 | Lindströmmebäcken | 24:1 | 0.19 | 42240 | 42240 | 1.3 | 44.6 | 0.0 | 44.6 | 44.6 | 0.0 | 0 | 44.6 | 1.056 | | | | |
| ASM002467B | Vadvikebäcken | 23:1 | 0.30 | 65560 | 65560 | 2.1 | 69.2 | 0.0 | 69.2 | 69.2 | 0.0 | 0 | 69.2 | 1.056 | PSM107735 | 0.002 | 1.381 | 24 |
| ASM002467A | Vadvikebäcken | 23:1 | 0.01 | 1980 | 67540 | 2.1 | 2.1 | 0.0 | 2.1 | 71.3 | 0.0 | 0 | 71.3 | 1.056 | | | | |
| | **Kärrviksån** | 5:1-20 | 27.31 | 6007100 | 6007100 | 26.9 | 8157.7 | 0.0 | 8157.7 | | 82.3 | 1 | 8075.4 | 1.344 | | | | |
| | **Laxemarån** | 10:1-32 | 40.97 | 9014280 | 9014280 | 37.5 | 12831.1 | 0.0 | 12831.1 | | 613.8 | 5 | 12217.2 | 1.355 | | | | |
| | **All catchments** | | 129.97 | 28593620 | 28593620 | 22.3 | 40409.1 | 0.0 | 40409.1 | | 1364.3 | 3 | 39044.8 | 1.366 | | | | |

| **Total organic carbon (TOC)** | | | | Water balance | | | Total per catchment | | | Total including contributions from upstream catchments | | | | | Calibration data | | | |
|---|---|---|---|---|---|---|---|---|---|---|---|---|---|---|---|---|---|---|
| Idcode | Name | ARO | Area | $Q_{catch}$ | $Q_{out}$ | q | Diffuse | Point | Total | Total IN | Retention | | Total OUT | Conc. | Reference | q | Conc. | Deviation |
| | | | $km^2$ | $m^3 \cdot yr^{-1}$ | $m^3 \cdot yr^{-1}$ | $L \cdot s^{-1}$ | $kg \cdot yr^{-1}$ | $kg \cdot yr^{-1}$ | $kg \cdot yr^{-1}$ | $kg \cdot yr^{-1}$ | $kg \cdot yr^{-1}$ | % | $kg \cdot yr^{-1}$ | $mg \cdot L^{-1}$ | | $L \cdot s^{-1}$ | $mg \cdot L^{-1}$ | % |
| ASM002474 | Kärrviksån | 5:20 | 0.12 | 25740 | 25740 | 0.8 | 559.4 | 0.0 | 559.4 | 559.4 | 0.0 | 0 | 559.4 | 21.732 | | | | |
| ASM002493 | Kärrviksån | 5:19 | 0.84 | 184140 | 209880 | 6.7 | 4002.9 | 0.0 | 4002.9 | 4562.2 | 0.0 | 0 | 4562.2 | 21.737 | | | | |
| ASM001483 | Kärrviksån | 5:17 | 0.15 | 33220 | 33220 | 1.1 | 721.9 | 0.0 | 721.9 | 721.9 | 0.0 | 0 | 721.9 | 21.729 | | | | |
| ASM002492 | Kärrviksån | 5:16 | 1.11 | 243980 | 277200 | 8.8 | 5300.5 | 0.0 | 5300.5 | 6022.4 | 0.0 | 0 | 6022.4 | 21.726 | | | | |
| ASM002491 | Kärrviksån | 5:15 | 1.87 | 411840 | 689040 | 21.8 | 8827.4 | 0.0 | 8827.4 | 14849.7 | 10.1 | 0 | 14839.6 | 21.537 | | | | |
| ASM001474 | Kärrviksån | 5:7 | 0.45 | 99000 | 99000 | 3.1 | 2100.2 | 0.0 | 2100.2 | 2100.2 | 0.0 | 0 | 2100.2 | 21.214 | | | | |
| ASM002487 | Kärrviksån | 5:6 | 1.20 | 264000 | 363000 | 11.5 | 5737.2 | 0.0 | 5737.2 | 7837.4 | 0.0 | 0 | 7837.4 | 21.591 | | | | |
| ASM001472 | Kärrviksån | 5:4 | 1.10 | 242880 | 242880 | 7.7 | 4845.9 | 0.0 | 4845.9 | 4845.9 | 465.3 | 10 | 4380.6 | 18.036 | | | | |
| ASM001470 | Kärrviksån | 5:3 | 0.40 | 87560 | 87560 | 2.8 | 1902.8 | 0.0 | 1902.8 | 1902.8 | 0.0 | 0 | 1902.8 | 21.732 | | | | |
| ASM001469 | Kärrviksån | 5:2 | 0.97 | 212960 | 212960 | 6.8 | 4628.4 | 0.0 | 4628.4 | 4628.4 | 0.0 | 0 | 4628.4 | 21.734 | | | | |
| ASM001471 | Kärrviksån | 5:5 | 2.79 | 614680 | 614680 | 19.5 | 13356.7 | 0.0 | 13356.7 | 13356.7 | 0.0 | 0 | 13356.7 | 21.729 | | | | |
| ASM001479 | Kärrviksån | 5:13 | 0.65 | 142340 | 142340 | 4.5 | 3093.3 | 0.0 | 3093.3 | 3093.3 | 0.0 | 0 | 3093.3 | 21.732 | | | | |
| ASM001480 | Kärrviksån | 5:14 | 0.10 | 22660 | 22660 | 0.7 | 492.4 | 0.0 | 492.4 | 492.4 | 0.0 | 0 | 492.4 | 21.729 | | | | |
| ASM002490 | Kärrviksån | 5:12 | 0.84 | 183920 | 348920 | 11.1 | 3977.3 | 0.0 | 3977.3 | 7563.0 | 51.2 | 1 | 7511.8 | 21.529 | | | | |
| ASM001478 | Kärrviksån | 5:11 | 0.49 | 108460 | 108460 | 3.4 | 2357.3 | 0.0 | 2357.3 | 2357.3 | 0.0 | 0 | 2357.3 | 21.734 | | | | |
| ASM002489 | Kärrviksån | 5:10 | 1.20 | 263560 | 372020 | 11.8 | 5726.5 | 0.0 | 5726.5 | 8083.7 | 0.0 | 0 | 8083.7 | 21.729 | | | | |
| ASM001476 | Kärrviksån | 5:9 | 3.62 | 796180 | 796180 | 25.2 | 17300.6 | 0.0 | 17300.6 | 17300.6 | 0.0 | 0 | 17300.6 | 21.729 | | | | |
| ASM001475B | Kärrviksån | 5:8 | 1.38 | 302940 | 1820060 | 57.7 | 6484.5 | 0.0 | 6484.5 | 39380.5 | 0.0 | 0 | 39380.5 | 21.637 | PSM002081 | 0.058 | 24.202 | 11 |
| ASM001475A | Kärrviksån | 5:8 | 0.04 | 9680 | 1829740 | 58.0 | 308.6 | 0.0 | 308.6 | 39689.1 | 0.0 | 0 | 39689.1 | 21.691 | | | | |
| ASM002479 | Kärrviksån | 5:18 | 1.18 | 259600 | 259600 | 8.2 | 5641.0 | 0.0 | 5641.0 | 5641.0 | 0.0 | 0 | 5641.0 | 21.729 | | | | |
| ASM002486C | Kärrviksån | 5:1 | 2.75 | 604560 | 1074040 | 34.1 | 13019.5 | 0.0 | 13019.5 | 23222.7 | 78.8 | 0 | 23143.9 | 21.548 | PSM002080 | | | |
| ASM002486B | Kärrviksån | 5:1 | 1.13 | 247940 | 3840760 | 121.8 | 4842.0 | 0.0 | 4842.0 | 82514.7 | 0.0 | 0 | 82514.7 | 21.484 | PSM002082 | 0.121 | 23.906 | 10 |
| ASM002486A | Kärrviksån | 5:1 | 2.93 | 645260 | 6007100 | 190.5 | 14070.4 | 0.0 | 14070.4 | 128691.0 | 14.8 | 0 | 128676.2 | 21.421 | PSM002083 | 0.190 | 22.914 | 7 |
| ASM002449 | Bjurhidebäcken | 4:1 | 0.63 | 139040 | 139040 | 4.4 | 3021.9 | 0.0 | 3021.9 | 3021.9 | 0.0 | 0 | 3021.9 | 21.734 | | | | |
| ASM002472 | Sörviksån | 3:2 | 0.47 | 103400 | 103400 | 3.3 | 2247.3 | 0.0 | 2247.3 | 2247.3 | 0.5 | 0 | 2246.8 | 21.729 | | | | |
| ASM002473 | Sörviksån | 3:1 | 0.53 | 116600 | 220000 | 7.0 | 2534.2 | 0.0 | 2534.2 | 4780.9 | 0.0 | 0 | 4780.9 | 21.732 | | | | |
| ASM002651 | Coastal area | | 1.67 | 368280 | 368280 | 11.7 | 7908.1 | 0.0 | 7908.1 | 7908.1 | 240.2 | 3 | 7667.9 | 20.821 | | | | |
| ASM002447 | Bodvikebäcken | 2:1 | 0.38 | 83600 | 83600 | 2.7 | 1446.5 | 0.0 | 1446.5 | 1446.5 | 456.1 | 32 | 990.4 | 11.847 | | | | |
| ASM002446 | Långbonäsbäcken | 1:1 | 0.07 | 15400 | 15400 | 0.5 | 334.6 | 0.0 | 334.6 | 334.6 | 0.0 | 0 | 334.6 | 21.729 | | | | |
| ASM002464 | Flakvarpebäcken | 19:1 | 0.18 | 40480 | 40480 | 1.3 | 814.6 | 0.0 | 814.6 | 814.6 | 131.2 | 16 | 683.4 | 16.882 | | | | |
| ASM002465 | Jössesbäcken | 20:1 | 0.11 | 24420 | 24420 | 0.8 | 530.7 | 0.0 | 530.7 | 530.7 | 0.0 | 0 | 530.7 | 21.732 | | | | |
| ASM002471 | Äspöbäcken | 21:1 | 0.06 | 13860 | 13860 | 0.4 | 301.2 | 0.0 | 301.2 | 301.2 | 0.0 | 0 | 301.2 | 21.732 | | | | |
| ASM002652 | Coastal area | | 1.39 | 305140 | 305140 | 9.7 | 6537.0 | 0.0 | 6537.0 | 6537.0 | 213.8 | 3 | 6323.2 | 20.722 | | | | |
| ASM001445 | Friskasjön | 7:2 | 1.85 | 406560 | 406560 | 12.9 | 8272.4 | 0.0 | 8272.4 | 8272.4 | 1055.0 | 13 | 7217.4 | 17.752 | | | | |
| ASM001484 | Kåreviksån | 7:1 | 0.21 | 46860 | 453420 | 14.4 | 1018.3 | 0.0 | 1018.3 | 8235.8 | 0.0 | 0 | 8235.8 | 18.164 | | | | |
| ASM001486B | Mederhultsån | 6:1 | 1.92 | 422620 | 422620 | 13.4 | 9185.2 | 0.0 | 9185.2 | 9185.2 | 0.0 | 0 | 9185.2 | 21.734 | PSM002084 | 0.013 | 21.734 | 0 |
| ASM001486A | Mederhultsån | 6:1 | 0.08 | 18040 | 440660 | 14.0 | 394.7 | 0.0 | 394.7 | 9579.8 | 0.0 | 0 | 9579.8 | 21.740 | | | | |
| ASM002654 | Coastal area | | 1.86 | 409420 | 409420 | 13.0 | 8747.9 | 0.0 | 8747.9 | 8747.9 | 289.9 | 3 | 8458.0 | 20.659 | | | | |
| ASM002460 | Pistlanbäcken | 8:1 | 0.50 | 109780 | 109780 | 3.5 | 2365.2 | 0.0 | 2365.2 | 2365.2 | 51.0 | 2 | 2314.2 | 21.081 | | | | |
| ASM001490 | Ekerumsån | 9:3 | 0.22 | 48840 | 48840 | 1.5 | 1061.7 | 0.0 | 1061.7 | 1061.7 | 0.0 | 0 | 1061.7 | 21.738 | | | | |
| ASM001489 | Ekerumsån | 9:2 | 0.77 | 168740 | 168740 | 5.4 | 3667.4 | 0.0 | 3667.4 | 3667.4 | 0.0 | 0 | 3667.4 | 21.734 | | | | |
| ASM002483B | Ekerumsån | 9:1 | 1.50 | 330880 | 548460 | 17.4 | 7187.6 | 0.0 | 7187.6 | 11916.7 | 0.0 | 0 | 11916.7 | 21.728 | PSM002085 | 0.017 | 21.103 | 3 |
| ASM002483A | Ekerumsån | 9:1 | 0.34 | 75020 | 623480 | 19.8 | 1634.1 | 0.0 | 1634.1 | 13550.8 | 0.0 | 0 | 13550.8 | 21.734 | | | | |
| ASM002478 | Laxemarån | 10:32 | 0.02 | 5060 | 5060 | 0.2 | 110.0 | 0.0 | 110.0 | 110.0 | 0.0 | 0 | 110.0 | 21.734 | | | | |
| ASM002482 | Laxemarån | 10:31 | 0.87 | 190740 | 195800 | 6.2 | 4144.7 | 0.0 | 4144.7 | 4254.7 | 0.0 | 0 | 4254.7 | 21.730 | | | | |
| ASM002480B | Laxemarån | 10:30 | 4.23 | 931480 | 1127280 | 35.7 | 19407.6 | 0.0 | 19407.6 | 23662.3 | 1583.6 | 7 | 22078.7 | 19.586 | PSM002068 | 0.036 | 22.969 | 15 |
| ASM002480A | Jämsen | 10:30 | 1.83 | 403480 | 1530760 | 48.5 | 7169.9 | 0.0 | 7169.9 | 29248.6 | 2001.8 | 7 | 27246.8 | 17.800 | PSM002069 | 0.049 | 17.800 | 0 |
| ASM001516 | Laxemarån | 10:29 | 0.53 | 117260 | 117260 | 3.7 | 2548.5 | 0.0 | 2548.5 | 2548.5 | 0.0 | 0 | 2548.5 | 21.734 | | | | |
| ASM001515 | Laxemarån | 10:28 | 0.34 | 74140 | 74140 | 2.4 | 1464.4 | 0.0 | 1464.4 | 1464.4 | 0.0 | 0 | 1464.4 | 19.752 | | | | |
| ASM001514 | Laxemarån | 10:27 | 0.49 | 107140 | 107140 | 3.4 | 2328.3 | 0.0 | 2328.3 | 2328.3 | 0.0 | 0 | 2328.3 | 21.732 | | | | |
| ASM001446 | Plittorpsgöl | 10:26 | 0.68 | 149160 | 149160 | 4.7 | 3081.4 | 0.0 | 3081.4 | 3081.4 | 314.1 | 10 | 2767.3 | 18.553 | | | | |
| ASM002459 | Laxemarån | 10:25 | 0.10 | 21780 | 170940 | 5.4 | 473.3 | 0.0 | 473.3 | 3240.6 | 0.0 | 0 | 3240.6 | 18.957 | | | | |
| ASM001512 | Laxemarån | 10:24 | 0.49 | 108680 | 108680 | 3.4 | 2361.3 | 0.0 | 2361.3 | 2361.3 | 0.0 | 0 | 2361.3 | 21.727 | | | | |
| ASM002476E | Laxemarån | 10:1 | 3.95 | 868780 | 2977700 | 94.4 | 18382.8 | 0.0 | 18382.8 | 57572.8 | 25.2 | 0 | 57547.6 | 19.326 | PSM002071 | 0.094 | 15.971 | 21 |
| ASM001510 | Laxemarån | 10:22 | 0.56 | 123640 | 123640 | 3.9 | 2686.9 | 0.0 | 2686.9 | 2686.9 | 0.0 | 0 | 2686.9 | 21.732 | | | | |
| ASM002453 | Laxemarån | 10:21 | 0.45 | 97900 | 221540 | 7.0 | 2121.1 | 0.0 | 2121.1 | 4808.0 | 14.9 | 0 | 4793.1 | 21.636 | | | | |
| ASM002450B | Laxemarån | 10:20 | 2.39 | 526240 | 747780 | 23.7 | 11408.0 | 0.0 | 11408.0 | 16201.2 | 58.4 | 0 | 16142.8 | 21.588 | PSM002072 | | | |
| ASM002450A | Laxemarån | 10:20 | 0.19 | 41140 | 788920 | 25.0 | 897.4 | 0.0 | 897.4 | 17040.2 | 0.0 | 0 | 17040.2 | 21.599 | | | | |
| ASM001511 | Laxemarån | 10:23 | 0.74 | 162800 | 162800 | 5.2 | 3537.9 | 0.0 | 3537.9 | 3537.9 | 0.0 | 0 | 3537.9 | 21.732 | | | | |
| ASM001448 | Grangöl | 10:19 | 0.50 | 108900 | 108900 | 3.5 | 2236.4 | 0.0 | 2236.4 | 2236.4 | 247.0 | 11 | 1989.4 | 18.268 | | | | |
| ASM002499 | Laxemarån | 10:18 | 0.06 | 12760 | 121660 | 3.9 | 277.3 | 0.0 | 277.3 | 2266.7 | 0.0 | 0 | 2266.7 | 18.631 | | | | |
| ASM001506 | Laxemarån | 10:17 | 0.40 | 87560 | 87560 | 2.8 | 1902.8 | 0.0 | 1902.8 | 1902.8 | 0.0 | 0 | 1902.8 | 21.732 | | | | |
| ASM001447 | Fjällgöl | 10:16 | 0.30 | 64900 | 64900 | 2.1 | 1310.8 | 0.0 | 1310.8 | 1310.8 | 181.0 | 14 | 1129.8 | 17.408 | | | | |
| ASM002451 | Laxemarån | 10:15 | 0.33 | 71500 | 136400 | 4.3 | 1553.7 | 0.0 | 1553.7 | 2683.4 | 0.0 | 0 | 2683.4 | 19.673 | | | | |
| ASM002452 | Laxemarån | 10:14 | 2.38 | 522500 | 868120 | 27.5 | 11348.0 | 0.0 | 11348.0 | 18200.9 | 19.9 | 0 | 18181.1 | 20.943 | | | | |
| ASM001503 | Laxemarån | 10:13 | 0.42 | 91520 | 91520 | 2.9 | 1988.9 | 0.0 | 1988.9 | 1988.9 | 0.0 | 0 | 1988.9 | 21.732 | | | | |
| ASM002454 | Laxemarån | 10:12 | 0.81 | 177760 | 269280 | 8.5 | 3862.2 | 0.0 | 3862.2 | 5851.1 | 0.0 | 0 | 5851.1 | 21.729 | | | | |
| ASM001501 | Laxemarån | 10:11 | 0.81 | 177320 | 177320 | 5.6 | 3853.8 | 0.0 | 3853.8 | 3853.8 | 0.0 | 0 | 3853.8 | 21.734 | | | | |
| ASM002457 | Laxemarån | 10:10 | 1.39 | 305580 | 482900 | 15.3 | 6639.4 | 0.0 | 6639.4 | 10493.3 | 0.0 | 0 | 10493.3 | 21.730 | | | | |
| ASM002476D | Laxemarån | 10:1 | 4.96 | 1091860 | 6641580 | 210.6 | 23716.7 | 0.0 | 23716.7 | 136367.9 | 0.0 | 0 | 136367.9 | 20.532 | PSM002077 | | | |
| ASM001499 | Laxemarån | 10:9 | 0.71 | 156420 | 156420 | 5.0 | 3398.9 | 0.0 | 3398.9 | 3398.9 | 0.0 | 0 | 3398.9 | 21.729 | | | | |
| ASM001498 | Laxemarån | 10:8 | 2.77 | 609620 | 766040 | 24.3 | 13248.1 | 0.0 | 13248.1 | 16647.0 | 0.0 | 0 | 16647.0 | 21.731 | PSM002078 | 0.024 | 18.623 | 17 |
| ASM001497 | Laxemarån | 10:7 | 0.61 | 133980 | 133980 | 4.2 | 2911.9 | 0.0 | 2911.9 | 2911.9 | 0.0 | 0 | 2911.9 | 21.734 | | | | |
| ASM002476C | Laxemarån | 10:1 | 0.32 | 69300 | 7610900 | 241.3 | 1560.3 | 0.0 | 1560.3 | 157487.1 | 8.9 | 0 | 157478.1 | 20.691 | PSM002079 | 0.242 | 19.351 | 7 |
| ASM001494 | Laxemarån | 10:4 | 1.00 | 220220 | 220220 | 7.0 | 4784.8 | 0.0 | 4784.8 | 4784.8 | 0.0 | 0 | 4784.8 | 21.727 | | | | |
| ASM001493 | Laxemarån | 10:3 | 0.32 | 70180 | 70180 | 2.2 | 1525.3 | 0.0 | 1525.3 | 1525.3 | 0.0 | 0 | 1525.3 | 21.734 | | | | |
| ASM001492 | Laxemarån | 10:2 | 0.46 | 101200 | 101200 | 3.2 | 2198.8 | 0.0 | 2198.8 | 2198.8 | 0.0 | 0 | 2198.8 | 21.727 | | | | |
| ASM001496 | Laxemarån | 10:6 | 0.89 | 195800 | 195800 | 6.2 | 4254.6 | 0.0 | 4254.6 | 4254.6 | 0.0 | 0 | 4254.6 | 21.729 | | | | |
| ASM001495 | Laxemarån | 10:5 | 0.29 | 63800 | 63800 | 2.0 | 1386.2 | 0.0 | 1386.2 | 1386.2 | 0.0 | 0 | 1386.2 | 21.727 | | | | |
| ASM002476B | Laxemarån | 10:1 | 3.23 | 710820 | 8972920 | 284.5 | 15469.9 | 0.0 | 15469.9 | 187097.7 | 46.7 | 0 | 187051.1 | 20.846 | PSM002087 | 0.285 | 19.327 | 8 |
| ASM002476A | Laxemarån | 10:1 | 0.19 | 41360 | 9014280 | 285.8 | 913.2 | 0.0 | 913.2 | 187964.3 | 0.0 | 0 | 187964.3 | 20.852 | | | | |
| ASM002495 | Glostadsbäcken | 12:3 | 0.13 | 27720 | 27720 | 0.9 | 602.4 | 0.0 | 602.4 | 602.4 | 0.0 | 0 | 602.4 | 21.732 | | | | |
| ASM002485 | Glostadsbäcken | 12:2 | 0.33 | 72820 | 72820 | 2.3 | 1582.3 | 0.0 | 1582.3 | 1582.3 | 0.0 | 0 | 1582.3 | 21.729 | | | | |
| ASM002498 | Glostadsbäcken | 12:1 | 1.60 | 351340 | 451880 | 14.3 | 7636.7 | 0.0 | 7636.7 | 9821.5 | 89.3 | 1 | 9732.2 | 21.537 | | | | |
| ASM001518B | Stålglobäcken | 13:1 | 0.68 | 149380 | 149380 | 4.7 | 3246.6 | 0.0 | 3246.6 | 3246.6 | 0.0 | 0 | 3246.6 | 21.734 | PSM002086 | 0.005 | 27.574 | 21 |
| ASM001518A | Stålglobäcken | 13:1 | 0.35 | 77880 | 227260 | 7.2 | 1690.7 | 0.0 | 1690.7 | 4937.3 | 0.0 | 0 | 4937.3 | 21.725 | | | | |
| ASM002462 | Uvöbäcken | 15:1 | 0.97 | 212740 | 212740 | 6.7 | 4623.7 | 0.0 | 4623.7 | 4623.7 | 0.0 | 0 | 4623.7 | 21.734 | | | | |
| ASM002497 | Stekebäcken | 14:2 | 0.44 | 95700 | 95700 | 3.0 | 2079.9 | 0.0 | 2079.9 | 2079.9 | 0.0 | 0 | 2079.9 | 21.734 | | | | |
| ASM001517 | Stekebäcken | 14:1 | 0.90 | 198660 | 294360 | 9.3 | 4316.8 | 0.0 | 4316.8 | 6396.7 | 0.0 | 0 | 6396.7 | 21.731 | | | | |
| ASM002463 | Svartebäck | 16:1 | 0.50 | 110880 | 110880 | 3.5 | 2404.3 | 0.0 | 2404.3 | 2404.3 | 17.3 | 1 | 2387.0 | 21.527 | | | | |
| ASM002655 | Coastal area | | 2.71 | 596420 | 596420 | 18.9 | 12643.6 | 0.0 | 12643.6 | 12643.6 | 778.3 | 6 | 11865.3 | 19.894 | | | | |
| ASM002658 | Coastal area | | 1.26 | 277420 | 277420 | 8.8 | 5922.1 | 0.0 | 5922.1 | 5922.1 | 178.6 | 3 | 5743.5 | 20.703 | | | | |
| ASM002656 | Coastal area | | 0.22 | 48400 | 48400 | 1.5 | 1001.7 | 0.0 | 1001.7 | 1001.7 | 91.7 | 9 | 910.0 | 18.802 | | | | |
| ASM002660 | Coastal area | | 0.14 | 30360 | 30360 | 1.0 | 627.2 | 0.0 | 627.2 | 627.2 | 61.6 | 10 | 565.6 | 18.629 | | | | |
| ASM002659 | Coastal area | | 15.70 | 3453780 | 3453780 | 109.5 | 70688.1 | 0.0 | 70688.1 | 70688.1 | 367.1 | 1 | 70321.0 | 20.361 | | | | |
| ASM002657 | Coastal area | | 2.60 | 571340 | 571340 | 18.1 | 11912.1 | 0.0 | 11912.1 | 11912.1 | 93.9 | 1 | 11818.2 | 20.685 | | | | |
| ASM001522 | Uthammarsån | 17:5 | 0.57 | 125620 | 125620 | 4.0 | 2730.8 | 0.0 | 2730.8 | 2730.8 | 0.0 | 0 | 2730.8 | 21.738 | | | | |
| ASM001523 | Uthammarsån | 17:6 | 0.96 | 210760 | 210760 | 6.7 | 4580.6 | 0.0 | 4580.6 | 4580.6 | 0.0 | 0 | 4580.6 | 21.734 | | | | |
| ASM001521 | Uthammarsån | 17:4 | 0.20 | 44880 | 44880 | 1.4 | 975.2 | 0.0 | 975.2 | 975.2 | 0.0 | 0 | 975.2 | 21.729 | | | | |
| ASM001520 | Uthammarsån | 17:3 | 0.08 | 17820 | 17820 | 0.6 | 387.2 | 0.0 | 387.2 | 387.2 | 0.0 | 0 | 387.2 | 21.729 | | | | |
| ASM002494B | Uthammarsån | 17:1 | 2.91 | 640860 | 1039940 | 33.0 | 13924.3 | 0.0 | 13924.3 | 22598.1 | 0.0 | 0 | 22598.1 | 21.730 | PSM002076 | 0.033 | 31.273 | 31 |
| ASM001533 | Uthammarsån | 17:2 | 0.51 | 112640 | 112640 | 3.6 | 2448.3 | 0.0 | 2448.3 | 2448.3 | 0.0 | 0 | 2448.3 | 21.736 | | | | |
| ASM002494A | Uthammarsån | 17:1 | 1.78 | 391820 | 1544400 | 49.0 | 8518.1 | 0.0 | 8518.1 | 33564.6 | 10.2 | 0 | 33554.4 | 21.726 | | | | |
| ASM001528 | Släthultebäcken | 18:5 | 0.32 | 70400 | 70400 | 2.2 | 1529.6 | 0.0 | 1529.6 | 1529.6 | 0.0 | 0 | 1529.6 | 21.727 | | | | |
| ASM002477 | Släthultebäcken | 18:4 | 0.66 | 144980 | 215380 | 6.8 | 3038.8 | 0.0 | 3038.8 | 4568.4 | 235.7 | 5 | 4332.7 | 20.117 | | | | |
| ASM001531 | Släthultebäcken | 18:8 | 0.30 | 66440 | 66440 | 2.1 | 1443.7 | 0.0 | 1443.7 | 1443.7 | 0.0 | 0 | 1443.7 | 21.729 | | | | |
| ASM001532 | Släthultebäcken | 18:9 | 0.11 | 24420 | 24420 | 0.8 | 530.7 | 0.0 | 530.7 | 530.7 | 0.0 | 0 | 530.7 | 21.734 | | | | |
| ASM002455 | Släthultebäcken | 18:7 | 0.76 | 167420 | 258280 | 8.2 | 3638.3 | 0.0 | 3638.3 | 5612.8 | 0.0 | 0 | 5612.8 | 21.731 | | | | |
| ASM002475 | Släthultebäcken | 18:6 | 1.06 | 232100 | 490380 | 15.5 | 5042.9 | 0.0 | 5042.9 | 10655.7 | 0.0 | 0 | 10655.7 | 21.729 | | | | |
| ASM001526 | Släthultebäcken | 18:3 | 0.40 | 88220 | 88220 | 2.8 | 1904.1 | 0.0 | 1904.1 | 1904.1 | 8.2 | 0 | 1896.0 | 21.491 | | | | |
| ASM002481C | Släthultebäcken | 18:1 | 2.44 | 537020 | 1027400 | 32.6 | 11175.8 | 0.0 | 11175.8 | 21831.4 | 0.0 | 0 | 21831.4 | 21.249 | PSM002070 | | | |
| ASM002481B | Släthultebäcken | 18:1 | 2.13 | 469260 | 1800260 | 57.1 | 10122.8 | 0.0 | 10122.8 | 38182.9 | 89.9 | 0 | 38093.0 | 21.160 | PSM002075 | | | |
| ASM001525 | Släthultebäcken | 18:2 | 0.77 | 169620 | 169620 | 5.4 | 3440.6 | 0.0 | 3440.6 | 3440.6 | 0.0 | 0 | 3440.6 | 20.284 | | | | |
| ASM002481A | Släthultebäcken | 18:1 | 0.00 | 220 | 1970100 | 62.5 | 4.6 | 0.0 | 4.6 | 41538.2 | 0.0 | 0 | 41538.2 | 21.084 | | | | |
| ASM001444 | Sörämagasinet | 11:1 | 0.52 | 115060 | 115060 | 3.6 | 1694.3 | 0.0 | 1694.3 | 1694.3 | 487.7 | 29 | 1206.6 | 10.486 | | | | |
| ASM002466 | Stekflagebäcken | 22:1 | 0.36 | 78980 | 78980 | 2.5 | 1599.5 | 0.0 | 1599.5 | 1599.5 | 218.7 | 14 | 1380.7 | 17.482 | | | | |
| ASM002653 | Coastal area | | 0.76 | 166980 | 166980 | 5.3 | 3589.9 | 0.0 | 3589.9 | 3589.9 | 103.7 | 3 | 3486.3 | 20.878 | | | | |
| ASM002470 | Skölkebäcken | 26:1 | 0.17 | 36300 | 36300 | 1.2 | 788.8 | 0.0 | 788.8 | 788.8 | 0.0 | 0 | 788.8 | 21.729 | | | | |
| ASM002469 | Gloebäcken | 25:1 | 0.13 | 28820 | 28820 | 0.9 | 626.3 | 0.0 | 626.3 | 626.3 | 0.0 | 0 | 626.3 | 21.732 | | | | |
| ASM002468 | Lindströmmebäcken | 24:1 | 0.19 | 42240 | 42240 | 1.3 | 917.9 | 0.0 | 917.9 | 917.9 | 0.0 | 0 | 917.9 | 21.729 | | | | |
| ASM002467B | Vadvikebäcken | 23:1 | 0.30 | 65560 | 65560 | 2.1 | 1424.7 | 0.0 | 1424.7 | 1424.7 | 0.0 | 0 | 1424.7 | 21.731 | PSM107735 | 0.002 | 33.123 | 34 |
| ASM002467A | Vadvikebäcken | 23:1 | 0.01 | 1980 | 67540 | 2.1 | 42.9 | 0.0 | 42.9 | 1467.6 | 0.0 | 0 | 1467.6 | 21.729 | | | | |
| | **Kärrviksån** | 5:1-20 | 27.31 | 6007100 | 6007100 | 26.9 | 129296.4 | 0.0 | 129296.4 | | 620.3 | 0 | 128676.2 | 21.421 | | | | |
| | **Laxemarån** | 10:1-32 | 40.97 | 9014280 | 9014280 | 37.5 | 192465.6 | 0.0 | 192465.6 | | 4501.4 | 2 | 187964.3 | 20.852 | | | | |
| | **All catchments** | | 129.97 | 28593620 | 28593620 | 22.3 | 608071.6 | 0.0 | 608071.6 | | 10391.3 | 2 | 597680.4 | 20.903 | | | | |

| **Bicarbonate ($HCO_3^-$)** | | | | Water balance | | | Total per catchment | | | Total including contributions from upstream catchments | | | | Calibration data | | | |
|---|---|---|---|---|---|---|---|---|---|---|---|---|---|---|---|---|---|
| Idcode | Name | ARO | Area | $Q_{catch}$ | $Q_{out}$ | q | Diffuse | Point | Total | Total IN | Retention | | Total OUT | Conc. | Reference | q | Conc. | Deviation |
| | | | $km^2$ | $m^3 \cdot yr^{-1}$ | $m^3 \cdot yr^{-1}$ | $L \cdot s^{-1}$ | $kg \cdot yr^{-1}$ | $kg \cdot yr^{-1}$ | $kg \cdot yr^{-1}$ | $kg \cdot yr^{-1}$ | $kg \cdot yr^{-1}$ | % | $kg \cdot yr^{-1}$ | $mg \cdot L^{-1}$ | | $L \cdot s^{-1}$ | $mg \cdot L^{-1}$ | % |
| ASM002474 | Kärrviksån | 5:20 | 0.12 | 25740 | 25740 | 0.8 | 319.6 | 0.0 | 319.6 | 319.6 | 0.0 | 0 | 319.6 | 12.415 | | | | |
| ASM002493 | Kärrviksån | 5:19 | 0.84 | 184140 | 209880 | 6.7 | 2286.9 | 0.0 | 2286.9 | 2606.4 | 0.0 | 0 | 2606.4 | 12.419 | | | | |
| ASM001483 | Kärrviksån | 5:17 | 0.15 | 33220 | 33220 | 1.1 | 412.4 | 0.0 | 412.4 | 412.4 | 0.0 | 0 | 412.4 | 12.414 | | | | |
| ASM002492 | Kärrviksån | 5:16 | 1.11 | 243980 | 277200 | 8.8 | 3029.7 | 0.0 | 3029.7 | 3442.1 | 0.0 | 0 | 3442.1 | 12.417 | | | | |
| ASM002491 | Kärrviksån | 5:15 | 1.87 | 411840 | 689040 | 21.8 | 5113.7 | 0.0 | 5113.7 | 8555.8 | 0.0 | 0 | 8555.8 | 12.417 | | | | |
| ASM001474 | Kärrviksån | 5:7 | 0.45 | 99000 | 99000 | 3.1 | 1199.9 | 0.0 | 1199.9 | 1199.9 | 0.0 | 0 | 1199.9 | 12.120 | | | | |
| ASM002487 | Kärrviksån | 5:6 | 1.20 | 264000 | 363000 | 11.5 | 3277.7 | 0.0 | 3277.7 | 4477.5 | 0.0 | 0 | 4477.5 | 12.335 | | | | |
| ASM001472 | Kärrviksån | 5:4 | 1.10 | 242880 | 242880 | 7.7 | 2887.3 | 0.0 | 2887.3 | 2887.3 | 0.0 | 0 | 2887.3 | 11.888 | | | | |
| ASM001470 | Kärrviksån | 5:3 | 0.40 | 87560 | 87560 | 2.8 | 1087.1 | 0.0 | 1087.1 | 1087.1 | 0.0 | 0 | 1087.1 | 12.415 | | | | |
| ASM001469 | Kärrviksån | 5:2 | 0.97 | 212960 | 212960 | 6.8 | 2644.2 | 0.0 | 2644.2 | 2644.2 | 0.0 | 0 | 2644.2 | 12.417 | | | | |
| ASM001471 | Kärrviksån | 5:5 | 2.79 | 614680 | 614680 | 19.5 | 7630.7 | 0.0 | 7630.7 | 7630.7 | 0.0 | 0 | 7630.7 | 12.414 | | | | |
| ASM001479 | Kärrviksån | 5:13 | 0.65 | 142340 | 142340 | 4.5 | 1767.2 | 0.0 | 1767.2 | 1767.2 | 0.0 | 0 | 1767.2 | 12.415 | | | | |
| ASM001480 | Kärrviksån | 5:14 | 0.10 | 22660 | 22660 | 0.7 | 281.3 | 0.0 | 281.3 | 281.3 | 0.0 | 0 | 281.3 | 12.414 | | | | |
| ASM002490 | Kärrviksån | 5:12 | 0.84 | 183920 | 348920 | 11.1 | 2283.7 | 0.0 | 2283.7 | 4332.2 | 0.0 | 0 | 4332.2 | 12.416 | | | | |
| ASM001478 | Kärrviksån | 5:11 | 0.49 | 108460 | 108460 | 3.4 | 1346.7 | 0.0 | 1346.7 | 1346.7 | 0.0 | 0 | 1346.7 | 12.417 | | | | |
| ASM002489 | Kärrviksån | 5:10 | 1.20 | 263560 | 372020 | 11.8 | 3271.5 | 0.0 | 3271.5 | 4618.3 | 0.0 | 0 | 4618.3 | 12.414 | | | | |
| ASM001476 | Kärrviksån | 5:9 | 3.62 | 796180 | 796180 | 25.2 | 9883.9 | 0.0 | 9883.9 | 9883.9 | 0.0 | 0 | 9883.9 | 12.414 | | | | |
| ASM001475B | Kärrviksån | 5:8 | 1.38 | 302940 | 1820060 | 57.7 | 3704.6 | 0.0 | 3704.6 | 22538.9 | 0.0 | 0 | 22538.9 | 12.384 | PSM002081 | 0.058 | 20.227 | 39 |
| ASM001475A | Kärrviksån | 5:8 | 0.04 | 9680 | 1829740 | 58.0 | 176.4 | 0.0 | 176.4 | 22715.4 | 0.0 | 0 | 22715.4 | 12.415 | | | | |
| ASM002479 | Kärrviksån | 5:18 | 1.18 | 259600 | 259600 | 8.2 | 3222.7 | 0.0 | 3222.7 | 3222.7 | 0.0 | 0 | 3222.7 | 12.414 | | | | |
| ASM002486C | Kärrviksån | 5:1 | 2.75 | 604560 | 1074040 | 34.1 | 7503.4 | 0.0 | 7503.4 | 13332.6 | 0.0 | 0 | 13332.6 | 12.413 | PSM002080 | | | |
| ASM002486B | Kärrviksån | 5:1 | 1.13 | 247940 | 3840760 | 121.8 | 3085.4 | 0.0 | 3085.4 | 47689.2 | 0.0 | 0 | 47689.2 | 12.417 | PSM002082 | 0.121 | 17.447 | 29 |
| ASM002486A | Kärrviksån | 5:1 | 2.93 | 645260 | 6007100 | 190.5 | 8041.2 | 0.0 | 8041.2 | 74457.2 | 0.0 | 0 | 74457.2 | 12.395 | PSM002083 | 0.190 | 13.816 | 10 |
| ASM002449 | Bjurhidebäcken | 4:1 | 0.63 | 139040 | 139040 | 4.4 | 1726.4 | 0.0 | 1726.4 | 1726.4 | 0.0 | 0 | 1726.4 | 12.417 | | | | |
| ASM002472 | Sörviksån | 3:2 | 0.47 | 103400 | 103400 | 3.3 | 1283.9 | 0.0 | 1283.9 | 1283.9 | 0.0 | 0 | 1283.9 | 12.417 | | | | |
| ASM002473 | Sörviksån | 3:1 | 0.53 | 116600 | 220000 | 7.0 | 1447.8 | 0.0 | 1447.8 | 2731.7 | 0.0 | 0 | 2731.7 | 12.417 | | | | |
| ASM002651 | Coastal area | | 1.67 | 368280 | 368280 | 11.7 | 4570.5 | 0.0 | 4570.5 | 4570.5 | 0.0 | 0 | 4570.5 | 12.410 | | | | |
| ASM002447 | Bodvikebäcken | 2:1 | 0.38 | 83600 | 83600 | 2.7 | 1037.9 | 0.0 | 1037.9 | 1037.9 | 0.0 | 0 | 1037.9 | 12.415 | | | | |
| ASM002446 | Långbonäsbäcken | 1:1 | 0.07 | 15400 | 15400 | 0.5 | 191.2 | 0.0 | 191.2 | 191.2 | 0.0 | 0 | 191.2 | 12.414 | | | | |
| ASM002464 | Flakvarpebäcken | 19:1 | 0.18 | 40480 | 40480 | 1.3 | 502.6 | 0.0 | 502.6 | 502.6 | 0.0 | 0 | 502.6 | 12.415 | | | | |
| ASM002465 | Jössesbäcken | 20:1 | 0.11 | 24420 | 24420 | 0.8 | 303.2 | 0.0 | 303.2 | 303.2 | 0.0 | 0 | 303.2 | 12.415 | | | | |
| ASM002471 | Äspöbäcken | 21:1 | 0.06 | 13860 | 13860 | 0.4 | 172.1 | 0.0 | 172.1 | 172.1 | 0.0 | 0 | 172.1 | 12.415 | | | | |
| ASM002652 | Coastal area | | 1.39 | 305140 | 305140 | 9.7 | 3788.8 | 0.0 | 3788.8 | 3788.8 | 0.0 | 0 | 3788.8 | 12.417 | | | | |
| ASM001445 | Frisksjön | 7:2 | 1.85 | 406560 | 406560 | 12.9 | 5047.1 | 0.0 | 5047.1 | 5047.1 | 0.0 | 0 | 5047.1 | 12.414 | | | | |
| ASM001484 | Käreviksån | 7:1 | 0.21 | 46860 | 453420 | 14.4 | 581.8 | 0.0 | 581.8 | 5628.9 | 0.0 | 0 | 5628.9 | 12.414 | | | | |
| ASM001486B | Mederhultsån | 6:1 | 1.92 | 422620 | 422620 | 13.4 | 5247.5 | 0.0 | 5247.5 | 5247.5 | 0.0 | 0 | 5247.5 | 12.417 | PSM002084 | 0.013 | 25.006 | 50 |
| ASM001486A | Mederhultsån | 6:1 | 0.08 | 18040 | 440660 | 14.0 | 225.5 | 0.0 | 225.5 | 5473.0 | 0.0 | 0 | 5473.0 | 12.420 | | | | |
| ASM002654 | Coastal area | | 1.86 | 409420 | 409420 | 13.0 | 5083.1 | 0.0 | 5083.1 | 5083.1 | 0.0 | 0 | 5083.1 | 12.415 | | | | |
| ASM002460 | Pistlanbäcken | 8:1 | 0.50 | 109780 | 109780 | 3.5 | 1363.0 | 0.0 | 1363.0 | 1363.0 | 0.0 | 0 | 1363.0 | 12.415 | | | | |
| ASM001490 | Ekerumsån | 9:3 | 0.22 | 48840 | 48840 | 1.5 | 606.5 | 0.0 | 606.5 | 606.5 | 0.0 | 0 | 606.5 | 12.419 | | | | |
| ASM001489 | Ekerumsån | 9:2 | 0.77 | 168740 | 168740 | 5.4 | 2095.2 | 0.0 | 2095.2 | 2095.2 | 0.0 | 0 | 2095.2 | 12.417 | | | | |
| ASM002483B | Ekerumsån | 9:1 | 1.50 | 330880 | 548460 | 17.4 | 4106.3 | 0.0 | 4106.3 | 6808.1 | 0.0 | 0 | 6808.1 | 12.413 | PSM002085 | 0.017 | 64.803 | 81 |
| ASM002483A | Ekerumsån | 9:1 | 0.34 | 75020 | 623480 | 19.8 | 933.6 | 0.0 | 933.6 | 7741.6 | 0.0 | 0 | 7741.6 | 12.417 | | | | |
| ASM002478 | Laxemarån | 10:32 | 0.02 | 5060 | 5060 | 0.2 | 62.8 | 0.0 | 62.8 | 62.8 | 0.0 | 0 | 62.8 | 12.417 | | | | |
| ASM002482 | Laxemarån | 10:31 | 0.87 | 190740 | 195800 | 6.2 | 2367.9 | 0.0 | 2367.9 | 2430.7 | 0.0 | 0 | 2430.7 | 12.414 | | | | |
| ASM002480B | Laxemarån | 10:30 | 4.23 | 931480 | 1127280 | 35.7 | 11517.3 | 0.0 | 11517.3 | 13948.0 | 0.0 | 0 | 13948.0 | 12.373 | PSM002068 | 0.036 | 12.373 | 0 |
| ASM002480A | Jämsen | 10:30 | 1.83 | 403480 | 1530760 | 48.5 | 4704.1 | 0.0 | 4704.1 | 18652.1 | 0.0 | 0 | 18652.1 | 12.185 | PSM002069 | 0.049 | 15.747 | 23 |
| ASM001516 | Laxemarån | 10:29 | 0.53 | 117260 | 117260 | 3.7 | 1456.0 | 0.0 | 1456.0 | 1456.0 | 0.0 | 0 | 1456.0 | 12.417 | | | | |
| ASM001515 | Laxemarån | 10:28 | 0.34 | 74140 | 74140 | 2.4 | 836.6 | 0.0 | 836.6 | 836.6 | 0.0 | 0 | 836.6 | 11.284 | | | | |
| ASM001514 | Laxemarån | 10:27 | 0.49 | 107140 | 107140 | 3.4 | 1330.2 | 0.0 | 1330.2 | 1330.2 | 0.0 | 0 | 1330.2 | 12.415 | | | | |
| ASM001446 | Plittorpsgöl | 10:26 | 0.68 | 149160 | 149160 | 4.7 | 1851.5 | 0.0 | 1851.5 | 1851.5 | 0.0 | 0 | 1851.5 | 12.413 | | | | |
| ASM002459 | Laxemarån | 10:25 | 0.10 | 21780 | 170940 | 5.4 | 270.4 | 0.0 | 270.4 | 2121.9 | 0.0 | 0 | 2121.9 | 12.413 | | | | |
| ASM001512 | Laxemarån | 10:24 | 0.49 | 108680 | 108680 | 3.4 | 1349.0 | 0.0 | 1349.0 | 1349.0 | 0.0 | 0 | 1349.0 | 12.413 | | | | |
| ASM002476E | Laxemarån | 10:1 | 3.95 | 868780 | 2977700 | 94.4 | 10502.2 | 0.0 | 10502.2 | 36248.0 | 0.0 | 0 | 36248.0 | 12.173 | PSM002071 | 0.094 | 14.000 | 13 |
| ASM001510 | Laxemarån | 10:22 | 0.56 | 123640 | 123640 | 3.9 | 1535.0 | 0.0 | 1535.0 | 1535.0 | 0.0 | 0 | 1535.0 | 12.415 | | | | |
| ASM002453 | Laxemarån | 10:21 | 0.45 | 97900 | 221540 | 7.0 | 1215.3 | 0.0 | 1215.3 | 2750.4 | 0.0 | 0 | 2750.4 | 12.415 | | | | |
| ASM002450B | Laxemarån | 10:20 | 2.39 | 526240 | 747780 | 23.7 | 6530.8 | 0.0 | 6530.8 | 9281.2 | 0.0 | 0 | 9281.2 | 12.412 | PSM002072 | | | |
| ASM002450A | Laxemarån | 10:20 | 0.19 | 41140 | 788920 | 25.0 | 512.7 | 0.0 | 512.7 | 9793.9 | 0.0 | 0 | 9793.9 | 12.414 | | | | |
| ASM001511 | Laxemarån | 10:23 | 0.74 | 162800 | 162800 | 5.2 | 2021.2 | 0.0 | 2021.2 | 2021.2 | 0.0 | 0 | 2021.2 | 12.415 | | | | |
| ASM001448 | Grangöl | 10:19 | 0.50 | 108900 | 108900 | 3.5 | 1351.9 | 0.0 | 1351.9 | 1351.9 | 0.0 | 0 | 1351.9 | 12.414 | | | | |
| ASM002499 | Laxemarån | 10:18 | 0.06 | 12760 | 121660 | 3.9 | 158.4 | 0.0 | 158.4 | 1510.3 | 0.0 | 0 | 1510.3 | 12.414 | | | | |
| ASM001506 | Laxemarån | 10:17 | 0.40 | 87560 | 87560 | 2.8 | 1087.1 | 0.0 | 1087.1 | 1087.1 | 0.0 | 0 | 1087.1 | 12.415 | | | | |
| ASM001447 | Fjällgöl | 10:16 | 0.30 | 64900 | 64900 | 2.1 | 805.8 | 0.0 | 805.8 | 805.8 | 0.0 | 0 | 805.8 | 12.415 | | | | |
| ASM002451 | Laxemarån | 10:15 | 0.33 | 71500 | 136400 | 4.3 | 887.6 | 0.0 | 887.6 | 1693.4 | 0.0 | 0 | 1693.4 | 12.415 | | | | |
| ASM002452 | Laxemarån | 10:14 | 2.38 | 522500 | 868120 | 27.5 | 6487.0 | 0.0 | 6487.0 | 10777.8 | 0.0 | 0 | 10777.8 | 12.415 | | | | |
| ASM001503 | Laxemarån | 10:13 | 0.42 | 91520 | 91520 | 2.9 | 1136.3 | 0.0 | 1136.3 | 1136.3 | 0.0 | 0 | 1136.3 | 12.415 | | | | |
| ASM002454 | Laxemarån | 10:12 | 0.81 | 177760 | 269280 | 8.5 | 2206.5 | 0.0 | 2206.5 | 3342.8 | 0.0 | 0 | 3342.8 | 12.414 | | | | |
| ASM001501 | Laxemarån | 10:11 | 0.81 | 177320 | 177320 | 5.6 | 2201.7 | 0.0 | 2201.7 | 2201.7 | 0.0 | 0 | 2201.7 | 12.417 | | | | |
| ASM002457 | Laxemarån | 10:10 | 1.39 | 305580 | 482900 | 15.3 | 3793.1 | 0.0 | 3793.1 | 5994.9 | 0.0 | 0 | 5994.9 | 12.414 | | | | |
| ASM002476D | Laxemarån | 10:1 | 4.96 | 1091860 | 6641580 | 210.6 | 13549.4 | 0.0 | 13549.4 | 81728.0 | 0.0 | 0 | 81728.0 | 12.306 | PSM002077 | | | |
| ASM001499 | Laxemarån | 10:9 | 0.71 | 156420 | 156420 | 5.0 | 1941.8 | 0.0 | 1941.8 | 1941.8 | 0.0 | 0 | 1941.8 | 12.414 | | | | |
| ASM001498 | Laxemarån | 10:8 | 2.77 | 609620 | 766040 | 24.3 | 7568.7 | 0.0 | 7568.7 | 9510.5 | 0.0 | 0 | 9510.5 | 12.415 | PSM002078 | 0.024 | 2.830 | 339 |
| ASM001497 | Laxemarån | 10:7 | 0.61 | 133980 | 133980 | 4.2 | 1663.6 | 0.0 | 1663.6 | 1663.6 | 0.0 | 0 | 1663.6 | 12.417 | | | | |
| ASM002476C | Laxemarån | 10:1 | 0.32 | 69300 | 7610900 | 241.3 | 898.4 | 0.0 | 898.4 | 93800.5 | 0.0 | 0 | 93800.5 | 12.324 | PSM002079 | 0.242 | 11.677 | 6 |
| ASM001494 | Laxemarån | 10:4 | 1.00 | 220220 | 220220 | 7.0 | 2733.6 | 0.0 | 2733.6 | 2733.6 | 0.0 | 0 | 2733.6 | 12.413 | | | | |
| ASM001493 | Laxemarån | 10:3 | 0.32 | 70180 | 70180 | 2.2 | 871.4 | 0.0 | 871.4 | 871.4 | 0.0 | 0 | 871.4 | 12.417 | | | | |
| ASM001492 | Laxemarån | 10:2 | 0.46 | 101200 | 101200 | 3.2 | 1256.2 | 0.0 | 1256.2 | 1256.2 | 0.0 | 0 | 1256.2 | 12.413 | | | | |
| ASM001496 | Laxemarån | 10:6 | 0.89 | 195800 | 195800 | 6.2 | 2430.7 | 0.0 | 2430.7 | 2430.7 | 0.0 | 0 | 2430.7 | 12.414 | | | | |
| ASM001495 | Laxemarån | 10:5 | 0.29 | 63800 | 63800 | 2.0 | 791.9 | 0.0 | 791.9 | 791.9 | 0.0 | 0 | 791.9 | 12.413 | | | | |
| ASM002476B | Laxemarån | 10:1 | 3.23 | 710820 | 8972920 | 284.5 | 8838.0 | 0.0 | 8838.0 | 110722.3 | 0.0 | 0 | 110722.3 | 12.340 | PSM002087 | 0.285 | 13.816 | 11 |
| ASM002476A | Laxemarån | 10:1 | 0.19 | 41360 | 9014280 | 285.8 | 521.7 | 0.0 | 521.7 | 111244.0 | 0.0 | 0 | 111244.0 | 12.341 | | | | |
| ASM002495 | Glostadsbäcken | 12:3 | 0.13 | 27720 | 27720 | 0.9 | 344.2 | 0.0 | 344.2 | 344.2 | 0.0 | 0 | 344.2 | 12.415 | | | | |
| ASM002485 | Glostadsbäcken | 12:2 | 0.33 | 72820 | 72820 | 2.3 | 904.0 | 0.0 | 904.0 | 904.0 | 0.0 | 0 | 904.0 | 12.414 | | | | |
| ASM002498 | Glostadsbäcken | 12:1 | 1.60 | 351340 | 451880 | 14.3 | 4362.9 | 0.0 | 4362.9 | 5611.1 | 0.0 | 0 | 5611.1 | 12.417 | | | | |
| ASM001518B | Stålglobäcken | 13:1 | 0.68 | 149380 | 149380 | 4.7 | 1854.8 | 0.0 | 1854.8 | 1854.8 | 0.0 | 0 | 1854.8 | 12.417 | PSM002086 | 0.005 | 13.361 | 7 |
| ASM001518A | Stålglobäcken | 13:1 | 0.35 | 77880 | 227260 | 7.2 | 965.9 | 0.0 | 965.9 | 2820.7 | 0.0 | 0 | 2820.7 | 12.412 | | | | |
| ASM002462 | Uvobäcken | 15:1 | 0.97 | 212740 | 212740 | 6.7 | 2641.5 | 0.0 | 2641.5 | 2641.5 | 0.0 | 0 | 2641.5 | 12.417 | | | | |
| ASM002497 | Stekebäcken | 14:2 | 0.44 | 95700 | 95700 | 3.0 | 1188.3 | 0.0 | 1188.3 | 1188.3 | 0.0 | 0 | 1188.3 | 12.417 | | | | |
| ASM001517 | Stekebäcken | 14:1 | 0.90 | 198660 | 294360 | 9.3 | 2466.2 | 0.0 | 2466.2 | 3654.5 | 0.0 | 0 | 3654.5 | 12.415 | | | | |
| ASM002463 | Svarteback | 16:1 | 0.50 | 110880 | 110880 | 3.5 | 1376.6 | 0.0 | 1376.6 | 1376.6 | 0.0 | 0 | 1376.6 | 12.415 | | | | |
| ASM002655 | Coastal area | | 2.71 | 596420 | 596420 | 18.9 | 7404.8 | 0.0 | 7404.8 | 7404.8 | 0.0 | 0 | 7404.8 | 12.415 | | | | |
| ASM002658 | Coastal area | | 1.26 | 277420 | 277420 | 8.8 | 3443.9 | 0.0 | 3443.9 | 3443.9 | 0.0 | 0 | 3443.9 | 12.414 | | | | |
| ASM002656 | Coastal area | | 0.22 | 48400 | 48400 | 1.5 | 600.9 | 0.0 | 600.9 | 600.9 | 0.0 | 0 | 600.9 | 12.415 | | | | |
| ASM002660 | Coastal area | | 0.14 | 30360 | 30360 | 1.0 | 376.9 | 0.0 | 376.9 | 376.9 | 0.0 | 0 | 376.9 | 12.415 | | | | |
| ASM002659 | Coastal area | | 15.70 | 3453780 | 3453780 | 109.5 | 42700.0 | 0.0 | 42700.0 | 42700.0 | 0.0 | 0 | 42700.0 | 12.363 | | | | |
| ASM002657 | Coastal area | | 2.60 | 571340 | 571340 | 18.1 | 7094.1 | 0.0 | 7094.1 | 7094.1 | 0.0 | 0 | 7094.1 | 12.417 | | | | |
| ASM001522 | Uthammarsån | 17:5 | 0.57 | 125620 | 125620 | 4.0 | 1560.1 | 0.0 | 1560.1 | 1560.1 | 0.0 | 0 | 1560.1 | 12.419 | | | | |
| ASM001523 | Uthammarsån | 17:6 | 0.96 | 210760 | 210760 | 6.7 | 2616.9 | 0.0 | 2616.9 | 2616.9 | 0.0 | 0 | 2616.9 | 12.417 | | | | |
| ASM001521 | Uthammarsån | 17:4 | 0.20 | 44880 | 44880 | 1.4 | 557.1 | 0.0 | 557.1 | 557.1 | 0.0 | 0 | 557.1 | 12.414 | | | | |
| ASM001520 | Uthammarsån | 17:3 | 0.08 | 17820 | 17820 | 0.6 | 221.2 | 0.0 | 221.2 | 221.2 | 0.0 | 0 | 221.2 | 12.414 | | | | |
| ASM002494B | Uthammarsån | 17:1 | 2.91 | 640860 | 1039940 | 33.0 | 7955.0 | 0.0 | 7955.0 | 12910.4 | 0.0 | 0 | 12910.4 | 12.415 | PSM002076 | 0.033 | 17.872 | 31 |
| ASM001533 | Uthammarsån | 17:2 | 0.51 | 112640 | 112640 | 3.6 | 1398.7 | 0.0 | 1398.7 | 1398.7 | 0.0 | 0 | 1398.7 | 12.418 | | | | |
| ASM002494A | Uthammarsån | 17:1 | 1.78 | 391820 | 1544400 | 49.0 | 4866.4 | 0.0 | 4866.4 | 19175.6 | 0.0 | 0 | 19175.6 | 12.416 | | | | |
| ASM001528 | Släthultebäcken | 18:5 | 0.32 | 70400 | 70400 | 2.2 | 873.9 | 0.0 | 873.9 | 873.9 | 0.0 | 0 | 873.9 | 12.413 | | | | |
| ASM002477 | Släthultebäcken | 18:4 | 0.66 | 144980 | 215380 | 6.8 | 1800.2 | 0.0 | 1800.2 | 2674.0 | 0.0 | 0 | 2674.0 | 12.415 | | | | |
| ASM001531 | Släthultebäcken | 18:8 | 0.30 | 66440 | 66440 | 2.1 | 824.8 | 0.0 | 824.8 | 824.8 | 0.0 | 0 | 824.8 | 12.414 | | | | |
| ASM001532 | Släthultebäcken | 18:9 | 0.11 | 24420 | 24420 | 0.8 | 303.2 | 0.0 | 303.2 | 303.2 | 0.0 | 0 | 303.2 | 12.417 | | | | |
| ASM002455 | Släthultebäcken | 18:7 | 0.76 | 167420 | 258280 | 8.2 | 2078.6 | 0.0 | 2078.6 | 3206.6 | 0.0 | 0 | 3206.6 | 12.415 | | | | |
| ASM002475 | Släthultebäcken | 18:6 | 1.06 | 232100 | 490380 | 15.5 | 2881.0 | 0.0 | 2881.0 | 6087.6 | 0.0 | 0 | 6087.6 | 12.414 | | | | |
| ASM001526 | Släthultebäcken | 18:3 | 0.40 | 88220 | 88220 | 2.8 | 1095.4 | 0.0 | 1095.4 | 1095.4 | 0.0 | 0 | 1095.4 | 12.417 | | | | |
| ASM002481C | Släthultebäcken | 18:1 | 2.44 | 537020 | 1027400 | 32.6 | 6540.4 | 0.0 | 6540.4 | 12628.0 | 0.0 | 0 | 12628.0 | 12.291 | PSM002070 | | | |
| ASM002481B | Släthultebäcken | 18:1 | 2.13 | 469260 | 1800260 | 57.1 | 5835.3 | 0.0 | 5835.3 | 22232.8 | 0.0 | 0 | 22232.8 | 12.350 | PSM002075 | | | |
| ASM001525 | Släthultebäcken | 18:2 | 0.77 | 169620 | 169620 | 5.4 | 2105.9 | 0.0 | 2105.9 | 2105.9 | 0.0 | 0 | 2105.9 | 12.415 | | | | |
| ASM002481A | Släthultebäcken | 18:1 | 0.00 | 220 | 1970100 | 62.5 | 2.6 | 0.0 | 2.6 | 24341.3 | 0.0 | 0 | 24341.3 | 12.355 | | | | |
| ASM001444 | Söråmagasinet | 11:1 | 0.52 | 115060 | 115060 | 3.6 | 1428.7 | 0.0 | 1428.7 | 1428.7 | 0.0 | 0 | 1428.7 | 12.417 | | | | |
| ASM002466 | Stekflagebäcken | 22:1 | 0.36 | 78980 | 78980 | 2.5 | 980.5 | 0.0 | 980.5 | 980.5 | 0.0 | 0 | 980.5 | 12.414 | | | | |
| ASM002653 | Coastal area | | 0.76 | 166980 | 166980 | 5.3 | 2073.5 | 0.0 | 2073.5 | 2073.5 | 0.0 | 0 | 2073.5 | 12.418 | | | | |
| ASM002470 | Skölkebäcken | 26:1 | 0.17 | 36300 | 36300 | 1.2 | 450.6 | 0.0 | 450.6 | 450.6 | 0.0 | 0 | 450.6 | 12.414 | | | | |
| ASM002469 | Gloebäcken | 25:1 | 0.13 | 28820 | 28820 | 0.9 | 357.8 | 0.0 | 357.8 | 357.8 | 0.0 | 0 | 357.8 | 12.415 | | | | |
| ASM002468 | Lindströmmebäcken | 24:1 | 0.19 | 42240 | 42240 | 1.3 | 524.4 | 0.0 | 524.4 | 524.4 | 0.0 | 0 | 524.4 | 12.414 | | | | |
| ASM002467B | Vadvikebäcken | 23:1 | 0.30 | 65560 | 65560 | 2.1 | 813.9 | 0.0 | 813.9 | 813.9 | 0.0 | 0 | 813.9 | 12.415 | PSM107735 | 0.002 | 6.898 | 80 |
| ASM002467A | Vadvikebäcken | 23:1 | 0.01 | 1980 | 67540 | 2.1 | 24.5 | 0.0 | 24.5 | 838.5 | 0.0 | 0 | 838.5 | 12.414 | | | | |
| | **Kärrviksån** | 5:1-20 | 27.31 | 6007100 | 6007100 | 26.9 | 74457.2 | 0.0 | 74457.2 | | 0.0 | 0 | 74457.2 | 12.395 | | | | |
| | **Laxemarån** | 10:1-32 | 40.97 | 9014280 | 9014280 | 37.5 | 111244.0 | 0.0 | 111244.0 | | 0.0 | 0 | 111244.0 | 12.341 | | | | |
| | **All catchments** | | 129.97 | 28593620 | 28593620 | 22.3 | 353911.0 | 0.0 | 353911.0 | | 0.0 | 0 | 353911.0 | 12.377 | | | | |

| **Magnesium (Mg)** | | | | Water balance | | | Total per catchment | | | Total including contributions from upstream catchments | | | | | Calibration data | | | |
|---|---|---|---|---|---|---|---|---|---|---|---|---|---|---|---|---|---|---|
| Idcode | Name | ARO | Area | $Q_{catch}$ | $Q_{out}$ | q | Diffuse | Point | Total | Total IN | Retention | | Total OUT | Conc. | Reference | q | Conc. | Deviation |
| | | | $km^2$ | $m^3 \cdot yr^{-1}$ | $m^3 \cdot yr^{-1}$ | $L \cdot s^{-1}$ | $kg \cdot yr^{-1}$ | $kg \cdot yr^{-1}$ | $kg \cdot yr^{-1}$ | $kg \cdot yr^{-1}$ | $kg \cdot yr^{-1}$ | % | $kg \cdot yr^{-1}$ | $mg \cdot L^{-1}$ | | $L \cdot s^{-1}$ | $mg \cdot L^{-1}$ | % |
| ASM002474 | Kärrviksån | 5:20 | 0.12 | 25740 | 25740 | 0.8 | 112.3 | 0.0 | 112.3 | 112.3 | 0.0 | 0 | 112.3 | 4.362 | | | | |
| ASM002493 | Kärrviksån | 5:19 | 0.84 | 184140 | 209880 | 6.7 | 656.7 | 0.0 | 656.7 | 769.0 | 0.0 | 0 | 769.0 | 3.664 | | | | |
| ASM001483 | Kärrviksån | 5:17 | 0.15 | 33220 | 33220 | 1.1 | 83.2 | 0.0 | 83.2 | 83.2 | 0.0 | 0 | 83.2 | 2.503 | | | | |
| ASM002492 | Kärrviksån | 5:16 | 1.11 | 243980 | 277200 | 8.8 | 769.2 | 0.0 | 769.2 | 852.4 | 0.0 | 0 | 852.4 | 3.075 | | | | |
| ASM002491 | Kärrviksån | 5:15 | 1.87 | 411840 | 689040 | 21.8 | 673.0 | 0.0 | 673.0 | 1525.4 | 0.0 | 0 | 1525.4 | 2.214 | | | | |
| ASM001474 | Kärrviksån | 5:7 | 0.45 | 99000 | 99000 | 3.1 | 154.3 | 0.0 | 154.3 | 154.3 | 0.0 | 0 | 154.3 | 1.559 | | | | |
| ASM002487 | Kärrviksån | 5:6 | 1.20 | 264000 | 363000 | 11.5 | 411.4 | 0.0 | 411.4 | 565.7 | 0.0 | 0 | 565.7 | 1.559 | | | | |
| ASM001472 | Kärrviksån | 5:4 | 1.10 | 242880 | 242880 | 7.7 | 422.6 | 0.0 | 422.6 | 422.6 | 0.0 | 0 | 422.6 | 1.740 | | | | |
| ASM001470 | Kärrviksån | 5:3 | 0.40 | 87560 | 87560 | 2.8 | 247.0 | 0.0 | 247.0 | 247.0 | 0.0 | 0 | 247.0 | 2.821 | | | | |
| ASM001469 | Kärrviksån | 5:2 | 0.97 | 212960 | 212960 | 6.8 | 365.8 | 0.0 | 365.8 | 365.8 | 0.0 | 0 | 365.8 | 1.718 | | | | |
| ASM001471 | Kärrviksån | 5:5 | 2.79 | 614680 | 614680 | 19.5 | 1054.4 | 0.0 | 1054.4 | 1054.4 | 0.0 | 0 | 1054.4 | 1.715 | | | | |
| ASM001479 | Kärrviksån | 5:13 | 0.65 | 142340 | 142340 | 4.5 | 221.8 | 0.0 | 221.8 | 221.8 | 0.0 | 0 | 221.8 | 1.559 | | | | |
| ASM001480 | Kärrviksån | 5:14 | 0.10 | 22660 | 22660 | 0.7 | 39.5 | 0.0 | 39.5 | 39.5 | 0.0 | 0 | 39.5 | 1.745 | | | | |
| ASM002490 | Kärrviksån | 5:12 | 0.84 | 183920 | 348920 | 11.1 | 299.4 | 0.0 | 299.4 | 560.8 | 0.0 | 0 | 560.8 | 1.607 | | | | |
| ASM001478 | Kärrviksån | 5:11 | 0.49 | 108460 | 108460 | 3.4 | 169.0 | 0.0 | 169.0 | 169.0 | 0.0 | 0 | 169.0 | 1.559 | | | | |
| ASM002489 | Kärrviksån | 5:10 | 1.20 | 263560 | 372020 | 11.8 | 442.5 | 0.0 | 442.5 | 611.6 | 0.0 | 0 | 611.6 | 1.644 | | | | |
| ASM001476 | Kärrviksån | 5:9 | 3.62 | 796180 | 796180 | 25.2 | 1814.1 | 0.0 | 1814.1 | 1814.1 | 0.0 | 0 | 1814.1 | 2.278 | | | | |
| ASM001475B | Kärrviksån | 5:8 | 1.38 | 302940 | 1820060 | 57.7 | 546.0 | 0.0 | 546.0 | 3532.4 | 0.0 | 0 | 3532.4 | 1.941 | PSM002081 | 0.058 | 1.753 | 11 |
| ASM001475A | Kärrviksån | 5:8 | 0.04 | 9680 | 1829740 | 58.0 | 16.5 | 0.0 | 16.5 | 3548.9 | 0.0 | 0 | 3548.9 | 1.940 | | | | |
| ASM002479 | Kärrviksån | 5:18 | 1.18 | 259600 | 259600 | 8.2 | 404.6 | 0.0 | 404.6 | 404.6 | 0.0 | 0 | 404.6 | 1.559 | | | | |
| ASM002486C | Kärrviksån | 5:1 | 2.75 | 604560 | 1074040 | 34.1 | 966.7 | 0.0 | 966.7 | 2140.3 | 0.0 | 0 | 2140.3 | 1.993 | PSM002080 | | | |
| ASM002486B | Kärrviksån | 5:1 | 1.13 | 247940 | 3840760 | 121.8 | 414.5 | 0.0 | 414.5 | 7629.1 | 0.0 | 0 | 7629.1 | 1.986 | PSM002082 | 0.121 | 1.833 | 8 |
| ASM002486A | Kärrviksån | 5:1 | 2.93 | 645260 | 6007100 | 190.5 | 1842.5 | 0.0 | 1842.5 | 12127.2 | 0.0 | 0 | 12127.2 | 2.019 | PSM002083 | 0.190 | 2.019 | 0 |
| ASM002449 | Bjurhidebäcken | 4:1 | 0.63 | 139040 | 139040 | 4.4 | 280.1 | 0.0 | 280.1 | 280.1 | 0.0 | 0 | 280.1 | 2.015 | | | | |
| ASM002472 | Sörviksån | 3:2 | 0.47 | 103400 | 103400 | 3.3 | 216.2 | 0.0 | 216.2 | 216.2 | 0.0 | 0 | 216.2 | 2.091 | | | | |
| ASM002473 | Sörviksån | 3:1 | 0.53 | 116600 | 220000 | 7.0 | 202.1 | 0.0 | 202.1 | 418.4 | 0.0 | 0 | 418.4 | 1.902 | | | | |
| ASM002651 | Coastal area | | 1.67 | 368280 | 368280 | 11.7 | 618.6 | 0.0 | 618.6 | 618.6 | 0.0 | 0 | 618.6 | 1.680 | | | | |
| ASM002447 | Bodvikebäcken | 2:1 | 0.38 | 83600 | 83600 | 2.7 | 103.9 | 0.0 | 103.9 | 103.9 | 0.0 | 0 | 103.9 | 1.243 | | | | |
| ASM002446 | Långbonäsbäcken | 1:1 | 0.07 | 15400 | 15400 | 0.5 | 24.0 | 0.0 | 24.0 | 24.0 | 0.0 | 0 | 24.0 | 1.559 | | | | |
| ASM002464 | Flakvarpebäcken | 19:1 | 0.18 | 40480 | 40480 | 1.3 | 58.1 | 0.0 | 58.1 | 58.1 | 0.0 | 0 | 58.1 | 1.435 | | | | |
| ASM002465 | Jössesbäcken | 20:1 | 0.11 | 24420 | 24420 | 0.8 | 38.1 | 0.0 | 38.1 | 38.1 | 0.0 | 0 | 38.1 | 1.559 | | | | |
| ASM002471 | Åspöbäcken | 21:1 | 0.06 | 13860 | 13860 | 0.4 | 21.6 | 0.0 | 21.6 | 21.6 | 0.0 | 0 | 21.6 | 1.559 | | | | |
| ASM002652 | Coastal area | | 1.39 | 305140 | 305140 | 9.7 | 472.8 | 0.0 | 472.8 | 472.8 | 0.0 | 0 | 472.8 | 1.549 | | | | |
| ASM001445 | Frisksjön | 7:2 | 1.85 | 406560 | 406560 | 12.9 | 874.8 | 0.0 | 874.8 | 874.8 | 0.0 | 0 | 874.8 | 2.152 | | | | |
| ASM001484 | Käreviksån | 7:1 | 0.21 | 46860 | 453420 | 14.4 | 73.0 | 0.0 | 73.0 | 947.8 | 0.0 | 0 | 947.8 | 2.090 | | | | |
| ASM001486B | Mederhultsån | 6:1 | 1.92 | 422620 | 422620 | 13.4 | 1296.5 | 0.0 | 1296.5 | 1296.5 | 0.0 | 0 | 1296.5 | 3.068 | PSM002084 | 0.013 | 3.356 | 9 |
| ASM001486A | Mederhultsån | 6:1 | 0.08 | 18040 | 440660 | 14.0 | 28.1 | 0.0 | 28.1 | 1324.7 | 0.0 | 0 | 1324.7 | 3.006 | | | | |
| ASM002654 | Coastal area | | 1.86 | 409420 | 409420 | 13.0 | 636.3 | 0.0 | 636.3 | 636.3 | 0.0 | 0 | 636.3 | 1.554 | | | | |
| ASM002460 | Pistlanbäcken | 8:1 | 0.50 | 109780 | 109780 | 3.5 | 169.6 | 0.0 | 169.6 | 169.6 | 0.0 | 0 | 169.6 | 1.545 | | | | |
| ASM001490 | Ekerumsån | 9:3 | 0.22 | 48840 | 48840 | 1.5 | 179.6 | 0.0 | 179.6 | 179.6 | 0.0 | 0 | 179.6 | 3.678 | | | | |
| ASM001489 | Ekerumsån | 9:2 | 0.77 | 168740 | 168740 | 5.4 | 559.1 | 0.0 | 559.1 | 559.1 | 0.0 | 0 | 559.1 | 3.313 | | | | |
| ASM002483B | Ekerumsån | 9:1 | 1.50 | 330880 | 548460 | 17.4 | 987.1 | 0.0 | 987.1 | 1725.8 | 0.0 | 0 | 1725.8 | 3.147 | PSM002085 | 0.017 | 3.147 | 0 |
| ASM002483A | Ekerumsån | 9:1 | 0.34 | 75020 | 623480 | 19.8 | 176.3 | 0.0 | 176.3 | 1902.0 | 0.0 | 0 | 1902.0 | 3.051 | | | | |
| ASM002478 | Laxemarån | 10:32 | 0.02 | 5060 | 5060 | 0.2 | 7.9 | 0.0 | 7.9 | 7.9 | 0.0 | 0 | 7.9 | 1.559 | | | | |
| ASM002482 | Laxemarån | 10:31 | 0.87 | 190740 | 195800 | 6.2 | 358.0 | 0.0 | 358.0 | 365.9 | 0.0 | 0 | 365.9 | 1.869 | | | | |
| ASM002480B | Laxemarån | 10:30 | 4.23 | 931480 | 1127280 | 35.7 | 1799.0 | 0.0 | 1799.0 | 2164.9 | 0.0 | 0 | 2164.9 | 1.920 | PSM002068 | 0.036 | 1.830 | 5 |
| ASM002480A | Jämsen | 10:30 | 1.83 | 403480 | 1530760 | 48.5 | 797.4 | 0.0 | 797.4 | 2962.4 | 0.0 | 0 | 2962.4 | 1.935 | PSM002069 | 0.049 | 2.195 | 12 |
| ASM001516 | Laxemarån | 10:29 | 0.53 | 117260 | 117260 | 3.7 | 212.4 | 0.0 | 212.4 | 212.4 | 0.0 | 0 | 212.4 | 1.811 | | | | |
| ASM001515 | Laxemarån | 10:28 | 0.34 | 74140 | 74140 | 2.4 | 159.4 | 0.0 | 159.4 | 159.4 | 0.0 | 0 | 159.4 | 2.150 | | | | |
| ASM001514 | Laxemarån | 10:27 | 0.49 | 107140 | 107140 | 3.4 | 472.5 | 0.0 | 472.5 | 472.5 | 0.0 | 0 | 472.5 | 4.410 | | | | |
| ASM001446 | Plittorpsgöl | 10:26 | 0.68 | 149160 | 149160 | 4.7 | 232.3 | 0.0 | 232.3 | 232.3 | 0.0 | 0 | 232.3 | 1.557 | | | | |
| ASM002459 | Laxemarån | 10:25 | 0.10 | 21780 | 170940 | 5.4 | 40.4 | 0.0 | 40.4 | 272.7 | 0.0 | 0 | 272.7 | 1.595 | | | | |
| ASM001512 | Laxemarån | 10:24 | 0.49 | 108680 | 108680 | 3.4 | 170.7 | 0.0 | 170.7 | 170.7 | 0.0 | 0 | 170.7 | 1.571 | | | | |
| ASM002476E | Laxemarån | 10:1 | 3.95 | 868780 | 2977700 | 94.4 | 1657.4 | 0.0 | 1657.4 | 5907.4 | 0.0 | 0 | 5907.4 | 1.984 | PSM002071 | 0.094 | 2.436 | 19 |
| ASM001510 | Laxemarån | 10:22 | 0.56 | 123640 | 123640 | 3.9 | 192.7 | 0.0 | 192.7 | 192.7 | 0.0 | 0 | 192.7 | 1.559 | | | | |
| ASM002453 | Laxemarån | 10:21 | 0.45 | 97900 | 221540 | 7.0 | 152.1 | 0.0 | 152.1 | 344.8 | 0.0 | 0 | 344.8 | 1.556 | | | | |
| ASM002450B | Laxemarån | 10:20 | 2.39 | 526240 | 747780 | 23.7 | 818.4 | 0.0 | 818.4 | 1163.2 | 0.0 | 0 | 1163.2 | 1.556 | PSM002072 | | | |
| ASM002450A | Laxemarån | 10:20 | 0.19 | 41140 | 788920 | 25.0 | 64.0 | 0.0 | 64.0 | 1227.2 | 0.0 | 0 | 1227.2 | 1.556 | | | | |
| ASM001511 | Laxemarån | 10:23 | 0.74 | 162800 | 162800 | 5.2 | 253.7 | 0.0 | 253.7 | 253.7 | 0.0 | 0 | 253.7 | 1.558 | | | | |
| ASM001448 | Grangöl | 10:19 | 0.50 | 108900 | 108900 | 3.5 | 160.5 | 0.0 | 160.5 | 160.5 | 0.0 | 0 | 160.5 | 1.474 | | | | |
| ASM002499 | Laxemarån | 10:18 | 0.06 | 12760 | 121660 | 3.9 | 29.0 | 0.0 | 29.0 | 189.5 | 0.0 | 0 | 189.5 | 1.557 | | | | |
| ASM001506 | Laxemarån | 10:17 | 0.40 | 87560 | 87560 | 2.8 | 209.3 | 0.0 | 209.3 | 209.3 | 0.0 | 0 | 209.3 | 2.390 | | | | |
| ASM001447 | Fjällgöl | 10:16 | 0.30 | 64900 | 64900 | 2.1 | 112.1 | 0.0 | 112.1 | 112.1 | 0.0 | 0 | 112.1 | 1.727 | | | | |
| ASM002451 | Laxemarån | 10:15 | 0.33 | 71500 | 136400 | 4.3 | 152.1 | 0.0 | 152.1 | 264.2 | 0.0 | 0 | 264.2 | 1.937 | | | | |
| ASM002452 | Laxemarån | 10:14 | 2.38 | 522500 | 868120 | 27.5 | 1117.4 | 0.0 | 1117.4 | 1780.4 | 0.0 | 0 | 1780.4 | 2.051 | | | | |
| ASM001503 | Laxemarån | 10:13 | 0.42 | 91520 | 91520 | 2.9 | 262.3 | 0.0 | 262.3 | 262.3 | 0.0 | 0 | 262.3 | 2.866 | | | | |
| ASM002454 | Laxemarån | 10:12 | 0.81 | 177760 | 269280 | 8.5 | 657.9 | 0.0 | 657.9 | 920.2 | 0.0 | 0 | 920.2 | 3.417 | | | | |
| ASM001501 | Laxemarån | 10:11 | 0.81 | 177320 | 177320 | 5.6 | 387.6 | 0.0 | 387.6 | 387.6 | 0.0 | 0 | 387.6 | 2.186 | | | | |
| ASM002457 | Laxemarån | 10:10 | 1.39 | 305580 | 482900 | 15.3 | 934.5 | 0.0 | 934.5 | 1322.1 | 0.0 | 0 | 1322.1 | 2.738 | | | | |
| ASM002476D | Laxemarån | 10:1 | 4.96 | 1091860 | 6641580 | 210.6 | 2429.4 | 0.0 | 2429.4 | 13840.5 | 0.0 | 0 | 13840.5 | 2.084 | PSM002077 | | | |
| ASM001499 | Laxemarån | 10:9 | 0.71 | 156420 | 156420 | 5.0 | 249.1 | 0.0 | 249.1 | 249.1 | 0.0 | 0 | 249.1 | 1.593 | | | | |
| ASM001498 | Laxemarån | 10:8 | 2.77 | 609620 | 766040 | 24.3 | 1210.3 | 0.0 | 1210.3 | 1459.5 | 0.0 | 0 | 1459.5 | 1.905 | PSM002078 | 0.024 | 1.777 | 7 |
| ASM001497 | Laxemarån | 10:7 | 0.61 | 133980 | 133980 | 4.2 | 256.4 | 0.0 | 256.4 | 256.4 | 0.0 | 0 | 256.4 | 1.913 | | | | |
| ASM002476C | Laxemarån | 10:1 | 0.32 | 69300 | 7610900 | 241.3 | 153.2 | 0.0 | 153.2 | 15709.6 | 0.0 | 0 | 15709.6 | 2.064 | PSM002079 | 0.242 | 2.315 | 11 |
| ASM001494 | Laxemarån | 10:4 | 1.00 | 220220 | 220220 | 7.0 | 732.4 | 0.0 | 732.4 | 732.4 | 0.0 | 0 | 732.4 | 3.326 | | | | |
| ASM001493 | Laxemarån | 10:3 | 0.32 | 70180 | 70180 | 2.2 | 171.5 | 0.0 | 171.5 | 171.5 | 0.0 | 0 | 171.5 | 2.444 | | | | |
| ASM001492 | Laxemarån | 10:2 | 0.46 | 101200 | 101200 | 3.2 | 295.6 | 0.0 | 295.6 | 295.6 | 0.0 | 0 | 295.6 | 2.921 | | | | |
| ASM001496 | Laxemarån | 10:6 | 0.89 | 195800 | 195800 | 6.2 | 390.2 | 0.0 | 390.2 | 390.2 | 0.0 | 0 | 390.2 | 1.993 | | | | |
| ASM001495 | Laxemarån | 10:5 | 0.29 | 63800 | 63800 | 2.0 | 133.8 | 0.0 | 133.8 | 133.8 | 0.0 | 0 | 133.8 | 2.097 | | | | |
| ASM002476B | Laxemarån | 10:1 | 3.23 | 710820 | 8972920 | 284.5 | 1716.0 | 0.0 | 1716.0 | 19149.0 | 0.0 | 0 | 19149.0 | 2.134 | PSM002087 | 0.285 | 2.547 | 16 |
| ASM002476A | Laxemarån | 10:1 | 0.19 | 41360 | 9014280 | 285.8 | 64.6 | 0.0 | 64.6 | 19213.6 | 0.0 | 0 | 19213.6 | 2.131 | | | | |
| ASM002495 | Glostadsbäcken | 12:3 | 0.13 | 27720 | 27720 | 0.9 | 98.1 | 0.0 | 98.1 | 98.1 | 0.0 | 0 | 98.1 | 3.538 | | | | |
| ASM002485 | Glostadsbäcken | 12:2 | 0.33 | 72820 | 72820 | 2.3 | 113.5 | 0.0 | 113.5 | 113.5 | 0.0 | 0 | 113.5 | 1.559 | | | | |
| ASM002498 | Glostadsbäcken | 12:1 | 1.60 | 351340 | 451880 | 14.3 | 633.0 | 0.0 | 633.0 | 844.6 | 0.0 | 0 | 844.6 | 1.869 | | | | |
| ASM001518B | Stålglobäcken | 13:1 | 0.68 | 149380 | 149380 | 4.7 | 562.7 | 0.0 | 562.7 | 562.7 | 0.0 | 0 | 562.7 | 3.767 | PSM002086 | 0.005 | 3.649 | 3 |
| ASM001518A | Stålglobäcken | 13:1 | 0.35 | 77880 | 227260 | 7.2 | 166.0 | 0.0 | 166.0 | 728.7 | 0.0 | 0 | 728.7 | 3.207 | | | | |
| ASM002462 | Uvöbäcken | 15:1 | 0.97 | 212740 | 212740 | 6.7 | 486.4 | 0.0 | 486.4 | 486.4 | 0.0 | 0 | 486.4 | 2.287 | | | | |
| ASM002497 | Stekebäcken | 14:2 | 0.44 | 95700 | 95700 | 3.0 | 299.2 | 0.0 | 299.2 | 299.2 | 0.0 | 0 | 299.2 | 3.126 | | | | |
| ASM001517 | Stekebäcken | 14:1 | 0.90 | 198660 | 294360 | 9.3 | 364.9 | 0.0 | 364.9 | 664.1 | 0.0 | 0 | 664.1 | 2.256 | | | | |
| ASM002463 | Svartebäck | 16:1 | 0.50 | 110880 | 110880 | 3.5 | 187.0 | 0.0 | 187.0 | 187.0 | 0.0 | 0 | 187.0 | 1.687 | | | | |
| ASM002655 | Coastal area | | 2.71 | 596420 | 596420 | 18.9 | 979.7 | 0.0 | 979.7 | 979.7 | 0.0 | 0 | 979.7 | 1.643 | | | | |
| ASM002658 | Coastal area | | 1.26 | 277420 | 277420 | 8.8 | 430.7 | 0.0 | 430.7 | 430.7 | 0.0 | 0 | 430.7 | 1.552 | | | | |
| ASM002656 | Coastal area | | 0.22 | 48400 | 48400 | 1.5 | 74.6 | 0.0 | 74.6 | 74.6 | 0.0 | 0 | 74.6 | 1.541 | | | | |
| ASM002660 | Coastal area | | 0.14 | 30360 | 30360 | 1.0 | 46.9 | 0.0 | 46.9 | 46.9 | 0.0 | 0 | 46.9 | 1.544 | | | | |
| ASM002659 | Coastal area | | 15.70 | 3453780 | 3453780 | 109.5 | 7189.1 | 0.0 | 7189.1 | 7189.1 | 0.0 | 0 | 7189.1 | 2.082 | | | | |
| ASM002657 | Coastal area | | 2.60 | 571340 | 571340 | 18.1 | 1052.3 | 0.0 | 1052.3 | 1052.3 | 0.0 | 0 | 1052.3 | 1.842 | | | | |
| ASM001522 | Uthammarsån | 17:5 | 0.57 | 125620 | 125620 | 4.0 | 341.8 | 0.0 | 341.8 | 341.8 | 0.0 | 0 | 341.8 | 2.721 | | | | |
| ASM001523 | Uthammarsån | 17:6 | 0.96 | 210760 | 210760 | 6.7 | 579.9 | 0.0 | 579.9 | 579.9 | 0.0 | 0 | 579.9 | 2.752 | | | | |
| ASM001521 | Uthammarsån | 17:4 | 0.20 | 44880 | 44880 | 1.4 | 151.1 | 0.0 | 151.1 | 151.1 | 0.0 | 0 | 151.1 | 3.367 | | | | |
| ASM001520 | Uthammarsån | 17:3 | 0.08 | 17820 | 17820 | 0.6 | 57.1 | 0.0 | 57.1 | 57.1 | 0.0 | 0 | 57.1 | 3.202 | | | | |
| ASM002494B | Uthammarsån | 17:1 | 2.91 | 640860 | 1039940 | 33.0 | 1353.4 | 0.0 | 1353.4 | 2483.2 | 0.0 | 0 | 2483.2 | 2.388 | PSM002076 | 0.033 | 2.442 | 2 |
| ASM001533 | Uthammarsån | 17:2 | 0.51 | 112640 | 112640 | 3.6 | 403.2 | 0.0 | 403.2 | 403.2 | 0.0 | 0 | 403.2 | 3.580 | | | | |
| ASM002494A | Uthammarsån | 17:1 | 1.78 | 391820 | 1544400 | 49.0 | 1445.2 | 0.0 | 1445.2 | 4331.7 | 0.0 | 0 | 4331.7 | 2.805 | | | | |
| ASM001528 | Släthultebäcken | 18:5 | 0.32 | 70400 | 70400 | 2.2 | 109.7 | 0.0 | 109.7 | 109.7 | 0.0 | 0 | 109.7 | 1.559 | | | | |
| ASM002477 | Släthultebäcken | 18:4 | 0.66 | 144980 | 215380 | 6.8 | 218.0 | 0.0 | 218.0 | 327.7 | 0.0 | 0 | 327.7 | 1.521 | | | | |
| ASM001531 | Släthultebäcken | 18:8 | 0.30 | 66440 | 66440 | 2.1 | 103.6 | 0.0 | 103.6 | 103.6 | 0.0 | 0 | 103.6 | 1.560 | | | | |
| ASM001532 | Släthultebäcken | 18:9 | 0.11 | 24420 | 24420 | 0.8 | 107.6 | 0.0 | 107.6 | 107.6 | 0.0 | 0 | 107.6 | 4.404 | | | | |
| ASM002455 | Släthultebäcken | 18:7 | 0.76 | 167420 | 258280 | 8.2 | 547.4 | 0.0 | 547.4 | 758.6 | 0.0 | 0 | 758.6 | 2.937 | | | | |
| ASM002475 | Släthultebäcken | 18:6 | 1.06 | 232100 | 490380 | 15.5 | 433.1 | 0.0 | 433.1 | 1191.7 | 0.0 | 0 | 1191.7 | 2.430 | | | | |
| ASM001526 | Släthultebäcken | 18:3 | 0.40 | 88220 | 88220 | 2.8 | 147.7 | 0.0 | 147.7 | 147.7 | 0.0 | 0 | 147.7 | 1.674 | | | | |
| ASM002481C | Släthultebäcken | 18:1 | 2.44 | 537020 | 1027400 | 32.6 | 1285.2 | 0.0 | 1285.2 | 2476.9 | 0.0 | 0 | 2476.9 | 2.411 | PSM002070 | | | |
| ASM002481B | Släthultebäcken | 18:1 | 2.13 | 469260 | 1800260 | 57.1 | 869.3 | 0.0 | 869.3 | 3821.6 | 0.0 | 0 | 3821.6 | 2.123 | PSM002075 | | | |
| ASM001525 | Släthultebäcken | 18:2 | 0.77 | 169620 | 169620 | 5.4 | 368.3 | 0.0 | 368.3 | 368.3 | 0.0 | 0 | 368.3 | 2.172 | | | | |
| ASM002481A | Släthultebäcken | 18:1 | 0.00 | 220 | 1970100 | 62.5 | 0.2 | 0.0 | 0.2 | 4190.2 | 0.0 | 0 | 4190.2 | 2.127 | | | | |
| ASM001444 | Sörämagasinet | 11:1 | 0.52 | 115060 | 115060 | 3.6 | 148.7 | 0.0 | 148.7 | 148.7 | 0.0 | 0 | 148.7 | 1.292 | | | | |
| ASM002466 | Stekflagebäcken | 22:1 | 0.36 | 78980 | 78980 | 2.5 | 114.7 | 0.0 | 114.7 | 114.7 | 0.0 | 0 | 114.7 | 1.453 | | | | |
| ASM002653 | Coastal area | | 0.76 | 166980 | 166980 | 5.3 | 259.7 | 0.0 | 259.7 | 259.7 | 0.0 | 0 | 259.7 | 1.555 | | | | |
| ASM002470 | Skölkebäcken | 26:1 | 0.17 | 36300 | 36300 | 1.2 | 56.6 | 0.0 | 56.6 | 56.6 | 0.0 | 0 | 56.6 | 1.559 | | | | |
| ASM002469 | Gloebäcken | 25:1 | 0.13 | 28820 | 28820 | 0.9 | 44.9 | 0.0 | 44.9 | 44.9 | 0.0 | 0 | 44.9 | 1.559 | | | | |
| ASM002468 | Lindströmmebäcken | 24:1 | 0.19 | 42240 | 42240 | 1.3 | 65.8 | 0.0 | 65.8 | 65.8 | 0.0 | 0 | 65.8 | 1.559 | | | | |
| ASM002467B | Vadvikebäcken | 23:1 | 0.30 | 65560 | 65560 | 2.1 | 102.2 | 0.0 | 102.2 | 102.2 | 0.0 | 0 | 102.2 | 1.559 | PSM107735 | 0.002 | 3.850 | 60 |
| ASM002467A | Vadvikebäcken | 23:1 | 0.01 | 1980 | 67540 | 2.1 | 3.1 | 0.0 | 3.1 | 105.3 | 0.0 | 0 | 105.3 | 1.559 | | | | |
| | **Kärrviksån** | 5:1-20 | 27.31 | 6007100 | 6007100 | 26.9 | 12127.2 | 0.0 | 12127.2 | | 0.0 | 0 | 12127.2 | 2.019 | | | | |
| | **Laxemarån** | 10:1-32 | 40.97 | 9014280 | 9014280 | 37.5 | 19213.6 | 0.0 | 19213.6 | | 0.0 | 0 | 19213.6 | 2.131 | | | | |
| | **All catchments** | | 129.97 | 28593620 | 28593620 | 22.3 | 60358.4 | 0.0 | 60358.4 | | 0.0 | 0 | 60358.4 | 2.111 | | | | |

| **Total silicon (Si)** | | | | Water balance | | | Total per catchment | | | Total including contributions from upstream catchments | | | | | Calibration data | | | |
|---|---|---|---|---|---|---|---|---|---|---|---|---|---|---|---|---|---|---|
| Idcode | Name | ARO | Area | $Q_{catch}$ | $Q_{out}$ | q | Diffuse | Point | Total | Total IN | Retention | | Total OUT | Conc. | Reference | q | Conc. | Deviation |
| | | | $km^2$ | $m^3 \cdot yr^{-1}$ | $m^3 \cdot yr^{-1}$ | $L \cdot s^{-1}$ | $kg \cdot yr^{-1}$ | $kg \cdot yr^{-1}$ | $kg \cdot yr^{-1}$ | $kg \cdot yr^{-1}$ | $kg \cdot yr^{-1}$ | % | $kg \cdot yr^{-1}$ | $mg \cdot L^{-1}$ | | $L \cdot s^{-1}$ | $mg \cdot L^{-1}$ | % |
| ASM002474 | Kärrviksån | 5:20 | 0.12 | 25740 | 25740 | 0.8 | 229.3 | 0.0 | 229.3 | 229.3 | 0.0 | 0 | 229.3 | 8.907 | | | | |
| ASM002493 | Kärrviksån | 5:19 | 0.84 | 184140 | 209880 | 6.7 | 1701.4 | 0.0 | 1701.4 | 1930.6 | 0.0 | 0 | 1930.6 | 9.199 | | | | |
| ASM001483 | Kärrviksån | 5:17 | 0.15 | 33220 | 33220 | 1.1 | 414.4 | 0.0 | 414.4 | 414.4 | 0.0 | 0 | 414.4 | 12.475 | | | | |
| ASM002492 | Kärrviksån | 5:16 | 1.11 | 243980 | 277200 | 8.8 | 2556.1 | 0.0 | 2556.1 | 2970.5 | 0.0 | 0 | 2970.5 | 10.716 | | | | |
| ASM002491 | Kärrviksån | 5:15 | 1.87 | 411840 | 689040 | 21.8 | 3814.9 | 0.0 | 3814.9 | 6785.4 | 26.3 | 0 | 6759.1 | 9.809 | | | | |
| ASM001474 | Kärrviksån | 5:7 | 0.45 | 99000 | 99000 | 3.1 | 918.7 | 0.0 | 918.7 | 918.7 | 0.0 | 0 | 918.7 | 9.280 | | | | |
| ASM002487 | Kärrviksån | 5:6 | 1.20 | 264000 | 363000 | 11.5 | 2736.0 | 0.0 | 2736.0 | 3654.7 | 0.0 | 0 | 3654.7 | 10.068 | | | | |
| ASM001472 | Kärrviksån | 5:4 | 1.10 | 242880 | 242880 | 7.7 | 1738.0 | 0.0 | 1738.0 | 1738.0 | 657.5 | 38 | 1080.5 | 4.449 | | | | |
| ASM001470 | Kärrviksån | 5:3 | 0.40 | 87560 | 87560 | 2.8 | 761.3 | 0.0 | 761.3 | 761.3 | 0.0 | 0 | 761.3 | 8.695 | | | | |
| ASM001469 | Kärrviksån | 5:2 | 0.97 | 212960 | 212960 | 6.8 | 1741.0 | 0.0 | 1741.0 | 1741.0 | 0.0 | 0 | 1741.0 | 8.175 | | | | |
| ASM001471 | Kärrviksån | 5:5 | 2.79 | 614680 | 614680 | 19.5 | 4841.6 | 0.0 | 4841.6 | 4841.6 | 0.0 | 0 | 4841.6 | 7.877 | | | | |
| ASM001479 | Kärrviksån | 5:13 | 0.65 | 142340 | 142340 | 4.5 | 1211.3 | 0.0 | 1211.3 | 1211.3 | 0.0 | 0 | 1211.3 | 8.510 | | | | |
| ASM001480 | Kärrviksån | 5:14 | 0.10 | 22660 | 22660 | 0.7 | 210.8 | 0.0 | 210.8 | 210.8 | 0.0 | 0 | 210.8 | 9.302 | | | | |
| ASM002490 | Kärrviksån | 5:12 | 0.84 | 183920 | 348920 | 11.1 | 1582.9 | 0.0 | 1582.9 | 3004.9 | 113.0 | 4 | 2892.0 | 8.288 | | | | |
| ASM001478 | Kärrviksån | 5:11 | 0.49 | 108460 | 108460 | 3.4 | 834.6 | 0.0 | 834.6 | 834.6 | 0.0 | 0 | 834.6 | 7.695 | | | | |
| ASM002489 | Kärrviksån | 5:10 | 1.20 | 263560 | 372020 | 11.8 | 2119.7 | 0.0 | 2119.7 | 2954.3 | 0.0 | 0 | 2954.3 | 7.941 | | | | |
| ASM001476 | Kärrviksån | 5:9 | 3.62 | 796180 | 796180 | 25.2 | 8027.5 | 0.0 | 8027.5 | 8027.5 | 0.0 | 0 | 8027.5 | 10.083 | | | | |
| ASM001475B | Kärrviksån | 5:8 | 1.38 | 302940 | 1820060 | 57.7 | 2535.1 | 0.0 | 2535.1 | 16408.9 | 0.0 | 0 | 16408.9 | 9.016 | PSM002081 | 0.058 | 8.616 | 5 |
| ASM001475A | Kärrviksån | 5:8 | 0.04 | 9680 | 1829740 | 58.0 | 61.9 | 0.0 | 61.9 | 16470.8 | 0.0 | 0 | 16470.8 | 9.002 | | | | |
| ASM002479 | Kärrviksån | 5:18 | 1.18 | 259600 | 259600 | 8.2 | 2143.0 | 0.0 | 2143.0 | 2143.0 | 0.0 | 0 | 2143.0 | 8.255 | | | | |
| ASM002486C | Kärrviksån | 5:1 | 2.75 | 604560 | 1074040 | 34.1 | 5161.2 | 0.0 | 5161.2 | 9234.8 | 176.7 | 2 | 9058.1 | 8.434 | PSM002080 | | | |
| ASM002486B | Kärrviksån | 5:1 | 1.13 | 247940 | 3840760 | 121.8 | 2106.3 | 0.0 | 2106.3 | 34394.3 | 0.0 | 0 | 34394.3 | 8.955 | PSM002082 | 0.121 | 8.547 | 5 |
| ASM002486A | Kärrviksån | 5:1 | 2.93 | 645260 | 6007100 | 190.5 | 5583.7 | 0.0 | 5583.7 | 52057.1 | 34.4 | 0 | 52022.8 | 8.660 | PSM002083 | 0.190 | 8.660 | 0 |
| ASM002449 | Bjurhidebäcken | 4:1 | 0.63 | 139040 | 139040 | 4.4 | 1170.4 | 0.0 | 1170.4 | 1170.4 | 0.0 | 0 | 1170.4 | 8.418 | | | | |
| ASM002472 | Sörviksån | 3:2 | 0.47 | 103400 | 103400 | 3.3 | 858.6 | 0.0 | 858.6 | 858.6 | 1.1 | 0 | 857.5 | 8.293 | | | | |
| ASM002473 | Sörviksån | 3:1 | 0.53 | 116600 | 220000 | 7.0 | 986.4 | 0.0 | 986.4 | 1843.9 | 0.0 | 0 | 1843.9 | 8.381 | | | | |
| ASM002651 | Coastal area | | 1.67 | 368280 | 368280 | 11.7 | 3000.1 | 0.0 | 3000.1 | 3000.1 | 456.4 | 15 | 2543.7 | 6.907 | | | | |
| ASM002447 | Bodvikebäcken | 2:1 | 0.38 | 83600 | 83600 | 2.7 | 522.3 | 0.0 | 522.3 | 522.3 | 378.7 | 73 | 143.6 | 1.717 | | | | |
| ASM002446 | Långbonäsbäcken | 1:1 | 0.07 | 15400 | 15400 | 0.5 | 100.1 | 0.0 | 100.1 | 100.1 | 0.0 | 0 | 100.1 | 6.499 | | | | |
| ASM002464 | Flakvarpebäcken | 19:1 | 0.18 | 40480 | 40480 | 1.3 | 269.7 | 0.0 | 269.7 | 269.7 | 141.3 | 52 | 128.4 | 3.173 | | | | |
| ASM002465 | Jössesbäcken | 20:1 | 0.11 | 24420 | 24420 | 0.8 | 276.2 | 0.0 | 276.2 | 276.2 | 0.0 | 0 | 276.2 | 11.310 | | | | |
| ASM002471 | Åspöbäcken | 21:1 | 0.06 | 13860 | 13860 | 0.4 | 111.4 | 0.0 | 111.4 | 111.4 | 0.0 | 0 | 111.4 | 8.041 | | | | |
| ASM002652 | Coastal area | | 1.39 | 305140 | 305140 | 9.7 | 2610.3 | 0.0 | 2610.3 | 2610.3 | 423.6 | 16 | 2186.7 | 7.166 | | | | |
| ASM001445 | Frisksjön | 7:2 | 1.85 | 406560 | 406560 | 12.9 | 3561.2 | 0.0 | 3561.2 | 3561.2 | 1622.9 | 46 | 1938.3 | 4.768 | | | | |
| ASM001484 | Kåreviksån | 7:1 | 0.21 | 46860 | 453420 | 14.4 | 357.9 | 0.0 | 357.9 | 2296.1 | 0.0 | 0 | 2296.1 | 5.064 | | | | |
| ASM001486B | Mederhultsån | 6:1 | 1.92 | 422620 | 422620 | 13.4 | 3909.8 | 0.0 | 3909.8 | 3909.8 | 0.0 | 0 | 3909.8 | 9.251 | PSM002084 | 0.013 | 9.895 | 7 |
| ASM001486A | Mederhultsån | 6:1 | 0.08 | 18040 | 440660 | 14.0 | 162.3 | 0.0 | 162.3 | 4072.1 | 0.0 | 0 | 4072.1 | 9.241 | | | | |
| ASM002654 | Coastal area | | 1.86 | 409420 | 409420 | 13.0 | 3500.3 | 0.0 | 3500.3 | 3500.3 | 574.4 | 16 | 2925.9 | 7.146 | | | | |
| ASM002460 | Pistlanbäcken | 8:1 | 0.50 | 109780 | 109780 | 3.5 | 933.1 | 0.0 | 933.1 | 933.1 | 104.5 | 11 | 828.6 | 7.548 | | | | |
| ASM001490 | Ekerumsån | 9:3 | 0.22 | 48840 | 48840 | 1.5 | 588.3 | 0.0 | 588.3 | 588.3 | 0.0 | 0 | 588.3 | 12.045 | | | | |
| ASM001489 | Ekerumsån | 9:2 | 0.77 | 168740 | 168740 | 5.4 | 2226.8 | 0.0 | 2226.8 | 2226.8 | 0.0 | 0 | 2226.8 | 13.196 | | | | |
| ASM002483B | Ekerumsån | 9:1 | 1.50 | 330880 | 548460 | 17.4 | 3078.0 | 0.0 | 3078.0 | 5893.0 | 0.0 | 0 | 5893.0 | 10.745 | PSM002085 | 0.017 | 10.738 | 0 |
| ASM002483A | Ekerumsån | 9:1 | 0.34 | 75020 | 623480 | 19.8 | 673.2 | 0.0 | 673.2 | 6566.3 | 0.0 | 0 | 6566.3 | 10.532 | | | | |
| ASM002478 | Laxemarån | 10:32 | 0.02 | 5060 | 5060 | 0.2 | 45.1 | 0.0 | 45.1 | 45.1 | 0.0 | 0 | 45.1 | 8.907 | | | | |
| ASM002482 | Laxemarån | 10:31 | 0.87 | 190740 | 195800 | 6.2 | 1492.0 | 0.0 | 1492.0 | 1537.0 | 0.0 | 0 | 1537.0 | 7.850 | | | | |
| ASM002480B | Laxemarån | 10:30 | 4.23 | 931480 | 1127280 | 35.7 | 7001.7 | 0.0 | 7001.7 | 8538.7 | 2486.5 | 29 | 6052.2 | 5.369 | PSM002068 | 0.036 | 5.369 | 0 |
| ASM002480A | Jämsen | 10:30 | 1.83 | 403480 | 1530760 | 48.5 | 3136.1 | 0.0 | 3136.1 | 9188.3 | 2721.5 | 30 | 6466.8 | 4.225 | PSM002069 | 0.049 | 4.237 | 0 |
| ASM001516 | Laxemarån | 10:29 | 0.53 | 117260 | 117260 | 3.7 | 1101.3 | 0.0 | 1101.3 | 1101.3 | 0.0 | 0 | 1101.3 | 9.392 | | | | |
| ASM001515 | Laxemarån | 10:28 | 0.34 | 74140 | 74140 | 2.4 | 726.7 | 0.0 | 726.7 | 726.7 | 0.0 | 0 | 726.7 | 9.802 | | | | |
| ASM001514 | Laxemarån | 10:27 | 0.49 | 107140 | 107140 | 3.4 | 1288.6 | 0.0 | 1288.6 | 1288.6 | 0.0 | 0 | 1288.6 | 12.027 | | | | |
| ASM001446 | Plittorpsgöl | 10:26 | 0.68 | 149160 | 149160 | 4.7 | 1223.7 | 0.0 | 1223.7 | 1223.7 | 482.1 | 39 | 741.6 | 4.972 | | | | |
| ASM002459 | Laxemarån | 10:25 | 0.10 | 21780 | 170940 | 5.4 | 176.5 | 0.0 | 176.5 | 918.0 | 0.0 | 0 | 918.0 | 5.370 | | | | |
| ASM001512 | Laxemarån | 10:24 | 0.49 | 108680 | 108680 | 3.4 | 899.4 | 0.0 | 899.4 | 899.4 | 0.0 | 0 | 899.4 | 8.275 | | | | |
| ASM002476E | Laxemarån | 10:1 | 3.95 | 868780 | 2977700 | 94.4 | 7313.6 | 0.0 | 7313.6 | 18714.4 | 46.8 | 0 | 18667.7 | 6.269 | PSM002071 | 0.094 | 5.980 | 5 |
| ASM001510 | Laxemarån | 10:22 | 0.56 | 123640 | 123640 | 3.9 | 952.6 | 0.0 | 952.6 | 952.6 | 0.0 | 0 | 952.6 | 7.704 | | | | |
| ASM002453 | Laxemarån | 10:21 | 0.45 | 97900 | 221540 | 7.0 | 829.4 | 0.0 | 829.4 | 1781.9 | 31.2 | 2 | 1750.8 | 7.903 | | | | |
| ASM002450B | Laxemarån | 10:20 | 2.39 | 526240 | 747780 | 23.7 | 4204.0 | 0.0 | 4204.0 | 5954.8 | 120.9 | 2 | 5833.9 | 7.802 | PSM002072 | | | |
| ASM002450A | Laxemarån | 10:20 | 0.19 | 41140 | 788920 | 25.0 | 238.6 | 0.0 | 238.6 | 6072.5 | 0.0 | 0 | 6072.5 | 7.697 | | | | |
| ASM001511 | Laxemarån | 10:23 | 0.74 | 162800 | 162800 | 5.2 | 1271.8 | 0.0 | 1271.8 | 1271.8 | 0.0 | 0 | 1271.8 | 7.812 | | | | |
| ASM001448 | Grangöl | 10:19 | 0.50 | 108900 | 108900 | 3.5 | 927.7 | 0.0 | 927.7 | 927.7 | 385.5 | 42 | 542.1 | 4.978 | | | | |
| ASM002499 | Laxemarån | 10:18 | 0.06 | 12760 | 121660 | 3.9 | 169.2 | 0.0 | 169.2 | 711.3 | 0.0 | 0 | 711.3 | 5.847 | | | | |
| ASM001506 | Laxemarån | 10:17 | 0.40 | 87560 | 87560 | 2.8 | 955.1 | 0.0 | 955.1 | 955.1 | 0.0 | 0 | 955.1 | 10.907 | | | | |
| ASM001447 | Fjällgöl | 10:16 | 0.30 | 64900 | 64900 | 2.1 | 491.2 | 0.0 | 491.2 | 491.2 | 235.1 | 48 | 256.1 | 3.946 | | | | |
| ASM002451 | Laxemarån | 10:15 | 0.33 | 71500 | 136400 | 4.3 | 809.7 | 0.0 | 809.7 | 1065.8 | 0.0 | 0 | 1065.8 | 7.814 | | | | |
| ASM002452 | Laxemarån | 10:14 | 2.38 | 522500 | 868120 | 27.5 | 5321.9 | 0.0 | 5321.9 | 8054.1 | 50.1 | 1 | 8004.0 | 9.220 | | | | |
| ASM001503 | Laxemarån | 10:13 | 0.42 | 91520 | 91520 | 2.9 | 1080.2 | 0.0 | 1080.2 | 1080.2 | 0.0 | 0 | 1080.2 | 11.803 | | | | |
| ASM002454 | Laxemarån | 10:12 | 0.81 | 177760 | 269280 | 8.5 | 1901.7 | 0.0 | 1901.7 | 2982.0 | 0.0 | 0 | 2982.0 | 11.074 | | | | |
| ASM001501 | Laxemarån | 10:11 | 0.81 | 177320 | 177320 | 5.6 | 1875.3 | 0.0 | 1875.3 | 1875.3 | 0.0 | 0 | 1875.3 | 10.576 | | | | |
| ASM002457 | Laxemarån | 10:10 | 1.39 | 305580 | 482900 | 15.3 | 3936.8 | 0.0 | 3936.8 | 5812.1 | 0.0 | 0 | 5812.1 | 12.036 | | | | |
| ASM002476D | Laxemarån | 10:1 | 4.96 | 1091860 | 6641580 | 210.6 | 9337.7 | 0.0 | 9337.7 | 52147.8 | 0.0 | 0 | 52147.8 | 7.852 | PSM002077 | | | |
| ASM001499 | Laxemarån | 10:9 | 0.71 | 156420 | 156420 | 5.0 | 1398.0 | 0.0 | 1398.0 | 1398.0 | 0.0 | 0 | 1398.0 | 8.938 | | | | |
| ASM001498 | Laxemarån | 10:8 | 2.77 | 609620 | 766040 | 24.3 | 5159.8 | 0.0 | 5159.8 | 6557.8 | 0.0 | 0 | 6557.8 | 8.561 | PSM002078 | 0.024 | 11.777 | 27 |
| ASM001497 | Laxemarån | 10:7 | 0.61 | 133980 | 133980 | 4.2 | 1318.3 | 0.0 | 1318.3 | 1318.3 | 0.0 | 0 | 1318.3 | 9.839 | | | | |
| ASM002476C | Laxemarån | 10:1 | 0.32 | 69300 | 7610900 | 241.3 | 602.3 | 0.0 | 602.3 | 60626.2 | 19.7 | 0 | 60606.5 | 7.963 | PSM002079 | 0.242 | 7.917 | 1 |
| ASM001494 | Laxemarån | 10:4 | 1.00 | 220220 | 220220 | 7.0 | 2646.2 | 0.0 | 2646.2 | 2646.2 | 0.0 | 0 | 2646.2 | 12.016 | | | | |
| ASM001493 | Laxemarån | 10:3 | 0.32 | 70180 | 70180 | 2.2 | 737.1 | 0.0 | 737.1 | 737.1 | 0.0 | 0 | 737.1 | 10.504 | | | | |
| ASM001492 | Laxemarån | 10:2 | 0.46 | 101200 | 101200 | 3.2 | 1146.1 | 0.0 | 1146.1 | 1146.1 | 0.0 | 0 | 1146.1 | 11.325 | | | | |
| ASM001496 | Laxemarån | 10:6 | 0.89 | 195800 | 195800 | 6.2 | 2004.7 | 0.0 | 2004.7 | 2004.7 | 0.0 | 0 | 2004.7 | 10.238 | | | | |
| ASM001495 | Laxemarån | 10:5 | 0.29 | 63800 | 63800 | 2.0 | 562.9 | 0.0 | 562.9 | 562.9 | 0.0 | 0 | 562.9 | 8.823 | | | | |
| ASM002476B | Laxemarån | 10:1 | 3.23 | 710820 | 8972920 | 284.5 | 7160.5 | 0.0 | 7160.5 | 74864.0 | 106.8 | 0 | 74757.2 | 8.331 | PSM002087 | 0.285 | 8.426 | 1 |
| ASM002476A | Laxemarån | 10:1 | 0.19 | 41360 | 9014280 | 285.8 | 332.8 | 0.0 | 332.8 | 75089.9 | 0.0 | 0 | 75089.9 | 8.330 | | | | |
| ASM002495 | Glostadsbäcken | 12:3 | 0.13 | 27720 | 27720 | 0.9 | 219.5 | 0.0 | 219.5 | 219.5 | 0.0 | 0 | 219.5 | 7.917 | | | | |
| ASM002485 | Glostadsbäcken | 12:2 | 0.33 | 72820 | 72820 | 2.3 | 802.5 | 0.0 | 802.5 | 802.5 | 0.0 | 0 | 802.5 | 11.021 | | | | |
| ASM002498 | Glostadsbäcken | 12:1 | 1.60 | 351340 | 451880 | 14.3 | 3799.7 | 0.0 | 3799.7 | 4821.7 | 240.8 | 5 | 4580.9 | 10.137 | | | | |
| ASM001518B | Stålglobäcken | 13:1 | 0.68 | 149380 | 149380 | 4.7 | 1685.7 | 0.0 | 1685.7 | 1685.7 | 0.0 | 0 | 1685.7 | 11.284 | PSM002086 | 0.005 | 12.800 | 12 |
| ASM001518A | Stålglobäcken | 13:1 | 0.35 | 77880 | 227260 | 7.2 | 820.4 | 0.0 | 820.4 | 2506.0 | 0.0 | 0 | 2506.0 | 11.027 | | | | |
| ASM002462 | Uvöbäcken | 15:1 | 0.97 | 212740 | 212740 | 6.7 | 1877.5 | 0.0 | 1877.5 | 1877.5 | 0.0 | 0 | 1877.5 | 8.825 | | | | |
| ASM002497 | Stekebäcken | 14:2 | 0.44 | 95700 | 95700 | 3.0 | 1001.6 | 0.0 | 1001.6 | 1001.6 | 0.0 | 0 | 1001.6 | 10.466 | | | | |
| ASM001517 | Stekebäcken | 14:1 | 0.90 | 198660 | 294360 | 9.3 | 1693.6 | 0.0 | 1693.6 | 2695.2 | 0.0 | 0 | 2695.2 | 9.156 | | | | |
| ASM002463 | Svartebäck | 16:1 | 0.50 | 110880 | 110880 | 3.5 | 970.6 | 0.0 | 970.6 | 970.6 | 38.8 | 4 | 931.8 | 8.404 | | | | |
| ASM002655 | Coastal area | | 2.71 | 596420 | 596420 | 18.9 | 5330.3 | 0.0 | 5330.3 | 5330.3 | 1455.8 | 27 | 3874.5 | 6.496 | | | | |
| ASM002658 | Coastal area | | 1.26 | 277420 | 277420 | 8.8 | 2444.3 | 0.0 | 2444.3 | 2444.3 | 369.6 | 15 | 2074.8 | 7.479 | | | | |
| ASM002656 | Coastal area | | 0.22 | 48400 | 48400 | 1.5 | 404.9 | 0.0 | 404.9 | 404.9 | 148.2 | 37 | 256.7 | 5.304 | | | | |
| ASM002660 | Coastal area | | 0.14 | 30360 | 30360 | 1.0 | 257.4 | 0.0 | 257.4 | 257.4 | 98.9 | 38 | 158.5 | 5.221 | | | | |
| ASM002659 | Coastal area | | 15.70 | 3453780 | 3453780 | 109.5 | 30994.8 | 0.0 | 30994.8 | 30994.8 | 899.9 | 3 | 30094.9 | 8.714 | | | | |
| ASM002657 | Coastal area | | 2.60 | 571340 | 571340 | 18.1 | 5302.2 | 0.0 | 5302.2 | 5302.2 | 230.8 | 4 | 5071.4 | 8.876 | | | | |
| ASM001522 | Uthammarsån | 17:5 | 0.57 | 125620 | 125620 | 4.0 | 1180.0 | 0.0 | 1180.0 | 1180.0 | 0.0 | 0 | 1180.0 | 9.394 | | | | |
| ASM001523 | Uthammarsån | 17:6 | 0.96 | 210760 | 210760 | 6.7 | 2267.3 | 0.0 | 2267.3 | 2267.3 | 0.0 | 0 | 2267.3 | 10.758 | | | | |
| ASM001521 | Uthammarsån | 17:4 | 0.20 | 44880 | 44880 | 1.4 | 534.5 | 0.0 | 534.5 | 534.5 | 0.0 | 0 | 534.5 | 11.910 | | | | |
| ASM001520 | Uthammarsån | 17:3 | 0.08 | 17820 | 17820 | 0.6 | 239.0 | 0.0 | 239.0 | 239.0 | 0.0 | 0 | 239.0 | 13.410 | | | | |
| ASM002494B | Uthammarsån | 17:1 | 2.91 | 640860 | 1039940 | 33.0 | 6071.4 | 0.0 | 6071.4 | 10292.2 | 0.0 | 0 | 10292.2 | 9.897 | PSM002076 | 0.033 | 11.101 | 11 |
| ASM001533 | Uthammarsån | 17:2 | 0.51 | 112640 | 112640 | 3.6 | 1338.0 | 0.0 | 1338.0 | 1338.0 | 0.0 | 0 | 1338.0 | 11.878 | | | | |
| ASM002494A | Uthammarsån | 17:1 | 1.78 | 391820 | 1544400 | 49.0 | 4966.0 | 0.0 | 4966.0 | 16596.1 | 28.8 | 0 | 16567.3 | 10.727 | | | | |
| ASM001528 | Släthultebäcken | 18:5 | 0.32 | 70400 | 70400 | 2.2 | 605.3 | 0.0 | 605.3 | 605.3 | 0.0 | 0 | 605.3 | 8.598 | | | | |
| ASM002477 | Släthultebäcken | 18:4 | 0.66 | 144980 | 215380 | 6.8 | 1143.3 | 0.0 | 1143.3 | 1748.6 | 415.4 | 24 | 1333.2 | 6.190 | | | | |
| ASM001531 | Släthultebäcken | 18:8 | 0.30 | 66440 | 66440 | 2.1 | 592.9 | 0.0 | 592.9 | 592.9 | 0.0 | 0 | 592.9 | 8.924 | | | | |
| ASM001532 | Släthultebäcken | 18:9 | 0.11 | 24420 | 24420 | 0.8 | 358.7 | 0.0 | 358.7 | 358.7 | 0.0 | 0 | 358.7 | 14.690 | | | | |
| ASM002455 | Släthultebäcken | 18:7 | 0.76 | 167420 | 258280 | 8.2 | 1912.7 | 0.0 | 1912.7 | 2864.4 | 0.0 | 0 | 2864.4 | 11.090 | | | | |
| ASM002475 | Släthultebäcken | 18:6 | 1.06 | 232100 | 490380 | 15.5 | 1819.2 | 0.0 | 1819.2 | 4683.6 | 0.0 | 0 | 4683.6 | 9.551 | | | | |
| ASM001526 | Släthultebäcken | 18:3 | 0.40 | 88220 | 88220 | 2.8 | 712.1 | 0.0 | 712.1 | 712.1 | 17.2 | 2 | 694.9 | 7.877 | | | | |
| ASM002481C | Släthultebäcken | 18:1 | 2.44 | 537020 | 1027400 | 32.6 | 4895.8 | 0.0 | 4895.8 | 9579.4 | 0.0 | 0 | 9579.4 | 9.324 | PSM002070 | | | |
| ASM002481B | Släthultebäcken | 18:1 | 2.13 | 469260 | 1800260 | 57.1 | 4695.2 | 0.0 | 4695.2 | 16302.7 | 217.5 | 1 | 16085.2 | 8.935 | PSM002075 | | | |
| ASM001525 | Släthultebäcken | 18:2 | 0.77 | 169620 | 169620 | 5.4 | 2023.3 | 0.0 | 2023.3 | 2023.3 | 0.0 | 0 | 2023.3 | 11.929 | | | | |
| ASM002481A | Släthultebäcken | 18:1 | 0.00 | 220 | 1970100 | 62.5 | 3.1 | 0.0 | 3.1 | 18111.7 | 0.0 | 0 | 18111.7 | 9.193 | | | | |
| ASM001444 | Sörämagasinet | 11:1 | 0.52 | 115060 | 115060 | 3.6 | 828.8 | 0.0 | 828.8 | 828.8 | 578.8 | 70 | 250.0 | 2.172 | | | | |
| ASM002466 | Stekflagebäcken | 22:1 | 0.36 | 78980 | 78980 | 2.5 | 589.1 | 0.0 | 589.1 | 589.1 | 280.3 | 48 | 308.9 | 3.911 | | | | |
| ASM002653 | Coastal area | | 0.76 | 166980 | 166980 | 5.3 | 1477.2 | 0.0 | 1477.2 | 1477.2 | 215.0 | 15 | 1262.2 | 7.559 | | | | |
| ASM002470 | Skölkebäcken | 26:1 | 0.17 | 36300 | 36300 | 1.2 | 335.4 | 0.0 | 335.4 | 335.4 | 0.0 | 0 | 335.4 | 9.239 | | | | |
| ASM002469 | Gloebäcken | 25:1 | 0.13 | 28820 | 28820 | 0.9 | 266.3 | 0.0 | 266.3 | 266.3 | 0.0 | 0 | 266.3 | 9.240 | | | | |
| ASM002468 | Lindströmmebäcken | 24:1 | 0.19 | 42240 | 42240 | 1.3 | 440.9 | 0.0 | 440.9 | 440.9 | 0.0 | 0 | 440.9 | 10.438 | | | | |
| ASM002467B | Vadvikebäcken | 23:1 | 0.30 | 65560 | 65560 | 2.1 | 519.2 | 0.0 | 519.2 | 519.2 | 0.0 | 0 | 519.2 | 7.919 | PSM107735 | 0.002 | 8.571 | 8 |
| ASM002467A | Vadvikebäcken | 23:1 | 0.01 | 1980 | 67540 | 2.1 | 17.7 | 0.0 | 17.7 | 536.8 | 0.0 | 0 | 536.8 | 7.948 | | | | |
| | **Kärrviksån** | 5:1-20 | 27.31 | 6007100 | 6007100 | 26.9 | 53030.5 | 0.0 | 53030.5 | | 1007.7 | 2 | 52022.8 | 8.660 | | | | |
| | **Laxemarån** | 10:1-32 | 40.97 | 9014280 | 9014280 | 37.5 | 81776.1 | 0.0 | 81776.1 | | 6686.1 | 8 | 75089.9 | 8.330 | | | | |
| | **All catchments** | | 129.97 | 28593620 | 28593620 | 22.3 | 261140.3 | 0.0 | 261140.3 | | 16632.5 | 6 | 244507.8 | 8.551 | | | | |

| **Strontium (Sr)** | | | | Water balance | | | Total per catchment | | | Total including contributions from upstream catchments | | | | | Calibration data | | | |
|---|---|---|---|---|---|---|---|---|---|---|---|---|---|---|---|---|---|---|
| Idcode | Name | ARO | Area | $Q_{catch}$ | $Q_{out}$ | q | Diffuse | Point | Total | Total IN | Retention | | Total OUT | Conc. | Reference | q | Conc. | Deviation |
| | | | $km^2$ | $m^3 \cdot yr^{-1}$ | $m^3 \cdot yr^{-1}$ | $L \cdot s^{-1}$ | $kg \cdot yr^{-1}$ | $kg \cdot yr^{-1}$ | $kg \cdot yr^{-1}$ | $kg \cdot yr^{-1}$ | $kg \cdot yr^{-1}$ | % | $kg \cdot yr^{-1}$ | $mg \cdot L^{-1}$ | | $L \cdot s^{-1}$ | $mg \cdot L^{-1}$ | % |
| ASM002474 | Kärrviksån | 5:20 | 0.12 | 25740 | 25740 | 0.8 | 1.1 | 0.0 | 1.1 | 1.1 | 0.0 | 0 | 1.1 | 0.043 | | | | |
| ASM002493 | Kärrviksån | 5:19 | 0.84 | 184140 | 209880 | 6.7 | 9.1 | 0.0 | 9.1 | 10.2 | 0.0 | 0 | 10.2 | 0.048 | | | | |
| ASM001483 | Kärrviksån | 5:17 | 0.15 | 33220 | 33220 | 1.1 | 2.4 | 0.0 | 2.4 | 2.4 | 0.0 | 0 | 2.4 | 0.072 | | | | |
| ASM002492 | Kärrviksån | 5:16 | 1.11 | 243980 | 277200 | 8.8 | 13.9 | 0.0 | 13.9 | 16.3 | 0.0 | 0 | 16.3 | 0.059 | | | | |
| ASM002491 | Kärrviksån | 5:15 | 1.87 | 411840 | 689040 | 21.8 | 20.0 | 0.0 | 20.0 | 36.3 | 0.0 | 0 | 36.3 | 0.053 | | | | |
| ASM001474 | Kärrviksån | 5:7 | 0.45 | 99000 | 99000 | 3.1 | 5.0 | 0.0 | 5.0 | 5.0 | 0.0 | 0 | 5.0 | 0.051 | | | | |
| ASM002487 | Kärrviksån | 5:6 | 1.20 | 264000 | 363000 | 11.5 | 15.2 | 0.0 | 15.2 | 20.3 | 0.0 | 0 | 20.3 | 0.056 | | | | |
| ASM001472 | Kärrviksån | 5:4 | 1.10 | 242880 | 242880 | 7.7 | 10.0 | 0.0 | 10.0 | 10.0 | 0.0 | 0 | 10.0 | 0.041 | | | | |
| ASM001470 | Kärrviksån | 5:3 | 0.40 | 87560 | 87560 | 2.8 | 4.1 | 0.0 | 4.1 | 4.1 | 0.0 | 0 | 4.1 | 0.047 | | | | |
| ASM001469 | Kärrviksån | 5:2 | 0.97 | 212960 | 212960 | 6.8 | 10.2 | 0.0 | 10.2 | 10.2 | 0.0 | 0 | 10.2 | 0.048 | | | | |
| ASM001471 | Kärrviksån | 5:5 | 2.79 | 614680 | 614680 | 19.5 | 29.2 | 0.0 | 29.2 | 29.2 | 0.0 | 0 | 29.2 | 0.047 | | | | |
| ASM001479 | Kärrviksån | 5:13 | 0.65 | 142340 | 142340 | 4.5 | 6.1 | 0.0 | 6.1 | 6.1 | 0.0 | 0 | 6.1 | 0.043 | | | | |
| ASM001480 | Kärrviksån | 5:14 | 0.10 | 22660 | 22660 | 0.7 | 1.1 | 0.0 | 1.1 | 1.1 | 0.0 | 0 | 1.1 | 0.049 | | | | |
| ASM002490 | Kärrviksån | 5:12 | 0.84 | 183920 | 348920 | 11.1 | 8.7 | 0.0 | 8.7 | 15.9 | 0.0 | 0 | 15.9 | 0.046 | | | | |
| ASM001478 | Kärrviksån | 5:11 | 0.49 | 108460 | 108460 | 3.4 | 4.7 | 0.0 | 4.7 | 4.7 | 0.0 | 0 | 4.7 | 0.043 | | | | |
| ASM002489 | Kärrviksån | 5:10 | 1.20 | 263560 | 372020 | 11.8 | 11.7 | 0.0 | 11.7 | 16.4 | 0.0 | 0 | 16.4 | 0.044 | | | | |
| ASM001476 | Kärrviksån | 5:9 | 3.62 | 796180 | 796180 | 25.2 | 45.8 | 0.0 | 45.8 | 45.8 | 0.0 | 0 | 45.8 | 0.057 | | | | |
| ASM001475B | Kärrviksån | 5:8 | 1.38 | 302940 | 1820060 | 57.7 | 13.6 | 0.0 | 13.6 | 91.6 | 0.0 | 0 | 91.6 | 0.050 | PSM002081 | 0.058 | 0.037 | 36 |
| ASM001475A | Kärrviksån | 5:8 | 0.04 | 9680 | 1829740 | 58.0 | 0.4 | 0.0 | 0.4 | 92.1 | 0.0 | 0 | 92.1 | 0.050 | | | | |
| ASM002479 | Kärrviksån | 5:18 | 1.18 | 259600 | 259600 | 8.2 | 11.8 | 0.0 | 11.8 | 11.8 | 0.0 | 0 | 11.8 | 0.046 | | | | |
| ASM002486C | Kärrviksån | 5:1 | 2.75 | 604560 | 1074040 | 34.1 | 27.3 | 0.0 | 27.3 | 49.3 | 0.0 | 0 | 49.3 | 0.046 | PSM002080 | | | |
| ASM002486B | Kärrviksån | 5:1 | 1.13 | 247940 | 3840760 | 121.8 | 11.8 | 0.0 | 11.8 | 189.5 | 0.0 | 0 | 189.5 | 0.049 | PSM002082 | 0.121 | 0.042 | 19 |
| ASM002486A | Kärrviksån | 5:1 | 2.93 | 645260 | 6007100 | 190.5 | 31.3 | 0.0 | 31.3 | 294.5 | 0.0 | 0 | 294.5 | 0.049 | PSM002083 | 0.190 | 0.044 | 11 |
| ASM002449 | Bjurhidebäcken | 4:1 | 0.63 | 139040 | 139040 | 4.4 | 6.0 | 0.0 | 6.0 | 6.0 | 0.0 | 0 | 6.0 | 0.043 | | | | |
| ASM002472 | Sörviksån | 3:2 | 0.47 | 103400 | 103400 | 3.3 | 4.5 | 0.0 | 4.5 | 4.5 | 0.0 | 0 | 4.5 | 0.043 | | | | |
| ASM002473 | Sörviksån | 3:1 | 0.53 | 116600 | 220000 | 7.0 | 5.0 | 0.0 | 5.0 | 9.5 | 0.0 | 0 | 9.5 | 0.043 | | | | |
| ASM002651 | Coastal area | | 1.67 | 368280 | 368280 | 11.7 | 15.6 | 0.0 | 15.6 | 15.6 | 0.0 | 0 | 15.6 | 0.042 | | | | |
| ASM002447 | Bodvikebäcken | 2:1 | 0.38 | 83600 | 83600 | 2.7 | 2.9 | 0.0 | 2.9 | 2.9 | 0.0 | 0 | 2.9 | 0.034 | | | | |
| ASM002446 | Långbonäsbäcken | 1:1 | 0.07 | 15400 | 15400 | 0.5 | 0.7 | 0.0 | 0.7 | 0.7 | 0.0 | 0 | 0.7 | 0.043 | | | | |
| ASM002464 | Flakvarpebäcken | 19:1 | 0.18 | 40480 | 40480 | 1.3 | 1.6 | 0.0 | 1.6 | 1.6 | 0.0 | 0 | 1.6 | 0.039 | | | | |
| ASM002465 | Jössesbäcken | 20:1 | 0.11 | 24420 | 24420 | 0.8 | 1.6 | 0.0 | 1.6 | 1.6 | 0.0 | 0 | 1.6 | 0.068 | | | | |
| ASM002471 | Åspöbäcken | 21:1 | 0.06 | 13860 | 13860 | 0.4 | 0.6 | 0.0 | 0.6 | 0.6 | 0.0 | 0 | 0.6 | 0.043 | | | | |
| ASM002652 | Coastal area | | 1.39 | 305140 | 305140 | 9.7 | 13.8 | 0.0 | 13.8 | 13.8 | 0.0 | 0 | 13.8 | 0.045 | | | | |
| ASM001445 | Frisksjön | 7:2 | 1.85 | 406560 | 406560 | 12.9 | 19.1 | 0.0 | 19.1 | 19.1 | 0.0 | 0 | 19.1 | 0.047 | | | | |
| ASM001484 | Kåreviksån | 7:1 | 0.21 | 46860 | 453420 | 14.4 | 2.0 | 0.0 | 2.0 | 21.1 | 0.0 | 0 | 21.1 | 0.046 | | | | |
| ASM001486B | Mederhultsån | 6:1 | 1.92 | 422620 | 422620 | 13.4 | 22.1 | 0.0 | 22.1 | 22.1 | 0.0 | 0 | 22.1 | 0.052 | PSM002084 | 0.013 | 0.062 | 16 |
| ASM001486A | Mederhultsån | 6:1 | 0.08 | 18040 | 440660 | 14.0 | 0.8 | 0.0 | 0.8 | 22.9 | 0.0 | 0 | 22.9 | 0.052 | | | | |
| ASM002654 | Coastal area | | 1.86 | 409420 | 409420 | 13.0 | 18.1 | 0.0 | 18.1 | 18.1 | 0.0 | 0 | 18.1 | 0.044 | | | | |
| ASM002460 | Pistlanbäcken | 8:1 | 0.50 | 109780 | 109780 | 3.5 | 5.0 | 0.0 | 5.0 | 5.0 | 0.0 | 0 | 5.0 | 0.046 | | | | |
| ASM001490 | Ekerumsån | 9:3 | 0.22 | 48840 | 48840 | 1.5 | 3.5 | 0.0 | 3.5 | 3.5 | 0.0 | 0 | 3.5 | 0.072 | | | | |
| ASM001489 | Ekerumsån | 9:2 | 0.77 | 168740 | 168740 | 5.4 | 13.4 | 0.0 | 13.4 | 13.4 | 0.0 | 0 | 13.4 | 0.079 | | | | |
| ASM002483B | Ekerumsån | 9:1 | 1.50 | 330880 | 548460 | 17.4 | 17.2 | 0.0 | 17.2 | 34.0 | 0.0 | 0 | 34.0 | 0.062 | PSM002085 | 0.017 | 0.074 | 16 |
| ASM002483A | Ekerumsån | 9:1 | 0.34 | 75020 | 623480 | 19.8 | 4.0 | 0.0 | 4.0 | 38.0 | 0.0 | 0 | 38.0 | 0.061 | | | | |
| ASM002478 | Laxemarån | 10:32 | 0.02 | 5060 | 5060 | 0.2 | 0.2 | 0.0 | 0.2 | 0.2 | 0.0 | 0 | 0.2 | 0.043 | | | | |
| ASM002482 | Laxemarån | 10:31 | 0.87 | 190740 | 195800 | 6.2 | 8.2 | 0.0 | 8.2 | 8.4 | 0.0 | 0 | 8.4 | 0.043 | | | | |
| ASM002480B | Laxemarån | 10:30 | 4.23 | 931480 | 1127280 | 35.7 | 38.8 | 0.0 | 38.8 | 47.2 | 0.0 | 0 | 47.2 | 0.042 | PSM002068 | 0.036 | 0.042 | 0 |
| ASM002480A | Jämsen | 10:30 | 1.83 | 403480 | 1530760 | 48.5 | 16.1 | 0.0 | 16.1 | 63.3 | 0.0 | 0 | 63.3 | 0.041 | PSM002069 | 0.049 | 0.044 | 5 |
| ASM001516 | Laxemarån | 10:29 | 0.53 | 117260 | 117260 | 3.7 | 6.2 | 0.0 | 6.2 | 6.2 | 0.0 | 0 | 6.2 | 0.053 | | | | |
| ASM001515 | Laxemarån | 10:28 | 0.34 | 74140 | 74140 | 2.4 | 4.5 | 0.0 | 4.5 | 4.5 | 0.0 | 0 | 4.5 | 0.060 | | | | |
| ASM001514 | Laxemarån | 10:27 | 0.49 | 107140 | 107140 | 3.4 | 7.5 | 0.0 | 7.5 | 7.5 | 0.0 | 0 | 7.5 | 0.070 | | | | |
| ASM001446 | Plittorpsgöl | 10:26 | 0.68 | 149160 | 149160 | 4.7 | 6.4 | 0.0 | 6.4 | 6.4 | 0.0 | 0 | 6.4 | 0.043 | | | | |
| ASM002459 | Laxemarån | 10:25 | 0.10 | 21780 | 170940 | 5.4 | 0.9 | 0.0 | 0.9 | 7.3 | 0.0 | 0 | 7.3 | 0.043 | | | | |
| ASM001512 | Laxemarån | 10:24 | 0.49 | 108680 | 108680 | 3.4 | 4.9 | 0.0 | 4.9 | 4.9 | 0.0 | 0 | 4.9 | 0.046 | | | | |
| ASM002476E | Laxemarån | 10:1 | 3.95 | 868780 | 2977700 | 94.4 | 42.5 | 0.0 | 42.5 | 136.2 | 0.0 | 0 | 136.2 | 0.046 | PSM002071 | 0.094 | 0.050 | 9 |
| ASM001510 | Laxemarån | 10:22 | 0.56 | 123640 | 123640 | 3.9 | 5.4 | 0.0 | 5.4 | 5.4 | 0.0 | 0 | 5.4 | 0.044 | | | | |
| ASM002453 | Laxemarån | 10:21 | 0.45 | 97900 | 221540 | 7.0 | 4.3 | 0.0 | 4.3 | 9.7 | 0.0 | 0 | 9.7 | 0.044 | | | | |
| ASM002450B | Laxemarån | 10:20 | 2.39 | 526240 | 747780 | 23.7 | 24.3 | 0.0 | 24.3 | 34.0 | 0.0 | 0 | 34.0 | 0.045 | PSM002072 | | | |
| ASM002450A | Laxemarån | 10:20 | 0.19 | 41140 | 788920 | 25.0 | 1.9 | 0.0 | 1.9 | 35.9 | 0.0 | 0 | 35.9 | 0.045 | | | | |
| ASM001511 | Laxemarån | 10:23 | 0.74 | 162800 | 162800 | 5.2 | 7.2 | 0.0 | 7.2 | 7.2 | 0.0 | 0 | 7.2 | 0.044 | | | | |
| ASM001448 | Grangöl | 10:19 | 0.50 | 108900 | 108900 | 3.5 | 4.9 | 0.0 | 4.9 | 4.9 | 0.0 | 0 | 4.9 | 0.045 | | | | |
| ASM002499 | Laxemarån | 10:18 | 0.06 | 12760 | 121660 | 3.9 | 1.0 | 0.0 | 1.0 | 5.9 | 0.0 | 0 | 5.9 | 0.048 | | | | |
| ASM001506 | Laxemarån | 10:17 | 0.40 | 87560 | 87560 | 2.8 | 5.2 | 0.0 | 5.2 | 5.2 | 0.0 | 0 | 5.2 | 0.060 | | | | |
| ASM001447 | Fjällgöl | 10:16 | 0.30 | 64900 | 64900 | 2.1 | 2.6 | 0.0 | 2.6 | 2.6 | 0.0 | 0 | 2.6 | 0.040 | | | | |
| ASM002451 | Laxemarån | 10:15 | 0.33 | 71500 | 136400 | 4.3 | 4.5 | 0.0 | 4.5 | 7.1 | 0.0 | 0 | 7.1 | 0.052 | | | | |
| ASM002452 | Laxemarån | 10:14 | 2.38 | 522500 | 868120 | 27.5 | 29.6 | 0.0 | 29.6 | 47.8 | 0.0 | 0 | 47.8 | 0.055 | | | | |
| ASM001503 | Laxemarån | 10:13 | 0.42 | 91520 | 91520 | 2.9 | 6.2 | 0.0 | 6.2 | 6.2 | 0.0 | 0 | 6.2 | 0.067 | | | | |
| ASM002454 | Laxemarån | 10:12 | 0.81 | 177760 | 269280 | 8.5 | 11.9 | 0.0 | 11.9 | 18.1 | 0.0 | 0 | 18.1 | 0.067 | | | | |
| ASM001501 | Laxemarån | 10:11 | 0.81 | 177320 | 177320 | 5.6 | 10.9 | 0.0 | 10.9 | 10.9 | 0.0 | 0 | 10.9 | 0.062 | | | | |
| ASM002457 | Laxemarån | 10:10 | 1.39 | 305580 | 482900 | 15.3 | 23.6 | 0.0 | 23.6 | 34.5 | 0.0 | 0 | 34.5 | 0.071 | | | | |
| ASM002476D | Laxemarån | 10:1 | 4.96 | 1091860 | 6641580 | 210.6 | 54.1 | 0.0 | 54.1 | 333.8 | 0.0 | 0 | 333.8 | 0.050 | PSM002077 | | | |
| ASM001499 | Laxemarån | 10:9 | 0.71 | 156420 | 156420 | 5.0 | 7.6 | 0.0 | 7.6 | 7.6 | 0.0 | 0 | 7.6 | 0.049 | | | | |
| ASM001498 | Laxemarån | 10:8 | 2.77 | 609620 | 766040 | 24.3 | 29.0 | 0.0 | 29.0 | 36.6 | 0.0 | 0 | 36.6 | 0.048 | PSM002078 | 0.024 | 0.036 | 31 |
| ASM001497 | Laxemarån | 10:7 | 0.61 | 133980 | 133980 | 4.2 | 7.5 | 0.0 | 7.5 | 7.5 | 0.0 | 0 | 7.5 | 0.056 | | | | |
| ASM002476C | Laxemarån | 10:1 | 0.32 | 69300 | 7610900 | 241.3 | 3.5 | 0.0 | 3.5 | 381.5 | 0.0 | 0 | 381.5 | 0.050 | PSM002079 | 0.242 | 0.048 | 4 |
| ASM001494 | Laxemarån | 10:4 | 1.00 | 220220 | 220220 | 7.0 | 15.5 | 0.0 | 15.5 | 15.5 | 0.0 | 0 | 15.5 | 0.071 | | | | |
| ASM001493 | Laxemarån | 10:3 | 0.32 | 70180 | 70180 | 2.2 | 4.1 | 0.0 | 4.1 | 4.1 | 0.0 | 0 | 4.1 | 0.058 | | | | |
| ASM001492 | Laxemarån | 10:2 | 0.46 | 101200 | 101200 | 3.2 | 6.5 | 0.0 | 6.5 | 6.5 | 0.0 | 0 | 6.5 | 0.064 | | | | |
| ASM001496 | Laxemarån | 10:6 | 0.89 | 195800 | 195800 | 6.2 | 11.1 | 0.0 | 11.1 | 11.1 | 0.0 | 0 | 11.1 | 0.057 | | | | |
| ASM001495 | Laxemarån | 10:5 | 0.29 | 63800 | 63800 | 2.0 | 3.0 | 0.0 | 3.0 | 3.0 | 0.0 | 0 | 3.0 | 0.046 | | | | |
| ASM002476B | Laxemarån | 10:1 | 3.23 | 710820 | 8972920 | 284.5 | 40.0 | 0.0 | 40.0 | 461.7 | 0.0 | 0 | 461.7 | 0.051 | PSM002087 | 0.285 | 0.051 | 0 |
| ASM002476A | Laxemarån | 10:1 | 0.19 | 41360 | 9014280 | 285.8 | 2.0 | 0.0 | 2.0 | 463.7 | 0.0 | 0 | 463.7 | 0.051 | | | | |
| ASM002495 | Glostadsbäcken | 12:3 | 0.13 | 27720 | 27720 | 0.9 | 1.2 | 0.0 | 1.2 | 1.2 | 0.0 | 0 | 1.2 | 0.044 | | | | |
| ASM002485 | Glostadsbäcken | 12:2 | 0.33 | 72820 | 72820 | 2.3 | 4.4 | 0.0 | 4.4 | 4.4 | 0.0 | 0 | 4.4 | 0.060 | | | | |
| ASM002498 | Glostadsbäcken | 12:1 | 1.60 | 351340 | 451880 | 14.3 | 21.8 | 0.0 | 21.8 | 27.5 | 0.0 | 0 | 27.5 | 0.061 | | | | |
| ASM001518B | Stålglobäcken | 13:1 | 0.68 | 149380 | 149380 | 4.7 | 9.8 | 0.0 | 9.8 | 9.8 | 0.0 | 0 | 9.8 | 0.066 | PSM002086 | 0.005 | 0.066 | 0 |
| ASM001518A | Stålglobäcken | 13:1 | 0.35 | 77880 | 227260 | 7.2 | 4.7 | 0.0 | 4.7 | 14.5 | 0.0 | 0 | 14.5 | 0.064 | | | | |
| ASM002462 | Uvöbäcken | 15:1 | 0.97 | 212740 | 212740 | 6.7 | 10.5 | 0.0 | 10.5 | 10.5 | 0.0 | 0 | 10.5 | 0.050 | | | | |
| ASM002497 | Stekebäcken | 14:2 | 0.44 | 95700 | 95700 | 3.0 | 5.7 | 0.0 | 5.7 | 5.7 | 0.0 | 0 | 5.7 | 0.060 | | | | |
| ASM001517 | Stekebäcken | 14:1 | 0.90 | 198660 | 294360 | 9.3 | 9.6 | 0.0 | 9.6 | 15.3 | 0.0 | 0 | 15.3 | 0.052 | | | | |
| ASM002463 | Svartebäck | 16:1 | 0.50 | 110880 | 110880 | 3.5 | 4.8 | 0.0 | 4.8 | 4.8 | 0.0 | 0 | 4.8 | 0.043 | | | | |
| ASM002655 | Coastal area | | 2.71 | 596420 | 596420 | 18.9 | 27.1 | 0.0 | 27.1 | 27.1 | 0.0 | 0 | 27.1 | 0.045 | | | | |
| ASM002658 | Coastal area | | 1.26 | 277420 | 277420 | 8.8 | 12.4 | 0.0 | 12.4 | 12.4 | 0.0 | 0 | 12.4 | 0.045 | | | | |
| ASM002656 | Coastal area | | 0.22 | 48400 | 48400 | 1.5 | 2.0 | 0.0 | 2.0 | 2.0 | 0.0 | 0 | 2.0 | 0.041 | | | | |
| ASM002660 | Coastal area | | 0.14 | 30360 | 30360 | 1.0 | 1.2 | 0.0 | 1.2 | 1.2 | 0.0 | 0 | 1.2 | 0.041 | | | | |
| ASM002659 | Coastal area | | 15.70 | 3453780 | 3453780 | 109.5 | 165.6 | 0.0 | 165.6 | 165.6 | 0.0 | 0 | 165.6 | 0.048 | | | | |
| ASM002657 | Coastal area | | 2.60 | 571340 | 571340 | 18.1 | 27.1 | 0.0 | 27.1 | 27.1 | 0.0 | 0 | 27.1 | 0.047 | | | | |
| ASM001522 | Uthammarsån | 17:5 | 0.57 | 125620 | 125620 | 4.0 | 6.7 | 0.0 | 6.7 | 6.7 | 0.0 | 0 | 6.7 | 0.053 | | | | |
| ASM001523 | Uthammarsån | 17:6 | 0.96 | 210760 | 210760 | 6.7 | 12.7 | 0.0 | 12.7 | 12.7 | 0.0 | 0 | 12.7 | 0.060 | | | | |
| ASM001521 | Uthammarsån | 17:4 | 0.20 | 44880 | 44880 | 1.4 | 3.2 | 0.0 | 3.2 | 3.2 | 0.0 | 0 | 3.2 | 0.071 | | | | |
| ASM001520 | Uthammarsån | 17:3 | 0.08 | 17820 | 17820 | 0.6 | 1.4 | 0.0 | 1.4 | 1.4 | 0.0 | 0 | 1.4 | 0.080 | | | | |
| ASM002494B | Uthammarsån | 17:1 | 2.91 | 640860 | 1039940 | 33.0 | 34.6 | 0.0 | 34.6 | 58.6 | 0.0 | 0 | 58.6 | 0.056 | PSM002076 | 0.033 | 0.060 | 7 |
| ASM001533 | Uthammarsån | 17:2 | 0.51 | 112640 | 112640 | 3.6 | 7.9 | 0.0 | 7.9 | 7.9 | 0.0 | 0 | 7.9 | 0.071 | | | | |
| ASM002494A | Uthammarsån | 17:1 | 1.78 | 391820 | 1544400 | 49.0 | 29.0 | 0.0 | 29.0 | 95.6 | 0.0 | 0 | 95.6 | 0.062 | | | | |
| ASM001528 | Släthultebäcken | 18:5 | 0.32 | 70400 | 70400 | 2.2 | 3.0 | 0.0 | 3.0 | 3.0 | 0.0 | 0 | 3.0 | 0.043 | | | | |
| ASM002477 | Släthultebäcken | 18:4 | 0.66 | 144980 | 215380 | 6.8 | 6.0 | 0.0 | 6.0 | 9.1 | 0.0 | 0 | 9.1 | 0.042 | | | | |
| ASM001531 | Släthultebäcken | 18:8 | 0.30 | 66440 | 66440 | 2.1 | 2.9 | 0.0 | 2.9 | 2.9 | 0.0 | 0 | 2.9 | 0.043 | | | | |
| ASM001532 | Släthultebäcken | 18:9 | 0.11 | 24420 | 24420 | 0.8 | 2.2 | 0.0 | 2.2 | 2.2 | 0.0 | 0 | 2.2 | 0.091 | | | | |
| ASM002455 | Släthultebäcken | 18:7 | 0.76 | 167420 | 258280 | 8.2 | 11.2 | 0.0 | 11.2 | 16.3 | 0.0 | 0 | 16.3 | 0.063 | | | | |
| ASM002475 | Släthultebäcken | 18:6 | 1.06 | 232100 | 490380 | 15.5 | 10.0 | 0.0 | 10.0 | 26.2 | 0.0 | 0 | 26.2 | 0.054 | | | | |
| ASM001526 | Släthultebäcken | 18:3 | 0.40 | 88220 | 88220 | 2.8 | 3.8 | 0.0 | 3.8 | 3.8 | 0.0 | 0 | 3.8 | 0.043 | | | | |
| ASM002481C | Släthultebäcken | 18:1 | 2.44 | 537020 | 1027400 | 32.6 | 27.8 | 0.0 | 27.8 | 54.1 | 0.0 | 0 | 54.1 | 0.053 | PSM002070 | | | |
| ASM002481B | Släthultebäcken | 18:1 | 2.13 | 469260 | 1800260 | 57.1 | 26.0 | 0.0 | 26.0 | 92.9 | 0.0 | 0 | 92.9 | 0.052 | PSM002075 | | | |
| ASM001525 | Släthultebäcken | 18:2 | 0.77 | 169620 | 169620 | 5.4 | 11.5 | 0.0 | 11.5 | 11.5 | 0.0 | 0 | 11.5 | 0.068 | | | | |
| ASM002481A | Släthultebäcken | 18:1 | 0.00 | 220 | 1970100 | 62.5 | 0.0 | 0.0 | 0.0 | 104.4 | 0.0 | 0 | 104.4 | 0.053 | | | | |
| ASM001444 | Sörämagasinet | 11:1 | 0.52 | 115060 | 115060 | 3.6 | 4.1 | 0.0 | 4.1 | 4.1 | 0.0 | 0 | 4.1 | 0.035 | | | | |
| ASM002466 | Stekflagebäcken | 22:1 | 0.36 | 78980 | 78980 | 2.5 | 3.2 | 0.0 | 3.2 | 3.2 | 0.0 | 0 | 3.2 | 0.040 | | | | |
| ASM002653 | Coastal area | | 0.76 | 166980 | 166980 | 5.3 | 7.3 | 0.0 | 7.3 | 7.3 | 0.0 | 0 | 7.3 | 0.044 | | | | |
| ASM002470 | Skölkebäcken | 26:1 | 0.17 | 36300 | 36300 | 1.2 | 1.7 | 0.0 | 1.7 | 1.7 | 0.0 | 0 | 1.7 | 0.047 | | | | |
| ASM002469 | Gloebäcken | 25:1 | 0.13 | 28820 | 28820 | 0.9 | 1.3 | 0.0 | 1.3 | 1.3 | 0.0 | 0 | 1.3 | 0.046 | | | | |
| ASM002468 | Lindströmmebäcken | 24:1 | 0.19 | 42240 | 42240 | 1.3 | 2.4 | 0.0 | 2.4 | 2.4 | 0.0 | 0 | 2.4 | 0.056 | | | | |
| ASM002467B | Vadvikebäcken | 23:1 | 0.30 | 65560 | 65560 | 2.1 | 2.8 | 0.0 | 2.8 | 2.8 | 0.0 | 0 | 2.8 | 0.043 | PSM107735 | 0.002 | 0.060 | 28 |
| ASM002467A | Vadvikebäcken | 23:1 | 0.01 | 1980 | 67540 | 2.1 | 0.1 | 0.0 | 0.1 | 2.9 | 0.0 | 0 | 2.9 | 0.043 | | | | |
| | **Kärrviksån** | 5:1-20 | 27.31 | 6007100 | 6007100 | 26.9 | 294.5 | 0.0 | 294.5 | | 0.0 | 0 | 294.5 | 0.049 | | | | |
| | **Laxemarån** | 10:1-32 | 40.97 | 9014280 | 9014280 | 37.5 | 463.7 | 0.0 | 463.7 | | 0.0 | 0 | 463.7 | 0.051 | | | | |
| | **All catchments** | | 129.97 | 28593620 | 28593620 | 22.3 | 1446.4 | 0.0 | 1446.4 | | 0.0 | 0 | 1446.4 | 0.051 | | | | |

| Calcium (Ca) | | | | Water balance | | | Total per catchment | | | Total including contributions from upstream catchments | | | | | Calibration data | | | |
|---|---|---|---|---|---|---|---|---|---|---|---|---|---|---|---|---|---|---|
| Idcode | Name | ARO | Area | $Q_{catch}$ | $Q_{out}$ | q | Diffuse | Point | Total | Total IN | Retention | | Total OUT | Conc. | Reference | q | Conc. | Deviation |
| | | | $km^2$ | $m^3 \cdot yr^{-1}$ | $m^3 \cdot yr^{-1}$ | $L \cdot s^{-1}$ | $kg \cdot yr^{-1}$ | $kg \cdot yr^{-1}$ | $kg \cdot yr^{-1}$ | $kg \cdot yr^{-1}$ | $kg \cdot yr^{-1}$ | % | $kg \cdot yr^{-1}$ | $mg \cdot L^{-1}$ | | $L \cdot s^{-1}$ | $mg \cdot L^{-1}$ | % |
| ASM002474 | Kärrviksån | 5:20 | 0.12 | 25740 | 25740 | 0.8 | 195.8 | 66.9 | 262.8 | 262.8 | 0.0 | 0 | 262.8 | 10.208 | | | | |
| ASM002493 | Kärrviksån | 5:19 | 0.84 | 184140 | 209880 | 6.7 | 1842.2 | 0.0 | 1842.2 | 2105.0 | 0.0 | 0 | 2105.0 | 10.030 | | | | |
| ASM001483 | Kärrviksån | 5:17 | 0.15 | 33220 | 33220 | 1.1 | 634.0 | 0.0 | 634.0 | 634.0 | 0.0 | 0 | 634.0 | 19.086 | | | | |
| ASM002492 | Kärrviksån | 5:16 | 1.11 | 243980 | 277200 | 8.8 | 3169.1 | 0.0 | 3169.1 | 3803.2 | 0.0 | 0 | 3803.2 | 13.720 | | | | |
| ASM002491 | Kärrviksån | 5:15 | 1.87 | 411840 | 689040 | 21.8 | 4022.4 | 0.0 | 4022.4 | 7825.6 | 0.0 | 0 | 7825.6 | 11.357 | | | | |
| ASM001474 | Kärrviksån | 5:7 | 0.45 | 99000 | 99000 | 3.1 | 1057.2 | 0.0 | 1057.2 | 1057.2 | 0.0 | 0 | 1057.2 | 10.679 | | | | |
| ASM002487 | Kärrviksån | 5:6 | 1.20 | 264000 | 363000 | 11.5 | 3524.6 | 0.0 | 3524.6 | 4581.9 | 0.0 | 0 | 4581.9 | 12.622 | | | | |
| ASM001472 | Kärrviksån | 5:4 | 1.10 | 242880 | 242880 | 7.7 | 1761.2 | 0.0 | 1761.2 | 1761.2 | 0.0 | 0 | 1761.2 | 7.251 | | | | |
| ASM001470 | Kärrviksån | 5:3 | 0.40 | 87560 | 87560 | 2.8 | 785.3 | 0.0 | 785.3 | 785.3 | 0.0 | 0 | 785.3 | 8.969 | | | | |
| ASM001469 | Kärrviksån | 5:2 | 0.97 | 212960 | 212960 | 6.8 | 2041.7 | 0.0 | 2041.7 | 2041.7 | 0.0 | 0 | 2041.7 | 9.587 | | | | |
| ASM001471 | Kärrviksån | 5:5 | 2.79 | 614680 | 614680 | 19.5 | 5744.4 | 0.0 | 5744.4 | 5744.4 | 0.0 | 0 | 5744.4 | 9.345 | | | | |
| ASM001479 | Kärrviksån | 5:13 | 0.65 | 142340 | 142340 | 4.5 | 1083.0 | 0.0 | 1083.0 | 1083.0 | 0.0 | 0 | 1083.0 | 7.608 | | | | |
| ASM001480 | Kärrviksån | 5:14 | 0.10 | 22660 | 22660 | 0.7 | 222.8 | 0.0 | 222.8 | 222.8 | 0.0 | 0 | 222.8 | 9.834 | | | | |
| ASM002490 | Kärrviksån | 5:12 | 0.84 | 183920 | 348920 | 11.1 | 1712.0 | 160.8 | 1872.8 | 3178.6 | 0.0 | 0 | 3178.6 | 9.110 | | | | |
| ASM001478 | Kärrviksån | 5:11 | 0.49 | 108460 | 108460 | 3.4 | 825.2 | 0.0 | 825.2 | 825.2 | 0.0 | 0 | 825.2 | 7.608 | | | | |
| ASM002489 | Kärrviksån | 5:10 | 1.20 | 263560 | 372020 | 11.8 | 2137.9 | 0.0 | 2137.9 | 2963.1 | 0.0 | 0 | 2963.1 | 7.965 | | | | |
| ASM001476 | Kärrviksån | 5:9 | 3.62 | 796180 | 796180 | 25.2 | 10550.7 | 0.0 | 10550.7 | 10550.7 | 0.0 | 0 | 10550.7 | 13.252 | | | | |
| ASM001475B | Kärrviksån | 5:8 | 1.38 | 302940 | 1820060 | 57.7 | 2519.4 | 0.0 | 2519.4 | 19211.8 | 0.0 | 0 | 19211.8 | 10.556 | PSM002081 | 0.058 | 10.919 | 3 |
| ASM001475A | Kärrviksån | 5:8 | 0.04 | 9680 | 1829740 | 58.0 | 81.3 | 0.0 | 81.3 | 19293.1 | 0.0 | 0 | 19293.1 | 10.544 | | | | |
| ASM002479 | Kärrviksån | 5:18 | 1.18 | 259600 | 259600 | 8.2 | 2223.6 | 0.0 | 2223.6 | 2223.6 | 0.0 | 0 | 2223.6 | 8.565 | | | | |
| ASM002486C | Kärrviksån | 5:1 | 2.75 | 604560 | 1074040 | 34.1 | 5123.7 | 164.2 | 5287.8 | 9616.4 | 0.0 | 0 | 9616.4 | 8.953 | PSM002080 | | | |
| ASM002486B | Kärrviksån | 5:1 | 1.13 | 247940 | 3840760 | 121.8 | 2314.4 | 0.0 | 2314.4 | 39049.6 | 0.0 | 0 | 39049.6 | 10.167 | PSM002082 | 0.121 | 10.267 | 1 |
| ASM002486A | Kärrviksån | 5:1 | 2.93 | 645260 | 6007100 | 190.5 | 6269.8 | 0.0 | 6269.8 | 60233.8 | 0.0 | 0 | 60233.8 | 10.027 | PSM002083 | 0.190 | 9.393 | 7 |
| ASM002449 | Bjurhidebäcken | 4:1 | 0.63 | 139040 | 139040 | 4.4 | 1058.0 | 0.0 | 1058.0 | 1058.0 | 0.0 | 0 | 1058.0 | 7.609 | | | | |
| ASM002472 | Sörviksån | 3:2 | 0.47 | 103400 | 103400 | 3.3 | 786.7 | 0.0 | 786.7 | 786.7 | 0.0 | 0 | 786.7 | 7.608 | | | | |
| ASM002473 | Sörviksån | 3:1 | 0.53 | 116600 | 220000 | 7.0 | 887.1 | 0.0 | 887.1 | 1673.8 | 0.0 | 0 | 1673.8 | 7.608 | | | | |
| ASM002651 | Coastal area | | 1.67 | 368280 | 368280 | 11.7 | 2763.3 | 0.0 | 2763.3 | 2763.3 | 0.0 | 0 | 2763.3 | 7.503 | | | | |
| ASM002447 | Bodvikebäcken | 2:1 | 0.38 | 83600 | 83600 | 2.7 | 506.9 | 0.0 | 506.9 | 506.9 | 0.0 | 0 | 506.9 | 6.064 | | | | |
| ASM002446 | Långbonäsbäcken | 1:1 | 0.07 | 15400 | 15400 | 0.5 | 117.2 | 0.0 | 117.2 | 117.2 | 0.0 | 0 | 117.2 | 7.608 | | | | |
| ASM002464 | Flakvarpebäcken | 19:1 | 0.18 | 40480 | 40480 | 1.3 | 281.9 | 0.0 | 281.9 | 281.9 | 0.0 | 0 | 281.9 | 6.965 | | | | |
| ASM002465 | Jössesbäcken | 20:1 | 0.11 | 24420 | 24420 | 0.8 | 419.3 | 0.0 | 419.3 | 419.3 | 0.0 | 0 | 419.3 | 17.172 | | | | |
| ASM002471 | Äspöbäcken | 21:1 | 0.06 | 13860 | 13860 | 0.4 | 105.5 | 0.0 | 105.5 | 105.5 | 0.0 | 0 | 105.5 | 7.608 | | | | |
| ASM002652 | Coastal area | | 1.39 | 305140 | 305140 | 9.7 | 2635.5 | 0.0 | 2635.5 | 2635.5 | 0.0 | 0 | 2635.5 | 8.637 | | | | |
| ASM001445 | Frisksjön | 7:2 | 1.85 | 406560 | 406560 | 12.9 | 3940.3 | 0.0 | 3940.3 | 3940.3 | 0.0 | 0 | 3940.3 | 9.692 | | | | |
| ASM001484 | Kåreviksån | 7:1 | 0.21 | 46860 | 453420 | 14.4 | 356.5 | 0.0 | 356.5 | 4296.9 | 0.0 | 0 | 4296.9 | 9.477 | | | | |
| ASM001486B | Mederhultsån | 6:1 | 1.92 | 422620 | 422620 | 13.4 | 4740.5 | 0.0 | 4740.5 | 4740.5 | 0.0 | 0 | 4740.5 | 11.217 | PSM002084 | 0.013 | 15.787 | 29 |
| ASM001486A | Mederhultsån | 6:1 | 0.08 | 18040 | 440660 | 14.0 | 141.2 | 0.0 | 141.2 | 4881.7 | 0.0 | 0 | 4881.7 | 11.078 | | | | |
| ASM002654 | Coastal area | | 1.86 | 409420 | 409420 | 13.0 | 3340.8 | 0.0 | 3340.8 | 3340.8 | 0.0 | 0 | 3340.8 | 8.160 | | | | |
| ASM002460 | Pistlanbäcken | 8:1 | 0.50 | 109780 | 109780 | 3.5 | 956.3 | 0.0 | 956.3 | 956.3 | 0.0 | 0 | 956.3 | 8.711 | | | | |
| ASM001490 | Ekerumsån | 9:3 | 0.22 | 48840 | 48840 | 1.5 | 924.3 | 0.0 | 924.3 | 924.3 | 0.0 | 0 | 924.3 | 18.924 | | | | |
| ASM001489 | Ekerumsån | 9:2 | 0.77 | 168740 | 168740 | 5.4 | 3664.5 | 0.0 | 3664.5 | 3664.5 | 0.0 | 0 | 3664.5 | 21.717 | | | | |
| ASM002483B | Ekerumsån | 9:1 | 1.50 | 330880 | 548460 | 17.4 | 3653.8 | 0.0 | 3653.8 | 8242.6 | 0.0 | 0 | 8242.6 | 15.029 | PSM002085 | 0.017 | 26.912 | 44 |
| ASM002483A | Ekerumsån | 9:1 | 0.34 | 75020 | 623480 | 19.8 | 864.6 | 0.0 | 864.6 | 9107.2 | 0.0 | 0 | 9107.2 | 14.607 | | | | |
| ASM002478 | Laxemarån | 10:32 | 0.02 | 5060 | 5060 | 0.2 | 38.5 | 0.0 | 38.5 | 38.5 | 0.0 | 0 | 38.5 | 7.608 | | | | |
| ASM002482 | Laxemarån | 10:31 | 0.87 | 190740 | 195800 | 6.2 | 1451.2 | 0.0 | 1451.2 | 1489.7 | 0.0 | 0 | 1489.7 | 7.608 | | | | |
| ASM002480B | Laxemarån | 10:30 | 4.23 | 931480 | 1127280 | 35.7 | 6896.3 | 0.0 | 6896.3 | 8386.0 | 0.0 | 0 | 8386.0 | 7.439 | PSM002068 | 0.036 | 7.439 | 0 |
| ASM002480A | Jämsen | 10:30 | 1.83 | 403480 | 1530760 | 48.5 | 3040.1 | 131.4 | 3171.5 | 11557.6 | 0.0 | 0 | 11557.6 | 7.550 | PSM002069 | 0.049 | 8.455 | 11 |
| ASM001516 | Laxemarån | 10:29 | 0.53 | 117260 | 117260 | 3.7 | 1326.1 | 0.0 | 1326.1 | 1326.1 | 0.0 | 0 | 1326.1 | 11.309 | | | | |
| ASM001515 | Laxemarån | 10:28 | 0.34 | 74140 | 74140 | 2.4 | 1069.2 | 88.6 | 1157.7 | 1157.7 | 0.0 | 0 | 1157.7 | 15.615 | | | | |
| ASM001514 | Laxemarån | 10:27 | 0.49 | 107140 | 107140 | 3.4 | 1932.5 | 50.6 | 1983.1 | 1983.1 | 0.0 | 0 | 1983.1 | 18.510 | | | | |
| ASM001446 | Plittorpsgöl | 10:26 | 0.68 | 149160 | 149160 | 4.7 | 1184.1 | 49.5 | 1233.6 | 1233.6 | 0.0 | 0 | 1233.6 | 8.271 | | | | |
| ASM002459 | Laxemarån | 10:25 | 0.10 | 21780 | 170940 | 5.4 | 165.7 | 47.3 | 213.0 | 1446.6 | 0.0 | 0 | 1446.6 | 8.463 | | | | |
| ASM001512 | Laxemarån | 10:24 | 0.49 | 108680 | 108680 | 3.4 | 932.4 | 0.0 | 932.4 | 932.4 | 0.0 | 0 | 932.4 | 8.580 | | | | |
| ASM002476E | Laxemarån | 10:1 | 3.95 | 868780 | 2977700 | 94.4 | 8621.2 | 304.6 | 8925.8 | 27329.3 | 0.0 | 0 | 27329.3 | 9.178 | PSM002071 | 0.094 | 9.178 | 0 |
| ASM001510 | Laxemarån | 10:22 | 0.56 | 123640 | 123640 | 3.9 | 979.3 | 94.5 | 1073.8 | 1073.8 | 0.0 | 0 | 1073.8 | 8.685 | | | | |
| ASM002453 | Laxemarån | 10:21 | 0.45 | 97900 | 221540 | 7.0 | 772.5 | 25.0 | 797.5 | 1871.2 | 0.0 | 0 | 1871.2 | 8.446 | | | | |
| ASM002450B | Laxemarån | 10:20 | 2.39 | 526240 | 747780 | 23.7 | 4650.2 | 188.4 | 4838.6 | 6709.8 | 0.0 | 0 | 6709.8 | 8.973 | PSM002072 | | | |
| ASM002450A | Laxemarån | 10:20 | 0.19 | 41140 | 788920 | 25.0 | 361.5 | 0.0 | 361.5 | 7071.3 | 0.0 | 0 | 7071.3 | 8.963 | | | | |
| ASM001511 | Laxemarån | 10:23 | 0.74 | 162800 | 162800 | 5.2 | 1326.5 | 0.0 | 1326.5 | 1326.5 | 0.0 | 0 | 1326.5 | 8.148 | | | | |
| ASM001448 | Grangöl | 10:19 | 0.50 | 108900 | 108900 | 3.5 | 953.9 | 0.0 | 953.9 | 953.9 | 0.0 | 0 | 953.9 | 8.760 | | | | |
| ASM002499 | Laxemarån | 10:18 | 0.06 | 12760 | 121660 | 3.9 | 275.7 | 0.0 | 275.7 | 1229.6 | 0.0 | 0 | 1229.6 | 10.107 | | | | |
| ASM001506 | Laxemarån | 10:17 | 0.40 | 87560 | 87560 | 2.8 | 1229.8 | 0.0 | 1229.8 | 1229.8 | 0.0 | 0 | 1229.8 | 14.045 | | | | |
| ASM001447 | Fjällgöl | 10:16 | 0.30 | 64900 | 64900 | 2.1 | 458.9 | 0.0 | 458.9 | 458.9 | 0.0 | 0 | 458.9 | 7.071 | | | | |
| ASM002451 | Laxemarån | 10:15 | 0.33 | 71500 | 136400 | 4.3 | 1100.1 | 0.0 | 1100.1 | 1559.0 | 0.0 | 0 | 1559.0 | 11.430 | | | | |
| ASM002452 | Laxemarån | 10:14 | 2.38 | 522500 | 868120 | 27.5 | 6761.5 | 0.0 | 6761.5 | 10779.9 | 0.0 | 0 | 10779.9 | 12.418 | | | | |
| ASM001503 | Laxemarån | 10:13 | 0.42 | 91520 | 91520 | 2.9 | 1561.2 | 0.0 | 1561.2 | 1561.2 | 0.0 | 0 | 1561.2 | 17.059 | | | | |
| ASM002454 | Laxemarån | 10:12 | 0.81 | 177760 | 269280 | 8.5 | 3022.3 | 0.0 | 3022.3 | 4583.5 | 0.0 | 0 | 4583.5 | 17.021 | | | | |
| ASM001501 | Laxemarån | 10:11 | 0.81 | 177320 | 177320 | 5.6 | 2630.0 | 0.0 | 2630.0 | 2630.0 | 0.0 | 0 | 2630.0 | 14.832 | | | | |
| ASM002457 | Laxemarån | 10:10 | 1.39 | 305580 | 482900 | 15.3 | 6408.7 | 0.0 | 6408.7 | 9038.7 | 0.0 | 0 | 9038.7 | 18.718 | | | | |
| ASM002476D | Laxemarån | 10:1 | 4.96 | 1091860 | 6641580 | 210.6 | 11064.4 | 0.0 | 11064.4 | 71193.6 | 0.0 | 0 | 71193.6 | 10.719 | PSM002077 | | | |
| ASM001499 | Laxemarån | 10:9 | 0.71 | 156420 | 156420 | 5.0 | 1539.4 | 0.0 | 1539.4 | 1539.4 | 0.0 | 0 | 1539.4 | 9.842 | | | | |
| ASM001498 | Laxemarån | 10:8 | 2.77 | 609620 | 766040 | 24.3 | 5719.1 | 0.0 | 5719.1 | 7258.6 | 0.0 | 0 | 7258.6 | 9.475 | PSM002078 | 0.024 | 7.080 | 34 |
| ASM001497 | Laxemarån | 10:7 | 0.61 | 133980 | 133980 | 4.2 | 1707.0 | 0.0 | 1707.0 | 1707.0 | 0.0 | 0 | 1707.0 | 12.740 | | | | |
| ASM002476C | Laxemarån | 10:1 | 0.32 | 69300 | 7610900 | 241.3 | 729.2 | 0.0 | 729.2 | 80888.4 | 0.0 | 0 | 80888.4 | 10.628 | PSM002079 | 0.242 | 9.190 | 16 |
| ASM001494 | Laxemarån | 10:4 | 1.00 | 220220 | 220220 | 7.0 | 4042.2 | 0.0 | 4042.2 | 4042.2 | 0.0 | 0 | 4042.2 | 18.355 | | | | |
| ASM001493 | Laxemarån | 10:3 | 0.32 | 70180 | 70180 | 2.2 | 945.4 | 0.0 | 945.4 | 945.4 | 0.0 | 0 | 945.4 | 13.471 | | | | |
| ASM001492 | Laxemarån | 10:2 | 0.46 | 101200 | 101200 | 3.2 | 1614.5 | 0.0 | 1614.5 | 1614.5 | 0.0 | 0 | 1614.5 | 15.954 | | | | |
| ASM001496 | Laxemarån | 10:6 | 0.89 | 195800 | 195800 | 6.2 | 2541.9 | 0.0 | 2541.9 | 2541.9 | 0.0 | 0 | 2541.9 | 12.982 | | | | |
| ASM001495 | Laxemarån | 10:5 | 0.29 | 63800 | 63800 | 2.0 | 569.5 | 0.0 | 569.5 | 569.5 | 0.0 | 0 | 569.5 | 8.926 | | | | |
| ASM002476B | Laxemarån | 10:1 | 3.23 | 710820 | 8972920 | 284.5 | 9061.7 | 0.0 | 9061.7 | 99663.7 | 0.0 | 0 | 99663.7 | 11.107 | PSM002087 | 0.285 | 10.163 | 9 |
| ASM002476A | Laxemarån | 10:1 | 0.19 | 41360 | 9014280 | 285.8 | 383.9 | 0.0 | 383.9 | 100047.6 | 0.0 | 0 | 100047.6 | 11.099 | | | | |
| ASM002495 | Glostadsbäcken | 12:3 | 0.13 | 27720 | 27720 | 0.9 | 226.0 | 0.0 | 226.0 | 226.0 | 0.0 | 0 | 226.0 | 8.153 | | | | |
| ASM002485 | Glostadsbäcken | 12:2 | 0.33 | 72820 | 72820 | 2.3 | 1049.1 | 0.0 | 1049.1 | 1049.1 | 0.0 | 0 | 1049.1 | 14.407 | | | | |
| ASM002498 | Glostadsbäcken | 12:1 | 1.60 | 351340 | 451880 | 14.3 | 5314.2 | 0.0 | 5314.2 | 6589.4 | 0.0 | 0 | 6589.4 | 14.582 | | | | |
| ASM001518B | Stålglobäcken | 13:1 | 0.68 | 149380 | 149380 | 4.7 | 2457.4 | 0.0 | 2457.4 | 2457.4 | 0.0 | 0 | 2457.4 | 16.451 | PSM002086 | 0.005 | 16.451 | 0 |
| ASM001518A | Stålglobäcken | 13:1 | 0.35 | 77880 | 227260 | 7.2 | 1129.5 | 0.0 | 1129.5 | 3586.9 | 0.0 | 0 | 3586.9 | 15.783 | | | | |
| ASM002462 | Uvöbäcken | 15:1 | 0.97 | 212740 | 212740 | 6.7 | 2157.0 | 0.0 | 2157.0 | 2157.0 | 0.0 | 0 | 2157.0 | 10.139 | | | | |
| ASM002497 | Stekebäcken | 14:2 | 0.44 | 95700 | 95700 | 3.0 | 1343.6 | 0.0 | 1343.6 | 1343.6 | 0.0 | 0 | 1343.6 | 14.040 | | | | |
| ASM001517 | Stekebäcken | 14:1 | 0.90 | 198660 | 294360 | 9.3 | 1939.6 | 0.0 | 1939.6 | 3283.3 | 0.0 | 0 | 3283.3 | 11.154 | | | | |
| ASM002463 | Svartebäck | 16:1 | 0.50 | 110880 | 110880 | 3.5 | 840.9 | 0.0 | 840.9 | 840.9 | 0.0 | 0 | 840.9 | 7.584 | | | | |
| ASM002655 | Coastal area | | 2.71 | 596420 | 596420 | 18.9 | 5252.3 | 0.0 | 5252.3 | 5252.3 | 0.0 | 0 | 5252.3 | 8.806 | | | | |
| ASM002658 | Coastal area | | 1.26 | 277420 | 277420 | 8.8 | 2335.5 | 0.0 | 2335.5 | 2335.5 | 0.0 | 0 | 2335.5 | 8.419 | | | | |
| ASM002656 | Coastal area | | 0.22 | 48400 | 48400 | 1.5 | 351.9 | 0.0 | 351.9 | 351.9 | 0.0 | 0 | 351.9 | 7.271 | | | | |
| ASM002660 | Coastal area | | 0.14 | 30360 | 30360 | 1.0 | 219.9 | 0.0 | 219.9 | 219.9 | 0.0 | 0 | 219.9 | 7.243 | | | | |
| ASM002659 | Coastal area | | 15.70 | 3453780 | 3453780 | 109.5 | 32950.7 | 386.7 | 33337.4 | 33337.4 | 0.0 | 0 | 33337.4 | 9.652 | | | | |
| ASM002657 | Coastal area | | 2.60 | 571340 | 571340 | 18.1 | 5332.7 | 0.0 | 5332.7 | 5332.7 | 0.0 | 0 | 5332.7 | 9.334 | | | | |
| ASM001522 | Uthammarsån | 17:5 | 0.57 | 125620 | 125620 | 4.0 | 1449.9 | 0.0 | 1449.9 | 1449.9 | 0.0 | 0 | 1449.9 | 11.542 | | | | |
| ASM001523 | Uthammarsån | 17:6 | 0.96 | 210760 | 210760 | 6.7 | 3032.2 | 0.0 | 3032.2 | 3032.2 | 0.0 | 0 | 3032.2 | 14.387 | | | | |
| ASM001521 | Uthammarsån | 17:4 | 0.20 | 44880 | 44880 | 1.4 | 826.4 | 0.0 | 826.4 | 826.4 | 0.0 | 0 | 826.4 | 18.414 | | | | |
| ASM001520 | Uthammarsån | 17:3 | 0.08 | 17820 | 17820 | 0.6 | 393.7 | 0.0 | 393.7 | 393.7 | 0.0 | 0 | 393.7 | 22.092 | | | | |
| ASM002494B | Uthammarsån | 17:1 | 2.91 | 640860 | 1039940 | 33.0 | 7606.4 | 0.0 | 7606.4 | 13308.6 | 0.0 | 0 | 13308.6 | 12.798 | PSM002076 | 0.033 | 13.606 | 6 |
| ASM001533 | Uthammarsån | 17:2 | 0.51 | 112640 | 112640 | 3.6 | 2066.0 | 0.0 | 2066.0 | 2066.0 | 0.0 | 0 | 2066.0 | 18.341 | | | | |
| ASM002494A | Uthammarsån | 17:1 | 1.78 | 391820 | 1544400 | 49.0 | 7737.9 | 0.0 | 7737.9 | 23112.5 | 0.0 | 0 | 23112.5 | 14.965 | | | | |
| ASM001528 | Släthultebäcken | 18:5 | 0.32 | 70400 | 70400 | 2.2 | 535.6 | 0.0 | 535.6 | 535.6 | 0.0 | 0 | 535.6 | 7.608 | | | | |
| ASM002477 | Släthultebäcken | 18:4 | 0.66 | 144980 | 215380 | 6.8 | 1063.8 | 0.0 | 1063.8 | 1599.4 | 0.0 | 0 | 1599.4 | 7.426 | | | | |
| ASM001531 | Släthultebäcken | 18:8 | 0.30 | 66440 | 66440 | 2.1 | 509.3 | 0.0 | 509.3 | 509.3 | 0.0 | 0 | 509.3 | 7.665 | | | | |
| ASM001532 | Släthultebäcken | 18:9 | 0.11 | 24420 | 24420 | 0.8 | 639.9 | 0.0 | 639.9 | 639.9 | 0.0 | 0 | 639.9 | 26.205 | | | | |
| ASM002455 | Släthultebäcken | 18:7 | 0.76 | 167420 | 258280 | 8.2 | 2822.8 | 0.0 | 2822.8 | 3971.9 | 0.0 | 0 | 3971.9 | 15.378 | | | | |
| ASM002475 | Släthultebäcken | 18:6 | 1.06 | 232100 | 490380 | 15.5 | 1765.9 | 0.0 | 1765.9 | 5737.8 | 0.0 | 0 | 5737.8 | 11.701 | | | | |
| ASM001526 | Släthultebäcken | 18:3 | 0.40 | 88220 | 88220 | 2.8 | 669.9 | 0.0 | 669.9 | 669.9 | 0.0 | 0 | 669.9 | 7.593 | | | | |
| ASM002481C | Släthultebäcken | 18:1 | 2.44 | 537020 | 1027400 | 32.6 | 5932.1 | 300.4 | 6232.6 | 11970.4 | 0.0 | 0 | 11970.4 | 11.651 | PSM002070 | | | |
| ASM002481B | Släthultebäcken | 18:1 | 2.13 | 469260 | 1800260 | 57.1 | 5835.5 | 0.0 | 5835.5 | 20075.2 | 0.0 | 0 | 20075.2 | 11.151 | PSM002075 | | | |
| ASM001525 | Släthultebäcken | 18:2 | 0.77 | 169620 | 169620 | 5.4 | 2940.4 | 0.0 | 2940.4 | 2940.4 | 0.0 | 0 | 2940.4 | 17.335 | | | | |
| ASM002481A | Släthultebäcken | 18:1 | 0.00 | 220 | 1970100 | 62.5 | 6.4 | 0.0 | 6.4 | 23022.0 | 0.0 | 0 | 23022.0 | 11.686 | | | | |
| ASM001444 | Sörämagasinet | 11:1 | 0.52 | 115060 | 115060 | 3.6 | 719.5 | 0.0 | 719.5 | 719.5 | 0.0 | 0 | 719.5 | 6.253 | | | | |
| ASM002466 | Stekflagebäcken | 22:1 | 0.36 | 78980 | 78980 | 2.5 | 559.0 | 0.0 | 559.0 | 559.0 | 0.0 | 0 | 559.0 | 7.077 | | | | |
| ASM002653 | Coastal area | | 0.76 | 166980 | 166980 | 5.3 | 1324.8 | 0.0 | 1324.8 | 1324.8 | 0.0 | 0 | 1324.8 | 7.934 | | | | |
| ASM002470 | Skölkebäcken | 26:1 | 0.17 | 36300 | 36300 | 1.2 | 328.9 | 0.0 | 328.9 | 328.9 | 0.0 | 0 | 328.9 | 9.062 | | | | |
| ASM002469 | Gloebäcken | 25:1 | 0.13 | 28820 | 28820 | 0.9 | 253.6 | 0.0 | 253.6 | 253.6 | 0.0 | 0 | 253.6 | 8.799 | | | | |
| ASM002468 | Lindströmmebäcken | 24:1 | 0.19 | 42240 | 42240 | 1.3 | 542.4 | 0.0 | 542.4 | 542.4 | 0.0 | 0 | 542.4 | 12.841 | | | | |
| ASM002467B | Vadvikebäcken | 23:1 | 0.30 | 65560 | 65560 | 2.1 | 498.8 | 0.0 | 498.8 | 498.8 | 0.0 | 0 | 498.8 | 7.608 | PSM107735 | 0.002 | 13.581 | 44 |
| ASM002467A | Vadvikebäcken | 23:1 | 0.01 | 1980 | 67540 | 2.1 | 15.1 | 0.0 | 15.1 | 513.9 | 0.0 | 0 | 513.9 | 7.609 | | | | |
| | **Kärrviksån** | 5:1-20 | 27.31 | 6007100 | 6007100 | 26.9 | 59841.9 | 391.9 | 60233.8 | | 0.0 | 0 | 60233.8 | 10.027 | | | | |
| | **Laxemarån** | 10:1-32 | 40.97 | 9014280 | 9014280 | 37.5 | 99067.7 | 979.8 | 100047.6 | | 0.0 | 0 | 100047.6 | 11.099 | | | | |
| | **All catchments** | | 129.97 | 28593620 | 28593620 | 22.3 | 304030.5 | 2058.9 | 306089.5 | | 0.0 | 0 | 306089.5 | 10.705 | | | | |

| **Potassium (K)** | | | | Water balance | | | Total per catchment | | | Total including contributions from upstream catchments | | | | | Calibration data | | | |
|---|---|---|---|---|---|---|---|---|---|---|---|---|---|---|---|---|---|---|
| Idcode | Name | ARO | Area | $Q_{catch}$ | $Q_{out}$ | q | Diffuse | Point | Total | Total IN | Retention | | Total OUT | Conc. | Reference | q | Conc. | Deviation |
| | | | $km^2$ | $m^3 \cdot yr^{-1}$ | $m^3 \cdot yr^{-1}$ | $L \cdot s^{-1}$ | $kg \cdot yr^{-1}$ | $kg \cdot yr^{-1}$ | $kg \cdot yr^{-1}$ | $kg \cdot yr^{-1}$ | $kg \cdot yr^{-1}$ | % | $kg \cdot yr^{-1}$ | $mg \cdot L^{-1}$ | | $L \cdot s^{-1}$ | $mg \cdot L^{-1}$ | % |
| ASM002474 | Kärrviksån | 5:20 | 0.12 | 25740 | 25740 | 0.8 | 22.6 | 140.2 | 162.8 | 162.8 | 0.0 | 0 | 162.8 | 6.326 | | | | |
| ASM002493 | Kärrviksån | 5:19 | 0.84 | 184140 | 209880 | 6.7 | 278.4 | 0.0 | 278.4 | 441.2 | 0.0 | 0 | 441.2 | 2.102 | | | | |
| ASM001483 | Kärrviksån | 5:17 | 0.15 | 33220 | 33220 | 1.1 | 80.8 | 0.0 | 80.8 | 80.8 | 0.0 | 0 | 80.8 | 2.431 | | | | |
| ASM002492 | Kärrviksån | 5:16 | 1.11 | 243980 | 277200 | 8.8 | 400.4 | 0.0 | 400.4 | 481.1 | 0.0 | 0 | 481.1 | 1.736 | | | | |
| ASM002491 | Kärrviksån | 5:15 | 1.87 | 411840 | 689040 | 21.8 | 378.3 | 0.0 | 378.3 | 859.5 | 0.0 | 0 | 859.5 | 1.247 | | | | |
| ASM001474 | Kärrviksån | 5:7 | 0.45 | 99000 | 99000 | 3.1 | 87.5 | 0.0 | 87.5 | 87.5 | 0.0 | 0 | 87.5 | 0.884 | | | | |
| ASM002487 | Kärrviksån | 5:6 | 1.20 | 264000 | 363000 | 11.5 | 262.8 | 0.0 | 262.8 | 350.3 | 0.0 | 0 | 350.3 | 0.965 | | | | |
| ASM001472 | Kärrviksån | 5:4 | 1.10 | 242880 | 242880 | 7.7 | 204.8 | 0.0 | 204.8 | 204.8 | 0.0 | 0 | 204.8 | 0.843 | | | | |
| ASM001470 | Kärrviksån | 5:3 | 0.40 | 87560 | 87560 | 2.8 | 74.9 | 0.0 | 74.9 | 74.9 | 0.0 | 0 | 74.9 | 0.855 | | | | |
| ASM001469 | Kärrviksån | 5:2 | 0.97 | 212960 | 212960 | 6.8 | 202.0 | 0.0 | 202.0 | 202.0 | 0.0 | 0 | 202.0 | 0.949 | | | | |
| ASM001471 | Kärrviksån | 5:5 | 2.79 | 614680 | 614680 | 19.5 | 533.6 | 0.0 | 533.6 | 533.6 | 0.0 | 0 | 533.6 | 0.868 | | | | |
| ASM001479 | Kärrviksån | 5:13 | 0.65 | 142340 | 142340 | 4.5 | 107.3 | 0.0 | 107.3 | 107.3 | 0.0 | 0 | 107.3 | 0.754 | | | | |
| ASM001480 | Kärrviksån | 5:14 | 0.10 | 22660 | 22660 | 0.7 | 19.2 | 0.0 | 19.2 | 19.2 | 0.0 | 0 | 19.2 | 0.847 | | | | |
| ASM002490 | Kärrviksån | 5:12 | 0.84 | 183920 | 348920 | 11.1 | 151.3 | 336.9 | 488.2 | 614.8 | 0.0 | 0 | 614.8 | 1.762 | | | | |
| ASM001478 | Kärrviksån | 5:11 | 0.49 | 108460 | 108460 | 3.4 | 81.8 | 0.0 | 81.8 | 81.8 | 0.0 | 0 | 81.8 | 0.754 | | | | |
| ASM002489 | Kärrviksån | 5:10 | 1.20 | 263560 | 372020 | 11.8 | 209.6 | 0.0 | 209.6 | 291.4 | 0.0 | 0 | 291.4 | 0.783 | | | | |
| ASM001476 | Kärrviksån | 5:9 | 3.62 | 796180 | 796180 | 25.2 | 792.0 | 0.0 | 792.0 | 792.0 | 0.0 | 0 | 792.0 | 0.995 | | | | |
| ASM001475B | Kärrviksån | 5:8 | 1.38 | 302940 | 1820060 | 57.7 | 237.4 | 0.0 | 237.4 | 1935.5 | 0.0 | 0 | 1935.5 | 1.063 | PSM002081 | 0.058 | 1.063 | 0 |
| ASM001475A | Kärrviksån | 5:8 | 0.04 | 9680 | 1829740 | 58.0 | 7.8 | 0.0 | 7.8 | 1943.3 | 0.0 | 0 | 1943.3 | 1.062 | | | | |
| ASM002479 | Kärrviksån | 5:18 | 1.18 | 259600 | 259600 | 8.2 | 206.2 | 0.0 | 206.2 | 206.2 | 0.0 | 0 | 206.2 | 0.794 | | | | |
| ASM002486C | Kärrviksån | 5:1 | 2.75 | 604560 | 1074040 | 34.1 | 484.1 | 343.9 | 828.0 | 1475.4 | 0.0 | 0 | 1475.4 | 1.374 | PSM002080 | | | |
| ASM002486B | Kärrviksån | 5:1 | 1.13 | 247940 | 3840760 | 121.8 | 344.9 | 0.0 | 344.9 | 4623.1 | 0.0 | 0 | 4623.1 | 1.204 | PSM002082 | 0.121 | 1.137 | 6 |
| ASM002486A | Kärrviksån | 5:1 | 2.93 | 645260 | 6007100 | 190.5 | 799.8 | 0.0 | 799.8 | 6788.4 | 0.0 | 0 | 6788.4 | 1.130 | PSM002083 | 0.190 | 1.176 | 4 |
| ASM002449 | Bjurhidebäcken | 4:1 | 0.63 | 139040 | 139040 | 4.4 | 105.7 | 0.0 | 105.7 | 105.7 | 0.0 | 0 | 105.7 | 0.760 | | | | |
| ASM002472 | Sörviksån | 3:2 | 0.47 | 103400 | 103400 | 3.3 | 78.0 | 0.0 | 78.0 | 78.0 | 0.0 | 0 | 78.0 | 0.754 | | | | |
| ASM002473 | Sörviksån | 3:1 | 0.53 | 116600 | 220000 | 7.0 | 87.9 | 0.0 | 87.9 | 165.9 | 0.0 | 0 | 165.9 | 0.754 | | | | |
| ASM002651 | Coastal area | | 1.67 | 368280 | 368280 | 11.7 | 303.2 | 0.0 | 303.2 | 303.2 | 0.0 | 0 | 303.2 | 0.823 | | | | |
| ASM002447 | Bodvikebäcken | 2:1 | 0.38 | 83600 | 83600 | 2.7 | 50.2 | 0.0 | 50.2 | 50.2 | 0.0 | 0 | 50.2 | 0.601 | | | | |
| ASM002446 | Långbonäsbäcken | 1:1 | 0.07 | 15400 | 15400 | 0.5 | 11.6 | 0.0 | 11.6 | 11.6 | 0.0 | 0 | 11.6 | 0.754 | | | | |
| ASM002464 | Flakvarpebäcken | 19:1 | 0.18 | 40480 | 40480 | 1.3 | 27.9 | 0.0 | 27.9 | 27.9 | 0.0 | 0 | 27.9 | 0.690 | | | | |
| ASM002465 | Jössesbäcken | 20:1 | 0.11 | 24420 | 24420 | 0.8 | 28.3 | 0.0 | 28.3 | 28.3 | 0.0 | 0 | 28.3 | 1.159 | | | | |
| ASM002471 | Åspöbäcken | 21:1 | 0.06 | 13860 | 13860 | 0.4 | 11.5 | 0.0 | 11.5 | 11.5 | 0.0 | 0 | 11.5 | 0.829 | | | | |
| ASM002652 | Coastal area | | 1.39 | 305140 | 305140 | 9.7 | 253.7 | 0.0 | 253.7 | 253.7 | 0.0 | 0 | 253.7 | 0.832 | | | | |
| ASM001445 | Frisksjön | 7:2 | 1.85 | 406560 | 406560 | 12.9 | 429.9 | 0.0 | 429.9 | 429.9 | 0.0 | 0 | 429.9 | 1.057 | | | | |
| ASM001484 | Kåreviksån | 7:1 | 0.21 | 46860 | 453420 | 14.4 | 35.3 | 0.0 | 35.3 | 465.2 | 0.0 | 0 | 465.2 | 1.026 | | | | |
| ASM001486B | Mederhultsån | 6:1 | 1.92 | 422620 | 422620 | 13.4 | 516.3 | 0.0 | 516.3 | 516.3 | 0.0 | 0 | 516.3 | 1.222 | PSM002084 | 0.013 | 2.664 | 54 |
| ASM001486A | Mederhultsån | 6:1 | 0.08 | 18040 | 440660 | 14.0 | 19.3 | 0.0 | 19.3 | 535.5 | 0.0 | 0 | 535.5 | 1.215 | | | | |
| ASM002654 | Coastal area | | 1.86 | 409420 | 409420 | 13.0 | 328.2 | 0.0 | 328.2 | 328.2 | 0.0 | 0 | 328.2 | 0.802 | | | | |
| ASM002460 | Pistlanbäcken | 8:1 | 0.50 | 109780 | 109780 | 3.5 | 95.8 | 0.0 | 95.8 | 95.8 | 0.0 | 0 | 95.8 | 0.872 | | | | |
| ASM001490 | Ekerumsån | 9:3 | 0.22 | 48840 | 48840 | 1.5 | 61.1 | 0.0 | 61.1 | 61.1 | 0.0 | 0 | 61.1 | 1.251 | | | | |
| ASM001489 | Ekerumsån | 9:2 | 0.77 | 168740 | 168740 | 5.4 | 240.6 | 0.0 | 240.6 | 240.6 | 0.0 | 0 | 240.6 | 1.426 | | | | |
| ASM002483B | Ekerumsån | 9:1 | 1.50 | 330880 | 548460 | 17.4 | 368.3 | 0.0 | 368.3 | 670.0 | 0.0 | 0 | 670.0 | 1.222 | PSM002085 | 0.017 | 1.222 | 0 |
| ASM002483A | Ekerumsån | 9:1 | 0.34 | 75020 | 623480 | 19.8 | 82.3 | 0.0 | 82.3 | 752.3 | 0.0 | 0 | 752.3 | 1.207 | | | | |
| ASM002478 | Laxemarån | 10:32 | 0.02 | 5060 | 5060 | 0.2 | 3.8 | 0.0 | 3.8 | 3.8 | 0.0 | 0 | 3.8 | 0.754 | | | | |
| ASM002482 | Laxemarån | 10:31 | 0.87 | 190740 | 195800 | 6.2 | 221.4 | 0.0 | 221.4 | 225.2 | 0.0 | 0 | 225.2 | 1.150 | | | | |
| ASM002480B | Laxemarån | 10:30 | 4.23 | 931480 | 1127280 | 35.7 | 861.9 | 0.0 | 861.9 | 1087.1 | 0.0 | 0 | 1087.1 | 0.964 | PSM002068 | 0.036 | 0.854 | 13 |
| ASM002480A | Jämsen | 10:30 | 1.83 | 403480 | 1530760 | 48.5 | 513.4 | 275.3 | 788.7 | 1875.8 | 0.0 | 0 | 1875.8 | 1.225 | PSM002069 | 0.049 | 1.296 | 5 |
| ASM001516 | Laxemarån | 10:29 | 0.53 | 117260 | 117260 | 3.7 | 106.6 | 0.0 | 106.6 | 106.6 | 0.0 | 0 | 106.6 | 0.909 | | | | |
| ASM001515 | Laxemarån | 10:28 | 0.34 | 74140 | 74140 | 2.4 | 147.5 | 185.5 | 333.0 | 333.0 | 0.0 | 0 | 333.0 | 4.491 | | | | |
| ASM001514 | Laxemarån | 10:27 | 0.49 | 107140 | 107140 | 3.4 | 127.8 | 106.0 | 233.8 | 233.8 | 0.0 | 0 | 233.8 | 2.182 | | | | |
| ASM001446 | Plittorpsgöl | 10:26 | 0.68 | 149160 | 149160 | 4.7 | 115.7 | 103.8 | 219.5 | 219.5 | 0.0 | 0 | 219.5 | 1.472 | | | | |
| ASM002459 | Laxemarån | 10:25 | 0.10 | 21780 | 170940 | 5.4 | 16.4 | 99.0 | 115.4 | 334.9 | 0.0 | 0 | 334.9 | 1.959 | | | | |
| ASM001512 | Laxemarån | 10:24 | 0.49 | 108680 | 108680 | 3.4 | 86.4 | 0.0 | 86.4 | 86.4 | 0.0 | 0 | 86.4 | 0.795 | | | | |
| ASM002476E | Laxemarån | 10:1 | 3.95 | 868780 | 2977700 | 94.4 | 1052.6 | 638.0 | 1690.7 | 4661.2 | 0.0 | 0 | 4661.2 | 1.565 | PSM002071 | 0.094 | 1.423 | 10 |
| ASM001510 | Laxemarån | 10:22 | 0.56 | 123640 | 123640 | 3.9 | 97.3 | 198.0 | 295.3 | 295.3 | 0.0 | 0 | 295.3 | 2.388 | | | | |
| ASM002453 | Laxemarån | 10:21 | 0.45 | 97900 | 221540 | 7.0 | 74.8 | 52.4 | 127.2 | 422.5 | 0.0 | 0 | 422.5 | 1.907 | | | | |
| ASM002450B | Laxemarån | 10:20 | 2.39 | 526240 | 747780 | 23.7 | 426.1 | 394.7 | 820.8 | 1243.2 | 0.0 | 0 | 1243.2 | 1.663 | PSM002072 | | | |
| ASM002450A | Laxemarån | 10:20 | 0.19 | 41140 | 788920 | 25.0 | 33.1 | 0.0 | 33.1 | 1276.3 | 0.0 | 0 | 1276.3 | 1.618 | | | | |
| ASM001511 | Laxemarån | 10:23 | 0.74 | 162800 | 162800 | 5.2 | 126.4 | 0.0 | 126.4 | 126.4 | 0.0 | 0 | 126.4 | 0.777 | | | | |
| ASM001448 | Grangöl | 10:19 | 0.50 | 108900 | 108900 | 3.5 | 84.8 | 0.0 | 84.8 | 84.8 | 0.0 | 0 | 84.8 | 0.779 | | | | |
| ASM002499 | Laxemarån | 10:18 | 0.06 | 12760 | 121660 | 3.9 | 17.1 | 0.0 | 17.1 | 101.9 | 0.0 | 0 | 101.9 | 0.838 | | | | |
| ASM001506 | Laxemarån | 10:17 | 0.40 | 87560 | 87560 | 2.8 | 89.7 | 0.0 | 89.7 | 89.7 | 0.0 | 0 | 89.7 | 1.024 | | | | |
| ASM001447 | Fjällgöl | 10:16 | 0.30 | 64900 | 64900 | 2.1 | 50.6 | 0.0 | 50.6 | 50.6 | 0.0 | 0 | 50.6 | 0.780 | | | | |
| ASM002451 | Laxemarån | 10:15 | 0.33 | 71500 | 136400 | 4.3 | 77.3 | 0.0 | 77.3 | 127.9 | 0.0 | 0 | 127.9 | 0.938 | | | | |
| ASM002452 | Laxemarån | 10:14 | 2.38 | 522500 | 868120 | 27.5 | 510.9 | 0.0 | 510.9 | 830.4 | 0.0 | 0 | 830.4 | 0.957 | | | | |
| ASM001503 | Laxemarån | 10:13 | 0.42 | 91520 | 91520 | 2.9 | 105.4 | 0.0 | 105.4 | 105.4 | 0.0 | 0 | 105.4 | 1.151 | | | | |
| ASM002454 | Laxemarån | 10:12 | 0.81 | 177760 | 269280 | 8.5 | 204.2 | 0.0 | 204.2 | 309.6 | 0.0 | 0 | 309.6 | 1.150 | | | | |
| ASM001501 | Laxemarån | 10:11 | 0.81 | 177320 | 177320 | 5.6 | 187.5 | 0.0 | 187.5 | 187.5 | 0.0 | 0 | 187.5 | 1.058 | | | | |
| ASM002457 | Laxemarån | 10:10 | 1.39 | 305580 | 482900 | 15.3 | 402.4 | 0.0 | 402.4 | 590.0 | 0.0 | 0 | 590.0 | 1.222 | | | | |
| ASM002476D | Laxemarån | 10:1 | 4.96 | 1091860 | 6641580 | 210.6 | 955.0 | 0.0 | 955.0 | 8748.9 | 0.0 | 0 | 8748.9 | 1.317 | PSM002077 | | | |
| ASM001499 | Laxemarån | 10:9 | 0.71 | 156420 | 156420 | 5.0 | 134.7 | 0.0 | 134.7 | 134.7 | 0.0 | 0 | 134.7 | 0.861 | | | | |
| ASM001498 | Laxemarån | 10:8 | 2.77 | 609620 | 766040 | 24.3 | 534.7 | 0.0 | 534.7 | 669.4 | 0.0 | 0 | 669.4 | 0.874 | PSM002078 | 0.024 | 0.587 | 49 |
| ASM001497 | Laxemarån | 10:7 | 0.61 | 133980 | 133980 | 4.2 | 132.2 | 0.0 | 132.2 | 132.2 | 0.0 | 0 | 132.2 | 0.987 | | | | |
| ASM002476C | Laxemarån | 10:1 | 0.32 | 69300 | 7610900 | 241.3 | 66.8 | 0.0 | 66.8 | 9617.3 | 0.0 | 0 | 9617.3 | 1.264 | PSM002079 | 0.242 | 1.264 | 0 |
| ASM001494 | Laxemarån | 10:4 | 1.00 | 220220 | 220220 | 7.0 | 269.5 | 0.0 | 269.5 | 269.5 | 0.0 | 0 | 269.5 | 1.224 | | | | |
| ASM001493 | Laxemarån | 10:3 | 0.32 | 70180 | 70180 | 2.2 | 70.2 | 0.0 | 70.2 | 70.2 | 0.0 | 0 | 70.2 | 1.000 | | | | |
| ASM001492 | Laxemarån | 10:2 | 0.46 | 101200 | 101200 | 3.2 | 112.9 | 0.0 | 112.9 | 112.9 | 0.0 | 0 | 112.9 | 1.116 | | | | |
| ASM001496 | Laxemarån | 10:6 | 0.89 | 195800 | 195800 | 6.2 | 198.7 | 0.0 | 198.7 | 198.7 | 0.0 | 0 | 198.7 | 1.015 | | | | |
| ASM001495 | Laxemarån | 10:5 | 0.29 | 63800 | 63800 | 2.0 | 52.3 | 0.0 | 52.3 | 52.3 | 0.0 | 0 | 52.3 | 0.819 | | | | |
| ASM002476B | Laxemarån | 10:1 | 3.23 | 710820 | 8972920 | 284.5 | 725.6 | 0.0 | 725.6 | 11046.4 | 0.0 | 0 | 11046.4 | 1.231 | PSM002087 | 0.285 | 1.492 | 17 |
| ASM002476A | Laxemarån | 10:1 | 0.19 | 41360 | 9014280 | 285.8 | 54.7 | 0.0 | 54.7 | 11101.1 | 0.0 | 0 | 11101.1 | 1.232 | | | | |
| ASM002495 | Glostadsbäcken | 12:3 | 0.13 | 27720 | 27720 | 0.9 | 22.0 | 0.0 | 22.0 | 22.0 | 0.0 | 0 | 22.0 | 0.794 | | | | |
| ASM002485 | Glostadsbäcken | 12:2 | 0.33 | 72820 | 72820 | 2.3 | 75.7 | 0.0 | 75.7 | 75.7 | 0.0 | 0 | 75.7 | 1.040 | | | | |
| ASM002498 | Glostadsbäcken | 12:1 | 1.60 | 351340 | 451880 | 14.3 | 380.0 | 0.0 | 380.0 | 477.8 | 0.0 | 0 | 477.8 | 1.057 | | | | |
| ASM001518B | Stålglobäcken | 13:1 | 0.68 | 149380 | 149380 | 4.7 | 173.1 | 0.0 | 173.1 | 173.1 | 0.0 | 0 | 173.1 | 1.159 | PSM002086 | 0.005 | 3.069 | 62 |
| ASM001518A | Stålglobäcken | 13:1 | 0.35 | 77880 | 227260 | 7.2 | 81.3 | 0.0 | 81.3 | 254.4 | 0.0 | 0 | 254.4 | 1.119 | | | | |
| ASM002462 | Uvöbäcken | 15:1 | 0.97 | 212740 | 212740 | 6.7 | 183.0 | 0.0 | 183.0 | 183.0 | 0.0 | 0 | 183.0 | 0.860 | | | | |
| ASM002497 | Stekebäcken | 14:2 | 0.44 | 95700 | 95700 | 3.0 | 98.0 | 0.0 | 98.0 | 98.0 | 0.0 | 0 | 98.0 | 1.024 | | | | |
| ASM001517 | Stekebäcken | 14:1 | 0.90 | 198660 | 294360 | 9.3 | 178.8 | 0.0 | 178.8 | 276.9 | 0.0 | 0 | 276.9 | 0.941 | | | | |
| ASM002463 | Svartebäck | 16:1 | 0.50 | 110880 | 110880 | 3.5 | 92.3 | 0.0 | 92.3 | 92.3 | 0.0 | 0 | 92.3 | 0.833 | | | | |
| ASM002655 | Coastal area | | 2.71 | 596420 | 596420 | 18.9 | 513.1 | 0.0 | 513.1 | 513.1 | 0.0 | 0 | 513.1 | 0.860 | | | | |
| ASM002658 | Coastal area | | 1.26 | 277420 | 277420 | 8.8 | 216.9 | 0.0 | 216.9 | 216.9 | 0.0 | 0 | 216.9 | 0.782 | | | | |
| ASM002656 | Coastal area | | 0.22 | 48400 | 48400 | 1.5 | 40.6 | 0.0 | 40.6 | 40.6 | 0.0 | 0 | 40.6 | 0.839 | | | | |
| ASM002660 | Coastal area | | 0.14 | 30360 | 30360 | 1.0 | 21.8 | 0.0 | 21.8 | 21.8 | 0.0 | 0 | 21.8 | 0.718 | | | | |
| ASM002659 | Coastal area | | 15.70 | 3453780 | 3453780 | 109.5 | 3692.2 | 810.2 | 4502.3 | 4502.3 | 0.0 | 0 | 4502.3 | 1.304 | | | | |
| ASM002657 | Coastal area | | 2.60 | 571340 | 571340 | 18.1 | 517.3 | 0.0 | 517.3 | 517.3 | 0.0 | 0 | 517.3 | 0.905 | | | | |
| ASM001522 | Uthammarsån | 17:5 | 0.57 | 125620 | 125620 | 4.0 | 115.5 | 0.0 | 115.5 | 115.5 | 0.0 | 0 | 115.5 | 0.919 | | | | |
| ASM001523 | Uthammarsån | 17:6 | 0.96 | 210760 | 210760 | 6.7 | 252.4 | 0.0 | 252.4 | 252.4 | 0.0 | 0 | 252.4 | 1.198 | | | | |
| ASM001521 | Uthammarsån | 17:4 | 0.20 | 44880 | 44880 | 1.4 | 54.2 | 0.0 | 54.2 | 54.2 | 0.0 | 0 | 54.2 | 1.208 | | | | |
| ASM001520 | Uthammarsån | 17:3 | 0.08 | 17820 | 17820 | 0.6 | 24.3 | 0.0 | 24.3 | 24.3 | 0.0 | 0 | 24.3 | 1.363 | | | | |
| ASM002494B | Uthammarsån | 17:1 | 2.91 | 640860 | 1039940 | 33.0 | 603.9 | 0.0 | 603.9 | 1050.2 | 0.0 | 0 | 1050.2 | 1.010 | PSM002076 | 0.033 | 1.170 | 14 |
| ASM001533 | Uthammarsån | 17:2 | 0.51 | 112640 | 112640 | 3.6 | 137.4 | 0.0 | 137.4 | 137.4 | 0.0 | 0 | 137.4 | 1.220 | | | | |
| ASM002494A | Uthammarsån | 17:1 | 1.78 | 391820 | 1544400 | 49.0 | 495.5 | 0.0 | 495.5 | 1683.1 | 0.0 | 0 | 1683.1 | 1.090 | | | | |
| ASM001528 | Släthultebäcken | 18:5 | 0.32 | 70400 | 70400 | 2.2 | 53.1 | 0.0 | 53.1 | 53.1 | 0.0 | 0 | 53.1 | 0.754 | | | | |
| ASM002477 | Släthultebäcken | 18:4 | 0.66 | 144980 | 215380 | 6.8 | 105.4 | 0.0 | 105.4 | 158.5 | 0.0 | 0 | 158.5 | 0.736 | | | | |
| ASM001531 | Släthultebäcken | 18:8 | 0.30 | 66440 | 66440 | 2.1 | 50.2 | 0.0 | 50.2 | 50.2 | 0.0 | 0 | 50.2 | 0.756 | | | | |
| ASM001532 | Släthultebäcken | 18:9 | 0.11 | 24420 | 24420 | 0.8 | 37.9 | 0.0 | 37.9 | 37.9 | 0.0 | 0 | 37.9 | 1.552 | | | | |
| ASM002455 | Släthultebäcken | 18:7 | 0.76 | 167420 | 258280 | 8.2 | 191.3 | 0.0 | 191.3 | 279.5 | 0.0 | 0 | 279.5 | 1.082 | | | | |
| ASM002475 | Släthultebäcken | 18:6 | 1.06 | 232100 | 490380 | 15.5 | 175.0 | 0.0 | 175.0 | 454.5 | 0.0 | 0 | 454.5 | 0.927 | | | | |
| ASM001526 | Släthultebäcken | 18:3 | 0.40 | 88220 | 88220 | 2.8 | 66.4 | 0.0 | 66.4 | 66.4 | 0.0 | 0 | 66.4 | 0.752 | | | | |
| ASM002481C | Släthultebäcken | 18:1 | 2.44 | 537020 | 1027400 | 32.6 | 830.3 | 629.4 | 1459.7 | 1914.2 | 0.0 | 0 | 1914.2 | 1.863 | PSM002070 | | | |
| ASM002481B | Släthultebäcken | 18:1 | 2.13 | 469260 | 1800260 | 57.1 | 448.6 | 0.0 | 448.6 | 2587.6 | 0.0 | 0 | 2587.6 | 1.437 | PSM002075 | | | |
| ASM001525 | Släthultebäcken | 18:2 | 0.77 | 169620 | 169620 | 5.4 | 197.2 | 0.0 | 197.2 | 197.2 | 0.0 | 0 | 197.2 | 1.163 | | | | |
| ASM002481A | Släthultebäcken | 18:1 | 0.00 | 220 | 1970100 | 62.5 | 0.6 | 0.0 | 0.6 | 2785.4 | 0.0 | 0 | 2785.4 | 1.414 | | | | |
| ASM001444 | Sörämagasinet | 11:1 | 0.52 | 115060 | 115060 | 3.6 | 136.8 | 0.0 | 136.8 | 136.8 | 0.0 | 0 | 136.8 | 1.189 | | | | |
| ASM002466 | Stekflagebäcken | 22:1 | 0.36 | 78980 | 78980 | 2.5 | 59.6 | 0.0 | 59.6 | 59.6 | 0.0 | 0 | 59.6 | 0.755 | | | | |
| ASM002653 | Coastal area | | 0.76 | 166980 | 166980 | 5.3 | 130.6 | 0.0 | 130.6 | 130.6 | 0.0 | 0 | 130.6 | 0.782 | | | | |
| ASM002470 | Skölkebäcken | 26:1 | 0.17 | 36300 | 36300 | 1.2 | 43.1 | 0.0 | 43.1 | 43.1 | 0.0 | 0 | 43.1 | 1.187 | | | | |
| ASM002469 | Gloebäcken | 25:1 | 0.13 | 28820 | 28820 | 0.9 | 34.9 | 0.0 | 34.9 | 34.9 | 0.0 | 0 | 34.9 | 1.211 | | | | |
| ASM002468 | Lindströmmebäcken | 24:1 | 0.19 | 42240 | 42240 | 1.3 | 41.9 | 0.0 | 41.9 | 41.9 | 0.0 | 0 | 41.9 | 0.992 | | | | |
| ASM002467B | Vadvikebäcken | 23:1 | 0.30 | 65560 | 65560 | 2.1 | 50.7 | 0.0 | 50.7 | 50.7 | 0.0 | 0 | 50.7 | 0.773 | PSM107735 | 0.002 | 1.464 | 47 |
| ASM002467A | Vadvikebäcken | 23:1 | 0.01 | 1980 | 67540 | 2.1 | 2.3 | 0.0 | 2.3 | 53.0 | 0.0 | 0 | 53.0 | 0.784 | | | | |
| | **Kärrviksån** | 5:1-20 | 27.31 | 6007100 | 6007100 | 26.9 | 5967.4 | 821.0 | 6788.4 | | 0.0 | 0 | 6788.4 | 1.130 | | | | |
| | **Laxemarån** | 10:1-32 | 40.97 | 9014280 | 9014280 | 37.5 | 9048.4 | 2052.7 | 11101.1 | | 0.0 | 0 | 11101.1 | 1.232 | | | | |
| | **All catchments** | | 129.97 | 28593620 | 28593620 | 22.3 | 28775.9 | 4313.4 | 33089.3 | | 0.0 | 0 | 33089.3 | 1.157 | | | | |

| Sodium (Na) | | | | Water balance | | | Total per catchment | | | Total including contributions from upstream catchments | | | | | Calibration data | | | |
|---|---|---|---|---|---|---|---|---|---|---|---|---|---|---|---|---|---|---|
| Idcode | Name | ARO | Area | $Q_{catch}$ | $Q_{out}$ | q | Diffuse | Point | Total | Total IN | Retention | | Total OUT | Conc. | Reference | q | Conc. | Deviation |
| | | | $km^2$ | $m^3 \cdot yr^{-1}$ | $m^3 \cdot yr^{-1}$ | $L \cdot s^{-1}$ | $kg \cdot yr^{-1}$ | $kg \cdot yr^{-1}$ | $kg \cdot yr^{-1}$ | $kg \cdot yr^{-1}$ | $kg \cdot yr^{-1}$ | % | $kg \cdot yr^{-1}$ | $mg \cdot L^{-1}$ | | $L \cdot s^{-1}$ | $mg \cdot L^{-1}$ | % |
| ASM002474 | Kärrviksån | 5:20 | 0.12 | 25740 | 25740 | 0.8 | 109.4 | 1788.9 | 1898.3 | 1898.3 | 0.0 | 0 | 1898.3 | 73.750 | | | | |
| ASM002493 | Kärrviksån | 5:19 | 0.84 | 184140 | 209880 | 6.7 | 967.8 | 0.0 | 967.8 | 2866.1 | 0.0 | 0 | 2866.1 | 13.656 | | | | |
| ASM001483 | Kärrviksån | 5:17 | 0.15 | 33220 | 33220 | 1.1 | 301.2 | 0.0 | 301.2 | 301.2 | 0.0 | 0 | 301.2 | 9.067 | | | | |
| ASM002492 | Kärrviksån | 5:16 | 1.11 | 243980 | 277200 | 8.8 | 1588.0 | 0.0 | 1588.0 | 1889.2 | 0.0 | 0 | 1889.2 | 6.815 | | | | |
| ASM002491 | Kärrviksån | 5:15 | 1.87 | 411840 | 689040 | 21.8 | 2123.3 | 0.0 | 2123.3 | 4012.5 | 0.0 | 0 | 4012.5 | 5.823 | | | | |
| ASM001474 | Kärrviksån | 5:7 | 0.45 | 99000 | 99000 | 3.1 | 548.4 | 0.0 | 548.4 | 548.4 | 0.0 | 0 | 548.4 | 5.539 | | | | |
| ASM002487 | Kärrviksån | 5:6 | 1.20 | 264000 | 363000 | 11.5 | 1758.3 | 0.0 | 1758.3 | 2306.7 | 0.0 | 0 | 2306.7 | 6.355 | | | | |
| ASM001472 | Kärrviksån | 5:4 | 1.10 | 242880 | 242880 | 7.7 | 983.9 | 0.0 | 983.9 | 983.9 | 0.0 | 0 | 983.9 | 4.051 | | | | |
| ASM001470 | Kärrviksån | 5:3 | 0.40 | 87560 | 87560 | 2.8 | 422.1 | 0.0 | 422.1 | 422.1 | 0.0 | 0 | 422.1 | 4.821 | | | | |
| ASM001469 | Kärrviksån | 5:2 | 0.97 | 212960 | 212960 | 6.8 | 1082.0 | 0.0 | 1082.0 | 1082.0 | 0.0 | 0 | 1082.0 | 5.081 | | | | |
| ASM001471 | Kärrviksån | 5:5 | 2.79 | 614680 | 614680 | 19.5 | 3060.6 | 0.0 | 3060.6 | 3060.6 | 0.0 | 0 | 3060.6 | 4.979 | | | | |
| ASM001479 | Kärrviksån | 5:13 | 0.65 | 142340 | 142340 | 4.5 | 605.0 | 0.0 | 605.0 | 605.0 | 0.0 | 0 | 605.0 | 4.250 | | | | |
| ASM001480 | Kärrviksån | 5:14 | 0.10 | 22660 | 22660 | 0.7 | 117.5 | 0.0 | 117.5 | 117.5 | 0.0 | 0 | 117.5 | 5.184 | | | | |
| ASM002490 | Kärrviksån | 5:12 | 0.84 | 183920 | 348920 | 11.1 | 911.8 | 4299.1 | 5210.9 | 5933.4 | 0.0 | 0 | 5933.4 | 17.005 | | | | |
| ASM001478 | Kärrviksån | 5:11 | 0.49 | 108460 | 108460 | 3.4 | 461.0 | 0.0 | 461.0 | 461.0 | 0.0 | 0 | 461.0 | 4.250 | | | | |
| ASM002489 | Kärrviksån | 5:10 | 1.20 | 263560 | 372020 | 11.8 | 1175.8 | 0.0 | 1175.8 | 1636.8 | 0.0 | 0 | 1636.8 | 4.400 | | | | |
| ASM001476 | Kärrviksån | 5:9 | 3.62 | 796180 | 796180 | 25.2 | 5269.7 | 0.0 | 5269.7 | 5269.7 | 0.0 | 0 | 5269.7 | 6.619 | | | | |
| ASM001475B | Kärrviksån | 5:8 | 1.38 | 302940 | 1820060 | 57.7 | 1377.5 | 0.0 | 1377.5 | 14217.4 | 0.0 | 0 | 14217.4 | 7.811 | PSM002081 | 0.058 | 4.213 | 85 |
| ASM001475A | Kärrviksån | 5:8 | 0.04 | 9680 | 1829740 | 58.0 | 44.8 | 0.0 | 44.8 | 14262.1 | 0.0 | 0 | 14262.1 | 7.795 | | | | |
| ASM002479 | Kärrviksån | 5:18 | 1.18 | 259600 | 259600 | 8.2 | 1207.6 | 0.0 | 1207.6 | 1207.6 | 0.0 | 0 | 1207.6 | 4.652 | | | | |
| ASM002486C | Kärrviksån | 5:1 | 2.75 | 604560 | 1074040 | 34.1 | 2787.7 | 4388.8 | 7176.5 | 11250.2 | 0.0 | 0 | 11250.2 | 10.475 | PSM002080 | | | |
| ASM002486B | Kärrviksån | 5:1 | 1.13 | 247940 | 3840760 | 121.8 | 1234.0 | 0.0 | 1234.0 | 30758.8 | 0.0 | 0 | 30758.8 | 8.009 | PSM002082 | 0.121 | 6.493 | 23 |
| ASM002486A | Kärrviksån | 5:1 | 2.93 | 645260 | 6007100 | 190.5 | 3313.9 | 0.0 | 3313.9 | 41927.9 | 0.0 | 0 | 41927.9 | 6.980 | PSM002083 | 0.190 | 7.548 | 8 |
| ASM002449 | Bjurhidebäcken | 4:1 | 0.63 | 139040 | 139040 | 4.4 | 591.0 | 0.0 | 591.0 | 591.0 | 0.0 | 0 | 591.0 | 4.251 | | | | |
| ASM002472 | Sörviksån | 3:2 | 0.47 | 103400 | 103400 | 3.3 | 439.5 | 0.0 | 439.5 | 439.5 | 0.0 | 0 | 439.5 | 4.250 | | | | |
| ASM002473 | Sörviksån | 3:1 | 0.53 | 116600 | 220000 | 7.0 | 495.6 | 0.0 | 495.6 | 935.0 | 0.0 | 0 | 935.0 | 4.250 | | | | |
| ASM002651 | Coastal area | | 1.67 | 368280 | 368280 | 11.7 | 1543.6 | 0.0 | 1543.6 | 1543.6 | 0.0 | 0 | 1543.6 | 4.191 | | | | |
| ASM002447 | Bodvikebäcken | 2:1 | 0.38 | 83600 | 83600 | 2.7 | 283.2 | 0.0 | 283.2 | 283.2 | 0.0 | 0 | 283.2 | 3.387 | | | | |
| ASM002446 | Långbonäsbäcken | 1:1 | 0.07 | 15400 | 15400 | 0.5 | 65.4 | 0.0 | 65.4 | 65.4 | 0.0 | 0 | 65.4 | 4.250 | | | | |
| ASM002464 | Flakvarpebäcken | 19:1 | 0.18 | 40480 | 40480 | 1.3 | 157.5 | 0.0 | 157.5 | 157.5 | 0.0 | 0 | 157.5 | 3.891 | | | | |
| ASM002465 | Jössesbäcken | 20:1 | 0.11 | 24420 | 24420 | 0.8 | 201.8 | 0.0 | 201.8 | 201.8 | 0.0 | 0 | 201.8 | 8.264 | | | | |
| ASM002471 | Äspöbäcken | 21:1 | 0.06 | 13860 | 13860 | 0.4 | 58.9 | 0.0 | 58.9 | 58.9 | 0.0 | 0 | 58.9 | 4.250 | | | | |
| ASM002652 | Coastal area | | 1.39 | 305140 | 305140 | 9.7 | 1423.9 | 0.0 | 1423.9 | 1423.9 | 0.0 | 0 | 1423.9 | 4.666 | | | | |
| ASM001445 | Frisksjön | 7:2 | 1.85 | 406560 | 406560 | 12.9 | 2055.8 | 0.0 | 2055.8 | 2055.8 | 0.0 | 0 | 2055.8 | 5.057 | | | | |
| ASM001484 | Kåreviksån | 7:1 | 0.21 | 46860 | 453420 | 14.4 | 199.2 | 0.0 | 199.2 | 2255.0 | 0.0 | 0 | 2255.0 | 4.973 | | | | |
| ASM001486B | Mederhultsån | 6:1 | 1.92 | 422620 | 422620 | 13.4 | 2436.3 | 0.0 | 2436.3 | 2436.3 | 0.0 | 0 | 2436.3 | 5.765 | PSM002084 | 0.013 | 8.619 | 33 |
| ASM001486A | Mederhultsån | 6:1 | 0.08 | 18040 | 440660 | 14.0 | 78.4 | 0.0 | 78.4 | 2514.7 | 0.0 | 0 | 2514.7 | 5.707 | | | | |
| ASM002654 | Coastal area | | 1.86 | 409420 | 409420 | 13.0 | 1828.3 | 0.0 | 1828.3 | 1828.3 | 0.0 | 0 | 1828.3 | 4.466 | | | | |
| ASM002460 | Pistlanbäcken | 8:1 | 0.50 | 109780 | 109780 | 3.5 | 516.2 | 0.0 | 516.2 | 516.2 | 0.0 | 0 | 516.2 | 4.702 | | | | |
| ASM001490 | Ekerumsån | 9:3 | 0.22 | 48840 | 48840 | 1.5 | 439.5 | 0.0 | 439.5 | 439.5 | 0.0 | 0 | 439.5 | 9.000 | | | | |
| ASM001489 | Ekerumsån | 9:2 | 0.77 | 168740 | 168740 | 5.4 | 1716.4 | 0.0 | 1716.4 | 1716.4 | 0.0 | 0 | 1716.4 | 10.172 | | | | |
| ASM002483B | Ekerumsån | 9:1 | 1.50 | 330880 | 548460 | 17.4 | 1883.2 | 0.0 | 1883.2 | 4039.1 | 0.0 | 0 | 4039.1 | 7.364 | PSM002085 | 0.017 | 7.337 | 0 |
| ASM002483A | Ekerumsån | 9:1 | 0.34 | 75020 | 623480 | 19.8 | 442.2 | 0.0 | 442.2 | 4481.3 | 0.0 | 0 | 4481.3 | 7.188 | | | | |
| ASM002478 | Laxemarån | 10:32 | 0.02 | 5060 | 5060 | 0.2 | 21.5 | 0.0 | 21.5 | 21.5 | 0.0 | 0 | 21.5 | 4.250 | | | | |
| ASM002482 | Laxemarån | 10:31 | 0.87 | 190740 | 195800 | 6.2 | 810.7 | 0.0 | 810.7 | 832.2 | 0.0 | 0 | 832.2 | 4.250 | | | | |
| ASM002480B | Laxemarån | 10:30 | 4.23 | 931480 | 1127280 | 35.7 | 3841.3 | 0.0 | 3841.3 | 4673.5 | 0.0 | 0 | 4673.5 | 4.146 | PSM002068 | 0.036 | 4.146 | 0 |
| ASM002480A | Jämsen | 10:30 | 1.83 | 403480 | 1530760 | 48.5 | 1650.2 | 3512.7 | 5162.9 | 9836.3 | 0.0 | 0 | 9836.3 | 6.426 | PSM002069 | 0.049 | 8.321 | 23 |
| ASM001516 | Laxemarån | 10:29 | 0.53 | 117260 | 117260 | 3.7 | 680.5 | 0.0 | 680.5 | 680.5 | 0.0 | 0 | 680.5 | 5.803 | | | | |
| ASM001515 | Laxemarån | 10:28 | 0.34 | 74140 | 74140 | 2.4 | 527.1 | 2367.6 | 2894.7 | 2894.7 | 0.0 | 0 | 2894.7 | 39.043 | | | | |
| ASM001514 | Laxemarån | 10:27 | 0.49 | 107140 | 107140 | 3.4 | 924.3 | 1352.9 | 2277.2 | 2277.2 | 0.0 | 0 | 2277.2 | 21.255 | | | | |
| ASM001446 | Plittorpsgöl | 10:26 | 0.68 | 149160 | 149160 | 4.7 | 646.8 | 1324.4 | 1971.1 | 1971.1 | 0.0 | 0 | 1971.1 | 13.215 | | | | |
| ASM002459 | Laxemarån | 10:25 | 0.10 | 21780 | 170940 | 5.4 | 92.6 | 1263.3 | 1355.8 | 3327.0 | 0.0 | 0 | 3327.0 | 19.463 | | | | |
| ASM001512 | Laxemarån | 10:24 | 0.49 | 108680 | 108680 | 3.4 | 506.2 | 0.0 | 506.2 | 506.2 | 0.0 | 0 | 506.2 | 4.658 | | | | |
| ASM002476E | Laxemarån | 10:1 | 3.95 | 868780 | 2977700 | 94.4 | 4535.9 | 8141.9 | 12677.7 | 32199.6 | 0.0 | 0 | 32199.6 | 10.814 | PSM002071 | 0.094 | 10.814 | 0 |
| ASM001510 | Laxemarån | 10:22 | 0.56 | 123640 | 123640 | 3.9 | 541.7 | 2526.5 | 3068.2 | 3068.2 | 0.0 | 0 | 3068.2 | 24.815 | | | | |
| ASM002453 | Laxemarån | 10:21 | 0.45 | 97900 | 221540 | 7.0 | 427.4 | 668.3 | 1095.7 | 4163.8 | 0.0 | 0 | 4163.8 | 18.795 | | | | |
| ASM002450B | Laxemarån | 10:20 | 2.39 | 526240 | 747780 | 23.7 | 2506.6 | 5036.7 | 7543.3 | 11707.2 | 0.0 | 0 | 11707.2 | 15.656 | PSM002072 | | | |
| ASM002450A | Laxemarån | 10:20 | 0.19 | 41140 | 788920 | 25.0 | 195.2 | 0.0 | 195.2 | 11902.4 | 0.0 | 0 | 11902.4 | 15.087 | | | | |
| ASM001511 | Laxemarån | 10:23 | 0.74 | 162800 | 162800 | 5.2 | 728.8 | 0.0 | 728.8 | 728.8 | 0.0 | 0 | 728.8 | 4.477 | | | | |
| ASM001448 | Grangöl | 10:19 | 0.50 | 108900 | 108900 | 3.5 | 509.2 | 0.0 | 509.2 | 509.2 | 0.0 | 0 | 509.2 | 4.676 | | | | |
| ASM002499 | Laxemarån | 10:18 | 0.06 | 12760 | 121660 | 3.9 | 129.2 | 0.0 | 129.2 | 638.4 | 0.0 | 0 | 638.4 | 5.247 | | | | |
| ASM001506 | Laxemarån | 10:17 | 0.40 | 87560 | 87560 | 2.8 | 608.7 | 0.0 | 608.7 | 608.7 | 0.0 | 0 | 608.7 | 6.952 | | | | |
| ASM001447 | Fjällgöl | 10:16 | 0.30 | 64900 | 64900 | 2.1 | 256.4 | 0.0 | 256.4 | 256.4 | 0.0 | 0 | 256.4 | 3.950 | | | | |
| ASM002451 | Laxemarån | 10:15 | 0.33 | 71500 | 136400 | 4.3 | 537.3 | 0.0 | 537.3 | 793.6 | 0.0 | 0 | 793.6 | 5.818 | | | | |
| ASM002452 | Laxemarån | 10:14 | 2.38 | 522500 | 868120 | 27.5 | 3389.7 | 0.0 | 3389.7 | 5430.4 | 0.0 | 0 | 5430.4 | 6.255 | | | | |
| ASM001503 | Laxemarån | 10:13 | 0.42 | 91520 | 91520 | 2.9 | 752.0 | 0.0 | 752.0 | 752.0 | 0.0 | 0 | 752.0 | 8.217 | | | | |
| ASM002454 | Laxemarån | 10:12 | 0.81 | 177760 | 269280 | 8.5 | 1456.4 | 0.0 | 1456.4 | 2208.4 | 0.0 | 0 | 2208.4 | 8.201 | | | | |
| ASM001501 | Laxemarån | 10:11 | 0.81 | 177320 | 177320 | 5.6 | 1291.2 | 0.0 | 1291.2 | 1291.2 | 0.0 | 0 | 1291.2 | 7.282 | | | | |
| ASM002457 | Laxemarån | 10:10 | 1.39 | 305580 | 482900 | 15.3 | 3012.8 | 0.0 | 3012.8 | 4304.0 | 0.0 | 0 | 4304.0 | 8.913 | | | | |
| ASM002476D | Laxemarån | 10:1 | 4.96 | 1091860 | 6641580 | 210.6 | 5798.2 | 0.0 | 5798.2 | 62571.7 | 0.0 | 0 | 62571.7 | 9.421 | PSM002077 | | | |
| ASM001499 | Laxemarån | 10:9 | 0.71 | 156420 | 156420 | 5.0 | 811.4 | 0.0 | 811.4 | 811.4 | 0.0 | 0 | 811.4 | 5.187 | | | | |
| ASM001498 | Laxemarån | 10:8 | 2.77 | 609620 | 766040 | 24.3 | 3044.7 | 0.0 | 3044.7 | 3856.1 | 0.0 | 0 | 3856.1 | 5.034 | PSM002078 | 0.024 | 4.079 | 23 |
| ASM001497 | Laxemarån | 10:7 | 0.61 | 133980 | 133980 | 4.2 | 858.0 | 0.0 | 858.0 | 858.0 | 0.0 | 0 | 858.0 | 6.404 | | | | |
| ASM002476C | Laxemarån | 10:1 | 0.32 | 69300 | 7610900 | 241.3 | 381.2 | 0.0 | 381.2 | 67667.1 | 0.0 | 0 | 67667.1 | 8.891 | PSM002079 | 0.242 | 8.797 | 1 |
| ASM001494 | Laxemarån | 10:4 | 1.00 | 220220 | 220220 | 7.0 | 1929.3 | 0.0 | 1929.3 | 1929.3 | 0.0 | 0 | 1929.3 | 8.761 | | | | |
| ASM001493 | Laxemarån | 10:3 | 0.32 | 70180 | 70180 | 2.2 | 470.9 | 0.0 | 470.9 | 470.9 | 0.0 | 0 | 470.9 | 6.711 | | | | |
| ASM001492 | Laxemarån | 10:2 | 0.46 | 101200 | 101200 | 3.2 | 784.6 | 0.0 | 784.6 | 784.6 | 0.0 | 0 | 784.6 | 7.753 | | | | |
| ASM001496 | Laxemarån | 10:6 | 0.89 | 195800 | 195800 | 6.2 | 1273.8 | 0.0 | 1273.8 | 1273.8 | 0.0 | 0 | 1273.8 | 6.506 | | | | |
| ASM001495 | Laxemarån | 10:5 | 0.29 | 63800 | 63800 | 2.0 | 306.4 | 0.0 | 306.4 | 306.4 | 0.0 | 0 | 306.4 | 4.803 | | | | |
| ASM002476B | Laxemarån | 10:1 | 3.23 | 710820 | 8972920 | 284.5 | 4554.9 | 0.0 | 4554.9 | 76987.1 | 0.0 | 0 | 76987.1 | 8.580 | PSM002087 | 0.285 | 9.013 | 5 |
| ASM002476A | Laxemarån | 10:1 | 0.19 | 41360 | 9014280 | 285.8 | 205.8 | 0.0 | 205.8 | 77192.9 | 0.0 | 0 | 77192.9 | 8.563 | | | | |
| ASM002495 | Glostadsbäcken | 12:3 | 0.13 | 27720 | 27720 | 0.9 | 124.2 | 0.0 | 124.2 | 124.2 | 0.0 | 0 | 124.2 | 4.479 | | | | |
| ASM002485 | Glostadsbäcken | 12:2 | 0.33 | 72820 | 72820 | 2.3 | 517.3 | 0.0 | 517.3 | 517.3 | 0.0 | 0 | 517.3 | 7.104 | | | | |
| ASM002498 | Glostadsbäcken | 12:1 | 1.60 | 351340 | 451880 | 14.3 | 2599.8 | 0.0 | 2599.8 | 3241.2 | 0.0 | 0 | 3241.2 | 7.173 | | | | |
| ASM001518B | Stålglobäcken | 13:1 | 0.68 | 149380 | 149380 | 4.7 | 1189.3 | 0.0 | 1189.3 | 1189.3 | 0.0 | 0 | 1189.3 | 7.961 | PSM002086 | 0.005 | 11.637 | 32 |
| ASM001518A | Stålglobäcken | 13:1 | 0.35 | 77880 | 227260 | 7.2 | 556.4 | 0.0 | 556.4 | 1745.7 | 0.0 | 0 | 1745.7 | 7.682 | | | | |
| ASM002462 | Uvöbäcken | 15:1 | 0.97 | 212740 | 212740 | 6.7 | 1130.2 | 0.0 | 1130.2 | 1130.2 | 0.0 | 0 | 1130.2 | 5.312 | | | | |
| ASM002497 | Stekebäcken | 14:2 | 0.44 | 95700 | 95700 | 3.0 | 665.1 | 0.0 | 665.1 | 665.1 | 0.0 | 0 | 665.1 | 6.950 | | | | |
| ASM001517 | Stekebäcken | 14:1 | 0.90 | 198660 | 294360 | 9.3 | 1024.0 | 0.0 | 1024.0 | 1689.1 | 0.0 | 0 | 1689.1 | 5.738 | | | | |
| ASM002463 | Svartebäck | 16:1 | 0.50 | 110880 | 110880 | 3.5 | 469.7 | 0.0 | 469.7 | 469.7 | 0.0 | 0 | 469.7 | 4.237 | | | | |
| ASM002655 | Coastal area | | 2.71 | 596420 | 596420 | 18.9 | 2816.5 | 0.0 | 2816.5 | 2816.5 | 0.0 | 0 | 2816.5 | 4.722 | | | | |
| ASM002658 | Coastal area | | 1.26 | 277420 | 277420 | 8.8 | 1269.4 | 0.0 | 1269.4 | 1269.4 | 0.0 | 0 | 1269.4 | 4.576 | | | | |
| ASM002656 | Coastal area | | 0.22 | 48400 | 48400 | 1.5 | 196.6 | 0.0 | 196.6 | 196.6 | 0.0 | 0 | 196.6 | 4.061 | | | | |
| ASM002660 | Coastal area | | 0.14 | 30360 | 30360 | 1.0 | 122.8 | 0.0 | 122.8 | 122.8 | 0.0 | 0 | 122.8 | 4.046 | | | | |
| ASM002659 | Coastal area | | 15.70 | 3453780 | 3453780 | 109.5 | 17471.5 | 10338.3 | 27809.8 | 27809.8 | 0.0 | 0 | 27809.8 | 8.052 | | | | |
| ASM002657 | Coastal area | | 2.60 | 571340 | 571340 | 18.1 | 2839.9 | 0.0 | 2839.9 | 2839.9 | 0.0 | 0 | 2839.9 | 4.971 | | | | |
| ASM001522 | Uthammarsån | 17:5 | 0.57 | 125620 | 125620 | 4.0 | 741.3 | 0.0 | 741.3 | 741.3 | 0.0 | 0 | 741.3 | 5.901 | | | | |
| ASM001523 | Uthammarsån | 17:6 | 0.96 | 210760 | 210760 | 6.7 | 1495.4 | 0.0 | 1495.4 | 1495.4 | 0.0 | 0 | 1495.4 | 7.095 | | | | |
| ASM001521 | Uthammarsån | 17:4 | 0.20 | 44880 | 44880 | 1.4 | 394.3 | 0.0 | 394.3 | 394.3 | 0.0 | 0 | 394.3 | 8.786 | | | | |
| ASM001520 | Uthammarsån | 17:3 | 0.08 | 17820 | 17820 | 0.6 | 184.1 | 0.0 | 184.1 | 184.1 | 0.0 | 0 | 184.1 | 10.329 | | | | |
| ASM002494B | Uthammarsån | 17:1 | 2.91 | 640860 | 1039940 | 33.0 | 3869.7 | 0.0 | 3869.7 | 6684.8 | 0.0 | 0 | 6684.8 | 6.428 | PSM002076 | 0.033 | 6.574 | 2 |
| ASM001533 | Uthammarsån | 17:2 | 0.51 | 112640 | 112640 | 3.6 | 986.1 | 0.0 | 986.1 | 986.1 | 0.0 | 0 | 986.1 | 8.755 | | | | |
| ASM002494A | Uthammarsån | 17:1 | 1.78 | 391820 | 1544400 | 49.0 | 3661.6 | 0.0 | 3661.6 | 11332.5 | 0.0 | 0 | 11332.5 | 7.338 | | | | |
| ASM001528 | Släthultebäcken | 18:5 | 0.32 | 70400 | 70400 | 2.2 | 299.2 | 0.0 | 299.2 | 299.2 | 0.0 | 0 | 299.2 | 4.250 | | | | |
| ASM002477 | Släthultebäcken | 18:4 | 0.66 | 144980 | 215380 | 6.8 | 594.2 | 0.0 | 594.2 | 893.5 | 0.0 | 0 | 893.5 | 4.148 | | | | |
| ASM001531 | Släthultebäcken | 18:8 | 0.30 | 66440 | 66440 | 2.1 | 284.0 | 0.0 | 284.0 | 284.0 | 0.0 | 0 | 284.0 | 4.274 | | | | |
| ASM001532 | Släthultebäcken | 18:9 | 0.11 | 24420 | 24420 | 0.8 | 294.4 | 0.0 | 294.4 | 294.4 | 0.0 | 0 | 294.4 | 12.056 | | | | |
| ASM002455 | Släthultebäcken | 18:7 | 0.76 | 167420 | 258280 | 8.2 | 1361.7 | 0.0 | 1361.7 | 1940.1 | 0.0 | 0 | 1940.1 | 7.511 | | | | |
| ASM002475 | Släthultebäcken | 18:6 | 1.06 | 232100 | 490380 | 15.5 | 986.5 | 0.0 | 986.5 | 2926.5 | 0.0 | 0 | 2926.5 | 5.968 | | | | |
| ASM001526 | Släthultebäcken | 18:3 | 0.40 | 88220 | 88220 | 2.8 | 374.2 | 0.0 | 374.2 | 374.2 | 0.0 | 0 | 374.2 | 4.242 | | | | |
| ASM002481C | Släthultebäcken | 18:1 | 2.44 | 537020 | 1027400 | 32.6 | 3057.3 | 8031.9 | 11089.2 | 14015.7 | 0.0 | 0 | 14015.7 | 13.642 | PSM002070 | | | |
| ASM002481B | Släthultebäcken | 18:1 | 2.13 | 469260 | 1800260 | 57.1 | 2943.7 | 0.0 | 2943.7 | 18227.0 | 0.0 | 0 | 18227.0 | 10.125 | PSM002075 | | | |
| ASM001525 | Släthultebäcken | 18:2 | 0.77 | 169620 | 169620 | 5.4 | 1413.4 | 0.0 | 1413.4 | 1413.4 | 0.0 | 0 | 1413.4 | 8.333 | | | | |
| ASM002481A | Släthultebäcken | 18:1 | 0.00 | 220 | 1970100 | 62.5 | 2.9 | 0.0 | 2.9 | 19643.3 | 0.0 | 0 | 19643.3 | 9.971 | | | | |
| ASM001444 | Sörämagasinet | 11:1 | 0.52 | 115060 | 115060 | 3.6 | 401.9 | 0.0 | 401.9 | 401.9 | 0.0 | 0 | 401.9 | 3.493 | | | | |
| ASM002466 | Stekflagebäcken | 22:1 | 0.36 | 78980 | 78980 | 2.5 | 312.2 | 0.0 | 312.2 | 312.2 | 0.0 | 0 | 312.2 | 3.953 | | | | |
| ASM002653 | Coastal area | | 0.76 | 166980 | 166980 | 5.3 | 730.2 | 0.0 | 730.2 | 730.2 | 0.0 | 0 | 730.2 | 4.373 | | | | |
| ASM002470 | Skölkebäcken | 26:1 | 0.17 | 36300 | 36300 | 1.2 | 176.4 | 0.0 | 176.4 | 176.4 | 0.0 | 0 | 176.4 | 4.860 | | | | |
| ASM002469 | Gloebäcken | 25:1 | 0.13 | 28820 | 28820 | 0.9 | 136.9 | 0.0 | 136.9 | 136.9 | 0.0 | 0 | 136.9 | 4.750 | | | | |
| ASM002468 | Lindströmmebäcken | 24:1 | 0.19 | 42240 | 42240 | 1.3 | 272.3 | 0.0 | 272.3 | 272.3 | 0.0 | 0 | 272.3 | 6.447 | | | | |
| ASM002467B | Vadvikebäcken | 23:1 | 0.30 | 65560 | 65560 | 2.1 | 278.6 | 0.0 | 278.6 | 278.6 | 0.0 | 0 | 278.6 | 4.250 | PSM107735 | 0.002 | 5.272 | 19 |
| ASM002467A | Vadvikebäcken | 23:1 | 0.01 | 1980 | 67540 | 2.1 | 8.5 | 0.0 | 8.5 | 287.1 | 0.0 | 0 | 287.1 | 4.251 | | | | |
| | **Kärrviksån** | 5:1-20 | 27.31 | 6007100 | 6007100 | 26.9 | 31451.1 | 10476.9 | 41927.9 | | 0.0 | 0 | 41927.9 | 6.980 | | | | |
| | **Laxemarån** | 10:1-32 | 40.97 | 9014280 | 9014280 | 37.5 | 50998.8 | 26194.2 | 77192.9 | | 0.0 | 0 | 77192.9 | 8.563 | | | | |
| | **All catchments** | | 129.97 | 28593620 | 28593620 | 22.3 | 157559.6 | 55041.2 | 212600.8 | | 0.0 | 0 | 212600.8 | 7.435 | | | | |

| Sulphate ($SO_4^{2-}$) | | | | Water balance | | | Total per catchment | | | Total including contributions from upstream catchments | | | | | Calibration data | | | |
|---|---|---|---|---|---|---|---|---|---|---|---|---|---|---|---|---|---|---|
| Idcode | Name | ARO | Area | $Q_{catch}$ | $Q_{out}$ | q | Diffuse | Point | Total | Total IN | Retention | | Total OUT | Conc. | Reference | q | Conc. | Deviation |
| | | | $km^2$ | $m^3 \cdot yr^{-1}$ | $m^3 \cdot yr^{-1}$ | $L \cdot s^{-1}$ | $kg \cdot yr^{-1}$ | $kg \cdot yr^{-1}$ | $kg \cdot yr^{-1}$ | $kg \cdot yr^{-1}$ | $kg \cdot yr^{-1}$ | % | $kg \cdot yr^{-1}$ | $mg \cdot L^{-1}$ | | $L \cdot s^{-1}$ | $mg \cdot L^{-1}$ | % |
| ASM002474 | Kärrviksån | 5:20 | 0.12 | 25740 | 25740 | 0.8 | 229.7 | 0.0 | 229.7 | 229.7 | 0.0 | 0 | 229.7 | 8.924 | | | | |
| ASM002493 | Kärrviksån | 5:19 | 0.84 | 184140 | 209880 | 6.7 | 2031.0 | 0.0 | 2031.0 | 2260.7 | 0.0 | 0 | 2260.7 | 10.771 | | | | |
| ASM001483 | Kärrviksån | 5:17 | 0.15 | 33220 | 33220 | 1.1 | 302.4 | 0.0 | 302.4 | 302.4 | 0.0 | 0 | 302.4 | 9.104 | | | | |
| ASM002492 | Kärrviksån | 5:16 | 1.11 | 243980 | 277200 | 8.8 | 2571.1 | 0.0 | 2571.1 | 2873.5 | 0.0 | 0 | 2873.5 | 10.366 | | | | |
| ASM002491 | Kärrviksån | 5:15 | 1.87 | 411840 | 689040 | 21.8 | 7083.3 | 0.0 | 7083.3 | 9956.8 | 0.0 | 0 | 9956.8 | 14.450 | | | | |
| ASM001474 | Kärrviksån | 5:7 | 0.45 | 99000 | 99000 | 3.1 | 2129.8 | 0.0 | 2129.8 | 2129.8 | 0.0 | 0 | 2129.8 | 21.513 | | | | |
| ASM002487 | Kärrviksån | 5:6 | 1.20 | 264000 | 363000 | 11.5 | 4977.0 | 0.0 | 4977.0 | 7106.9 | 0.0 | 0 | 7106.9 | 19.578 | | | | |
| ASM001472 | Kärrviksån | 5:4 | 1.10 | 242880 | 242880 | 7.7 | 6725.6 | 0.0 | 6725.6 | 6725.6 | 0.0 | 0 | 6725.6 | 27.691 | | | | |
| ASM001470 | Kärrviksån | 5:3 | 0.40 | 87560 | 87560 | 2.8 | 2892.4 | 0.0 | 2892.4 | 2892.4 | 0.0 | 0 | 2892.4 | 33.033 | | | | |
| ASM001469 | Kärrviksån | 5:2 | 0.97 | 212960 | 212960 | 6.8 | 8423.1 | 0.0 | 8423.1 | 8423.1 | 0.0 | 0 | 8423.1 | 39.552 | | | | |
| ASM001471 | Kärrviksån | 5:5 | 2.79 | 614680 | 614680 | 19.5 | 20361.8 | 0.0 | 20361.8 | 20361.8 | 0.0 | 0 | 20361.8 | 33.126 | | | | |
| ASM001479 | Kärrviksån | 5:13 | 0.65 | 142340 | 142340 | 4.5 | 1270.3 | 0.0 | 1270.3 | 1270.3 | 0.0 | 0 | 1270.3 | 8.924 | | | | |
| ASM001480 | Kärrviksån | 5:14 | 0.10 | 22660 | 22660 | 0.7 | 202.2 | 0.0 | 202.2 | 202.2 | 0.0 | 0 | 202.2 | 8.924 | | | | |
| ASM002490 | Kärrviksån | 5:12 | 0.84 | 183920 | 348920 | 11.1 | 1641.4 | 0.0 | 1641.4 | 3113.9 | 0.0 | 0 | 3113.9 | 8.924 | | | | |
| ASM001478 | Kärrviksån | 5:11 | 0.49 | 108460 | 108460 | 3.4 | 968.0 | 0.0 | 968.0 | 968.0 | 0.0 | 0 | 968.0 | 8.924 | | | | |
| ASM002489 | Kärrviksån | 5:10 | 1.20 | 263560 | 372020 | 11.8 | 2355.1 | 0.0 | 2355.1 | 3323.0 | 0.0 | 0 | 3323.0 | 8.932 | | | | |
| ASM001476 | Kärrviksån | 5:9 | 3.62 | 796180 | 796180 | 25.2 | 12217.6 | 0.0 | 12217.6 | 12217.6 | 0.0 | 0 | 12217.6 | 15.345 | | | | |
| ASM001475B | Kärrviksån | 5:8 | 1.38 | 302940 | 1820060 | 57.7 | 3497.4 | 0.0 | 3497.4 | 22151.9 | 0.0 | 0 | 22151.9 | 12.171 | PSM002081 | 0.058 | 9.861 | 23 |
| ASM001475A | Kärrviksån | 5:8 | 0.04 | 9680 | 1829740 | 58.0 | 344.5 | 0.0 | 344.5 | 22496.5 | 0.0 | 0 | 22496.5 | 12.295 | | | | |
| ASM002479 | Kärrviksån | 5:18 | 1.18 | 259600 | 259600 | 8.2 | 3790.9 | 0.0 | 3790.9 | 3790.9 | 0.0 | 0 | 3790.9 | 14.603 | | | | |
| ASM002486C | Kärrviksån | 5:1 | 2.75 | 604560 | 1074040 | 34.1 | 7313.6 | 0.0 | 7313.6 | 13365.3 | 0.0 | 0 | 13365.3 | 12.444 | PSM002080 | | | |
| ASM002486B | Kärrviksån | 5:1 | 1.13 | 247940 | 3840760 | 121.8 | 6888.1 | 0.0 | 6888.1 | 52706.7 | 0.0 | 0 | 52706.7 | 13.723 | PSM002082 | 0.121 | 10.524 | 30 |
| ASM002486A | Kärrviksån | 5:1 | 2.93 | 645260 | 6007100 | 190.5 | 24081.5 | 0.0 | 24081.5 | 122297.9 | 0.0 | 0 | 122297.9 | 20.359 | PSM002083 | 0.190 | 13.281 | 53 |
| ASM002449 | Bjurhidebäcken | 4:1 | 0.63 | 139040 | 139040 | 4.4 | 4925.5 | 0.0 | 4925.5 | 4925.5 | 0.0 | 0 | 4925.5 | 35.425 | | | | |
| ASM002472 | Sörviksån | 3:2 | 0.47 | 103400 | 103400 | 3.3 | 3891.9 | 0.0 | 3891.9 | 3891.9 | 0.0 | 0 | 3891.9 | 37.640 | | | | |
| ASM002473 | Sörviksån | 3:1 | 0.53 | 116600 | 220000 | 7.0 | 4919.2 | 0.0 | 4919.2 | 8811.1 | 0.0 | 0 | 8811.1 | 40.050 | | | | |
| ASM002651 | Coastal area | | 1.67 | 368280 | 368280 | 11.7 | 15132.1 | 0.0 | 15132.1 | 15132.1 | 0.0 | 0 | 15132.1 | 41.089 | | | | |
| ASM002447 | Bodvikebäcken | 2:1 | 0.38 | 83600 | 83600 | 2.7 | 3546.0 | 0.0 | 3546.0 | 3546.0 | 0.0 | 0 | 3546.0 | 42.416 | | | | |
| ASM002446 | Långbonäsbäcken | 1:1 | 0.07 | 15400 | 15400 | 0.5 | 653.2 | 0.0 | 653.2 | 653.2 | 0.0 | 0 | 653.2 | 42.416 | | | | |
| ASM002464 | Flakvarpebäcken | 19:1 | 0.18 | 40480 | 40480 | 1.3 | 1717.0 | 0.0 | 1717.0 | 1717.0 | 0.0 | 0 | 1717.0 | 42.416 | | | | |
| ASM002465 | Jössesbäcken | 20:1 | 0.11 | 24420 | 24420 | 0.8 | 1035.8 | 0.0 | 1035.8 | 1035.8 | 0.0 | 0 | 1035.8 | 42.416 | | | | |
| ASM002471 | Åspöbäcken | 21:1 | 0.06 | 13860 | 13860 | 0.4 | 587.9 | 0.0 | 587.9 | 587.9 | 0.0 | 0 | 587.9 | 42.416 | | | | |
| ASM002652 | Coastal area | | 1.39 | 305140 | 305140 | 9.7 | 12936.6 | 0.0 | 12936.6 | 12936.6 | 0.0 | 0 | 12936.6 | 42.396 | | | | |
| ASM001445 | Frisksjön | 7:2 | 1.85 | 406560 | 406560 | 12.9 | 14094.3 | 0.0 | 14094.3 | 14094.3 | 0.0 | 0 | 14094.3 | 34.667 | | | | |
| ASM001484 | Käreviksån | 7:1 | 0.21 | 46860 | 453420 | 14.4 | 1981.7 | 0.0 | 1981.7 | 16076.0 | 0.0 | 0 | 16076.0 | 35.455 | | | | |
| ASM001486B | Mederhultsån | 6:1 | 1.92 | 422620 | 422620 | 13.4 | 10848.8 | 0.0 | 10848.8 | 10848.8 | 0.0 | 0 | 10848.8 | 25.670 | PSM002084 | 0.013 | 27.197 | 6 |
| ASM001486A | Mederhultsån | 6:1 | 0.08 | 18040 | 440660 | 14.0 | 753.5 | 0.0 | 753.5 | 11602.2 | 0.0 | 0 | 11602.2 | 26.329 | | | | |
| ASM002654 | Coastal area | | 1.86 | 409420 | 409420 | 13.0 | 17150.5 | 0.0 | 17150.5 | 17150.5 | 0.0 | 0 | 17150.5 | 41.890 | | | | |
| ASM002460 | Pistlanbäcken | 8:1 | 0.50 | 109780 | 109780 | 3.5 | 4199.4 | 0.0 | 4199.4 | 4199.4 | 0.0 | 0 | 4199.4 | 38.253 | | | | |
| ASM001490 | Ekerumsån | 9:3 | 0.22 | 48840 | 48840 | 1.5 | 825.1 | 0.0 | 825.1 | 825.1 | 0.0 | 0 | 825.1 | 16.893 | | | | |
| ASM001489 | Ekerumsån | 9:2 | 0.77 | 168740 | 168740 | 5.4 | 2662.7 | 0.0 | 2662.7 | 2662.7 | 0.0 | 0 | 2662.7 | 15.780 | | | | |
| ASM002483B | Ekerumsån | 9:1 | 1.50 | 330880 | 548460 | 17.4 | 6700.8 | 0.0 | 6700.8 | 10188.6 | 0.0 | 0 | 10188.6 | 18.577 | PSM002085 | 0.017 | 21.410 | 13 |
| ASM002483A | Ekerumsån | 9:1 | 0.34 | 75020 | 623480 | 19.8 | 3035.1 | 0.0 | 3035.1 | 13223.7 | 0.0 | 0 | 13223.7 | 21.210 | | | | |
| ASM002478 | Laxemarån | 10:32 | 0.02 | 5060 | 5060 | 0.2 | 45.2 | 0.0 | 45.2 | 45.2 | 0.0 | 0 | 45.2 | 8.924 | | | | |
| ASM002482 | Laxemarån | 10:31 | 0.87 | 190740 | 195800 | 6.2 | 1702.3 | 0.0 | 1702.3 | 1747.4 | 0.0 | 0 | 1747.4 | 8.924 | | | | |
| ASM002480B | Laxemarån | 10:30 | 4.23 | 931480 | 1127280 | 35.7 | 8313.0 | 0.0 | 8313.0 | 10060.4 | 0.0 | 0 | 10060.4 | 8.924 | PSM002068 | 0.036 | 7.375 | 21 |
| ASM002480A | Jämsen | 10:30 | 1.83 | 403480 | 1530760 | 48.5 | 3600.9 | 0.0 | 3600.9 | 13661.3 | 0.0 | 0 | 13661.3 | 8.924 | PSM002069 | 0.049 | 8.924 | 0 |
| ASM001516 | Laxemarån | 10:29 | 0.53 | 117260 | 117260 | 3.7 | 1061.1 | 0.0 | 1061.1 | 1061.1 | 0.0 | 0 | 1061.1 | 9.049 | | | | |
| ASM001515 | Laxemarån | 10:28 | 0.34 | 74140 | 74140 | 2.4 | 761.9 | 0.0 | 761.9 | 761.9 | 0.0 | 0 | 761.9 | 10.277 | | | | |
| ASM001514 | Laxemarån | 10:27 | 0.49 | 107140 | 107140 | 3.4 | 1062.9 | 0.0 | 1062.9 | 1062.9 | 0.0 | 0 | 1062.9 | 9.921 | | | | |
| ASM001446 | Plittorpsgöl | 10:26 | 0.68 | 149160 | 149160 | 4.7 | 1331.2 | 0.0 | 1331.2 | 1331.2 | 0.0 | 0 | 1331.2 | 8.924 | | | | |
| ASM002459 | Laxemarån | 10:25 | 0.10 | 21780 | 170940 | 5.4 | 273.5 | 0.0 | 273.5 | 1604.6 | 0.0 | 0 | 1604.6 | 9.387 | | | | |
| ASM001512 | Laxemarån | 10:24 | 0.49 | 108680 | 108680 | 3.4 | 1002.2 | 0.0 | 1002.2 | 1002.2 | 0.0 | 0 | 1002.2 | 9.221 | | | | |
| ASM002476E | Laxemarån | 10:1 | 3.95 | 868780 | 2977700 | 94.4 | 9142.9 | 0.0 | 9142.9 | 28296.9 | 0.0 | 0 | 28296.9 | 9.503 | PSM002071 | 0.094 | 13.727 | 31 |
| ASM001510 | Laxemarån | 10:22 | 0.56 | 123640 | 123640 | 3.9 | 1103.4 | 0.0 | 1103.4 | 1103.4 | 0.0 | 0 | 1103.4 | 8.924 | | | | |
| ASM002453 | Laxemarån | 10:21 | 0.45 | 97900 | 221540 | 7.0 | 903.2 | 0.0 | 903.2 | 2006.6 | 0.0 | 0 | 2006.6 | 9.058 | | | | |
| ASM002450B | Laxemarån | 10:20 | 2.39 | 526240 | 747780 | 23.7 | 5002.2 | 0.0 | 5002.2 | 7008.8 | 0.0 | 0 | 7008.8 | 9.373 | PSM002072 | | | |
| ASM002450A | Laxemarån | 10:20 | 0.19 | 41140 | 788920 | 25.0 | 1497.7 | 0.0 | 1497.7 | 8506.5 | 0.0 | 0 | 8506.5 | 10.782 | | | | |
| ASM001511 | Laxemarån | 10:23 | 0.74 | 162800 | 162800 | 5.2 | 1653.1 | 0.0 | 1653.1 | 1653.1 | 0.0 | 0 | 1653.1 | 10.154 | | | | |
| ASM001448 | Grangöl | 10:19 | 0.50 | 108900 | 108900 | 3.5 | 971.9 | 0.0 | 971.9 | 971.9 | 0.0 | 0 | 971.9 | 8.924 | | | | |
| ASM002499 | Laxemarån | 10:18 | 0.06 | 12760 | 121660 | 3.9 | 113.9 | 0.0 | 113.9 | 1085.8 | 0.0 | 0 | 1085.8 | 8.924 | | | | |
| ASM001506 | Laxemarån | 10:17 | 0.40 | 87560 | 87560 | 2.8 | 781.4 | 0.0 | 781.4 | 781.4 | 0.0 | 0 | 781.4 | 8.924 | | | | |
| ASM001447 | Fjällgöl | 10:16 | 0.30 | 64900 | 64900 | 2.1 | 579.2 | 0.0 | 579.2 | 579.2 | 0.0 | 0 | 579.2 | 8.924 | | | | |
| ASM002451 | Laxemarån | 10:15 | 0.33 | 71500 | 136400 | 4.3 | 646.9 | 0.0 | 646.9 | 1226.1 | 0.0 | 0 | 1226.1 | 8.989 | | | | |
| ASM002452 | Laxemarån | 10:14 | 2.38 | 522500 | 868120 | 27.5 | 5002.1 | 0.0 | 5002.1 | 8095.4 | 0.0 | 0 | 8095.4 | 9.325 | | | | |
| ASM001503 | Laxemarån | 10:13 | 0.42 | 91520 | 91520 | 2.9 | 2296.3 | 0.0 | 2296.3 | 2296.3 | 0.0 | 0 | 2296.3 | 25.091 | | | | |
| ASM002454 | Laxemarån | 10:12 | 0.81 | 177760 | 269280 | 8.5 | 5324.2 | 0.0 | 5324.2 | 7620.5 | 0.0 | 0 | 7620.5 | 28.300 | | | | |
| ASM001501 | Laxemarån | 10:11 | 0.81 | 177320 | 177320 | 5.6 | 2254.7 | 0.0 | 2254.7 | 2254.7 | 0.0 | 0 | 2254.7 | 12.716 | | | | |
| ASM002457 | Laxemarån | 10:10 | 1.39 | 305580 | 482900 | 15.3 | 5172.4 | 0.0 | 5172.4 | 7427.2 | 0.0 | 0 | 7427.2 | 15.380 | | | | |
| ASM002476D | Laxemarån | 10:1 | 4.96 | 1091860 | 6641580 | 210.6 | 19064.4 | 0.0 | 19064.4 | 80664.1 | 0.0 | 0 | 80664.1 | 12.145 | PSM002077 | | | |
| ASM001499 | Laxemarån | 10:9 | 0.71 | 156420 | 156420 | 5.0 | 2988.2 | 0.0 | 2988.2 | 2988.2 | 0.0 | 0 | 2988.2 | 19.104 | | | | |
| ASM001498 | Laxemarån | 10:8 | 2.77 | 609620 | 766040 | 24.3 | 10638.2 | 0.0 | 10638.2 | 13626.4 | 0.0 | 0 | 13626.4 | 17.788 | PSM002078 | 0.024 | 18.457 | 4 |
| ASM001497 | Laxemarån | 10:7 | 0.61 | 133980 | 133980 | 4.2 | 1665.7 | 0.0 | 1665.7 | 1665.7 | 0.0 | 0 | 1665.7 | 12.432 | | | | |
| ASM002476C | Laxemarån | 10:1 | 0.32 | 69300 | 7610900 | 241.3 | 2100.6 | 0.0 | 2100.6 | 98056.7 | 0.0 | 0 | 98056.7 | 12.884 | PSM002079 | 0.242 | 15.322 | 16 |
| ASM001494 | Laxemarån | 10:4 | 1.00 | 220220 | 220220 | 7.0 | 6926.5 | 0.0 | 6926.5 | 6926.5 | 0.0 | 0 | 6926.5 | 31.452 | | | | |
| ASM001493 | Laxemarån | 10:3 | 0.32 | 70180 | 70180 | 2.2 | 2470.1 | 0.0 | 2470.1 | 2470.1 | 0.0 | 0 | 2470.1 | 35.197 | | | | |
| ASM001492 | Laxemarån | 10:2 | 0.46 | 101200 | 101200 | 3.2 | 4086.7 | 0.0 | 4086.7 | 4086.7 | 0.0 | 0 | 4086.7 | 40.383 | | | | |
| ASM001496 | Laxemarån | 10:6 | 0.89 | 195800 | 195800 | 6.2 | 3857.9 | 0.0 | 3857.9 | 3857.9 | 0.0 | 0 | 3857.9 | 19.703 | | | | |
| ASM001495 | Laxemarån | 10:5 | 0.29 | 63800 | 63800 | 2.0 | 1812.6 | 0.0 | 1812.6 | 1812.6 | 0.0 | 0 | 1812.6 | 28.411 | | | | |
| ASM002476B | Laxemarån | 10:1 | 3.23 | 710820 | 8972920 | 284.5 | 25694.3 | 0.0 | 25694.3 | 142904.9 | 0.0 | 0 | 142904.9 | 15.926 | PSM002087 | 0.285 | 16.861 | 6 |
| ASM002476A | Laxemarån | 10:1 | 0.19 | 41360 | 9014280 | 285.8 | 1754.3 | 0.0 | 1754.3 | 144659.2 | 0.0 | 0 | 144659.2 | 16.048 | | | | |
| ASM002495 | Glostadsbäcken | 12:3 | 0.13 | 27720 | 27720 | 0.9 | 1175.8 | 0.0 | 1175.8 | 1175.8 | 0.0 | 0 | 1175.8 | 42.416 | | | | |
| ASM002485 | Glostadsbäcken | 12:2 | 0.33 | 72820 | 72820 | 2.3 | 3030.0 | 0.0 | 3030.0 | 3030.0 | 0.0 | 0 | 3030.0 | 41.610 | | | | |
| ASM002498 | Glostadsbäcken | 12:1 | 1.60 | 351340 | 451880 | 14.3 | 13690.4 | 0.0 | 13690.4 | 17896.3 | 0.0 | 0 | 17896.3 | 39.604 | | | | |
| ASM001518B | Stålglobäcken | 13:1 | 0.68 | 149380 | 149380 | 4.7 | 5662.4 | 0.0 | 5662.4 | 5662.4 | 0.0 | 0 | 5662.4 | 37.906 | PSM002086 | 0.005 | 37.906 | 0 |
| ASM001518A | Stålglobäcken | 13:1 | 0.35 | 77880 | 227260 | 7.2 | 3300.4 | 0.0 | 3300.4 | 8962.8 | 0.0 | 0 | 8962.8 | 39.439 | | | | |
| ASM002462 | Uvöbäcken | 15:1 | 0.97 | 212740 | 212740 | 6.7 | 8982.3 | 0.0 | 8982.3 | 8982.3 | 0.0 | 0 | 8982.3 | 42.222 | | | | |
| ASM002497 | Stekebäcken | 14:2 | 0.44 | 95700 | 95700 | 3.0 | 3977.2 | 0.0 | 3977.2 | 3977.2 | 0.0 | 0 | 3977.2 | 41.559 | | | | |
| ASM001517 | Stekebäcken | 14:1 | 0.90 | 198660 | 294360 | 9.3 | 8426.4 | 0.0 | 8426.4 | 12403.5 | 0.0 | 0 | 12403.5 | 42.137 | | | | |
| ASM002463 | Svartebäck | 16:1 | 0.50 | 110880 | 110880 | 3.5 | 4565.3 | 0.0 | 4565.3 | 4565.3 | 0.0 | 0 | 4565.3 | 41.174 | | | | |
| ASM002655 | Coastal area | | 2.71 | 596420 | 596420 | 18.9 | 25291.3 | 0.0 | 25291.3 | 25291.3 | 0.0 | 0 | 25291.3 | 42.405 | | | | |
| ASM002658 | Coastal area | | 1.26 | 277420 | 277420 | 8.8 | 11745.4 | 0.0 | 11745.4 | 11745.4 | 0.0 | 0 | 11745.4 | 42.338 | | | | |
| ASM002656 | Coastal area | | 0.22 | 48400 | 48400 | 1.5 | 2052.9 | 0.0 | 2052.9 | 2052.9 | 0.0 | 0 | 2052.9 | 42.416 | | | | |
| ASM002660 | Coastal area | | 0.14 | 30360 | 30360 | 1.0 | 1287.7 | 0.0 | 1287.7 | 1287.7 | 0.0 | 0 | 1287.7 | 42.416 | | | | |
| ASM002659 | Coastal area | | 15.70 | 3453780 | 3453780 | 109.5 | 95403.9 | 0.0 | 95403.9 | 95403.9 | 0.0 | 0 | 95403.9 | 27.623 | | | | |
| ASM002657 | Coastal area | | 2.60 | 571340 | 571340 | 18.1 | 19652.5 | 0.0 | 19652.5 | 19652.5 | 0.0 | 0 | 19652.5 | 34.397 | | | | |
| ASM001522 | Uthammarsån | 17:5 | 0.57 | 125620 | 125620 | 4.0 | 3114.1 | 0.0 | 3114.1 | 3114.1 | 0.0 | 0 | 3114.1 | 24.790 | | | | |
| ASM001523 | Uthammarsån | 17:6 | 0.96 | 210760 | 210760 | 6.7 | 4014.7 | 0.0 | 4014.7 | 4014.7 | 0.0 | 0 | 4014.7 | 19.049 | | | | |
| ASM001521 | Uthammarsån | 17:4 | 0.20 | 44880 | 44880 | 1.4 | 1517.6 | 0.0 | 1517.6 | 1517.6 | 0.0 | 0 | 1517.6 | 33.815 | | | | |
| ASM001520 | Uthammarsån | 17:3 | 0.08 | 17820 | 17820 | 0.6 | 702.9 | 0.0 | 702.9 | 702.9 | 0.0 | 0 | 702.9 | 39.446 | | | | |
| ASM002494B | Uthammarsån | 17:1 | 2.91 | 640860 | 1039940 | 33.0 | 8483.9 | 0.0 | 8483.9 | 17833.3 | 0.0 | 0 | 17833.3 | 17.148 | PSM002076 | 0.033 | 18.694 | 8 |
| ASM001533 | Uthammarsån | 17:2 | 0.51 | 112640 | 112640 | 3.6 | 4335.1 | 0.0 | 4335.1 | 4335.1 | 0.0 | 0 | 4335.1 | 38.487 | | | | |
| ASM002494A | Uthammarsån | 17:1 | 1.78 | 391820 | 1544400 | 49.0 | 16481.0 | 0.0 | 16481.0 | 38649.5 | 0.0 | 0 | 38649.5 | 25.026 | | | | |
| ASM001528 | Slåthultebäcken | 18:5 | 0.32 | 70400 | 70400 | 2.2 | 628.3 | 0.0 | 628.3 | 628.3 | 0.0 | 0 | 628.3 | 8.924 | | | | |
| ASM002477 | Slåthultebäcken | 18:4 | 0.66 | 144980 | 215380 | 6.8 | 1293.9 | 0.0 | 1293.9 | 1922.2 | 0.0 | 0 | 1922.2 | 8.924 | | | | |
| ASM001531 | Slåthultebäcken | 18:8 | 0.30 | 66440 | 66440 | 2.1 | 592.9 | 0.0 | 592.9 | 592.9 | 0.0 | 0 | 592.9 | 8.924 | | | | |
| ASM001532 | Slåthultebäcken | 18:9 | 0.11 | 24420 | 24420 | 0.8 | 217.9 | 0.0 | 217.9 | 217.9 | 0.0 | 0 | 217.9 | 8.924 | | | | |
| ASM002455 | Slåthultebäcken | 18:7 | 0.76 | 167420 | 258280 | 8.2 | 1494.1 | 0.0 | 1494.1 | 2305.0 | 0.0 | 0 | 2305.0 | 8.924 | | | | |
| ASM002475 | Slåthultebäcken | 18:6 | 1.06 | 232100 | 490380 | 15.5 | 2071.4 | 0.0 | 2071.4 | 4376.4 | 0.0 | 0 | 4376.4 | 8.924 | | | | |
| ASM001526 | Slåthultebäcken | 18:3 | 0.40 | 88220 | 88220 | 2.8 | 2640.2 | 0.0 | 2640.2 | 2640.2 | 0.0 | 0 | 2640.2 | 29.928 | | | | |
| ASM002481C | Slåthultebäcken | 18:1 | 2.44 | 537020 | 1027400 | 32.6 | 4792.6 | 0.0 | 4792.6 | 9169.0 | 0.0 | 0 | 9169.0 | 8.924 | PSM002070 | | | |
| ASM002481B | Slåthultebäcken | 18:1 | 2.13 | 469260 | 1800260 | 57.1 | 8650.1 | 0.0 | 8650.1 | 22381.5 | 0.0 | 0 | 22381.5 | 12.432 | PSM002075 | | | |
| ASM001525 | Slåthultebäcken | 18:2 | 0.77 | 169620 | 169620 | 5.4 | 4430.9 | 0.0 | 4430.9 | 4430.9 | 0.0 | 0 | 4430.9 | 26.122 | | | | |
| ASM002481A | Slåthultebäcken | 18:1 | 0.00 | 220 | 1970100 | 62.5 | 0.0 | 0.0 | 0.0 | 26812.4 | 0.0 | 0 | 26812.4 | 13.610 | | | | |
| ASM001444 | Sörämagasinet | 11:1 | 0.52 | 115060 | 115060 | 3.6 | 4880.4 | 0.0 | 4880.4 | 4880.4 | 0.0 | 0 | 4880.4 | 42.416 | | | | |
| ASM002466 | Stekflagebäcken | 22:1 | 0.36 | 78980 | 78980 | 2.5 | 3350.0 | 0.0 | 3350.0 | 3350.0 | 0.0 | 0 | 3350.0 | 42.416 | | | | |
| ASM002653 | Coastal area | | 0.76 | 166980 | 166980 | 5.3 | 7073.2 | 0.0 | 7073.2 | 7073.2 | 0.0 | 0 | 7073.2 | 42.360 | | | | |
| ASM002470 | Skölkebäcken | 26:1 | 0.17 | 36300 | 36300 | 1.2 | 1539.7 | 0.0 | 1539.7 | 1539.7 | 0.0 | 0 | 1539.7 | 42.416 | | | | |
| ASM002469 | Gloebäcken | 25:1 | 0.13 | 28820 | 28820 | 0.9 | 1222.4 | 0.0 | 1222.4 | 1222.4 | 0.0 | 0 | 1222.4 | 42.416 | | | | |
| ASM002468 | Lindströmmebäcken | 24:1 | 0.19 | 42240 | 42240 | 1.3 | 1791.7 | 0.0 | 1791.7 | 1791.7 | 0.0 | 0 | 1791.7 | 42.416 | | | | |
| ASM002467B | Vadvikebäcken | 23:1 | 0.30 | 65560 | 65560 | 2.1 | 2780.8 | 0.0 | 2780.8 | 2780.8 | 0.0 | 0 | 2780.8 | 42.416 | PSM107735 | 0.002 | 36.359 | 17 |
| ASM002467A | Vadvikebäcken | 23:1 | 0.01 | 1980 | 67540 | 2.1 | 84.0 | 0.0 | 84.0 | 2864.8 | 0.0 | 0 | 2864.8 | 42.416 | | | | |
| | **Kärrviksån** | 5:1-20 | 27.31 | 6007100 | 6007100 | 26.9 | 122297.9 | 0.0 | 122297.9 | | 0.0 | 0 | 122297.9 | 20.359 | | | | |
| | **Laxemarån** | 10:1-32 | 40.97 | 9014280 | 9014280 | 37.5 | 144659.2 | 0.0 | 144659.2 | | 0.0 | 0 | 144659.2 | 16.048 | | | | |
| | **All catchments** | | 129.97 | 28593620 | 28593620 | 22.3 | 674982.2 | 0.0 | 674982.2 | | 0.0 | 0 | 674982.2 | 23.606 | | | | |

| Chloride ($Cl^-$) | | | | Water balance | | | Total per catchment | | | Total including contributions from upstream catchments | | | | | Calibration data | | | |
|---|---|---|---|---|---|---|---|---|---|---|---|---|---|---|---|---|---|---|
| Idcode | Name | ARO | Area | $Q_{catch}$ | $Q_{out}$ | q | Diffuse | Point | Total | Total IN | Retention | | Total OUT | Conc. | Reference | q | Conc. | Deviation |
| | | | $km^2$ | $m^3 \cdot yr^{-1}$ | $m^3 \cdot yr^{-1}$ | $L \cdot s^{-1}$ | $kg \cdot yr^{-1}$ | $kg \cdot yr^{-1}$ | $kg \cdot yr^{-1}$ | $kg \cdot yr^{-1}$ | $kg \cdot yr^{-1}$ | % | $kg \cdot yr^{-1}$ | $mg \cdot L^{-1}$ | | $L \cdot s^{-1}$ | $mg \cdot L^{-1}$ | % |
| ASM002474 | Kärrviksån | 5:20 | 0.12 | 25740 | 25740 | 0.8 | 116.4 | 3843.3 | 3959.7 | 3959.7 | 0.0 | 0 | 3959.7 | 153.836 | | | | |
| ASM002493 | Kärrviksån | 5:19 | 0.84 | 184140 | 209880 | 6.7 | 833.0 | 0.0 | 833.0 | 4792.7 | 0.0 | 0 | 4792.7 | 22.835 | | | | |
| ASM001483 | Kärrviksån | 5:17 | 0.15 | 33220 | 33220 | 1.1 | 150.3 | 0.0 | 150.3 | 150.3 | 0.0 | 0 | 150.3 | 4.524 | | | | |
| ASM002492 | Kärrviksån | 5:16 | 1.11 | 243980 | 277200 | 8.8 | 1103.7 | 0.0 | 1103.7 | 1253.9 | 0.0 | 0 | 1253.9 | 4.524 | | | | |
| ASM002491 | Kärrviksån | 5:15 | 1.87 | 411840 | 689040 | 21.8 | 1892.1 | 0.0 | 1892.1 | 3146.1 | 0.0 | 0 | 3146.1 | 4.566 | | | | |
| ASM001474 | Kärrviksån | 5:7 | 0.45 | 99000 | 99000 | 3.1 | 453.8 | 0.0 | 453.8 | 453.8 | 0.0 | 0 | 453.8 | 4.584 | | | | |
| ASM002487 | Kärrviksån | 5:6 | 1.20 | 264000 | 363000 | 11.5 | 1243.0 | 0.0 | 1243.0 | 1696.8 | 0.0 | 0 | 1696.8 | 4.674 | | | | |
| ASM001472 | Kärrviksån | 5:4 | 1.10 | 242880 | 242880 | 7.7 | 1497.7 | 0.0 | 1497.7 | 1497.7 | 0.0 | 0 | 1497.7 | 6.167 | | | | |
| ASM001470 | Kärrviksån | 5:3 | 0.40 | 87560 | 87560 | 2.8 | 598.7 | 0.0 | 598.7 | 598.7 | 0.0 | 0 | 598.7 | 6.837 | | | | |
| ASM001469 | Kärrviksån | 5:2 | 0.97 | 212960 | 212960 | 6.8 | 1142.6 | 0.0 | 1142.6 | 1142.6 | 0.0 | 0 | 1142.6 | 5.366 | | | | |
| ASM001471 | Kärrviksån | 5:5 | 2.79 | 614680 | 614680 | 19.5 | 5092.7 | 0.0 | 5092.7 | 5092.7 | 0.0 | 0 | 5092.7 | 8.285 | | | | |
| ASM001479 | Kärrviksån | 5:13 | 0.65 | 142340 | 142340 | 4.5 | 643.9 | 0.0 | 643.9 | 643.9 | 0.0 | 0 | 643.9 | 4.524 | | | | |
| ASM001480 | Kärrviksån | 5:14 | 0.10 | 22660 | 22660 | 0.7 | 102.5 | 0.0 | 102.5 | 102.5 | 0.0 | 0 | 102.5 | 4.524 | | | | |
| ASM002490 | Kärrviksån | 5:12 | 0.84 | 183920 | 348920 | 11.1 | 832.0 | 9236.2 | 10068.1 | 10814.5 | 0.0 | 0 | 10814.5 | 30.994 | | | | |
| ASM001478 | Kärrviksån | 5:11 | 0.49 | 108460 | 108460 | 3.4 | 490.6 | 0.0 | 490.6 | 490.6 | 0.0 | 0 | 490.6 | 4.524 | | | | |
| ASM002489 | Kärrviksån | 5:10 | 1.20 | 263560 | 372020 | 11.8 | 1192.2 | 0.0 | 1192.2 | 1682.9 | 0.0 | 0 | 1682.9 | 4.524 | | | | |
| ASM001476 | Kärrviksån | 5:9 | 3.62 | 796180 | 796180 | 25.2 | 3641.4 | 0.0 | 3641.4 | 3641.4 | 0.0 | 0 | 3641.4 | 4.574 | | | | |
| ASM001475B | Kärrviksån | 5:8 | 1.38 | 302940 | 1820060 | 57.7 | 1377.9 | 0.0 | 1377.9 | 17516.7 | 0.0 | 0 | 17516.7 | 9.624 | PSM002081 | 0.058 | 4.438 | 117 |
| ASM001475A | Kärrviksån | 5:8 | 0.04 | 9680 | 1829740 | 58.0 | 52.3 | 0.0 | 52.3 | 17569.0 | 0.0 | 0 | 17569.0 | 9.602 | | | | |
| ASM002479 | Kärrviksån | 5:18 | 1.18 | 259600 | 259600 | 8.2 | 1182.5 | 0.0 | 1182.5 | 1182.5 | 0.0 | 0 | 1182.5 | 4.555 | | | | |
| ASM002486C | Kärrviksån | 5:1 | 2.75 | 604560 | 1074040 | 34.1 | 2744.3 | 9428.8 | 12173.0 | 18148.3 | 0.0 | 0 | 18148.3 | 16.897 | PSM002080 | | | |
| ASM002486B | Kärrviksån | 5:1 | 1.13 | 247940 | 3840760 | 121.8 | 1242.9 | 0.0 | 1242.9 | 40106.3 | 0.0 | 0 | 40106.3 | 10.442 | PSM002082 | 0.121 | 8.285 | 26 |
| ASM002486A | Kärrviksån | 5:1 | 2.93 | 645260 | 6007100 | 190.5 | 6156.2 | 0.0 | 6156.2 | 56291.0 | 0.0 | 0 | 56291.0 | 9.371 | PSM002083 | 0.190 | 9.371 | 0 |
| ASM002449 | Bjurhidebäcken | 4:1 | 0.63 | 139040 | 139040 | 4.4 | 703.6 | 0.0 | 703.6 | 703.6 | 0.0 | 0 | 703.6 | 5.060 | | | | |
| ASM002472 | Sörviksån | 3:2 | 0.47 | 103400 | 103400 | 3.3 | 657.2 | 0.0 | 657.2 | 657.2 | 0.0 | 0 | 657.2 | 6.356 | | | | |
| ASM002473 | Sörviksån | 3:1 | 0.53 | 116600 | 220000 | 7.0 | 1004.0 | 0.0 | 1004.0 | 1661.2 | 0.0 | 0 | 1661.2 | 7.551 | | | | |
| ASM002651 | Coastal area | | 1.67 | 368280 | 368280 | 11.7 | 6276.9 | 0.0 | 6276.9 | 6276.9 | 0.0 | 0 | 6276.9 | 17.044 | | | | |
| ASM002447 | Bodvikebäcken | 2:1 | 0.38 | 83600 | 83600 | 2.7 | 1836.3 | 0.0 | 1836.3 | 1836.3 | 0.0 | 0 | 1836.3 | 21.965 | | | | |
| ASM002446 | Långbonäsbäcken | 1:1 | 0.07 | 15400 | 15400 | 0.5 | 309.5 | 0.0 | 309.5 | 309.5 | 0.0 | 0 | 309.5 | 20.097 | | | | |
| ASM002464 | Flakvarpebäcken | 19:1 | 0.18 | 40480 | 40480 | 1.3 | 877.3 | 0.0 | 877.3 | 877.3 | 0.0 | 0 | 877.3 | 21.673 | | | | |
| ASM002465 | Jössesbäcken | 20:1 | 0.11 | 24420 | 24420 | 0.8 | 585.5 | 0.0 | 585.5 | 585.5 | 0.0 | 0 | 585.5 | 23.975 | | | | |
| ASM002471 | Åspöbäcken | 21:1 | 0.06 | 13860 | 13860 | 0.4 | 229.3 | 0.0 | 229.3 | 229.3 | 0.0 | 0 | 229.3 | 16.545 | | | | |
| ASM002652 | Coastal area | | 1.39 | 305140 | 305140 | 9.7 | 6186.6 | 0.0 | 6186.6 | 6186.6 | 0.0 | 0 | 6186.6 | 20.275 | | | | |
| ASM001445 | Frisksjön | 7:2 | 1.85 | 406560 | 406560 | 12.9 | 3484.4 | 0.0 | 3484.4 | 3484.4 | 0.0 | 0 | 3484.4 | 8.570 | | | | |
| ASM001484 | Käreviksån | 7:1 | 0.21 | 46860 | 453420 | 14.4 | 742.8 | 0.0 | 742.8 | 4227.2 | 0.0 | 0 | 4227.2 | 9.323 | | | | |
| ASM001486B | Mederhultsån | 6:1 | 1.92 | 422620 | 422620 | 13.4 | 2078.9 | 0.0 | 2078.9 | 2078.9 | 0.0 | 0 | 2078.9 | 4.919 | PSM002084 | 0.013 | 9.374 | 48 |
| ASM001486A | Mederhultsån | 6:1 | 0.08 | 18040 | 440660 | 14.0 | 192.9 | 0.0 | 192.9 | 2271.8 | 0.0 | 0 | 2271.8 | 5.155 | | | | |
| ASM002654 | Coastal area | | 1.86 | 409420 | 409420 | 13.0 | 8075.1 | 0.0 | 8075.1 | 8075.1 | 0.0 | 0 | 8075.1 | 19.723 | | | | |
| ASM002460 | Pistlanbäcken | 8:1 | 0.50 | 109780 | 109780 | 3.5 | 982.4 | 0.0 | 982.4 | 982.4 | 0.0 | 0 | 982.4 | 8.949 | | | | |
| ASM001490 | Ekerumsån | 9:3 | 0.22 | 48840 | 48840 | 1.5 | 220.9 | 0.0 | 220.9 | 220.9 | 0.0 | 0 | 220.9 | 4.524 | | | | |
| ASM001489 | Ekerumsån | 9:2 | 0.77 | 168740 | 168740 | 5.4 | 763.3 | 0.0 | 763.3 | 763.3 | 0.0 | 0 | 763.3 | 4.524 | | | | |
| ASM002483B | Ekerumsån | 9:1 | 1.50 | 330880 | 548460 | 17.4 | 1532.1 | 0.0 | 1532.1 | 2516.3 | 0.0 | 0 | 2516.3 | 4.588 | PSM002085 | 0.017 | 5.728 | 20 |
| ASM002483A | Ekerumsån | 9:1 | 0.34 | 75020 | 623480 | 19.8 | 1238.5 | 0.0 | 1238.5 | 3754.8 | 0.0 | 0 | 3754.8 | 6.022 | | | | |
| ASM002478 | Laxemarån | 10:32 | 0.02 | 5060 | 5060 | 0.2 | 22.9 | 0.0 | 22.9 | 22.9 | 0.0 | 0 | 22.9 | 4.524 | | | | |
| ASM002482 | Laxemarån | 10:31 | 0.87 | 190740 | 195800 | 6.2 | 862.8 | 0.0 | 862.8 | 885.7 | 0.0 | 0 | 885.7 | 4.524 | | | | |
| ASM002480B | Laxemarån | 10:30 | 4.23 | 931480 | 1127280 | 35.7 | 4213.6 | 0.0 | 4213.6 | 5099.4 | 0.0 | 0 | 5099.4 | 4.524 | PSM002068 | 0.036 | 4.524 | 0 |
| ASM002480A | Jämsen | 10:30 | 1.83 | 403480 | 1530760 | 48.5 | 1825.2 | 7546.5 | 9371.7 | 14471.1 | 0.0 | 0 | 14471.1 | 9.454 | PSM002069 | 0.049 | 12.646 | 25 |
| ASM001516 | Laxemarån | 10:29 | 0.53 | 117260 | 117260 | 3.7 | 530.4 | 0.0 | 530.4 | 530.4 | 0.0 | 0 | 530.4 | 4.524 | | | | |
| ASM001515 | Laxemarån | 10:28 | 0.34 | 74140 | 74140 | 2.4 | 335.4 | 5086.5 | 5421.8 | 5421.8 | 0.0 | 0 | 5421.8 | 73.130 | | | | |
| ASM001514 | Laxemarån | 10:27 | 0.49 | 107140 | 107140 | 3.4 | 484.7 | 2906.5 | 3391.2 | 3391.2 | 0.0 | 0 | 3391.2 | 31.652 | | | | |
| ASM001446 | Plittorpsgöl | 10:26 | 0.68 | 149160 | 149160 | 4.7 | 674.7 | 2845.3 | 3520.0 | 3520.0 | 0.0 | 0 | 3520.0 | 23.599 | | | | |
| ASM002459 | Laxemarån | 10:25 | 0.10 | 21780 | 170940 | 5.4 | 98.5 | 2713.9 | 2812.5 | 6332.5 | 0.0 | 0 | 6332.5 | 37.045 | | | | |
| ASM001512 | Laxemarån | 10:24 | 0.49 | 108680 | 108680 | 3.4 | 491.6 | 0.0 | 491.6 | 491.6 | 0.0 | 0 | 491.6 | 4.524 | | | | |
| ASM002476E | Laxemarån | 10:1 | 3.95 | 868780 | 2977700 | 94.4 | 3930.0 | 17491.8 | 21421.8 | 52060.4 | 0.0 | 0 | 52060.4 | 17.483 | PSM002071 | 0.094 | 17.488 | 0 |
| ASM001510 | Laxemarån | 10:22 | 0.56 | 123640 | 123640 | 3.9 | 559.3 | 5427.9 | 5987.2 | 5987.2 | 0.0 | 0 | 5987.2 | 48.424 | | | | |
| ASM002453 | Laxemarån | 10:21 | 0.45 | 97900 | 221540 | 7.0 | 442.9 | 1435.8 | 1878.6 | 7865.8 | 0.0 | 0 | 7865.8 | 35.505 | | | | |
| ASM002450B | Laxemarån | 10:20 | 2.39 | 526240 | 747780 | 23.7 | 2380.5 | 10820.8 | 13201.3 | 21067.1 | 0.0 | 0 | 21067.1 | 28.173 | PSM002072 | | | |
| ASM002450A | Laxemarån | 10:20 | 0.19 | 41140 | 788920 | 25.0 | 197.4 | 0.0 | 197.4 | 21264.5 | 0.0 | 0 | 21264.5 | 26.954 | | | | |
| ASM001511 | Laxemarån | 10:23 | 0.74 | 162800 | 162800 | 5.2 | 736.4 | 0.0 | 736.4 | 736.4 | 0.0 | 0 | 736.4 | 4.524 | | | | |
| ASM001448 | Grangöl | 10:19 | 0.50 | 108900 | 108900 | 3.5 | 492.6 | 0.0 | 492.6 | 492.6 | 0.0 | 0 | 492.6 | 4.524 | | | | |
| ASM002499 | Laxemarån | 10:18 | 0.06 | 12760 | 121660 | 3.9 | 57.7 | 0.0 | 57.7 | 550.3 | 0.0 | 0 | 550.3 | 4.524 | | | | |
| ASM001506 | Laxemarån | 10:17 | 0.40 | 87560 | 87560 | 2.8 | 396.1 | 0.0 | 396.1 | 396.1 | 0.0 | 0 | 396.1 | 4.524 | | | | |
| ASM001447 | Fjällgöl | 10:16 | 0.30 | 64900 | 64900 | 2.1 | 293.6 | 0.0 | 293.6 | 293.6 | 0.0 | 0 | 293.6 | 4.524 | | | | |
| ASM002451 | Laxemarån | 10:15 | 0.33 | 71500 | 136400 | 4.3 | 323.4 | 0.0 | 323.4 | 617.0 | 0.0 | 0 | 617.0 | 4.524 | | | | |
| ASM002452 | Laxemarån | 10:14 | 2.38 | 522500 | 868120 | 27.5 | 2372.8 | 0.0 | 2372.8 | 3936.2 | 0.0 | 0 | 3936.2 | 4.534 | | | | |
| ASM001503 | Laxemarån | 10:13 | 0.42 | 91520 | 91520 | 2.9 | 431.7 | 0.0 | 431.7 | 431.7 | 0.0 | 0 | 431.7 | 4.717 | | | | |
| ASM002454 | Laxemarån | 10:12 | 0.81 | 177760 | 269280 | 8.5 | 818.1 | 0.0 | 818.1 | 1249.8 | 0.0 | 0 | 1249.8 | 4.641 | | | | |
| ASM001501 | Laxemarån | 10:11 | 0.81 | 177320 | 177320 | 5.6 | 802.1 | 0.0 | 802.1 | 802.1 | 0.0 | 0 | 802.1 | 4.524 | | | | |
| ASM002457 | Laxemarån | 10:10 | 1.39 | 305580 | 482900 | 15.3 | 1388.0 | 0.0 | 1388.0 | 2190.1 | 0.0 | 0 | 2190.1 | 4.535 | | | | |
| ASM002476D | Laxemarån | 10:1 | 4.96 | 1091860 | 6641580 | 210.6 | 5093.0 | 0.0 | 5093.0 | 86530.5 | 0.0 | 0 | 86530.5 | 13.029 | PSM002077 | | | |
| ASM001499 | Laxemarån | 10:9 | 0.71 | 156420 | 156420 | 5.0 | 710.7 | 0.0 | 710.7 | 710.7 | 0.0 | 0 | 710.7 | 4.543 | | | | |
| ASM001498 | Laxemarån | 10:8 | 2.77 | 609620 | 766040 | 24.3 | 2789.6 | 0.0 | 2789.6 | 3500.3 | 0.0 | 0 | 3500.3 | 4.569 | PSM002078 | 0.024 | 3.945 | 16 |
| ASM001497 | Laxemarån | 10:7 | 0.61 | 133980 | 133980 | 4.2 | 607.8 | 0.0 | 607.8 | 607.8 | 0.0 | 0 | 607.8 | 4.536 | | | | |
| ASM002476C | Laxemarån | 10:1 | 0.32 | 69300 | 7610900 | 241.3 | 344.6 | 0.0 | 344.6 | 90983.1 | 0.0 | 0 | 90983.1 | 11.954 | PSM002079 | 0.242 | 12.902 | 7 |
| ASM001494 | Laxemarån | 10:4 | 1.00 | 220220 | 220220 | 7.0 | 1075.1 | 0.0 | 1075.1 | 1075.1 | 0.0 | 0 | 1075.1 | 4.882 | | | | |
| ASM001493 | Laxemarån | 10:3 | 0.32 | 70180 | 70180 | 2.2 | 359.9 | 0.0 | 359.9 | 359.9 | 0.0 | 0 | 359.9 | 5.128 | | | | |
| ASM001492 | Laxemarån | 10:2 | 0.46 | 101200 | 101200 | 3.2 | 773.1 | 0.0 | 773.1 | 773.1 | 0.0 | 0 | 773.1 | 7.639 | | | | |
| ASM001496 | Laxemarån | 10:6 | 0.89 | 195800 | 195800 | 6.2 | 940.6 | 0.0 | 940.6 | 940.6 | 0.0 | 0 | 940.6 | 4.804 | | | | |
| ASM001495 | Laxemarån | 10:5 | 0.29 | 63800 | 63800 | 2.0 | 304.4 | 0.0 | 304.4 | 304.4 | 0.0 | 0 | 304.4 | 4.772 | | | | |
| ASM002476B | Laxemarån | 10:1 | 3.23 | 710820 | 8972920 | 284.5 | 5291.8 | 0.0 | 5291.8 | 99728.0 | 0.0 | 0 | 99728.0 | 11.114 | PSM002087 | 0.285 | 13.200 | 16 |
| ASM002476A | Laxemarån | 10:1 | 0.19 | 41360 | 9014280 | 285.8 | 736.1 | 0.0 | 736.1 | 100464.1 | 0.0 | 0 | 100464.1 | 11.145 | | | | |
| ASM002495 | Glostadsbäcken | 12:3 | 0.13 | 27720 | 27720 | 0.9 | 360.2 | 0.0 | 360.2 | 360.2 | 0.0 | 0 | 360.2 | 12.993 | | | | |
| ASM002485 | Glostadsbäcken | 12:2 | 0.33 | 72820 | 72820 | 2.3 | 825.3 | 0.0 | 825.3 | 825.3 | 0.0 | 0 | 825.3 | 11.333 | | | | |
| ASM002498 | Glostadsbäcken | 12:1 | 1.60 | 351340 | 451880 | 14.3 | 4086.8 | 0.0 | 4086.8 | 5272.3 | 0.0 | 0 | 5272.3 | 11.667 | | | | |
| ASM001518B | Stålglobäcken | 13:1 | 0.68 | 149380 | 149380 | 4.7 | 827.8 | 0.0 | 827.8 | 827.8 | 0.0 | 0 | 827.8 | 5.541 | PSM002086 | 0.005 | 13.514 | 59 |
| ASM001518A | Stålglobäcken | 13:1 | 0.35 | 77880 | 227260 | 7.2 | 1265.5 | 0.0 | 1265.5 | 2093.2 | 0.0 | 0 | 2093.2 | 9.211 | | | | |
| ASM002462 | Uvöbäcken | 15:1 | 0.97 | 212740 | 212740 | 6.7 | 3282.4 | 0.0 | 3282.4 | 3282.4 | 0.0 | 0 | 3282.4 | 15.429 | | | | |
| ASM002497 | Stekebäcken | 14:2 | 0.44 | 95700 | 95700 | 3.0 | 856.8 | 0.0 | 856.8 | 856.8 | 0.0 | 0 | 856.8 | 8.953 | | | | |
| ASM001517 | Stekebäcken | 14:1 | 0.90 | 198660 | 294360 | 9.3 | 3357.3 | 0.0 | 3357.3 | 4214.0 | 0.0 | 0 | 4214.0 | 14.316 | | | | |
| ASM002463 | Svartebäck | 16:1 | 0.50 | 110880 | 110880 | 3.5 | 959.9 | 0.0 | 959.9 | 959.9 | 0.0 | 0 | 959.9 | 8.657 | | | | |
| ASM002655 | Coastal area | | 2.71 | 596420 | 596420 | 18.9 | 12761.9 | 0.0 | 12761.9 | 12761.9 | 0.0 | 0 | 12761.9 | 21.397 | | | | |
| ASM002658 | Coastal area | | 1.26 | 277420 | 277420 | 8.8 | 4601.8 | 0.0 | 4601.8 | 4601.8 | 0.0 | 0 | 4601.8 | 16.588 | | | | |
| ASM002656 | Coastal area | | 0.22 | 48400 | 48400 | 1.5 | 1191.0 | 0.0 | 1191.0 | 1191.0 | 0.0 | 0 | 1191.0 | 24.608 | | | | |
| ASM002660 | Coastal area | | 0.14 | 30360 | 30360 | 1.0 | 678.4 | 0.0 | 678.4 | 678.4 | 0.0 | 0 | 678.4 | 22.345 | | | | |
| ASM002659 | Coastal area | | 15.70 | 3453780 | 3453780 | 109.5 | 33517.1 | 22210.6 | 55727.6 | 55727.6 | 0.0 | 0 | 55727.6 | 16.135 | | | | |
| ASM002657 | Coastal area | | 2.60 | 571340 | 571340 | 18.1 | 5578.0 | 0.0 | 5578.0 | 5578.0 | 0.0 | 0 | 5578.0 | 9.763 | | | | |
| ASM001522 | Uthammarsån | 17:5 | 0.57 | 125620 | 125620 | 4.0 | 579.5 | 0.0 | 579.5 | 579.5 | 0.0 | 0 | 579.5 | 4.613 | | | | |
| ASM001523 | Uthammarsån | 17:6 | 0.96 | 210760 | 210760 | 6.7 | 955.7 | 0.0 | 955.7 | 955.7 | 0.0 | 0 | 955.7 | 4.534 | | | | |
| ASM001521 | Uthammarsån | 17:4 | 0.20 | 44880 | 44880 | 1.4 | 206.0 | 0.0 | 206.0 | 206.0 | 0.0 | 0 | 206.0 | 4.589 | | | | |
| ASM001520 | Uthammarsån | 17:3 | 0.08 | 17820 | 17820 | 0.6 | 83.9 | 0.0 | 83.9 | 83.9 | 0.0 | 0 | 83.9 | 4.706 | | | | |
| ASM002494B | Uthammarsån | 17:1 | 2.91 | 640860 | 1039940 | 33.0 | 2911.9 | 0.0 | 2911.9 | 4736.8 | 0.0 | 0 | 4736.8 | 4.555 | PSM002076 | 0.033 | 7.410 | 39 |
| ASM001533 | Uthammarsån | 17:2 | 0.51 | 112640 | 112640 | 3.6 | 560.3 | 0.0 | 560.3 | 560.3 | 0.0 | 0 | 560.3 | 4.974 | | | | |
| ASM002494A | Uthammarsån | 17:1 | 1.78 | 391820 | 1544400 | 49.0 | 4412.3 | 0.0 | 4412.3 | 9709.4 | 0.0 | 0 | 9709.4 | 6.287 | | | | |
| ASM001528 | Släthultebäcken | 18:5 | 0.32 | 70400 | 70400 | 2.2 | 318.5 | 0.0 | 318.5 | 318.5 | 0.0 | 0 | 318.5 | 4.524 | | | | |
| ASM002477 | Släthultebäcken | 18:4 | 0.66 | 144980 | 215380 | 6.8 | 655.8 | 0.0 | 655.8 | 974.3 | 0.0 | 0 | 974.3 | 4.524 | | | | |
| ASM001531 | Släthultebäcken | 18:8 | 0.30 | 66440 | 66440 | 2.1 | 300.5 | 0.0 | 300.5 | 300.5 | 0.0 | 0 | 300.5 | 4.524 | | | | |
| ASM001532 | Släthultebäcken | 18:9 | 0.11 | 24420 | 24420 | 0.8 | 110.5 | 0.0 | 110.5 | 110.5 | 0.0 | 0 | 110.5 | 4.524 | | | | |
| ASM002455 | Släthultebäcken | 18:7 | 0.76 | 167420 | 258280 | 8.2 | 757.3 | 0.0 | 757.3 | 1168.4 | 0.0 | 0 | 1168.4 | 4.524 | | | | |
| ASM002475 | Släthultebäcken | 18:6 | 1.06 | 232100 | 490380 | 15.5 | 1049.9 | 0.0 | 1049.9 | 2218.3 | 0.0 | 0 | 2218.3 | 4.524 | | | | |
| ASM001526 | Släthultebäcken | 18:3 | 0.40 | 88220 | 88220 | 2.8 | 495.3 | 0.0 | 495.3 | 495.3 | 0.0 | 0 | 495.3 | 5.614 | | | | |
| ASM002481C | Släthultebäcken | 18:1 | 2.44 | 537020 | 1027400 | 32.6 | 2429.3 | 17255.4 | 19684.7 | 21903.0 | 0.0 | 0 | 21903.0 | 21.319 | PSM002070 | | | |
| ASM002481B | Släthultebäcken | 18:1 | 2.13 | 469260 | 1800260 | 57.1 | 2446.9 | 0.0 | 2446.9 | 25819.4 | 0.0 | 0 | 25819.4 | 14.342 | PSM002075 | | | |
| ASM001525 | Släthultebäcken | 18:2 | 0.77 | 169620 | 169620 | 5.4 | 824.9 | 0.0 | 824.9 | 824.9 | 0.0 | 0 | 824.9 | 4.863 | | | | |
| ASM002481A | Släthultebäcken | 18:1 | 0.00 | 220 | 1970100 | 62.5 | 0.0 | 0.0 | 0.0 | 26644.4 | 0.0 | 0 | 26644.4 | 13.524 | | | | |
| ASM001444 | Söråmagasinet | 11:1 | 0.52 | 115060 | 115060 | 3.6 | 1785.6 | 0.0 | 1785.6 | 1785.6 | 0.0 | 0 | 1785.6 | 15.519 | | | | |
| ASM002466 | Stekflagebäcken | 22:1 | 0.36 | 78980 | 78980 | 2.5 | 1542.7 | 0.0 | 1542.7 | 1542.7 | 0.0 | 0 | 1542.7 | 19.533 | | | | |
| ASM002653 | Coastal area | | 0.76 | 166980 | 166980 | 5.3 | 2923.6 | 0.0 | 2923.6 | 2923.6 | 0.0 | 0 | 2923.6 | 17.509 | | | | |
| ASM002470 | Skölkebäcken | 26:1 | 0.17 | 36300 | 36300 | 1.2 | 531.6 | 0.0 | 531.6 | 531.6 | 0.0 | 0 | 531.6 | 14.644 | | | | |
| ASM002469 | Gloebäcken | 25:1 | 0.13 | 28820 | 28820 | 0.9 | 276.9 | 0.0 | 276.9 | 276.9 | 0.0 | 0 | 276.9 | 9.610 | | | | |
| ASM002468 | Lindströmmebäcken | 24:1 | 0.19 | 42240 | 42240 | 1.3 | 569.9 | 0.0 | 569.9 | 569.9 | 0.0 | 0 | 569.9 | 13.492 | | | | |
| ASM002467B | Vadvikebäcken | 23:1 | 0.30 | 65560 | 65560 | 2.1 | 370.7 | 0.0 | 370.7 | 370.7 | 0.0 | 0 | 370.7 | 5.654 | PSM107735 | 0.002 | 5.654 | 0 |
| ASM002467A | Vadvikebäcken | 23:1 | 0.01 | 1980 | 67540 | 2.1 | 22.3 | 0.0 | 22.3 | 393.0 | 0.0 | 0 | 393.0 | 5.818 | | | | |
| | **Kärrviksån** | 5:1-20 | 27.31 | 6007100 | 6007100 | 26.9 | 33782.8 | 22508.2 | 56291.0 | | 0.0 | 0 | 56291.0 | 9.371 | | | | |
| | **Laxemarån** | 10:1-32 | 40.97 | 9014280 | 9014280 | 37.5 | 44189.2 | 56274.9 | 100464.1 | | 0.0 | 0 | 100464.1 | 11.145 | | | | |
| | **All catchments** | | 129.97 | 28593620 | 28593620 | 22.3 | 217221.0 | 118249.1 | 335470.2 | | 0.0 | 0 | 335470.2 | 11.732 | | | | |

# Appendix D

Compilation of the number of observations behind mean values in data selection C. Data from surface water, shallow groundwater and groundwater of the bedrock.

| Idcode | Water type | Label | Elevation | pH | Cl | Sr | Si | Fe | $S^{2-}$ | $N_{tot}$ | DOC | D | $^{13}C$ | $^{14}C$ | $^{34}S$ | $^{87}Sr$ | Cu | La | U | $^{222}Rn$ |
|---|---|---|---|---|---|---|---|---|---|---|---|---|---|---|---|---|---|---|---|---|
| HAS13 | Ground Water | HAS13-65 | -65 | 1 | 1 | 1 | 1 | 0 | 1 | 0 | 1 | 1 | 0 | 0 | 0 | 0 | 0 | 0 | 0 | 1 |
| HAV06 | Ground Water | HAV06-63 | -63 | 1 | 1 | 0 | 0 | 0 | 0 | 0 | 1 | 1 | 0 | 0 | 0 | 0 | 0 | 0 | 0 | 0 |
| HLX10 | Ground Water | HLX10-28 | -29 | 1 | 1 | 1 | 1 | 1 | 0 | 0 | 0 | 1 | 1 | 1 | 1 | 1 | 0 | 0 | 0 | 0 |
| HLX14 | Ground Water | HLX14-43 | -42 | 1 | 1 | 1 | 1 | 1 | 0 | 0 | 0 | 1 | 1 | 1 | 1 | 0 | 0 | 0 | 0 | 0 |
| HLX20 | Ground Water | HLX20-55 | -54 | 1 | 1 | 1 | 1 | 1 | 1 | 0 | 1 | 1 | 1 | 1 | 1 | 1 | 0 | 1 | 1 | 1 |
| HLX28 | Ground Water | HLX28-54 | -54 | 1 | 1 | 1 | 1 | 1 | 0 | 0 | 0 | 1 | 1 | 1 | 1 | 1 | 0 | 0 | 0 | 0 |
| HLX30 | Ground Water | HLX30-61 | -60 | 1 | 1 | 1 | 1 | 1 | 0 | 0 | 0 | 1 | 1 | 1 | 1 | 1 | 0 | 0 | 0 | 0 |
| HLX35 | Ground Water | HLX35-53 | -53 | 1 | 1 | 1 | 1 | 1 | 0 | 0 | 0 | 1 | 1 | 1 | 1 | 1 | 0 | 0 | 0 | 0 |
| HSH02 | Ground Water | HSH02-91 | -91 | 1 | 1 | 1 | 1 | 1 | 0 | 0 | 0 | 1 | 1 | 1 | 1 | 1 | 0 | 0 | 0 | 0 |
| KAS02 | Ground Water | KAS02-200 | -200 | 1 | 1 | 1 | 1 | 0 | 1 | 0 | 1 | 1 | 0 | 0 | 0 | 0 | 0 | 0 | 1 | 1 |
| KAS02 | Ground Water | KAS02-308 | -308 | 1 | 1 | 1 | 1 | 0 | 1 | 0 | 1 | 1 | 0 | 0 | 0 | 0 | 0 | 0 | 0 | 1 |
| KAS02 | Ground Water | KAS02-318 | -317 | 1 | 1 | 1 | 1 | 0 | 1 | 0 | 1 | 1 | 0 | 0 | 0 | 0 | 0 | 0 | 1 | 1 |
| KAS02 | Ground Water | KAS02-457 | -456 | 1 | 1 | 1 | 0 | 0 | 1 | 0 | 1 | 1 | 1 | 0 | 0 | 0 | 0 | 0 | 0 | 1 |
| KAS02 | Ground Water | KAS02-523 | -523 | 1 | 1 | 0 | 1 | 0 | 1 | 0 | 0 | 1 | 0 | 0 | 0 | 0 | 0 | 0 | 1 | 1 |
| KAS02 | Ground Water | KAS02-853 | -852 | 1 | 1 | 1 | 1 | 0 | 1 | 0 | 1 | 1 | 0 | 0 | 0 | 0 | 0 | 0 | 0 | 1 |
| KAS02 | Ground Water | KAS02-882 | -881 | 1 | 1 | 1 | 1 | 0 | 1 | 0 | 1 | 1 | 0 | 0 | 0 | 0 | 0 | 0 | 0 | 1 |
| KAS03 | Ground Water | KAS03-122 | -122 | 1 | 1 | 1 | 1 | 0 | 1 | 0 | 1 | 1 | 0 | 0 | 0 | 0 | 0 | 0 | 0 | 1 |
| KAS03 | Ground Water | KAS03-239 | -239 | 1 | 1 | 1 | 1 | 0 | 1 | 0 | 1 | 1 | 1 | 0 | 0 | 0 | 0 | 0 | 0 | 1 |
| KAS03 | Ground Water | KAS03-349 | -349 | 0 | 1 | 1 | 1 | 0 | 1 | 0 | 1 | 1 | 0 | 0 | 0 | 0 | 0 | 0 | 0 | 1 |
| KAS03 | Ground Water | KAS03-455 | -454 | 1 | 1 | 1 | 1 | 0 | 1 | 0 | 1 | 1 | 0 | 0 | 0 | 0 | 0 | 0 | 0 | 1 |
| KAS03 | Ground Water | KAS03-603 | -602 | 1 | 1 | 1 | 1 | 0 | 1 | 0 | 1 | 1 | 0 | 0 | 0 | 0 | 0 | 0 | 0 | 1 |
| KAS03 | Ground Water | KAS03-831 | -830 | 1 | 1 | 1 | 1 | 0 | 1 | 0 | 1 | 1 | 0 | 0 | 0 | 0 | 0 | 0 | 0 | 1 |
| KAS03 | Ground Water | KAS03-915 | -914 | 1 | 1 | 1 | 1 | 0 | 1 | 0 | 0 | 1 | 0 | 0 | 0 | 0 | 0 | 0 | 0 | 1 |
| KAS04 | Ground Water | KAS04-186 | -185 | 1 | 1 | 1 | 1 | 0 | 1 | 0 | 1 | 1 | 0 | 0 | 0 | 0 | 0 | 0 | 0 | 1 |
| KAS04 | Ground Water | KAS04-276 | -276 | 1 | 1 | 1 | 1 | 0 | 1 | 0 | 1 | 1 | 0 | 0 | 0 | 0 | 0 | 0 | 1 | 1 |
| KAS04 | Ground Water | KAS04-377 | -377 | 1 | 1 | 1 | 1 | 0 | 1 | 0 | 1 | 1 | 0 | 0 | 0 | 0 | 0 | 0 | 0 | 1 |
| KAS06 | Ground Water | KAS06-285 | -284 | 1 | 1 | 1 | 1 | 0 | 1 | 0 | 1 | 1 | 0 | 0 | 0 | 0 | 0 | 0 | 0 | 1 |
| KAS06 | Ground Water | KAS06-332 | -332 | 1 | 1 | 1 | 1 | 1 | 1 | 0 | 1 | 1 | 0 | 0 | 0 | 0 | 0 | 0 | 0 | 1 |
| KAS06 | Ground Water | KAS06-434 | -433 | 1 | 1 | 1 | 1 | 0 | 1 | 0 | 1 | 1 | 0 | 0 | 0 | 0 | 0 | 0 | 0 | 1 |
| KAV01 | Ground Water | KAV01-675 | -675 | 0 | 1 | 0 | 1 | 0 | 0 | 0 | 0 | 1 | 0 | 0 | 0 | 0 | 0 | 0 | 0 | 1 |
| KLX01 | Ground Water | KLX01-258 | -257 | 1 | 1 | 1 | 1 | 0 | 1 | 0 | 1 | 1 | 0 | 0 | 0 | 0 | 0 | 0 | 0 | 1 |
| KLX01 | Ground Water | KLX01-673 | -673 | 1 | 1 | 1 | 1 | 0 | 1 | 0 | 1 | 1 | 0 | 0 | 0 | 0 | 0 | 0 | 0 | 1 |
| KLX02 | Ground Water | KLX02-1069 | -1068 | 1 | 1 | 1 | 1 | 1 | 1 | 0 | 1 | 1 | 0 | 0 | 0 | 0 | 0 | 0 | 0 | 0 |
| KLX02 | Ground Water | KLX02-1323 | -1323 | 1 | 1 | 1 | 1 | 1 | 1 | 0 | 1 | 1 | 0 | 1 | 0 | 1 | 0 | 1 | 0 | 1 |
| KLX02 | Ground Water | KLX02-1531 | -1531 | 1 | 1 | 1 | 1 | 1 | 1 | 0 | 1 | 1 | 0 | 0 | 0 | 0 | 0 | 0 | 0 | 0 |
| KLX03 | Ground Water | KLX03-171 | -171 | 1 | 1 | 1 | 1 | 1 | 1 | 0 | 1 | 1 | 1 | 1 | 1 | 0 | 0 | 1 | 1 | 1 |
| KLX03 | Ground Water | KLX03-380 | -380 | 1 | 1 | 1 | 1 | 1 | 1 | 0 | 1 | 1 | 1 | 1 | 1 | 1 | 0 | 1 | 1 | 1 |
| KLX03 | Ground Water | KLX03-923 | -922 | 1 | 1 | 1 | 1 | 1 | 1 | 0 | 1 | 1 | 0 | 0 | 1 | 1 | 0 | 1 | 1 | 1 |
| KLX04 | Ground Water | KLX04+6 | 7 | 1 | 1 | 1 | 1 | 1 | 0 | 0 | 0 | 1 | 0 | 0 | 0 | 0 | 0 | 0 | 0 | 0 |
| KLX04 | Ground Water | KLX04-487 | -487 | 1 | 1 | 1 | 1 | 1 | 1 | 0 | 1 | 1 | 0 | 1 | 1 | 1 | 0 | 1 | 1 | 1 |
| KLX04 | Ground Water | KLX04-945 | -944 | 1 | 1 | 1 | 1 | 1 | 1 | 0 | 1 | 1 | 0 | 0 | 1 | 1 | 0 | 1 | 1 | 1 |
| KLX05 | Ground Water | KLX05-205 | -205 | 1 | 1 | 1 | 1 | 1 | 1 | 0 | 1 | 1 | 1 | 1 | 1 | 1 | 0 | 1 | 1 | 1 |
| KLX05 | Ground Water | KLX05-550 | -550 | 1 | 1 | 1 | 1 | 1 | 0 | 0 | 0 | 1 | 0 | 0 | 0 | 0 | 0 | 0 | 0 | 0 |
| KLX06 | Ground Water | KLX06-1 | 0 | 1 | 1 | 1 | 1 | 1 | 0 | 0 | 0 | 1 | 0 | 0 | 0 | 0 | 0 | 0 | 0 | 0 |
| KLX06 | Ground Water | KLX06-219 | -219 | 1 | 1 | 1 | 1 | 1 | 1 | 0 | 0 | 1 | 0 | 0 | 0 | 0 | 0 | 0 | 0 | 0 |
| KLX06 | Ground Water | KLX06-222 | -221 | 1 | 1 | 1 | 1 | 1 | 1 | 0 | 1 | 1 | 1 | 1 | 1 | 1 | 0 | 1 | 1 | 1 |
| KLX06 | Ground Water | KLX06-476 | -475 | 1 | 1 | 1 | 1 | 1 | 1 | 0 | 1 | 1 | 1 | 1 | 1 | 1 | 0 | 1 | 1 | 1 |
| KLX08 | Ground Water | KLX08-391 | -391 | 1 | 1 | 1 | 1 | 1 | 1 | 0 | 1 | 1 | 0 | 0 | 1 | 1 | 0 | 1 | 1 | 1 |
| KLX08 | Ground Water | KLX08-505 | -505 | 1 | 1 | 1 | 1 | 1 | 1 | 0 | 1 | 1 | 0 | 0 | 1 | 1 | 0 | 1 | 1 | 1 |
| KLX13A | Ground Water | KLX13A-409 | -408 | 1 | 1 | 1 | 1 | 1 | 1 | 0 | 1 | 1 | 1 | 1 | 1 | 1 | 0 | 1 | 1 | 0 |
| KLX15A | Ground Water | KLX15A-468 | -467 | 1 | 1 | 1 | 1 | 1 | 1 | 0 | 1 | 1 | 0 | 0 | 1 | 1 | 0 | 1 | 1 | 1 |
| KLX17A | Ground Water | KLX17A-343 | -342 | 1 | 1 | 1 | 1 | 1 | 1 | 0 | 1 | 1 | 1 | 1 | 1 | 1 | 0 | 1 | 1 | 0 |
| KLX19A | Ground Water | KLX19A-414 | -414 | 1 | 1 | 1 | 1 | 1 | 1 | 0 | 1 | 1 | 1 | 1 | 1 | 1 | 0 | 1 | 1 | 1 |
| KSH01A | Ground Water | KSH01A-153 | -153 | 1 | 1 | 1 | 1 | 1 | 1 | 0 | 1 | 1 | 1 | 0 | 1 | 1 | 1 | 1 | 1 | 1 |
| KSH01A | Ground Water | KSH01A-242 | -242 | 1 | 1 | 1 | 1 | 1 | 1 | 0 | 1 | 1 | 0 | 0 | 1 | 1 | 1 | 1 | 1 | 1 |
| KSH01A | Ground Water | KSH01A-246 | -246 | 1 | 1 | 1 | 1 | 1 | 1 | 0 | 1 | 1 | 0 | 0 | 1 | 1 | 0 | 1 | 1 | 1 |
| KSH01A | Ground Water | KSH01A-532 | -532 | 1 | 1 | 1 | 1 | 1 | 1 | 0 | 1 | 1 | 0 | 0 | 1 | 1 | 0 | 1 | 1 | 1 |
| KSH01A | Ground Water | KSH01A-537 | -536 | 1 | 1 | 1 | 1 | 1 | 0 | 0 | 1 | 1 | 0 | 0 | 1 | 1 | 0 | 1 | 1 | 1 |
| KSH02 | Ground Water | KSH02-416 | -415 | 1 | 1 | 1 | 1 | 1 | 0 | 0 | 1 | 1 | 0 | 0 | 1 | 1 | 0 | 1 | 1 | 0 |
| KSH02 | Ground Water | KSH02-419 | -419 | 1 | 1 | 1 | 1 | 1 | 0 | 0 | 1 | 1 | 1 | 0 | 1 | 1 | 0 | 1 | 1 | 1 |
| KSH02 | Ground Water | KSH02-571 | -571 | 1 | 1 | 1 | 1 | 1 | 0 | 0 | 1 | 1 | 0 | 0 | 1 | 1 | 0 | 1 | 1 | 0 |
| KSH02 | Ground Water | KSH02-952 | -952 | 1 | 1 | 1 | 1 | 1 | 1 | 0 | 1 | 1 | 0 | 0 | 1 | 1 | 0 | 1 | 1 | 1 |
| PSM002060 | Sea Water | PO60B | | 33 | 33 | 33 | 33 | 33 | 2 | 32 | 33 | 5 | 4 | 4 | 5 | 4 | 1 | 1 | 1 | 2 |
| PSM002060 | Sea Water | PO60S | | 35 | 35 | 35 | 35 | 35 | 2 | 35 | 35 | 5 | 5 | 5 | 6 | 4 | 1 | 1 | 1 | 2 |
| PSM002061 | Sea Water | PO61B | | 35 | 35 | 35 | 35 | 34 | 2 | 35 | 35 | 7 | 6 | 6 | 7 | 5 | 1 | 1 | 1 | 2 |
| PSM002061 | Sea Water | PO61S | | 36 | 36 | 36 | 36 | 36 | 2 | 35 | 36 | 7 | 7 | 6 | 8 | 6 | 1 | 1 | 1 | 2 |
| PSM002062 | Sea Water | PO62B | | 38 | 38 | 38 | 38 | 38 | 2 | 38 | 38 | 8 | 6 | 6 | 8 | 6 | 1 | 1 | 1 | 2 |
| PSM002062 | Sea Water | PO62S | | 37 | 37 | 37 | 37 | 37 | 2 | 37 | 37 | 7 | 5 | 5 | 7 | 5 | 1 | 1 | 1 | 2 |
| PSM002063 | Sea Water | PO63B | | 17 | 17 | 17 | 17 | 17 | 0 | 17 | 17 | 0 | 1 | 1 | 1 | 1 | 0 | 0 | 0 | 0 |
| PSM002063 | Sea Water | PO63S | | 17 | 17 | 17 | 17 | 17 | 0 | 17 | 17 | 0 | 1 | 1 | 1 | 1 | 0 | 0 | 0 | 0 |

| Idcode | Water type | Label | Elevation | pH | Cl | Sr | Si | Fe | $S^{2-}$ | $N_{tot}$ | DOC | D | $^{13}C$ | $^{14}C$ | $^{34}S$ | $^{87}Sr$ | Cu | La | U | $^{222}Rn$ |
|---|---|---|---|---|---|---|---|---|---|---|---|---|---|---|---|---|---|---|---|---|
| PSM002064 | Sea Water | PO64B | | 66 | 66 | 66 | 66 | 66 | 3 | 61 | 61 | 8 | 6 | 6 | 8 | 6 | 6 | 6 | 6 | 3 |
| PSM002064 | Sea Water | PO64S | | 61 | 62 | 62 | 62 | 62 | 4 | 59 | 59 | 8 | 6 | 6 | 8 | 6 | 7 | 7 | 7 | 4 |
| PSM002065 | Lake Water | PL65B | | 59 | 59 | 59 | 59 | 58 | 3 | 54 | 54 | 8 | 2 | 2 | 7 | 6 | 5 | 5 | 5 | 3 |
| PSM002065 | Lake Water | PL65S | | 58 | 58 | 58 | 58 | 58 | 3 | 55 | 55 | 5 | 1 | 1 | 5 | 5 | 7 | 7 | 7 | 3 |
| PSM002066 | Lake Water | PL66B | | 17 | 17 | 17 | 17 | 17 | 0 | 17 | 17 | 1 | 1 | 1 | 1 | 1 | 0 | 0 | 0 | 0 |
| PSM002066 | Lake Water | PL66S | | 18 | 18 | 18 | 18 | 18 | 0 | 18 | 18 | 1 | 1 | 1 | 1 | 1 | 0 | 0 | 0 | 0 |
| PSM002067 | Lake Water | PL67B | | 35 | 35 | 35 | 35 | 34 | 0 | 35 | 35 | 1 | 1 | 1 | 1 | 1 | 0 | 0 | 0 | 0 |
| PSM002067 | Lake Water | PL67S | | 30 | 30 | 30 | 30 | 30 | 0 | 30 | 30 | 1 | 1 | 1 | 1 | 1 | 0 | 0 | 0 | 0 |
| PSM002068 | Stream Water | PW068 | | 17 | 17 | 17 | 17 | 17 | 0 | 17 | 17 | 0 | 0 | 0 | 0 | 0 | 0 | 0 | 0 | 0 |
| PSM002069 | Stream Water | PW069 | | 31 | 31 | 31 | 31 | 31 | 0 | 31 | 31 | 0 | 0 | 0 | 0 | 0 | 0 | 0 | 0 | 0 |
| PSM002070 | Stream Water | PW070 | | 15 | 15 | 15 | 15 | 15 | 0 | 15 | 15 | 0 | 0 | 0 | 0 | 0 | 0 | 0 | 0 | 0 |
| PSM002071 | Stream Water | PW071 | | 37 | 37 | 37 | 37 | 36 | 2 | 37 | 37 | 8 | 2 | 2 | 8 | 6 | 1 | 1 | 1 | 2 |
| PSM002072 | Stream Water | PW072 | | 3 | 3 | 3 | 3 | 3 | 0 | 3 | 3 | 1 | 0 | 0 | 1 | 1 | 0 | 0 | 0 | 0 |
| PSM002075 | Stream Water | PW075 | | 12 | 12 | 12 | 12 | 12 | 0 | 12 | 12 | 0 | 0 | 0 | 0 | 0 | 0 | 0 | 0 | 0 |
| PSM002076 | Stream Water | PW076 | | 22 | 22 | 22 | 22 | 22 | 0 | 22 | 22 | 5 | 1 | 1 | 5 | 4 | 0 | 0 | 0 | 0 |
| PSM002077 | Stream Water | PW077 | | 15 | 15 | 15 | 15 | 15 | 0 | 15 | 15 | 0 | 0 | 0 | 0 | 0 | 0 | 0 | 0 | 0 |
| PSM002078 | Stream Water | PW078 | | 16 | 16 | 16 | 16 | 16 | 0 | 16 | 16 | 0 | 0 | 0 | 0 | 0 | 0 | 0 | 0 | 0 |
| PSM002079 | Stream Water | PW079 | | 60 | 60 | 60 | 60 | 60 | 3 | 56 | 56 | 7 | 2 | 2 | 7 | 5 | 6 | 6 | 6 | 3 |
| PSM002080 | Stream Water | PW080 | | 8 | 8 | 8 | 8 | 8 | 0 | 8 | 8 | 0 | 0 | 0 | 0 | 0 | 0 | 0 | 0 | 0 |
| PSM002081 | Stream Water | PW081 | | 18 | 19 | 19 | 19 | 19 | 0 | 18 | 19 | 0 | 0 | 0 | 0 | 0 | 0 | 0 | 0 | 0 |
| PSM002082 | Stream Water | PW082 | | 23 | 23 | 23 | 23 | 23 | 1 | 23 | 23 | 5 | 2 | 2 | 5 | 3 | 0 | 0 | 0 | 1 |
| PSM002083 | Stream Water | PW083 | | 55 | 55 | 55 | 55 | 55 | 2 | 52 | 52 | 6 | 1 | 1 | 6 | 4 | 4 | 4 | 4 | 2 |
| PSM002084 | Stream Water | PW084 | | 37 | 37 | 37 | 37 | 37 | 2 | 37 | 37 | 8 | 4 | 4 | 8 | 6 | 1 | 1 | 1 | 2 |
| PSM002085 | Stream Water | PW085 | | 55 | 55 | 55 | 55 | 55 | 2 | 50 | 50 | 8 | 6 | 6 | 8 | 6 | 5 | 5 | 5 | 2 |
| PSM002086 | Stream Water | PW086 | | 23 | 23 | 23 | 23 | 23 | 0 | 23 | 23 | 6 | 1 | 1 | 6 | 5 | 0 | 0 | 0 | 0 |
| PSM002087 | Stream Water | PW087 | | 64 | 64 | 64 | 64 | 64 | 4 | 60 | 60 | 8 | 2 | 2 | 8 | 6 | 8 | 8 | 8 | 4 |
| PSM002170 | Precipitation | PN170 | 6 | 18 | 18 | 18 | 18 | 18 | 0 | 0 | 0 | 18 | 0 | 0 | 0 | 0 | 0 | 0 | 0 | 0 |
| PSM005964 | Lake Water | PL64B | | 22 | 22 | 22 | 22 | 22 | 0 | 22 | 22 | 0 | 0 | 0 | 0 | 0 | 0 | 0 | 0 | 0 |
| PSM005964 | Lake Water | PL64S | | 22 | 22 | 22 | 22 | 22 | 0 | 22 | 21 | 0 | 0 | 0 | 0 | 0 | 0 | 0 | 0 | 0 |
| PSM007097 | Sea Water | PO97B | | 25 | 25 | 25 | 25 | 25 | 1 | 21 | 21 | 0 | 0 | 0 | 0 | 0 | 5 | 5 | 5 | 1 |
| PSM007097 | Sea Water | PO97S | | 23 | 23 | 23 | 23 | 23 | 1 | 19 | 18 | 0 | 0 | 0 | 0 | 0 | 5 | 5 | 5 | 1 |
| PSM107735 | Stream Water | PW735 | | 11 | 11 | 11 | 11 | 11 | 0 | 11 | 11 | 1 | 0 | 0 | 1 | 1 | 0 | 0 | 0 | 0 |
| SSM000002 | Near Surface GW | S002+0 | 0 | 1 | 1 | 1 | 1 | 1 | 0 | 0 | 0 | 0 | 0 | 0 | 0 | 1 | 0 | 0 | 0 | 0 |
| SSM000008 | Near Surface GW | S008+0 | 1 | 5 | 5 | 5 | 5 | 5 | 3 | 0 | 1 | 5 | 3 | 3 | 3 | 3 | 2 | 2 | 2 | 2 |
| SSM000010 | Near Surface GW | S010+2 | 3 | 6 | 6 | 6 | 6 | 6 | 3 | 0 | 1 | 6 | 3 | 3 | 3 | 3 | 2 | 2 | 2 | 2 |
| SSM000012 | Near Surface GW | S012-4 | -4 | 6 | 6 | 6 | 5 | 6 | 3 | 0 | 1 | 6 | 3 | 3 | 3 | 3 | 2 | 2 | 2 | 2 |
| SSM000014 | Near Surface GW | S014-1 | -1 | 5 | 5 | 5 | 5 | 5 | 2 | 0 | 1 | 5 | 3 | 3 | 3 | 3 | 1 | 1 | 1 | 2 |
| SSM000016 | Near Surface GW | S016-1 | 0 | 5 | 5 | 5 | 5 | 5 | 2 | 0 | 0 | 5 | 1 | 1 | 2 | 2 | 1 | 1 | 1 | 1 |
| SSM000018 | Near Surface GW | S018-2 | -2 | 5 | 5 | 5 | 5 | 5 | 3 | 0 | 1 | 5 | 2 | 2 | 3 | 3 | 2 | 2 | 2 | 2 |
| SSM000020 | Near Surface GW | S020+3 | 4 | 5 | 5 | 5 | 5 | 5 | 2 | 0 | 1 | 5 | 2 | 2 | 3 | 3 | 1 | 1 | 1 | 2 |
| SSM000022 | Near Surface GW | S022-1 | -1 | 14 | 14 | 14 | 14 | 14 | 9 | 7 | 9 | 14 | 4 | 4 | 7 | 4 | 10 | 10 | 10 | 3 |
| SSM000024 | Near Surface GW | S024+0 | 0 | 1 | 1 | 1 | 1 | 1 | 1 | 0 | 0 | 1 | 1 | 1 | 1 | 1 | 0 | 0 | 0 | 1 |
| SSM000026 | Near Surface GW | S026-1 | 0 | 4 | 4 | 4 | 4 | 4 | 1 | 0 | 0 | 4 | 0 | 0 | 2 | 2 | 0 | 0 | 0 | 1 |
| SSM000027 | Near Surface GW | S027+5 | 5 | 4 | 4 | 4 | 4 | 4 | 2 | 1 | 3 | 4 | 0 | 0 | 3 | 2 | 3 | 3 | 3 | 2 |
| SSM000029 | Near Surface GW | S029-5 | -5 | 5 | 5 | 5 | 5 | 5 | 3 | 3 | 4 | 5 | 1 | 1 | 4 | 1 | 5 | 5 | 5 | 1 |
| SSM000030 | Near Surface GW | S030+6 | 7 | 12 | 12 | 12 | 12 | 12 | 9 | 8 | 10 | 12 | 2 | 2 | 5 | 2 | 10 | 10 | 10 | 2 |
| SSM000031 | Near Surface GW | S031+2 | 3 | 6 | 6 | 6 | 6 | 6 | 3 | 3 | 4 | 6 | 0 | 0 | 4 | 1 | 5 | 5 | 5 | 1 |
| SSM000034 | Near Surface GW | S034-4 | -3 | 6 | 6 | 6 | 6 | 6 | 4 | 3 | 5 | 6 | 2 | 2 | 0 | 2 | 6 | 6 | 6 | 2 |
| SSM000035 | Near Surface GW | S035+23 | 24 | 1 | 1 | 1 | 1 | 1 | 0 | 1 | 1 | 1 | 0 | 0 | 1 | 0 | 1 | 1 | 1 | 0 |
| SSM000037 | Near Surface GW | S037+9 | 9 | 11 | 11 | 11 | 11 | 11 | 8 | 8 | 9 | 11 | 1 | 1 | 4 | 1 | 10 | 10 | 10 | 1 |
| SSM000039 | Near Surface GW | S039+7 | 8 | 2 | 2 | 2 | 2 | 2 | 1 | 2 | 2 | 2 | 0 | 0 | 2 | 0 | 2 | 2 | 2 | 0 |
| SSM000040 | Near Surface GW | S040-2 | -1 | 5 | 5 | 5 | 5 | 5 | 0 | 0 | 0 | 5 | 0 | 0 | 0 | 1 | 3 | 3 | 3 | 0 |
| SSM000041 | Near Surface GW | S041+1 | 1 | 4 | 4 | 4 | 4 | 4 | 3 | 2 | 3 | 4 | 1 | 1 | 1 | 1 | 3 | 3 | 3 | 1 |
| SSM000042 | Near Surface GW | S042-1 | -1 | 11 | 11 | 11 | 11 | 11 | 7 | 7 | 8 | 11 | 1 | 1 | 4 | 1 | 9 | 9 | 9 | 1 |
| SSM000224 | Near Surface GW | S224-10 | -10 | 4 | 4 | 4 | 4 | 4 | 2 | 3 | 4 | 4 | 0 | 0 | 4 | 1 | 4 | 4 | 4 | 1 |
| SSM000226 | Near Surface GW | S226+2 | 2 | 2 | 2 | 2 | 2 | 2 | 1 | 1 | 2 | 2 | 1 | 1 | 2 | 1 | 2 | 2 | 2 | 1 |
| SSM000227 | Near Surface GW | S227+5 | 6 | 1 | 1 | 1 | 1 | 1 | 0 | 1 | 1 | 1 | 0 | 0 | 1 | 0 | 1 | 1 | 1 | 0 |
| SSM000228 | Near Surface GW | S228+6 | 7 | 7 | 7 | 7 | 7 | 7 | 6 | 7 | 7 | 7 | 0 | 0 | 2 | 0 | 7 | 7 | 7 | 0 |
| SSM000230 | Near Surface GW | S230+0 | 1 | 3 | 3 | 3 | 3 | 3 | 1 | 3 | 3 | 3 | 0 | 0 | 3 | 0 | 3 | 3 | 3 | 0 |
| SSM000238 | Near Surface GW | S238-12 | -11 | 1 | 1 | 1 | 1 | 1 | 0 | 1 | 1 | 1 | 0 | 0 | 1 | 0 | 1 | 1 | 1 | 0 |
| SSM000239 | Near Surface GW | S239-4 | -4 | 1 | 1 | 1 | 1 | 1 | 0 | 1 | 1 | 1 | 0 | 0 | 1 | 0 | 1 | 1 | 1 | 0 |
| SSM000240 | Near Surface GW | S240-5 | -5 | 5 | 5 | 5 | 5 | 5 | 4 | 5 | 5 | 5 | 0 | 0 | 1 | 0 | 5 | 5 | 5 | 0 |
| SSM000241 | Near Surface GW | S241-3 | -3 | 1 | 1 | 1 | 1 | 1 | 1 | 1 | 1 | 1 | 0 | 0 | 0 | 0 | 1 | 1 | 1 | 0 |
| SSM000241 | Near Surface GW | S241-33 | -32 | 1 | 1 | 1 | 1 | 1 | 1 | 1 | 1 | 1 | 0 | 0 | 0 | 0 | 1 | 1 | 1 | 0 |
| SSM000242 | Near Surface GW | S242-16 | -15 | 1 | 1 | 1 | 1 | 1 | 0 | 1 | 1 | 1 | 0 | 0 | 1 | 1 | 1 | 1 | 1 | 0 |
| SSM000260 | Near Surface GW | S260+2 | 2 | 1 | 1 | 1 | 1 | 1 | 1 | 1 | 1 | 0 | 0 | 0 | 0 | 0 | 1 | 1 | 1 | 0 |
| SSM000261 | Near Surface GW | S261+0 | 1 | 1 | 1 | 1 | 1 | 1 | 1 | 1 | 1 | 0 | 0 | 0 | 0 | 0 | 1 | 1 | 1 | 0 |
| SSM000262 | Near Surface GW | S262-2 | -2 | 1 | 1 | 1 | 1 | 1 | 1 | 1 | 1 | 0 | 0 | 0 | 0 | 0 | 1 | 1 | 1 | 0 |
| SSM000263 | Near Surface GW | S263-3 | -3 | 1 | 1 | 1 | 1 | 1 | 1 | 1 | 1 | 0 | 0 | 0 | 0 | 0 | 1 | 1 | 1 | 0 |

# Appendix E

Compilation of mean values of data selection C. Data from surface water, shallow groundwater and groundwater of the bedrock.

| IDCODE | WATER_TYPE | label | Elevation | First | Last | Na | K | Ca | Mg | $HCO_3^-$ | Cl | $SO_4^{2-}$ | Br | Li | Sr | Fe | Mn | pH | U | Th | La | $^2H$ | $^{18}O$ | $^3H$ | $^{14}C$ | $^{13}C$ | $\delta^{34}S$ | $^{87}Sr$ | $N_{tot}$ | $P_{tot}$ | DOC |
|---|---|---|---|---|---|---|---|---|---|---|---|---|---|---|---|---|---|---|---|---|---|---|---|---|---|---|---|---|---|---|---|
| | | | masl | date | date | mg·L$^{-1}$ | mg·L$^{-1}$ | mg·L$^{-1}$ | mg·L$^{-1}$ | mg·L$^{-1}$ | mg·L$^{-1}$ | mg·L$^{-1}$ | mg·L$^{-1}$ | mg·L$^{-1}$ | mg·L$^{-1}$ | mg·L$^{-1}$ | mg·L$^{-1}$ | | µg·L$^{-1}$ | µg·L$^{-1}$ | µg·L$^{-1}$ | ‰ SMOW | ‰ SMOW | TU | pMC | ‰ PCB | ‰ CDT | ratio | mg·L$^{-1}$ | mg·L$^{-1}$ | mg·L$^{-1}$ |
| HAS13 | Ground Water | HAS13-65 | -65 | 1989-07-03 | 1989-07-03 | 1880 | 32.8 | 1 040 | 219.0 | 132 | 5070 | 136 | 37 | 0.260 | 11.9 | | 2.57 | 7.30 | | | | -69 | -7.2 | 1.2 | | | | | | | 1.7 |
| HAV06 | Ground Water | HAV06-63 | -63 | 1987-07-31 | 1987-07-31 | 127 | 1.6 | 11 | 1.4 | 228 | 36 | 71 | | | | | | 8.30 | | | | -70 | -10.2 | 0.5 | | | | | | | 2.7 |
| HLX10 | Ground Water | HLX10-28 | -29 | 2005-10-28 | 2005-10-28 | 104 | 3.2 | 12 | 4.1 | 219 | 32 | 49 | 0 | 0.011 | 0.1 | 0.10 | 0.06 | 7.03 | | | | -77 | -10.8 | 5.7 | 53 | -16.1 | 16.4 | 0.716 | | | |
| HLX14 | Ground Water | HLX14-43 | -42 | 2006-11-04 | 2006-11-04 | 248 | 5.4 | 44 | 12.9 | 223 | 357 | 54 | 1 | 0.024 | 0.8 | 0.36 | 0.15 | 7.97 | | | | -84 | -11.2 | 2.5 | 50 | -17.2 | 26.9 | | | | |
| HLX20 | Ground Water | HLX20-55 | -54 | 2007-06-18 | 2007-06-18 | 103 | 1.8 | 12 | 3.4 | 198 | 50 | 37 | 0 | 0.015 | 0.2 | 0.03 | 0.04 | 8.27 | 0.08 | 0.0 | 0.12 | -81 | -11.5 | 1.0 | 42 | -16.8 | 27.3 | 0.715 | | 0.030 | 3.1 |
| HLX28 | Ground Water | HLX28-54 | -54 | 2005-04-12 | 2005-04-12 | 110 | 3.0 | 11 | 3.6 | 265 | 23 | 36 | 0 | 0.011 | 0.1 | 0.08 | 0.06 | 8.17 | | | | -77 | -10.9 | 1.0 | 47 | -16.2 | 30.0 | 0.716 | | | |
| HLX30 | Ground Water | HLX30-61 | -60 | 2005-09-05 | 2005-09-05 | 357 | 4.3 | 62 | 8.7 | 146 | 520 | 72 | | 0.056 | 1.2 | 0.06 | 0.07 | 8.03 | | | | -100 | -13.5 | 0.4 | 34 | -13.4 | 18.2 | 0.715 | | | |
| HLX35 | Ground Water | HLX35-53 | -53 | 2006-01-18 | 2006-01-18 | 217 | 4.4 | 21 | 6.5 | 244 | 203 | 59 | 1 | 0.017 | 0.3 | 0.08 | 0.09 | 8.19 | | | | -85 | -11.4 | 2.2 | 42 | -16.1 | 30.6 | 0.716 | | | |
| HSH02 | Ground Water | HSH02-91 | -91 | 2003-02-03 | 2003-02-03 | 122 | 2.2 | 5 | 1.4 | 266 | 23 | 29 | 0 | 0.016 | 0.1 | 0.36 | 0.02 | 8.58 | | | | -76 | -10.7 | 11.0 | 67 | -16.9 | 17.2 | 0.715 | | | |
| KAS02 | Ground Water | KAS02-200 | -200 | 1989-01-11 | 1989-01-11 | 1300 | 6.6 | 990 | 65.0 | 71 | 3820 | 106 | 13 | 0.380 | 18.0 | | 0.91 | 7.40 | 0.25 | 0.2 | | -109 | -13.9 | 0.3 | | | | | | | 6.0 |
| KAS02 | Ground Water | KAS02-308 | -308 | 1988-04-11 | 1988-04-11 | 1700 | 9.0 | 1 540 | 72.0 | 27 | 5340 | 270 | 21 | 0.560 | 26.0 | | 0.80 | 8.00 | | | | -101 | -12.3 | 8.0 | | | | | | | 2.4 |
| KAS02 | Ground Water | KAS02-318 | -317 | 1988-09-27 | 1988-09-27 | 1710 | 8.8 | 1 480 | 75.0 | 33 | 5360 | 291 | 29 | 0.550 | 27.0 | | 0.67 | 7.50 | 0.21 | 0.3 | | -100 | -12.7 | 4.0 | | | | | | | 2.0 |
| KAS02 | Ground Water | KAS02-457 | -456 | 1988-04-25 | 1988-04-25 | 1800 | 8.1 | 1 580 | 66.0 | 25 | 5440 | 290 | 28 | 0.810 | 30.0 | | 0.73 | 8.20 | | | | -100 | -12.8 | 8.0 | | -6.5 | | | | | 3.0 |
| KAS02 | Ground Water | KAS02-523 | -523 | 1988-05-05 | 1988-05-05 | 2200 | | 1 890 | | 10 | 6330 | 550 | 42 | | | | | 8.00 | 0.23 | 0.2 | | -97 | -12.3 | 8.0 | | | | | | | |
| KAS02 | Ground Water | KAS02-853 | -852 | 1988-09-20 | 1988-09-20 | 2850 | 11.5 | 3 690 | 31.0 | 7 | 11100 | 522 | 79 | 1.800 | 61.0 | | 0.19 | 7.50 | | | | -97 | -13.0 | 8.0 | | | | | | | 0.5 |
| KAS02 | Ground Water | KAS02-882 | -881 | 1989-01-31 | 1989-01-31 | 3000 | 10.9 | 3 830 | 31.0 | 11 | 11100 | 519 | 74 | 1.900 | 63.0 | | 0.23 | 8.30 | | | | -97 | -13.1 | 0.2 | | | | | | | 0.3 |
| KAS03 | Ground Water | KAS03-122 | -122 | 1989-02-21 | 1989-02-21 | 613 | 2.4 | 162 | 21.0 | 61 | 1220 | 31 | 5 | 0.129 | 3.3 | | 0.10 | 8.00 | | | | -125 | -15.8 | 0.1 | | | | | | | 2.0 |
| KAS03 | Ground Water | KAS03-239 | -239 | 1988-08-28 | 1988-08-28 | 1290 | 6.5 | 490 | 58.0 | 53 | 2950 | 39 | 18 | 0.300 | 9.7 | | 0.35 | 8.00 | | | | -118 | -14.5 | 8.0 | | -15.1 | | | | | 0.3 |
| KAS03 | Ground Water | KAS03-349 | -349 | 1988-08-16 | 1988-08-16 | 1770 | 5.9 | 1 400 | 40.0 | 12 | 5180 | 370 | 27 | 0.630 | 26.0 | | 0.27 | | | | | -105 | -13.3 | 4.0 | | | | | | | 0.3 |
| KAS03 | Ground Water | KAS03-455 | -454 | 1988-08-22 | 1988-08-22 | 1550 | 6.2 | 1 190 | 40.0 | 27 | 4600 | 300 | 21 | 0.610 | 21.0 | | 0.27 | 7.60 | | | | -110 | -13.6 | 4.0 | | | | | | | 0.3 |
| KAS03 | Ground Water | KAS03-603 | -602 | 1988-09-03 | 1988-09-03 | 1920 | 6.2 | 1 740 | 38.0 | 11 | 5880 | 470 | 46 | 0.730 | 28.0 | | 0.24 | 8.00 | | | | -103 | -13.3 | 4.0 | | | | | | | 1.1 |
| KAS03 | Ground Water | KAS03-831 | -830 | 1988-09-08 | 1988-09-08 | 2130 | 6.6 | 2 670 | 45.0 | 11 | 8080 | 680 | 51 | 0.830 | 44.0 | | 0.23 | 7.90 | | | | -100 | -13.0 | 4.0 | | | | | | | 0.3 |
| KAS03 | Ground Water | KAS03-915 | -914 | 1989-03-15 | 1989-03-15 | 3020 | 7.3 | 4 380 | 49.5 | 11 | 12300 | 709 | 85 | 1.650 | 78.0 | | 0.20 | 8.10 | | | | -96 | -12.7 | 0.4 | | | | | | | |
| KAS04 | Ground Water | KAS04-186 | -185 | 1989-04-17 | 1989-04-17 | 382 | 2.4 | 91 | 6.2 | 222 | 508 | 180 | 3 | | 1.8 | | | 8.20 | | | | -85 | -11.0 | 4.3 | | | | | | | 6.9 |
| KAS04 | Ground Water | KAS04-276 | -276 | 1989-04-27 | 1989-04-27 | 1180 | 6.1 | 740 | 30.0 | 69 | 3030 | 220 | 16 | 0.380 | 12.6 | | 0.31 | 8.00 | 0.48 | 0.4 | | -100 | -13.0 | 0.5 | | | | | | | 5.3 |
| KAS04 | Ground Water | KAS04-377 | -377 | 1989-04-03 | 1989-04-03 | 1890 | 7.8 | 1 660 | 61.0 | 21 | 5840 | 407 | 24 | 0.940 | 28.9 | | 0.44 | 8.10 | | | | -92 | -11.9 | 0.0 | | | | | | | 1.3 |
| KAS06 | Ground Water | KAS06-285 | -284 | 1989-06-07 | 1989-06-07 | 1820 | 9.1 | 1 490 | 119.0 | 49 | 5680 | 283 | 24 | 0.660 | 24.9 | | 0.83 | 7.50 | | | | -78 | -9.2 | 0.3 | | | | | | | 0.1 |
| KAS06 | Ground Water | KAS06-332 | -332 | 1989-06-14 | 1989-06-14 | 2070 | 11.7 | 1 410 | 153.0 | 64 | 5970 | 362 | 23 | 0.550 | 22.4 | 0.85 | 1.11 | 7.50 | | | | -69 | -7.4 | 0.6 | | | | | | | 0.1 |
| KAS06 | Ground Water | KAS06-434 | -433 | 1989-06-21 | 1989-06-21 | 2200 | 11.1 | 1 570 | 130.0 | 50 | 6150 | 459 | 30 | 0.740 | 25.8 | | 0.88 | 7.50 | | | | -71 | -8.2 | 3.5 | | | | | | | 0.5 |
| KAV01 | Ground Water | KAV01-675 | -675 | 1987-04-21 | 1987-04-21 | 3200 | | 2 800 | | 10 | 9700 | 390 | 74 | | | | | | | | | -93 | -12.8 | 1.5 | | | | | | | |
| KLX01 | Ground Water | KLX01-258 | -257 | 1988-12-08 | 1988-12-08 | 1040 | 6.2 | 243 | 28.0 | 83 | 2050 | 48 | 9 | 0.130 | 5.0 | | 0.20 | 8.10 | | | | -90 | -11.5 | 8.0 | | | | | | | 1.5 |
| KLX01 | Ground Water | KLX01-673 | -673 | 1988-11-03 | 1988-11-03 | 1680 | 7.1 | 1 400 | 23.0 | 24 | 4870 | 351 | 38 | 0.530 | 24.0 | | 0.20 | 8.10 | | | | -102 | -13.3 | 4.0 | | | | | | | 1.2 |
| KLX02 | Ground Water | KLX02-1069 | -1068 | 1993-12-16 | 1993-12-16 | 3800 | 10.4 | 5 620 | 2.1 | 8 | 15800 | 1010 | 130 | 1.710 | 80.7 | 0.00 | 0.01 | 8.50 | | | | -79 | -11.7 | | | | | | | | 1.1 |
| KLX02 | Ground Water | KLX02-1323 | -1323 | 1999-08-10 | 1999-08-10 | 6210 | 17.9 | 11 200 | 2.7 | 9 | 31230 | 1024 | 196 | 4.450 | 191.0 | 0.20 | 0.08 | 7.90 | | | 0.02 | -62 | -9.7 | 0.4 | 0 | | | 0.717 | | | 98.0 |
| KLX02 | Ground Water | KLX02-1531 | -1531 | 1994-01-17 | 1994-01-17 | 8030 | 29.0 | 18 600 | 2.7 | 9 | 45500 | 832 | 312 | 4.250 | 275.0 | 0.41 | 0.14 | 7.90 | | | | -47 | -8.9 | | | | | | | | 0.9 |
| KLX03 | Ground Water | KLX03-171 | -171 | 2004-12-15 | 2004-12-15 | 255 | 2.8 | 32 | 4.9 | 328 | 259 | 37 | | 0.029 | 0.6 | 0.26 | 0.06 | 8.20 | 0.63 | 0.1 | 0.16 | -85 | -11.5 | 0.4 | 46 | -17.0 | 37.2 | | | 0.004 | 21.0 |
| KLX03 | Ground Water | KLX03-380 | -380 | 2005-03-22 | 2005-03-22 | 791 | 5.5 | 234 | 10.8 | 189 | 1390 | 127 | | 0.087 | 4.8 | 0.41 | 0.11 | 7.89 | 0.42 | 0.0 | 0.08 | -98 | -13.0 | | 65 | -27.1 | 15.1 | 0.715 | | 0.006 | 13.0 |
| KLX03 | Ground Water | KLX03-923 | -922 | 2005-02-14 | 2005-02-14 | 2880 | 8.6 | 3 780 | 2.1 | 8 | 10500 | 758 | | 0.467 | 72.2 | 0.00 | 0.02 | 8.68 | 0.01 | 0.1 | 0.03 | -95 | -12.2 | 0.4 | | | 11.1 | 0.716 | | 0.020 | 1.4 |
| KLX04 | Ground Water | KLX04+6 | 7 | 2004-07-08 | 2004-07-08 | 94 | 3.1 | 41 | 8.3 | 268 | 44 | 20 | 0 | 0.021 | 0.5 | 0.13 | 0.19 | 7.93 | | | | -79 | -10.5 | 3.7 | | | | | | | |
| KLX04 | Ground Water | KLX04-487 | -487 | 2004-09-29 | 2004-09-29 | 691 | 3.2 | 234 | 6.9 | 51 | 1480 | 104 | 8 | 0.152 | 4.7 | 0.09 | 0.11 | 7.83 | 0.25 | 0.4 | 0.14 | -113 | -15.1 | 1.2 | 43 | | 12.7 | 0.716 | | 0.005 | 2.2 |
| KLX04 | Ground Water | KLX04-945 | -944 | 2004-09-16 | 2004-09-16 | 2010 | 7.7 | 2 710 | 5.0 | 8 | 7910 | 845 | 62 | 0.665 | 47.7 | 0.16 | 0.07 | 7.61 | 0.29 | 0.2 | 0.09 | -101 | -13.8 | 0.4 | | | 9.1 | 0.716 | | 0.020 | 0.5 |
| KLX05 | Ground Water | KLX05-205 | -205 | 2007-08-14 | 2007-08-14 | 446 | 4.3 | 55 | 7.2 | 194 | 592 | 146 | 3 | 0.050 | 1.0 | 0.36 | 0.08 | 8.42 | 3.59 | 0.0 | 0.03 | -88 | -12.1 | 0.4 | 30 | -14.9 | 24.9 | 0.715 | | 0.011 | 7.0 |
| KLX05 | Ground Water | KLX05-550 | -550 | 2006-12-05 | 2006-12-05 | 2500 | 12.2 | 1 360 | 8.7 | 12 | 5690 | 415 | 39 | 0.189 | 23.6 | 0.12 | 0.11 | 7.38 | | | | -88 | -12.2 | 0.4 | | | | | | | |
| KLX06 | Ground Water | KLX06-1 | 0 | 2004-12-21 | 2004-12-21 | 69 | 2.1 | 23 | 3.5 | 157 | 43 | 26 | 0 | 0.014 | 0.2 | 0.08 | 0.21 | 7.72 | | | | -74 | -10.5 | 4.6 | | | | | | | |
| KLX06 | Ground Water | KLX06-219 | -219 | 2005-03-09 | 2005-03-09 | 114 | 1.5 | 7 | 1.2 | 226 | 37 | 34 | 0 | 0.018 | 0.2 | 0.06 | 0.01 | 8.72 | | | | -80 | -11.1 | 0.4 | | | | | | | |
| KLX06 | Ground Water | KLX06-222 | -221 | 2006-10-24 | 2006-10-24 | 130 | 2.6 | 8 | 1.3 | 224 | 59 | 41 | 0 | 0.021 | 0.2 | 0.06 | 0.01 | 8.85 | 1.66 | 0.0 | 0.15 | -75 | -11.3 | 0.4 | 36 | -16.5 | 30.9 | 0.716 | | 0.028 | 3.5 |
| KLX06 | Ground Water | KLX06-476 | -475 | 2006-10-24 | 2006-10-24 | 514 | 8.3 | 169 | 10.6 | 86 | 778 | 376 | 4 | 0.087 | 3.3 | 0.05 | 0.06 | 8.49 | 0.21 | 0.0 | 0.07 | -88 | -13.0 | 0.4 | 38 | -18.8 | 13.5 | 0.716 | | 0.014 | 3.6 |
| KLX08 | Ground Water | KLX08-391 | -391 | 2006-06-19 | 2006-06-19 | 796 | 3.5 | 298 | 6.8 | 32 | 1590 | 133 | 8 | 0.165 | 5.5 | 0.30 | 0.09 | 7.85 | 0.03 | 0.0 | 0.01 | -117 | -15.6 | 2.1 | | | 17.0 | 0.716 | | 0.015 | 2.5 |
| KLX08 | Ground Water | KLX08-505 | -505 | 2006-07-26 | 2006-07-26 | 947 | 5.9 | 367 | 8.0 | 21 | 2030 | 145 | 11 | 0.174 | 6.8 | 0.02 | 0.09 | 8.19 | 0.03 | 0.1 | 0.01 | -113 | -15.2 | 2.5 | | | 13.2 | 0.716 | | 0.014 | 1.8 |
| KLX13A | Ground Water | KLX13A-409 | -408 | 2007-01-11 | 2007-01-11 | 449 | 1.8 | 52 | 3.1 | 74 | 744 | 37 | 3 | 0.072 | 1.2 | 0.00 | 0.03 | 8.35 | 0.05 | 0.0 | 0.00 | -120 | -15.9 | 3.6 | 22 | -16.6 | 29.0 | 0.715 | | 0.002 | 2.7 |
| KLX15A | Ground Water | KLX15A-468 | -467 | 2007-08-06 | 2007-08-06 | 2080 | 13.8 | 1 540 | 54.0 | 14 | 5890 | 425 | 29 | 0.293 | 27.7 | 0.54 | 0.55 | 7.42 | 0.14 | 0.1 | 0.03 | -81 | -10.8 | 0.4 | | | 17.3 | 0.716 | | 0.020 | 1.5 |
| KLX17A | Ground Water | KLX17A-343 | -342 | 2007-04-12 | 2007-04-12 | 322 | 4.0 | 68 | 9.4 | 122 | 565 | 23 | 2 | 0.045 | 1.7 | 0.79 | 0.10 | 7.96 | 0.12 | 0.0 | 0.07 | -111 | -14.4 | 0.9 | 44 | -16.8 | 31.3 | 0.715 | | 0.004 | 3.4 |
| KLX19A | Ground Water | KLX19A-414 | -414 | 2007-08-21 | 2007-08-21 | 962 | 8.3 | 152 | 10.1 | 36 | 1750 | 122 | 10 | 0.085 | 2.7 | 0.07 | 0.07 | 8.22 | 0.08 | 0.1 | 0.02 | -105 | -13.9 | 0.4 | 31 | -17.8 | 22.0 | 0.716 | | 0.002 | 1.5 |
| KSH01A | Ground Water | KSH01A-153 | -153 | 2003-04-22 | 2003-04-22 | 2280 | 14.7 | 960 | 70.8 | 26 | 5590 | 32 | 31 | 0.308 | 15.9 | 1.15 | 0.54 | 7.36 | 0.14 | 0.1 | 0.51 | -98 | -13.0 | 0.4 | | -13.5 | 23.1 | 0.715 | | | 0.9 |
| KSH01A | Ground Water | KSH01A-242 | -242 | 2003-05-05 | 2003-05-05 | 2580 | 12.0 | 1 160 | 63.5 | 18 | 6322 | 48 | 36 | 0.369 | 19.0 | 1.03 | 0.55 | 7.40 | 0.16 | 0.1 | 0.49 | -100 | -13.4 | 0.4 | | | 20.2 | 0.715 | | | 0.5 |
| KSH01A | Ground Water | KSH01A-246 | -246 | 2006-06-30 | 2006-06-30 | 2610 | 11.9 | 1 220 | 62.5 | 20 | 6320 | 25 | 35 | 0.477 | 21.3 | 0.61 | 0.63 | 7.57 | 0.07 | 0.1 | 0.14 | -100 | -13.7 | 0.4 | | | 28.0 | 0.711 | | 0.133 | 1.0 |
| KSH01A | Ground Water | KSH01A-532 | -532 | 2006-06-20 | 2006-06-20 | 3180 | 12.6 | 2 140 | 39.7 | 19 | 8560 | 209 | 63 | 0.716 | 36.8 | 0.32 | 0.46 | 7.51 | 0.10 | 0.1 | 0.31 | -91 | -12.6 | 0.4 | | | 19.3 | 0.716 | | 0.020 | 1.2 |
| KSH01A | Ground Water | KSH01A-537 | -536 | 2003-09-15 | 2003-09-15 | 3210 | 12.8 | 2 220 | 43.4 | 11 | 8876 | 230 | 73 | 0.606 | 36.3 | 0.46 | 0.48 | 7.63 | 0.15 | 0.1 | 0.05 | -92 | -12.7 | 1.1 | | | 17.7 | 0.715 | | | 0.5 |
| KSH02 | Ground Water | KSH02-416 | -415 | 2003-09-05 | 2003-09-05 | 3100 | 9.8 | 1 710 | 11.1 | 5 | 7803 | 227 | 59 | 0.366 | 26.7 | 0.08 | 0.13 | 6.83 | 0.57 | 0.1 | 0.03 | -94 | -12.8 | 0.4 | | | 17.7 | 0.715 | | | 0.5 |
| KSH02 | Ground Water | KSH02-419 | -419 | 2006-06-27 | 2006-06-27 | 3100 | 10.4 | 1 770 | 13.4 | 98 | 7910 | 27 | 58 | 0.439 | 28.5 | 0.03 | 0.16 | 7.38 | 0.03 | 0.1 | 0.68 | -91 | -12.8 | 0.4 | | 21.4 | 21.3 | 0.715 | | 0.005 | 240.0 |
| KSH02 | Ground Water | KSH02-571 | -571 | 2003-09-15 | 2003-09-15 | 3310 | 10.2 | 1 790 | 7.3 | 7 | 8262 | 303 | 67 | 0.359 | 28.9 | 0.03 | 0.14 | 8.13 | 0.10 | 0.1 | 0.03 | -93 | -12.9 | 0.4 | | | 17.1 | 0.715 | | | 0.5 |
| KSH02 | Ground Water | KSH02-952 | -952 | 2006-06-27 | 2006-06-27 | 4920 | 15.8 | 5 510 | 5.7 | 7 | 17100 | 592 | 127 | 0.997 | 95.4 | 0.05 | 0.08 | 8.32 | 0.00 | 0.1 | 0.46 | -74 | -10.9 | 0.8 | | | 13.3 | 0.716 | | 0.005 | 1.0 |
| PSM002060 | Sea Water | PO60B | | 2002-10-30 | 2005-01-26 | 2032 | 76.8 | 98 | 242.1 | 94 | 3755 | 547 | 14.8 | 0.032 | 1.48 | 0.01 | 0.00 | 7.77 | 0.77 | 0.1 | 0.03 | -56 | -7.0 | 14.4 | 109 | -2.6 | 20.3 | 0.710 | 0.27 | 0.027 | 3.8 |
| PSM002060 | Sea Water | PO60S | | 2002-10-30 | 2005-01-26 | 1979 | 74.4 | 95 | 235.3 | 92 | 3603 | 534 | 14.6 | 0.032 | 1.44 | 0.01 | 0.00 | 7.94 | 0.78 | 0.1 | 0.03 | -56 | -7.0 | 15.9 | 109 | -0.2 | 20.2 | 0.709 | 0.28 | 0.022 | 3.9 |
| PSM002061 | Sea Water | PO61B | | 2002-11-19 | 2004-12-01 | 2005 | 75.9 | 97 | 238.5 | 94 | 3701 | 539 | 14.6 | 0.032 | 1.46 | 0.02 | 0.00 | 7.84 | 0.77 | 0.1 | 0.03 | -56 | -7.0 | 13.8 | 109 | -1.0 | 19.9 | 0.709 | 0.32 | 0.038 | 4.0 |
| PSM002061 | Sea Water | PO61S | | 2002-10-30 | 2004-12-01 | 1988 | 74.9 | 96 | 235.7 | 92 | 3626 | 529 | 14.4 | 0.032 | 1.44 | 0.01 | 0.00 | 7.99 | 0.78 | 0.1 | 0.03 | -56 | -7.0 | 13.4 | 109 | -0.8 | 20.4 | 0.709 | 0.30 | 0.023 | 4.0 |
| PSM002062 | Sea Water | PO62B | | 2002-12-02 | 2005-04-26 | 1494 | 56.4 | 75 | 178.7 | 75 | 2774 | 401 | 10.7 | 0.025 | 1.10 | 0.10 | 0.02 | 7.46 | 0.74 | 0.1 | 0.03 | -61 | -7.7 | 13.3 | 108 | -3.6 | 19.8 | 0.710 | 0.61 | 0.022 | 7.4 |
| PSM002062 | Sea Water | PO62S | | 2002-12-02 | 2005-04-26 | 1274 | 48.6 | 65 | 153.1 | 64 | 2314 | 335 | 9.2 | 0.021 | 0.95 | 0.18 | 0.02 | 7.55 | 0.74 | 0.1 | 0.03 | -63 | -8.1 | 14.2 | 109 | -4.5 | 19.5 | 0.710 | 0.71 | 0.023 | 9.4 |
| PSM002063 | Sea Water | PO63B | | 2002-10-30 | 2003-10-28 | 1909 | 71.8 | 90 | 226.1 | 90 | 3531 | 515 | 12.5 | 0.031 | 1.38 | 0.01 | 0.01 | 7.90 | | | | | | | 110 | -1.0 | 21.9 | 0.709 | 0.33 | 0.022 | 4.2 |
| PSM002063 | Sea Water | PO63S | | 2002-10-30 | 2003-10-28 | 1907 | 71.3 | 90 | 226.7 | 90 | 3484 | 500 | 12.1 | 0.031 | 1.38 | 0.01 | 0.00 | 7.93 | | | | | | | 110 | -1.3 | 21.4 | 0.709 | 0.34 | 0.021 | 4.4 |

| IDCODE | WATER_TYPE | label | Elevation | First | Last | Na | K | Ca | Mg | $HCO_3^-$ | Cl | $SO_4^{2-}$ | Br | Li | Sr | Fe | Mn | pH | U | Th | La | $^2H$ | $^{18}O$ | $^3H$ | $^{14}C$ | $^{13}C$ | $\delta^{34}S$ | $^{87}Sr$ | $N_{tot}$ | $P_{tot}$ | DOC |
|---|---|---|---|---|---|---|---|---|---|---|---|---|---|---|---|---|---|---|---|---|---|---|---|---|---|---|---|---|---|---|---|
| | | | masl | date | date | mg·L$^{-1}$ | mg·L$^{-1}$ | mg·L$^{-1}$ | mg·L$^{-1}$ | mg·L$^{-1}$ | mg·L$^{-1}$ | mg·L$^{-1}$ | mg·L$^{-1}$ | mg·L$^{-1}$ | mg·L$^{-1}$ | mg·L$^{-1}$ | mg·L$^{-1}$ | | µg·L$^{-1}$ | µg·L$^{-1}$ | µg·L$^{-1}$ | ‰ SMOW | ‰ SMOW | TU | pMC | ‰ PCB | ‰ CDT | ratio | mg·L$^{-1}$ | mg·L$^{-1}$ | mg·L$^{-1}$ |
| PSM002064 | Sea Water | PO64B | | 2002-11-19 | 2007-07-24 | 1874 | 72.2 | 93 | 227.6 | 93 | 3489 | 497 | 12.8 | 0.031 | 1.42 | 0.22 | 0.04 | 7.29 | 0.75 | 0.1 | 0.07 | -57 | -7.0 | 14.3 | 107 | -5.1 | 20.1 | 0.709 | 0.56 | 0.039 | 5.2 |
| PSM002064 | Sea Water | PO64S | | 2002-11-19 | 2007-07-02 | 1620 | 62.5 | 81 | 197.5 | 78 | 3032 | 430 | 11.0 | 0.028 | 1.23 | 0.09 | 0.01 | 7.69 | 0.77 | 0.1 | 0.16 | -62 | -7.9 | 13.7 | 108 | -4.2 | 19.6 | 0.710 | 0.53 | 0.020 | 7.1 |
| PSM002065 | Lake Water | PL65B | | 2002-11-20 | 2007-07-24 | 10 | 1.6 | 7.5 | 2.4 | 14 | 13 | 13 | 0.1 | 0.002 | 0.04 | 0.88 | 0.06 | 6.71 | 0.32 | 0.1 | 1.22 | -66 | -8.4 | 12.0 | 105 | -19.8 | 3.6 | 0.722 | 1.08 | 0.025 | 15.2 |
| PSM002065 | Lake Water | PL65S | | 2002-11-20 | 2007-06-27 | 10 | 1.6 | 8.2 | 2.5 | 14 | 14 | 14 | 0.1 | 0.002 | 0.04 | 0.84 | 0.05 | 6.78 | 0.33 | 0.1 | 1.50 | -68 | -9.0 | 11.7 | 106 | -18.8 | 2.9 | 0.722 | 1.08 | 0.023 | 15.2 |
| PSM002066 | Lake Water | PL66B | | 2002-10-31 | 2003-10-28 | 11 | 1.6 | 10.2 | 3.0 | 14 | 15 | 22 | 0.1 | 0.003 | 0.06 | 0.26 | 0.29 | 6.69 | | | | -56 | -7.1 | 14.2 | 66 | -15.7 | 0.9 | 0.720 | 0.68 | 0.010 | 9.1 |
| PSM002066 | Lake Water | PL66S | | 2002-10-31 | 2003-10-28 | 11 | 1.6 | 9.9 | 2.9 | 11 | 15 | 22 | 0.1 | 0.002 | 0.05 | 0.06 | 0.03 | 6.99 | | | | -54 | -6.7 | 10.7 | 66 | -12.9 | 0.9 | 0.721 | 0.59 | 0.008 | 9.0 |
| PSM002067 | Lake Water | PL67B | | 2002-10-31 | 2005-03-16 | 10 | 1.3 | 9.2 | 2.4 | 19 | 15 | 10 | 0.2 | 0.002 | 0.05 | 2.50 | 0.30 | 6.49 | | | | -65 | -8.7 | 10.0 | 78 | -21.1 | 8.3 | 0.728 | 1.10 | 0.021 | 16.8 |
| PSM002067 | Lake Water | PL67S | | 2002-10-31 | 2005-03-16 | 9 | 1.3 | 8.5 | 2.2 | 15 | 13 | 9 | 0.1 | 0.002 | 0.04 | 1.30 | 0.09 | 6.77 | | | | -65 | -8.5 | 11.3 | 76 | -18.5 | 8.8 | 0.728 | 0.93 | 0.016 | 17.0 |
| PSM002068 | Stream Water | PW068 | | 2003-01-13 | 2004-11-16 | 6 | 1.1 | 9.8 | 2.4 | 23 | 7 | 8 | 0.1 | 0.002 | 0.10 | 1.77 | 0.20 | 6.56 | | | | | | | | | | | 1.30 | 0.029 | 18.2 |
| PSM002069 | Stream Water | PW069 | | 2002-11-20 | 2004-12-01 | 8 | 1.3 | 8.4 | 2.2 | 15 | 12 | 9 | 0.1 | 0.002 | 0.04 | 1.26 | 0.08 | 6.67 | | | | | | | | | | | 0.94 | 0.017 | 16.8 |
| PSM002070 | Stream Water | PW070 | | 2002-12-02 | 2003-10-28 | 11 | 0.9 | 12.5 | 2.8 | 31 | 16 | 7 | 0.1 | 0.002 | 0.11 | 1.25 | 0.23 | 6.59 | | | | | | | | | | | 1.07 | 0.028 | 18.3 |
| PSM002071 | Stream Water | PW071 | | 2002-12-02 | 2005-03-16 | 12 | 1.5 | 9.8 | 2.6 | 17 | 19 | 12 | 0.1 | 0.002 | 0.05 | 1.29 | 0.08 | 6.48 | 0.16 | 0.0 | 0.22 | -73 | -9.8 | 11.9 | 101 | -20.6 | 6.7 | 0.726 | 0.93 | 0.023 | 14.8 |
| PSM002072 | Stream Water | PW072 | | 2002-12-02 | 2003-10-28 | 9 | 0.8 | 4.3 | 1.1 | 3 | 10 | 5 | 0.1 | 0.002 | 0.02 | 0.86 | 0.04 | 5.53 | | | | -79 | -11.6 | 12.6 | | | 12.0 | 0.721 | 0.85 | 0.024 | 25.5 |
| PSM002075 | Stream Water | PW075 | | 2003-01-13 | 2003-10-28 | 10 | 1.2 | 13.0 | 3.2 | 31 | 14 | 10 | 0.1 | 0.003 | 0.07 | 2.03 | 0.19 | 6.48 | | | | | | | | | | | 1.39 | 0.040 | 22.4 |
| PSM002076 | Stream Water | PW076 | | 2003-01-13 | 2005-03-16 | 8 | 1.1 | 14.4 | 2.6 | 22 | 9 | 20 | 0.2 | 0.003 | 0.06 | 2.59 | 0.10 | 6.26 | | | | -78 | -11.0 | 12.0 | 93 | -19.8 | 8.5 | 0.720 | 2.11 | 0.070 | 29.0 |
| PSM002077 | Stream Water | PW077 | | 2002-12-03 | 2003-10-29 | 10 | 1.4 | 9.7 | 2.6 | 17 | 15 | 13 | 0.1 | 0.003 | 0.05 | 1.33 | 0.06 | 6.34 | | | | | | | | | | | 0.97 | 0.030 | 16.6 |
| PSM002078 | Stream Water | PW078 | | 2003-01-14 | 2004-12-01 | 4 | 0.5 | 7.4 | 1.9 | 4 | 5 | 20 | 0.2 | 0.002 | 0.04 | 0.79 | 0.05 | 5.71 | | | | | | | | | | | 1.00 | 0.020 | 16.7 |
| PSM002079 | Stream Water | PW079 | | 2002-12-18 | 2007-07-25 | 12 | 1.7 | 12.0 | 3.1 | 18 | 19 | 19 | 0.1 | 0.003 | 0.06 | 1.11 | 0.07 | 6.40 | 0.28 | 0.1 | 3.49 | -74 | -10.2 | 11.5 | 97 | -19.2 | 7.6 | 0.723 | 1.04 | 0.028 | 16.0 |
| PSM002080 | Stream Water | PW080 | | 2003-01-13 | 2003-10-28 | 9 | 1.8 | 10.8 | 2.1 | 27 | 11 | 8 | 0.1 | 0.002 | 0.05 | 1.37 | 0.06 | 6.35 | | | | | | | | | | | 1.40 | 0.056 | 21.8 |
| PSM002081 | Stream Water | PW081 | | 2003-01-14 | 2004-11-16 | 5 | 1.1 | 12.9 | 2.0 | 29 | 5 | 10 | 0.1 | 0.002 | 0.04 | 2.87 | 0.19 | 6.44 | | | | | | | | | | | 1.58 | 0.059 | 24.0 |
| PSM002082 | Stream Water | PW082 | | 2003-01-14 | 2004-11-16 | 9 | 1.8 | 14.3 | 2.5 | 35 | 11 | 11 | 0.1 | 0.002 | 0.06 | 1.99 | 0.12 | 6.40 | | | | -78 | -10.8 | 11.9 | 98 | -18.5 | 8.6 | 0.722 | 1.73 | 0.048 | 23.4 |
| PSM002083 | Stream Water | PW083 | | 2002-12-18 | 2007-06-28 | 11 | 1.5 | 13.0 | 2.9 | 21 | 14 | 20 | 0.1 | 0.004 | 0.06 | 1.48 | 0.07 | 6.38 | 0.57 | 0.2 | 3.16 | -78 | -11.0 | 11.3 | 104 | -16.7 | 6.1 | 0.721 | 1.28 | 0.046 | 19.7 |
| PSM002084 | Stream Water | PW084 | | 2002-12-03 | 2006-09-20 | 11 | 3.0 | 17.3 | 3.7 | 32 | 12 | 27 | 0.1 | 0.004 | 0.07 | 1.62 | 0.08 | 6.60 | 0.80 | 0.0 | 0.39 | -79 | -11.1 | 11.8 | 100 | -17.2 | 3.4 | 0.720 | 1.60 | 0.049 | 20.1 |
| PSM002085 | Stream Water | PW085 | | 2002-12-04 | 2007-07-25 | 15 | 1.3 | 30.9 | 3.9 | 74 | 15 | 30 | 0.1 | 0.004 | 0.09 | 1.09 | 0.06 | 7.39 | 1.15 | 0.1 | 1.75 | -78 | -11.0 | 12.9 | 95 | -13.7 | 7.1 | 0.721 | 1.88 | 0.045 | 20.2 |
| PSM002086 | Stream Water | PW086 | | 2002-12-03 | 2004-11-30 | 14 | 3.3 | 19.1 | 4.3 | 19 | 16 | 46 | 0.7 | 0.006 | 0.08 | 1.55 | 0.13 | 6.12 | | | | -78 | -11.2 | 12.3 | 93 | -17.9 | 3.8 | 0.719 | 2.66 | 0.062 | 25.5 |
| PSM002087 | Stream Water | PW087 | | 2002-12-04 | 2007-07-25 | 13 | 1.9 | 13.4 | 3.4 | 22 | 20 | 22 | 0.1 | 0.003 | 0.07 | 1.19 | 0.06 | 6.52 | 0.30 | 0.1 | 3.10 | -75 | -10.4 | 11.9 | 96 | -18.2 | 6.4 | 0.723 | 1.16 | 0.033 | 16.6 |
| PSM002170 | Precipitation | PN170 | 6 | 2002-09-09 | 2006-12-20 | 2 | 0.8 | 0.9 | 0.3 | 1 | 2 | 2 | 0.1 | 0.002 | 0.01 | 0.05 | 0.03 | 4.94 | | | | -71 | -9.9 | 11.9 | | | | | | | |
| PSM005964 | Lake Water | PL64B | | 2003-08-14 | 2004-11-17 | 14 | 2.7 | 11.1 | 3.6 | 38 | 19 | 14 | 0.1 | 0.002 | 0.05 | 0.94 | 0.05 | 7.06 | | | | | | | | | | | 0.91 | 0.026 | 11.9 |
| PSM005964 | Lake Water | PL64S | | 2003-08-14 | 2004-11-16 | 14 | 2.6 | 11.0 | 3.6 | 36 | 19 | 15 | 0.1 | 0.002 | 0.05 | 0.82 | 0.02 | 7.21 | | | | | | | | | | | 0.85 | 0.023 | 11.9 |
| PSM007097 | Sea Water | PO97B | | 2005-05-25 | 2007-07-24 | 1864 | 73.7 | 95.8 | 230.2 | 92 | 3529 | 489 | 11.9 | 0.033 | 1.47 | 0.05 | 0.07 | 7.38 | 0.76 | 0.1 | 0.17 | | | | | | | | 0.59 | 0.034 | 5.5 |
| PSM007097 | Sea Water | PO97S | | 2005-04-25 | 2007-07-24 | 1580 | 62.5 | 82.8 | 194.8 | 76 | 2987 | 424 | 9.9 | 0.029 | 1.24 | 0.05 | 0.01 | 7.90 | 0.70 | 0.1 | 0.57 | | | | | | | | 0.60 | 0.020 | 7.7 |
| PSM107735 | Stream Water | PW735 | | 2003-12-10 | 2004-12-01 | 5 | 1.5 | 13.8 | 3.9 | 7 | 6 | 37 | 0.2 | 0.009 | 0.06 | 1.87 | 0.14 | 5.71 | | | | -73 | -10.5 | 12.9 | | | 3.6 | 0.721 | 1.35 | 0.030 | 32.1 |
| SSM000002 | Near Surface GW | S002+0 | 0 | 2003-04-22 | 2003-04-22 | 59 | 11.5 | 31.8 | 28.8 | 371 | 9 | 13 | 0.1 | 0.012 | 0.27 | 0.99 | 0.34 | 7.75 | | | | | | | | | 0.712 | | | | |
| SSM000008 | Near Surface GW | S008+0 | 1 | 2004-03-23 | 2005-06-01 | 9 | 1.9 | 31.9 | 3.4 | 110 | 4 | 8 | 0.1 | 0.003 | 0.09 | 1.57 | 0.28 | 6.83 | 3.41 | 0.8 | 11.25 | -78 | -10.9 | 13.0 | 84 | -17.3 | 0.8 | 0.719 | | 0.047 | 15.0 |
| SSM000010 | Near Surface GW | S010+2 | 3 | 2004-03-23 | 2005-06-01 | 10 | 3.9 | 40.9 | 6.8 | 138 | 5 | 20 | 0.1 | 0.010 | 0.13 | 4.95 | 0.59 | 6.86 | 8.00 | 1.5 | 24.95 | -77 | -10.8 | 13.4 | 78 | -17.5 | -8.8 | 0.719 | | 0.071 | 15.0 |
| SSM000012 | Near Surface GW | S012-4 | -4 | 2004-03-25 | 2005-05-31 | 44 | 5.7 | 55.0 | 8.8 | 209 | 18 | 69 | 0.1 | 0.017 | 0.18 | 2.44 | 0.56 | 7.51 | 3.37 | 1.6 | 5.22 | -75 | -10.4 | 10.0 | 66 | -11.4 | 6.7 | 0.720 | | 0.055 | 8.3 |
| SSM000014 | Near Surface GW | S014-1 | -1 | 2004-03-23 | 2005-03-22 | 16 | 5.5 | 21.5 | 11.1 | 58 | 12 | 58 | 0.1 | 0.036 | 0.09 | 12.52 | 0.60 | 6.29 | 11.80 | 2.2 | 16.30 | -75 | -10.3 | 14.3 | 90 | -18.2 | -11.4 | 0.720 | | 0.104 | 7.4 |
| SSM000016 | Near Surface GW | S016-1 | 0 | 2004-03-23 | 2005-05-31 | 5 | 2.9 | 50.1 | 6.1 | 140 | 7 | 19 | 0.1 | 0.008 | 0.06 | 4.66 | 0.08 | 6.58 | 27.60 | 2.4 | 19.30 | -81 | -11.0 | 13.0 | 84 | -17.0 | -0.6 | 0.733 | | 0.168 | |
| SSM000018 | Near Surface GW | S018-2 | -2 | 2004-03-23 | 2005-05-31 | 63 | 38.9 | 42.1 | 16.4 | 64 | 118 | 102 | 0.7 | 0.022 | 0.16 | 2.11 | 0.38 | 6.22 | 4.05 | 1.5 | 19.00 | -76 | -10.5 | 12.2 | 98 | -19.6 | -2.3 | 0.716 | | 0.194 | 9.4 |
| SSM000020 | Near Surface GW | S020+3 | 4 | 2004-03-23 | 2005-03-17 | 6 | 3.2 | 28.2 | 6.3 | 40 | 5 | 51 | 0.1 | 0.012 | 0.09 | 5.46 | 0.34 | 6.17 | 1.90 | 0.8 | 22.10 | -76 | -10.3 | 13.3 | 85 | -18.8 | -6.4 | 0.722 | | 0.026 | 12.0 |
| SSM000022 | Near Surface GW | S022-1 | -1 | 2004-03-23 | 2007-09-06 | 212 | 6.3 | 21.8 | 7.4 | 275 | 139 | 129 | 1.1 | 0.022 | 0.26 | 0.68 | 0.09 | 7.88 | 4.54 | 0.3 | 1.76 | -77 | -10.6 | 1.6 | 46 | -11.2 | 22.2 | 0.716 | 0.93 | 0.035 | 5.9 |
| SSM000024 | Near Surface GW | S024+0 | 0 | 2004-06-22 | 2004-06-22 | 6 | 2.5 | 15.3 | 4.0 | 99 | 4 | 5 | 0.1 | 0.007 | 0.07 | 5.89 | 0.29 | 6.89 | | | | -79 | -10.5 | 12.6 | 89 | -16.5 | 6.4 | 0.722 | | | |
| SSM000026 | Near Surface GW | S026-1 | 0 | 2004-03-23 | 2005-03-17 | 7 | 1.8 | 21.0 | 3.8 | 55 | 6 | 16 | 0.1 | 0.004 | 0.05 | 6.27 | 0.38 | 6.41 | | | | -76 | -10.2 | 14.0 | | | 3.5 | 0.724 | | | |
| SSM000027 | Near Surface GW | S027+5 | 5 | 2004-09-28 | 2006-03-21 | 6 | 1.2 | 5.2 | 1.3 | 13 | 6 | 15 | 0.1 | 0.002 | 0.02 | 3.45 | 0.11 | 5.68 | 0.62 | 0.5 | 8.22 | -80 | -11.1 | 10.0 | | | -0.9 | 0.718 | 0.73 | 0.026 | 3.9 |
| SSM000029 | Near Surface GW | S029-5 | -5 | 2005-06-14 | 2006-05-16 | 98 | 8.1 | 19.2 | 9.8 | 199 | 84 | 22 | 0.7 | 0.013 | 0.12 | 7.05 | 0.22 | 6.73 | 1.43 | 2.8 | 12.37 | -79 | -11.0 | 9.8 | 85 | -17.9 | 26.3 | 0.718 | 1.78 | 0.173 | 11.3 |
| SSM000030 | Near Surface GW | S030+6 | 7 | 2004-09-27 | 2007-09-04 | 30 | 2.6 | 70.0 | 8.6 | 254 | 15 | 42 | 0.1 | 0.010 | 0.27 | 2.87 | 0.62 | 7.13 | 0.64 | 0.5 | 2.57 | -78 | -10.9 | 9.1 | 69 | -15.3 | 10.9 | 0.715 | 2.10 | 0.185 | 8.7 |
| SSM000031 | Near Surface GW | S031+2 | 3 | 2004-12-09 | 2006-05-16 | 8 | 1.1 | 13.0 | 2.9 | 41 | 8 | 14 | 0.1 | 0.002 | 0.04 | 4.65 | 0.13 | 6.29 | 0.78 | 0.9 | 10.31 | -78 | -11.0 | 11.1 | | | -0.4 | 0.720 | 0.27 | 0.017 | 9.8 |
| SSM000034 | Near Surface GW | S034-4 | -3 | 2004-09-14 | 2006-05-30 | 74 | 12.8 | 102.4 | 44.9 | 529 | 119 | 0 | 1.1 | 0.025 | 0.51 | 6.67 | 1.35 | 6.91 | 0.09 | 0.3 | 0.93 | -78 | -11.0 | 14.5 | 106 | -13.1 | | 0.712 | 0.81 | 0.091 | 7.2 |
| SSM000035 | Near Surface GW | S035+23 | 24 | 2006-03-21 | 2006-03-21 | 8 | 2.9 | 15.8 | 5.8 | 69 | 4 | 15 | 0.1 | 0.004 | 0.05 | 5.90 | 0.70 | 6.49 | 1.80 | 2.1 | 16.70 | -76 | -11.0 | 9.0 | | | 3.1 | | 0.26 | 0.109 | 4.5 |
| SSM000037 | Near Surface GW | S037+9 | 9 | 2005-03-22 | 2007-09-04 | 43 | 3.9 | 49.8 | 7.8 | 194 | 31 | 39 | 0.1 | 0.015 | 0.21 | 5.43 | 0.66 | 6.84 | 1.21 | 0.9 | 9.01 | -79 | -11.0 | 7.7 | 69 | -17.8 | 14.1 | 0.717 | 0.63 | 0.070 | 8.4 |
| SSM000039 | Near Surface GW | S039+7 | 8 | 2006-03-23 | 2006-05-23 | 6 | 1.9 | 30.6 | 4.3 | 35 | 9 | 70 | 0.1 | 0.003 | 0.07 | 0.57 | 0.07 | 6.13 | 2.58 | 0.4 | 14.85 | -81 | -11.4 | 11.7 | | | -18.1 | | 0.85 | 0.026 | 6.7 |
| SSM000040 | Near Surface GW | S040-2 | -1 | 2004-09-09 | 2005-09-08 | 90 | 9.7 | 27.3 | 19.6 | 157 | 147 | 18 | 0.7 | 0.017 | 0.19 | 16.59 | 0.37 | 6.71 | 5.59 | 1.2 | 16.95 | -78 | -10.8 | 12.2 | | | | 0.714 | | 0.196 | |
| SSM000041 | Near Surface GW | S041+1 | 1 | 2005-03-22 | 2007-09-06 | 10 | 5.1 | 47.9 | 8.6 | 113 | 24 | 36 | 0.1 | 0.012 | 0.14 | 14.77 | 0.66 | 6.49 | 0.62 | 0.8 | 8.59 | -79 | -10.9 | 10.0 | 69 | -16.7 | 5.4 | 0.720 | 0.54 | 0.106 | 9.8 |
| SSM000042 | Near Surface GW | S042-1 | -1 | 2004-12-16 | 2007-09-06 | 71 | 4.6 | 58.8 | 13.3 | 163 | 81 | 87 | 0.6 | 0.010 | 0.15 | 10.97 | 0.85 | 6.80 | 1.86 | 1.4 | 16.15 | -77 | -10.8 | 8.4 | 77 | -17.5 | -4.0 | 0.718 | 0.61 | 0.088 | 6.7 |
| SSM000224 | Near Surface GW | S224-10 | -10 | 2005-09-15 | 2006-05-16 | 28 | 3.8 | 15.9 | 3.9 | 38 | 45 | 16 | 0.1 | 0.002 | 0.06 | 0.30 | 0.05 | 6.16 | 3.35 | 0.4 | 7.19 | -79 | -11.1 | 10.7 | | | -0.9 | 0.722 | 0.48 | 0.005 | 7.8 |
| SSM000226 | Near Surface GW | S226+2 | 2 | 2005-09-20 | 2006-03-28 | 11 | 2.2 | 32.3 | 4.5 | 115 | 6 | 12 | 0.1 | 0.002 | 0.11 | 0.91 | 0.11 | 6.82 | 4.26 | 0.4 | 9.93 | -79 | -11.1 | 10.7 | 63 | -14.5 | 4.4 | 0.718 | 0.76 | 0.018 | 10.7 |
| SSM000227 | Near Surface GW | S227+5 | 6 | 2005-12-09 | 2005-12-09 | 7 | 3.6 | 13.7 | 5.3 | | 10 | 28 | 0.1 | 0.006 | 0.09 | 2.04 | 0.17 | 4.94 | 1.21 | 0.3 | 19.80 | -75 | -10.9 | 13.5 | | | 27.1 | | 5.08 | 0.051 | 21.7 |
| SSM000228 | Near Surface GW | S228+6 | 7 | 2005-12-13 | 2007-09-04 | 38 | 2.4 | 36.8 | 6.1 | 126 | 40 | 39 | 0.2 | 0.011 | 0.10 | 5.97 | 0.53 | 6.61 | 2.49 | 0.8 | 13.03 | -79 | -10.9 | 9.1 | | | 1.2 | | 0.51 | 0.025 | 12.6 |
| SSM000230 | Near Surface GW | S230+0 | 1 | 2005-12-13 | 2006-05-18 | 96 | 5.9 | 32.5 | 4.8 | 37 | 173 | 19 | 0.1 | 0.008 | 0.15 | 1.06 | 0.05 | 6.43 | 0.93 | 0.3 | 6.40 | -81 | -11.4 | 11.6 | | | 1.7 | | 7.20 | 1.777 | 11.6 |
| SSM000238 | Near Surface GW | S238-12 | -11 | 2006-03-14 | 2006-03-14 | 1910 | 67.8 | 110.0 | 243.0 | 194 | 3610 | 480 | 12.2 | 0.033 | 1.52 | 0.57 | 0.26 | 7.11 | 0.26 | 0.1 | 1.17 | -54 | -7.0 | 13.5 | | | 19.8 | | 3.55 | 0.641 | 7.6 |
| SSM000239 | Near Surface GW | S239-4 | -4 | 2006-03-14 | 2006-03-14 | 1290 | 51.8 | 89.6 | 155.0 | 504 | 2480 | 130 | 9.9 | 0.027 | 1.35 | 1.06 | 0.26 | 7.31 | 0.54 | 0.2 | 2.14 | -60 | -7.6 | 9.7 | | | 32.1 | | 11.40 | 0.719 | 9.9 |
| SSM000240 | Near Surface GW | S240-5 | -5 | 2006-03-15 | 2007-09-12 | 327 | 14.3 | 84.9 | 44.1 | 264 | 609 | 57 | 2.8 | 0.020 | 0.60 | 1.17 | 0.68 | 7.37 | 0.65 | 0.4 | 1.44 | -75 | -10.3 | 9.0 | | | 23.0 | | 1.96 | 0.360 | 10.4 |
| SSM000241 | Near Surface GW | S241-3 | -3 | 2006-09-12 | 2006-09-12 | 12 | 5.3 | 56.7 | 8.2 | 147 | 20 | 37 | 0.2 | 0.010 | 0.16 | 8.22 | 0.72 | 6.68 | 0.87 | 1.1 | 7.87 | -78 | -10.8 | 11.3 | | | | | 0.68 | 0.134 | 9.4 |
| SSM000241 | Near Surface GW | S241-33 | -32 | 2007-05-31 | 2007-05-31 | 2650 | 129.0 | 323.0 | 419.0 | 5170 | 4770 | 24 | 171.0 | 0.145 | 5.12 | 2.34 | 0.94 | 6.69 | 0.49 | 0.1 | 0.14 | -65 | -8.5 | 1.9 | | | | | 625.00 | 58.500 | 106.0 |
| SSM000242 | Near Surface GW | S242-16 | -15 | 2006-02-16 | 2006-02-16 | 2230 | 94.0 | 258.0 | 341.0 | 3520 | 3570 | 1 | 63.0 | 0.099 | 3.63 | 6.67 | 2.02 | 6.74 | 1.02 | 0.2 | 0.62 | -64 | -8.1 | 1.4 | | | 10.1 | 0.712 | 270.00 | 27.000 | 71.3 |
| SSM000260 | Near Surface GW | S260+2 | 2 | 2007-03-20 | 2007-03-20 | 21 | 3.6 | 68.9 | 11.1 | 239 | 12 | 52 | 0.1 | 0.010 | 0.25 | 1.34 | 0.38 | 7.25 | 0.23 | 0.3 | 1.76 | | | | | | | | 1.90 | 0.166 | 9.5 |
| SSM000261 | Near Surface GW | S261+0 | 1 | 2007-03-20 | 2007-03-20 | 28 | 5.7 | 63.3 | 13.7 | 249 | 13 | 44 | 0.1 | 0.017 | 0.27 | 8.18 | 0.64 | 6.97 | 4.80 | 1.6 | 14.30 | | | | | | | | 5.40 | 1.210 | 11.5 |
| SSM000262 | Near Surface GW | S262-2 | -2 | 2007-03-22 | 2007-03-22 | 35 | 3.8 | 43.0 | 8.0 | 152 | 41 | 36 | 0.2 | 0.009 | 0.22 | 3.63 | 0.48 | 7.05 | 1.37 | 0.2 | 0.66 | | | | | | | | 2.18 | 0.126 | 12.6 |
| SSM000263 | Near Surface GW | S263-3 | -3 | 2007-03-22 | 2007-03-22 | 138 | 19.8 | 96.0 | 14.3 | 135 | 331 | 58 | 1.4 | 0.016 | 0.48 | 0.90 | 0.51 | 7.17 | 1.59 | 0.6 | 2.72 | | | | | | | | 3.01 | 0.238 | 8.8 |